IDENTIFICATION AND EVALUATION OF NEW RESOURCE OIL PLAYS IN NORTHEAST BRITISH COLUMBIA'S PORTION OF THE WESTERN CANADA SEDIMENTARY BASIN

GEOSCIENCE BC REPORT 2018-20

July, 2018

Petrel Robertson Consulting Ltd.

Trican Geological Solutions
(now AGAT Laboratories)

Howard Anderson, P.Eng.

TABLE OF CONTENTS

APPENDICES

LIST OF TABLES

LIST OF MAPS

LIST OF CROSS-SECTIONS

EXECUTIVE SUMMARY

Horizontal drilling and multi-frac completions have greatly augmented B.C. gas and liquids resources and reserves by accessing unconventional (low-permeability) reservoirs. However, relatively little new unconventional oil potential has been identified in what is generally regarded as a gas-prone area of the Western Canada Sedimentary Basin.

Geoscience BC has tasked the PRCL project team with identifying new exploration and exploitation fairways for oil in unconventional reservoirs – “Resource Oil”. Our analysis spans the entire stratigraphic column, with the exception of the Montney Formation, which is the subject of numerous dedicated studies and is an active oil and liquids drilling target.

We identified resource oil targets using regional geological assessments of reservoir and production trends in conventional, tight, and shale reservoirs. We reviewed all existing files of analytical data – standard core analysis, geochemistry / maturity, mineralogy, geomechanical properties – submitted to the BC OGC, and tabulated them to support future detailed analyses. Where analytical data were lacking on promising plays, we sampled cores and completed comprehensive laboratory analyses, which are included in this report. Finally, we analyzed test and production data from a reservoir engineering perspective to better understand the scope and quality of potential resource oil fairways.

Of 19 reservoir intervals deemed suitable for analysis, 10 were judged to have little realistic prospectivity (a ‘**C**’ prospectivity grade) for reasons including: lack of extensive low-permeability reservoir facies, poor geomechanical properties (low “frackability”), and lack of viable oil charge. Six others were assigned a ‘**B**’ grade – indicating some real resource oil potential based on existing oil shows or production and favourable geological / geomechanical characteristics, but generally lacking either substantial horizontal / multi-frac testing, or good evidence of extensive resource oil fairways. One target – Doig Formation sandstones – was assigned an ‘**A/B**’ grade, as there is some very good existing production and possible scope to extend the development fairway into both conventional and tight areas. Only two reservoirs – the Halfway and Chinkeh formations, were seen as ‘**A**’ targets. The Chinkeh is prospective for tight oil across a broad, poorly-defined fairway downdip from the existing Maxhamish gas field, while the Halfway presents halo oil potential in lower-permeability shoreface sandstones offsetting historical conventional production focused on higher-quality tidal channel sandstones.

INTRODUCTION

Horizontal drilling and multi-frac completions have greatly augmented B.C. gas and liquids resources and reserves in recent years, by identifying and making accessible hydrocarbons in unconventional (low-permeability) reservoirs. Adams *et al*. (2016) demonstrated that by 2014, horizontal multi-frac drilling for gas and liquids-rich gas had come to dominate oil and gas industry drilling in British Columbia (Fig. 1).

However, relatively little new unconventional oil potential has been identified in what is generally regarded as a gas-prone area of the Western Canada Sedimentary Basin. The Oil and Gas Fields map of NE British Columbia shows a scattering of existing oil pools from Desan in the north to Brassey in the south, but many of these are fairly small and stratigraphically restricted (Fig. 2).

Geoscience BC has tasked the PRCL project team with identifying new exploration and exploitation fairways for oil in unconventional reservoirs – "Resource Oil" – accessible through modern drilling and completions technology. This report summarizes our study of this potential throughout northeastern British Columbia. Our work does not address the Montney Formation, which has been the subject of recent dedicated studies, and is currently being actively developed for oil and liquids-rich gas.

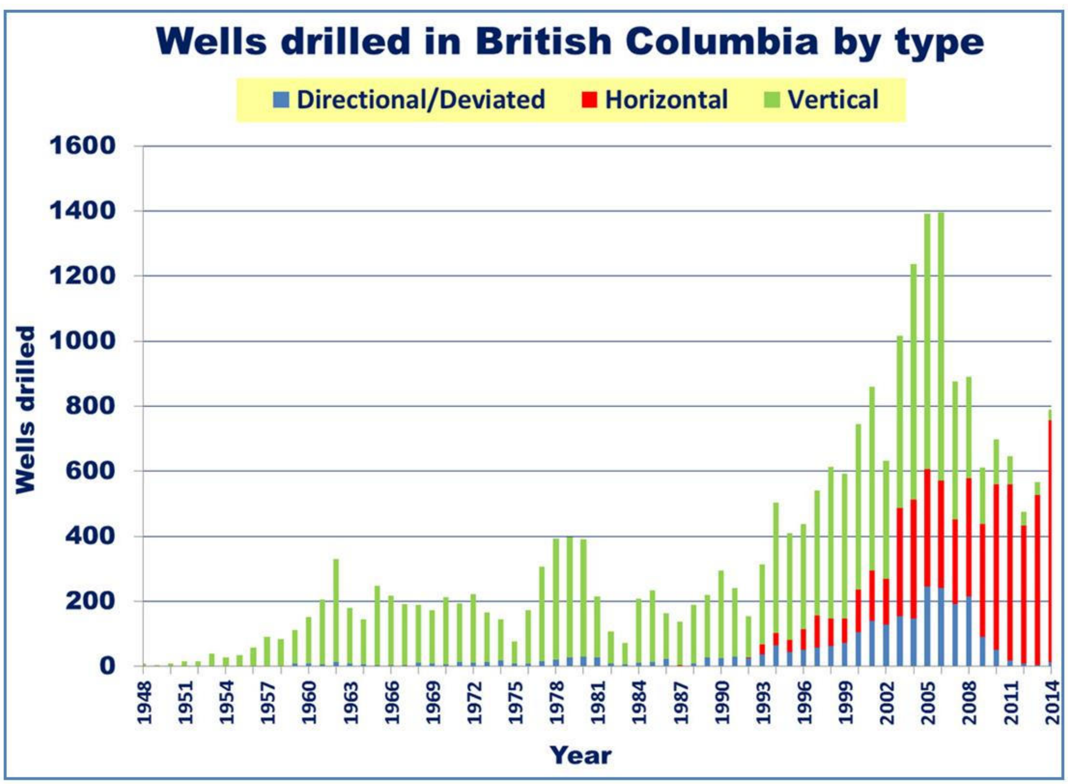

Figure 1. Wells drilled in British Columbia by type (from Adams *et al*., 2016).

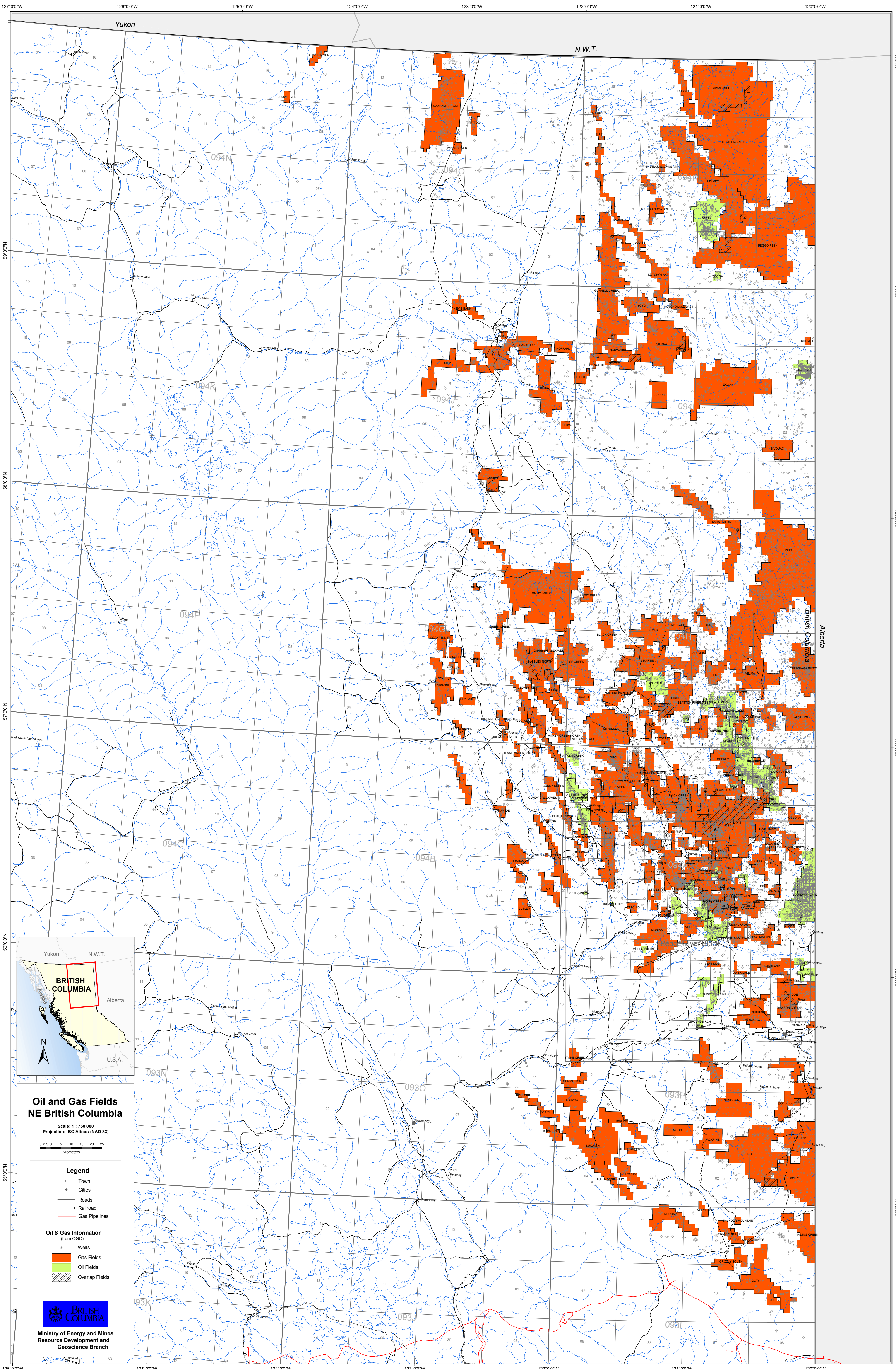

Figure 2. Oil and Gas Fields in NEBC (http://www2.gov.bc.ca/gov/content/industry/natural-gas-oil/petroleum-geoscience/petroleum-geoscience-publications/petroleum-maps-and-figures).

PROJECT TEAM

Petrel Robertson Consulting Ltd. (PRCL) (www.petrelrob.com) is a fully integrated petroleum geoscience consulting firm, with a wealth of expertise in unconventional oil and gas exploration, appraisal, and development in Canada. We have produced comprehensive regional assessments of petroleum and natural gas resources in Canada and internationally for more than thirty years, with a focus on unconventional reservoirs over the past decade. We have worked extensively in NEBC, evaluating conventional and unconventional plays in Devonian through Upper Cretaceous reservoirs.

Trican Geological Solutions (TGS) was founded in 2000 (formerly CBM Solutions Ltd.). TGS initially formed to evaluate coalbed methane projects throughout Canada and the United States and evolved through technical focus and research to become a leader in the field of unconventional resource analysis and testing. The *Geological Solutions* personnel provide evaluations and data instrumental in understanding reservoir development and ultimately enhancing well completion efforts. Current offerings include a complete array of laboratory analytical testing, geological studies, project evaluation and consulting for shale, tight-rock and coalbed methane reservoirs. In-house analyses and programs include rock mechanics, extensive testing of rock properties, gas-in-place and oil-in-place modeling, natural gas liquids yield modeling, petrophysical modeling and petrographic, SEM and CT imaging. Prior to completion of this project, the TGS team and facilities were acquired by AGAT Laboratories (www.agatlabs.com).

Howard Anderson is a professional engineer with over 35 years' experience in the oil and gas industry. Specializing in reservoir engineering, he has worked in both management and technical positions. Beginning at Imperial Oil, followed by 14 years at Canadian Hunter, he embarked on a series of entrepreneurial junior companies, including Rockyview Energy, Triangle Petroleum, and Tuzo Energy, organizations which specialized in developing and exploiting unconventional reservoirs, CBM, shale gas, and shale oil. Currently providing consulting services, he is also working with a team of colleagues to start a new company with a strategy of acquiring and redeveloping under-exploited light oil reservoirs.

EVALUATING RESOURCE OIL PLAYS

Unconventional gas and oil plays have come to dominate drilling activity in the Western Canada Sedimentary Basin in the 2010's. In the early days of unconventionals, attempts were made to delineate fixed boundaries – such as permeability values – between conventional and unconventional reservoirs. With continued evaluation of various plays, and with constantly-improving drilling and completion technologies, we now realize a near-continuous spectrum of reservoir characteristics that challenges fixed definitions.

Therefore, for the purpose of this study, we define unconventional reservoirs as follows:

> Unconventional reservoirs consist of low-permeability rock in which the pore spaces are poorly connected, making it difficult for oil and gas to flow. In order to produce oil and gas at economic rates, industry uses advanced stimulation techniques – primarily horizontal drilling and multi-stage hydraulic fracturing.

"Unconventional" is thus a moving target, dependent upon technology and economics as well as upon reservoir characteristics.

Clarkson and Pedersen (2011) analyzed the spectrum of unconventional oil plays, and assigned them to three categories:

- **Tight** oil plays – oil has migrated from source to reservoir, which consists of clastics or carbonates with low permeability, requiring horizontal drilling and multi-frac stimulation to produce oil at economic rates. The Middle Bakken sandstone of the Williston Basin and portions of the Montney in Alberta and B.C. are good examples;

- **Halo** oil plays – oil has migrated from source to reservoir, which includes lower-permeability fringes flanking conventional clastic and carbonate reservoirs. The halo play can be developed with horizontal, multi-frac wellbores to enlarge the original conventional play area. Halo plays may extend vertically from a conventional pool, as well as laterally. The Cardium Formation in west-central Alberta is the classical example;

- **Shale** oil plays – oil accumulations hosted by true shales / mudrocks – source and reservoir are the same, or are finely interbedded. Some research suggests that pore networks in true shales can produce liquids-rich gas, but are too small to flow actual oil (Dembicki, 2014). However, recent drilling successes point to appropriate combinations of brittle rock, organic content and thermal maturity, and effective fracturing being able to support economic oil production from shales, or shales with interbedded fine clastics or carbonates. Examples include: the Cretaceous Second White Specks of Alberta, the Devonian Duvernay

Formation of central Alberta, and Permian shales and distal clastics in the Permian Basin of Texas and New Mexico.

Our assessment of resource oil potential in northeastern B.C. is guided by the Clarkson and Pedersen classification. We discuss several examples of each of the three categories, specifying the category as we introduce each prospective unit. One key learning is that tight and halo oil reservoirs can occur in normal stratigraphic trap settings, and thus are not limited to regional, basin-centred settings that are typical of many unconventional gas plays. Our search has thus been very wide-ranging.

Another key point is that recovering oil from unconventional reservoirs is more difficult to accomplish than recovering gas. The U.S. Energy Information Administration (2013), in its first comprehensive world-wide review of both shale gas and shale oil resources, made the following critically-important point:

> "the production of shale oil requires that at least 15 percent to 25 percent of the pore fluids be in the form of natural gas so that there is sufficient gas-expansion to drive the oil to the well-bore. In the absence of natural gas to provide reservoir drive, shale oil production is problematic and potentially uneconomic at a low production rate. Consequently, producer drilling activity that currently targets oil production in the Eagle Ford shale is primarily focused on the condensate-rich portion of the formation rather than those portions that have a much greater proportion of oil and commensurately less natural gas."

Thus, simply identifying oil in place and reservoir characteristics is not sufficient to predict productive potential, particularly in shales. Operators in the Duvernay play of Alberta drilled hundreds of wells and experimented extensively with completion technologies for several years, and decided to focus development on liquids-rich gas reservoirs at Fox Creek / Kaybob, as they could not make economic oil wells in the area. Only recently has true oil production from the Duvernay been established in the shallower East Shale Basin area, although its productive potential is still being tested.

UNCONVENTIONAL OIL EVALUATION STRATEGY

Our strategy in this report is to define and describe potential resource oil plays in NEBC, and to set the stage for more detailed work in the future that will establish play viability and optimize economics. We are working largely at a conceptual level, as there has been little drilling dedicated to resource oil plays in B.C.

To fulfill this strategy, we do need to understand two key elements for each potential resource oil play:

1. The oil resource in place – governed by the distribution of the reservoir, its capacity to contain hydrocarbons, and the geochemistry and maturity of the source rocks (which may be the same as the reservoir for self-sourced / shale plays);

2. The produceability of the oil resource. Reservoir mineralogies and geomechanical properties can be measured to determine how readily the rock can be fracture stimulated. The reservoir stress regime, which depends upon rock properties, regional stress fields and their anisotropies, and reservoir pressure will also play a role in designing fracture stimulation programs, and determining how effectively the rock can be fractured.

In the future, we would look for our work to be built upon by systematic collection and analysis of supporting datasets, as has been undertaken on the Horn River play in NWT (e.g., Pyle *et al*., 2014). With such data, detailed unconventional play evaluation, as outlined by Stoneburner (2015) can be undertaken – and in the future, advanced resource potential models, such as those constructed for the Cardium Formation by Chen and Osadetz (2013), can be constructed.

WORKPLAN

PHASE 1. PLAY IDENTIFICATION

Our team completed an exhaustive review of known and possible petroleum systems in northeastern British Columbia, in order to identify potential resource oil plays. We incorporated a thorough investigation of the literature, built on the group's extensive experience in conventional and unconventional reservoirs. We compiled relevant evaluation data from all available literature and reports, including an exhaustive review of analytical reports submitted to the BC Oil & Gas Commission. These are summarized in Appendix 1; filters can be applied to the spreadsheet to identify data from particular formations or locations, or by data type. Finally, we reviewed all existing oil production to identify existing or potential unconventional plays.

PRCL qualitatively ranked potential Resource Oil plays on criteria including: oil in place potential, reservoir characteristics amenable to hydraulic fracturing, existing infrastructure, and ease of access. We identified three ranking levels:

- 'A' Plays – Best productive potential, will be the focus of analytical work in this project;

- 'B' Plays – Lesser productive potential, worthy of geological characterization, but limited or no new analytical work;

- 'C' Plays – Future productive potential seen, but potential is limited, and justifies only scoping-level geological analysis.

PHASE 2. LABORATORY AND ANALYTICAL WORK

Analytical test results support analysis of the two key resource oil play elements: oil resource in place, and produceability of the resource from the host reservoir.

Some of the most critical analyses include:

- ***Source Rock Analysis (SRA)*** – generally undertaken using Rock-Eval Pyrolysis, SRA generates a variety of data about organic matter in the reservoir, including:

    - Total Organic Carbon (TOC), a measure of the organic richness of the rocks.
    - T_{max}, a measure of organic maturity, which plays a role in determining what hydrocarbons have been and can be generated. T_{max} is measured at the S2 peak during Rock-Eval pyrolysis, and is generally regarded as valid

only where TOC is >0.3 wt %, and S2 exceeds 0.2 mg HC/g rock (Ferri *et al*., 2013). Bustin and Bustin (2016) defined the oil window to lie between T_{max} 435°C and 465°C, but recognized that these ranges depend upon the nature of the organic material in the reservoir. Other measures of organic maturity, such as Vitrinite Reflectance (VRo) data, may also be available; Bustin and Bustin (2016) defined the oil-generating window to lie between VRo 0.65% and 1.35%.

    - The S1 parameter measures residual oil compositions in rock samples, and can be important in calculation of hydrocarbon in place and reservoir fluid gravity.

- ***Adsorption Isotherm*** – Measures the net holding capacity for gases in the sorbed state. Depending on the gas compositions in the reservoir, multiple isotherms may be required. If a gas is present in compositions >5% (CH_4, CO_2 or C2+), separate isotherms are run for each gas and a "net" isotherm is modeled to show the total storage capacity based on the relative percentages of gases found in the reservoir. Isotherm data are used for total hydrocarbon in place calculations.

- ***Porosity*** – Measures total porosity using mercury immersion by Archimedes Principle (bulk density) and helium pycnometry (skeletal density). Porosity measurements provide a direct petrophysical measurement for well log calibration, and are critical inputs for resource in place calculations.

- ***Confined Permeability (Pulse Decay Method)*** – Designed for ultra-low permeability rocks, this method measures the permeability of samples under simulated reservoir conditions, as well as the stress sensitivity of permeability (change in permeability related to changes in effective confining pressure). Results indicate potential for fluid flow through the reservoir.

- ***Steady State Permeability*** – Measures the permeability of samples under ambient conditions up to net effective stress conditions. Steady state permeability is designed for rocks with higher (conventional) permeability (>0.01mD).

- ***X-Ray Diffraction (XRD) and Clay Speciation*** – Identifies the mineral phases and quantifies bulk mineralogical composition of the reservoir, which is key to determination of brittleness.

- ***Thin sections*** – Used to examine the fabric, mineral assemblages, and distribution of pore space, from which pore development and diagenesis can be interpreted.

- ***Scanning Electron Microscopy with XRF (SEM/EDS)*** – Complements thin section analysis and examines fabric, pore development, diagenesis (overgrowths, pore-filling, etc.) and mineral distribution at a micro-/nano-scale.

X-ray fluorescence is used to determine geochemical compositions of specific features.

- ***Mechanical Properties*** – Most critical of these are Young's modulus (YM) and Poisson's ratio (PR), which are used to model and understand behaviour of reservoir rocks when fractured. These are measured in the laboratory, and can be calculated from well logs, particularly dipole sonic logs. See Appendix 2 for further discussion.

After compiling existing datasets from the literature and BCOGC core files, we identified gaps hindering effective evaluation of prospective resource oil plays. We designed and completed a program of sampling from cores and sample cuttings, and undertook analytical procedures to best evaluate each play; complete results are presented in Appendix 3, along with more detail on laboratory procedures. While we did not undertake any interpretation of dipole sonic logs, wells with available dipole sonics are highlighted on play maps.

PHASE 3. PLAY CHARACTERIZATION

Characterizations completed for Resource Oil plays were governed by their overall prospectivity, and upon available datasets. Work included:

Reservoir mapping and facies characterization

- Depth to top formation and total thickness maps, outlining areal extent of the play;
- Facies and paleogeographic interpretations, backed by previous studies, literature, and core and sample observations
    - Cross-sections illustrate stratigraphic elements that are key controllers for productive potential;
- Where possible, reservoir mapping and characterization has been related to existing conventional pools.

Reservoir quality assessment

- Lithological / petrographic controls on reservoir quality;
- Porosity / permeability relationships, backed by core and sample data.

Hydrogeology, geochemistry, and fluid distribution

- Organic matter content, type and maturity in each play, as a guide to hydrocarbon types that would be expected to occur;
- Production and hydrogeology

    - Careful stratigraphic screening to identify and assign production and test data to the correct stratigraphic unit;

Reservoir engineering

- Our initial workplan included extensive use of mini-frac data and other modern datasets, but we found insufficient available information on most plays to provide useful and comprehensive assessment;
- A more conventional reservoir engineering analysis was instead completed on production and test data from specific wells and reservoirs identified from our screening.

Summary characterization

- Oil in place potential is described qualitatively, or semi-quantitatively where comparison can be drawn with quantitative assessments. We do not have sufficient data nor scope to undertake a proper probabilistic assessment, as outlined, for example, by National Energy Board / NTGS (2015).
- Describe key reservoir characteristics and their relevance to successful development and oil recovery
    - Address potential recovery factors and total recoverable volumes, with reference to geomechanical and reservoir engineering analysis
- Discuss productive analogues and relate development results in those to play potential.
- Assess success of drilling efforts to date, if any.

RESERVOIRS REVIEWED AND REJECTED

Resource oil targets in northeastern B.C. range in age from Devonian through Cretaceous. Figure 3 depicts the NEBC stratigraphic column, and highlights potential resource oil targets. We review these in stratigraphic order, from oldest to youngest, but first we discuss briefly reservoirs that were reviewed and rejected as insufficiently prospective for resource oil.

Keg River Formation

- **Reservoir**: Platform carbonates in Presqu'ile / Keg River barrier flanking Horn River Basin and Cordova Embayment; isolated reef buildups within evaporitic Muskeg section at Rainbow / Zama / Shekilie to east. Reefal outliers in eastern Horn River Basin at Yoyo and Sierra, in Klua Embayment at Klua. Grades southward to Muskeg evaporites. No evidence for systematic development of tight reservoir facies.
- **Source rocks**: Devonian shales in adjacent basins
- **Production and hydrogeology**: Regionally wet, conventional stratigraphic structural traps hosting gas in the west, oil to the east (in Alberta).
- **Assessment**: No evidence for development of extensive tight reservoir facies as seen in some other reefal units like the Swan Hills Formation; source rocks are gas prone where the Keg River exists in NEBC.

Horn River Shales (Evie / Otter Park / Klua)

- **Reservoir**: Shale, components of Horn River Basin and Cordova Embayment gas-producing package
- **Source rocks**: Self-sourced
- **Production and hydrogeology**: Produce gas from horizontal multi-frac wells in Horn River Basin and Cordova Embayment
- **Assessment**: Mature to over-mature for gas in Horn River, Liard, and Cordova basins.

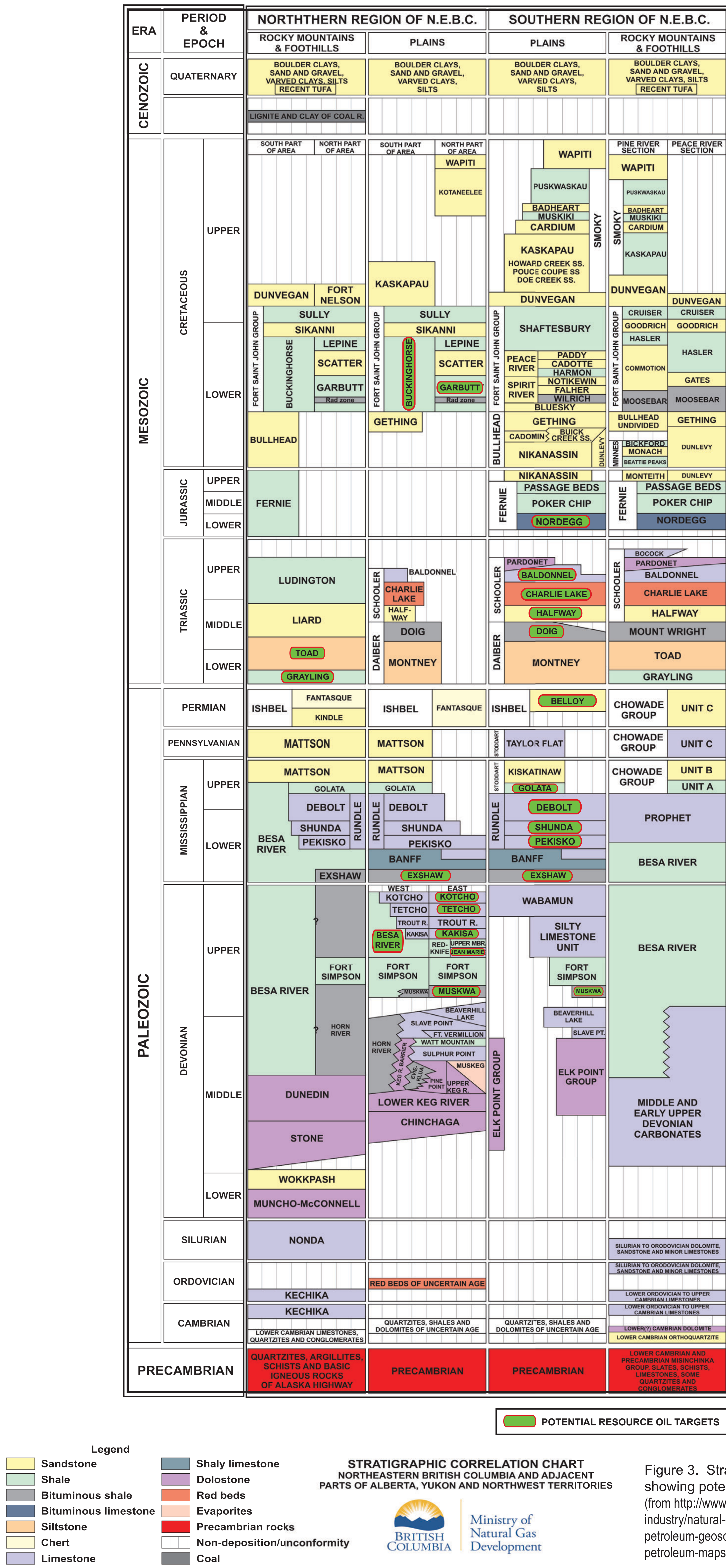

Figure 3. Stratigraphic column, NEBC, showing potential resource oil targets (from http://www2.gov.bc.ca/gov/content/industry/natural-gas-oil/petroleum-geoscience/petroleum-geoscience-publications/petroleum-maps-and-figures).

Slave Point Formation

- **Reservoir** Platform carbonates throughout NEBC and northwestern Alberta, flanking Horn River Basin and Cordova Embayment in north, and Peace River Arch in south.
- **Source rocks**: Devonian shales in adjacent basins
- **Production and hydrogeology**: Regionally wet, conventional stratigraphic structural traps hosting gas in the west, oil to the east (in Alberta).
- **Assessment**: No evidence for systematic development of tight reservoir facies as seen in some other reefal units like the Swan Hills Formation; source rocks are gas prone in NEBC.

Fort Simpson Formation

- **Reservoir**: Shale, regionally-extensive basin fill of Woodbend / Winterburn age
- **Source rocks**: Organic-poor, not recognized as a source rock
- **Production and hydrogeology**: No production or shows
- **Assessment**: Geochemical / source rock work indicates very low organic content and no substantial productive potential.

Mattson Formation

- **Reservoir**: Fluvial – marginal marine sandstones in northern and eastern Liard Basin. Sourced from north, shaling out southward into Liard Basin. Possible tight reservoir fairways in distal facies.
- **Source rocks**: Exshaw and Besa River shales
- **Production and hydrogeology**: Isolated, structurally controlled gas pools associated with Bovie Fault Zone on eastern flank of Liard Basin; conventional reservoir quality.
- **Assessment**: There is extensive conventional and probably tight reservoir potential, but not clearly associated with oil-prone source rocks. Well control is inadequate to evaluate oil potential.

Nikanassin Formation (including Buick Creek sandstone)

- **Reservoir**: Fluvial – deltaic / marginal marine sandstones with excellent reservoir quality where not degraded by burial diagenesis. The northern subcrop edge occurs in 94A and 94H.
- **Source rocks**: Self-sourced (? – coals), Nordegg / Gordondale, Triassic
- **Production and hydrogeology**: Deep Basin gas in south (93I, 93P), in tight, deeply-buried reservoirs. There are highly-productive gas wells in tight,

naturally-fractured Foothills reservoirs in 93I and west of Buick Creek (Town/Gundy) (PRCL, 1997).

- **Assessment**: Significant tight reservoir potential in Deep Basin area, but associated exclusively with gas-prone source rocks. Very small, structurally-bounded oil pools exist in the Buick Creek / Fireweed areas, probably associated with local migration of deeper oils.

Cadomin / Gething / Bluesky

- **Reservoir**: Fluvial – deltaic / marginal marine sandstones with fair-excellent reservoir quality where not degraded by burial diagenesis. Thick stacked section in southern Deep Basin through Peace River block and northward to major west-east valley fill at the northern flank of the Early Cretaceous continental drainage system in 94G/H (Hayes, 2005). Limited to thin fluvial and transgressive deposits filling valleys and mantling the sub-Cretaceous unconformity north of 94G/H (PRCL, 2000).
- **Source rocks**: Self-sourced (? – coals), Nordegg / Gordondale, Triassic
- **Production and hydrogeology**: Deep Basin gas in south (93I, 93P), limited by reservoir quality and generally limited continuity. Isolated conventional oil and gas pools in Peace River Block and northward. Major medium-gravity Bluesky oil pool at Hay River.
- **Assessment**: Significant tight reservoir potential in Deep Basin area, but associated exclusively with gas-prone source rocks. Local oil charge (e.g., Elm, Hay River) likely a function of deeper source rock maturity, but resource-scale low-permeability facies are not developed.

Dunvegan Formation (including Doe Creek sandstone)

- **Reservoir**: Deltaic / marginal marine sandstones deposited on fringes of extensive, northerly-sourced deltaic complex with numerous internal T/R cycles. Section is very shallow (to outcrop) in much of BC, and tends to be in non-marine facies with poorer reservoir quality and continuity.
- **Source rocks**: Cretaceous shales
- **Production and hydrogeology**: Relatively small oil and gas pools, predominantly in Alberta where source rocks and reservoirs are more marine and continuous, and source rocks are oil-prone. Very minor oil production at Tupper (93-P-1). Best-looking sands at substantial burial depths in 93P generally test tight with no significant oil shows.
- **Assessment**: Little regional reservoir potential, and no indications of oil prospectivity.

RESOURCE OIL RESERVOIRS

MUSKWA FORMATION

Age and Play Type

Upper Devonian – Shale Oil play;
Prospectivity: 'B' play – Limited data, productive potential not established.

Regional Geology

Ferri and Griffiths (2014) described the Muskwa Formation as:

> "a Late Devonian (Frasnian) unit that conformably underlies the Fort Simpson shale found throughout northeastern British Columbia, except in the region of the Peace River high (Fig. M1). It also overlies the Slave Point, Waterways and Keg River formations (Evie reef complex) and Otter Park carbonates as its lower contact moves from shelf to basin. In the Horn River Basin, Muskwa strata have been placed within the Horn River Formation and reduced to member status.
>
> The Muskwa is an approximate stratigraphic equivalent to the Duvernay Formation in Alberta and the Canol Formation in the Northwest Territories. In northwestern British Columbia, the Muskwa and the Horn River Formation become a subset of the Besa River Formation as one approaches the deformation belt.

The Muskwa is a pyritic, siliceous, variably calcareous and generally organic-rich dark grey to black shale, and is viewed as a principal source horizon in the Western Canada Sedimentary Basin."

On logs, the Muskwa is characterized by elevated gamma values, caused by the concentration of radioactive minerals in association with organic-rich intervals (see Cross-section MWA-MWA', MWB-MWB', MWC-MWC'). Resistivity values are moderate, reflecting the generally silica-rich, low-calcareous composition. We sampled a cored section at Husky Bivouac a-55-B/94-I-8, a thick Muskwa shale section lying on lighter-coloured Waterways shales with a sharp contact (Appendix 4).

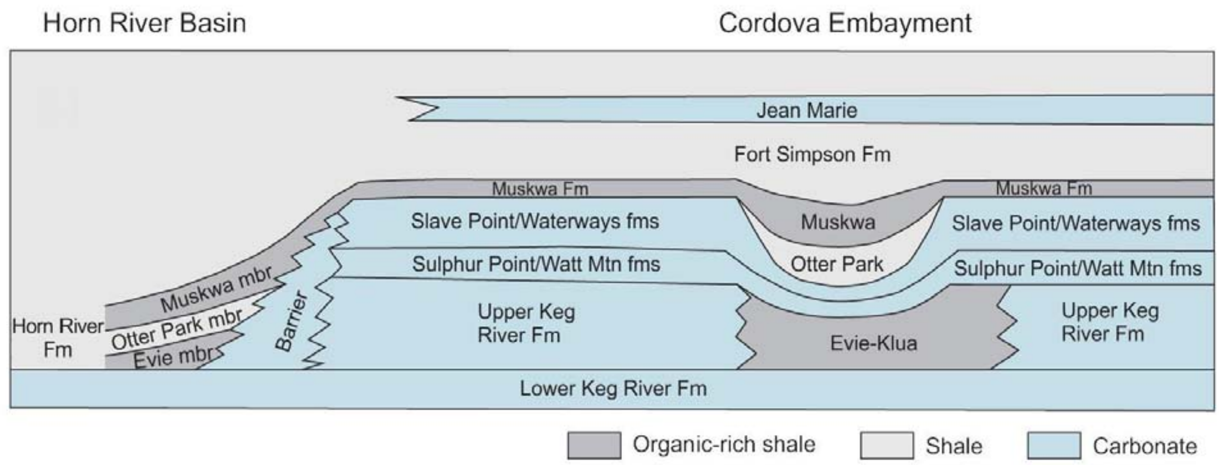

Figure M1. Stratigraphic relationships for Muskwa Formation in northern NEBC (from Ferri and Griffiths, 2014). Muskwa shales are generally thinner southward toward the Peace River Arch.

Figure M1 shows the Muskwa to be thick in the shale-dominated sections of the Horn River Basin and Cordova Embayment, and thinner where it caps the Slave Point / Waterways sections regionally. Cross-section MWA-MWA' demonstrates the thicker Muskwa in the Cordova Embayment to the north, and Cross-section MWB-MWB' demonstrates thicker Muskwa sections in the eastern Rainbow-Zama sub-basins. In the Hotchkiss Embayment to the south, Slave Point reefal facies are replaced by Waterways shales, but the Muskwa does not appear to thicken systematically (Cross-section MWA-MWA'). Further to the south, the Muskwa pinches out against the Peace River Arch, a positive feature during Devonian time.

Regional isopach Map M1 gives a general idea of Muskwa thickness throughout NEBC, but relies on commercial database tops which are not totally consistent, particularly to the west in the Liard Basin. Figure M2 shows more consistent regional westward thickening of the Muskwa into the Horn River and Liard Basins, but at a much larger scale. Burial depths to top Muskwa range from about 1500m in the east to >3500m in the southwest, and more than 4500m in the Liard Basin (Map M2).

Production and Test Data

Maps M1 and M2 show a number of horizontal Muskwa gas wells in the Horn River Basin and Cordova Embayment. In the Bivouac area (94-I-8) of the western Rainbow-Zama sub-basins (94-I-8 and adjacent Alberta), industry has tested Muskwa shales with horizontal multi-frac wells where they are liquids-prone (Adams *et al.*, 2016). Several producing wells are highlighted on Maps M1 and M2, and on Cross-section MWC-MWC'. Although large in-place oil and gas resources have been mapped in the Muskwa of northwestern Alberta (Rokosh et al., 2012), there has been little drilling and production other than the Rainbow-Zama sub-basin activity documented here, and no drilling since 2014.

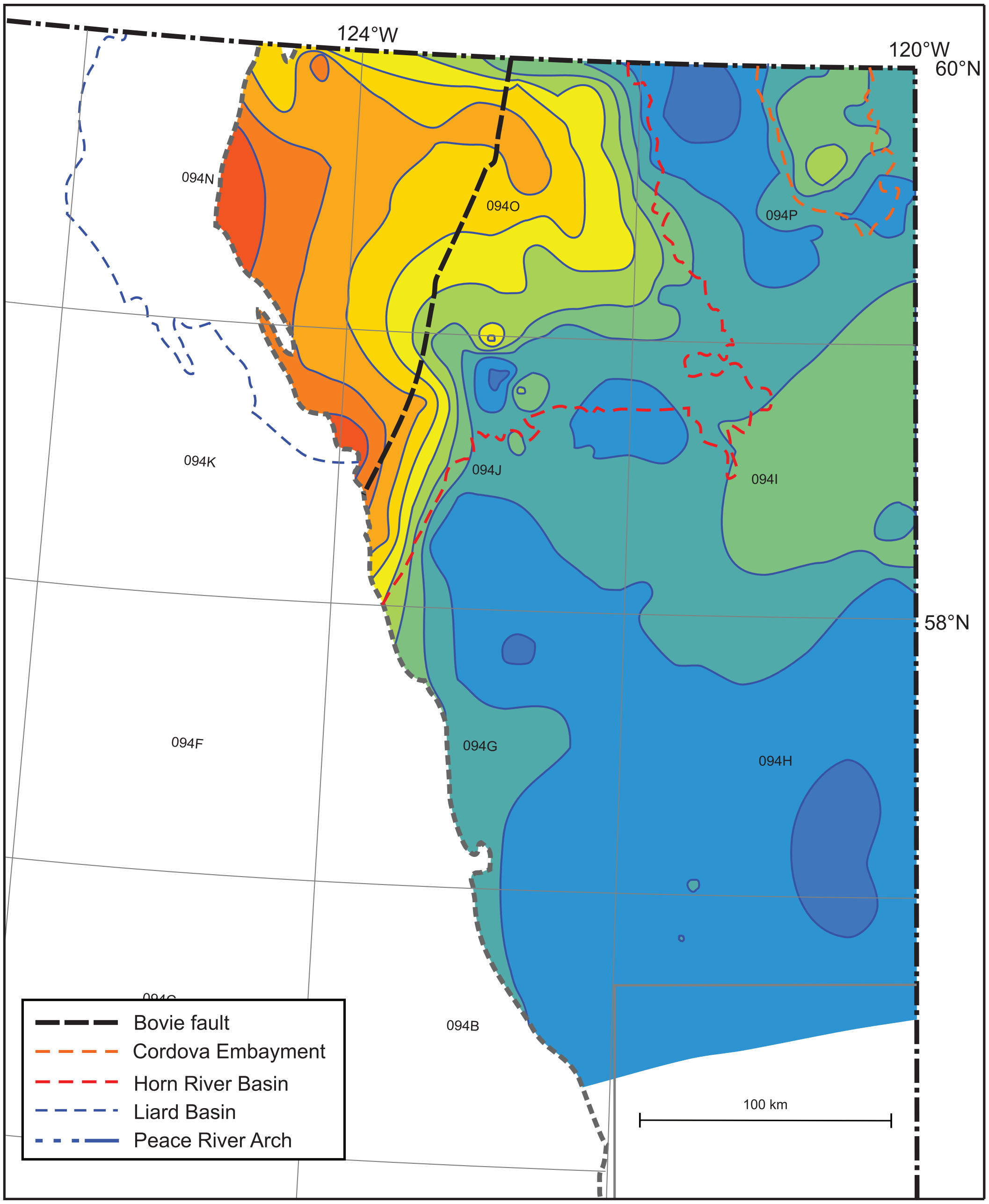

Figure M2. Regional thickness map, Muskwa Formation (from Ferri and Griffiths, 2014). Thickness increases from blue to red.

Reservoir Engineering Analysis

We studied production from 13 horizontal Muskwa wells south and east of the Horn River Basin and Cordova Embayment – nine oil wells drilled between 2009 and 2012 in Alberta, one gas well and one uncompleted well in Alberta, and two B.C. gas wells. Horizontal legs vary between 600m and 1700m, and all were fracked with 3 to 25 stages using both perf and open hole techniques (Table M1). We saw no correlation between completion characteristics and production results. None of the wells were drillstem tested; however, initial reservoir pressures were measured in most. Pressure gradients are as high as 0.49 psi/ft (11.08 kPa/m) to datum depth, indicating some degree of overpressure. We also noted gradients as low as 0.29 psi/ft, but it is not clear whether all pressure measurements are fully built up.

Well	Top Completion	Bottom Completion	Approx HZ Length	Completion Style	No of Fracs	IP bbl/d	EUR bbl
100/16-33-106-09W6/00	2015	3769	1754	Perf, acid, frac	16	54	13232
100/13-34-106-09W6/00	2060	3769	1709	Perf, frac	17	65	9572
100/02-28-107-09W6/02	1858	3179	1321	Perf, frac	3	23	2810
100/08-36-108-11W6/02	1961	3370	1409	Open hole	25	27	3079
100/02-30-109-08W6/00	2219	2990	771	Perf, frac	11	129	116000
100/03-30-109-08W6/00	2115	3120	1005	Open hole	12	51	10870
100/16-06-109-12W6/00	2020	3540	1520	Open hole	14	11	1033
100/04-30-110-09W6/00	2822	3380	558	Open hole	7	31	6993
100/02-25-110-10W6/00	2070	3807	1737	Perf, frac	20	97	55000

Table M1. Completion summary, Muskwa oil wells.

Table M2 summarizes production from each of the nine horizontal oil wells. They all appear to be connected to gathering systems, and intermittent production does not appear to be related to weather (see production plots, Appendix 5). Only one well, 2-30-109-8W6 can be deemed economic, with at IP rate of 20.5 m^3/d (129 BOPD), cumulative production of 10.2 e^3m^3 (64 MBO), and estimated ultimate recoverable resources of 18.4 e^3m^3 (116 MBO). Only one of the three gas wells recovered substantial gas – b-33-B/94-I-8/02 produced 0.46 BCF (13.0 e^6m^3), with a forecast EUR of >1 BCF (see Muskwa Report in Appendix 5 for more detail).

Well	Field	Pool	Status	Current Operator	First Prod	Last Prod	Cum OIL (Bbl)	Cum GAS (Mcf)	Cum CND (Bbl)	Cum WTR (Bbl)	IP bbl/d	EUR bbl
100/16-33-106-09W6/00	HARO	Muskwa	Susp OIL	Husky	2014/04	2016/10	13232	90136	0	2720	54	13232
100/13-34-106-09W6/00	HARO	Muskwa	Pump OIL	Husky	2014/04	2017/10	9572	110172	0	2351	63	9572
100/02-28-107-09W6/02	RAINBOW	Muskwa	Susp OIL	Husky	2011/04	2011/11	2810	4295	0	3210	23	2810
100/08-36-108-11W6/02	BLACK	Muskwa	ABD OIL	Murphy	2012/03	2012/08	3079	35827	0	3290	27	3079
100/02-30-109-08W6/00	RAINBOW	Muskwa	Pump OIL	Husky	2009/11	2018/01	63690	58746	0	3073	129	116000
100/03-30-109-08W6/00	RAINBOW	Muskwa	Susp OIL	Husky	2012/10	2017/04	10870	12263	0	1379	51	10870
100/16-06-109-12W6/00	BLACK	Muskwa	Susp OIL	Husky	2013/08	2013/12	1033	29140	0	0	11	1033
100/04-30-110-09W6/00	BLACK	Muskwa	Pump OIL	Husky	2013/10	2017/11	6993	17257	0	4192	31	6993
100/02-25-110-10W6/00	BLACK	Muskwa	Pump OIL	Husky	2013/04	2018/01	39803	95734	0	0	97	55000

Table M2. Production statistics, Muskwa oil wells.

Analytical Data

B.C. Ministry of Energy and Mines / CBM Solutions (2005) tabulated Rock-Eval data for twenty Muskwa samples from seven wells in NEBC. They found S2 values to be very low, suggesting the shales to be overmature with respect to the oil window, and T_{max} values unreliable for determination of maturity. Huge gas resources hosted by the Muskwa and older Horn River shales have been identified in the Horn River Basin and Cordova Embayment. BCMEM/NEB (2011) tabulated gas-in-place of $3729e^9m^3$ (132 TCF) and marketable gas of $711e^9m^3$ (25 TCF) (medium case) in the Muskwa in the Horn River Basin, while in the Cordova Embayment BCMNGD (2015) assigned $700.3e^9m^3$ (24.7 TCF) gas-in-place and $90.9e^9m^3$ (3.2 TCF) marketable gas in the Muskwa (P50 case). Gas in both basins is very dry, with significant CO_2 content – indicative of very low liquids potential. Wilson and Bustin (2017) have acquired additional Muskwa geochemical and maturity data in undertaking an analysis of petroleum systems in Devonian shales in the Horn River and Liard Basins.

We mapped Total Organic Carbon (TOC) for the Muskwa, using all available Rock-Eval and Source Rock Analyzer (SRA) data in NEBC (Appendix 6; Map M3). Where multiple data points are available from one wellbore, we selected median TOC values. In the major basins where thick sections are sampled, TOC values are generally moderate to high.

- The Rainbow-Zama area, part of the Alberta Muskwa Basin, has TOC values typically between 1-3 wt%, and shows decreasing TOC content with increasing rock burial and maturity from east to west. Downhole TOC analysis of the one core from the Rainbow-Zama area in BC, at well Husky Bivouac a-55-B/94-I-8, demonstrates large organic content variability (1.6-5.6 wt%) and richness despite the thermal maturity (T_{max} 443-473°C) (see Muskwa Core Analysis section below).

- The Horn River Basin shows TOC values ranging generally between 2 and 4 wt%, but up to 8 wt% TOC in some areas.

- The Cordova Embayment shows TOC values ranging up to >4 wt%. Using log analysis, Balogun (2014) determined the Muskwa to have fair to good source rock potential in the Cordova Embayment.

Relatively low TOC values outside the major basins reflect at least in part the thinner Muskwa section, and likely inadequate sampling and dilution with other shales where drill cuttings were analyzed. Overall, it is clear that the Muskwa is generally rich in organic matter.

Ferri and Griffiths (2014) mapped vitrinite reflectance data in NEBC to show generally high thermal maturities, although lower values indicate prospectivity for liquids-rich gas generation eastward along the Alberta border (Fig. M3). However, during the Devonian higher-order plants were just emerging and only limited vitrinite is present – and where it

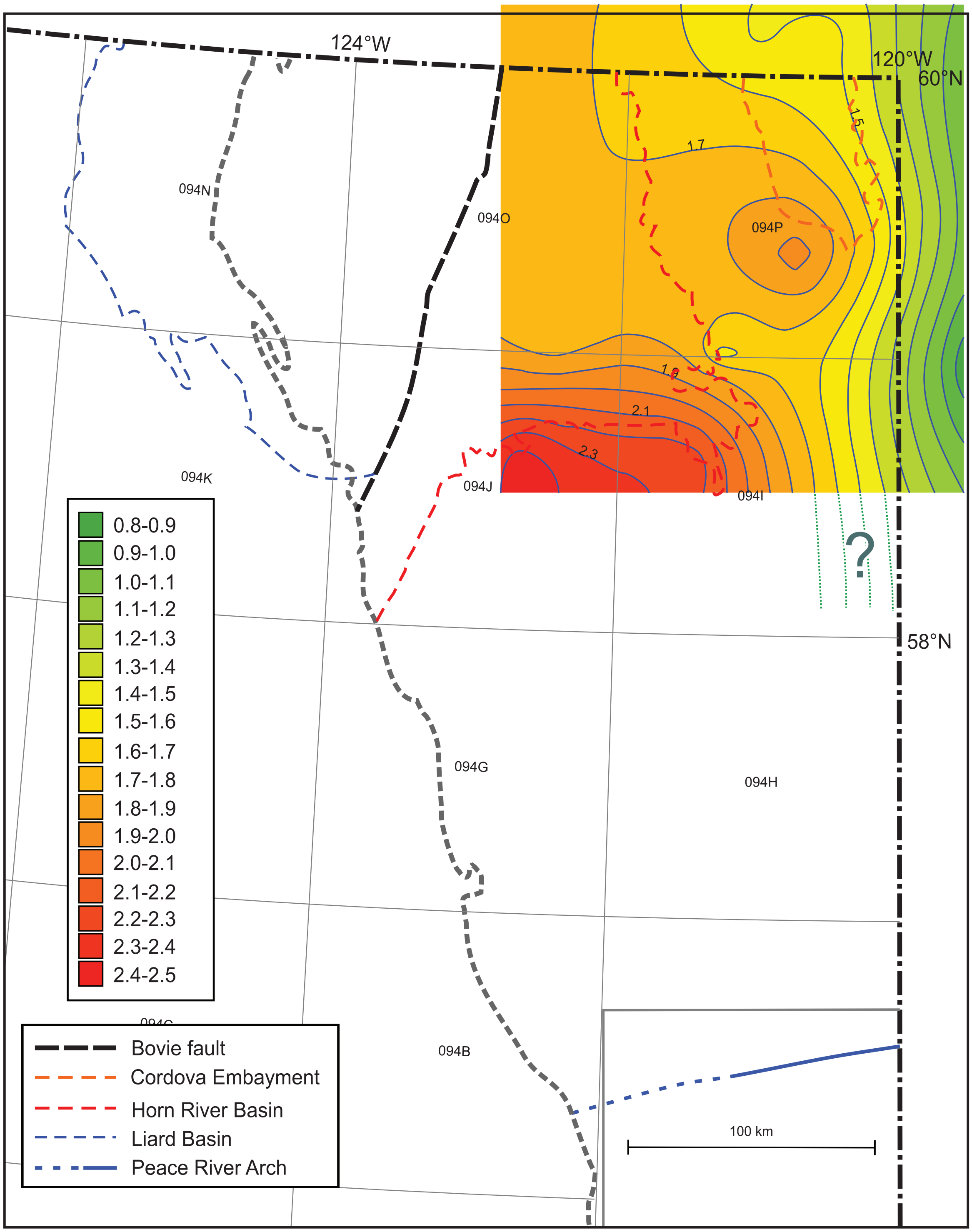

Figure M3. Isoreflectance map showing maturity of Muskwa shales in NEBC from vitrinite reflectance data. Values below Ro=1.3 are viewed as prospective for liquids-rich gas and hydrocarbon liquids (from Ferri and Griffiths, 2014).

does occur, the organic material is very fine-grained and not easily assessed for reflectivity. Additionally, what is typically measured is bitumen reflectance, which then requires a conversion to vitrinite equivalence, adding further uncertainty. Rokosh *et al*. (2012) similarly mapped the Muskwa in adjacent Alberta to be in the condensate-generating window, with even lower maturities to the south of the Hotchkiss Embayment (Fig. M4).

Dong *et al*. (2017) studied the impact of rock composition on geomechanical properties of shales in the Horn River Basin, and concluded that the Muskwa Formation in that area is relatively brittle because of high biogenic silica content.

Wilson and Bustin (2017) are currently evaluating Upper Devonian petroleum systems in NEBC, with an eye to predicting types and volumes of generated and retained hydrocarbons throughout basin evolution, focusing on distribution of wet gas, condensate, and oil.

Muskwa Core Analysis

We analyzed the Muskwa Formation in core from Husky Bivouac a-55-B/94-I-8 (1815-1851m), to provide a new comprehensive analytical dataset (Appendix 3). The Muskwa is a finely laminated, organic-rich siliceous shale with abundant silt-size quartz grains and recrystallized microfossils (radiolaria) and shell fragments (Appendix 4; Appendix 7; Fig. M5, M6). Algal material may also have been present, represented by short streaks or clusters of opaque organics, including bituminous material. Under the SEM, most quartz appears as microcrystallites (<5 µm); the grains are euhedral and neoformed and often covered by illitic clay (Fig. M7).

Mineralogy through the Muskwa section appears to vary cyclically, as does TOC content, which ranges between 1.6-5.6 wt% (Fig. M8). T_{max} values range between 443-473°C; however, an oil-based drilling mud was used, so it is likely that the lower temperatures reflect contamination from the fluid, while the upper temperature range represents the true organic maturity. Hence, the organic maturity of the Muskwa at this location is in the condensate to dry gas transition zone.

Unconfined porosity of Muskwa sample ranges between 6.45-7.85%, with matrix permeabilities of 6.5-14 nD (Table M3). Mercury injection capillary pressure (MICP) conformance-corrected porosity is much lower, ranging between 3.25-4.46% (Table M4). The difference between the two methods indicates that the majority of the pore throats are <3-4 nm, as illustrated in the pore throat distribution pattern (Fig. M9).

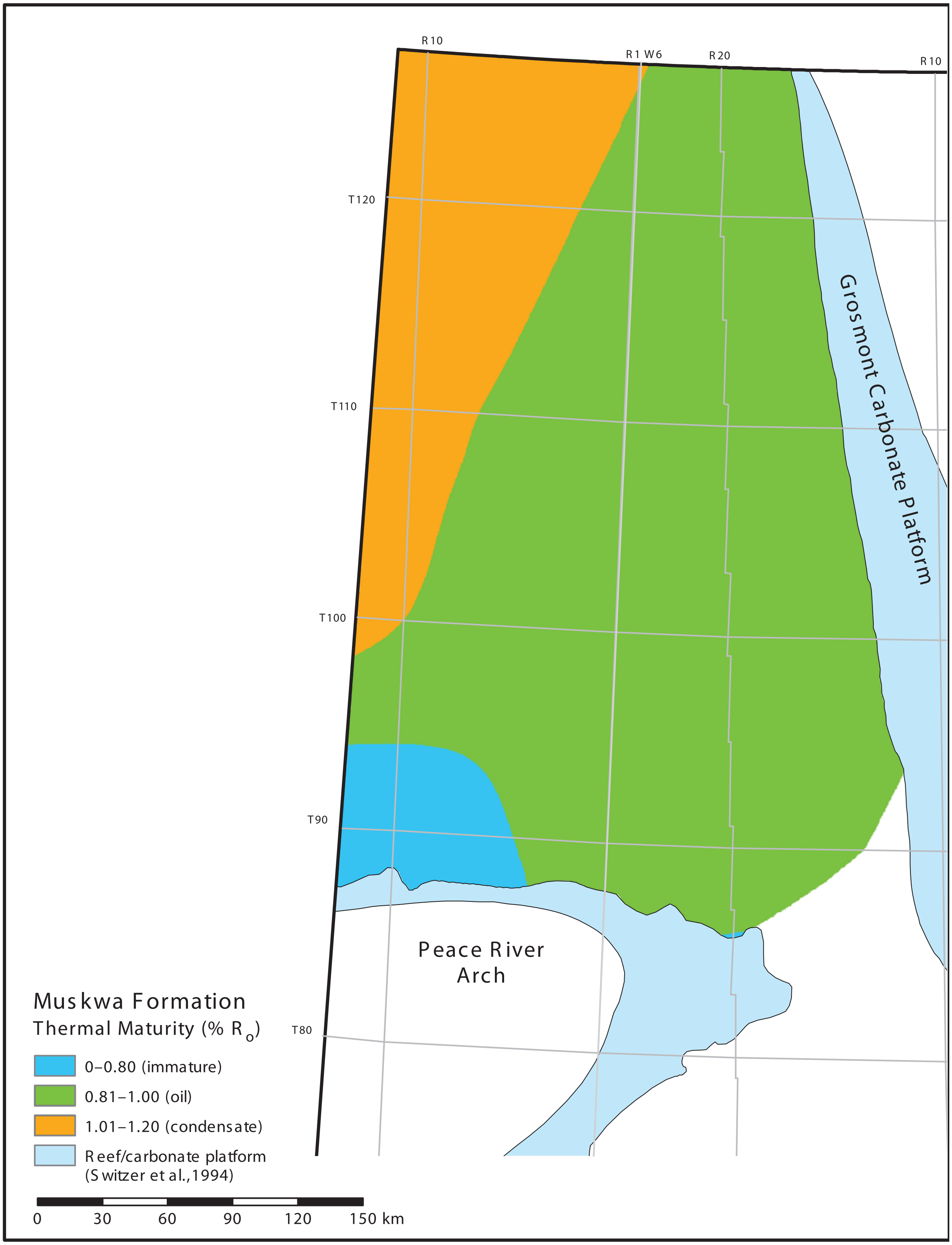

Figure M4. Thermal maturity map of the Muskwa Formation in Alberta, based on vitrinite reflectance data (from Rokosh et al., 2012).

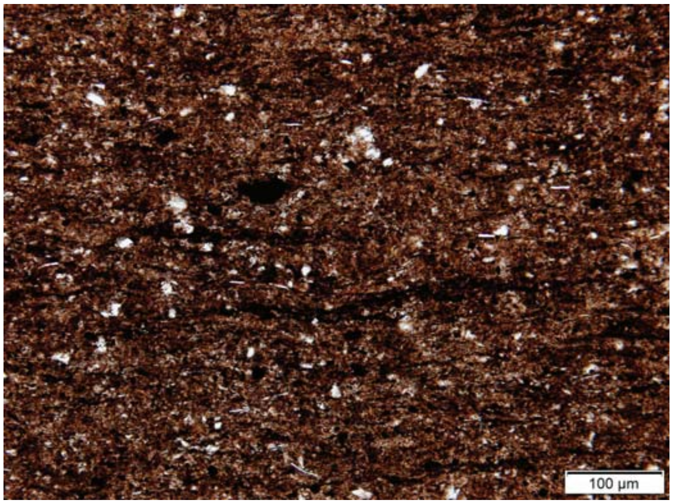

Figure M5. Photomicrograph, Muskwa Formation, Husky Hz Bivouac a-55-B/94-I-8 (1830.76m), under plane polarized light; typical organic-rich, finely-laminated siliceous shale.

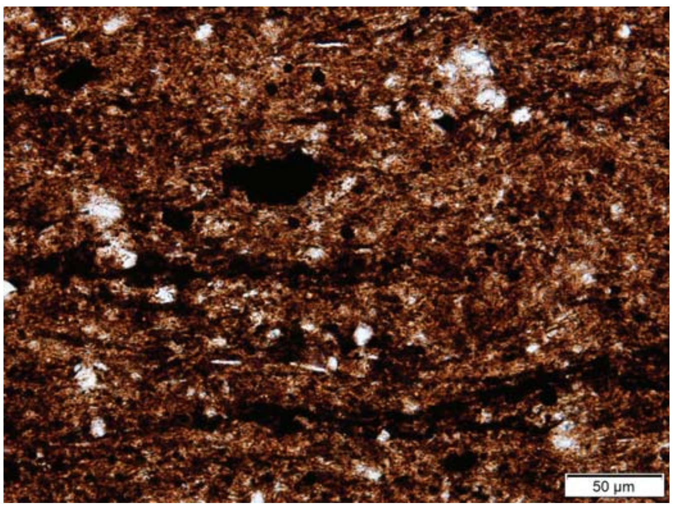

Figure M6. Photomicrograph, Muskwa Formation, Husky Hz Bivouac a-55-B/94-I-8 (1830.76m), under plane polarized light. Abundant silt-sized quartz grains float in a silica-rich clay matrix with bedding-parallel micas; note also opaque organic matter and pyrite.

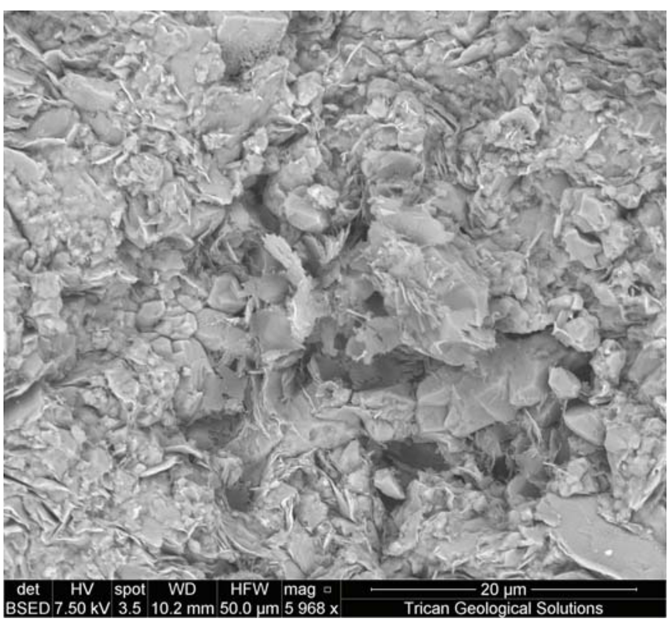

Figure M7. BSED SEM micrograph, Muskwa Formation, Husky Hz Bivouac a-55-B/94-I-8 (1830.76m). Note open pore spaces featuring euhedral neoformed quartz crystals and illitic clays. Organic material is finely dispersed throughout.

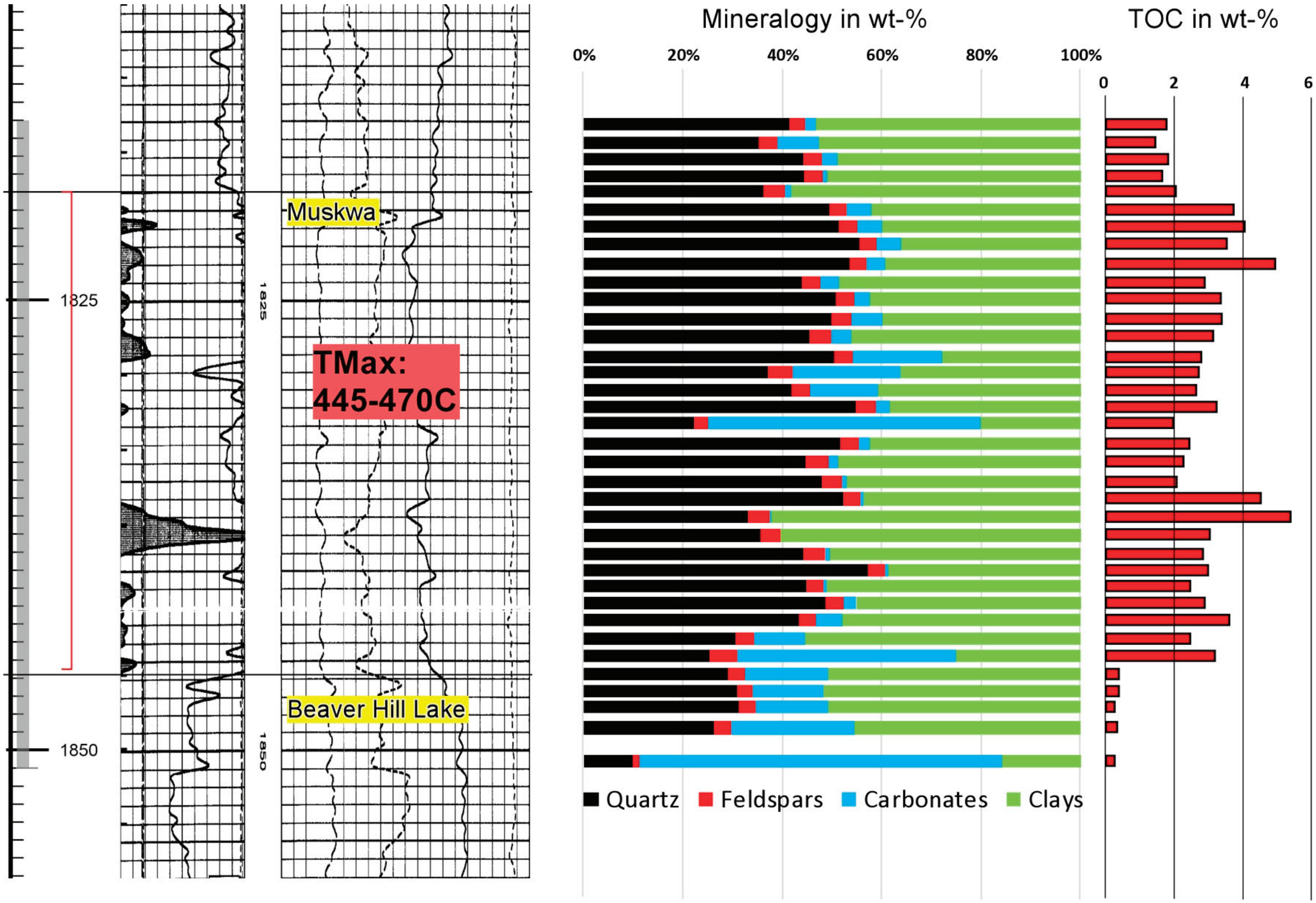

Figure M8. Mineralogy and TOC plots for samples from the Muskwa Formation, Husky Hz Bivouac a-55-B/94-I-8.

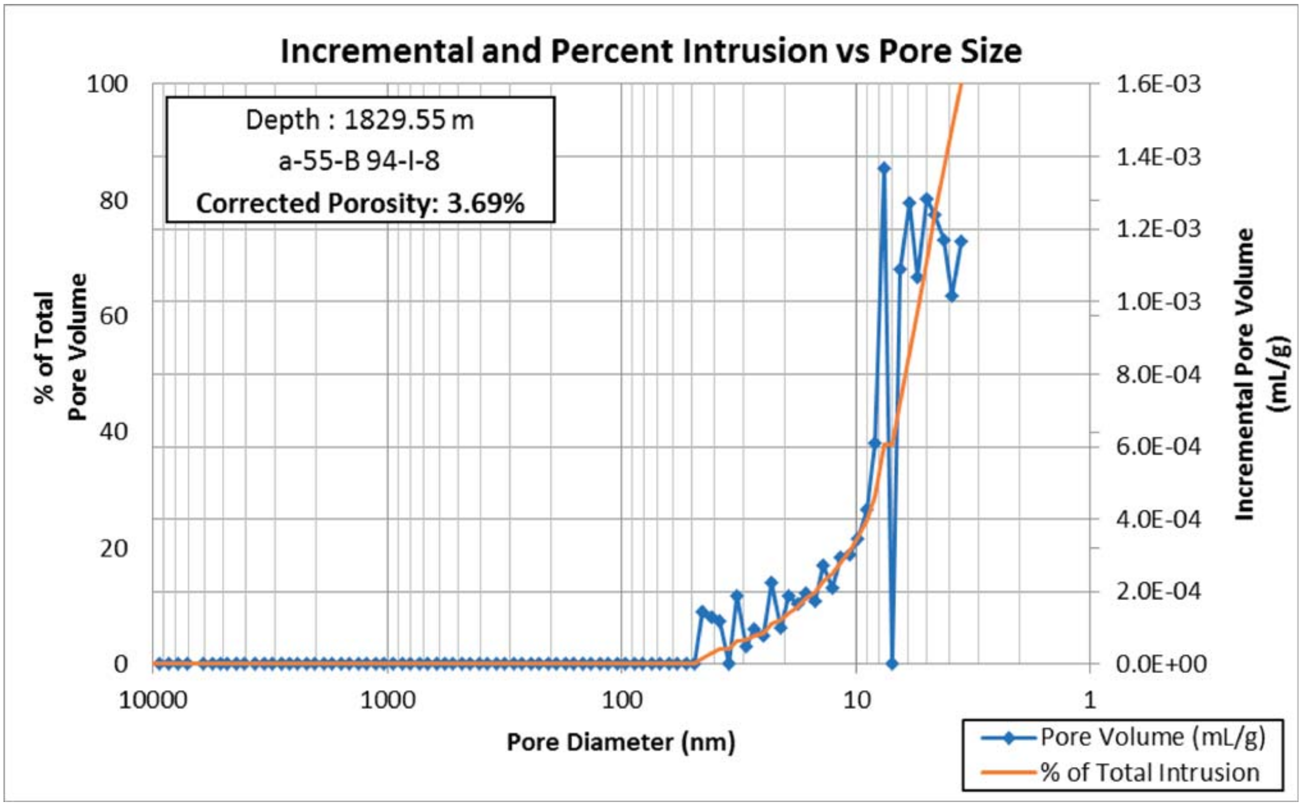

Figure M9. Incremental and percent intrusion vs pore size, Muskwa Formation, Husky Hz Bivouac a55-B/94-I-8 (1829.55m), highlighting large percentage of very small pore throats (<10 nm).

Unconfined Porosity and Matrix Permeability										
Well Name	Well Location	Core Depth (m)	Fm	Density		Porosity (%)	GRI Matrix Permeability (md)		GRI Matrix Permeability (nd)	
				Bulk Density (g/cc)	Skeletal Density (g/cc)		Avg	Std Dev	Avg	Std Dev
Husky Bivouac	a-055-B/094-I-08	1821.63	Muskwa	2.398	2.595	7.59	1.33E-05	5.83E-06	13.32	5.83
Husky Bivouac	a-055-B/094-I-08	1829.55	Muskwa	2.440	2.649	7.85	1.40E-05	4.13E-06	14.00	4.13
Husky Bivouac	a-055-B/094-I-08	1838.87	Muskwa	2.470	2.663	7.25	1.11E-05	4.62E-07	11.15	0.46
Husky Bivouac	a-055-B/094-I-08	1845.04	Muskwa	2.481	2.652	6.45	6.55E-06	9.41E-07	6.55	0.94

Table M3. Muskwa Formation – unconfined porosity and GRI matrix permeability measurements from core samples, Husky Hz Bivouac a-55-B/94-I-8.

MICP Porosity										
Well Name	Well Location	Core Depth (m)	Fm	Density g/cc		Porosity (%)	Corrected Porosity (%)	Peak Range		Stem Volume Used (%)
				Bulk Density (g/cc)	Skeletal Density (g/cc)			Peak Range	Modal Peak	
Husky Bivouac	a-055-B 094-I-08	1821.63	Muskwa	2.412	2.525	4.58	4.46	4 - 80	4	0
Husky Bivouac	a-055-B 094-I-08	1829.55	Muskwa	2.459	2.553	4.34	3.69	4 - 40	8	9
Husky Bivouac	a-055-B 094-I-08	1845.05	Muskwa	2.609	2.696	3.76	3.25	4 - 50	6	0

Table M4. Muskwa Formation – MICP porosity and conformance-corrected porosity measurements from core samples, Husky Hz Bivouac a-55-B/94-I-8.

Hydrocarbon analysis (S1) of core samples shows that residual hydrocarbons most commonly contain C_{10}-C_{25} chains with calculated API gravities of 35-40° (Fig. M10). Calculated specific gravities range between 0.83-0.85 (Table M5), and heavy and light condensates dominate (Fig. M11). However, while samples were collected from the centre of the core, the peak at C_8 may indicate contamination by invert drilling mud. Regardless, it is clear that liquid hydrocarbons are present in the Muskwa.

Hydrocarbon Composition by Thermal Desorption Gas Chromotography																
Well Name	Well Location	Core Depth (m)	Fm	% Light Condensate	% Heavy Condensate	% Naphthenes	% Aromatics	% Biomarkers	Peak	Initial Boiling Point (°C)	Carbon Number	Final Boiling Point (°C)	Carbon Number	Calculated Specific Gravity	Calculated API gravity	Chromatogram Quality
Husky Bivouac	a-055-B/094-I-08	1815.20	Muskwa	34.37	49.31	0.60	5.22	10.50	C8	62	<C6	456	C31	0.83	39.54	best
Husky Bivouac	a-055-B/094-I-08	1819.98	Muskwa	19.10	65.58	0.31	3.22	11.79	C8	85	C7	488	C35	0.85	35.19	best
Husky Bivouac	a-055-B/094-I-08	1830.13	Muskwa	34.05	52.11	0.35	2.16	11.33	C8	73	C6	471	C33	0.83	38.27	best
Husky Bivouac	a-055-B/094-I-08	1840.43	Muskwa	18.39	65.01	0.24	1.05	15.30	C8	97	C7	480	C34	0.85	34.70	best
Husky Bivouac	a-055-B/094-I-08	1851.70	Otter Park	44.12	45.33	0.23	0.99	9.32	C8	85	C7	480	C34	0.83	39.97	best

Table M5. Muskwa Formation – hydrocarbon composition data, Husky Hz Bivouac a-55-B/94-I-8.

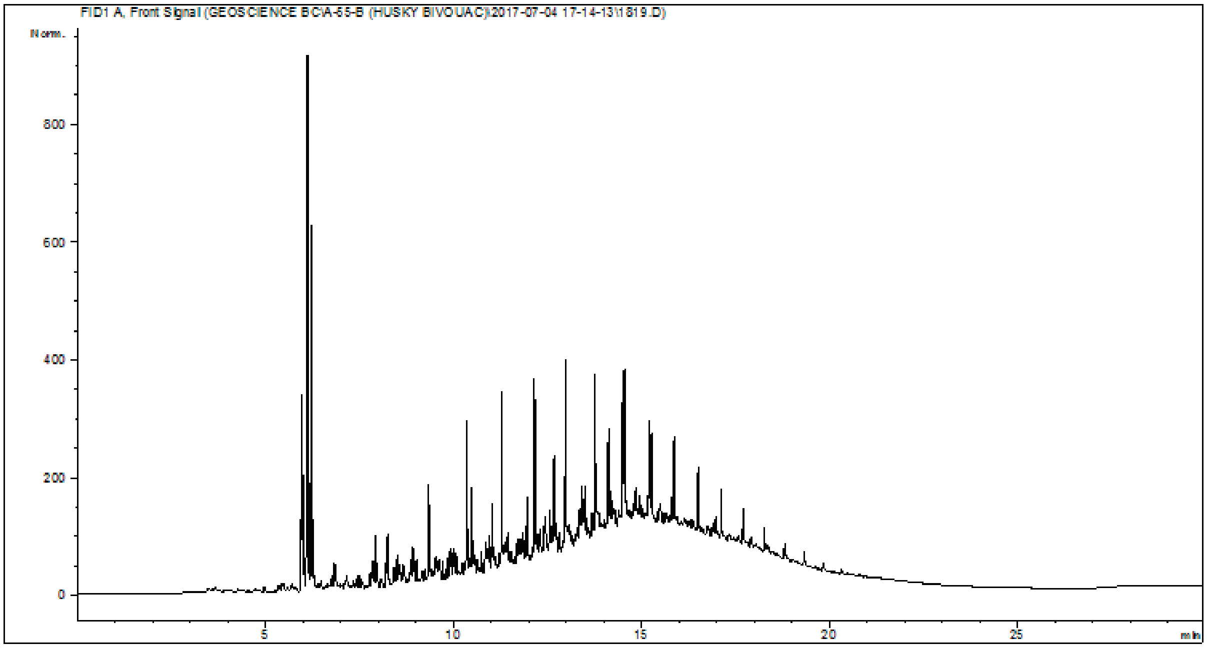

Figure M10. Bulk rock hydrocarbon analysis (S1), showing hydrocarbon chain distribution and detection. Note the C6 peak, which likely indicates invert drilling mud contamination of the core. Muskwa Formation, Husky Hz Bivouac a-55-B/94-I-8, 1819.89m.

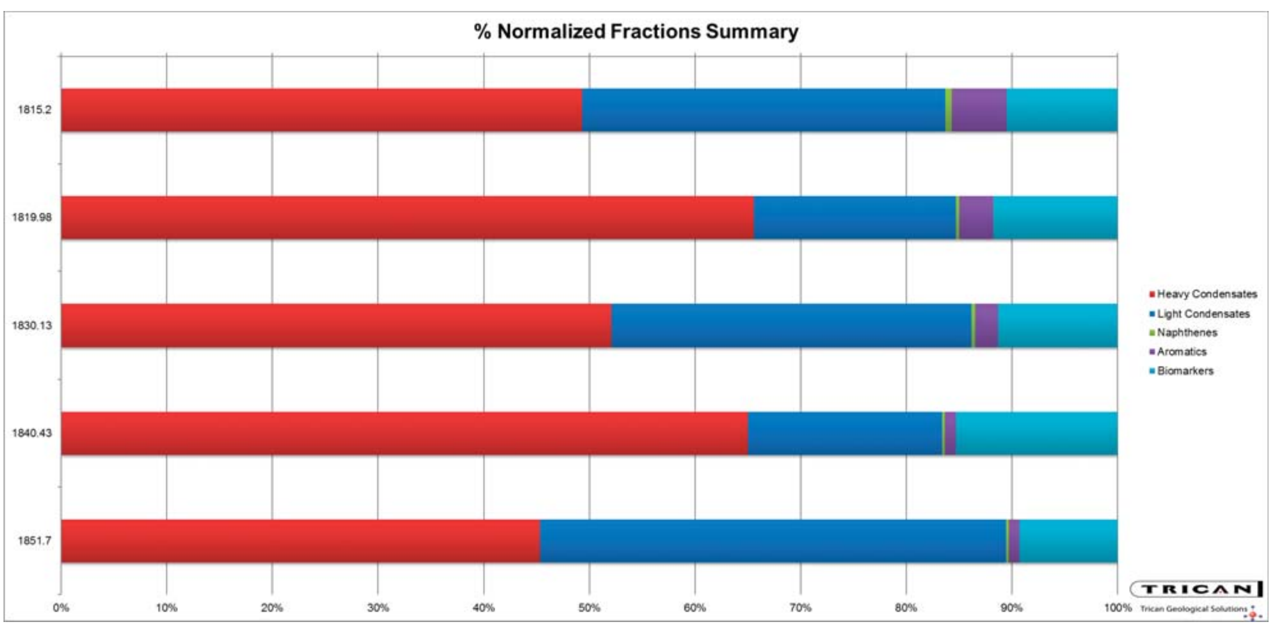

Figure M11. Normalized fraction plot of hydrocarbon groups, Muskwa Formation, Husky Hz Bivouac a-55-B/94-I-8 (five samples listed by depth).

Static mechanical properties of the Muskwa from two samples show Young's modulus ranging from 30.4 to 30.7 Gpa, and Poisson's ratio ranging 0.178 to 0.188 (Table M6). Compressive strength differs significantly between the two samples, but filled horizontal fractures in the 1840.39m sample may explain a lower strength value. Dynamic Young's modulus and Poisson's ratio are significantly higher than the static values (Table M7). Correlation between these values can help to understand dipole sonic logs used in the calculation of *in situ* stresses.

Well Location	Depth (m)	Formation	Confining Pressure (MPa)	Compressive Strength (MPa)	Residual Strength (MPa)	Static Young's Modulus (GPa)	Static Poisson's Ratio
200/a-055-B 094-I-08/00	1824.89	Muskwa	16.0	168.85	129.45	30.70	0.178
200/a-055-B 094-I-08/00	1840.39	Muskwa	16.0	137.94	108.57	30.40	0.188

Table M6. Muskwa Formation – static mechanical properties, Husky Hz Bivouac a-55-B/94-I-8.

Well Location	Depth (m)	Formation	P-Wave Velocity (m/s)	S-Wave Velocity (m/s)	Dynamic Poisson's Ratio	Dynamic Young's Modulus (GPa)
200/a-055-B 094-I-08/00	1824.89	Muskwa	4814.9	2514.2	0.312	40.58
200/a-055-B 094-I-08/00	1840.39	Muskwa	4793.0	2531.1	0.307	42.02

Table M7. Muskwa Formation – dynamic mechanical properties, Husky Hz Bivouac a-55-B/94-I-8.

Resource Oil Assessment

Muskwa Formation shales are rich regional source rocks, and have proven to be highly productive shale gas reservoirs in the Horn River Basin and Cordova Embayment. To the southeast, organic maturity levels are lower, and one might expect the same rocks to produce liquids-rich gas and even oil.

Analytical work confirms favourable organic content and maturity, backed up by our analysis at the Husky Bivouac well. Geomechanical properties may require further characterization, as parts of the Muskwa may be more clay-rich and less amenable to fracture stimulation. Limited oil and liquids production from the overlying Jean Marie and Tetcho carbonates in the Helmet area suggest that the Muskwa has generated liquid hydrocarbons, a viewpoint shared by Ferri and Griffiths (2014). Moreover, Rokosh *et al*. (2012) mapped the Muskwa to be rich in natural gas liquids in northwestern Alberta, immediately east of our study area.

However, horizontal wells drilled to test Muskwa oil and liquids production have produced some liquid hydrocarbons, but in generally subeconomic quantitites. Limited reservoir pressure data suggest some elevated pressures, but the presence of widespread overpressuring to support shale production has not been established. We saw no good relationship between drilling and completion procedures and production results, suggesting that insufficient work has been done to optimize methdologies.

Horizontals were drilled during the 2009-2012 period, during the first rush of evaluations for the Duvernay and Muskwa plays throughout Alberta. Results focused industry attention on the Duvernay at Kaybob / Fox Creek, and further assessment in other areas languished. However, smaller operators appear to have “cracked the nut” since early 2017 in obtaining economic oil production from the shallower, less mature Duvernay in the East Shale Basin. We suggest that the Muskwa in northeastern B.C. and adjacent Alberta deserves re-evaluation with the modern methodologies and successes of the East Shale Basin Duvernay in mind. A good initial step would be a vertical drilling program with extensive coring to better establish the distribution of reservoir properties.

JEAN MARIE MEMBER

Age and Play Type

Upper Devonian – Tight Oil play (tight carbonate);
Prospectivity: ‘B’ Play – Oil production established, but regional prospectivity appears unlikely.

Regional Geology

The Jean Marie was deposited as a broad, shallow marine limestone platform, under moderate energy conditions (McAdam, 1993). Belyea and McLaren (1962) described the Jean Marie in outcrop in the Northwest Territories, while Law (1971) and McAdam (1993) published regional overviews in the Northwest Territories and northeastern B.C. subsurface, respectively. Stoakes (1992) described the Jean Marie in the context of the basin-scale Winterburn megasequence. Wendte (2004) provided more detailed descriptions of internal facies and correlations in the Cordova Embayment area (94P).

The Jean Marie varies from 10 to 25 metres thick across northeastern British Columbia and adjacent Alberta, thickening abruptly westward to a shelf margin (Map JM1; Fig. JM1; Cross-section UDev-UDev’). McAdam (1993) noted that this margin is nearly coincident with the Slave Point carbonate bank edge in 94-P-5 and northward, and parallels the Keg River carbonate bank edge further south, implying deep control on development of the Jean Marie shelf edge.

Burial depths are 1000-1500 metres in the north, and increase southward (Map JM2). Redknife and Fort Simpson marine shales encase the Jean Marie, producing a closed reservoir system (Fig. JM1; Cross-section UDev-UDev’).

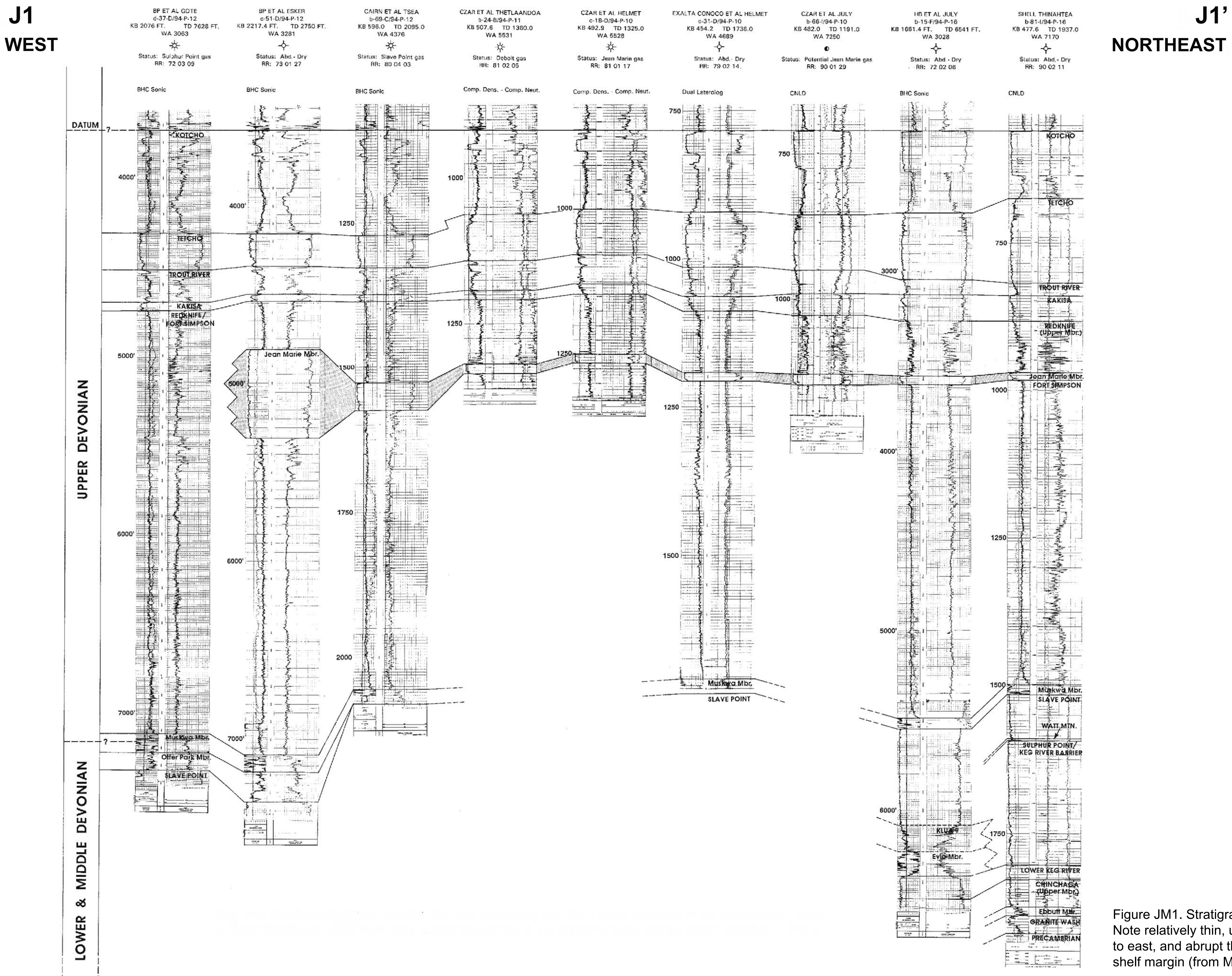

Figure JM1. Stratigraphic cross-section J1-J1'. Note relatively thin, uniform carbonate platform to east, and abrupt thickening at the westerly shelf margin (from McAdam, 1993).

Reservoir Description

Eastern Platform

Wendte (2004) subdivided the eastern platformal Jean Marie into four depositional successions. The basal unit consists of crinoidal wackestones deposited below fair-weather wave base on a widespread ramp. The upper three units comprise complete transgressive-regressive cycles, ranging from relatively deep-water, branching coral-bearing limestones, to shallower-water reefal limestones (Fig. JM2). In shoal areas, patch reefs up to 100 metres across grew with relief of only about seven metres above the sea floor. Thin, platy stromatoporoids created a cavernous framework; within this, shelter cavities hosted the algae *Renalcis*, and were later filled by lime muds (Fig. JM3, 4).

A permeability vs porosity cross-plot from core analysis data shows Jean Marie reservoirs in the Helmet area (blue) and other platform areas (red) to exhibit porosities up to 15% and permeabilities to a Darcy or more (Fig. JM5). Reservoir quality in the basal cycle wackestone is poor to non-existent. Within the upper three cycles, platform limestone facies exhibit porosities of 2-7%, and permeabilities ranging from 0.01 to 0.5 mD. Optimal Jean Marie reservoirs (stratigraphic sweet spots) occur within the patch reefs, where *Renalcis* is preferentially leached, and brittle cavity-filling mudstones are fractured (Stoakes, 1992; Wendte, 2004; Fig. JM4). Core analyses through these intervals are highly variable and often “spiky” – porosities range from 4 to 12%, and permeabilities from <1 mD to 10 darcies – reflecting the interplay of leached matrix porosity and short open fractures.

Reinson *et al*. (1993) and Hamilton *et al*. (1995) speculated that larger-scale natural fractures exerted control on Jean Marie productivity, and that fracture intensity could be related to compaction drape over Slave Point bank margins, or to regional tectonism. Jones (1980) proposed an association between deep-seated regional fault trends and preferential dolomitization in Devonian carbonates, including in the Jean Marie at Helmet.

Conventional well logs accurately distinguish stratigraphic sweet spots in the Jean Marie platform. However, there does not appear to be a good linear relationship between reservoir performance and application of porosity log cutoff values.

Western Platform Margin

Wackestones of the basal ramp thicken along the western margin, and appear to make up the basal third to half of the formation. The three platformal cycles are not readily correlated into the margin, and high-quality reef facies have not been observed. Instead, grainstones and broken reefal debris dominate the section (Fig. JM6). These rocks exhibit core analysis porosities of 3-10% and permeabilities of 0.1-2 mD, with scattered spikes of 10 mD+; Fig. JM5 demonstrates generally poorer reservoir quality in core analysis at Gunnell Creek along the western margin.

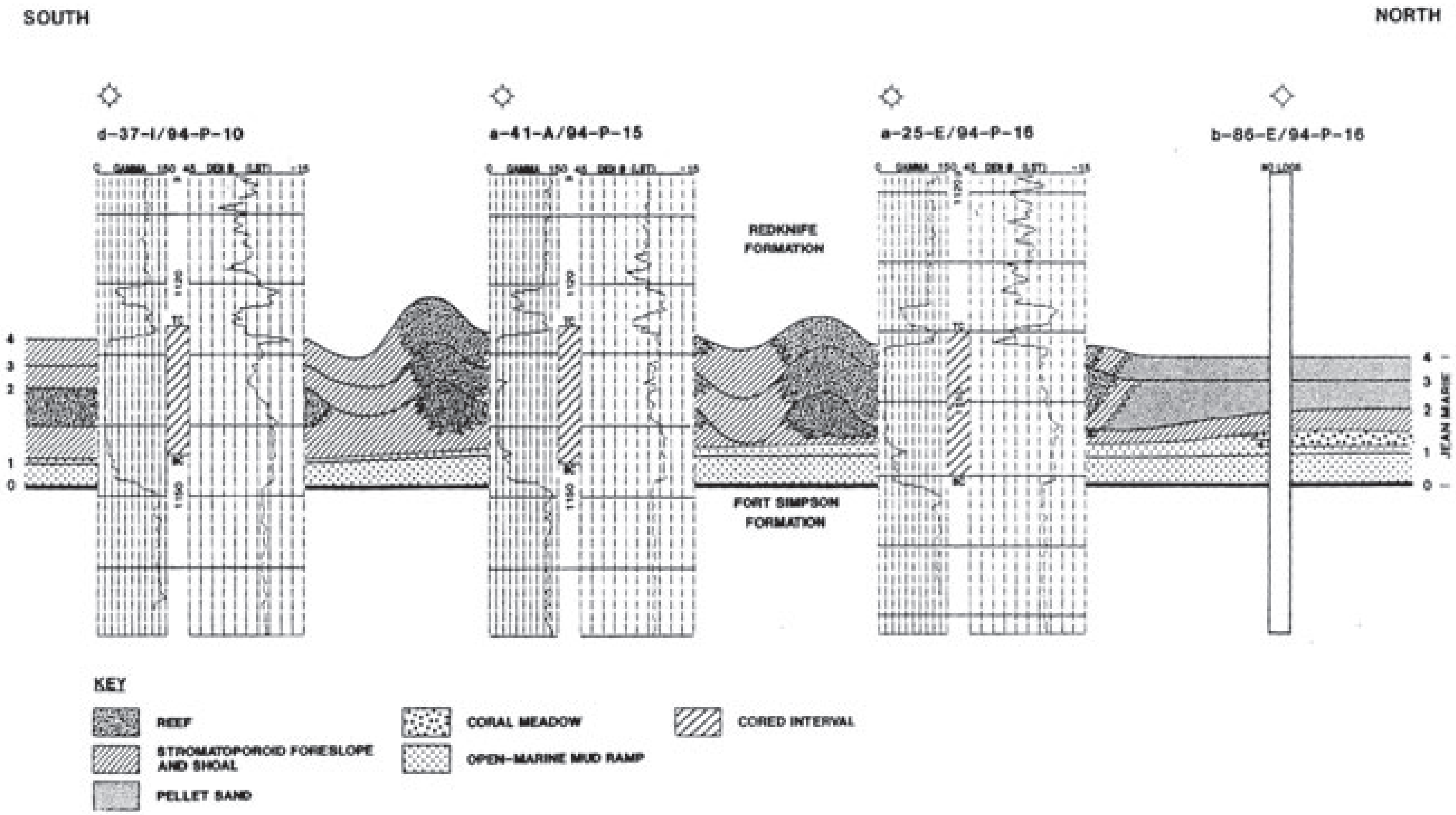

Figure JM2. Cross-section illustrating reefal buildups on regional Jean Marie platform (from Stoakes, 1992).

Figure JM3. Jean Marie reefal facies, dominated by tabular stromatoporoids, many in growth position. Well b-66-I/94-P-10, 1139.6-1140.9m.

Figure JM4. Closeup of Jean Marie reefal facies – note leached Renalcis (yellow-brown), tabular stromatoporoids, and grey cavity-filling muds with short fractures. Well b-66-I/94-P-10, 1137.7m

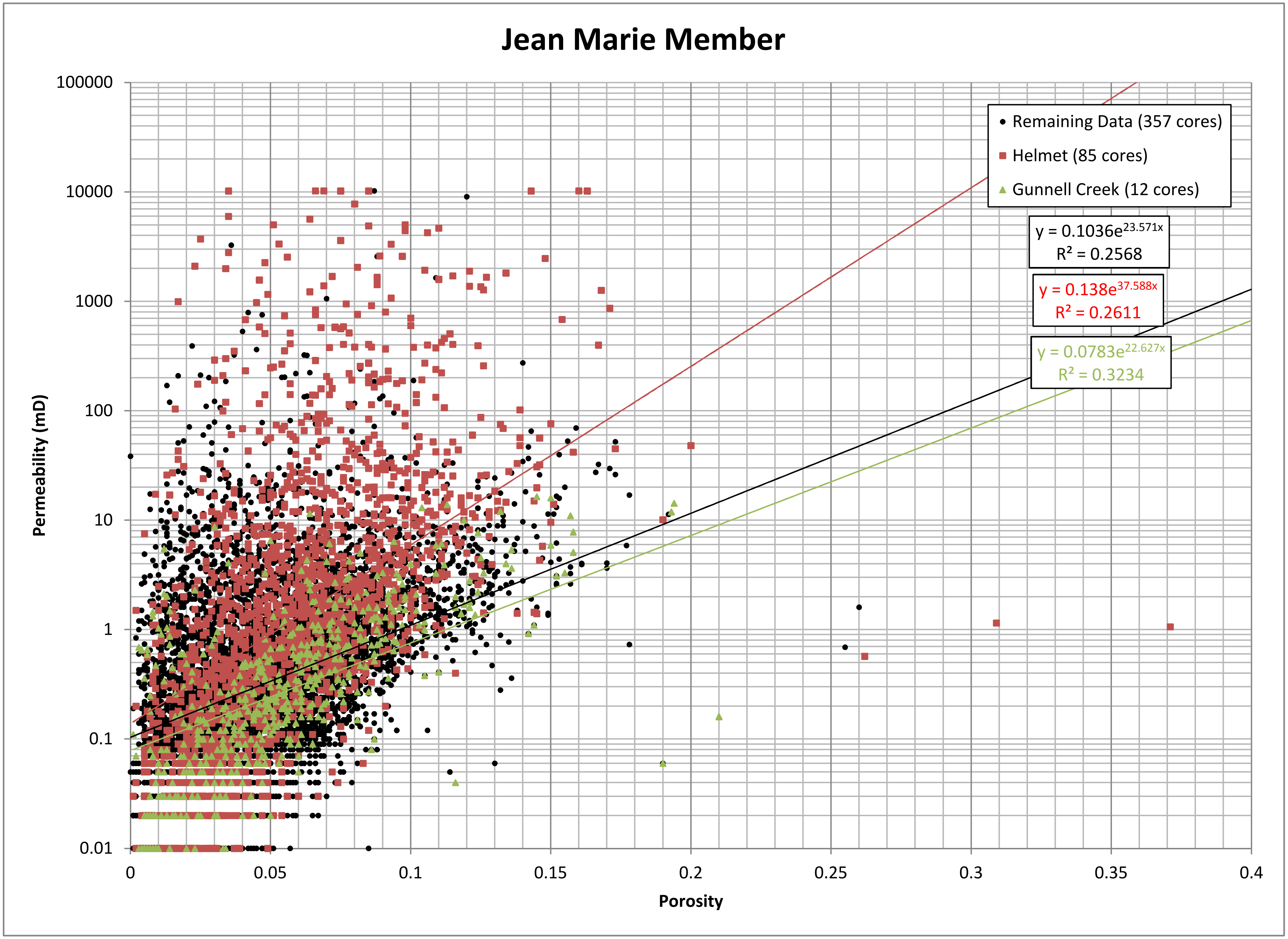

Figure JM5. Porosity / permeability cross-plot, Jean Marie Member, distinguishing cores from Helmet area, other platform areas, and Gunnell Creek (western margin buildup).

Figure JM6. Jean Marie reef debris and grainstones, the primary reservoir facies in the western thick platform margin. Well d-91-F/94-I-13, 1463.7-1465.1m.

Well logs accurately depict reservoir quality through the reef debris section, and demonstrate pay sections of up to 20 metres or greater. High-porosity zones exhibit lower peak values and more gradational boundaries than those on the platform, indicating that high-quality fractured reefal sweet spots are likely not present along the thick western margin.

Production and Test Data

Maps JM1 and JM2 demonstrate widespread Jean Marie gas production from about 2000 horizontal wells in northeastern B.C., with isolated oil production in the Helmet area (Cross-section JM-JM').

The Jean Marie is regionally gas saturated and underpressured (Letourneau, 1991; Reimer, 1994), and thus can be considered as a Deep Basin tight carbonate play. Reimer (1994) speculated that fracturing of the underlying Fort Simpson shales allowed CO_2 and methane, evolved through thermochemical sulphate reduction in the Keg River and Slave Point formations, access to the Jean Marie. Methane charged the reservoirs, while CO_2 dissolved in formation waters aided development of solution porosity, resulting in increased reservoir capacity and subnormal reservoir pressures. Adams (2014) listed remaining raw gas reserves in the BC Jean Marie at 1.46 TCF, with ultimate marketable gas potential of 6.5 TCF.

Reservoir Engineering Analysis

We found six Jean Marie oil wells in the Helmet area, five in British Columbia (Table JM1: Map JM1). Two closely-spaced wells, a-69-K (19.2e^{3}m^3 [121 MBO]) and a-80-K/94-P-7 (75.2e^{3}m^3 (473 MBO)) have produced significant oil volumes from thick, well-developed and structurally slightly low sections (Cross-section JM-JM'), but offsetting wells show no signs of oil production.

Well	First Prod	Cum OIL (mbbl)	Cum GAS (mmcf)	Cum CND (bbl)	Cum WTR (mbbl)	IP (bbl/d)	EUR (mbbl)	HZ Length (m)
100/07-01-111-08W6/00	1979/12	0.3	0.2	0	0.1	6	0.3	0
200/c-032-K 094-I-06/03	2003/03	0.7	4.4	0	0	24	0.7	182
200/b-054-L 094-P-02/00	2007/01	7.5	224	0	0.4	110	7.5	245
200/d-038-K 094-P-07/02	2003/07	2.0	492	0	0.3	8	2.0	1170
200/a-069-K 094-P-07/00	2002/09	121	443	0	5.7	156	132	717
200/a-080-K 094-P-07/00	2003/03	473	4821	0	61	307	646	0

Table JM1. Completion summary, Jean Marie oil wells

Looking at 722 gas wells in the surrounding area, condensate volumes are very small, averaging about 1 bbl/MMCF. Only eight wells produced more than 10,000 barrels condensate (the largest was about 22,000 barrels), and another 38 produced >5000 barrels (Fig. JM7). Figure JM8 shows the same data expressed as condensate-gas ratios, and on both maps, one can interpret a strong northwest-southeast trend of high-condensate wells. Two less pronounced trends of high condensate values, orthogonal to the main trend, are evident on the condensate production map, although only the southern trend shows on the ratio map.

Reviewing about 100 valid DST's in the Helmet area, there was significant oil recovery from only one at d-54-F/94-P-2 – which appears to lie on the southern orthogonal lineament of high condensate values (Fig. JM7, JM8). Reservoir pressures from DST's showed an underpressured gradient of about 0.2 psi/ft (4.5 kPa/m) overall, but a fair scatter of values with only suggestions of local compartmentalization. The Jean Marie report in Appendix 5 provides additional detail.

Analytical Data

While the Jean Marie has been cored extensively, database searches revealed almost no analytical data submitted other than routine core analyses (Appendix 1). Obviously, however, operators have completed many horizontal / multi-frac wells for gas production – and we assume that techniques have been perfected to efficiently stimulate the reservoir.

Hydrocarbon composition is at least in part a function of the underlying source rock, which is likely the Muskwa over most of the productive area. As noted above, the Muskwa is more liquids-prone away from the Horn River Basin, eastward toward the Alberta border – although Helmet lies tens of kilometres northwest of the area where the Muskwa itself has been tested horizontally for liquids.

Resource Oil Assessment

The Jean Marie Formation is a regionally extensive, well-studied carbonate platform, composed of stacked reefal carbonate cycles with intricate reservoir quality controls. It has been horizontally drilled over large areas for regionally-pervasive subnormally-pressured gas.

Oil has been produced only at a few wells at Helmet (94-P-7), in the same general area where other Paleozoic reservoirs (Tetcho and Rundle) produce oil as well. This area appears to be tens of kilometres northwest of the where Muskwa source rocks have themselves been drilled horizontally in an effort to produce liquids.

Jones (1980) mapped a series of northwest-southeast trending "isostatic adjustment" faults in NEBC, one of which trends directly through the Helmet area (Fig. JM9). While Jones envisioned these faults being conduits for dolomitizing fluids, they may have

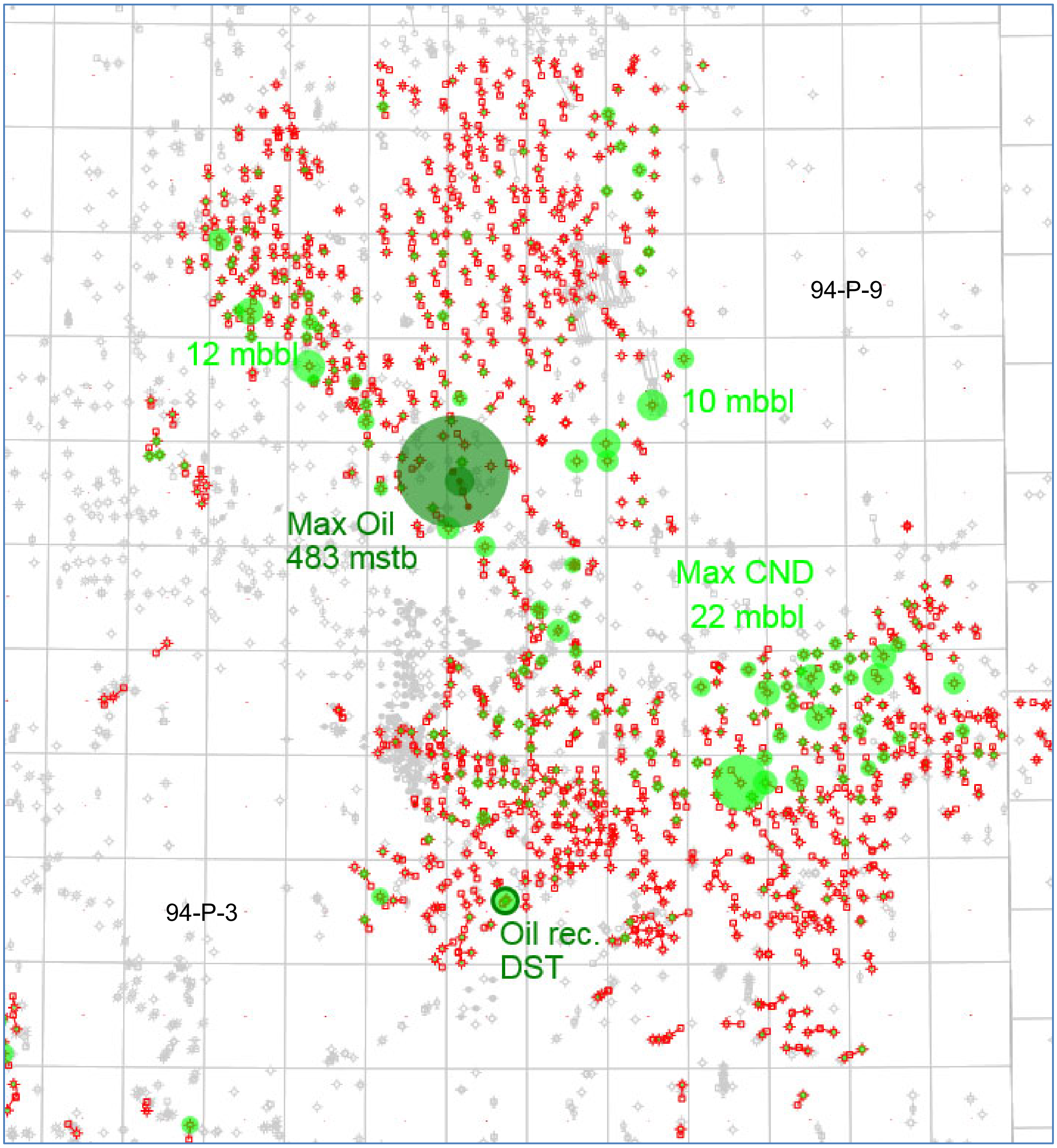

Figure JM7. Condensate production cumulative volumes from Jean Marie wells in the Helmet area.

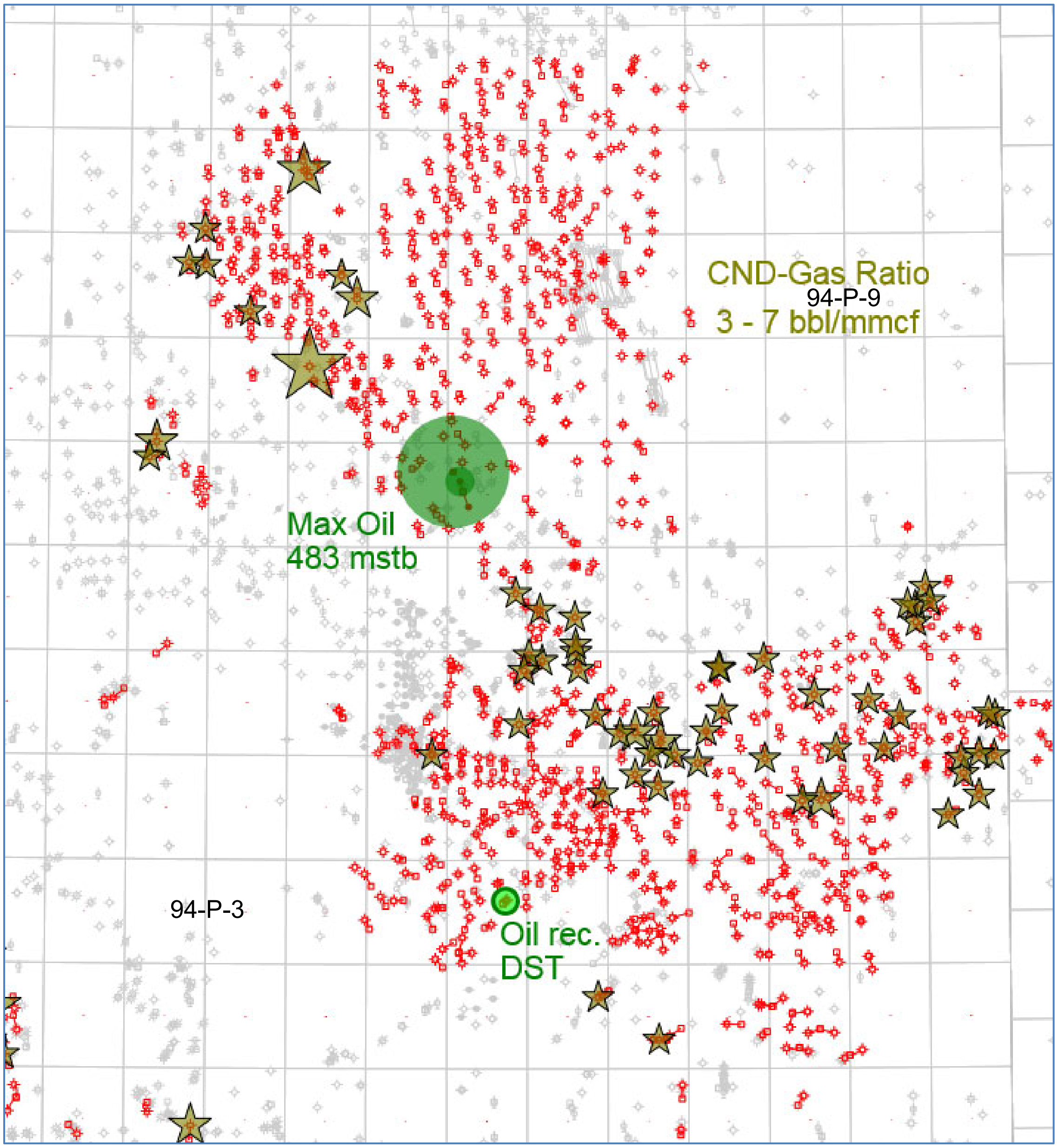

Figure JM8. Condensate production ratios from Jean Marie wells in the Helmet area.

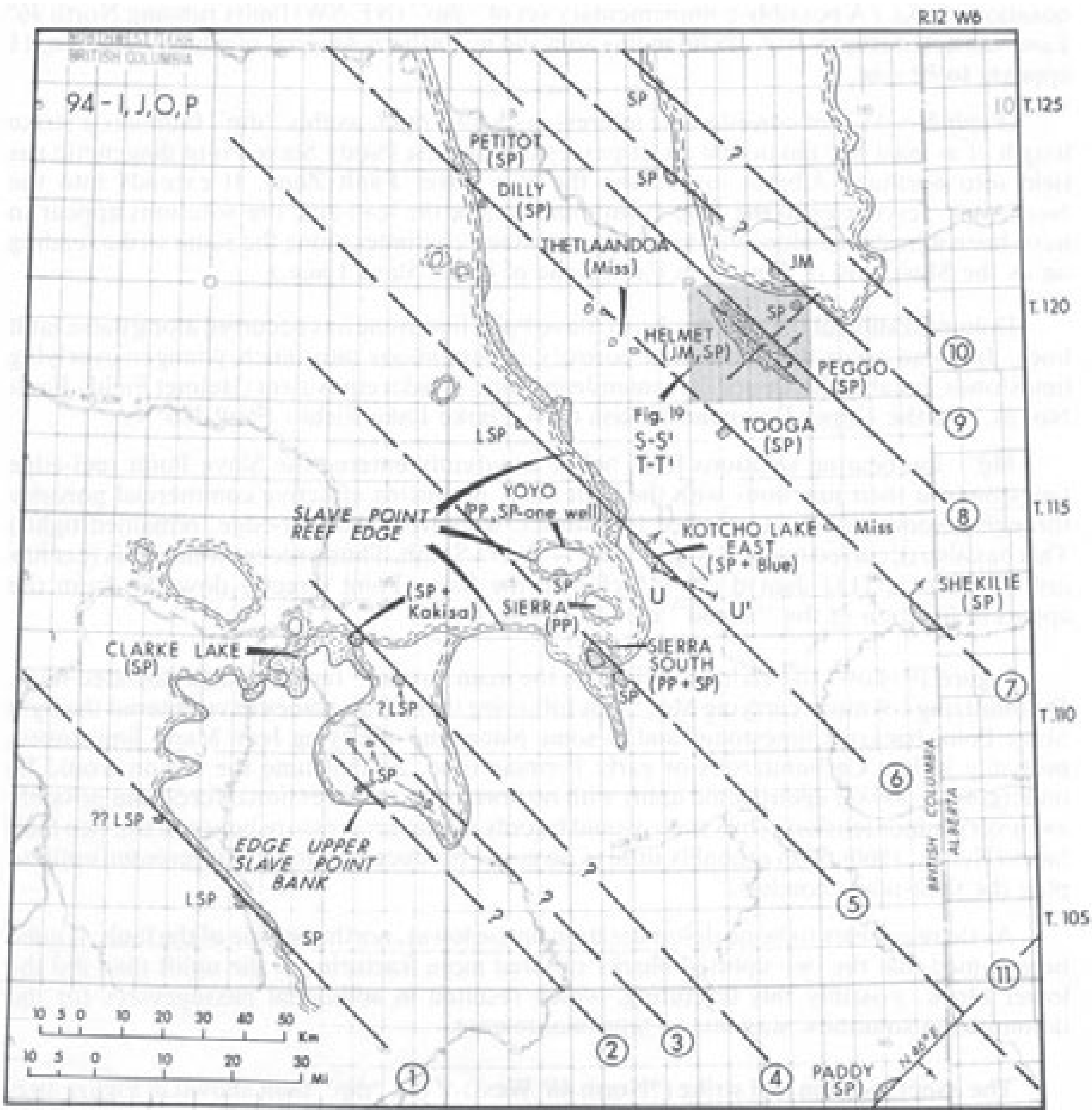

Figure JM9. Isostatic adjustment fault trends, NEBC, highlighting areas of oil production from Jean Marie, Tetcho and Rundle Group reservoirs (after Jones, 1980).

served to enhance migration of liquid hydrocarbons through the thick Fort Simpson shale section as well. Note that one of Jones' faults essentially coincides with the NW-SE trend of oil and elevated condensate production highlighted on Fig. JM8.

An analogue has been suggested in local production of oil from local structural lows in the low-permeability Viking play in eastern Alberta and adjacent Saskatchewan (Mark Otterson, David Foo, personal communications). Anecdotally, operators have proposed an initial oil charge, followed by gas charging the formation and displacing oil from local highs. Gas then moved updip at local spill points, bypassing much of the oil in local lows. Perhaps such a process may have operated in the Jean Marie in NEBC, particularly at Desan where complex local faulting and structure has been mapped (see Rundle Group / Desan Focus Area discussion).

We conclude that Jean Marie oil potential in NEBC is likely limited to small residual pools associated with structural lows, more likely toward the east and into northwestern Alberta, where the Muskwa source rock is less mature.

KAKISA FORMATION

Age and Play Type

Upper Devonian – Tight Oil play (tight carbonate);
Prospectivity: 'C' Play – no evidence for producible oil or liquids.

Regional Geology

The Kakisa Formation is defined in outcrop in the southern Northwest Territories as a quartzose, silty dolomitic limestone, with prominent bioclastic or reefoid buildups occurring at various levels throughout the formation (Glass, 1990). It conformably overlies shales of the Redknife Formation, and is conformably overlain by the Trout River Formation (Cross-section UDev-UDev').

In the subsurface of northeastern B.C., there are many Kakisa penetrations, but most wells target deeper reservoirs such as the Jean Marie and Slave Point, so the Kakisa has not been specifically evaluated. Detailed stratigraphic / sedimentological models have not been developed, but cores from c-A60-C/94-P-1, b-53-C/94-I-10 and c-52-I/94-I-10 exhibit abundant heterogeneous rubbled carbonate debris with variably-cemented vuggy/shelter porosity (Appendix 4), and logs show signatures ranging from clean and blocky to stacked shoaling-upward cycles (Cross-sections UDev-UDev', Kakisa-Kakisa').

The Kakisa maps as a broad shelfal carbonate across northeastern B.C. and into the Northwest Territories, ranging in thickness from 15-30m across much of the area

(Map KK1). It thins westward and northward to shelfal margins, and thickens southward toward the Peace River Arch where it loses its distinct identity (Cross-section UDev-UDev'). Burial depths are less than 900m in the northeast, and range to greater than 3200m in the Liard Basin (Map KK2).

Reservoir Quality

Kakisa porosities appear quite low on logs, although there are prominent porosity "notches" in some sections (Cross-section Kakisa-Kakisa'). A permeability-porosity cross-plot from core analysis shows low porosities (all samples <10%, most <5%), but with permeabilities ranging into the tens of millidarcies (Fig. KK1). Jones (1980) noted dolomitization in the Kakisa at Clarke Lake; one core at 02/d-91-L/94-J-9 shows several intervals with Kmax values of >10mD, but porosities are very low (1-4%), and the formation tested tight after acid and frac.

Production and Test Data

Reservoir Engineering Analysis

We analyzed 29 producing gas wells in the Ekwan-Tooga-Helmet area (94-I-10). All but one well are horizontal, with an average TD of 1100m and average horizontal length of 900m. All but two of the horizontal wells were completed open hole with no stimulation. Of the two, one horizontal was perf'd, and the other was perf'd and acidized; both showed very poor production. The vertical well was perf'd and acidized, and produced better than the average horizontal. We found no Kakisa oil producers.

Cumulative production from the 29 wells is 29 BCF to date, with expected ultimate recovery of about 39 BCF; cumulative production per well ranges from zero to 3.8 BCF, averaging 1.1 BCF (31 e^6m^3). No oil production was observed in any of the wells, and condensate averaged 7 Bbl/MMCF. Estimated ultimate recovery (EUR) per well ranges from zero to 4.5 BCF, averaging 1.4 BCF (40 e^6m^3). Initial production rates range from zero to 3.2 MMCF/D, averaging 900 MCF/D (25.5 e^3m^3/d). There is a poor correlation between IP and EUR.

Most wells at Ekwan show water production beginning at 2-5 Bbl/MMCF, steadily rising to 10 Bbl/MMCF (Fig. KK2). To the north, the small group of wells in Tooga/Helmet do not show as much water production, generally peaking at 5 Bbl/MMCF. It is not known how water is allocated back to wells in the production accounting process, so it is possible that these values are merely averages spread across the wells, or it is possible that all wells, regardless of structural position, perform similarly.

Most wells in the Ekwan main pool appear to decline in pressure more or less as expected, but in two wells, no pressure depletion was observed, despite significant production from the wells themselves and their neighbours (Fig. KK3). Neighbouring wells did not appear to follow the same pressure declines. In general, declines are not

Well ID	Sample ID	Zone	Sample Type	Depth (m)	Tmax	TOC %	Quartz	Feldspar		Carbonates		Clays			Sulphides	Apatite
					°C			Albite	K-fsp	Calcite	Dolomite, Fe-dolomite	Illite/mica	Chlorite	Kaolinite	Pyrite	
CNRL Hz Helmet C-A-046-K/94-P-01 WA 28724 aka: Devon Hz Helmet C-035-K/94-P-01 (int: 725.00 - 927.00 m)	720.8	Exshaw	Core	720.80	439	1.54	25.9	3	2.5	1.6		37.5	12.5	12.3	4.6	
	722.52	Exshaw	Core	722.52	439	1.82	31.1	3.5	3.2	1.6		37.3	9.8	8.5	5	
	723.57	Exshaw	Core	723.57	434	0.97	7.8			56.7	3.7	1.3		13.9	12.2	4.4
	723.71	Kotcho- U. Lst	Core	723.71	426	0.41	4.8			94.3	0.8				0.1	
	724.91	Kotcho- U. Lst	Core	724.91	418	0.45	2			90.5	6.3				1.2	
	726.19	Kotcho- U. Lst	Core	726.19	441	0.33	3.9			88.4	7.6				0.1	
	728.04	Kotcho- U. Lst	Core	728.04	441	0.32	2.6			91.7	5.7					
	729.76	Kotcho- U. Lst	Core	729.76	440	0.30	2.2			88.4	8.4			1		
	731.26	Kotcho- U. Lst	Core	731.26			0.9			92.1	7					
	731.28	Kotcho- U. Lst	Core	731.28	438	0.32	1.6			94.5	4					
	733.06	Kotcho- U. Lst	Core	733.06	441	0.27	2.4			91.3	5.1	0.4		0.8		
	737.16	Kotcho- U. Lst	Core	737.16	424	0.33	1.9			97.2	1					
	888.48	Tetcho- L. Lst	Core	888.48	437	0.30	1.3			95.7	1	0.7		0.7	0.6	
	890.54	Tetcho- L. Lst	Core	890.54	433	0.52	0.6			98.7	0.7					
	892.23	Tetcho- L. Lst	Core	892.23	440	0.45	0.9			98	1.1					
	894.28	Tetcho- L. Lst	Core	894.28	436	0.28	0.5			98.1	1.4					
	896.89	Tetcho- L. Lst	Core	896.89	435	0.33	1.1			91.6	7.3					
	900.03	Tetcho- L. Lst	Core	900.03	436	0.35	0.8			98.8	0.4					
	903.43	Tetcho- L. Lst	Core	903.43	438	0.32	0.9			98	1.1					
	907.62	Tetcho- L. Lst	Core	907.62	440	0.35	1			98.2	0.8					
	910.87	Tetcho- L. Lst	Core	910.87	440	0.36	1.4			89.9	8.6					
	913.9	Tetcho- L. Lst	Core	913.90	434	0.35	0.9			98	1.1					
	916.62	Tetcho- L. Lst	Core	916.62	441	0.30	2.4			97	0.6					
	919.53	Tetcho- L. Lst	Core	919.53	430	0.50	1.3			87.1	11.6					
	919.87	Tetcho- L. Lst	Core	919.87			1.8			91.4	6.8					
	921.54	Tetcho- L. Lst	Core	921.54	441	0.25	1.3			98.4	0.4					
	924.58	Tetcho- L. Lst	Core	924.58	437	0.33	3.8			95.8	0.5					

Table KT1. Mineralogical and TOC/T_{max} data of Exshaw-Tetcho interval, CNRL Hz Helmet 202/c-A46-K/94-P-1 (Devon Hz Helmet 202/c-35-K/94-P-1).

Unconfined Porosity and Matrix Permeability										
Well Name	Well Location	Core Depth (m)	Fm	Density		Porosity (%)	GRI Matrix Permeability (md)		GRI Matrix Permeability (nd)	
				Bulk Density (g/cc)	Skeletal Density (g/cc)		Avg	Std Dev	Avg	Std Dev
Husky Ekwan	c-052-I/094-I-10	973.43	Kakisa	2.631	2.715	3.12	5.26E-06	3.60E-06	5.26	3.60
Husky Ekwan	c-052-I/094-I-10	976.83	Kakisa	2.628	2.728	3.64	1.11E-05	1.08E-05	11.14	10.85
Husky Ekwan	c-052-I/094-I-10	980.33	Kakisa	2.622	2.717	3.52	1.54E-05	1.58E-05	15.43	15.78
Husky Ekwan	c-052-I/094-I-10	986.41	Kakisa	2.545	2.711	6.12	3.34E-05	1.94E-05	33.38	19.42
Encana Peggo	c-060-C/094-P-01	1061.92	Kakisa	2.651	2.688	1.36	9.42E-07	1.62E-07	0.94	0.16
Encana Peggo	c-060-C/094-P-01	1064.45	Kakisa	2.667	2.705	1.38	1.68E-06	2.46E-07	1.68	0.25
Encana Peggo	c-060-C/094-P-01	1066.25	Kakisa	2.678	2.700	0.83	7.20E-07	1.58E-07	0.72	0.16
Encana Peggo	c-060-C/094-P-01	1072.57	Kakisa	2.668	2.704	1.33	2.78E-06	7.94E-07	2.78	0.79
Encana Peggo	c-060-C/094-P-01	1075.33	Kakisa	2.584	2.715	4.82	3.60E-05	1.96E-05	35.97	19.59
Encana Peggo	c-060-C/094-P-01	1076.68	Kakisa	2.676	2.727	1.87	8.23E-06	7.46E-07	8.23	0.75
Husky Hz Ekwan	b-053-C/094-I-10	1108.42	Kakisa	2.652	2.706	2.01	3.30E-06	9.27E-07	3.30	0.93
Husky Hz Ekwan	b-053-C/094-I-10	1111.07	Kakisa	2.608	2.706	3.63	1.35E-05	1.55E-06	13.46	1.55
Husky Hz Ekwan	b-053-C/094-I-10	1113.47	Kakisa	2.609	2.709	3.67	2.11E-05	1.05E-05	21.06	10.49
Husky Hz Ekwan	b-053-C/094-I-10	1118.10	Kakisa	2.635	2.703	2.50	9.27E-06	1.13E-06	9.27	1.13
Husky Hz Ekwan	b-053-C/094-I-10	1120.47	Kakisa	2.521	2.707	6.88	1.22E-04	4.37E-05	122.49	43.69
Husky Hz Ekwan	b-053-C/094-I-10	1122.55	Kakisa	2.637	2.710	2.68	5.58E-06	1.81E-06	5.58	1.81
Husky Hz Ekwan	b-053-C/094-I-10	1125.26	Kakisa	2.637	2.723	3.17	6.78E-06	5.56E-07	6.78	0.56

Table KK2. Kakisa Formation – unconfined porosity and GRI matrix permeability measurements from core samples in three wells.

MICP Porosity										
Well Name	Well Location	Core Depth (m)	Fm	Density g/cc		Porosity (%)	Corrected Porosity (%)	Peak Range		Stem Volume Used (%)
				Bulk Density (g/cc)	Skeletal Density (g/cc)			Peak Range	Modal Peak	
Encana Peggo	c-060-C 094-P-01	1061.92	Kakisa	2.572	2.600	3.31	1.08	6 - 160	38	14
Encana Peggo	c-060-C 094-P-01	1066.25	Kakisa	2.631	2.670	1.80	1.47	4 - 70	4	6
Encana Peggo	c-060-C 094-P-01	1076.68	Kakisa	2.671	2.679	0.90	0.30	32 - 260	189	2
Husky Ekwan	c-052-I 094-I-10	973.43	Kakisa	3.957	4.023	1.91	1.64	4 - 60	6	12
Husky Ekwan	c-052-I 094-I-10	980.33	Kakisa	2.619	2.660	1.58	1.54	15 - 420	53	0
Husky Hz Ekwan	b-053-C 094-I-10	1108.42	Kakisa	2.670	2.692	1.49	0.81	6 - 150	41	9
Husky Hz Ekwan	b-053-C 094-I-10	1113.47	Kakisa	2.541	2.699	6.28	5.83	5 - 1100	522	25
Husky Hz Ekwan	b-053-C 094-I-10	1120.47	Kakisa	2.593	2.676	3.44	3.10	41 - 2260	1030	19
Husky Hz Ekwan	b-053-C 094-I-10	1125.26	Kakisa	2.669	2.712	1.87	1.57	4 - 40	4	7

Table KK3. Kakisa Formation – MICP porosity and conformance-corrected porosity measurements from core samples in three wells.

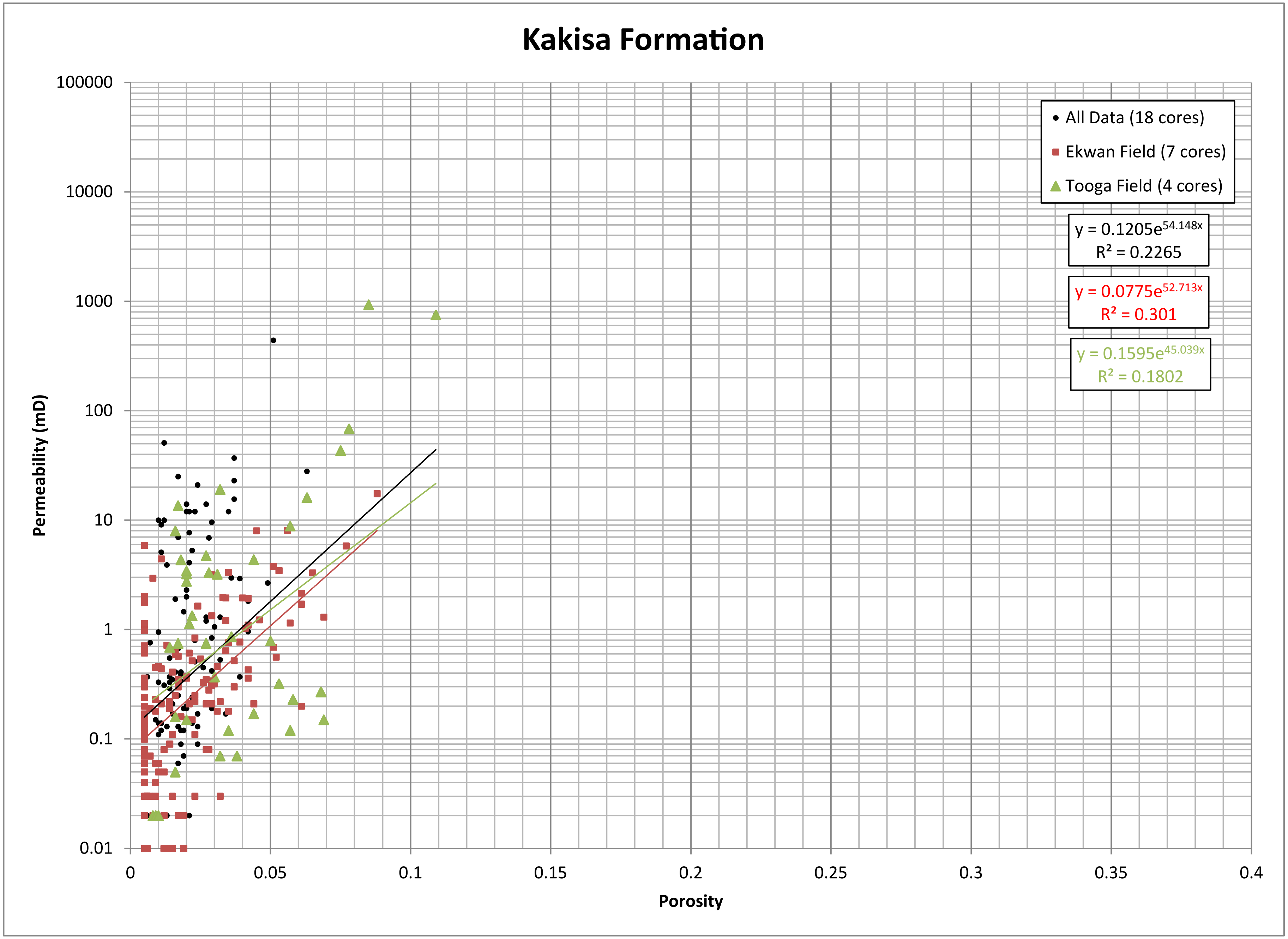

Figure KK1. Porosity / permeability cross-plot, Kakisa Formation.

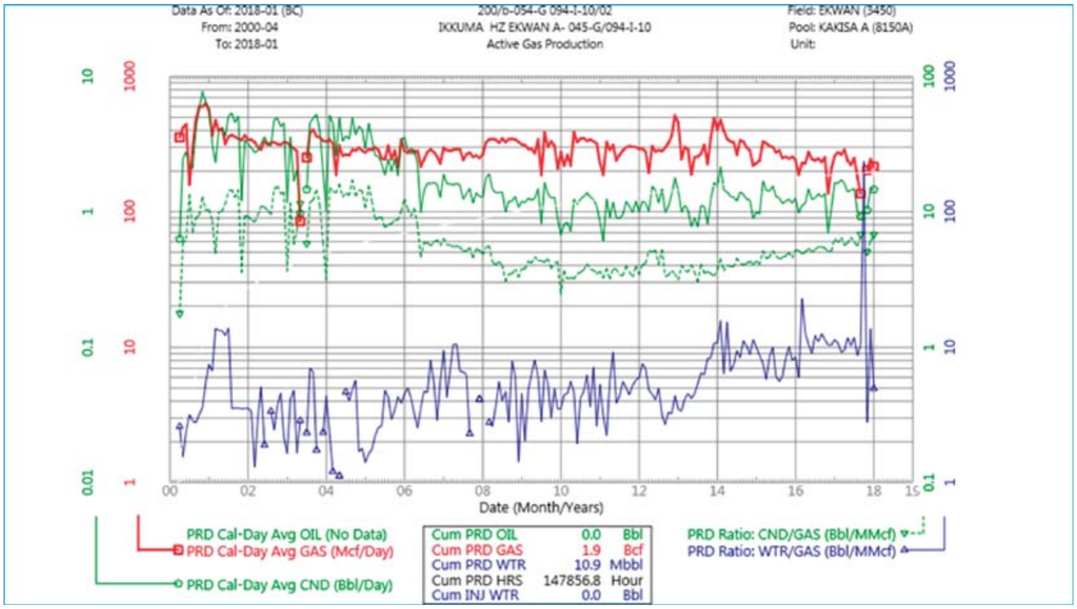

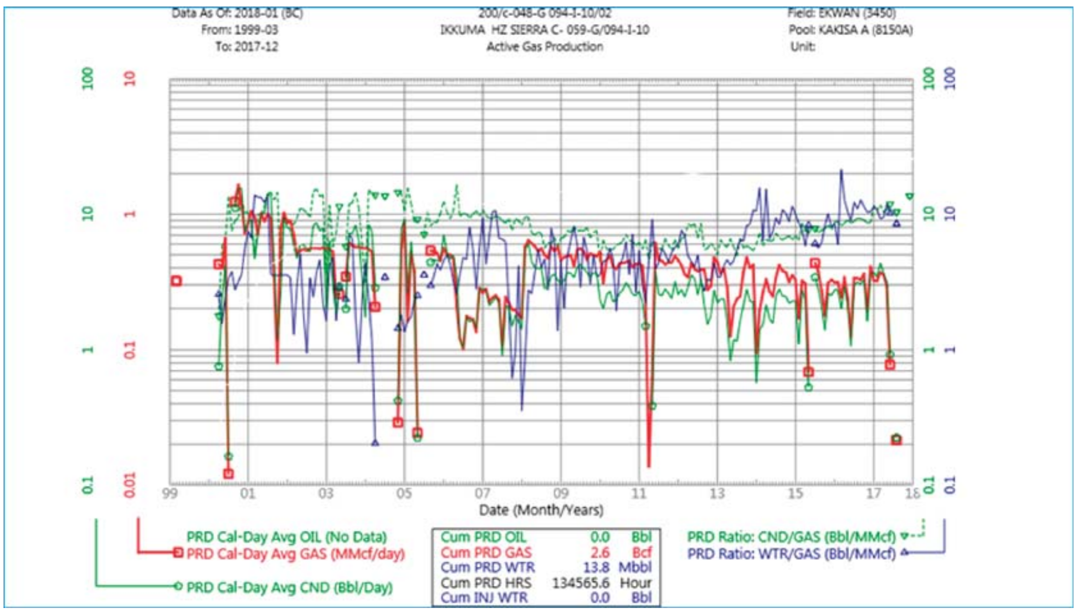

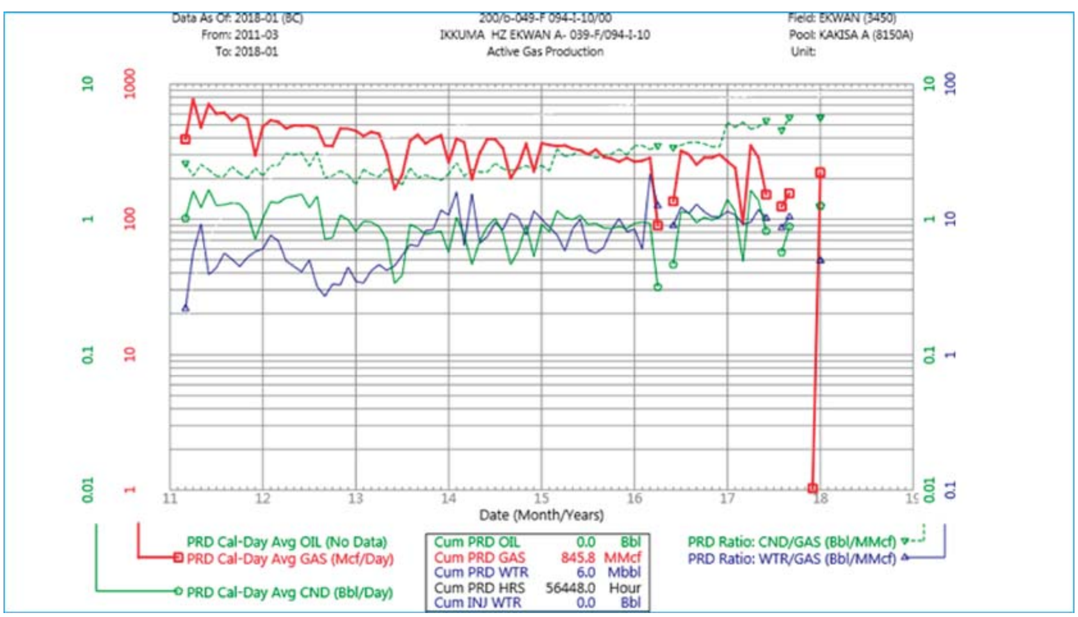

Figure KK2. Production plots, three representative horizontal Kakisa gas wells.

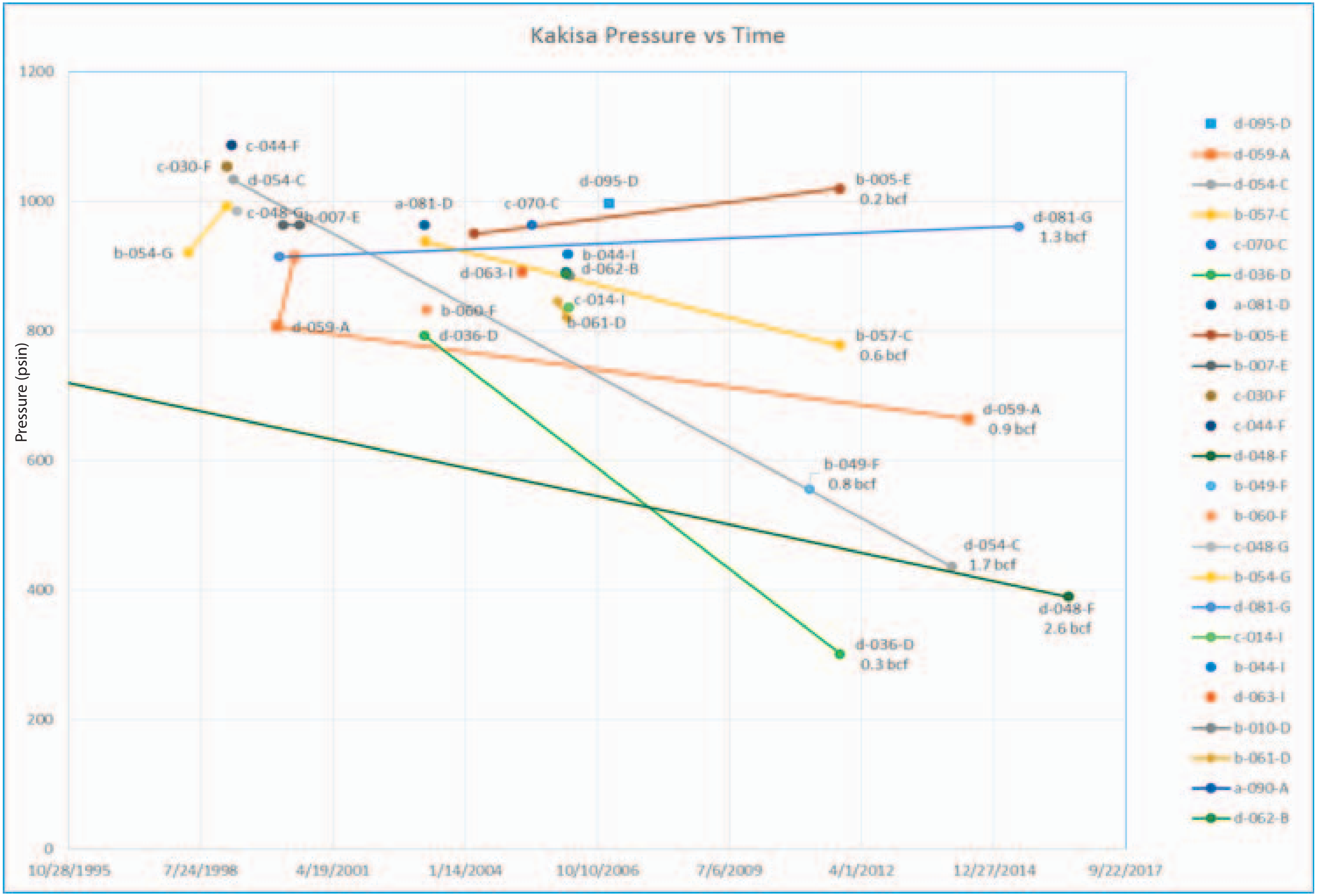

Figure KK3. Pressure vs time plots for several Kakisa gas wells in the Ekwan-Tooga-Helmet area. Note the anomalous increase of reservoir pressure with production and time in the b-5-E and d-81-G wells.

steep, and in a couple of cases almost too flat to get decline curves to converge. It is possible there is at least a partial water drive supporting gas production, but the reservoirs are underpressured, at an average datum pressure gradient of 0.25 psi/ft (5.7 kPa/m). Average depth is 1100m, average pressure 900 psia (6205 kPa).

Kakisa DST's are generally inconclusive, or indicate the formation has low permeability. A more detailed engineering analysis is available in Appendix 5.

Analytical Data

We analyzed cores from the Kakisa in three wells: Encana Peggo c-A60-C/94-P-1, Husky Ekwan b-53-C/94-I-10, and Husky Ekwan c-52-I/94-I-10 (Appendix 3). Lithologies including light grey nodular to laminated mudstones, wackestones, packstone, and stromatoporoid boundstones represent reef mounds and associated reefal debris. We felt this level of analysis was justified given the paucity of existing data, and an initial impression that oil prospectivity could be established.

Kakisa mineralogy is dominated by calcite (in many samples >95%), with small to trace amounts of quartz, dolomite and organics (Table KK1). Several samples also contain small amounts of feldspars, clay minerals (predominantly illite and chlorite), and pyrite.

Petrographically, we observed Kakisa bioclastic wackestones, packstones, boundstones and mudstones (Fig. KK4-KK7). Limestones are heavily recrystallized and in many cases micritic with some spar; micritic muds can impart a darker grey colour. Scattered large open pores are present, particular as fossiliferous shelter porosity (Fig. KK4, 5). Pressure solution features such as stylolites are common, and recrystallization and cementation markedly reduce porosity.

Unconfined porosities of Kakisa samples range between <1% to ~7%, and matrix permeabilities measure from 1.2 e^{-4} to 8 e^{-7} mD (Table KK2). MICP conformance-corrected porosity is <5.8%, reflecting pronounced porosity reduction through diagenetic overprint (Table KK3). The difference between the two porosity measures implies that a significant number of pore throats are <3-4 nm, although some samples feature larger pore throats – compare pore throat distribution patterns in two samples from the b-53-C well (Fig. KK8, KK9).

Total organic carbon is very low (generally <0.7 wt%) (Table KK1). T_{max} values range from ~425-440°C, but their validity is questionable given the low TOC values. Hydrocarbon analysis (S1) shows that residual hydrocarbons are present and most commonly contain C_{15}-C_{35} chains with calculated API gravities of 30-35°, and calculated specific gravities ranging between 0.85-0.89 (Table KK4, Fig. KK10); heavy condensates are dominant (Fig. KK11). We conclude that hydrocarbon liquids are present in the Kakisa Formation, despite observing no hydrocarbon staining in large pores.

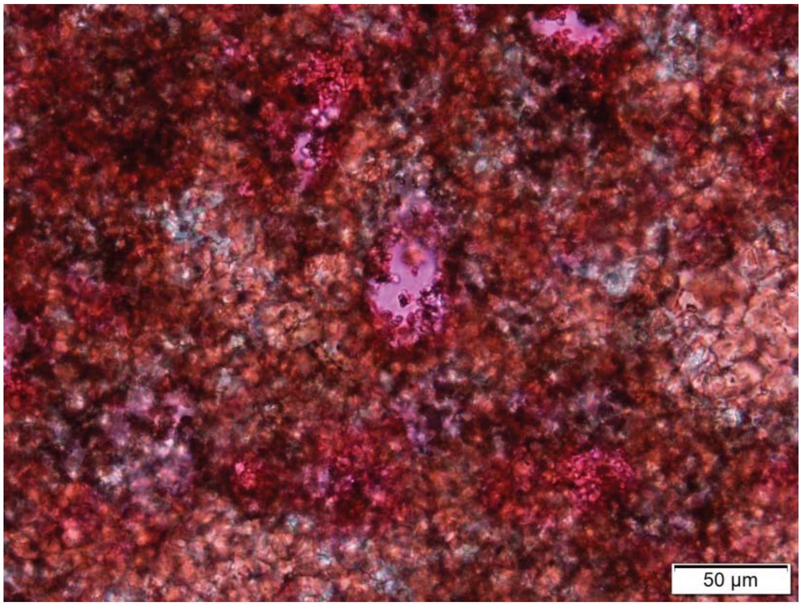

Figure KK4. Photomicrograph, Kakisa Formation, Husky Ekwan b-53-C/94-I-10 (1118.32-1118.39 m) under plane polarized light. Recrystallized stromatoporoid boundstone features isolated pores (pink epoxy) and abundant recrystallized micrite and neomorphic microspar.

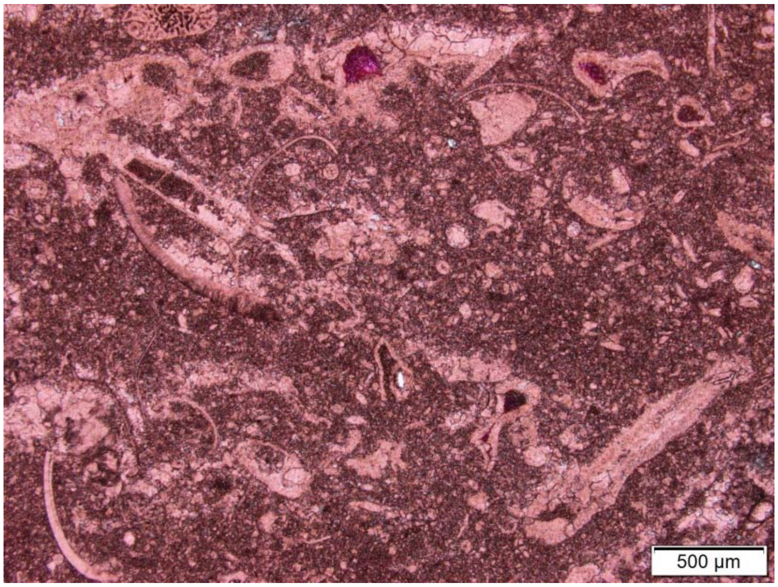

Figure KK5. Photomicrograph, Kakisa Formation, Husky Ekwan c-52-I/94-I-10 (970.51-970.55 m) under plane polarized light. Recrystallized bioclastic wackestone/packstone consists of coarse crystalline, replaced bivalve and brachiopod shells and shell fragments within micritic/microsparry calcite matrix. Pink epoxy highlights large shelter porosity, but the remainder is fully recrystallized and tightly cemented.

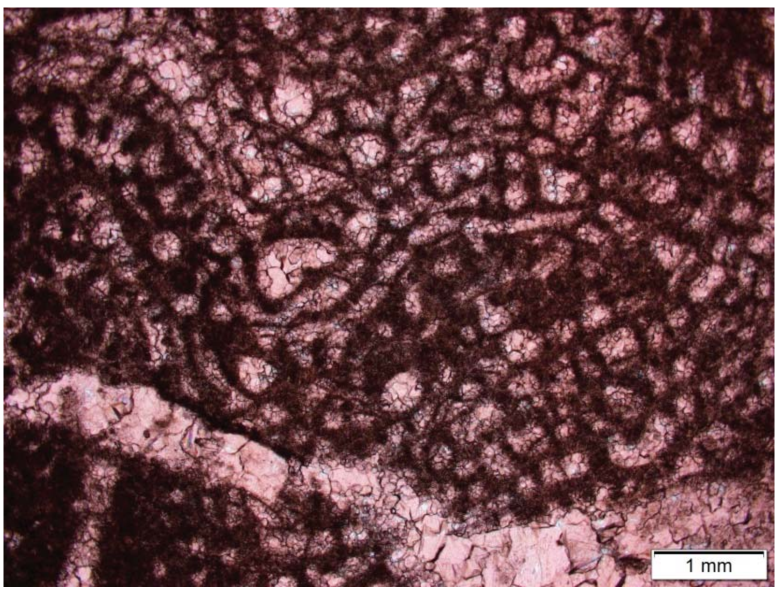

Figure KK6. Photomicrograph, Kakisa Formation, Husky Ekwan b-53-C/94-I-10 (1118.32-1118.39 m) under plane polarized light. A recrystallized stromatoporoid features inner chambers filled with coarse, interlocking calcite with interstitial micritic calcite. Note the lenticular coarse crystalline structure along the bottom is slightly displaced due to fracturing.

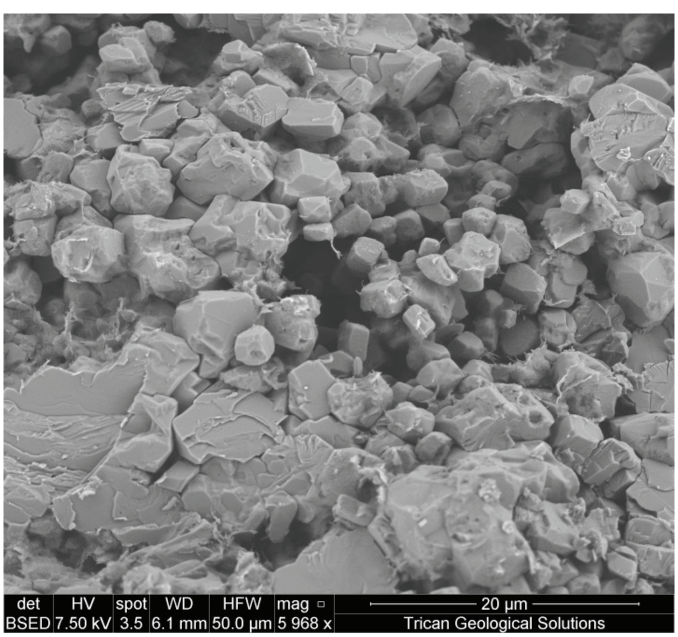

Figure KK7. BSED SEM micrograph of Kakisa Formation, Husky Ekwan b-53-C/94-I-10 (1118.32-1118.39 m) show “granular” euhedral micrite, with trace amounts of illitic clay needles/flakes, particularly in the upper right of photo.

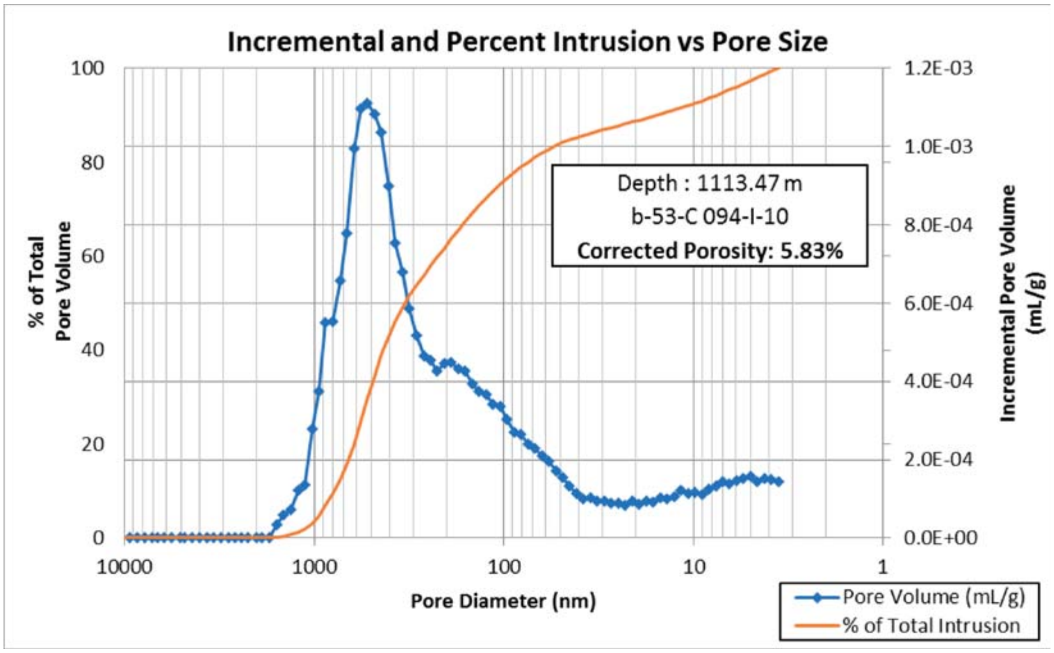

Figure KK8. Incremental and percent intrusion vs pore size, Kakisa Formation, Husky Ekwan b-53-C/94-I-10 (1113.47m), highlighting a wide range of pore throat diameters, with a major peak around 500 nm.

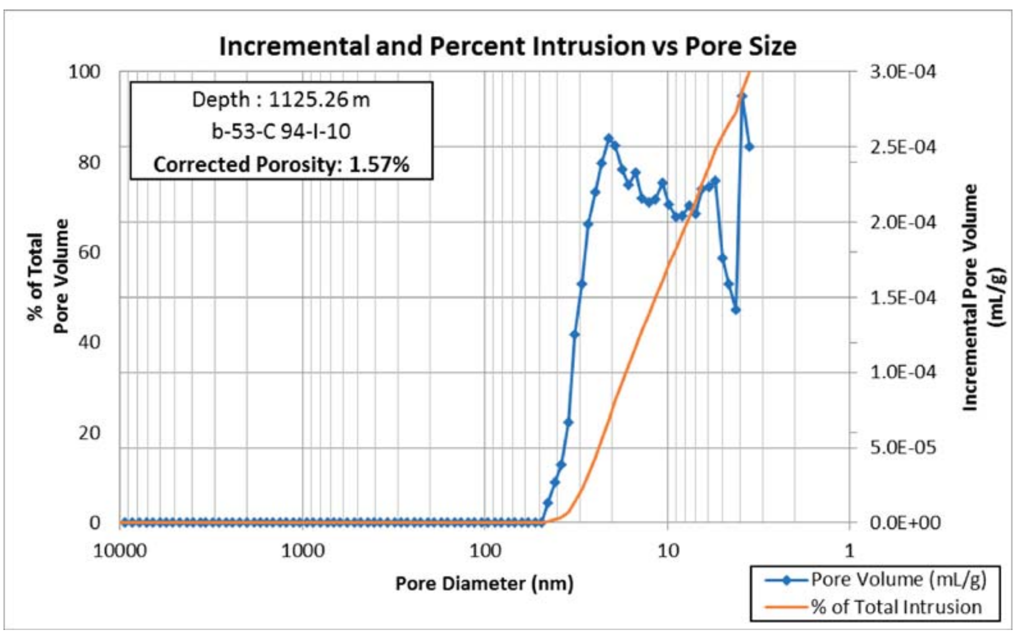

Figure KK9. Incremental and percent intrusion vs pore size, Kakisa Formation, Husky Ekwan b-53-C/94-I-10 (1125.26m), highlighting large percentage of small pore throats (<40 nm).

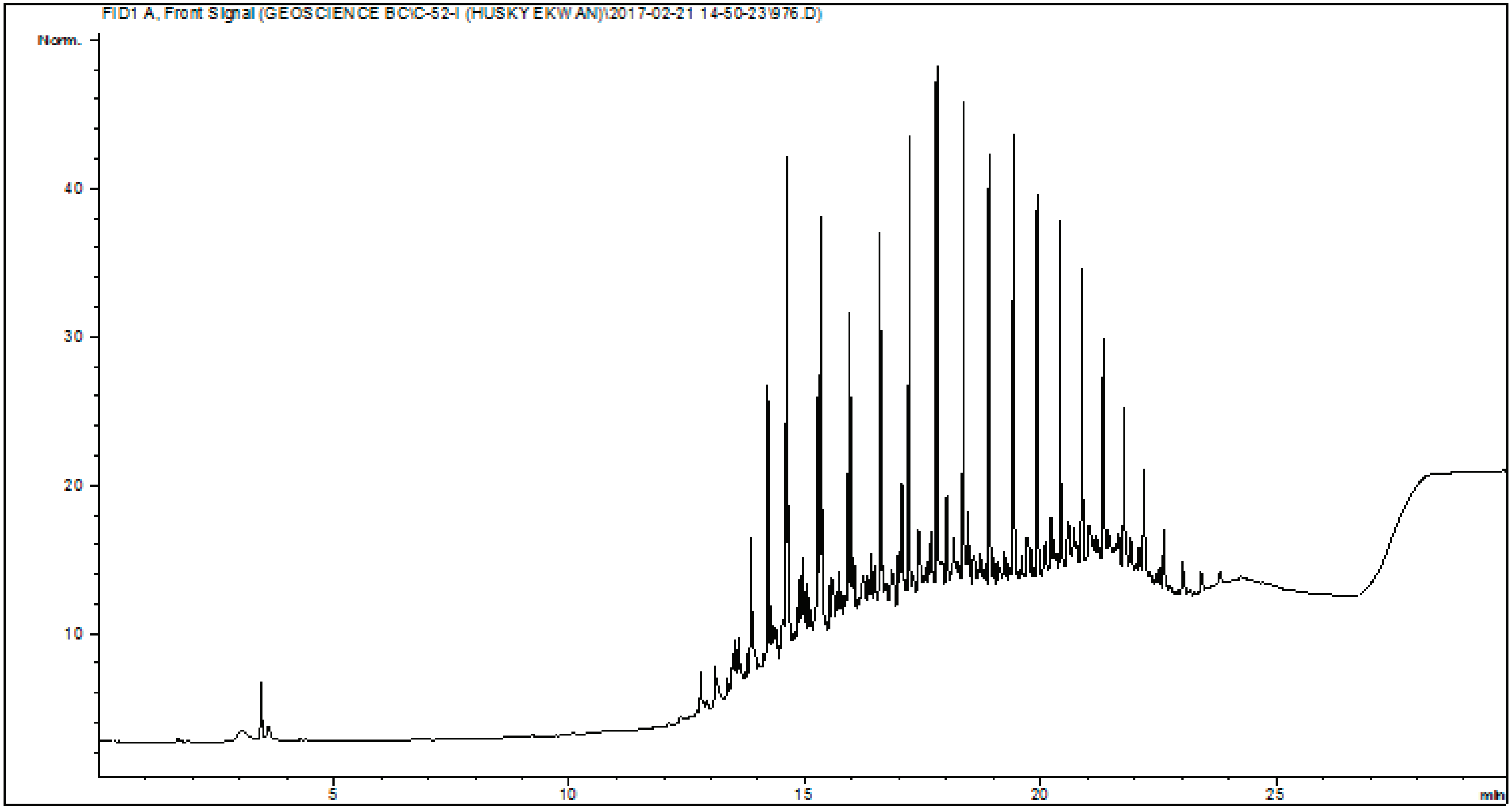

Figure KK10. Bulk rock hydrocarbon analysis (S1), showing hydrocarbon chain distribution and detection, Kakisa Formation, Husky Ekwan c 52 I/94 I 10, 976m.

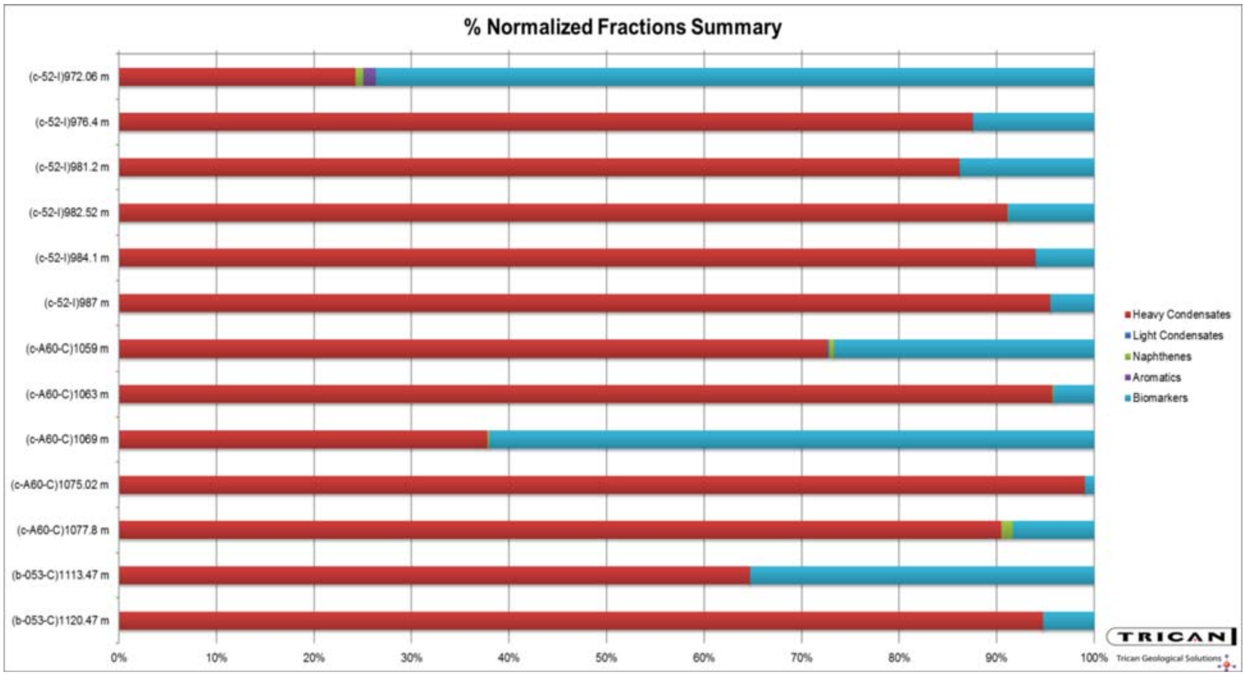

Figure KK11. Normalized fraction plot of hydrocarbon groups, Kakisa Formation, various wells (13 samples listed by well and depth).

Hydrocarbon Composition by Thermal Desorption Gas Chromatography

Well Name	Well Location	Core Depth (m)	Fm	% Light Condensate	% Heavy Condensate	% Naphthenes	% Aromatics	% Biomarkers	Peak	Initial Boiling Point (°C)	Carbon Number	Final Boiling Point (°C)	Carbon Number	Calculated Specific Gravity	Calculated API gravity	Chromatogram Quality
Husky Ekwan	c-052-I/094-I-10	972.06	Kakisa	0.00	24.25	0.79	1.30	73.67	pristane	264	C15	383	C23	0.87	31.87	no good
Husky Ekwan	c-052-I/094-I-10	976.40	Kakisa	0.00	87.51	0.02	0.04	12.43	C25	260	C14	461	C31	0.86	32.78	okay
Husky Ekwan	c-052-I/094-I-10	981.20	Kakisa	0.00	86.19	0.01	0.00	13.80	pristane	271	C15	463	C32	0.86	33.05	okay
Husky Ekwan	c-052-I/094-I-10	982.52	Kakisa	0.00	91.12	0.07	0.00	8.81	C30	273	C15	473	C33	0.87	31.68	okay
Husky Ekwan	c-052-I/094-I-10	984.10	Kakisa	0.02	93.98	0.00	0.00	6.00	C30	294	C16	468	C32	0.86	32.32	poor
Husky Ekwan	c-052-I/094-I-10	987.00	Kakisa	0.00	95.50	0.00	0.00	4.50	C26	294	C16	502	C37	0.88	29.66	good
ECA Peggo	c-A60-C/094-P-01	1059.00	Kakisa	0.13	72.66	0.57	0.00	26.64	pristane	35	<C6	409	C26	0.85	35.02	poor
ECA Peggo	c-A60-C/094-P-01	1063.00	Kakisa	0.00	95.73	0.09	0.00	4.19	C26	50	<C6	486	C35	0.87	31.74	poor
ECA Peggo	c-A60-C/094-P-01	1069.00	Kakisa	0.00	37.79	0.16	0.00	62.06	phytane	22	<C6	421	C27	0.85	34.25	no good
ECA Peggo	c-A60-C/094-P-01	1075.02	Kakisa	0.00	99.03	0.00	0.00	0.97	C35	66	<C6	514	C39	0.88	29.67	okay
ECA Peggo	c-A60-C/094-P-01	1077.80	Kakisa	0.00	90.47	1.20	0.00	8.34	C30	49	<C6	479	C34	0.85	35.36	very poor
Husky Hz Ekwan	b-053-C/094-I-10	1108.42	Kakisa	0.00	0.00	0.00	0.00	0.00	n/a	3	<C6	549	C40	n/a	n/a	no good
Husky Hz Ekwan	b-053-C/094-I-10	1111.07	Kakisa	0.00	0.00	0.00	0.00	0.00	n/a	4	<C6	549	C40	n/a	n/a	no good
Husky Hz Ekwan	b-053-C/094-I-10	1113.47	Kakisa	0.00	64.70	0.00	0.00	35.30	phytane	57	<C6	532	C40	0.90	25.83	no good
Husky Hz Ekwan	b-053-C/094-I-10	1118.10	Kakisa	0.00	0.00	0.00	0.00	0.00	n/a	2	<C6	549	C40	n/a	n/a	no good
Husky Hz Ekwan	b-053-C/094-I-10	1120.47	Kakisa	0.00	94.75	0.00	0.00	5.25	C25	98	C7	536	C40	0.87	31.32	poor
Husky Hz Ekwan	b-053-C/094-I-10	1122.55	Kakisa	0.00	0.00	0.00	0.00	0.00	n/a	6	<C6	488	C35	n/a	n/a	no good
Husky Hz Ekwan	b-053-C/094-I-10	1125.26	Kakisa	0.00	0.00	0.00	0.00	0.00	n/a	8	<C6	414	C26	n/a	n/a	no good

Table KK4. Kakisa Formation – hydrocarbon composition data, three wells.

We had difficulty obtaining competent and representative samples from the Kakisa Formation, as planes of weakness were common in most samples. Three samples of the eight obtained had a length:diameter ratio less than 2:1 (the minimum ratio suggested by ASTM Standard), and two were below 1.7. Results are variable, showing Young's modulus ranging from 42.9-60.0 GPa, and compressive strengths ranging from 123-220 Mpa (Table KK5). Variability could be related to density, and potentially cementation, but variability arising from distribution of weakness planes adds considerable uncertainty.

Well Location	Depth (m)	Confining Pressure (MPa)	Axial Strain at Failure (%)	Compressive Strength (MPa)	Residual Strength (MPa)	Static Young's Modulus (GPa)	Static Poisson's Ratio	Static Bulk Modulus (GPa)	Static Shear Modulus (GPa)
b-053-C 94-I-10	1109.64	15.5	0.513	185.54	120.85	55.04	0.270	39.88	21.67
b-053-C 94-I-10	116.34	15.5	0.484	172.22	150.16	48.79	0.252	32.81	19.48
b-053-C 94-I-10	1124.55	15.5	0.444	218.50	172.24	57.99	0.293	46.66	22.43
c-052-I 94-I-10	971.21	13.5	0.377	200.57	141.96	59.39	0.258	40.98	23.60
c-052-I 94-I-10	982.42	13.5	0.647	123.00	118.56	42.93	0.263	30.25	16.99
c-060-C 94-P-01	1062.91	15.0	0.549	145.27	100.99	46.93	0.286	36.47	18.25
c-060-C 94-P-01	1070.63	15.0	0.435	219.52	141.28	60.03	0.256	40.98	23.90
c-060-C 94-P-01	1077.54	15.0	0.532	162.33	124.92	44.87	0.271	32.72	17.65

Table KK5. Kakisa Formation – rock mechanical properties from three wells.

We found no analytical work completed on the Kakisa in the literature or in reports submitted to the B.C. Oil & Gas Commission.

Resource Oil Assessment

The Kakisa Formation is a regionally extensive carbonate platform reservoir, composed primarily of low-permeability limestones with isolated intervals of low-grade conventional reservoir. There has been little work published on cyclicity and depositional facies, but it appears likely that reservoir sweet spots could be identified and systematically mapped with some degree of confidence – which was likely been done before operators drilled the existing horizontal gas wells.

Given the occurrence of oil and hydrocarbon liquids in other Paleozoic reservoirs (Jean Marie, Tetcho, Rundle) in northern 94-I and southern 94-P, and the liquids-generating maturity of the Muskwa shales in the area, one would expect some oil production from the Kakisa. Evidence of residual heavier hydrocarbons in core is encouraging, but only gas has been produced. As well, condensate ratios are low, reservoirs appear relatively underpressured, and there may be some associated water.

While we cannot discount the possibility that oil may be discovered in the Kakisa, we have no real explanation for lack of oil shows to date, and therefore cannot confidently point to oil potential in the future.

KOTCHO / TETCHO FORMATIONS

Age and Play Type

Upper Devonian – Tight Oil play (tight carbonate);
Prospectivity: 'B' Play - Oil production established, but regional prospectivity appears unlikely.

Regional Geology

The Kotcho and Tetcho formations are outer shelf carbonates deposited on the northwestern flank of the Wabamun Group (Fig. KT1). At their type sections in outcrop in the Northwest Territories, they are described as argillaceous limestones with shale interbeds, reflecting relatiavely distal deposition. The Tetcho lies conformably on Trout River shales and argillaceous limestones, and is succeeded conformably by the Kotcho; the Kotcho is uniformly overlain by marine Exshaw shales, although not the relationship is somewhat unconformable (Halbertsma, 1994). Cross-section UDev-UDev' illustrates the northwestward transition from a dominantly clean carbonate section to basinal shales.

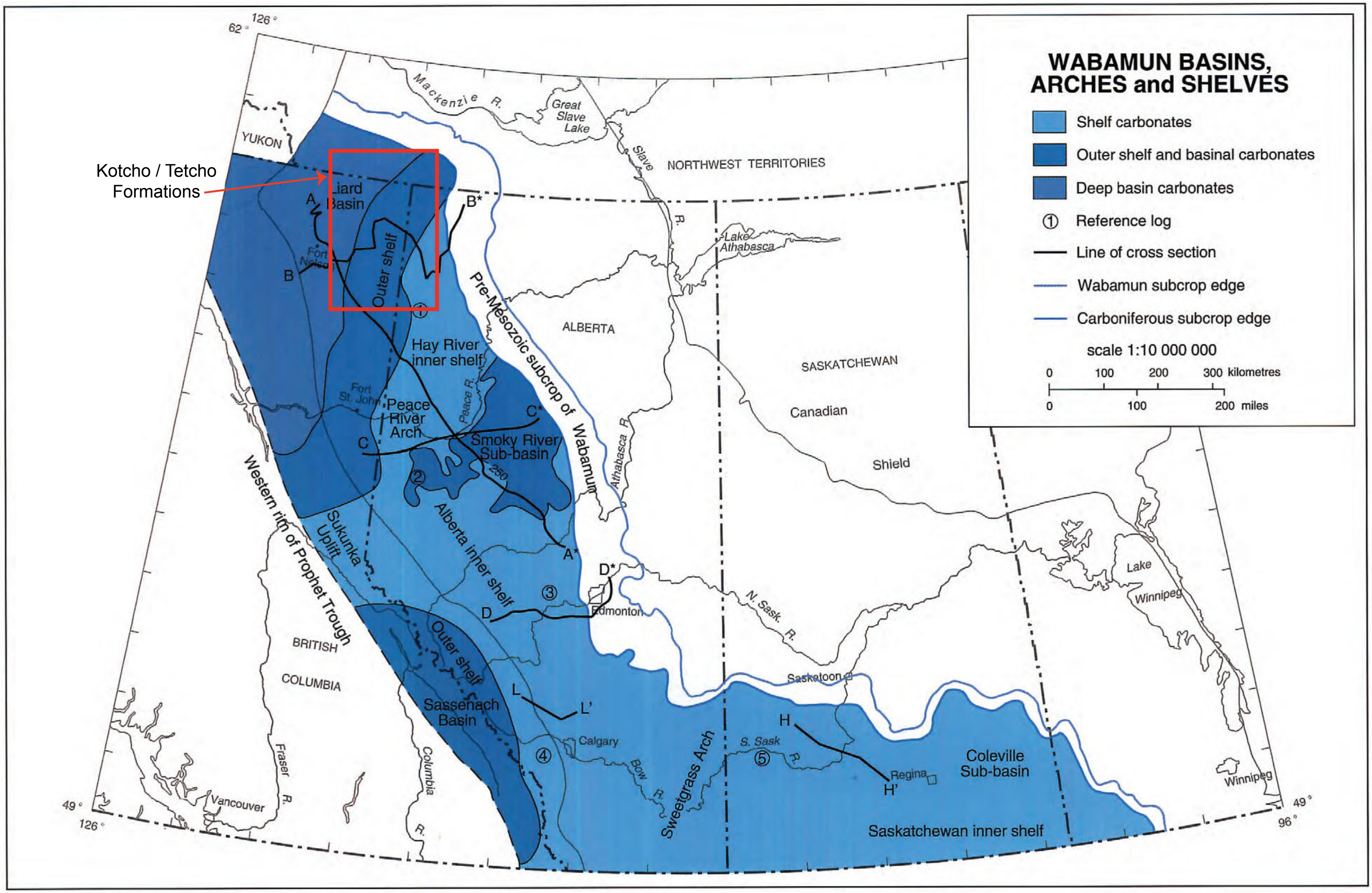

Figure KT1. Wabamun (Kotcho-Tetcho) paleogeography, WCSB (from Halbertsma, 1994).

In the subsurface of northeastern B.C., there are many Kotcho and Tetcho penetrations, but most wells target deeper reservoirs such as the Jean Marie and Slave Point, and so the Kotcho and Tetcho have not been extensively evaluated. Detailed stratigraphic / sedimentological models have not been developed, but cores from c-A46-K/94-P-1, d-A11-K/94-P-2, and d-13-C/94-P-9 exhibit mottled/burrowed argillaceous carbonates (Appendix 4), and logs show stacked shoaling- and cleaning-upward successions (Cross-sections UDev-UDev', Kakisa-Kakisa').

Clean limestones of the Kotcho range up to 100m thick (Cross-section UDev-UDev', Tetcho-Tetcho') along the BC/Alberta border, and thin / shale out westward (Map KT1). The Tetcho has a similar distribution, but is somewhat more extensive (Map KT2). Burial depths for the Kotcho range from about 600m in the northeast to more than 2200m in the southwest (Map KT3); the top Tetcho lies 200-600m deeper (Map KT4).

Reservoir Quality

Kotcho and Tetcho porosities appear quite low on logs in most wells; prominent porosity "notches" are generally lacking (Cross-section Tetcho-Tetcho'). A permeability-porosity cross-plot from core analysis shows low to moderate porosities up to 10%, and permeabilities of 10mD or less (Fig. KT2). Jones (1980) did not identify anomalous Kotcho / Tetcho dolomitization associated with deep faults, as he did for other carbonate reservoirs.

Production and Test Data

Kotcho – Very few DST's have been conducted, and none yielded indications of substantial reservoir quality. Our completions search yielded only three wells in the study area where a Kotcho completion was attempted (Map K1). At d-57-J/94-P-1 and c-28-D/94-P-2, porous zones at the top of the Kotcho were perfed and acidized, but only a slight gas flow was noted at c-28-D.

Tetcho – Tetcho DST's indicate the formation to be generally tight, but a number of completions have been attempted. In several vertical wells, perf / acid jobs have produced little or no hydrocarbon. There are six producing horizontal wells, three oil and three gas.

Reservoir Engineering Analysis

Three horizontal oil wells at c-35-K/94-P-1, c-65-C/94-P-8, and c-66-C/94-P-8, were drilled between 2012 and 2015 by Devon Canada (now CNRL) (Map KT2). These are highlighted on Cross-section Tetcho-Tetcho', where we show the entire vertical section in vertical wellbores adjacent to the actual producing horizontal. The oil wells are drilled to a true vertical depth of 900m, with measured depth of 2200m and average horizontal length of 1200m, and were completed open hole with 12 to 15 frac stages.

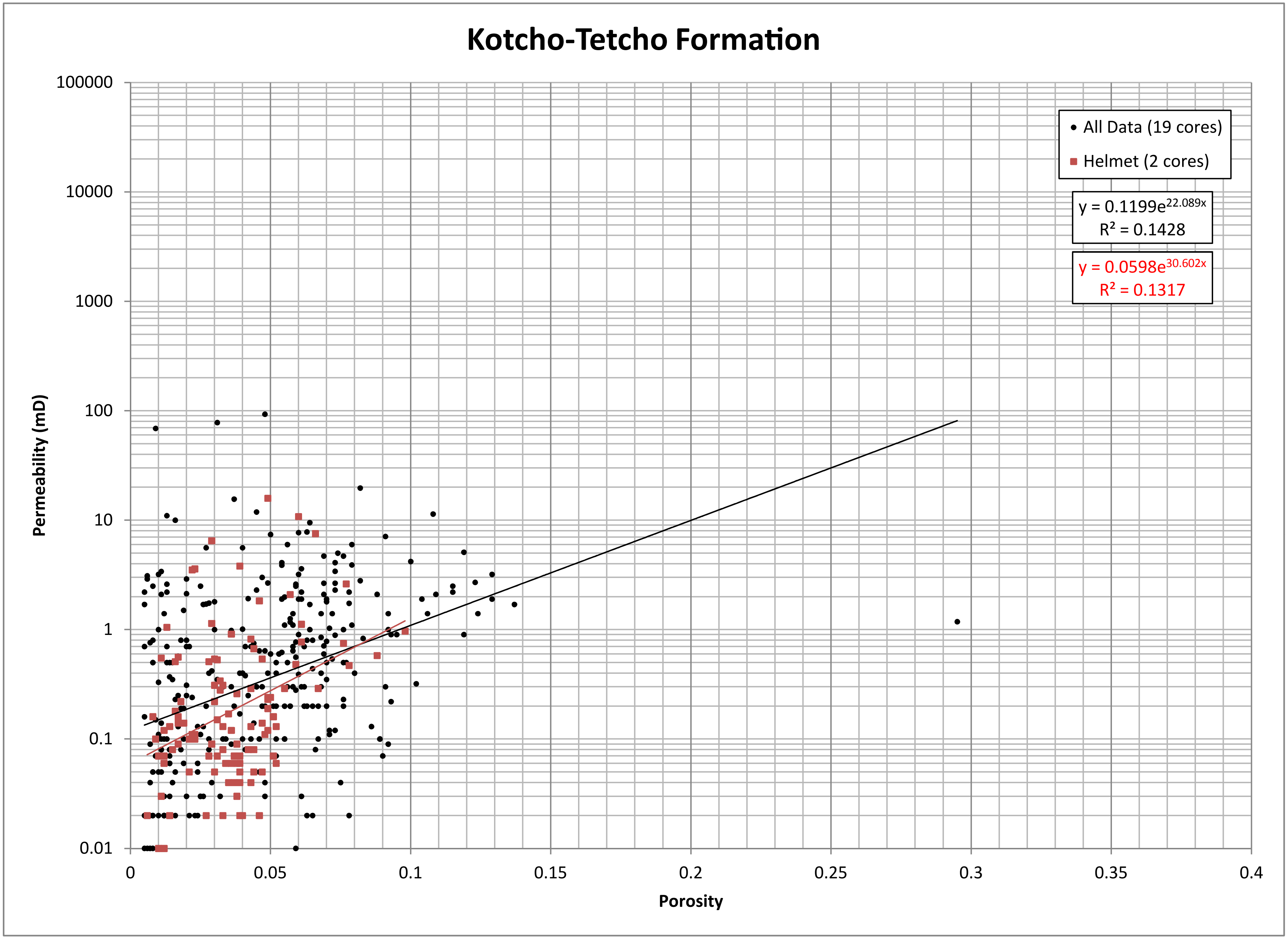

Figure KT2. Porosity / permeability cross-plot, Kotcho-Tetcho Formations.

Production performance has been encouraging, averaging 11.6 m^3/d (73 BOPD) initially with EUR's of about 7.6 e^3m^3 oil (48 MBO) (Fig. KT3). Water production has been negligible, and GOR behavior has been normal for primary production, rising from the mid 100's scf/bbl to low 1000's. No oil analysis was available, but a liquid sample from one of the gas producers indicated an API gravity of 45 degrees.

Three horizontal gas wells were also drilled by Devon (now CNRL), with poor production results. Two wells were suspended after producing less than 2.8 e^6m^3 gas (0.1 BCF), and one well is currently producing at 2.7 e^3m^3/d (95 MCF/D). All were drilled to a true vertical depth of 1100m, with measured depths of 2400m and average horizontal lengths of 1200m. Completions were open hole with 12 to 15 frac stages.

Eight Tetcho pressure points were found, seven from completed wells. Four of the six producing wells recorded initial pressures; two of the oil wells had pressures averaging 4070 kPa (590 psia) at depths of 870m, giving a datum gradient of 4.75 kPa/m (0.21 psi/ft). The two gas wells showed average gradients of 5.2 kPa/m (0.23 psi/ft) – significantly underpressured compared to a normal water gradient of 9.9 kPa/m (0.44 psi/ft).

Of the completed non-producing wells, three were production tested, but none recorded any flow data. Pressures at these three wells, all located downdip from the producing wells, showed pressure gradients of 5.4 kPa/m (0.24 psi/ft), which if correct and built-up, are also significantly underpressured.

A DST in the northeast corner of the study area at b-68-D/94-P-16 showed good pressure response and moderate permeability. Although not fully built-up or extrapolated, the test indicated gas recovery along with oily mud, and was overpressured at 0.46 psi/ft. Some depletion was noted on the charts.

A more detailed engineering analysis is available in Appendix 5.

Analytical Data

Database and literature searches showed very few existing analytical reports for the Kotcho / Tetcho (Appendix 1).

We analyzed cores from the Kotcho / Tetcho interval in three wells: CNRL Hz Helmet 02/c-A46-K/94-P-1 (Devon Hz Helmet 02/c-35-K/94-P-1) (Exshaw, Kotcho / Tetcho), CNRL Hz Helmet d-A11-K/94-P-2 (c-22-K/94-P-2) (Tetcho lower limestone), and Czar Venus d-13-C/94-P-9 (Tetcho) (Appendix 3). All are grey to dark grey, nodular to thinly bedded limestones with intervals containing abundant intraclasts (Appendix 4). As for the Kakisa, we felt this level of analysis was justified given the paucity of existing data, and an initial impression that oil prospectivity could be established.

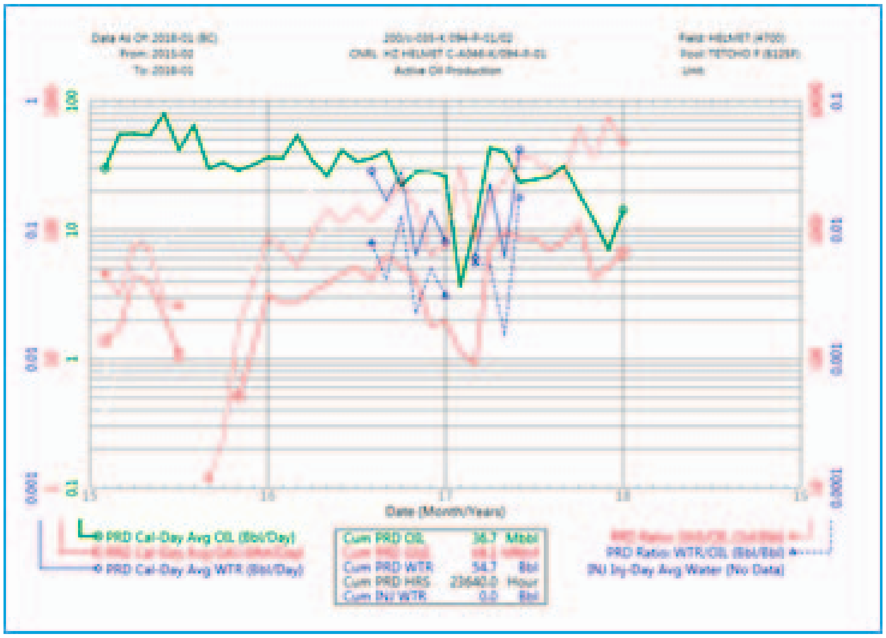

C-35-K

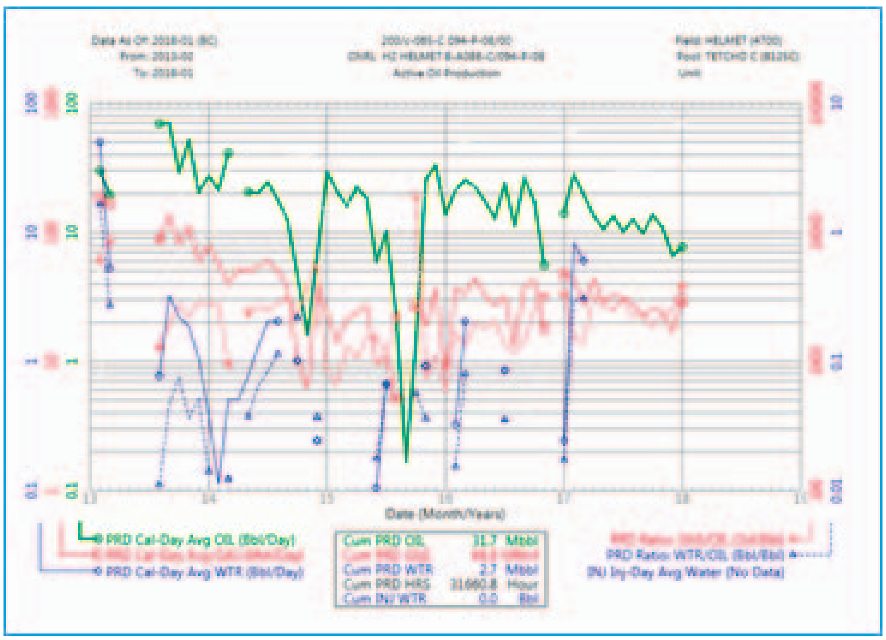

C-65-C

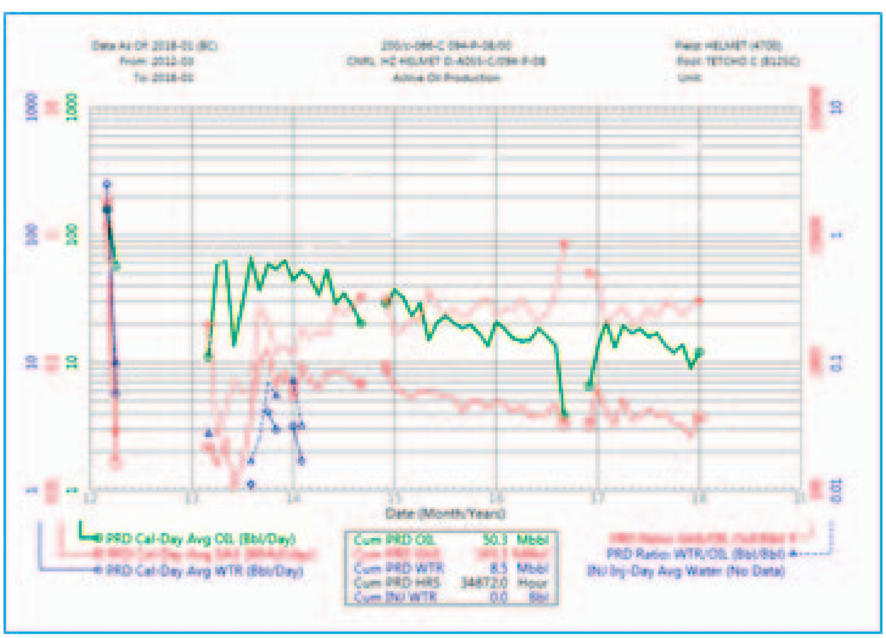

C-66-C

Figure KT3. Production plots for the three horizontal Tetcho oil wells.

Mineralogies are dominated by calcite (generally >95%) with small to trace amounts of quartz, dolomite and organics (Table KT1, KT2; Fig. KT4). A few samples also contain small to trace amounts of dolomite, feldspars, clay minerals (illite and chlorite) and pyrite.

Total organic carbon values are very low (mostly <0.4 wt%) (Table KT1, KT2). T_{max} values range from ~420-445°C, but their validity is questionable given the low TOC measurements. Residual hydrocarbons were not observed in core, but differential thermal GC analysis (S1) shows that small amounts of heavy condensates are present.

Petrographic analysis shows a variety of rock types, including bioclastic wackestones, packstones, and mudstones (Fig. KT5-KT9). Limestones are heavily recrystallized and in many cases micritic with some spar; micritic muds can impart a darker grey colour. Very thin mud layers are common and generate a nodular appearance. There are scattered large open pores. Stylolites, recrystallization and cementation have reduced porosity significantly.

Unconfined porosities of Kotcho samples range between 3.5-8.5%, with matrix permeabilities of 2.7 e^{-5} to 7 e^{-6} mD. Tetcho samples exhibit much lower porosities (1.5-4.5%) and matrix permeabilities ranging between 1.2 e^{-5} to 7 e^{-6} mD (Table KT3). MICP conformance-corrected porosities for Kotcho samples range between 0.9-7.4%, and for the Tetcho between 0.6-4.6% (Table KT4). Plots of incremental and percent intrusion vs pore size for a Kotcho sample show a wide range of pore throat diameters with a major peak around 1000 nm, and for a Tetcho sample show a similarly wide range but with the major peak at a much smaller 80 nm (Fig. KT10, KT11). More work is required to create reliable characterizations, but the wide pore size ranges suggest the potential for highly variable reservoir characteristics and responses.

Hydrocarbon analysis (S1) shows that residual hydrocarbons are present and most commonly contain C_{15}-C_{35} chains with a calculated API gravity of 30-35° (Fig. KT12). Calculated specific gravity ranges between 0.85-0.89, and heavy condensates dominate (Table KT5, Fig. KT13). We conclude that hydrocarbon liquids are present in the Kotcho / Tetcho reservoirs, although we observed no hydrocarbon staining in core.

Mechanical properties of Kotcho / Tetcho samples from d-A11-K/94-P-2 and d-13-C/94-P-9 show average compressive strength of 170-230 MPa and residual strengths of 120-195 MPa. Poisson's ratio measures ~0.25-0.33, and Young's modulus ~47-63, indicating strong and brittle rocks (Table KT6).

Resource Oil Assessment

Like the Kakisa, the Kotcho and Tetcho formations are regionally extensive carbonate platform reservoirs, composed primarily of low-permeability limestones with isolated intervals of low-grade conventional reservoir. There has been little work published on cyclicity and depositional facies, but it appears likely that reservoir sweet spots could be

Well ID	Sample ID	Zone	Sample Type	Depth (m)	Tmax	TOC %	Quartz	Feldspar		Carbonates		Clays			Sulphides	Apatite
					°C			Albite	K-fsp	Calcite	Dolomite, Fe-dolomite	Illite/mica	Chlorite	Kaolinite	Pyrite	
CNRL Hz Helmet C-A-046-K/94-P-01 WA 28724 aka: Devon Hz Helmet C-035-K/94-P-01 (int: 725.00 - 927.00 m)	720.8	Exshaw	Core	720.80	439	1.54	25.9	3	2.5	1.6		37.5	12.5	12.3	4.6	
	722.52	Exshaw	Core	722.52	439	1.82	31.1	3.5	3.2	1.6		37.3	9.8	8.5	5	
	723.57	Exshaw	Core	723.57	434	0.97	7.8			56.7	3.7	1.3		13.9	12.2	4.4
	723.71	Kotcho- U. Lst	Core	723.71	426	0.41	4.8			94.3	0.8				0.1	
	724.91	Kotcho- U. Lst	Core	724.91	418	0.45	2			90.5	6.3				1.2	
	726.19	Kotcho- U. Lst	Core	726.19	441	0.33	3.9			88.4	7.6				0.1	
	728.04	Kotcho- U. Lst	Core	728.04	441	0.32	2.6			91.7	5.7					
	729.76	Kotcho- U. Lst	Core	729.76	440	0.30	2.2			88.4	8.4			1		
	731.26	Kotcho- U. Lst	Core	731.26			0.9			92.1	7					
	731.28	Kotcho- U. Lst	Core	731.28	438	0.32	1.6			94.5	4					
	733.06	Kotcho- U. Lst	Core	733.06	441	0.27	2.4			91.3	5.1	0.4		0.8		
	737.16	Kotcho- U. Lst	Core	737.16	424	0.33	1.9			97.2	1					
	888.48	Tetcho- L. Lst	Core	888.48	437	0.30	1.3			95.7	1	0.7		0.7	0.6	
	890.54	Tetcho- L. Lst	Core	890.54	433	0.52	0.6			98.7	0.7					
	892.23	Tetcho- L. Lst	Core	892.23	440	0.45	0.9			98	1.1					
	894.28	Tetcho- L. Lst	Core	894.28	436	0.28	0.5			98.1	1.4					
	896.89	Tetcho- L. Lst	Core	896.89	435	0.33	1.1			91.6	7.3					
	900.03	Tetcho- L. Lst	Core	900.03	436	0.35	0.8			98.8	0.4					
	903.43	Tetcho- L. Lst	Core	903.43	438	0.32	0.9			98	1.1					
	907.62	Tetcho- L. Lst	Core	907.62	440	0.35	1			98.2	0.8					
	910.87	Tetcho- L. Lst	Core	910.87	440	0.36	1.4			89.9	8.6					
	913.9	Tetcho- L. Lst	Core	913.90	434	0.35	0.9			98	1.1					
	916.62	Tetcho- L. Lst	Core	916.62	441	0.30	2.4			97	0.6					
	919.53	Tetcho- L. Lst	Core	919.53	430	0.50	1.3			87.1	11.6					
	919.87	Tetcho- L. Lst	Core	919.87			1.8			91.4	6.8					
	921.54	Tetcho- L. Lst	Core	921.54	441	0.25	1.3			98.4	0.4					
	924.58	Tetcho- L. Lst	Core	924.58	437	0.33	3.8			95.8	0.5					

Table KT1. Mineralogical and TOC/T_{max} data of Exshaw-Tetcho interval, CNRL Hz Helmet 202/c-A46-K/94-P-1 (Devon Hz Helmet 202/c-35-K/94-P-1).

Well ID	Sample ID	Zone	Sample Type	Depth (m)	Tmax	TOC %	Quartz	Feldspar	Carbonates		Clays		Sulphides
					°C			Albite	Calcite	Dolomite, Fe-dolomite	Illite/mica	Chlorite	Pyrite
CNRL Hz Helmet D-A011-K/094-P-02 C-22-K/094-P-02 WA 27829 (int: 1196.96 - 1238.65m)	1197.39	Tetcho- L. Lst	Core	1197.39	439	0.53	3.5		88	1.4	2.6	1.5	2.9
	1197.55	Tetcho- L. Lst	Core	1197.55	449	0.26	0.9		99.1	0.1			
	1199.06	Tetcho- L. Lst	Core	1199.06	442	0.36	0.4		99.6				
	1201.13	Tetcho- L. Lst	Core	1201.13	443	0.37	0.7		99.3				
	1201.44	Tetcho- L. Lst	Core	1201.44	438	0.33	0.9		99.1				
	1203.85	Tetcho- L. Lst	Core	1203.85	444	0.35	3		89	4.6	1.5	0.7	1.2
	1205.34	Tetcho- L. Lst	Core	1205.34	443	0.34	1.1		94.6	1.9	0.6	0.5	1.2
	1206.77	Tetcho- L. Lst	Core	1206.77	444	0.46	1.6		95.4	1.5	0.6		0.8
	1209.44	Tetcho- L. Lst	Core	1209.44	441	0.26	1.8		95.4	2	0.9		
	1211.43	Tetcho- L. Lst	Core	1211.43	429	0.34	1		96.8	2.2			
	1212.54	Tetcho- L. Lst	Core	1212.54	447	0.31	1.4		95.9	2	0.8		
	1213.81	Tetcho- L. Lst	Core	1213.81	447	0.43	2.4		88.8	6.5	1.5	0.8	
	1215.7	Tetcho- L. Lst	Core	1215.70	423	0.33	1.3		98.1	0.7			
	1217.51	Tetcho- L. Lst	Core	1217.51	429	0.32	1.3		98	0.7			
	1219.14	Tetcho- L. Lst	Core	1219.14	475	0.28	1.2		98.4	0.4			
	1221.92	Tetcho- L. Lst	Core	1221.92	440	0.35	0.8		97.4	1	0.8		
	1224.5	Tetcho- L. Lst	Core	1224.50	464	0.29	0.6		99.1	0.3			
	1225.82	Tetcho- L. Lst	Core	1225.82	445	0.46	3.8		85.8	9.5	0.9		
	1228.98	Tetcho- L. Lst	Core	1228.98	447	0.68	6.8		71.3	17.1	2.5	2.3	
	1231.52	Tetcho- L. Lst	Core	1231.52	435	0.28	8.8		90	1.1			
	1232.9	Tetcho- L. Lst	Core	1232.90	428	0.26	5.2		88	6.8			
	1235.72	Tetcho- L. Lst	Core	1235.72	426	0.43	2.5		91.9	3.6	0.7	1.2	
	1237.54	Tetcho- L. Lst	Core	1237.54	433	0.33	7		77.8	12.9	0.9	1.4	
Czar Venus d-13-C/94-P-9	810.11	Tetcho	Core	810.11	440	0.28	1.7	0.1	96.8	0.8	0.3	0.4	
	812.74	Tetcho	Core	812.74	441	0.29	1.7	0.3	96.3	1.1	0.1	0.4	
	813.66	Tetcho	Core	813.66	438	0.27	1.1	0.2	97.7	0.4	0.4	0.2	
	815.82	Tetcho	Core	815.82	440	0.32	1.2	0.2	97.2	0.5	0.3	0.5	
	817.54	Tetcho	Core	817.54	429	0.26	2.5	0.5	94.7	0.8	0.5	0.4	0.5
	819.55	Tetcho	Core	819.55	440	0.27	1.8	0.3	96	1.1	0.4	0.4	
	821.4	Tetcho	Core	821.40	443	0.34	1.5	0.2	97.1	1	0.2	0.1	
	823.28	Tetcho	Core	823.28	440	0.28	1	0.1	98.1	0.6	0.1	0.2	
	824.6	Tetcho	Core	824.60	444	0.26	0.9	0.1	98	0.6	0.2	0.3	
	826.04	Tetcho	Core	826.04	423	0.30	0.8	0.2	97.8	0.7	0.2	0.2	
	827.17	Tetcho	Core	827.17	437	0.36	4.6	0.7	92.4	1.6	0.2	0.6	
	827.71	Tetcho	Core	827.71			1.4	0.2	97.2	0.6	0.2	0.3	
	828.84	Tetcho	Core	828.84	439	0.27	1.4	0.2	97.3	0.8	0.1	0.3	
	830.62	Tetcho	Core	830.62	439	0.35	1.8	0.2	91.4	5.9	0.6	0.1	
	832.4	Tetcho	Core	832.40	446	0.38	2.1	0.5	72.5	20.4	4.5	0.1	
	834	Tetcho	Core	834.00	440	0.34	2.8	0.3	95.7	0.8	0.2	0.2	
	835.38	Tetcho	Core	835.38	448	0.42	3.9	0.5	86.5	5	3.6	0.5	
	837.21	Tetcho	Core	837.21	438	0.46	2.4	0.5	87.4	8.7	0.5	0.4	
	839.02	Tetcho	Core	839.02	439	0.36	1.9	0.6	81.8	14.8	0.7	0.3	
	841	Tetcho	Core	841.00	442	0.32	10.1	1.1	86.1	2.1	0.3	0.2	
	842.9	Tetcho	Core	842.90	440	0.36							
	844.72	Tetcho	Core	844.72	444	0.41	16.5	1.1	59.9	14.8	6.9	0.9	0.1
	846.44	Tetcho	Core	846.44	434	0.26							
	847.69	Tetcho	Core	847.69	437	0.31	7	0.7	90.2	1.1	0.6	0.4	

Table KT2. Mineralogical and TOC/T_{max} data, Tetcho Formation, CNRL Hz Helmet d-A11-K/94-P-2 and Czar Venus d-13-C/94-P-9.

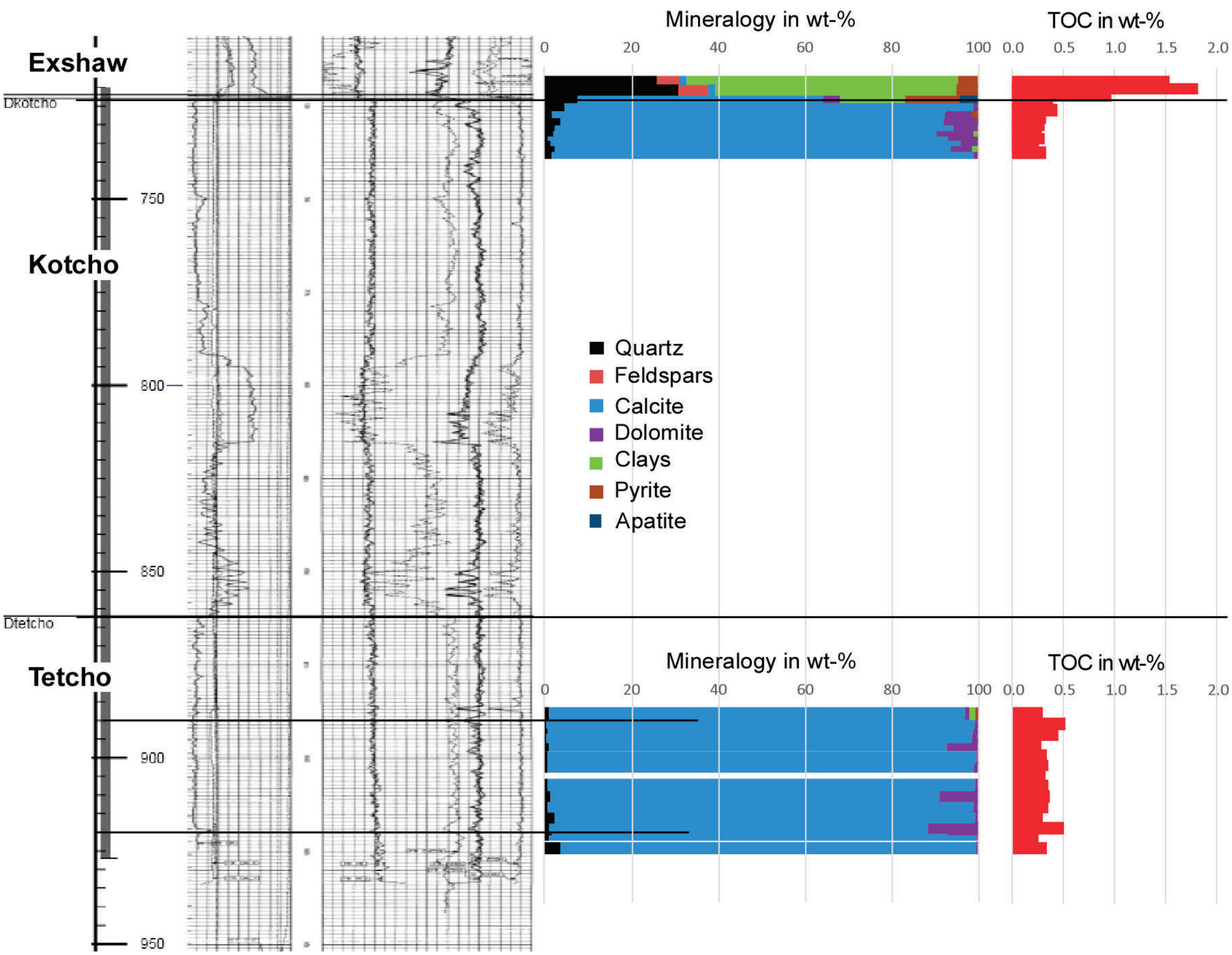

Figure KT4. Mineralogy and TOC plots for samples from the Kotcho and Tetcho formations, CNRL Hz Helmet 02/c-A46-K/94-P-1.

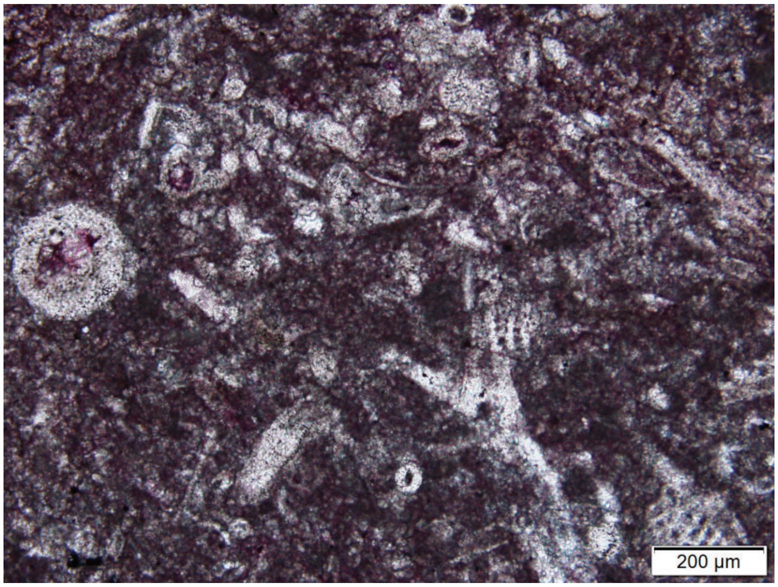

Figure KT5. Photomicrograph, Kotcho Formation, CNRL Hz Helmet 02/c-A46-K/94-P-1 (727.6-727.64 m) under plane polarized light. Fossiliferous packstone containing coarse crystalline shell fragments in a micritic matrix. Microcrystalline porosity is highlighted by pink epoxy.

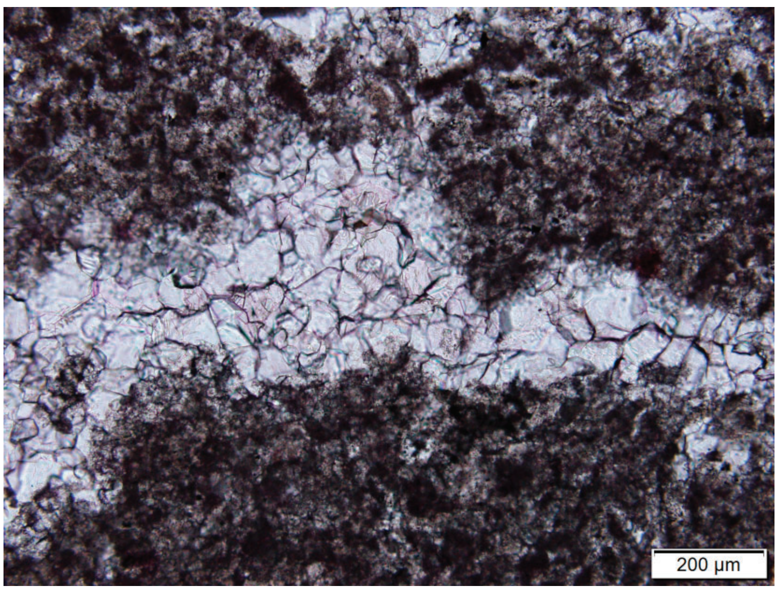

Figure KT6. Photomicrograph, Kotcho Formation, CNRL Hz Helmet 02/c-A46-K/94-P-1 (727.6-727.64 m) under plane polarized light. Sparry calcite fill of fenestral fabric or possibly fractures.

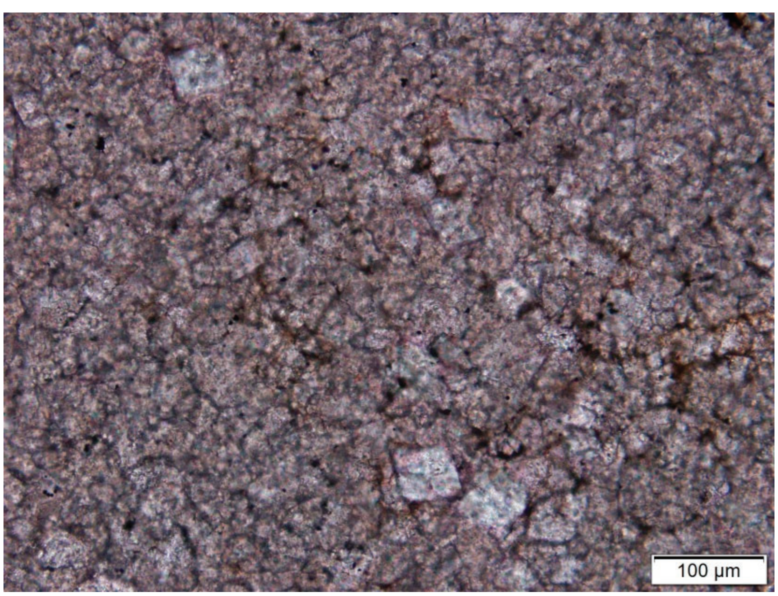

Figure KT7. Photomicrograph, Tetcho Formation, CNRL Hz Helmet 02/c-A46-K/94-P-1 (907.45-907.51 m) under plane polarized light. Wackestone with dolomitized patches preserved as interlocking anhedral to euhedral dolomite crystals up to 50 um. Finely dispersed opaques (clays, pyrite, organic matter) occur along crystal edges.

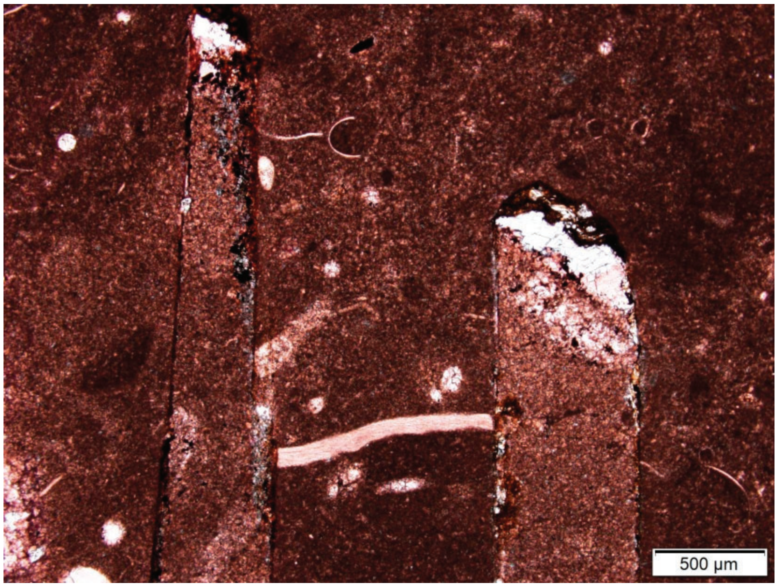

Figure KT8. Photomicrograph, Tetcho Formation, Czar Venus d-13-C/94-P-9 (812.69-812.73 m) under plane polarized light. Bioclastic wackestone with a microcrystalline calcite matrix and floating shell debris.

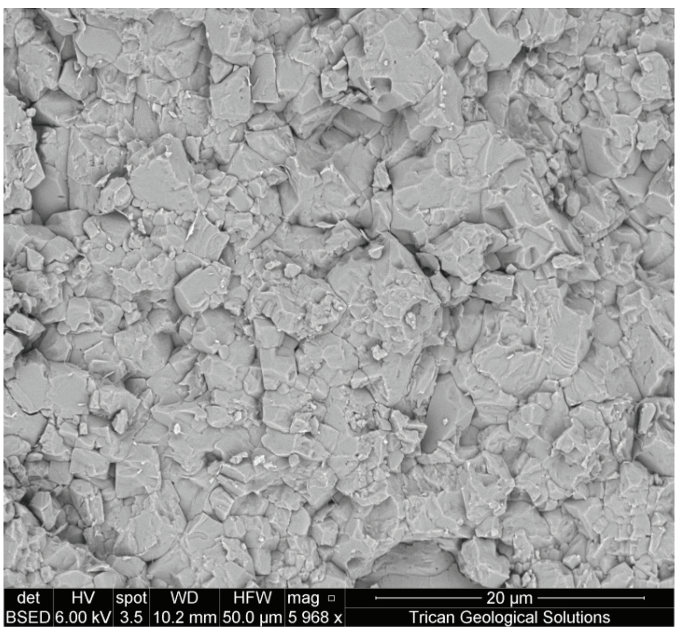

Figure KT9. BSED SEM micrograph of Tetcho Formation, Czar Venus d-13-C/94-P-9 (812.69-812.73 m). Fabric is dominated by interlocking microcrystalline calcite with pervasive overgrowths, with small amounts of euhedral secondary quartz.

Unconfined Porosity and Matrix Permeability										
Well Name	Well Location	Core Depth (m)	Fm	Density		Porosity (%)	GRI Matrix Permeability (md)		GRI Matrix Permeability (nd)	
				Bulk Density (g/cc)	Skeletal Density (g/cc)		Avg	Std Dev	Avg	Std Dev
CNRL Hz Helmet	d-011-K/094-O-02	1197.55	Tetcho	2.651	2.705	2.00				
CNRL Hz Helmet	d-011-K/094-O-02	1201.44	Tetcho	2.636	2.704	2.52				
CNRL Hz Helmet	d-011-K/094-O-02	1205.34	Tetcho	2.661	2.700	1.46				
CNRL Hz Helmet	d-011-K/094-O-02	1209.44	Tetcho	2.636	2.709	2.67				
CNRL Hz Helmet	d-011-K/094-O-02	1211.43	Tetcho	2.531	2.708	6.51				
CNRL Hz Helmet	d-011-K/094-O-02	1217.51	Tetcho	2.607	2.708	3.75				
CNRL Hz Helmet	d-011-K/094-O-02	1224.50	Tetcho	2.642	2.707	2.43				
CNRL Hz Helmet	d-011-K/094-O-02	1231.52	Tetcho	2.646	2.707	2.23				
CNRL Hz Helmet	d-011-K/094-O-02	1237.54	Tetcho	2.607	2.720	4.15				
Czar Venus	d-013-C/094-P-09	811.84	Tetcho	2.658	2.722	2.34	4.61E-06	3.19E-06	4.61	3.19
Czar Venus	d-013-C/094-P-09	822.99	Tetcho	2.653	2.723	2.54	4.01E-06	6.69E-07	4.01	0.67
Czar Venus	d-013-C/094-P-09	833.53	Tetcho	2.634	2.719	3.14	1.26E-05	4.21E-06	12.56	4.21
Czar Venus	d-013-C/094-P-09	844.97	Tetcho	2.671	2.726	2.00	3.35E-06	5.55E-07	3.35	0.56
CNRL Hz Helmet	c-046-K/094-P-01	724.91	Kotcho	2.501	2.734	8.52	5.46E-05	2.78E-05	54.57	27.76
CNRL Hz Helmet	c-046-K/094-P-01	729.76	Kotcho	2.550	2.723	6.36	2.66E-05	1.92E-06	26.63	1.92
CNRL Hz Helmet	c-046-K/094-P-01	733.06	Kotcho	2.619	2.716	3.58	6.99E-06	9.17E-07	6.99	0.92
CNRL Hz Helmet	c-046-K/094-P-01	888.48	Tetcho	2.654	2.714	2.20	1.13E-06	6.58E-08	1.13	0.07
CNRL Hz Helmet	c-046-K/094-P-01	892.23	Tetcho	2.584	2.707	4.56	3.16E-05	2.54E-06	31.60	2.54
CNRL Hz Helmet	c-046-K/094-P-01	896.89	Tetcho	2.607	2.731	4.51	1.25E-05	1.15E-06	12.49	1.15
CNRL Hz Helmet	c-046-K/094-P-01	903.43	Tetcho	2.599	2.713	4.21	6.68E-06	5.79E-07	6.68	0.58
CNRL Hz Helmet	c-046-K/094-P-01	907.62	Tetcho	2.624	2.707	3.08	1.83E-05	1.24E-06	18.34	1.24
CNRL Hz Helmet	c-046-K/094-P-01	910.87	Tetcho	2.630	2.719	3.25	6.44E-06	6.15E-07	6.44	0.61
CNRL Hz Helmet	c-046-K/094-P-01	916.62	Tetcho	2.647	2.711	2.37	4.84E-06	6.44E-07	4.84	0.64
CNRL Hz Helmet	c-046-K/094-P-01	921.54	Tetcho	2.618	2.714	3.52	1.18E-05	9.72E-07	11.82	0.97
CNRL Hz Helmet	c-046-K/094-P-01	924.58	Tetcho	2.635	2.707	2.66	1.73E-06	2.37E-07	1.73	0.24

Table KT3. Kotcho and Tetcho – unconfined porosity and GRI matrix permeability measurements from core samples in three wells.

MICP Porosity										
Well Name	Well Location	Core Depth (m)	Fm	Density g/cc		Porosity (%)	Corrected Porosity (%)	Peak Range		Stem Volume Used (%)
				Bulk Density (g/cc)	Skeletal Density (g/cc)			Peak Range	Modal Peak	
CNRL Hz Helmet	c-046-K 094-P-01	724.91	Kotcho- U. Lst	2.476	2.674	8.05	7.41	20 - 3120	1213	12
CNRL Hz Helmet	c-046-K 094-P-01	733.06	Kotcho- U. Lst	2.599	2.657	2.68	2.20	19 - 130	58	18
CNRL Hz Helmet	c-046-K 094-P-01	888.48	Tetcho- L. Lst	2.673	2.696	1.29	0.85	9 - 70	18	11
CNRL Hz Helmet	c-046-K 094-P-01	910.87	Tetcho- L. Lst	2.639	2.717	3.65	2.87	4 - 100	23	15
CNRL Hz Helmet	c-046-K 094-P-01	924.58	Tetcho- L. Lst	2.648	2.675	1.33	1.02	10 - 70	16	9
CNRL Hz Helmet	d-011-K 094-P-02	1197.55	Tetcho- L. Lst	2.666	2.690	1.10	0.90	15 - 90	41	14
CNRL Hz Helmet	d-011-K 094-P-02	1201.44	Tetcho- L. Lst	2.642	2.687	1.91	1.70	17 - 120	41	27
CNRL Hz Helmet	d-011-K 094-P-02	1205.34	Tetcho- L. Lst	2.674	2.687	0.61	0.50	10 - 60	16	9
CNRL Hz Helmet	d-011-K 094-P-02	1209.44	Tetcho- L. Lst	2.656	2.689	1.50	1.25	13 - 150	29	19
CNRL Hz Helmet	d-011-K 094-P-02	1211.43	Tetcho- L. Lst	2.574	2.692	4.62	4.39	18 - 1220	81	30
CNRL Hz Helmet	d-011-K 094-P-02	1217.51	Tetcho- L. Lst	2.634	2.689	2.20	2.03	19 - 890	41	24
CNRL Hz Helmet	d-011-K 094-P-02	1224.50	Tetcho- L. Lst	2.641	2.681	1.94	1.53	20 - 290	88	21
CNRL Hz Helmet	d-011-K 094-P-02	1231.52	Tetcho- L. Lst	2.655	2.688	1.43	1.22	18 - 190	41	12
CNRL Hz Helmet	d-011-K 094-P-02	1237.54	Tetcho- L. Lst	2.622	2.687	2.88	2.45	12 - 180	35	42
Czar Venus	d-013-C 094-P-09	811.84	Tetcho	2.640	2.676	1.59	1.35	4 - 30	12	11
Czar Venus	d-013-C 094-P-09	822.99	Tetcho	2.621	2.652	1.27	1.14	14 - 100	74	9
Czar Venus	d-013-C 094-P-09	833.53	Tetcho	2.631	2.680	2.27	1.83	16 - 200	53	30
Czar Venus	d-013-C 094-P-09	844.97	Tetcho	2.655	2.665	0.63	0.37	10 - 70	23	8

Table KT4. Kotcho and Tetcho – MICP porosity and conformance-corrected porosity measurements from core samples in three wells.

Hydrocarbon Composition by Thermal Desorption Gas Chromatography																
TRICAN Trican Geological Solutions																
Well Name	Well Location	Core Depth (m)	Fm	% Light Condensate	% Heavy Condensate	% Naphthenes	% Aromatics	% Biomarkers	Peak	Initial Boiling Point (°C)	Carbon Number	Final Boiling Point (°C)	Carbon Number	Calculated Specific Gravity	Calculated API gravity	Chromatogram Quality
Devon Hz Helmet	202/c-046-K 094-P-01/00	725.14	Kotcho- U. Lst	0.00	93.29	0.00	0.00	6.71	C29	169	C10	545	C40	0.88	29.50	good
Devon Hz Helmet	202/c-046-K 094-P-01/00	890.54	Tetcho- L. Lst	0.00	91.65	0.00	0.00	8.35	C25	188	C11	544	C40	0.88	30.10	good
Devon Hz Helmet	202/c-046-K 094-P-01/00	902.20	Tetcho- L. Lst	0.00	88.74	0.14	0.00	11.13	C30	72	C6	542	C40	0.87	31.11	okay
Czar Venus	200/d-013-C 094-P-09/00	812.74	Tetcho	0.00	100.00	0.00	0.00	0.00	C18	9	<C6	495	C36	0.86	33.35	no good
Czar Venus	200/d-013-C 094-P-09/00	819.55	Tetcho	0.00	8.12	0.00	0.00	91.88	phytane	11	<C6	476	C33	0.81	43.30	no good
Czar Venus	200/d-013-C 094-P-09/00	828.84	Tetcho	0.00	80.93	0.00	0.00	19.07	C29	6	<C6	516	C39	0.89	27.85	no good
Czar Venus	200/d-013-C 094-P-09/00	837.21	Tetcho	0.00	99.09	0.00	0.00	0.91	C34	58	<C6	538	C40	0.87	31.56	poor
Czar Venus	200/d-013-C 094-P-09/00	844.72	Tetcho	0.00	100.00	0.00	0.00	0.00	C17	15	<C6	452	C30	0.85	35.79	no good
CNRL Helmet	202/d-011-K 094-P-02/00	1209.55	Tetcho- L. Lst	0.00	90.82	0.16	0.00	9.02	C26	180	C10	491	C35	0.86	33.21	poor
CNRL Helmet	202/d-011-K 094-P-02/00	1210.94	Tetcho- L. Lst	1.36	81.75	0.13	0.18	16.59	C15	160	C9	438	C29	0.85	35.84	good

Table KT5. Kotcho and Tetcho – hydrocarbon composition data, three wells.

Well Name	Depth (m)	Confining Pressure (MPa)	Axial Strain at Failure (%)	Compressive Strength (MPa)	Residual Strength (MPa)	Static Young's Modulus (GPa)	Static Poisson's Ratio	Static Bulk Modulus (GPa)	Static Shear Modulus (GPa)
d-011-K 094-P-02	1200.83	17.0	0.360	173.49	134.36	53.77	0.268	38.63	21.20
d-011-K 094-P-02	1211.80	17.0	0.561	210.62	144.50	52.52	0.283	40.40	20.46
d-011-K 094-P-02	1229.99	17.0	0.585	216.22	195.93	47.55	0.251	31.85	19.00
d-013-C 094-P-09	816.25	14.5	0.385	229.15	183.88	63.28	0.295	51.56	24.42
d-013-C 094-P-09	834.28	14.5	0.444	234.45	120.65	62.68	0.331	61.75	23.55

Table KT6. Kotcho and Tetcho – rock mechanical properties from two wells.

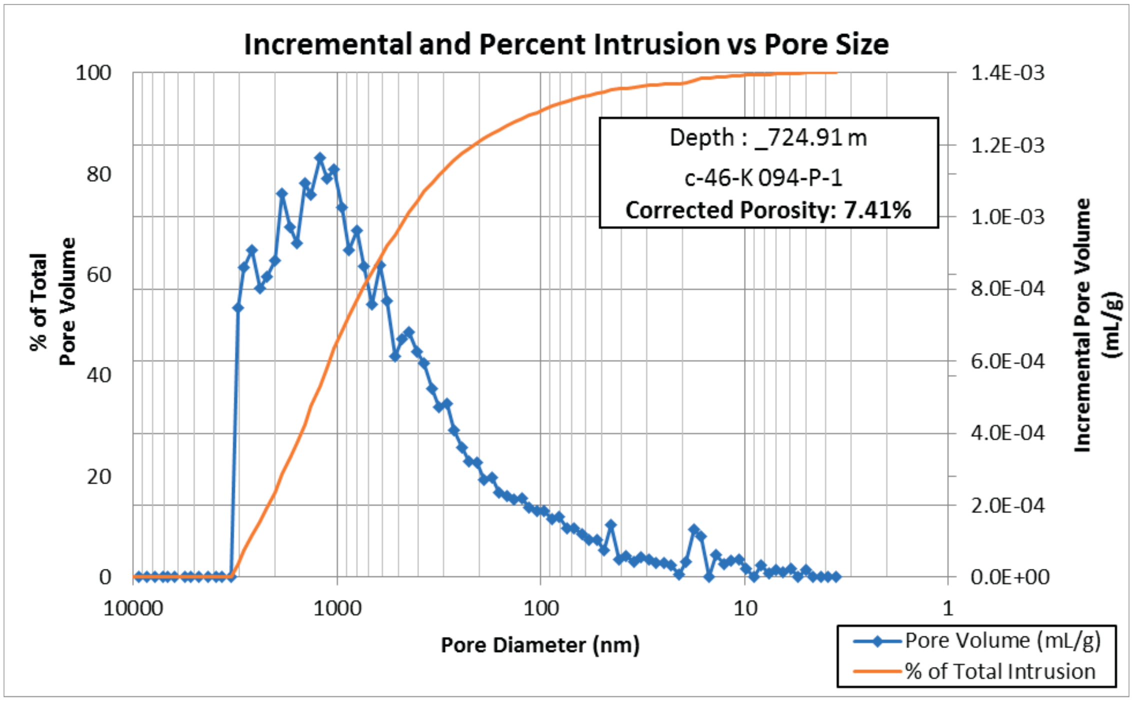

Figure KT10. Incremental and percent intrusion versus pore size, Kotcho Formation, CNRL Hz Helmet 02/c-A46-K/94-P-1 (724.91m), highlighting wide range of pore throat sizes with a major peak around 1000 nm.

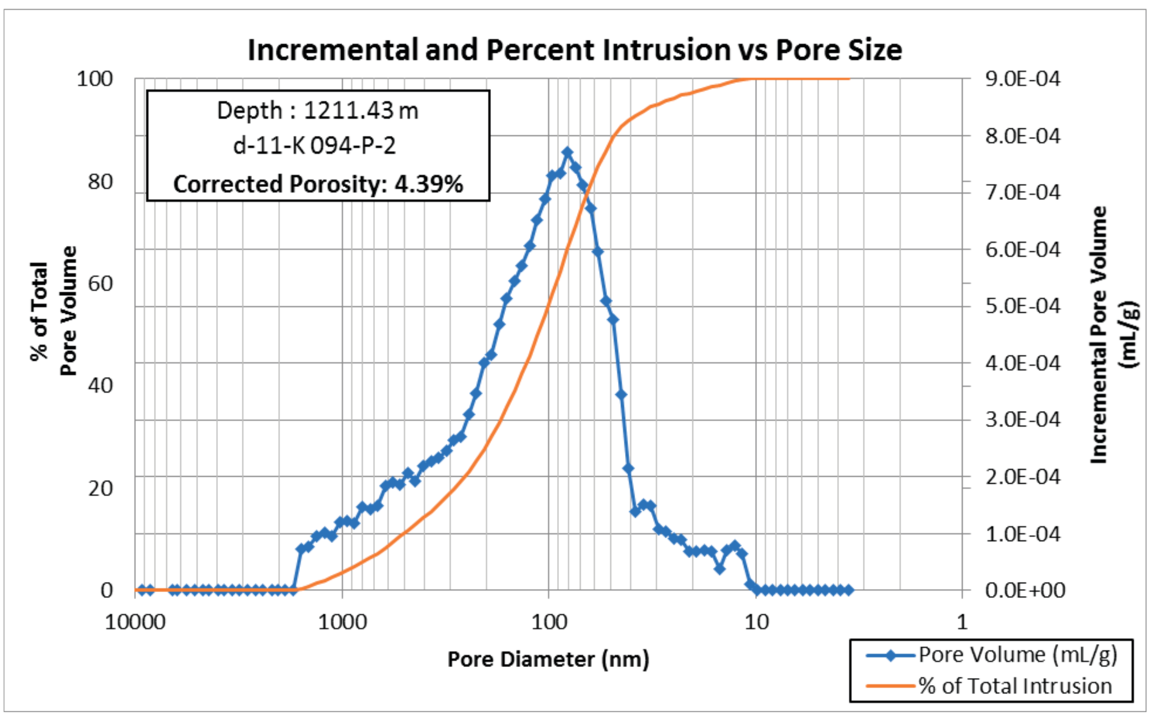

Figure KT11. Incremental and percent intrusion versus pore size, Tetcho Formation, CNRL Hz Helmet d-A11-K/94-P-2 (1211.43m), highlighting wide range of pore throat sizes with a major peak around 80 nm.

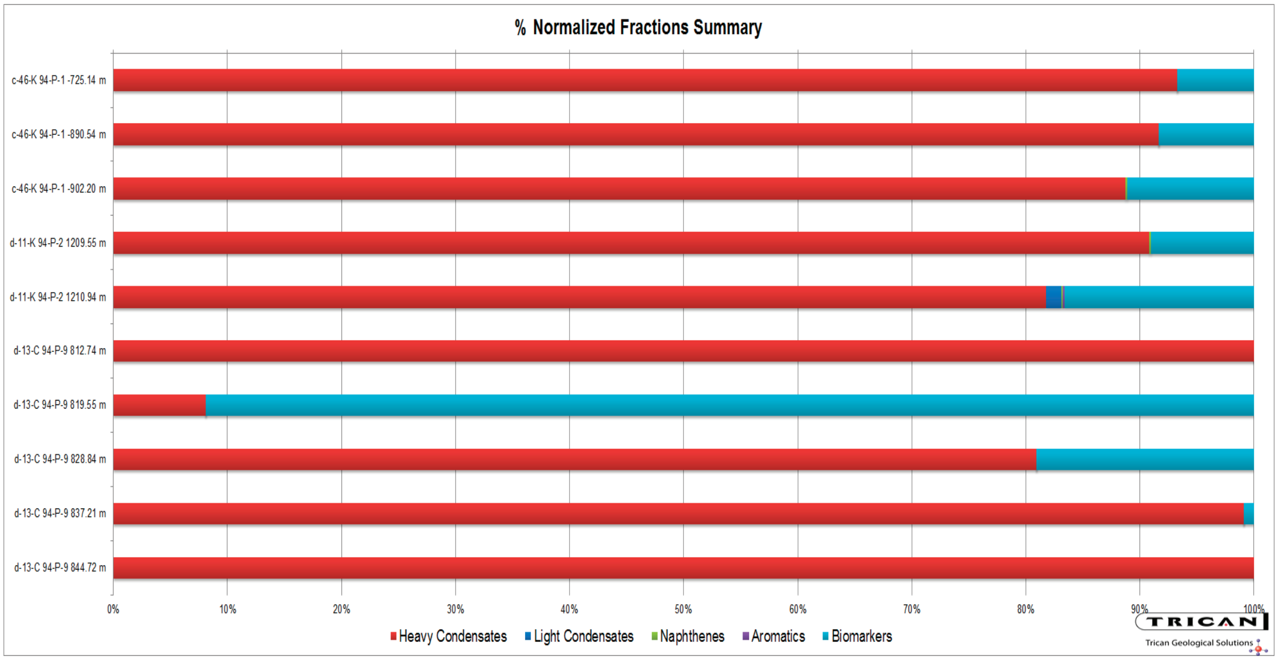

Figure KT12. Bulk rock hydrocarbon analysis (S1), showing hydrocarbon chain distribution and detection, Kotcho/Tetcho.

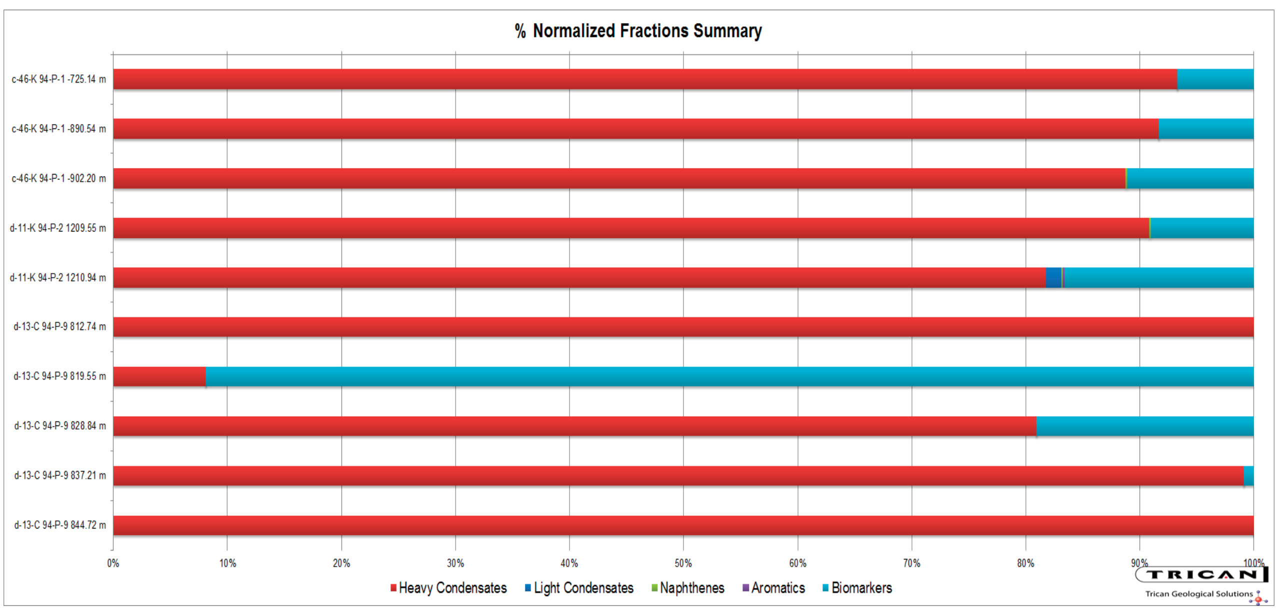

Figure KT13. Normalized fraction plot of hydrocarbon groups, Kotcho and Tetcho, three wells (10 samples listed by well and depth). Heavy condensates dominate in all but one sample.

identified and systematically mapped with some degree of confidence – which was likely been done before operators drilled the existing horizontal wells in the Tetcho.

Existing horizontal wells demonstrate that oil is present and can be produced from the Tetcho in the Helmet area. The Kotcho appears to be poorer-quality reservoir, and productivity has not been established. Analytical work suggests that the Tetcho has favourable frac characteristics, and more work could be done to optimize drilling and completion techniques to improve productive characteristics.

The biggest question around future resource oil potential in the Tetcho (and Kotcho) is that of oil charge – several Paleozoic reservoirs, including the Jean Marie and Rundle, produce oil in the Helmet / Tooga area and mostly gas elsewhere. As noted above for the Jean Marie, liquids migration to younger reservoirs may have been enhanced locally along regional NW-SE trending "isostatic adjustment faults" mapped by Jones (1980) (Fig. JM8) – but we don't understand why this mechanism would have been effective only locally. As for the Jean Marie, local structural controls may have been important.

If this is the case, additional oil potential in the Tetcho is likely limited to small, structurally-influenced pools, as opposed to regional resource oil potential.

EXSHAW / BESA RIVER FORMATIONS

Age and Play Type

Upper Devonian / Lower Mississippian – Shale Oil Play;
Prospectivity: 'C' Play – oil prospectivity not established in the study area.

Regional Geology

The Exshaw Formation is an organic-rich black marine shale, deposited across the entire Western Canada Sedimentary Basin during regional transgression in latest Devonian and earliest Mississippian time (Smith and Bustin, 2000). Stasiuk and Fowler (2004) described petrographic organic facies that make the Exshaw an excellent and well-recognized source rock.

While regionally extensive, the Exshaw is generally thin, and in many wells is not differentiated from overlying Banff shales and distal carbonates. In northeastern B.C., it thickens westward into the Liard Basin, and eventually becomes a component of the thick, basinal Besa River Formation (Fig. E1). Cross-section Exshaw-Exshaw' also demonstrates this relationship, and highlights the high-gamma log expression of the Exshaw interval. Note that the radioactive, organic-rich interval is less than 10m thick in most wells east of the Liard Basin.

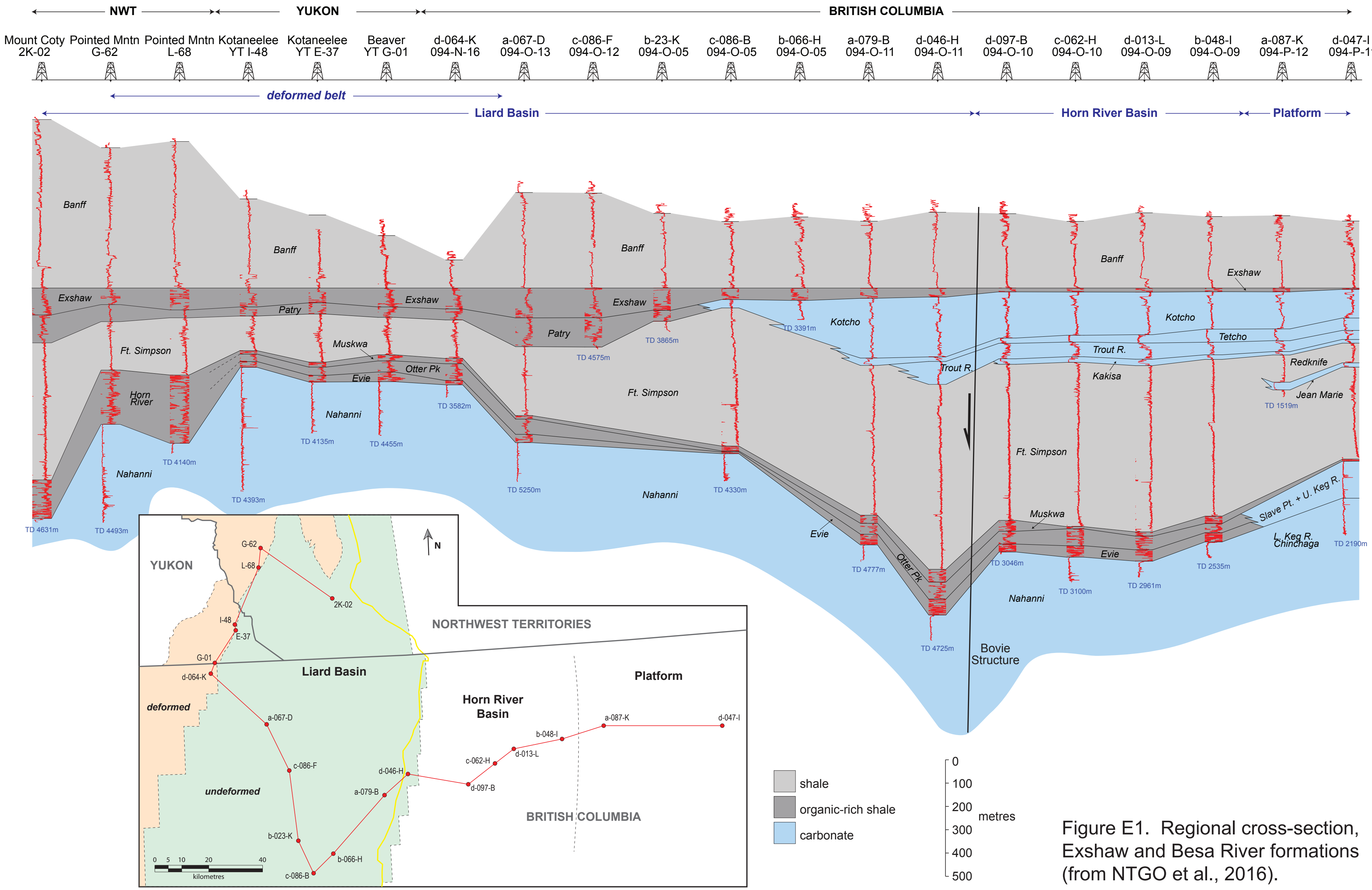

Figure E1. Regional cross-section, Exshaw and Besa River formations (from NTGO et al., 2016).

Production and Test Data

Adams *et al*. (2016) documented limited drilling for dry gas in Exshaw / Besa River shales in the Liard Basin; Ferri *et al*. (2015) showed the thick reservoir interval to be stratigraphically equivalent to the thin Exshaw Formation to the east.

During initial development of Horn River shale gas in the northwestern part of the Horn River Basin, Quicksilver Resources indicated that oil shows were encountered in the Exshaw interval. They did not produce any Exshaw oil, although a completion was attempted at d-28-A/94-O-15, which stands as a suspended Exshaw gas well.

Analytical Data

While database searches show that the Exshaw / Besa River interval has been sampled in a number of wells in northeastern B.C., many samples were taken from drill cuttings and sidewall cores – meaning considerable uncertainty as to how representative the sampling was. Analytical work has also been focused on gas-prone areas in and adjacent to the Liard Basin.

When we sampled core from CNRL Hz Helmet 02/c-A46-K/94-P-1 for the Kotcho and Tetcho, we analyzed three samples from the overlying Exshaw, which showed abundant clay minerals and substantial quartz, as well as high TOC measurements (Fig. KT4; Table KT1) (Appendix 3).

In northwestern Alberta adjacent to the B.C. border, Rokosh et al. (2012) recognized the presence of the basal Banff/Exshaw source rock succession but did not assess hydrocarbon resources because of scant data and lack of industry focus on the interval. BCMEM / CBM Solutions (2005) sampled the Exshaw in four wells in NEBC, and found TOC values ranging from very low to quite rich; however, low S2 values produced unreliable T_{max} measurements, and suggest highly mature organic material.

Ferri et al. (2015) found the upper Besa River equivalents to the Exshaw in the Liard Basin to be highly mature and silica- and organics-rich, and thus an excellent shale gas reservoir.

Resource Oil Assessment

We see little prospectivity for the Exshaw as a resource oil target in NEBC. It is thin and has received little attention in eastern areas where it might be expected to be oil prone. It thickens westward into the Liard Basin to form part of the Besa River package, but is clearly prospective for gas.

BANFF FORMATION

Age and Play Type

Lower Mississippian – Tight Oil Play (tight carbonate, sandstone);
Prospectivity: 'C' Play – generally poor reservoir potential with few oil shows.

Regional Geology

The Banff Formation is a basinal to slope assemblage of shales and muddy limestones, arranged in stacked shallowing-upward successions (O'Connell, 1990; Richards *et al.*, 1994). Higher-energy, shelfal lime grainstones and muddy tidal carbonates occur higher in the section, and may develop conventional reservoir quality, particularly where they subcrop beneath major unconformities (Barclay *et al*., 1997). We have designated this cleaner carbonate section the "upper Banff carbonate unit" in NEBC (Cross-section Banff-Banff').

A distinct mixed siliciclastic/carbonate succession overlies the shallow-water carbonate section in northeastern BC and adjacent Alberta; we have termed it the "upper Banff clastic unit" (Map B1; Cross-section Banff-Banff'). A similar unit was described in the greater Cessford area of southern Alberta by Goldthorpe (1996), and Richards *et al.* (1994) correlated a sand-dominated "Member D" at the top of the Banff over much of the western side of the Western Canada Sedimentary Basin. Petrel Robertson (2000) described upper Banff clastics in NEBC and adjacent Alberta in detail, based primarily on core in Alberta.

The Banff is overlain more or less conformably by shelfal carbonates of the Rundle Group, and is bevelled to the northeast by the pre-Cretaceous unconformity (Cross-section Banff-Banff'). It shales out northwestward and becomes a component of the basinal Besa River Formation in the Liard Basin. Burial depths range from <400m in the far northeast to >1000m at the southern edge of the prospective fairway (Map B3).

Lithology and Reservoir Quality

The upper Banff clastic unit consist of interbedded siltstone to very fine-grained sandstone, green-grey mudstones and shales (in places mottled brick red), and thin beds of fossiliferous mudstone. A typical section is dominantly shale in the upper and basal thirds, while the middle third is predominantly siltstone. In the upper and basal units, medium to dark green-grey shales contain isolated lenses and thin beds of quartzose siltstone and fossiliferous calcareous mudstone. Low resistivities and slow sonic transit times distinguish upper Banff non-calcareous shales from more calcareous rocks below, although thin siltstone and calcareous beds produce gamma, sonic and density spikes.

The middle section comprises quartzose siltstones, variably cemented by carbonate minerals, and variably interbedded with green-grey mudstones. Clean siltstones exhibit very well-developed current ripple cross-lamination, in places highlighted by flasers and mudstone partings or thin beds. They consist almost entirely of subrounded to rounded, well-sorted quartz grains, with accessory amounts of glauconite, phosphate, detrital dolomite and feldspar (Petrel Robertson, 2000). Porosity values can exceed 25%, while permeabilities range up to several hundred millidarcies in thin clean beds (Fig. B1). Detrital carbonate mud and chlorite occur either dispersed through the rock, or as laminae outlining sedimentary structures. Authigenic cements are composed primarily of carbonate minerals. Reservoir-quality siltstones range up to 3-4 metres thick (e.g. wells a-83-G/94-I-16, d-56-G/94-P-6/03, Cross-section Banff-Banff'), but are difficult to correlate from well to well.

Goldthorpe (1996) interpreted porosity development in the upper Banff at Cessford as being entirely secondary, and attributable to dolomitization and solution. These processes appear to have enhanced porosity in upper Banff clastics in NEBC and adjacent Alberta, as porous reservoir rock is most consistently developed along the subcrop edge (Map B2).

Core coverage is very poor in the underlying upper Banff carbonate unit, but logs and the few available cores suggest it is strongly heterolithic with little consistent reservoir development (Fig. B1). At the base of the upper Banff carbonates, however, there is a consistently-developed clean carbonate unit up to five metres thick (Cross-section Banff-Banff'). At 02/d-3-E/94-I-14, core across this section shows porosities of 3-18%, and permeabilities of 0.1-2.1mD. Logs from other wells suggest comparable reservoir quality is widespread. More intensive stratigraphic work may reveal the presence of multiple clean carbonate units in this part of the Banff.

Production and Test Data

Conventional gas pools have been developed locally along the upper Banff clastics subcrop edge at Haro and Kotcho in Alberta, and Shekilie in NEBC (Map B1). Pool reserves are small, reflecting thin net pay sections and shallow depths (and thus relatively low recovery factors); the three main pools total only 880 e^6m^3 (31.1 BCF) original marketable reserves. Petrel Robertson (2000) mapped a regional aquifer system in the relatively continuous upper Banff siltstones in Alberta, and showed these gas pools to be conventional stratigraphic traps associated with the aquifer. Further northwestward, however, where porous upper Banff sandstones are less continuously developed, we see very few water-bearing drillstem tests, and reservoir pressures from scattered gas tests show no regional continuity (Petrel Robertson, 2000).

In addition to oil and gas producers, upper Banff clastic and carbonate sections have been completed in more than 40 wells in northeastern BC (Map B1, B2). Acid squeezes and small fracs were attempted in most wells, generally resulting in small, non-commercial gas flows. A small amount of clean oil was produced from the uppermost upper Banff clastics at d-33-F/94-P-7 (Map B1, B2).

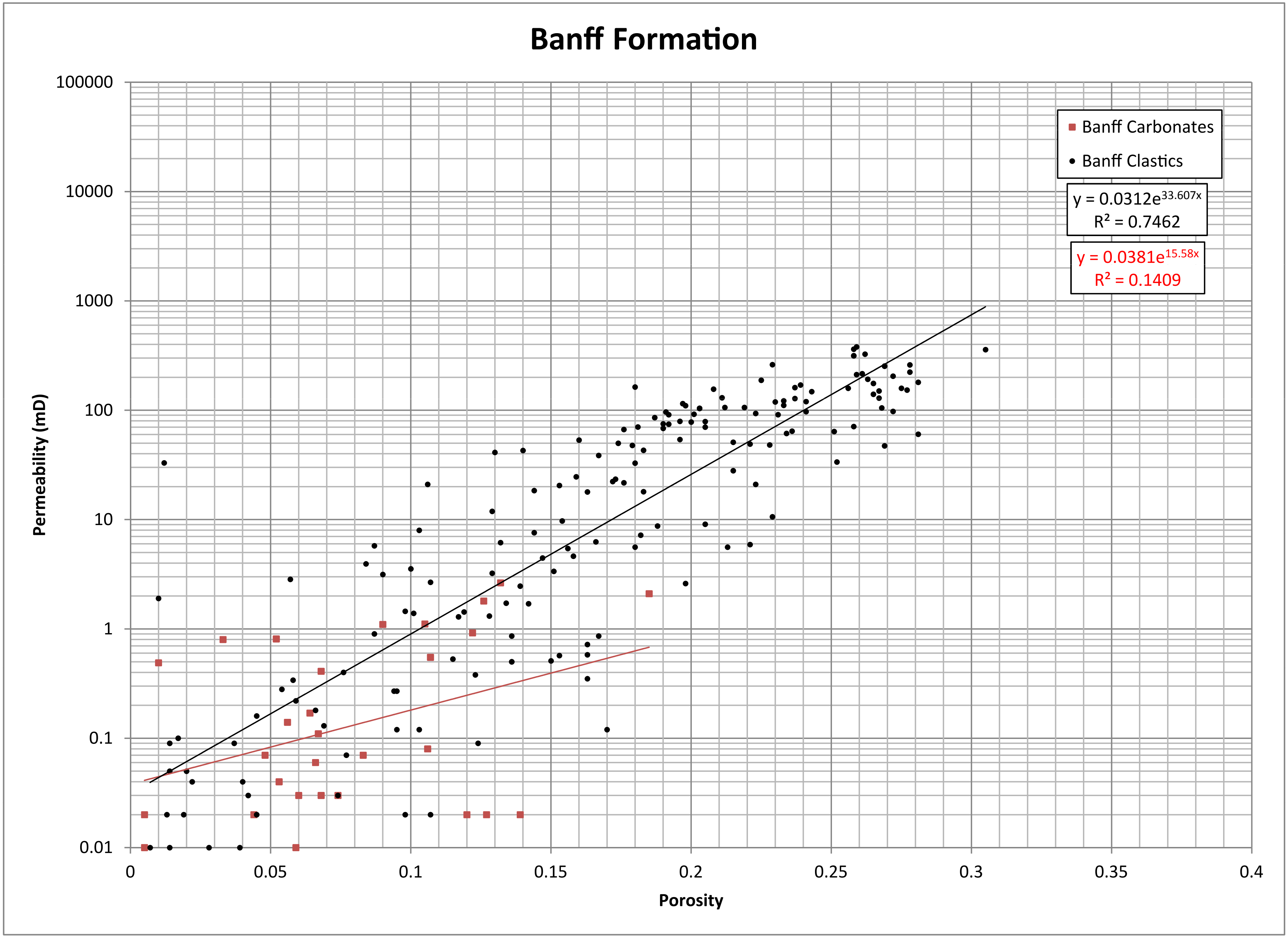

Figure B1. Porosity / permeability cross-plot, Banff Formation.

The basal clean carbonate of the upper Banff carbonate succession has tested gas in several locations, and appears consistenly hydrocarbon-bearing on logs (Cross-section Banff-Banff'). At d-56-G/94-P-6/03, the basal carbonate produced 4765 m^3 oil (30 MBO), offsetting a minor gas test in the nearby b-54-G well (Cross-section Banff-Banff'). Pore volumes of oil in the core at 02/d-3-E/94-I-14 measured up to 56%, although the zone was listed as suspended gas after frac.

Analytical Data

LIttle analytical data have been acquired for the upper Banff other than routine core analyses. Several source rock analyses and other tests have been completed in the equivalent shale-dominated Besa River section to the west in the Liard Basin.

Resource Oil Assessment

Inconsistently developed, conventional-quality upper Banff siltstones appear to have limited potential for oil, although they may be charged locally at Desan (94-P-7), where underlying Devonian carbonates and the overlying Rundle Group are also oil-charged.

Consistenly-developed basal carbonates of the upper Banff carbonate unit shows better potential:

- One producing oil well and a significant oil show in core;
- Mappable, consistently-developed moderate to tight reservoir quality;
- Continuous hydrocarbon saturation apparent from logs;
- Potential for effective trapping and pressure isolation between a thick underlying shale section and overlying tight shales and carbonates.

These are thinner and less mappable reservoir targets than the underlying Devonian platformal carbonates – but perhaps could have been charged with oil by Exshaw shales where they are in the oil maturity window.

RUNDLE GROUP

Age and Play Type

Mississippian – Tight / Halo Oil Play (tight carbonate);
Prospectivity: 'B' Play – Oil productivity established in marginal to conventional-quality reservoirs, with some potential to grow the play using more detailed mapping and effective horizontal drilling / multi-frac completion wells.

Regional Geology

Tectonic quiescence and Devonian basin-filling sedimentation allowed broad, shallow-water carbonate ramp settings to develop throughout Western Canada near the end of the Devonian, and to persist through much of Mississippian time. In northwestern Alberta and northeastern British Columbia, carbonate ramps sloped northwestward into the Prophet Trough, where slope to basin sediments accumulated at the western edge of the North American craton (Barclay *et al*., 1997; Richards *et al*., 1994) (Fig. R1). The Devonian/Mississippian Antler Orogeny had relatively little effect on the craton, but toward its western margin, structural deformation of the Devonian section can be observed, and reactivation of older basement features influenced the development of Mississippian reservoir facies (Hutton, 1995).

Rundle Group stratigraphy is consistently developed through western Alberta and northeastern British Columbia. It comprises three highly-correlative carbonate shelfal units (from oldest to youngest): the Pekisko, Shunda and Debolt formations (Fig. 3). Cross-section Rundle-Rundle' correlates them in NEBC, and also details the Elkton Member, recognized as a distinct basal unit within the Debolt Formation. In the northern and eastern parts of the study area, the Rundle is capped by the pre-Cretaceous unconformity, which incises northeastward, creating highly mappable subcrop edges (Cross-section Rundle-Rundle', Map R1). Northwestward, with the transition to more distal facies the constituent formations can no longer be differentiated, and we map the Rundle Group as a unit (Map R1; Petrel Robertson, 2000, 2010).

Burial depths range from <400m in the far northeast to more than 4100m in the southerly Deep Basin / foredeep (Map R1). Note also the abrupt deepening across the Bovie Fault Zone from the Horn River Basin into the Liard Basin.

Reservoir Development and Quality

Reservoir quality in Rundle carbonates is developed in three primary settings:

1. Reservoirs immediately beneath the pre-Cretaceous unconformity, where strata have been extensively altered by diagenetic processes;

2. Reservoirs which have retained primary (depositional) porosity, although diagenetically modified to some degree;

3. Highly-fractured reservoirs, found primarily in structurally-deformed settings.

Figure R2, a permeability vs porosity cross-plot for all Rundle cores in NEBC, demonstrates a tremendous range of reservoir quality.

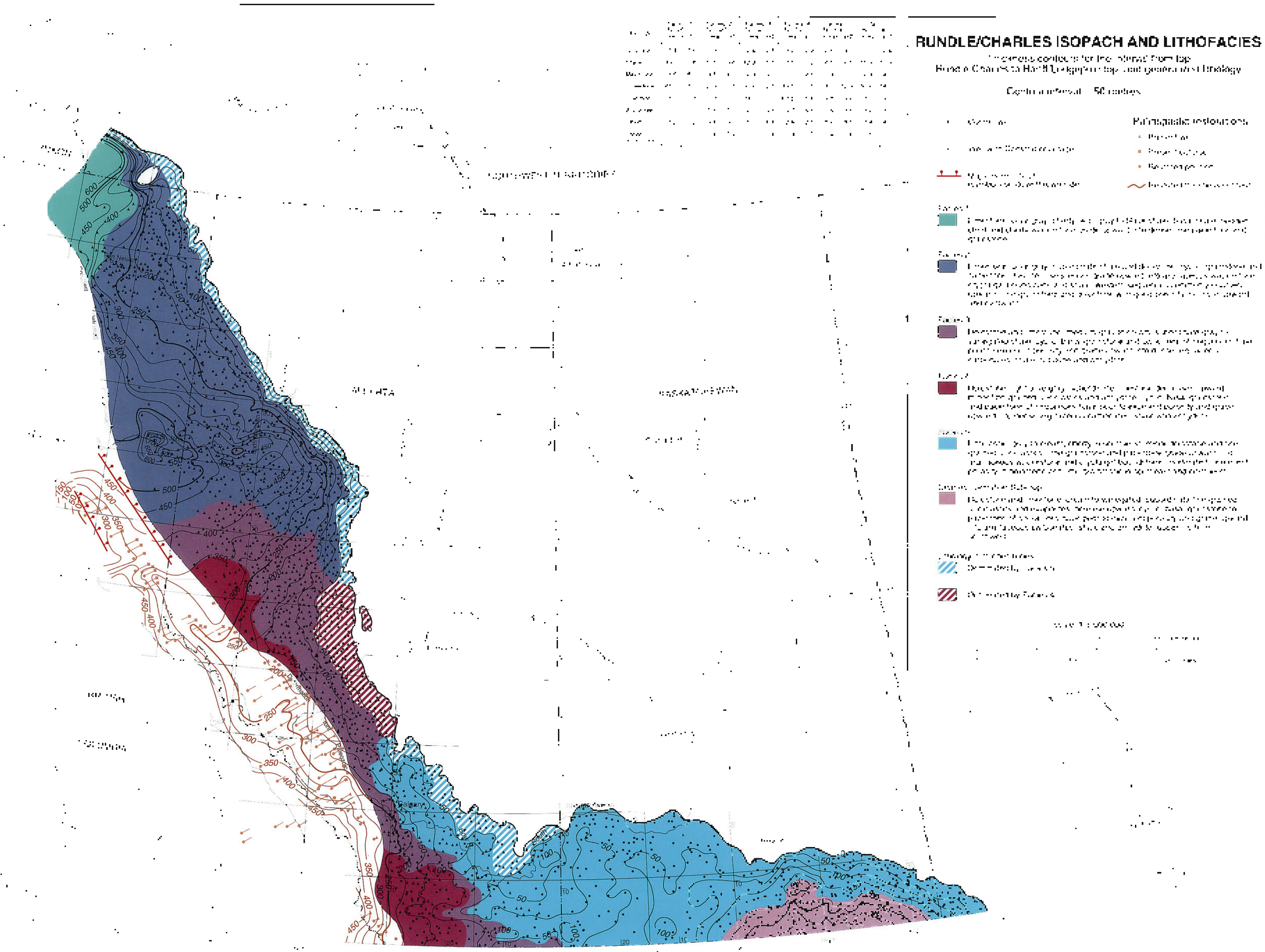

Figure R1. Regional isopach and lithofacies, Rundle Group, Western Canada (from Richards et al., 1994)

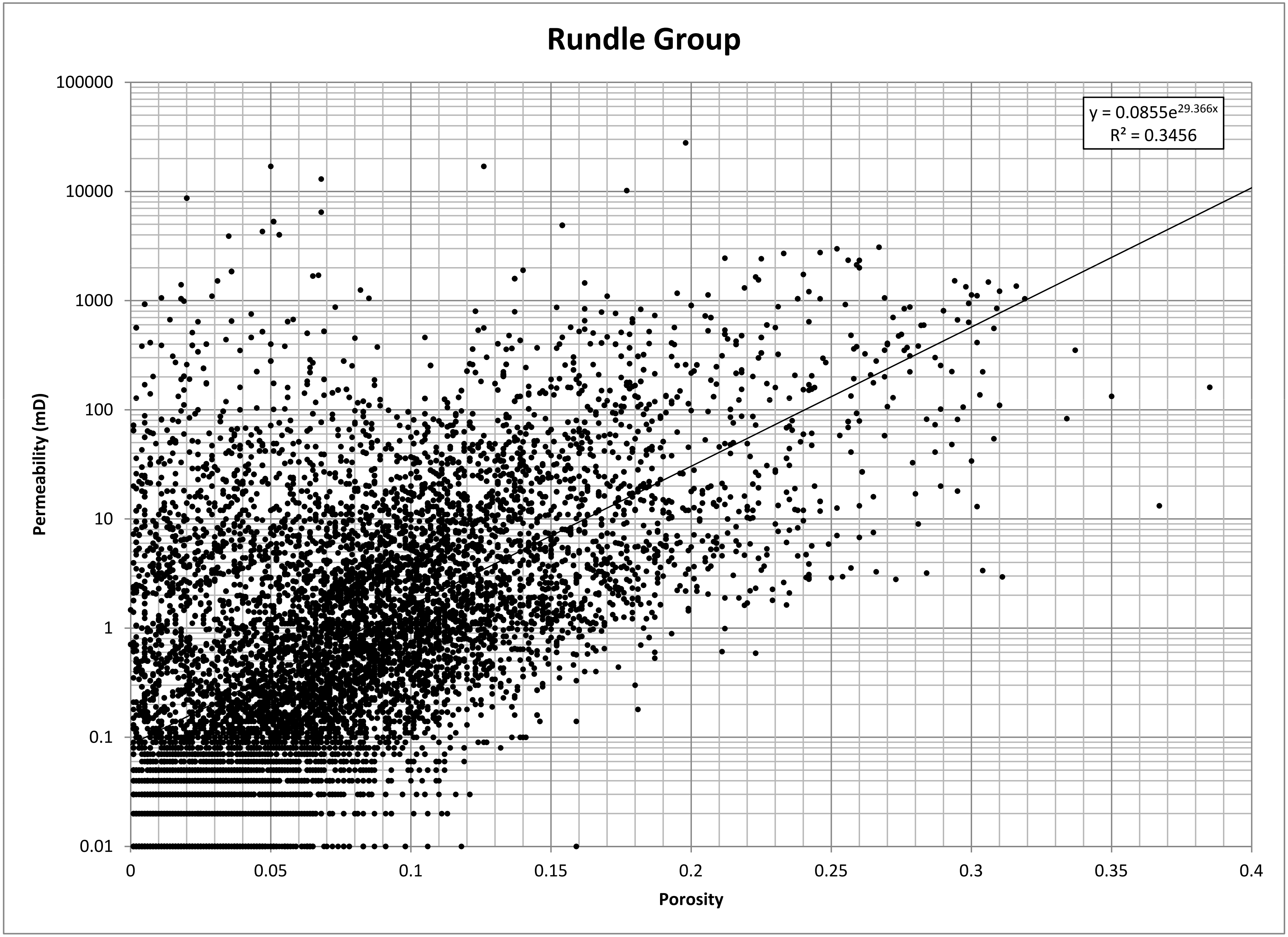

Figure R2. Porosity / permeability cross-plot, Rundle Group (regional).

Diagenetically-Modified Subcrop Reservoirs – Diagenetic processes are active where rocks have been exposed to long-term fluid flow at subcrop edges, but the effects are strongly dependent upon pre-existing facies and fabrics. Multiple stages of diagenesis have occurred in some places, including several early (prelithification) and later stages. For example, the Debolt in some areas experienced exposure and erosion at pre-Belloy, pre-Montney, and pre-Gething unconformities.

Petrel Robertson (2010) documented extensive and widespread solution, dolomitization, and diagenetic enhancement at the top of the Rundle in the Horn River Basin, forming a mappable "detrital zone". Similar "detrital zone" facies are seen elsewhere – e.g., wells a-17-F/94-I-14 and d-74-J/94-I-15 on Cross-section Rundle-Rundle'. Solution and diagenetic enhancement are noted most consistently along subcrop edges beneath the pre-Cretaceous unconformity, such as at the Bivouac, Haro, Charm and Venus gas pools (Map R1).

Subcrop reservoirs display highly variable but generally very good reservoir quality – to the point that quantitative measurements in cores, drill cuttings and on logs are not reliable. Consistent, mappable development of oil-bearing tight facies in this setting is very unlikely.

Modified Primary Porosity Reservoirs – Relatively coarse-grained bioclastic limestones may retain primary intergranular porosity if it is not destroyed by compaction or cementation. Such reservoirs occur downdip from the subcrop edge at Bivouac and Desan, particularly within shallow-water skeletal facies of the Shunda in B.C. (Petrel Robertson, 2000). Early structural movements may have isolated these facies in some areas, hindering free circulation of fluids which typically precipitate calcite cement and destroy reservoir quality. Some cementation has occurred, but subsequent cement and bioclast solution has enhanced reservoir quality.

Petrel Robertson (2015) demonstrated that upper Debolt shallow-water carbonates exhibit limited to good reservoir quality, enhanced by low-temperate solution and dolomitization, on the northern flank of the Fort St. John Graben ("injection favourability" area, Map R1). Figure R3, a permeability/porosity cross-plot from cores in the Fort St John Graben area and deformed belt immediately to the west, shows a substantial spread of reservoir quality. There is substantial low-quality rock, but samples clustering around the trend line for porosity values of 5% or greater show considerable conventional reservoir quality attributable to modified primary porosity. However, many of the high-permeability values above the trend line are from intervals that are fractured and/or have experienced hydrothermal dolomitization.

Fractured Reservoirs – Structural deformation, particularly west of the deformation front, causes fracturing and complex hydrothermal dolomitization of relatively brittle carbonate reservoirs, and is a primary mechanism for reservoir creation in Foothills gas pools (White and Al-Aasm, 1997). Core analysis points showing low porosities (<10%) and high permeabilities (>100 mD) in Figure R3 are generally from fractured sections.

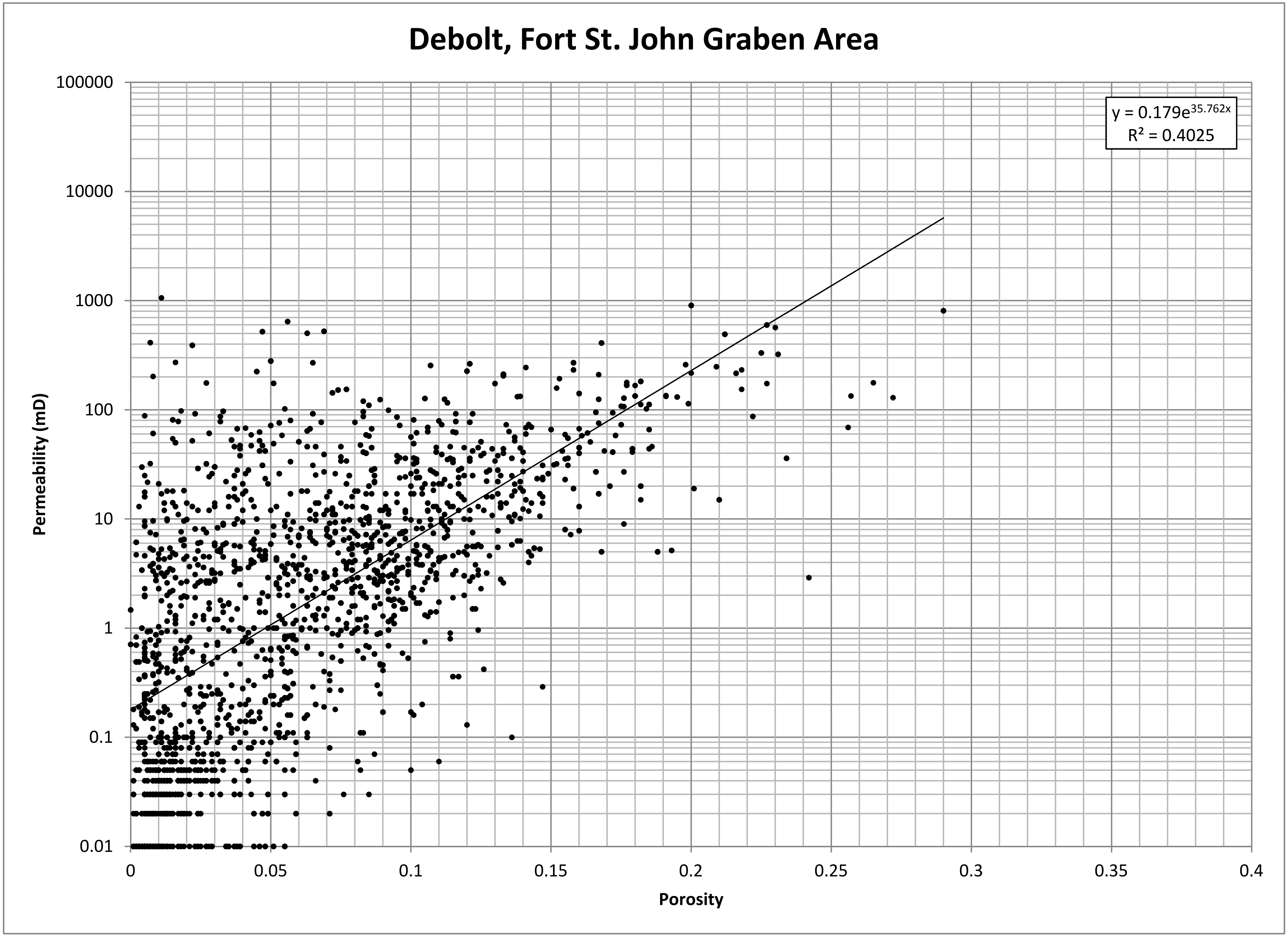

Figure R3. Porosity / permeability cross-plot, Rundle Group (Fort St John Graben area).

Resource oil potential is most likely to exist in modified primary porosity reservoirs, which host most existing Rundle oil pools in NEBC (see Desan Focus Area and Production and Test Data below). Subcrop reservoirs exhibit generally good reservoir quality, and are in trapping situations only along subcrop edges – which appear to be primarily gas-charged. Fractured reservoirs in the Foothills are almost exclusively gas-charged as well, except at Blueberry and Halfway (Map R1).

Desan Focus Area

Map R2 and Cross-section Desan-Desan' illustrate Rundle oil pools at Desan. Referencing local stratigraphy developed by Petrel Robertson (2000), production is primarily from the Shunda Formation, although some pools are officially designated as Pekisko. Although the Elkton is present, it is not a significant contributor to oil production. Several marker beds can be correlated locally within the Shunda, which highlights distinct porous zones within clean limestones at various stratigraphic levels. Cross-section Desan-Desan' also illustrates pervasive small-scale faulting, offsetting the local markers and influencing top Shunda structure (Map R2). Despite these obvious structural and stratigraphic variations in reservoir development, hydrodynamic analysis indicate general reservoir pressure continuity throughout Desan and southward to Tooga (PRCL, 2000). We have not undertaken detailed mapping of individual porous zones to assess their continuity, but it would be instructive to do so.

Reservoir development in the Shunda is typical of modified primary porosity limestones, and is controlled by two factors: i) optimum development of grainstone facies, partly controlled by local, syndepositional structural movements; and ii) diagenetic events preserving and enhancing depositional porosity (Fig. R4). Regional faults discussed by Jones (1980), which introduced dolomitizing fluids to older Devonian reservoirs, may be responsible for both structural offsets at the Shunda level, and introduction of fluids modifying Rundle reservoirs. Core analysis data in Fig. R5 show substantial conventional-quality reservoir rock (permeability > 1mD), but equally significant low-permeability rock – in accordance with our observation of interbedded porous and non-porous zones on logs (Cross-section Desan-Desan').

Production and Test Data

A number of large gas pools occur along the Debolt, Elkton and Pekisko subcrop edges in northwestern Alberta (Map R1). Moving northwestward into British Columbia, numerous gas wells have been completed along the Elkton and Debolt edges, but traps appear to be smaller and less continuous, and reservoirs are at the top of the Rundle section in subcrop reservoirs.

Desan Focus Area

At Desan and Tooga, medium-grade oil has been tested and produced from modified primary reservoirs in the Shunda (Map R2). OGC's 2015 Pool Reserve Report shows seven oil pools at Desan, with the bulk of the wells and reserves in two "Pekisko" pools.

Well: d-41-D/94-P-7	Depth: 640.1m	Magnification: 35x	Polarization: PL

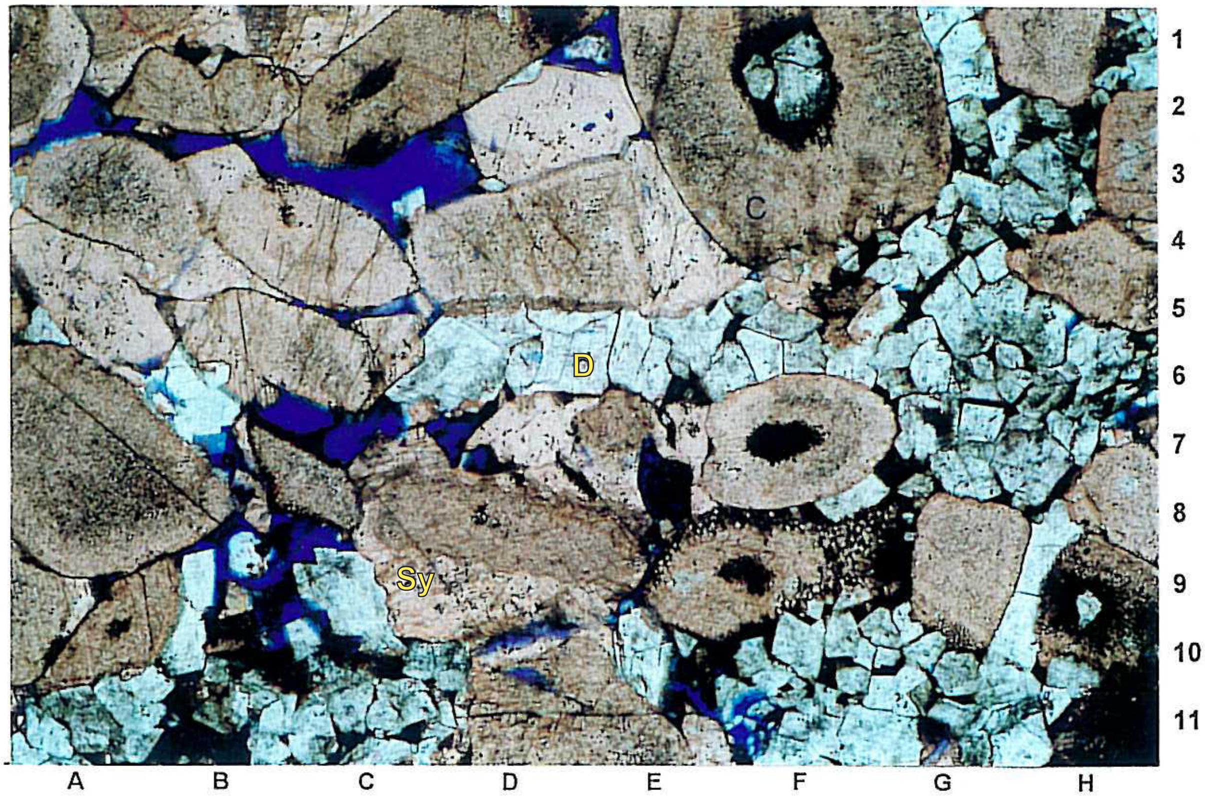

Figure R4. Partly dolomitized coarse-grained crinoidal limestone, Gulf AEC Desan d-41-D/94-P-7 (640.1m). Dolomite (D) is an early-stage cement, followed by syntaxial calcite cement (Sy). Fair enlarged interparticle porosity (core analysis porosity 5.3%, permeability 4.9 mD).

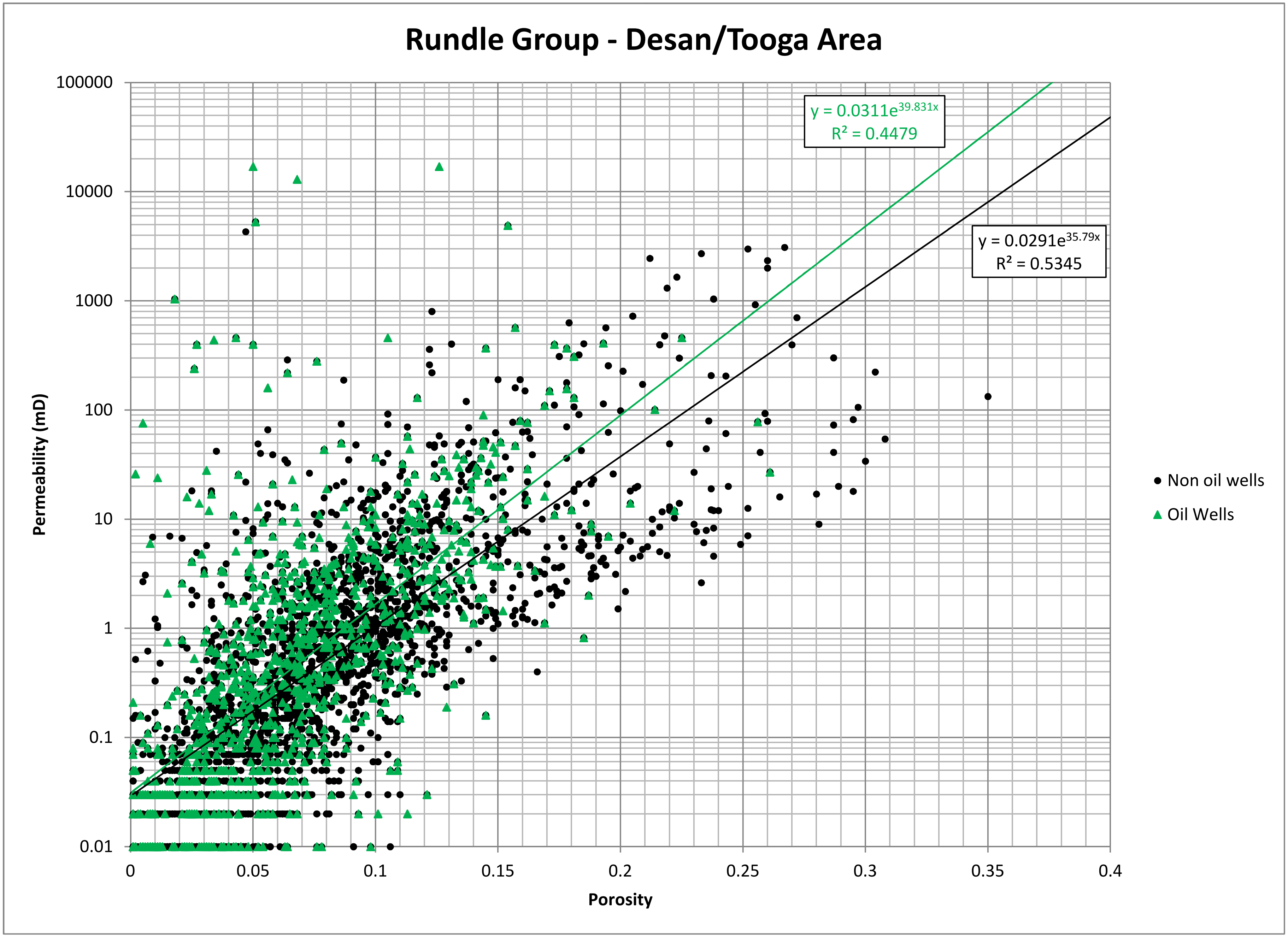

Figure R5. Porosity / permeability cross-plot, Rundle Group (Desan area).

Original oil in place is tabulated as 9,555e^3m^3 (60.1 MMBO), initial reserves as 1,228 e^3m^3 (7.7 MMBO), and current annual production as 43e^3m^3 (270 MBO). A recovery factor of 18% has been assigned to the largest pool, which is under active waterflood. Oil densities range from 900 to 909 kg/m^3. To the south, two "Debolt" pools at Tooga are assigned initial reserves of 31e^3m^3 (195 MBO), but have not been produced. There are additional Rundle oil shows in the area, as far west as D/94-P-6.

Reservoir Engineering Analysis

We studied approximately 130 oil wells in the greater Desan area, included 44 newer horizontal wells infilled amongst the older verticals (Appendix 5). A clear distinction can be made between the North Pool, which was not waterflooded, and the South Pool, which was (Map R2). The Tooga Pool was also evaluated.

Production from the earliest group of vertical wells began in January 1984, and proceeded intermittently for three winter seasons, presumably due to lack of all-weather roads and pipeline takeaway capacity. The wells were shut in from March 1986 until November 1994, when full field production commenced. In 1996, injection began in the South Pool, expanding from a single injector to 6 injectors by 1998 and ultimately 16 injectors by 2010.

South Pool Waterflood Area – Figure R6 shows vertical well configuration as it existed on waterflood prior to the commencement of horizontal drilling, and the subsequent addition of horizontal wells. Horizontal drilling began in 1996 and carried on through 2012. Average horizontal length is 800m. The horizontal wells appear to be intended to create polygons of production drainage patterns around the injection wells. All horizontal wells were completed open hole and acidized. Six wells within the waterflood area were re-acidized around 2014, and showed average improvement in rates of about 40%, improving as a group from 175 bbl/d to 245 bbl/d. Five of the six wells showed improvement; one well stayed the same.

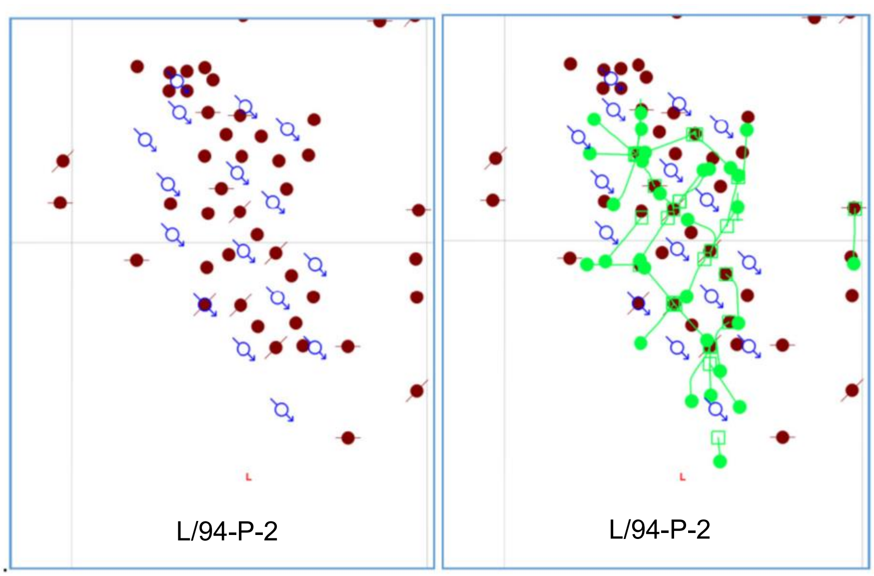

Figure R6. South Pool Waterflood Area map, Desan focus study. Map on left shows vertical well configuration prior to horizontal drilling, and map on right shows the subsequent addition of horizontal wells (in green).

Cumulative production from the South Pool is 859 e^3m^3 oil (5.4 MMBO), 23.3 e^6m^3 gas (0.82 BCF), and 334 e^3m^3 water (2.1 MMBW) (Fig. R7). Injection total is 1830 e^3m^3 water (11.5 MMBW). Decline is modest, and current pool production is about 79 m^3/d oil (500 BOPD). Current water cut is just above 50%, but water breakthrough has not been detrimental to performance. Gas/oil ratio is roughly 100 scf/bbl. Production performance appears quite good, but considerably more water has been injected than total voidage has been produced, begging the question of where the water may have gone. It is not known whether there is any water influx from an aquifer drive in the pool, although Petrel Robertson (2000) demonstrated the presence of a regional aquifer in the area.

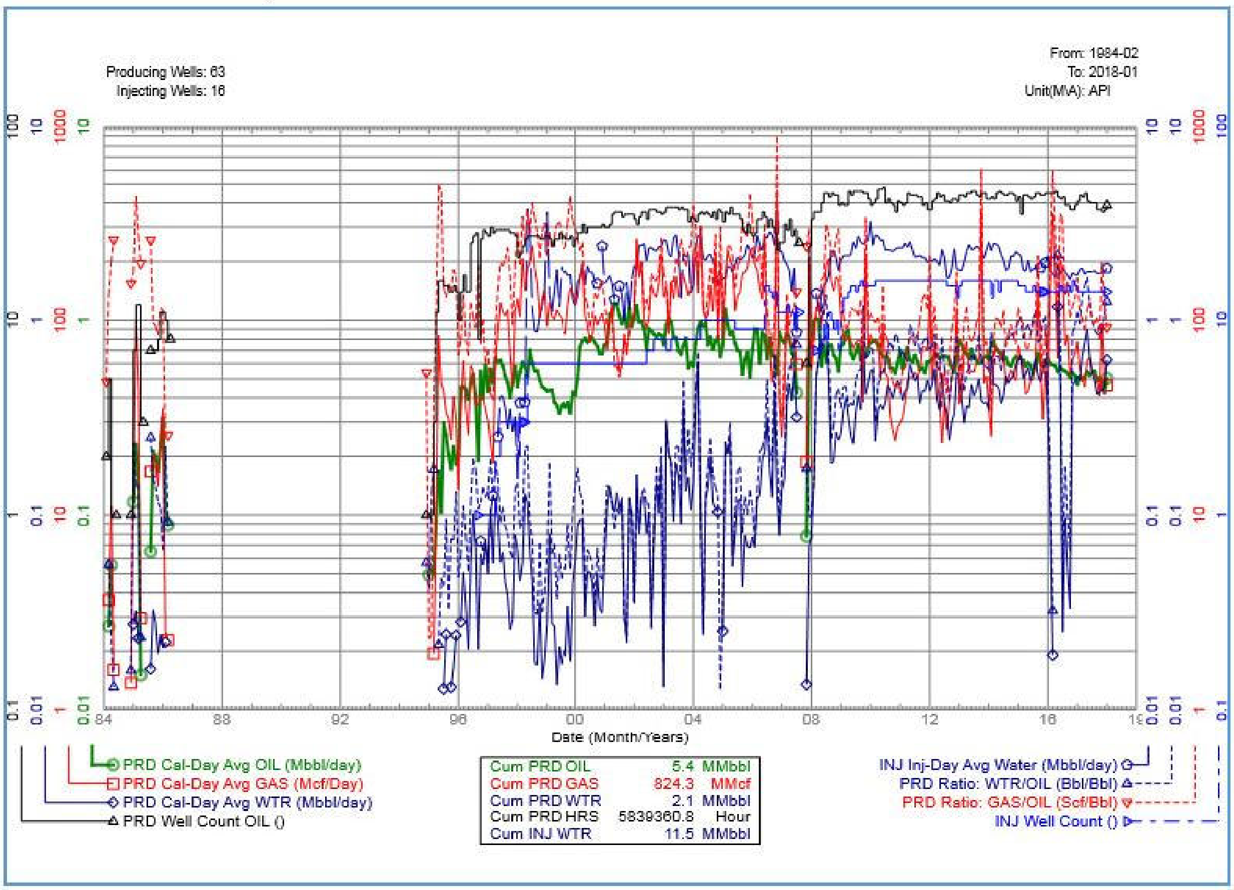

Figure R7. Production history plot, South Pool Waterflood, Desan Field.

Pressures were available on 56 producing wells, 37 in the waterflood area and 19 elsewhere; in many cases, however, only an initial pressure was recorded (Fig. R8). In the waterflood area, pressure has declined at many producing wells, but pressure at new wells has remained high, despite substantial nearby production and injection. This may indicate potential for further infill drilling because of heterogeneity and undrained compartments generated by local faulting and production from different porous intervals.

Figure R8. Pressure history plots, wells in South Pool Waterflood area.

North Pool Area - No waterflooding was undertaken in the North Pool, but a horizontal drilling program added wells in two stages, late 1990's and in 2011-12 (Fig. R9). Cumulative production from the North Pool is considerably less than the South pool, at 91 e^3m^3 oil (0.57 MMBO), 8.4 e^6m^3 gas (0.28 BCF), and 139 e^3m^3 water (0.88 MMBW) (Fig. R10). Cumulative water production is greater than oil production, but there has been no water injection. Current group water cut is about 73%.

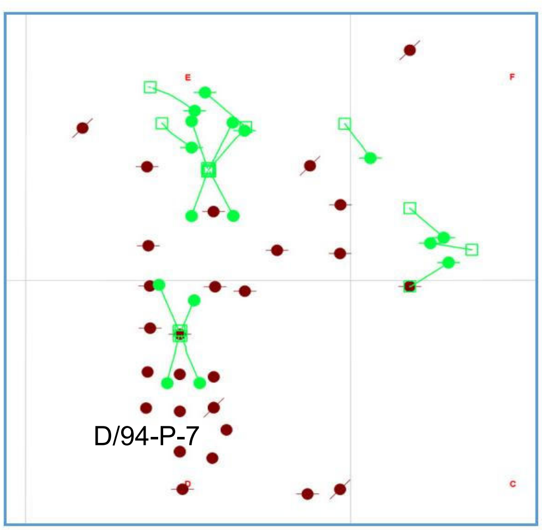

Figure R9. North Pool Area map, Desan focus study. Horizontal wells (in green) were added after initial drilling.

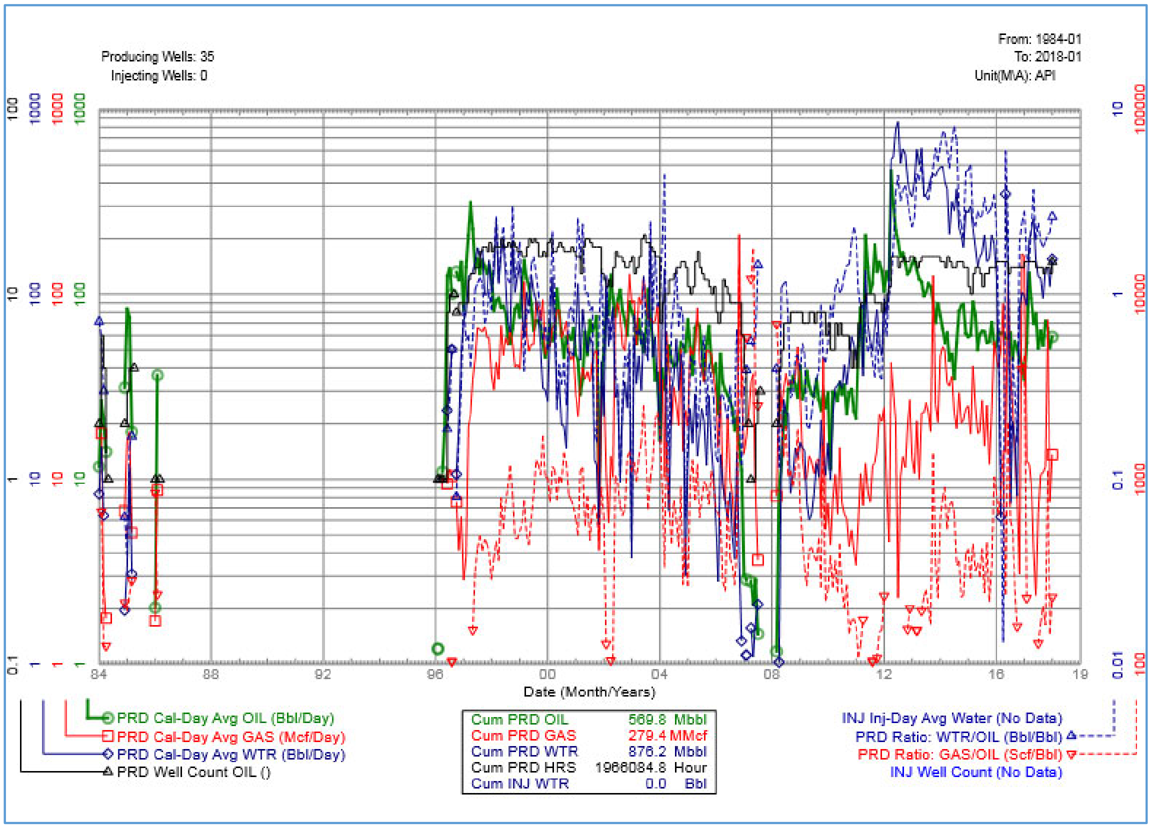

Figure R10. Production history plot, North Pool area, Desan Field.

Plotting reservoir pressures in non-waterflood wells, initial pressures remain high even in wells drilled quite late, further supporting the concept of significant reservoir heterogeneity and/or compartmentalization (Fig. R11).

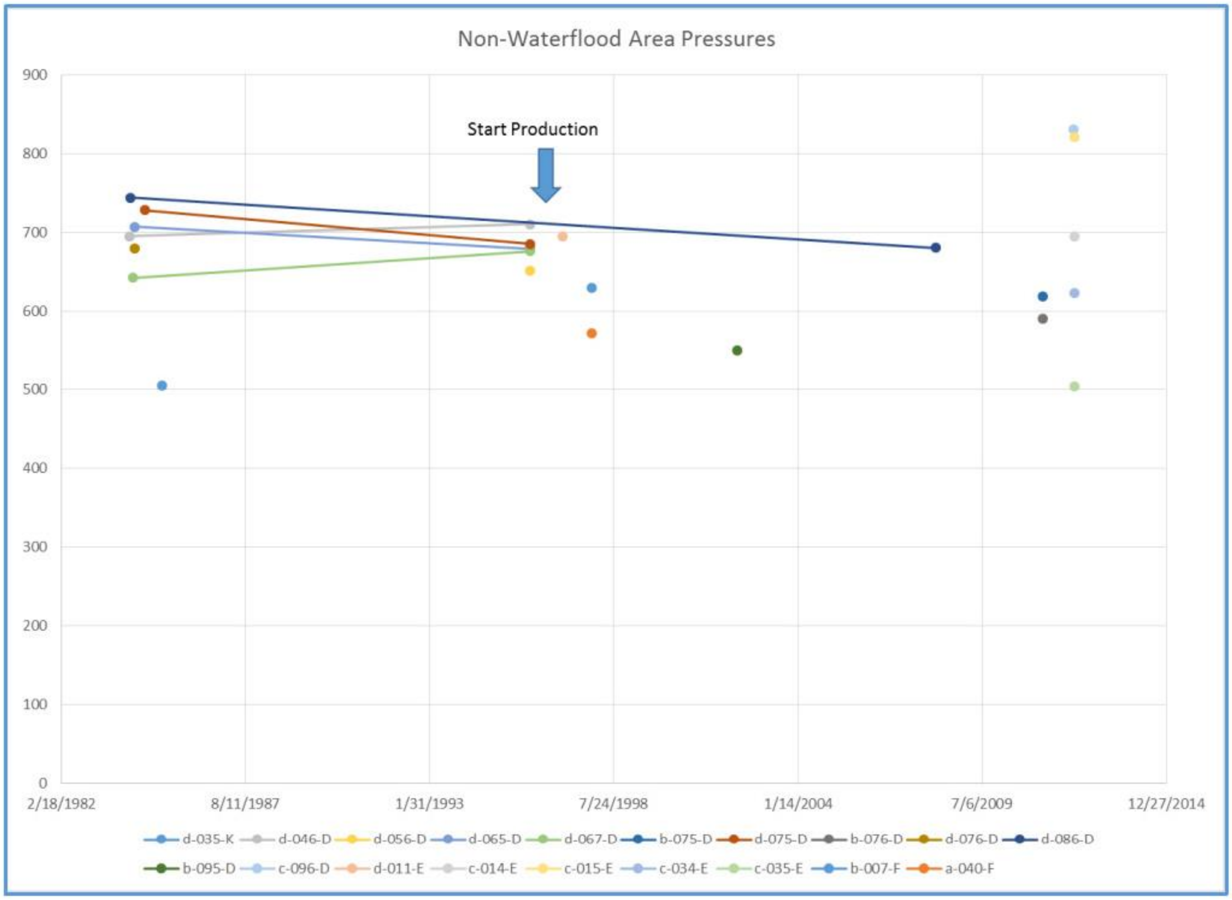

Figure R11. Pressure history plots, North Pool non-waterflood producing wells, Desan Field.

There are substantial differences in production performance between the South (waterflood) and North (non-waterflood) areas (Table R1). While waterflood support is partly responsible for better performance, it appears likely that the operator chose to waterflood the South Pool because better, more continuous reservoir quality was mapped there. It is particularly important to note that the performance of non-waterflood horizontal wells (IP 47 BOPD, EUR 20 MBO) is uneconomic by any measure.

Well Performance Comparison				
	Vertical		Horizontal	
	IP (bbl/d)	EUR (mbl)	IP (bbl/d)	EUR (mbl)
South (WF)	23	43	111	244
North (non-WF)	18	16	47	20

Table R1. Well performance comparison, waterflood (south) versus non-waterflood (North) areas, Desan Field.

Other Areas

To the south at Blueberry (94-A-12, 13), four Debolt oil pools have original oil in place of 12,946e^3m^3 (81.4 MMBO), initial reserves of 3,881e^3m^3 (24.4 MMBO), and current annual production of 27e^3m^3 (170 MBO) (Map R1). At Halfway (Twp 86-87, Rge 25W6), one Debolt oil pool has original oil in place of 950e^3m^3 (0.60 MMBO), and initial reserves of 95e^3m^3 (0.06 MMBO), which have been depleted. These pools were developed with vertical wells and a limited number of water injectors. Substantial variability of watercuts and pressures across the pools. suggests an opportunity to optimize the waterflooding.

There are also two single-well Debolt oil pools at Blueberry West (Twp 88-25W6). Blueberry and Halfway Debolt oil is much lighter (787-827 kg/m^3) than at Desan, and recovery factors are higher at Blueberry (20-35%). Both are discrete structural traps on the eastern flank of the outer Foothills. Blueberry West watered out despite there being no injection into the pool and no longer produces. The Halfway Debolt originally produced from 7 vertical wells, but over a span of five years wells went to 100% watercut and were shut in.

Analytical Data

Although many cores have been taken from the Rundle in NEBC, very little analytical work has been done other than routine core analyses. Appendix 1 and Map R1 highlight wells where source rock or other analyses have been reported in the literature or submitted in reports to the OGC. Other analyses are primarily petrographic reports, with little or no geomechanical testing reported.

Resource Oil Assessment

While we see a great deal of variability in reservoir quality in the Rundle Group, and substantial oil production from two different areas, actual Resource Oil potential is questionable.

As we saw for older reservoirs (Jean Marie, Tetcho, upper Banff), there appears to be an oil-prone “sweet spot” in southern 94P that could be related to deep-seated structure and maturity patterns in underlying source rocks – particularly the Muskwa and possibly the Exshaw (Fig. JM8). Bustin and Bustin (2016) suggested lower source rock maturities in the outer Foothills at Blueberry and Halfway as well.

Detailed stratigraphic and local structural analysis in the Desan area may well define additional oil potential, and effective horizontal / multi-frac drilling may enable economic access to both low-permeability carbonate reservoirs, and to higher-quality but structurally / stratigraphically discontinuous intervals. Operators must contend with relatively low reservoir pressures at fairly shallow depths.

GOLATA FORMATION

Age and Play Type

Upper Mississippian – Shale Oil Play;
Prospectivity: 'C' Play – Extensive, mappable marine shale – but low organic content and high maturity levels preclude significant oil prospectivity.

Regional Geology

After Rundle Group carbonate ramp deposition, profound subsidence of the former Peace River Arch took place, significantly influencing deposition of the upper Mississippian through Pennsylvanian and Permian Stoddart Group (Golata, Kiskatinaw, and Taylor Flat formations) and Belloy Formation (O'Connell *et al*., 1990). Barclay *et al.* (1990) showed deposition to have occurred within the broad, west-east trending Peace River Embayment, focused within the structurally-bounded Fort St. John Graben / Dawson Creek Graben Complex (Fig. G1). They documented up to 1200 metres of syndepositional subsidence in distinct, fault-bounded compartments (Fig. G2, G3; Cross-section Stoddart-Stoddart').

As the Fort St. John Graben subsided, shales and siltstones of the Golata Formation accumulated in a low-energy, restricted marine embayment that transgressed the Debolt platform and graded to open marine facies westward (Barclay, 1988; Barclay *et al*., 1990) (Fig. G4) (core photos 11-34-84-15W6 and 7-22-80-14W6, Appendix 4). Map G1 illustrates restriction of Golata deposition to the Fort St. John Graben area, although a southerly limit has not been defined because deep well control is lacking. Map G2, depth to top Golata, illustrates structural compartmentalization within the Fort St. John Graben, and significant deepening to >3500m southward. Post-Golata differential subsidence caused exposure and erosion over some structural blocks, and likely degraded Golata source rock quality (Fig. G5; Barclay, 1988; Barclay *et al.*, 2002). The Golata ranges up to more than 100m thick, but thicknesses change abruptly across faults as the result of both syn-depositional and post-depositional movements (Map G1).

While Golata and equivalent strata are present in the deformed belt and crop out to the west, stratigraphic changes and structural deformation make it difficult to map.

Golata-equivalent shales have also been identified in the Liard Basin and surrounding areas, where Rocheleau *et al.* (2014) found them to have good source rock characteristics.

Production and Test Data

There are no production or meaningful test data from the Golata, as it has not been targeted as a potential shale gas/oil play. Commercial database searches indicate

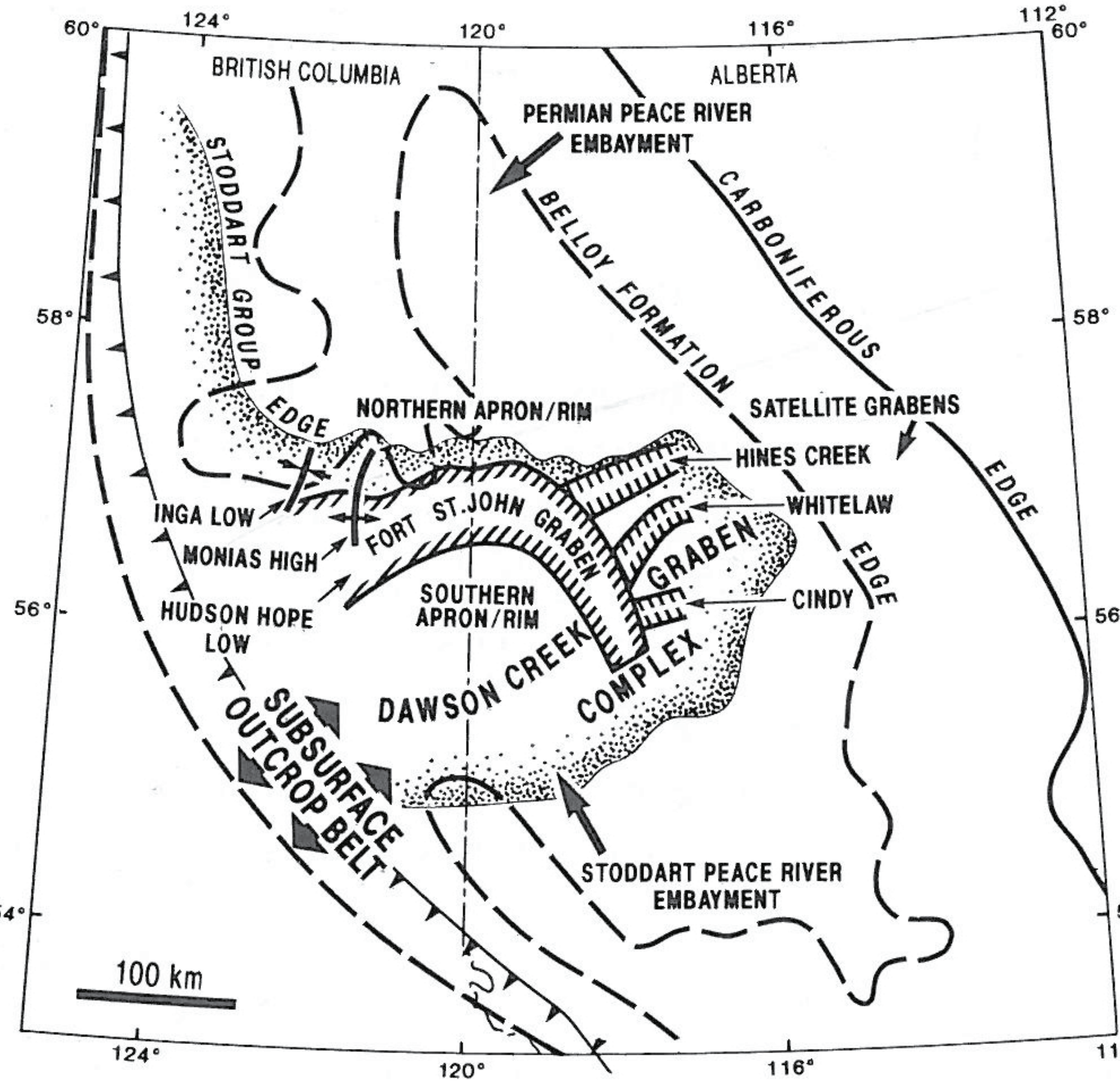

Figure G1. Peace River Embayment tectonostratigraphic elements, Mississippian-Permian time (from Barclay et al., 1990).

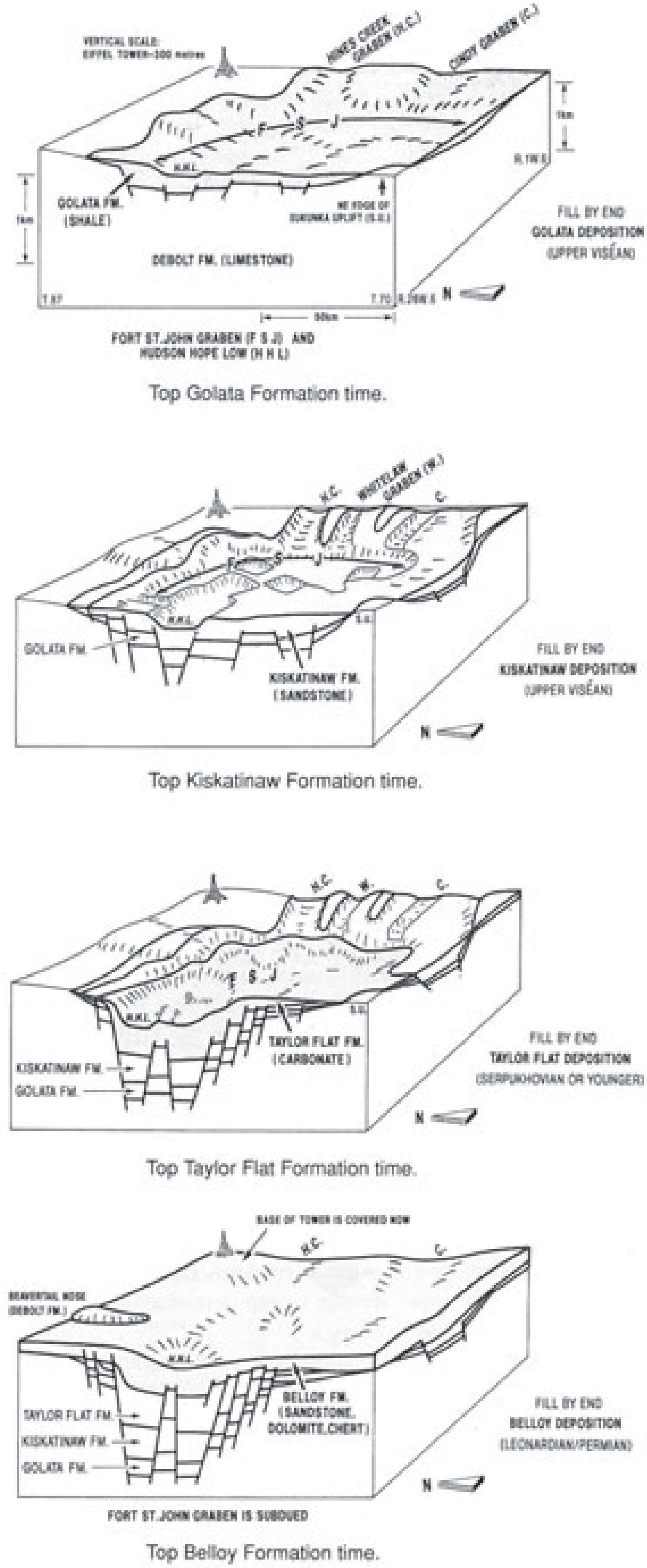

Figure G2. Schematic deposition of Stoddart Group and Belloy Formation during subsidence of Fort St. John Graben (from Barclay et al., 1990).

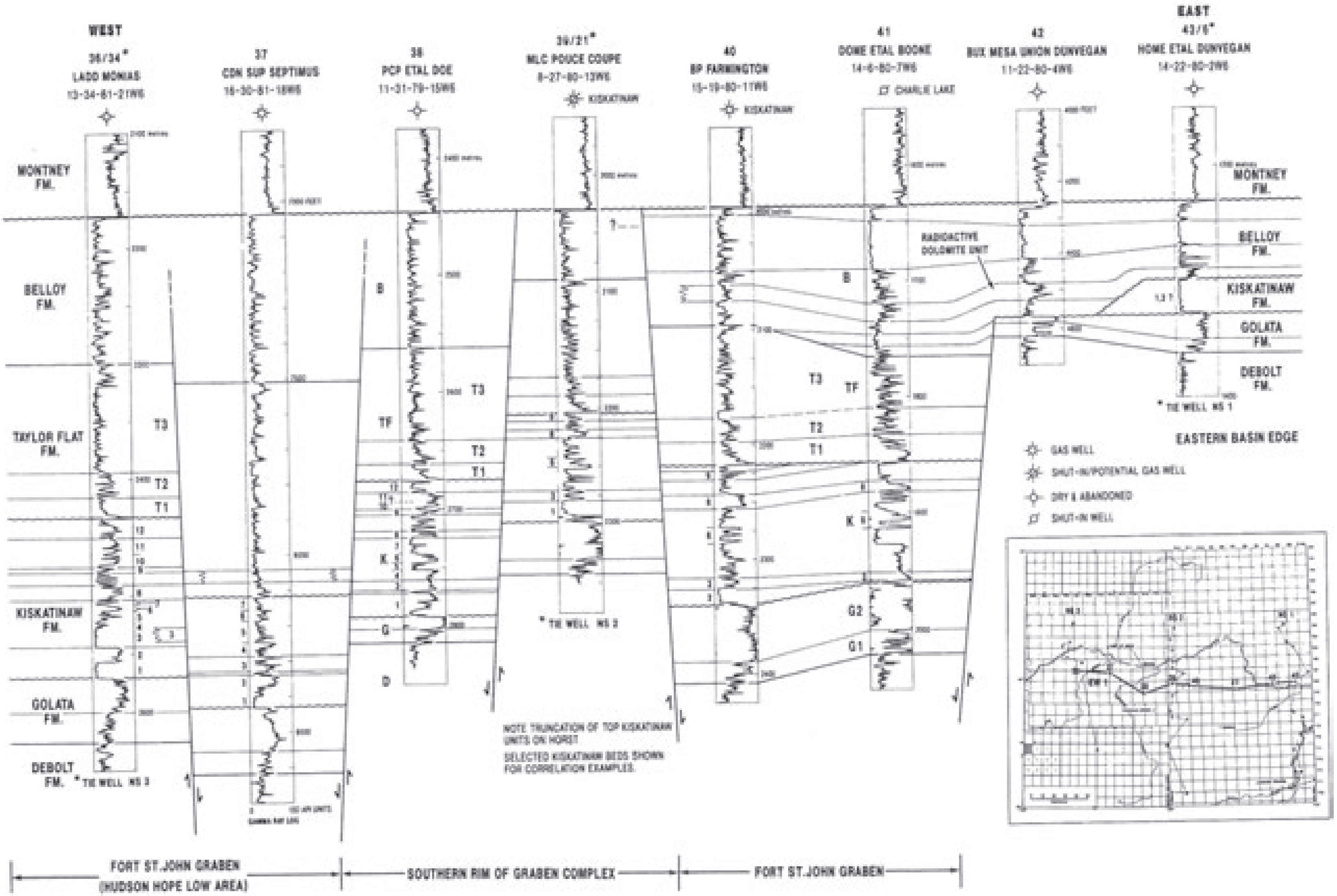

Figure G3. Belloy-Debolt cross-section in Fort St. John Graben, showing syndepositional faulting that profoundly affected depositional thicknesses (from Barclay et al., 1990).

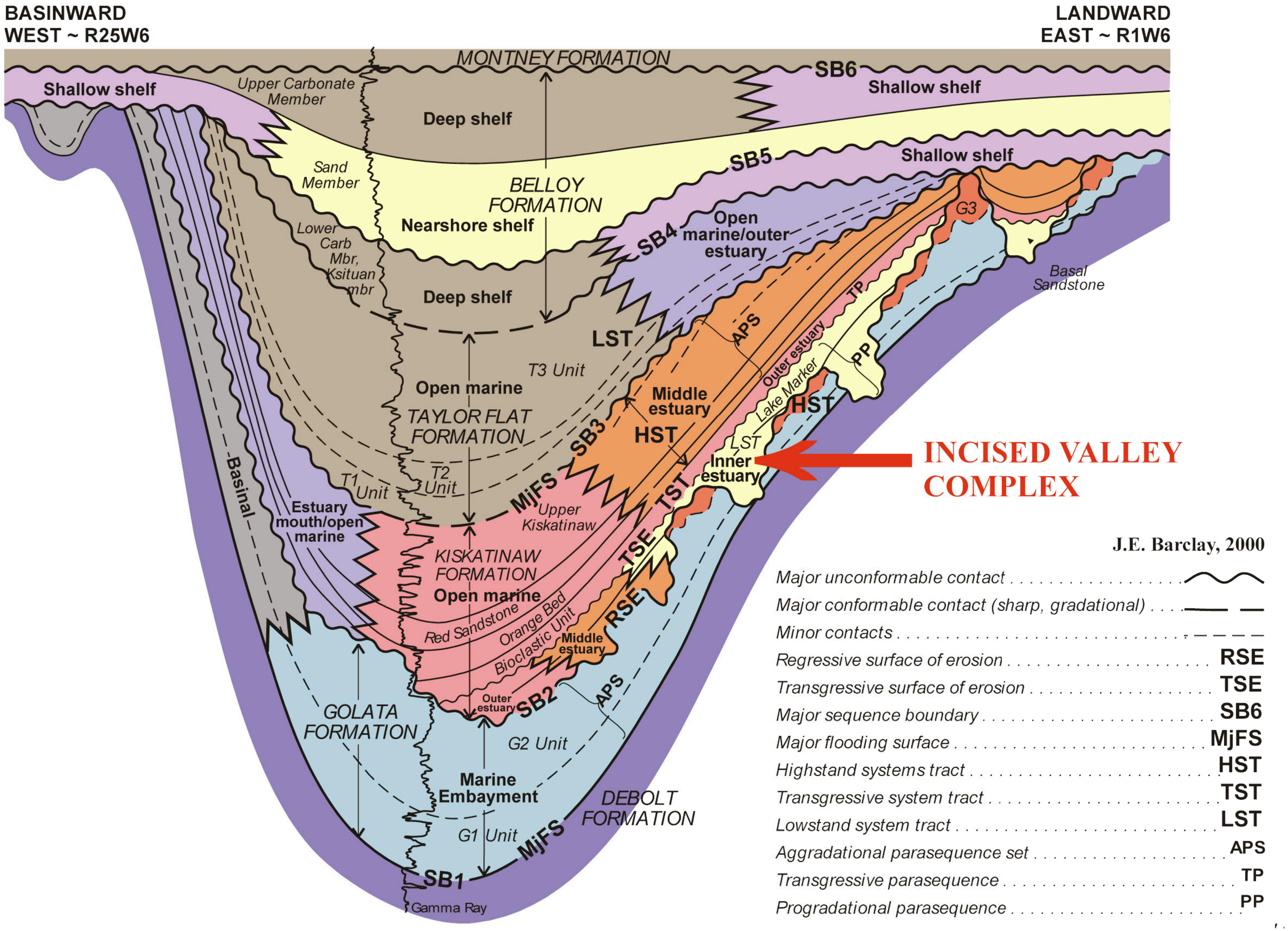

Figure G4. Schematic cross-section illustrating depositional relationships of Stoddart Group and Belloy Formation in Fort St. John Graben (from Barclay et al., 2002).

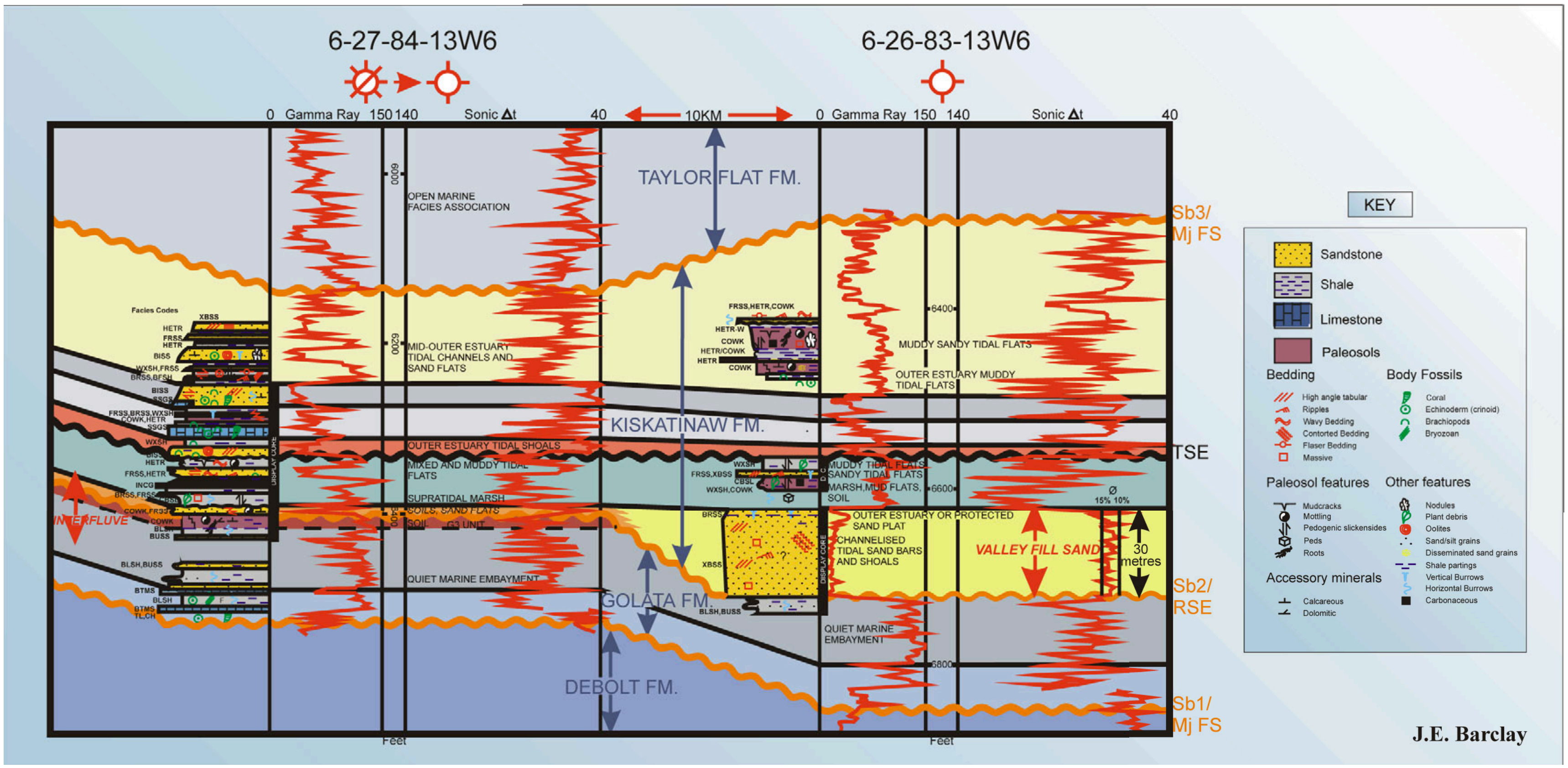

Figure G5. Kiskatinaw valley fill to interfluve relationship (from Barclay et al., 2002).

Golata production from some wells, but the producing zones are actually basal Kiskatinaw sandstones erroneously assigned to the Golata.

Analytical Data

Little analytical work has been completed on the Golata – our database search revealed only GSC Open File reports on source rock analysis from cuttings in two wells (Appendix 1; Map G1).

We analyzed one Golata core, from PCI Doe Creek 7-22-80-14W6, consisting of dark grey organic-rich shales, to ensure adequate characterization of the play (Appendix 3, 4).

Clay minerals and quartz dominate Golata mineralogies; small amounts of feldspars (<9%), siderite (<23%) and pyrite (<9%) are also present (Fig. G6; Table G1). A few samples contain apatite (<9%), and one sample has dolomite. Clay minerals include interstratified illite, mixed layers and mica (20-62%),with kaolinite (1-32%) and smaller amounts of chlorite (2-7%). Total Organic Carbon (TOC) ranges between 0.5-2.6 wt%, with higher values in the upper part of the cored section. T_{max} values range between 460-500°C, indicating high maturation of organic matter – wet to dry gas equivalent.

Well ID	Sample ID	Zone	Sample Type	Depth (m)	Tmax	TOC %	Quartz		Feldspar	Carbonates		Clays			Sulphides	Apatite
					°C			Albite	K-feldspar	Dolomite	Siderite	Illite/mica	Chlorite	Kaolinite	Pyrite	
	2400	Golata	Core	2400.00	544	0.90	59.7	2.3	1.9			26.5	2.9	5.9	0.9	
	2401	Golata	Core	2401.00		0.65	58.7	2.1	2.1			25.5	3.1	7.3	1.3	
	2402	Golata	Core	2402.00	481	1.20	57.8	2.0	1.5		6.5	20.1	3.4	7.7	1.0	
	2403	Golata	Core	2403.00	473	1.78	40.5	3.7	1.3		5.8	28.6	4.2	11.7	4.2	
	2404	Golata	Core	2404.00	500	0.90	7.9	0.1	0.1		0.3	54.4	3.4	32.5	1.4	
	2405	Golata	Core	2405.00	496	1.07	11.4	0.1	0.1		0.6	54.3	3.5	28.4	1.6	
	2406	Golata	Core	2406.00	498	0.78	8.8	0.1	0.1		2.1	55.5	3.7	28.6	1.2	
	2407	Golata	Core	2407.00	487	1.31	7.9	0.1	0.1		16.9	46.5	2.6	24.0	1.8	
	2408	Golata	Core	2408.00	488	1.76	24.4	2.3	2.8		0.4	41.6	4.3	22.2	1.8	
	2409	Golata	Core	2409.00	484	1.17	23.9	2.2	2.8		11.5	37.1	3.1	17.2	1.9	
	2410	Golata	Core	2410.00	488	2.02	24.3	2.2	2.7		0.9	42.1	4.6	21.3	1.7	
	2411	Golata	Core	2411.00	485	2.17	34.2	2.2	2.2		2.8	36.5	4.0	16.5	1.5	
	2412	Golata	Core	2412.00	487	1.52	26.1	2.4	2.6		1.3	42.1	4.6	19.0	1.8	
	2413	Golata	Core	2413.00	484	1.31	26.3	2.7	2.9		0.8	40.9	4.2	19.7	2.4	
PCI Doe Creek	2414	Golata	Core	2414.00	485	1.24	29.4	2.3	2.3		8.0	35.5	5.1	15.7	1.5	
7-22-80-14W6	2415	Golata	Core	2415.00	483	1.90	32.3	2.3	2.5		0.5	38.0	4.9	17.8	1.5	
WA:06823	2416	Golata	Core	2416.00	480	1.60	48.8	2.1	2.4		9.7	19.0	7.0	10.0	1.0	
	2417	Golata	Core	2417.00	474	1.86	42.0	2.2	2.6		2.1	31.2	6.1	9.1	4.6	
	2418	Golata	Core	2418.00	500	0.44	84.5	0.9	0.5		5.9	2.4	2.0	2.8	0.7	
	2422	Golata	Core	2422.00	506	0.71	46.2	2.5	1.9		9.8	28.0	4.2	6.8	0.5	
	2423	Golata	Core	2423.00	499	0.87	40.1	2.5	3.0		1.2	37.3	5.3	9.6	0.8	
	2424	Golata	Core	2424.00		1.00	12.1	2.2	3.3		23.8	46.3	4.4	6.3	1.4	
	2425	Golata	Core	2425.00	493	0.51	25.1	2.9	3.8		2.5	50.7	5.1	8.3	1.4	
	2426	Golata	Core	2426.00	482	0.56	13.7	2.8	2.9		0.1	55.5	3.7	10.4	1.5	9.4
	2427	Golata	Core	2427.00	484	0.57	30.5	3.4	4.5		0.1	49.7	2.1	2.9	1.7	4.8
	2428	Golata	Core	2428.00	493	0.73	25.2	3.1	2.9		0.2	55.0	1.9	2.7	8.8	
	2429	Golata	Core	2429.00	479	2.64	24.8	3.4	3.4	9.0		49.6	2.8	3.5	3.7	
	2430	Golata	Core	2430.00	483	0.64	29.7	3.7	4.4		0.7	56.0	1.9	0.9	2.6	0.1
	2431	Golata	Core	2431.00	468	0.45	22.1	4.0	4.6		1.1	61.6	2.0	0.8	3.6	0.2
	2432	Golata	Core	2432.00	461	0.55	26.3	3.8	4.1		0.6	56.2	2.4	1.4	5.0	
	2433	Golata	Core	2433.00	470	0.59	27.3	3.9	4.3		0.5	55.2	2.7	1.6	4.2	

Table G1. X-Ray diffraction analyses, Golata Formation, PCI Doe Creek 7-22-80-14W6.

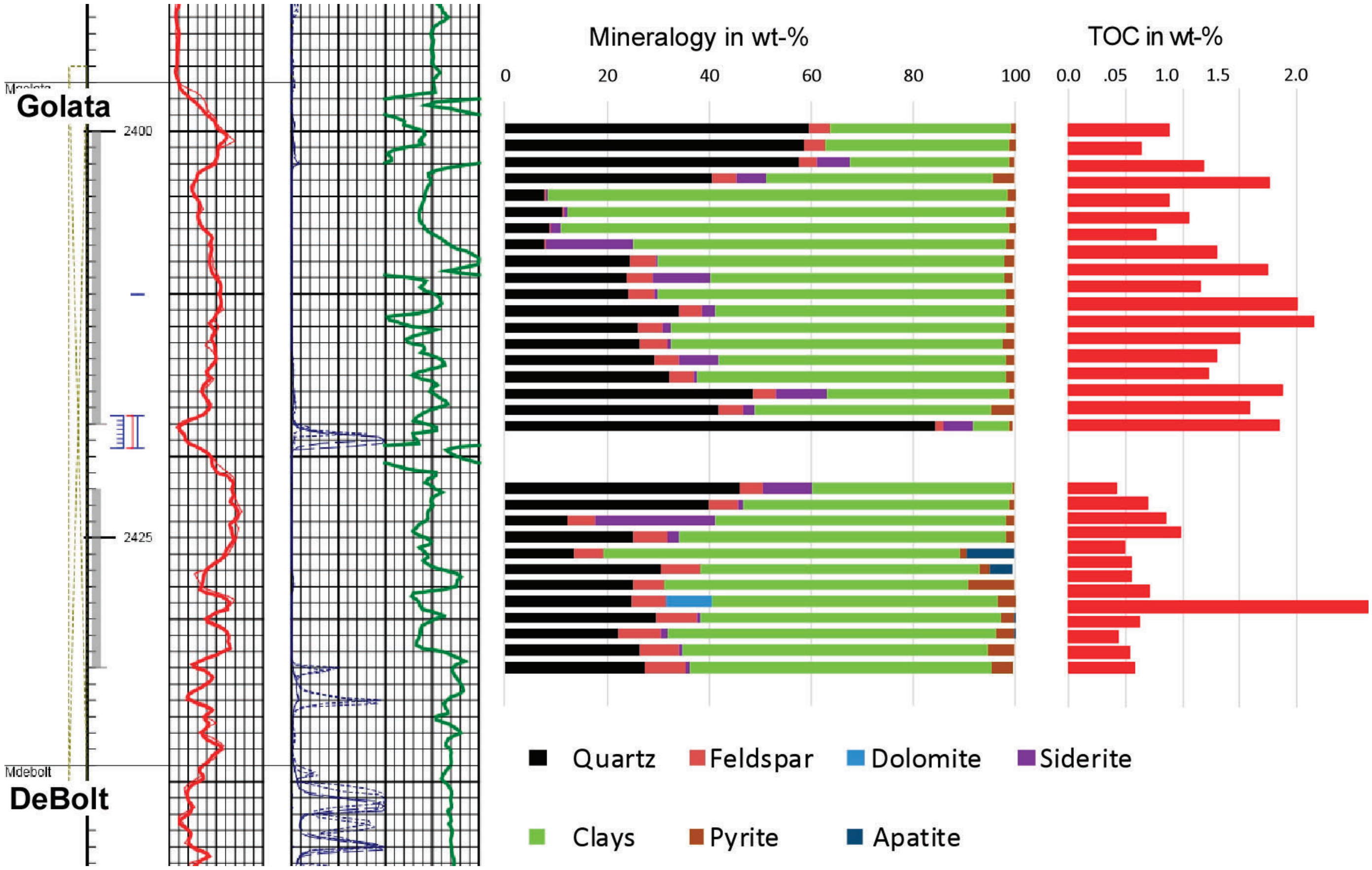

Figure G6. Mineralogy and TOC plots for samples from the Golata Formation, PCI Doe Creek 7-22-80-14W6.

Petrographically, the Golata consists of thinly-bedded dark shale with scattered sandy interbeds and abundant bioturbation (Fig. G7, G8). Quartz grains are silt-sized to fine-grained, with rare medium grains that are angular to subangular. Overall, sorting appears to be fairly good. Some secondary quartz cements are observed.

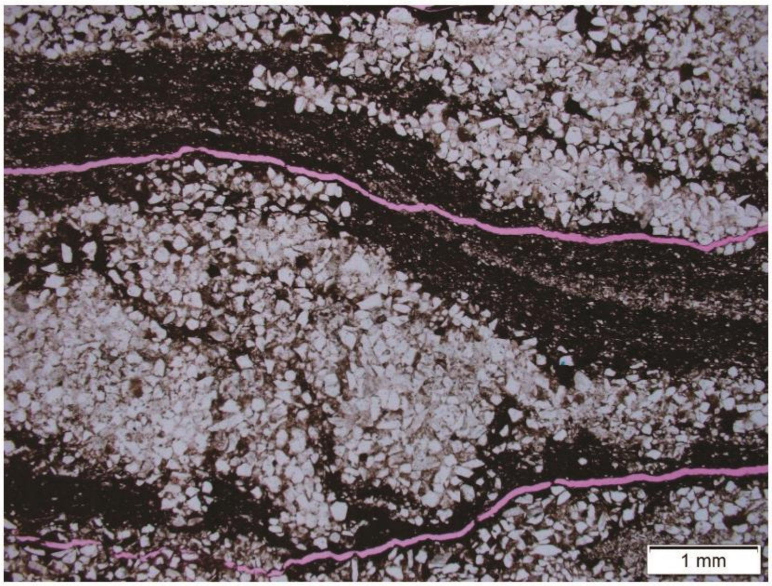

Figure G7. Photomicrograph, Golata Formation, PCI Doe Creek 7-22-80-14W6 (2416.14 m) under plane polarized light. Laminae of very fine- to fine-grained sandstone are interbedded with laminae rich in clays, organic matter and pyrite. Epoxy-filled (pink) fractures are a product of sample preparation.

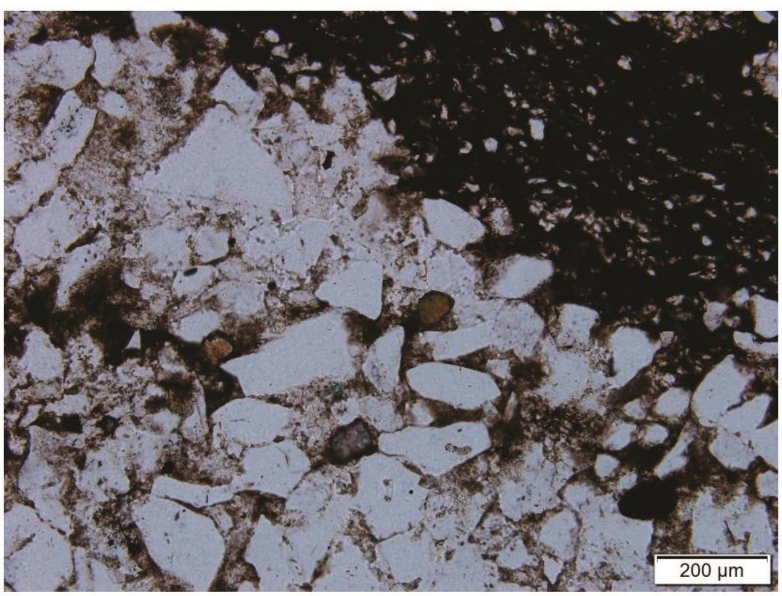

Figure G8. Photomicrograph, Golata Formation, PCI Doe Creek 7-22-80-14W6 (2416.14 m) under plane polarized light. Angular to subangular quartz grains with interstitial clays occur interbedded with and opaque-rich layer with silt-sized quartz grains.

Unconfined porosities in Golata samples range between 1-5.7%, with matrix permeabilities of 2.5-10.9 nD (Table G2). MICP conformance-corrected porosities are much lower (although only three samples were measured) and range between 0.5-2.8% (Table G3). The difference between the two methods implies that the majority of the pore throats are very small (nm-size). An incremental and percent intrusion vs pore size distribution plot indicates predominantly very small pore throat diameters (Fig. G9).

Unconfined Porosity and Matrix Permeability										
Well Name	Well Location	Core Depth (m)	Fm	Density		Porosity (%)	GRI Matrix Permeability (md)		GRI Matrix Permeability (nd)	
				Bulk Density (g/cc)	Skeletal Density (g/cc)		Avg	Std Dev	Avg	Std Dev
PCI Doe Creek	07-22-080-14W6	2401.29	Golata	2.599	2.689	3.34	1.09E-05	3.09E-06	10.94	3.09
PCI Doe Creek	07-22-080-14W6	2403.12	Golata	2.565	2.720	5.71	9.78E-06	2.41E-06	9.78	2.41
PCI Doe Creek	07-22-080-14W6	2405.00	Golata	2.551	2.633	3.14	6.55E-06	6.46E-07	6.55	0.65
PCI Doe Creek	07-22-080-14W6	2407.18	Golata	2.543	2.650	4.05	6.64E-06	1.87E-06	6.64	1.87
PCI Doe Creek	07-22-080-14W6	2408.62	Golata	2.591	2.687	3.58	8.79E-06	1.08E-06	8.79	1.08
PCI Doe Creek	07-22-080-14W6	2409.40	Golata	2.581	2.674	3.46	6.41E-06	8.51E-07	6.41	0.85
PCI Doe Creek	07-22-080-14W6	2410.51	Golata	2.562	2.627	2.46	4.15E-06	6.08E-07	4.15	0.61
PCI Doe Creek	07-22-080-14W6	2412.35	Golata	2.561	2.676	4.31	2.97E-06	1.83E-06	2.97	1.83
PCI Doe Creek	07-22-080-14W6	2413.94	Golata	2.603	2.698	3.52	3.87E-06	1.17E-06	3.87	1.17
PCI Doe Creek	07-22-080-14W6	2415.13	Golata	2.550	2.659	4.11	8.78E-06	4.23E-06	8.78	4.23
PCI Doe Creek	07-22-080-14W6	2416.64	Golata	2.551	2.574	0.89	4.01E-06	1.08E-06	4.01	1.08
PCI Doe Creek	07-22-080-14W6	2418.00	Golata	2.617	2.682	2.43	3.49E-06	1.09E-06	3.49	1.09
PCI Doe Creek	07-22-080-14W6	2422.40	Golata	2.588	2.686	3.64	7.03E-06	1.26E-06	7.03	1.26
PCI Doe Creek	07-22-080-14W6	2424.65	Golata	2.628	2.696	2.52	2.48E-06	9.48E-07	2.48	0.95
PCI Doe Creek	07-22-080-14W6	2426.80	Golata	2.740	2.789	1.77	2.99E-06	7.73E-07	2.99	0.77
PCI Doe Creek	07-22-080-14W6	2429.08	Golata	2.805	2.882	2.69	9.57E-06	4.40E-06	9.57	4.40
PCI Doe Creek	07-22-080-14W6	2433.00	Golata	2.596	2.702	3.94	8.84E-06	4.86E-06	8.84	4.86

Table G2. Golata Formation – unconfined porosity and GRI matrix permeability measurements from core samples, PCI Doe Creek 7-22-80-14W6.

MICP Porosity										
Well Name	Well Location	Core Depth (m)	Fm	Density g/cc		Porosity (%)	Corrected Porosity (%)	Peak Range		Stem Volume Used (%)
				Bulk Density (g/cc)	Skeletal Density (g/cc)			Peak Range	Modal Peak	
PCI Doe Creek	07-22-080-14W6	2401.29	Golata	2.590	2.602	0.93	0.46	5 - 80	18	12
PCI Doe Creek	07-22-080-14W6	2433.00	Golata	2.619	2.694	3.47	2.80	4 - 110	4	16
PCI Doe Creek	07-22-080-14W6	2408.62	Golata	2.713	2.751	1.98	1.39	4 - 70	4	11

Table G3. Golata Formation – MICP porosity and conformance-corrected porosity measurements from core samples, PCI Doe Creek 7-22-80-14W6.

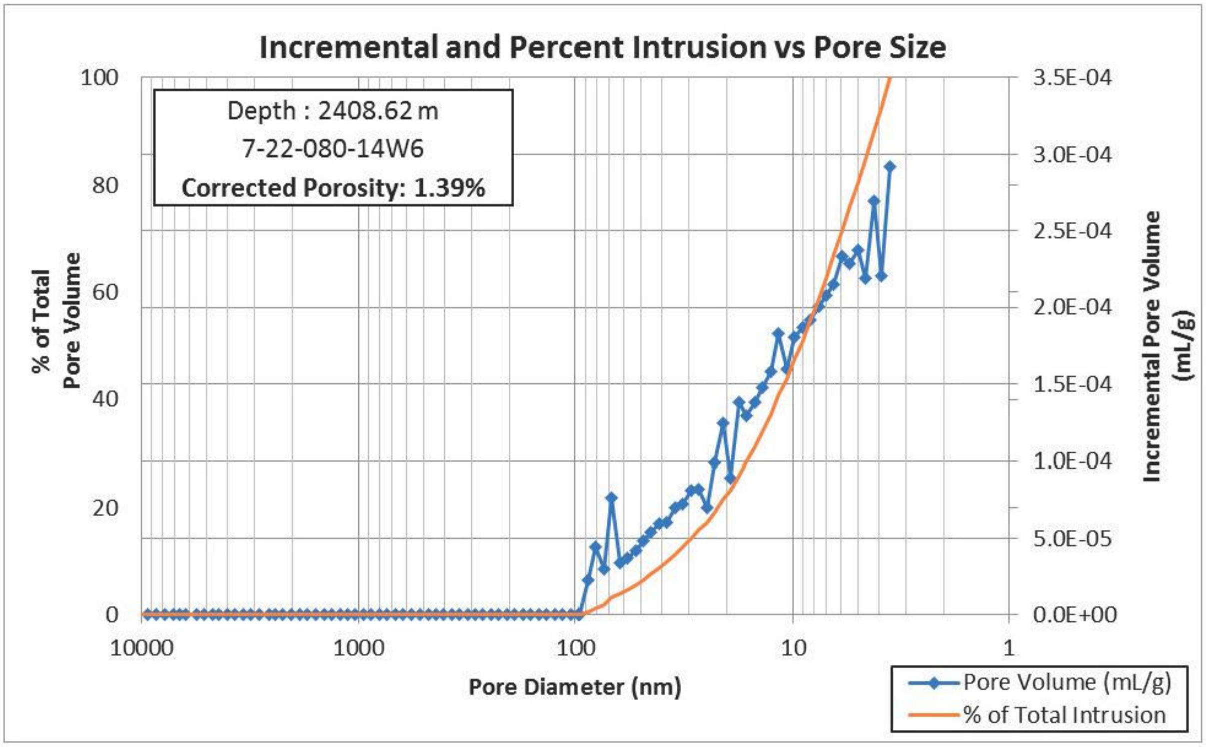

Figure G9. Incremental and percent intrusion vs pore size, Golata Formation, PCI Doe Creek 7-22-80-14W6 (2408.62 m), highlighting a range of pore throat diameters less than 90 nm.

Mechanical properties of the Golata are difficult to determine, as the fissile shales are difficult to sample. Only a few sample plugs were recovered, and these were from sand-rich intervals. They showed high compressive strength (168-297 MPa) and residual strength (112-191 MPa); Poisson's ratio is ~0.18-0.21 and Young's modulus ~30-47 (Table G4). These data indicate strong and brittle rocks, but they are not representative of clay-rich shale layers. Sufficiently thick sandstone units may represent fracturing barriers, or at least significant heterogeneities in the reservoir that would influence fracture behaviour.

Well Name	Depth (m)	Confining Pressure (MPa)	Axial Strain at Failure (%)	Compressive Strength (MPa)	Residual Strength (MPa)	Static Young's Modulus (GPa)	Static Poisson's Ratio	Static Bulk Modulus (GPa)	Static Shear Modulus (GPa)
07-22-080-14W6	2401.17	15.0	0.833	237.92	156.70	35.20	0.210	20.24	14.54
07-22-080-14W6	2417.85	15.0	0.658	168.26	112.14	29.61	0.180	15.44	12.54
07-22-080-14W6	2429.60	15.0	0.669	297.51	191.00	47.39	0.196	26.01	19.80

Table G4. Golata Formation - Rock mechanical analyses showing confining pressure, compressive strength, Young's modulus, Poisson's ratio and bulk and shear modulii from three samples in PCI Doe Creek 7-22-80-14W6.

Although existing TOC and maturity data are not encouraging, one would expect a regionally-extensive marine shale to be a viable shale reservoir target. We therefore completed Passey (petrophysical) analysis of the Golata in eleven wells with available and adequate digital log suites to provide a more widely-based check on organic richness, and contrasted results with a well from the organic-rich Nordegg. Figure G10a shows large sonic-resistivity separation (coloured pink) and a significant uranium anomaly indicating high organic matter content in the Nordegg; lack of these indicators demonstrate very low organic matter in the Golata (Fig. G10b). Passey analysis outputs for the Golata wells analyzed are presented in Appendix 8, and demonstrate low total organic carbon values throughout, thus reinforcing results from the analytical testing.

Resource Oil Assessment

Despite being a widespread, mappable marine shale, the Golata in the Peace River area is not prospective as a shale oil target because of low organic content and high thermal maturity. Abundant clay-rich shales may not be amenable to effective fracture stimulation.

KISKATINAW / TAYLOR FLAT FORMATIONS

Age and Play Type

Upper Mississippian – Halo Oil Play (tight sandstone);
Prospectivity: 'C' Play – Little evidence of mappable trends or productive characteristics to suggest halo or tight oil potential.

Regional Geology

After Golata deposition, fluvial/estuarine to shallow marine sediments of the Kiskatinaw Formation prograded from an eastern deltaic source, westward to channelized estuarine and marginal marine environments near the B.C./Alberta border (Barclay *et al*., 1990; Barclay *et al*., 2002) (Fig. KI1). The basal Kiskatinaw is dominated by channel sandstones, typically quartzose, exhibiting flaser bedding and other tidal features. To the west, it grades to more open marine limestones and shales (Fig. KI1, G4). As regional graben subsidence and marine transgression continued, Kiskatinaw sandstones became thinner and less continuous upward, and grade to marine shales and thin-bedded carbonates and sandstones (western three wells, Cross-section Stoddart-Stoddart').

A highly-correlative flooding surface caps the Kiskatinaw, and is succeeded by open marine carbonates and shales of the Taylor Flat Formation (Cross-section Stoddart-Stoddart'). Bioclastic sandy packstones to grainstones and calcareous and bioclastic sandstones are common, but bedding is generally thin compared to more massive reservoir facies in the basal Kiskatinaw and upper Belloy (Barclay *et al*., 1990). Facies

G10a

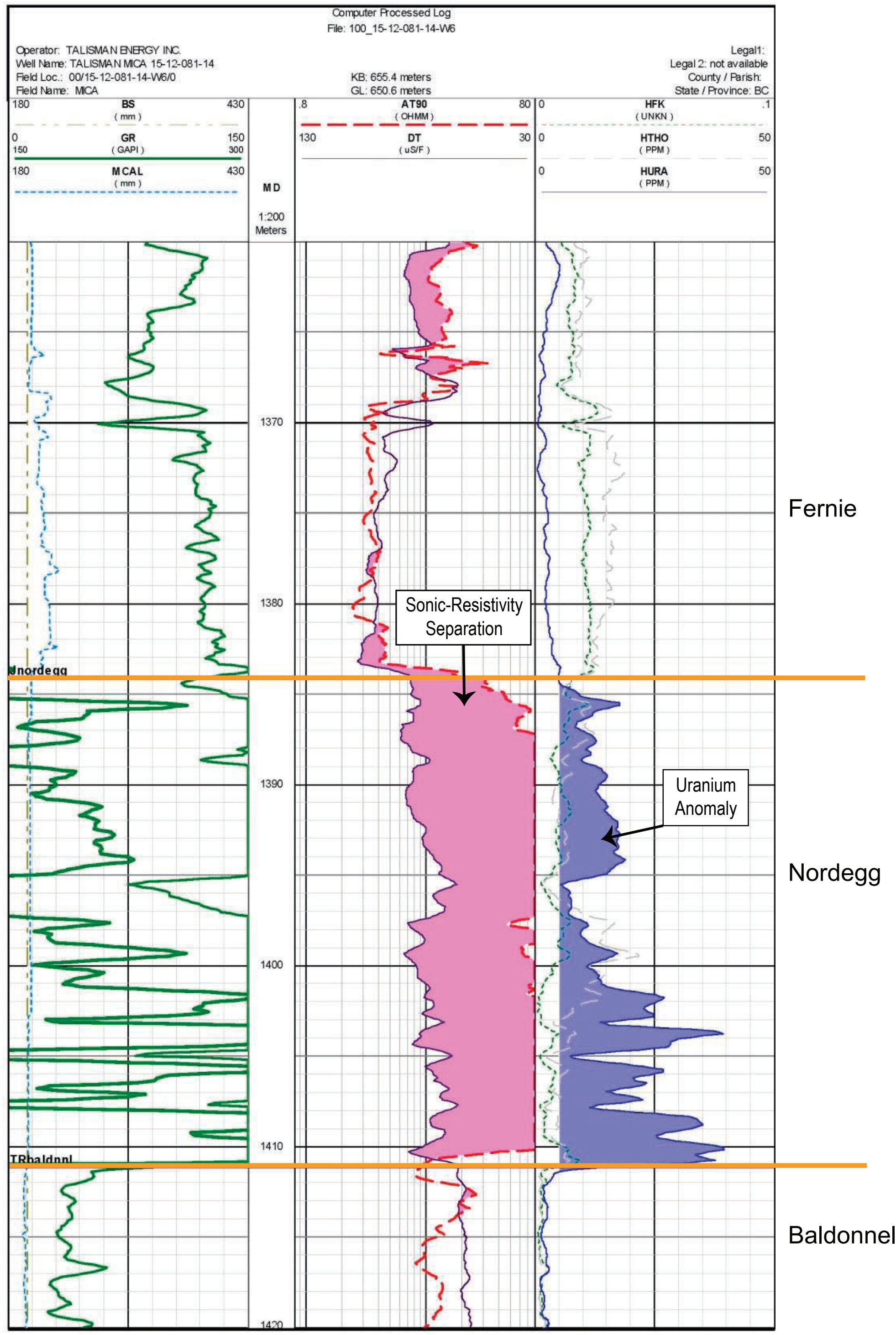

G10b

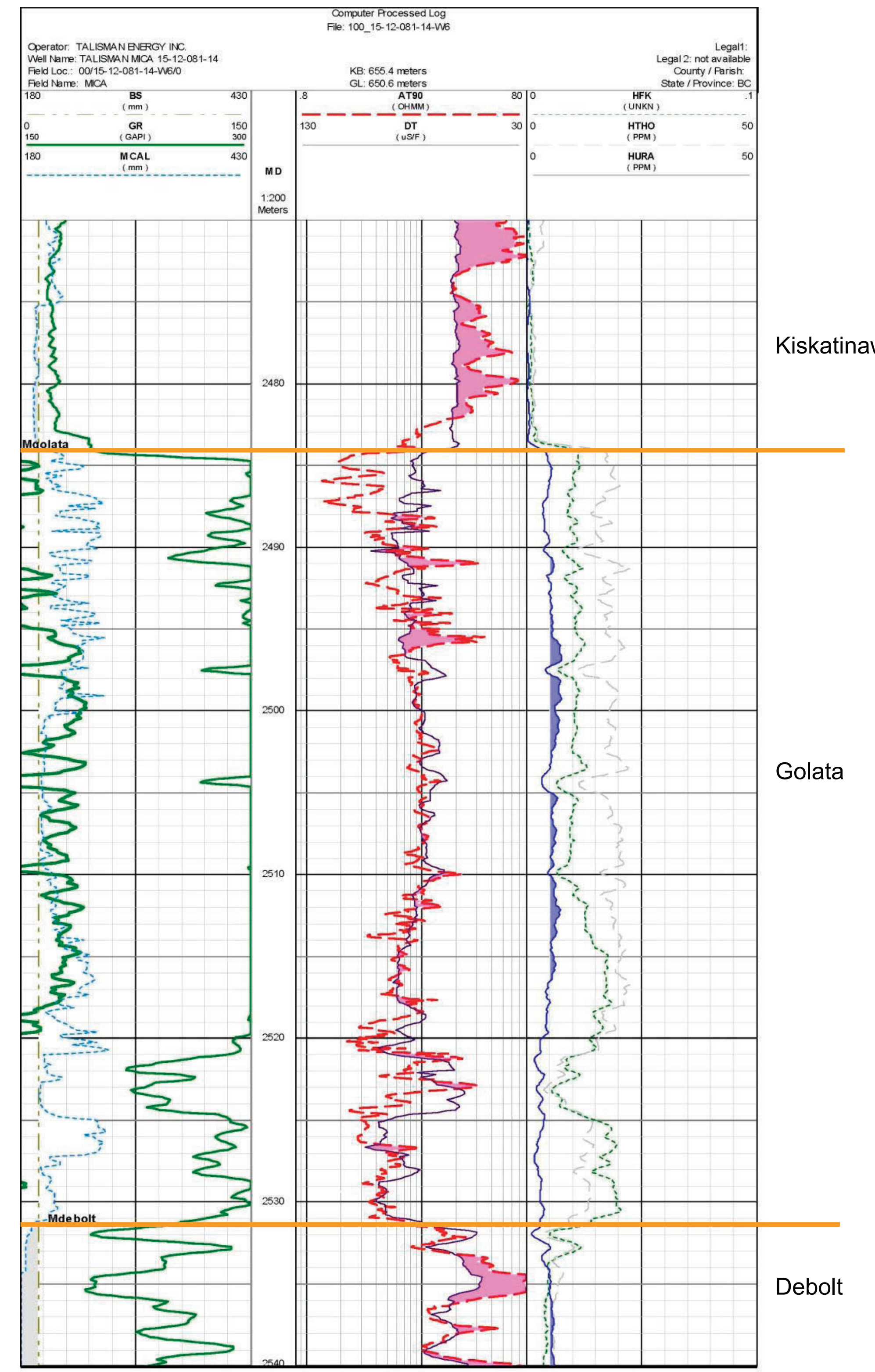

Figure G10. Passey analysis output logs for wells in the Nordegg (G10a) and Golata (G10b) sections. Large sonic-resistivity separation (coloured pink) and uranium anomaly indicate high organic matter content in the Nordegg; lack of these indicators demonstrate very low organic matter in the Golata.

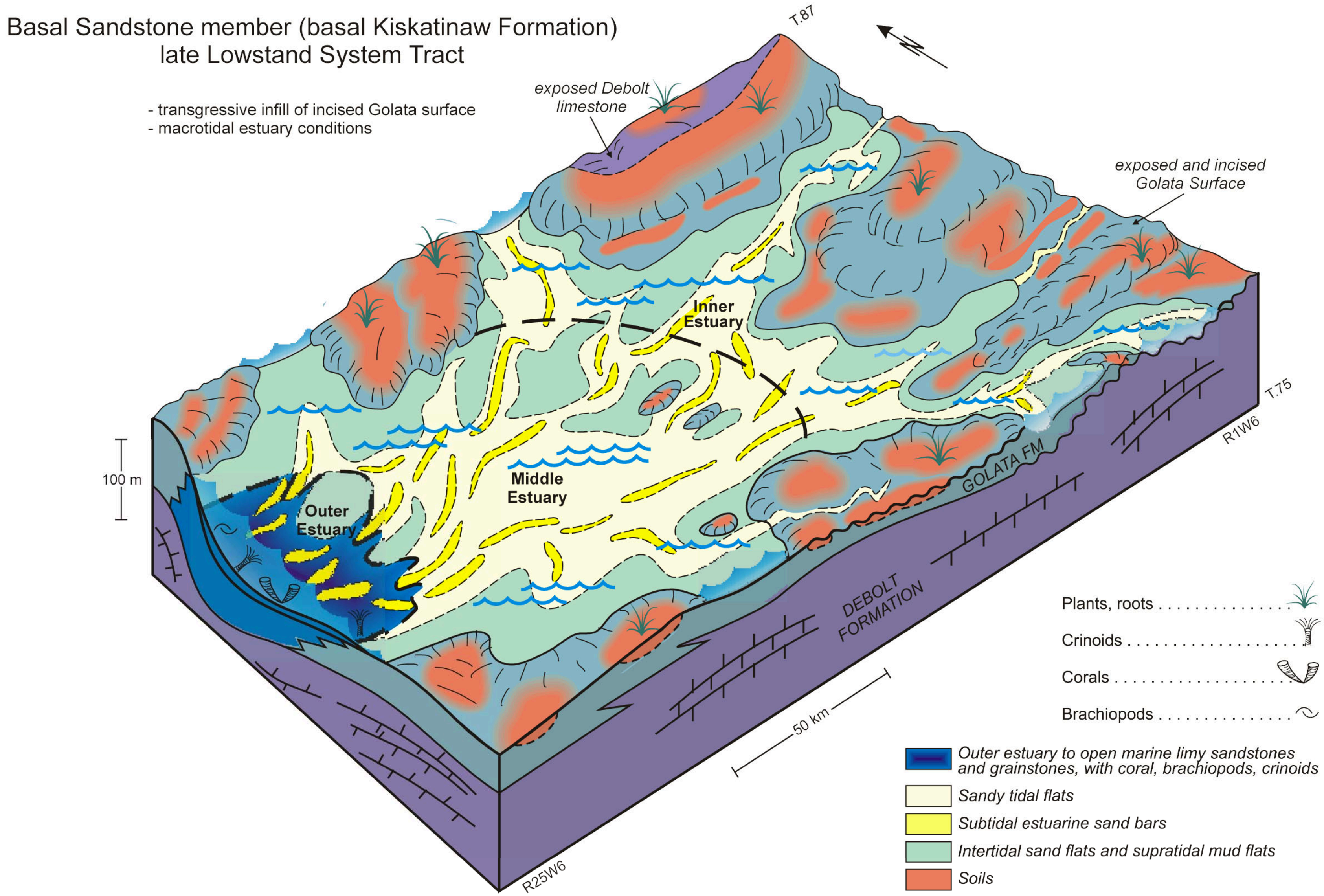

Figure KI1. Schematic deposition of basal Kiskatinaw Formation (from Barclay et al., 2002).

relationships are poorly understood within the Taylor Flat because of poor core control and lack of productive zones that would stimulate more detailed coring and study. Picking the top Taylor Flat is “problematic” because lithologies are similar to the lower part of the Belloy, and strong regional log markers are lacking (Barclay *et al*., 1990). To the northwest in the deformed belt, Kiskatinaw and Taylor Flat strata become more thinly-bedded and difficult to correlate as they pass to more distal marine facies. As well, significant structural deformation introduces correlation uncertainties.

Map KI1, a total isopach map of the Kiskatinaw (top Kiskatinaw to top Golata, or to top Debolt where the Golata was not picked), illustrates the influence of pre- and syn-depositional faulting on Kiskatinaw deposition. Substantial thickening occurs through the central axis of the Fort St. John Graben (Twp 81-83) (Cross-section Stoddart-Stoddart’). The northerly zero edge of the Kiskatinaw is controlled by faults on the northern side of the complex, some of which show throws up to 600 metres. Abrupt stratigraphic changes across faults in this area can make it difficult to distinguish Belloy sandstones where they lie directly on Kiskatinaw sandstones, as in the Eagle area. South of Twp 80, limited well control shows thinner but still substantial Kiskatinaw deposition. Locally, abrupt changes in Kiskatinaw thickness reflect syn-depositional movement along individual faults within the Fort St. John Graben, as illustrated schematically in Fig. G3. We have interpreted the presence of short fault segments in several locations to explain such thickness variations, particularly in the Monias (Twp 81-82, Rge 20-22W6) and Parkland (Twp 81, Rge 15-16W6) areas.

A burial depth map was not prepared for the Kiskatinaw; instead, refer to Map G2, the burial depth map for the Golata Formation, immediately below the Kiskatinaw.

Reservoir Development

Basal channel sandstones up to 30m thick are the primary reservoirs in the Kiskatinaw (Fig. KI2). Kirkland and Hutcheon (1991) noted that fine- to medium-grained quartzose sandstones are variably cemented with quartz overgrowths, dolomite, and anhydrite. However, there has also been substantial porosity enhancement through dissolution of these minerals, and substantial creation of microporosity through alteration of less abundant minerals. Kirkland and Hutcheon (1991) concluded that enhanced porosity may be the product of fluid interactions facilitated by faulting and unconformity relationships where the Kiskatinaw has been eroded.

Figure KI3 demonstrates a typical range of conventional reservoir quality in clean Kiskatinaw sandstones (grain density <2690 kg/m^3), with porosities ranging up to 14% and permeabilities to a few hundred millidarcies. There are a few low-porosity/high-perm samples likely representing fractures, and a substantial fraction of tight (<1mD) samples. A secondary “best fit” line fits a subset of the data at low porosities. This and the mathematical best fit line, which fits higher-porosity samples better, suggest there may be a bimodal population of rock types, possibly related to grain size or the degree of silica cementation. Using the secondary “best-fit” line, 6% porosity equates to a broad range of permeabilities around 2-3 mD.

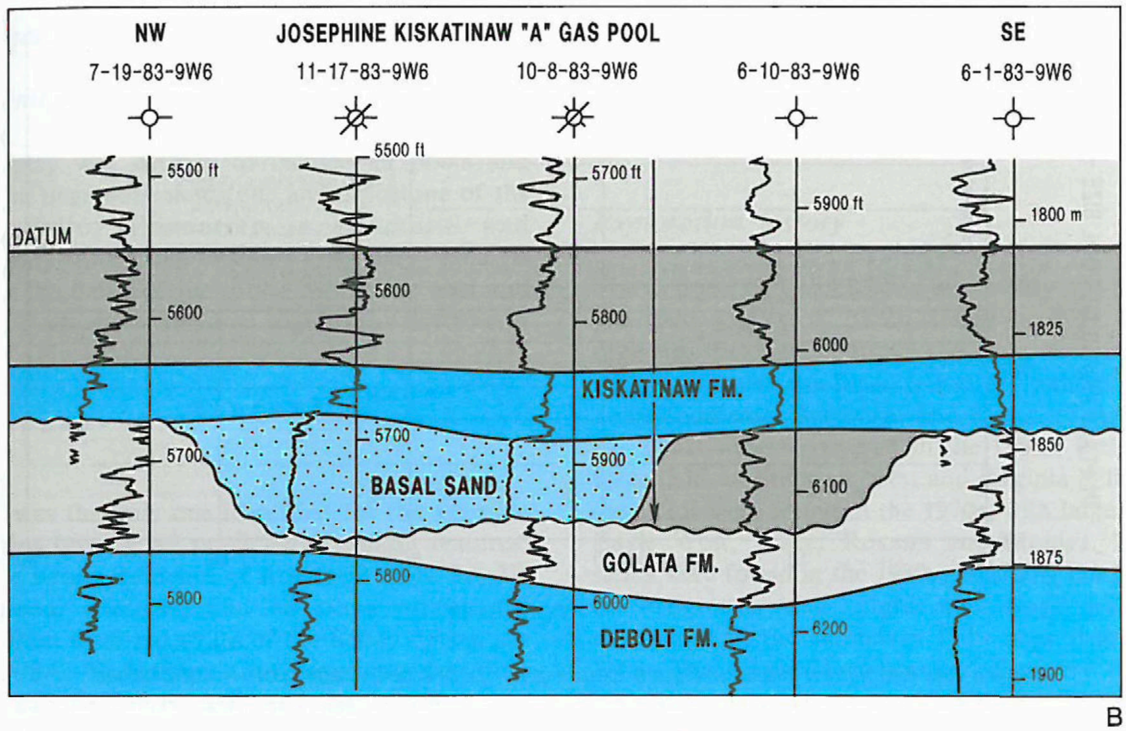

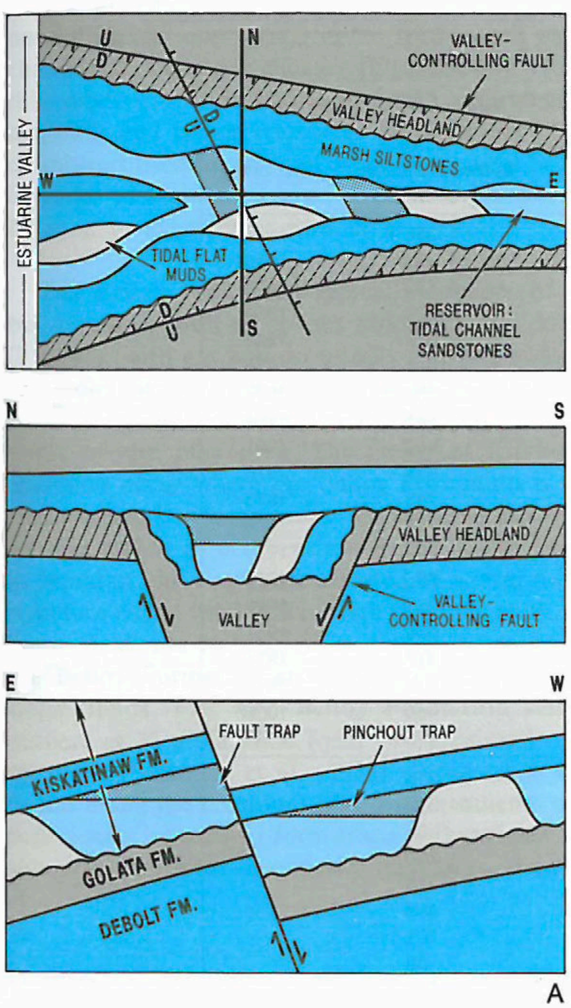

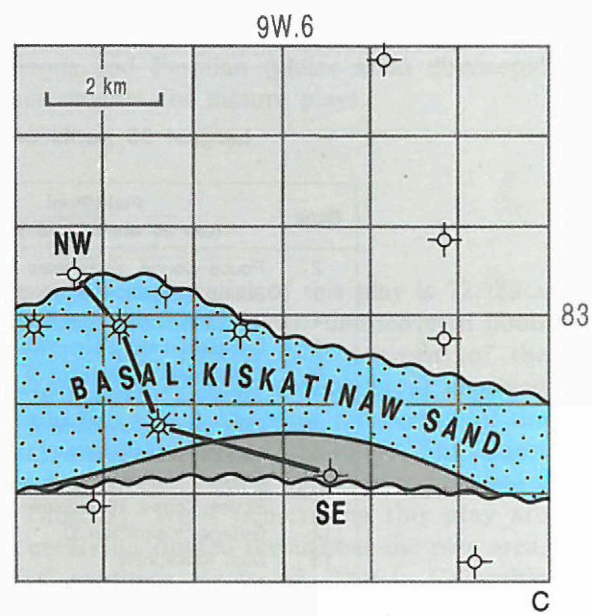

Figure KI2. Basal Kiskatinaw reservoir development and structural-stratigraphic trapping relationships (from Barclay et al., 1997).

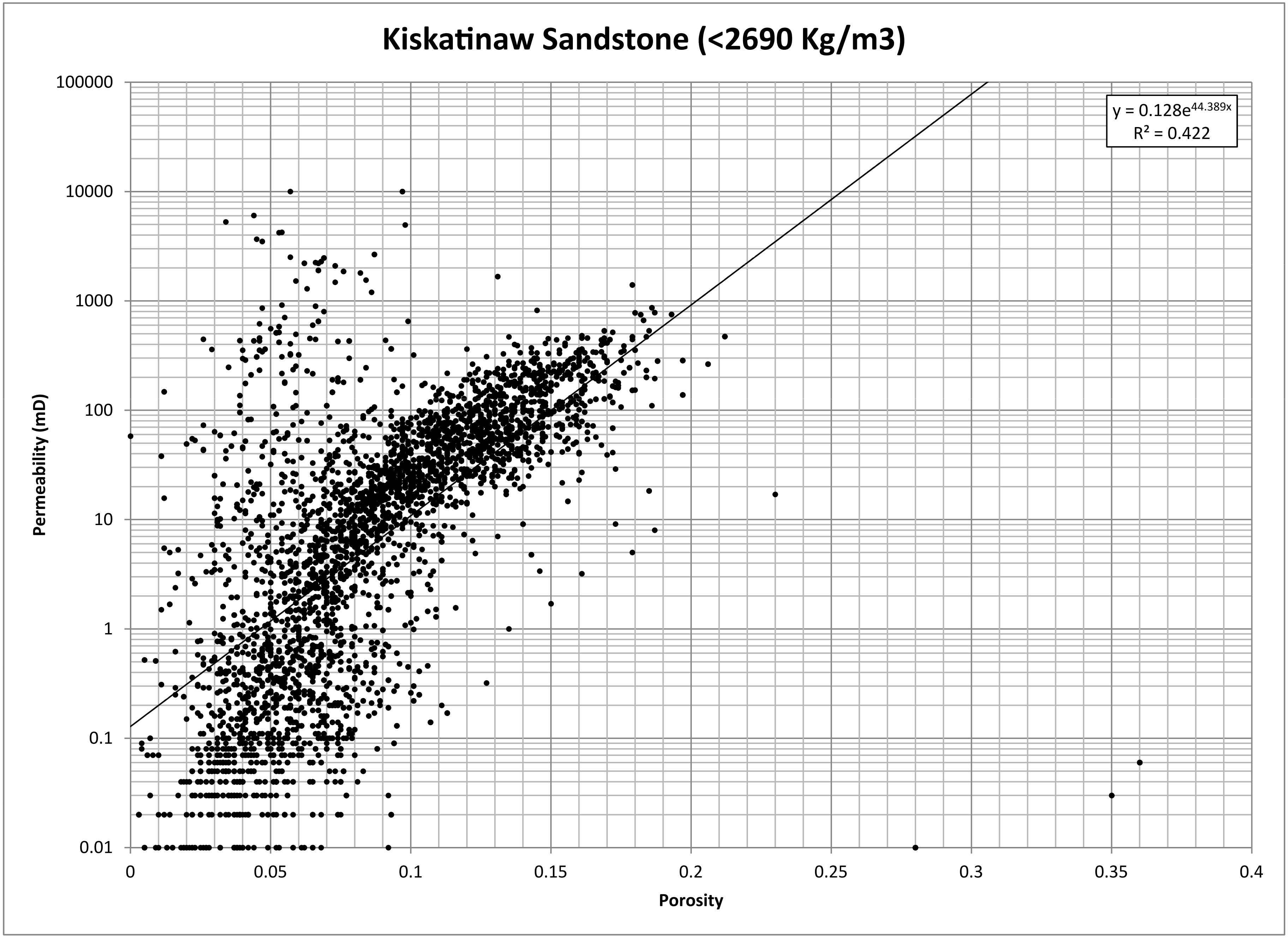

Figure KI3. Porosity / permeability cross-plot, Kiskatinaw sandstone.

Figure KI4 shows reservoir quality in Kiskatinaw mixed lithologies (grain density 2690 to 2770 kg/m^3, indicating substantial amounts of denser minerals and cements). There is more scatter, ranging from tightly-cemented samples to porosities up to 20%, probably the result of diagenetic enhancement.

Map KI2 illustrates distribution of net porous Kiskatinaw sandstones, using a porosity cut-off of 6% (sandstone density log) in combination with a soft gamma log cut-off of 75 API units. Contours are drawn on a regional basis and are generalized; more detailed local mapping using seismic would show more intricate, compartmentalized reservoir bodies. Almost all net porous reservoir sandstone occurs within thick basal sandstones; thinner sandstones higher in the section tend to be more cemented and less continuous. Based on Kirkland and Hutcheon's (1991) conclusions, the most continuous porous sandstones should occur close to the northern subcrop edge.

Production and Test Data

Kiskatinaw sandstones produce gas from structural / stratigraphic traps in the Fort St John graben in western Alberta and into the easternmost townships of the Peace River Block in B.C. (Map KI1). Oil production occurs only from the Eagle Field (Twp 84-18W6), where stacked Belloy and Kiskatinaw sandstones are both oil-bearing, and in scattered wells to the east near the Alberta border. Oil production at Eagle appears to be at least in part a function of local charge; both the Belloy and the Montney also produce oil in this area, and primarily gas elsewhere. We suggest there may be an element of deeper structure that favours oil migration in this area, as there appears to be in the Desan / Helmet area.

The Belloy/Kiskatinaw stacked reservoirs at Eagle are mature fields, under waterflood using vertical wells. Water cuts and pressures vary widely, suggesting stratigraphic and structural compartmentalization within the field area, and possible optimization potential. Overall, the field area is small – only several sections, and appears tightly bounded by both significant faults and abrupt reservoir facies changes.

There have been no horizontal wells drilled in the Kiskatinaw in NEBC.

Analytical Data

While there are many Stoddart / Kiskatinaw cores, the only analytical report for Stoddart Group strata in the BCOGC database other than routine core analyses and large-interval source rock analysis on cuttings is a petrography study on 12 samples from the Taylor Flat Formation in Township 80-19W6 (Appendix 1). We did not undertake any additional analytical work.

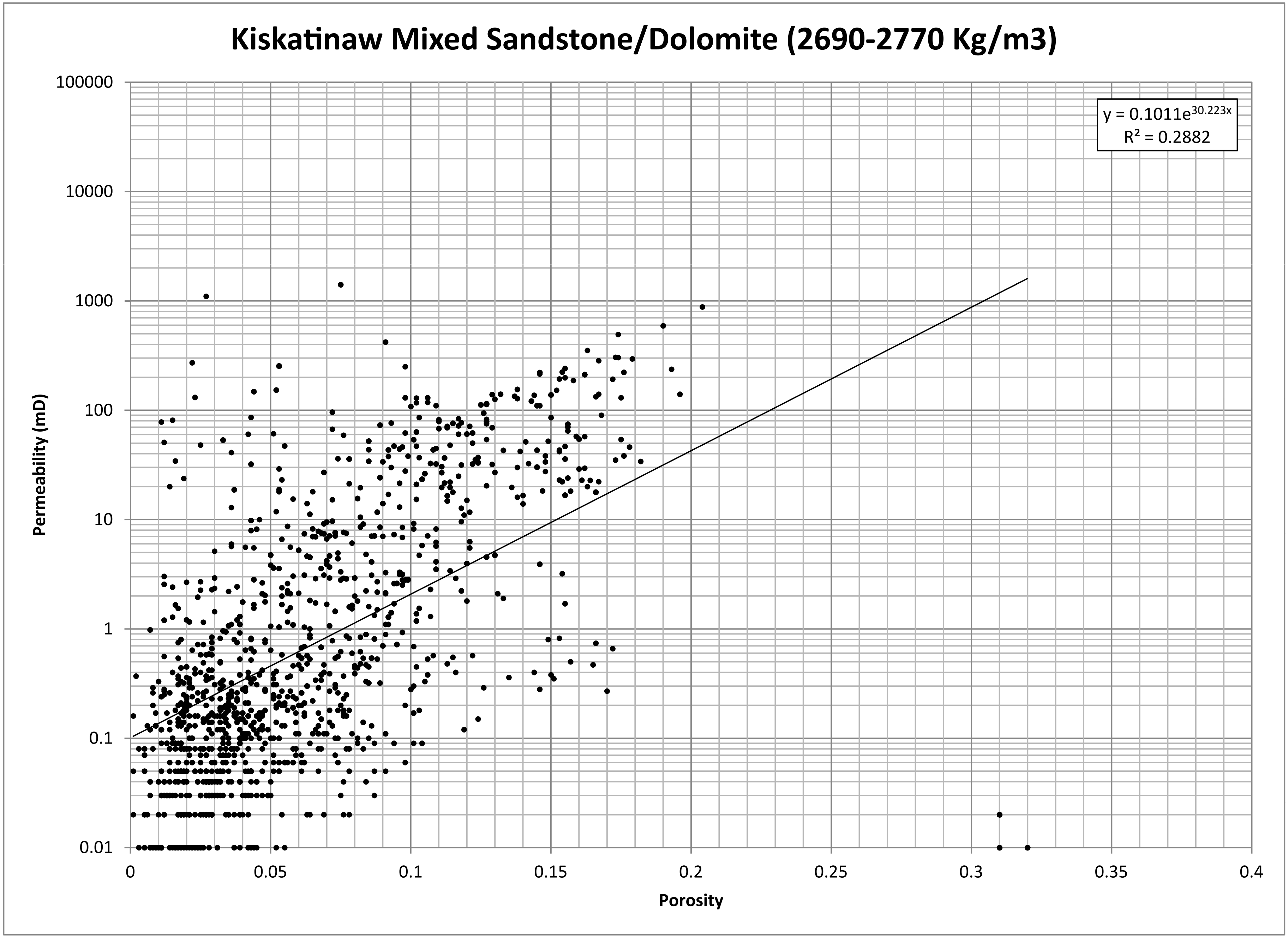

Figure KI4. Porosity / permeability cross-plot, Kiskatinaw mixed lithologies.

Resource Oil Assessment

Widespread gas production and only very local oil production preclude realistic potential for new areas with resource oil prospectivity in the Kiskatinaw and Taylor Flat.

We see little halo oil potential offsetting existing production for a number of reasons:

- The oil-producing area at Eagle is very tightly bounded by both structural and stratigraphic elements;
- Thick basal Kiskatinaw reservoirs are strongly channelized, and offer little potential for halo facies with unconventional reservoir potential;
- Thinner sandstones and sandy carbonates higher in the Kiskatinaw and Taylor Flat section tend to be thin and tightly cemented, making it difficult to map out unconventional potential in thin stacked reservoirs overlying the oil-bearing basal reservoirs.

BELLOY FORMATION

Age and Play Type

Permian – Halo Oil Play (tight sandstone)
Prospectivity: 'C' Play - Little evidence of mappable trends or productive characteristics to suggest halo or tight oil potential.

Regional Geology

Barclay *et al.* (1997) summarized the Belloy regionally:

> The Belloy was deposited within the Peace River Embayment in a relatively tectonically stable, shallow-water, marine shelf setting characterized by mixed carbonate and siliciclastic deposition. An eastern facies assemblage of dolomitic sandstone and dolostone coquinas belong to tidal shoreline environments. Thicker deposits consisting of siltstone and limestone in the western parts of the Peace River Embayment are interpreted as deeper water, outer shelf to basinal sediments. Exposure and erosion at the Permian-Triassic unconformity caused an influx of chert and silica cements into the uppermost Permian units and also caused the isolation of reservoir units at the top of the Belloy.

In northeastern B.C., the Belloy overlies interbedded sandstones and carbonates of the Taylor Flat Formation unconformably, and exhibits internal complexity marked by several unconformities (Fig. BL1). Taylor Flat and Belloy strata have not been

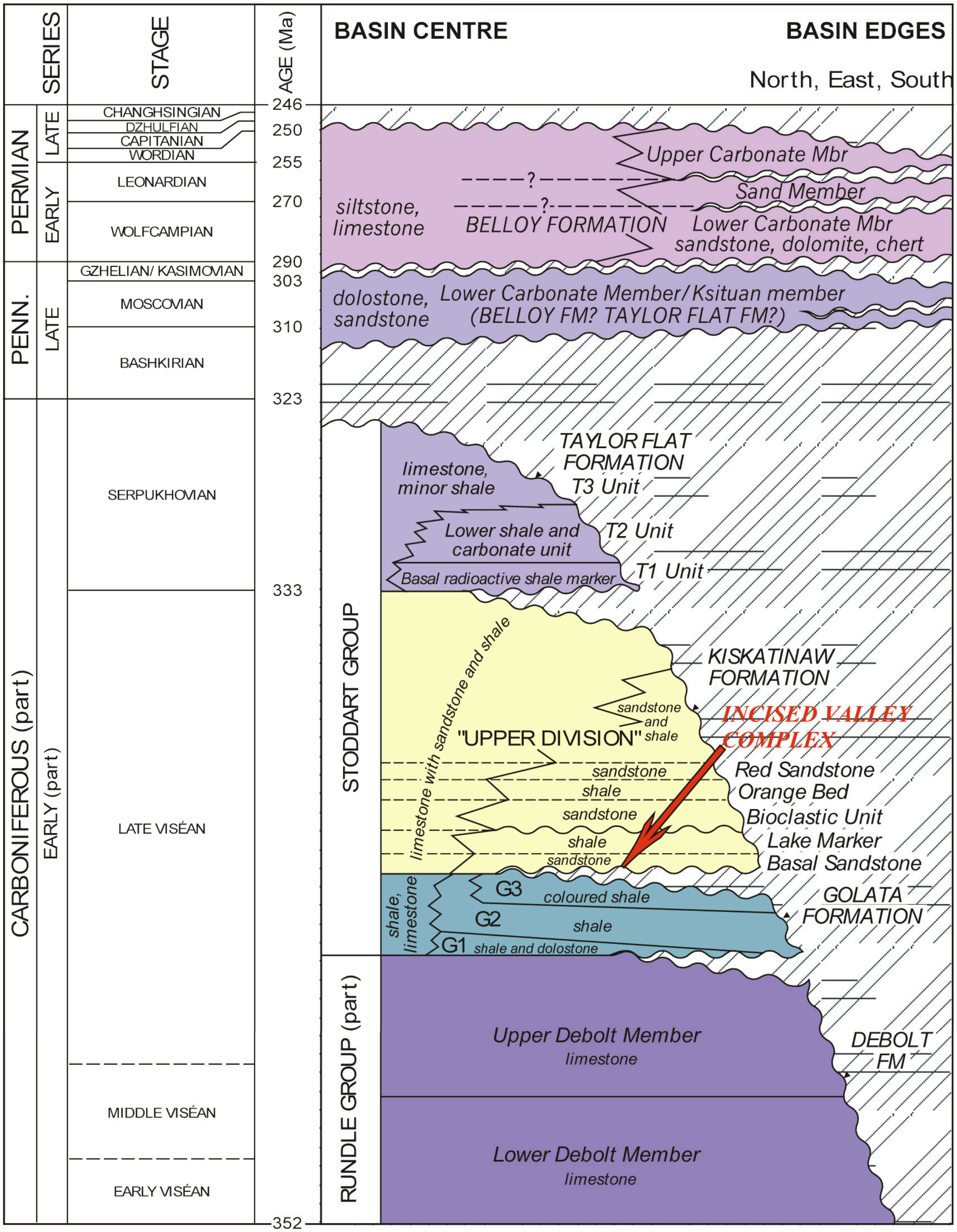

G1: *Basal transition unit of shales and carbonates*
G2: *Black shales*
G3: *Coloured shale exposure surface*

Figure BL1. Schematic internal stratigraphy of Kiskatinaw through Debolt succession, Fort St. John Graben of northeastern B.C. and adjacent Alberta (from Barclay et al., 2002). Note complex internal stratigraphy of Belloy Formation, including internal unconformities.

consistently and clearly distinguished in the literature, and thus were not differentiated for our mapping in this study. Fossenier (2001) completed a comprehensive analysis of Belloy strata in B.C., including core descriptions and extensive biostratigraphic analysis focused on conodonts, documenting extreme lithological and stratigraphic complexity. However, we cannot carry Fossenier's biostratigraphic correlations with confidence where core data are lacking, and for the purposes of this study have mapped the Belloy as a single unit.

Towards the margins of the Fort St. John Graben, Belloy strata lie unconformably on the Kiskatinaw and Golata (Fig. G4). The top of the Belloy is a regional unconformity surface, and is overlain everywhere by distinctive thick siltstones of the Montney Formation. In most places, the contact is marked by "hot" gamma log spikes on well logs and an unconformity surface mantled by chert-pebble conglomerate (Cross-section Stoddart-Stoddart').

Furthermore, where Belloy carbonates were deposited directly on the Debolt (as at the western and eastern edges of Fig. G4), they cannot be reliably distinguished without core and biostratigraphic control. For the purposes of this study, where the Montney lies directly on a carbonate section with no direct evidence of Stoddart Group strata below, we have chosen to assign the entire carbonate succession to the Debolt.

Map BL1, a total isopach map of the Belloy (top Belloy to top Kiskatinaw, or to top Golata where the Kiskatinaw was not picked), includes undifferentiated Taylor Flat Formation strata. Abrupt thickening of the succession south of the graben-bounding faults in Twp 83-85 reflects syn-depositional thickening, primarily within the Taylor Flat Formation (Fig. G3, Cross-section Stoddart-Stoddart'). Smaller faults exert more local control, as discussed above for the Kiskatinaw Formation. North of the main Fort St. John Graben bounding faults, where isopachs are 50m or less, there is little or no Taylor Flat, and the mapped section is made up entirely of Belloy strata. We can draw the 25m contour with confidence, but it is difficult to delineate a Belloy zero edge.

Map BL2 illustrates drill depth to the top of the Belloy. Fault lines were used to constrain computer contouring, which in places has produced unrealistic values (*e.g.*, fault wedge in Twp 83-84, Rge 20-21W6). While drill depths to the Belloy are 2300m or less over much of area, they are generally >3000m south of Twp 78.

Reservoir Description

Various workers have interpreted Belloy stratigraphy and reservoir distribution locally. In the Eagle / Stoddart area (Twp 83-86, Rge 17-21W6), Young et al. (1993) and Leggett et al. (1993a, b) documented sandstone-dominated shallow marine facies cut by a variety of channels filled with sandstones, exhibiting excellent reservoir quality in places (Fig. BL2).

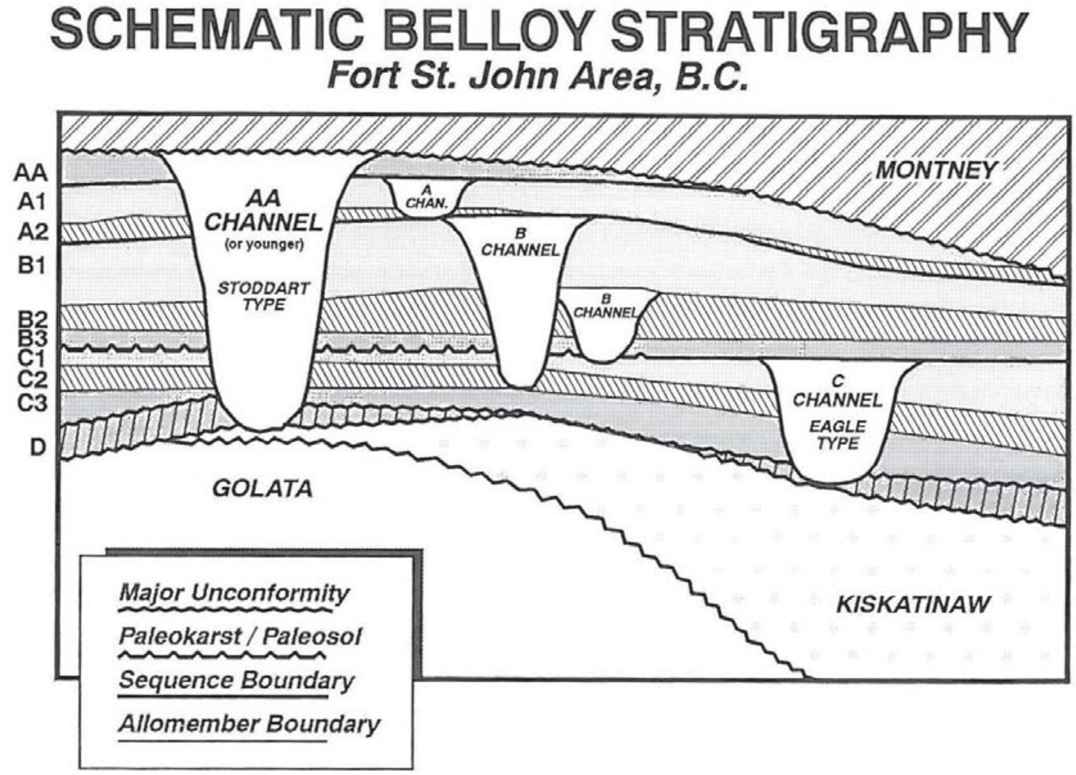

Figure BL2. Schematic Belloy stratigraphy, Eagle / Stoddart area (from Leggett *et al*., 1993b).

At Boundary Lake (Twp 84-14W6), Bloy and Scott (1993) showed Belloy reservoirs to occur in stacked shoaling-upward successions capped by carbonate grainstones and sandstones (Fig. BL3). Local faulting controlled both reservoir preservation (protecting it from post-Belloy erosion) and structural entrapment of gas. This study provides a good illustration of the intricate interbedding of sandstone and carbonate reservoirs in the Belloy.

Figures BL4 to BL6 show three porosity-permeability cross-plots for the Belloy. Data have been binned according to grain density as sandstone (grain density <2690 kg/m^3), mixed lithology (primarily carbonate-cemented sandstones and limestones) (grain density 2690 to 2770 kg/m^3), and dolomite (either dolomites or heavily cemented/mineralized sandstones (grain density >2770 kg/m^3). All three plots are dominated by a fairly good linear poro-perm relationship, with a scattering of low-porosity, high-permeability values that can be attributed primarily to fractures. The fracture values skew the mathematically-derived best-fit line, and make it difficult to achieve a high correlation coefficient. Unlike the Kiskatinaw, good reservoir quality occurs in all three lithological bins, consistent with the observation that there are porous / permeable carbonates in the Belloy.

Map BL3 illustrates distribution of net porous Belloy reservoir, primarily within the upper 50-75m of the formation. Recognizing the mixed lithologies present in the Belloy, we attempted to attain a porosity cut-off of approximately 6%, in combination with a soft

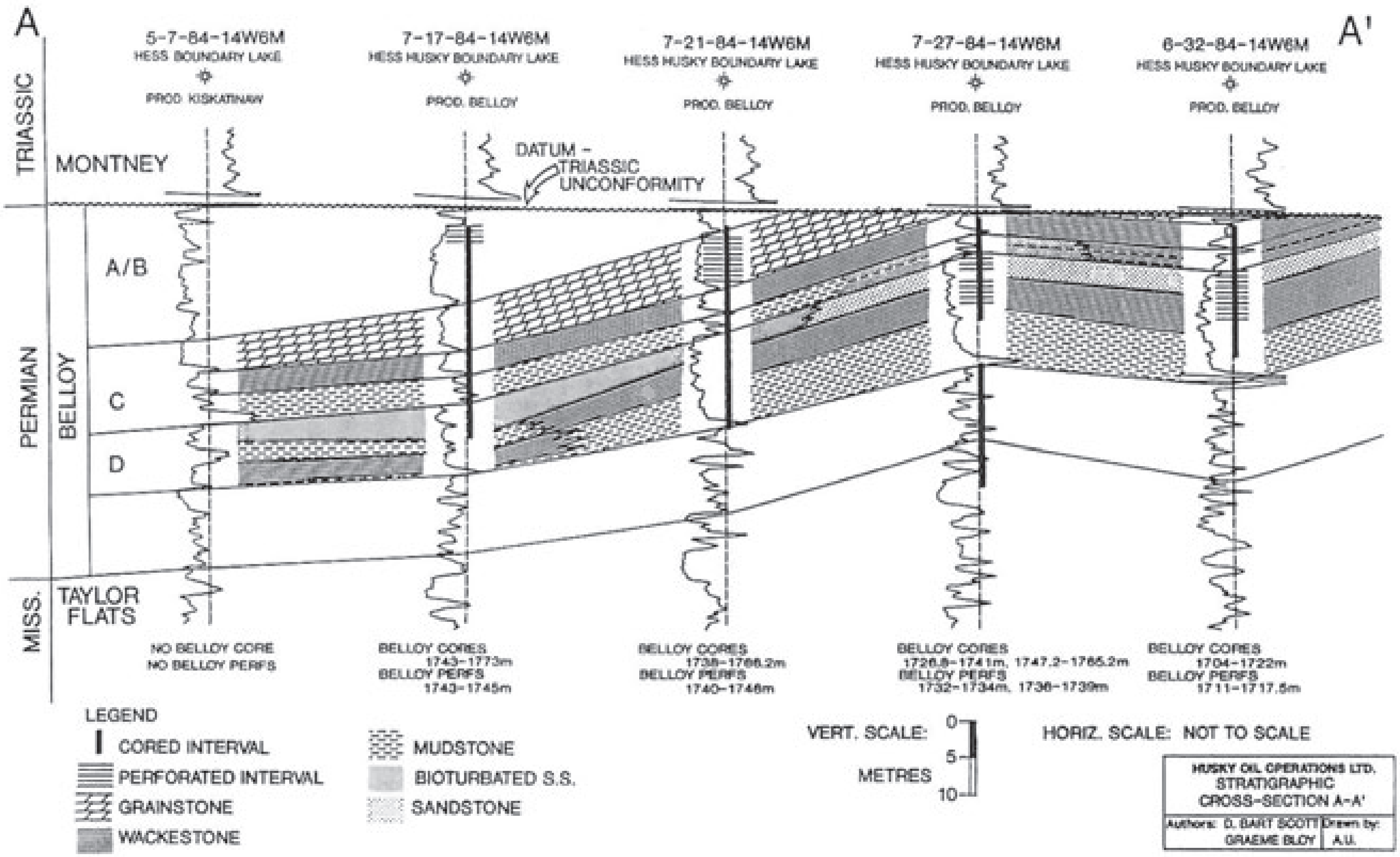

Figure BL3. Stacked shoaling-upward Belloy reservoirs at Boundary Lake (from Bloy and Scott, 1993).

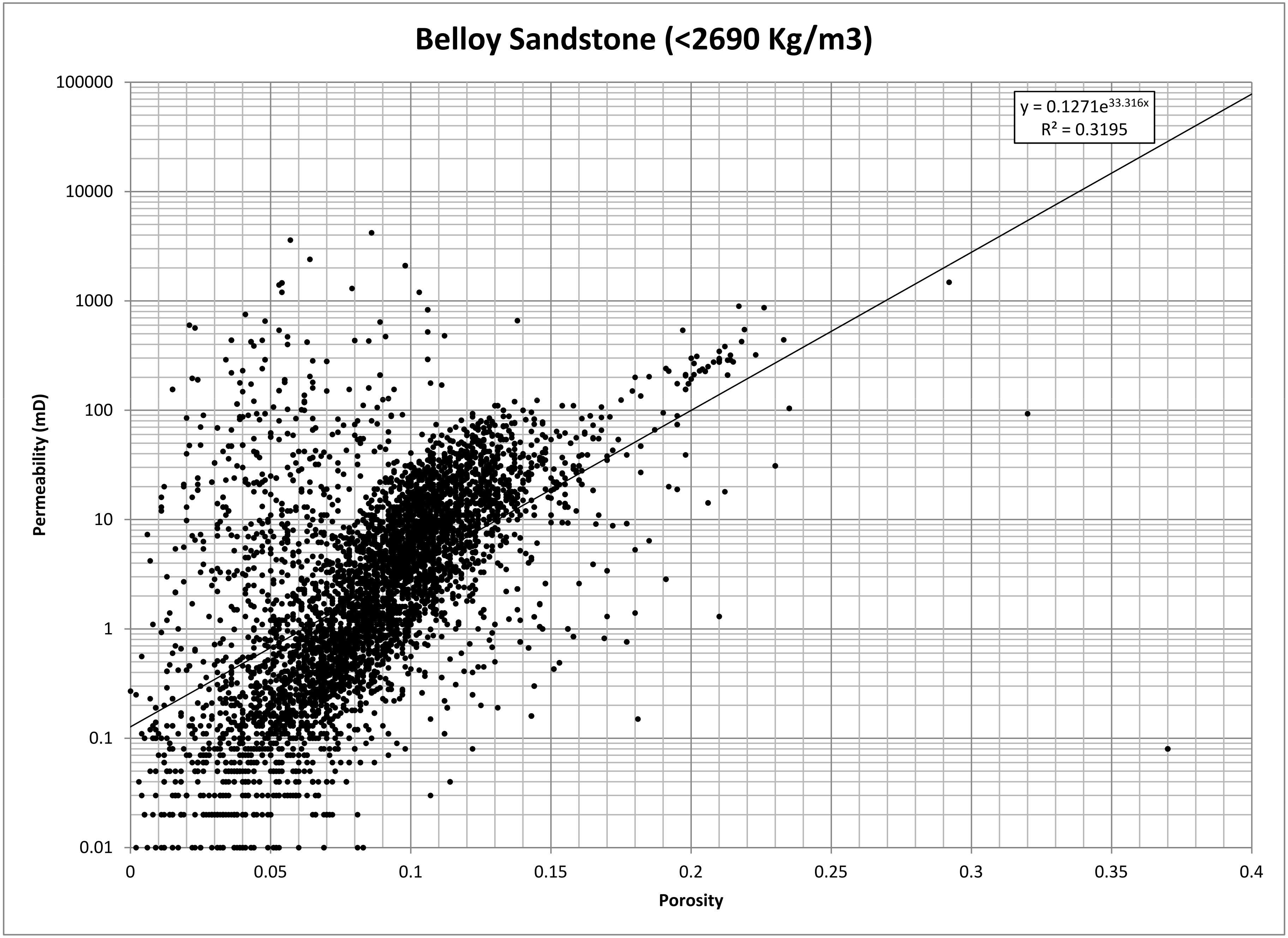

Figure BL4. Porosity / permeability cross-plot, Belloy sandstone.

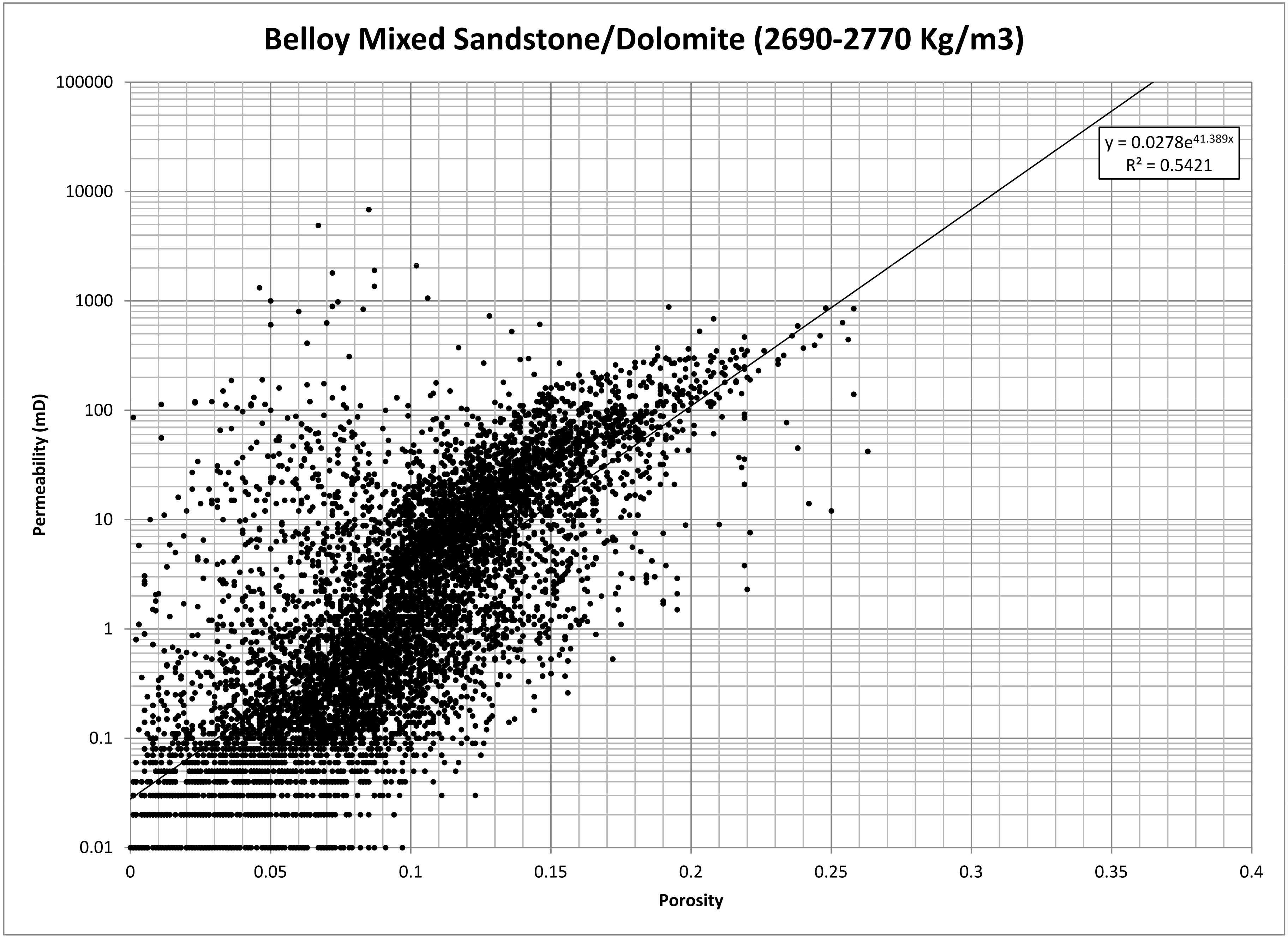

Figure BL5. Porosity / permeability cross-plot, Banff mixed lithologies.

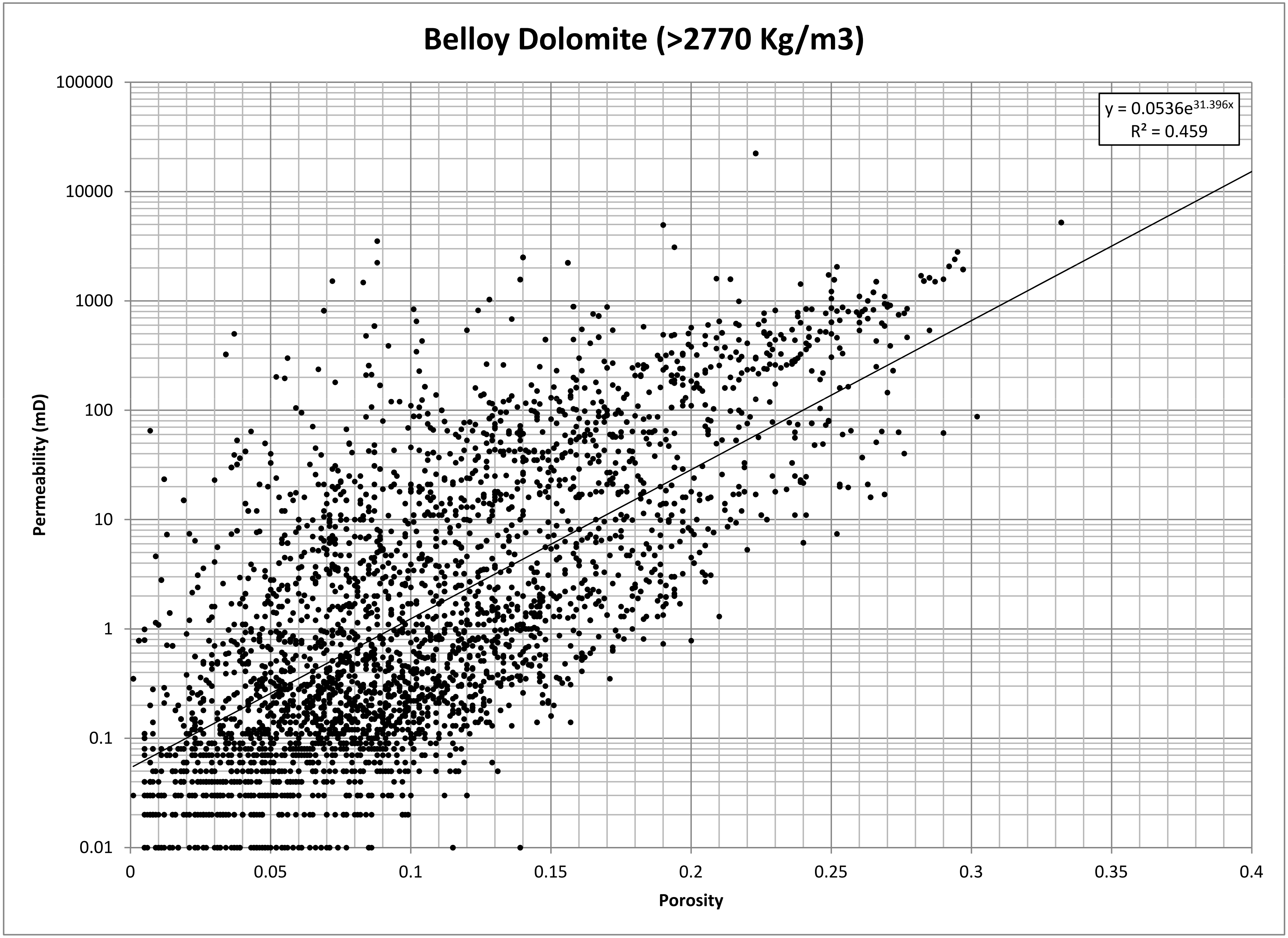

Figure BL6. Porosity / permeability cross-plot, Belloy dolomite.

gamma log cut-off of 75 API units. Where clean sandstone facies are present, as at Eagle and Stoddart, the sandstone density scale was used. Elsewhere, we looked for porosity log deviations from background and the presence of SP log deflections and even filter cake on the caliper log to indicate presence of permeability. Where information was inconclusive, we tended toward an optimistic interpretation of porous reservoir thickness. We calibrated porosity values to core where available; unfortunately, wellsite sample cuttings log interpretations are generally not adequate to support porosity / permeability assessment.

Substantial thicknesses of net porous reservoir are present in the Belloy in most wells in Twp 79-85, and as far west as Rge 19 and 20W6. Faults delineating the northern flank of the Fort St. John Graben do not appear to have exerted dramatic influence on net porous thickness. At a regional mapping scale, continuity of net porous zones is difficult to determine, but the widespread presence of some porous reservoir in almost every well in the northeast implies at least some degree of continuity. Systematic thinning of net porous section to the south and west suggests that burial diagenesis has degraded reservoir quality; there is little porous reservoir below a present-day burial depth of 2200m (compare Map BL2).

Production and Test Data

The Belloy is an important oil and gas producer in northeastern B.C.; smaller gas pools in the south are controlled primarily by structure, whereas the large oil and gas pools at Eagle and Stoddart exhibit both stratigraphic and structural controls (Barclay et al., 1997).

Appendix 9 summarizes important characteristics of Belloy oil pools in British Columbia (included in the 'other' tab). Key observations relevant to resource oil potential include:

- The largest existing pool is at Eagle West, where the Belloy 'A' pool contains 149 million barrels of oil originally in place (MMBOOIP) ($23.7e^6m^3$). Two other pools at Eagle and Stoddart contain 56 and 73 MMBOOIP, while the remaining pool each contain <10 MMBOOIP.
- Net pays range 1.5-10.5m, with most between 2m and 7m.
- Most pools are very mature and remaining reserves are relatively small.
- Oil gravities are light to very light.
- Pool average porosities (2-18%) and permeabilities (3-54mD) range from somewhat tight to conventional.
- Recovery factors are modest (20-31%) in many pools, but several pools are expected to recover only 10% or less.
- Only seven original reservoir pressure gradients are available; they range 7.5-9.4 kPa/m; all slightly underpressured.

- Major pools at Eagle and Stoddart are under waterflood.

As noted for the Kiskatinaw, Belloy oil production at Eagle and Stoddart appears to be more a function of local charge than due to particular properties of the reservoir; both the Kiskatinaw and the Montney show similar geographic patterns, producing oil in this small area and primarily gas in surrounding areas.

Horizontal Drilling

As discussed in more detail below for the Charlie Lake, routine database searches for Belloy horizonal wells produce a number of false positives – wells actually completed horizontally in the Montney – because of the way tops data are picked and submitted. Manual checking was required to extract true Belloy horizontals.

Between 1992 and 2010, fewer than 10 horizontal wells were completed in the Belloy, primarily on the fringes of the Eagle and Stoddart fields, looking to enhance oil production rates and recoverable reserves. While most of these wells did produce oil, lack of followup suggests that they were not seen to be economic. However, one horizontal well drilled in 2006 (4-15-85-19W6) has produced $19.2e^3m^3$ oil (121 MBO), and is still producing $9.55m^3/d$ oil with little water production.

Analytical Data

Our database search yielded analytical reports on Belloy cuttings and core from 25 wells (Appendix 1). The most common procedures have been source rock analysis, X-Ray diffraction analysis, and capillary pressure analysis. At least some of these reports are focused on the overlying Montney, with only a few upper Belloy samples included. There has been no geomechanical testing submitted, and just a few petrographic reports.

Resource Oil Assessment

We regard tight oil potential in the Belloy as being small, comparable to the underlying Kiskatinaw / Taylor Flat section. In particular, there is no evidence of oil charge for the Belloy outside of the Eagle-Stoddart area. While this is a larger productive area than for the Kiskatinaw, it is still tightly bounded by faulting and stratigraphic pinchouts. Also as for the Kiskatinaw, we have seen no evidence for systematic development of low-quality / halo facies around the conventional producing reservoirs.

TOAD - GRAYLING FORMATION

Age and Play Type

Lower / Middle Triassic – Tight Oil Play (tight sandstone)
Prospectivity: 'B' Play – May share continuous productive potential with the overlying Chinkeh is some areas, but these have not been mapped out.

Regional Geology

The Toad and Grayling formations were defined in the BC Foothills in the 1940's, and mapping was extended beneath the adjacent Plains as the Toad-Grayling Formation using wells drilled in the 1950's and 1960's. Ferri et al. (2010) described a 600m thick section of the Toad near the Halfway River (NW 94-B-14) as a coarsening-upward succession of distal turbidites, becoming more proximal to the top. They correlated the section with the Doig and Montney of the adjacent subsurface, but did not recognize any specific stratigraphic boundaries that could be matched from surface to subsurface.

For this study, we map the Toad-Grayling only in the Liard Basin – geographically distinct from the Montney-Doig succession further south (Fig. TG1). Some of the original field sections were described in the Triassic outcrop areas in western 94N (Map TG1). In the Liard Basin subsurface, the Toad-Grayling thickens westward from an abrupt, structurally controlled zero edge along the Bovie Fault Zone to more than 900m thick (Map TG1, Cross-section Liard1-Liard1'). Burial depths range from about 800m in the east to >2200m in the west, adjacent to the deformation front (Map TG2). The Toad-Grayling is capped unconformably by the Lower Cretaceous Chinkeh Formation, and unconformably overlies the Permian Fantasque / Kindle succession (Cross-section Liard1-Liard1', Liard2-Liard2').

We examined Toad-Grayling cores from seven locations (Appendix 4):

- Imperial Pan American Tattoo a-26-B/94-O-11;
- Legacy Maxhamish b-19-J/94-O-11;
- ECA Maxhamish b-39-J/94-O-11;
- AEC Maxhamish c-95-J/94-O-11;
- GSENR Maxhamish a-64-B/94-O-14;
- AEC Maxhamish c-16-G/94-O-14;
- ECA Maxhamish d-48-B/94-O-11.

All of these sampled the uppermost Toad-Grayling, as the primary target for coring was the overlying Chinkeh. The sections sampled consist primarily of laminated to rippled

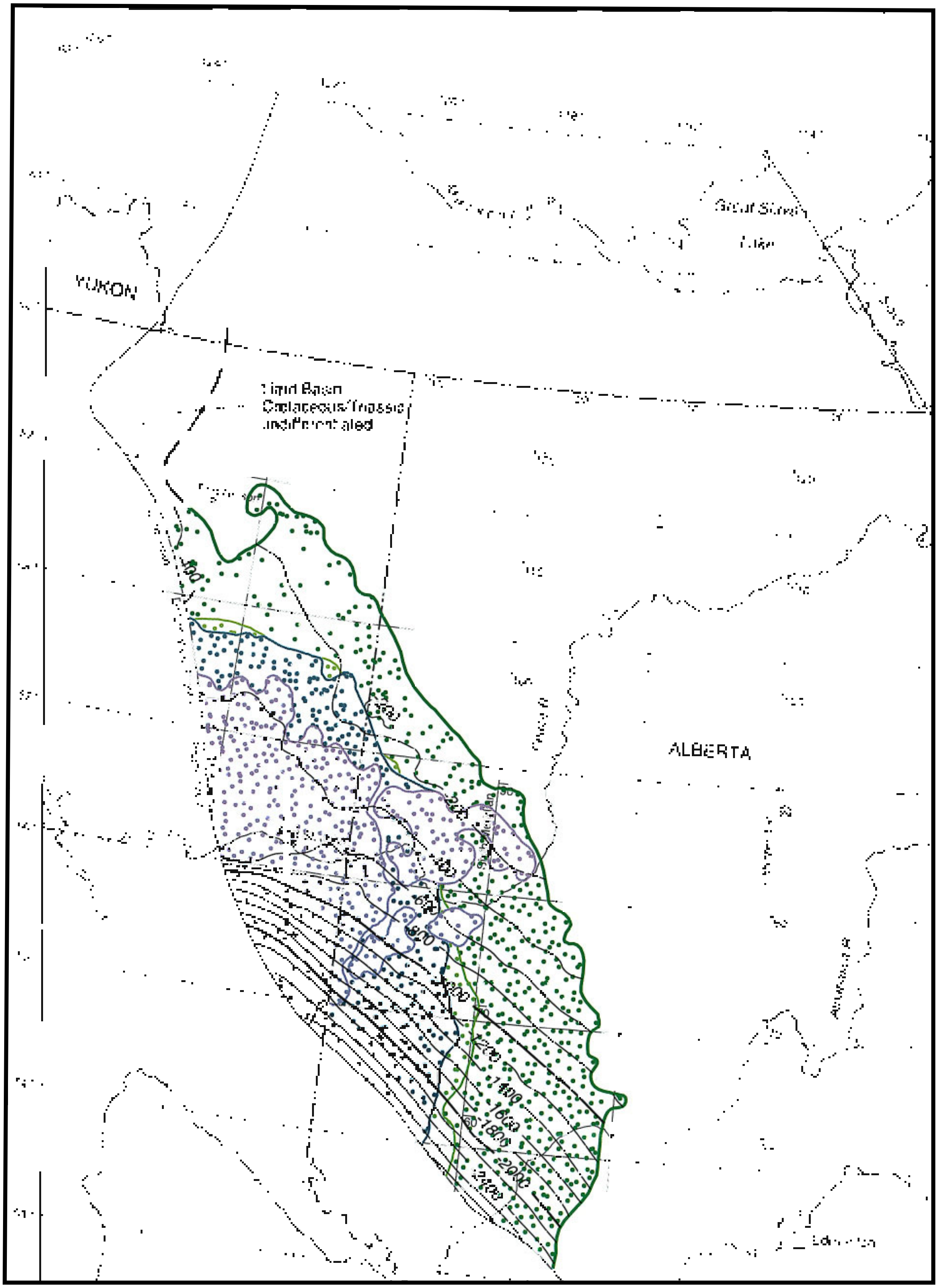

Figure TG1. Triassic structure, WCSB, showing separation of Liard Basin Triassic strata from Triassic units to the south (from Edwards et al., 1994).

lithic siltstones and very fine-grained sandstones, interbedded with dark argillaceous siltstones and silty shales. The Chinkeh/Toad contact is readily apparent in core, but the pick can be difficult on logs and in drill cuttings where the basal Chinkeh is not well developed.

Where the full Toad-Grayling section has been logged, an overall sandier-upward signature is apparent, but consistent internal stratigraphic markers have not been picked (Cross-section Liard1-Liard1', Liard2-Liard2'). Most full penetrations are unfortunately in older wells with less complete log suites; most recent wells have been drilled either for the Chinkeh (and therefore TD near the top of the Toad-Grayling), or for deep Devonian shale plays (and are either confidential or have incomplete uphole log suites). We expect that with better well control, specific stratigraphic subunits including reservoir-quality shoreline sandstones could be mapped as they are in the Montney and Doig in the south.

Reservoir Quality

The Toad-Grayling permeability vs porosity cross-plot demonstrates tight to moderate reservoir quality in the short cored sections sampled, with porosities ranging up to 19% and permeabilities generally <10mD (Fig. TG2). A cluster of data with porosities of 17-19% and permeabilities of 2-20mD may represent better-sorted, more proximal sandstones, while the poorer rock represents more argillaceous, distal units.

More well control and more extensive sampling is required to understand the distribution and continuity of reservoir quality in the Toad-Grayling. Systematic evaluation of available drill cuttings may be useful, even with current well control.

Production and Test Data

Some Chinkeh drillstem tests straddle the upper part of the Toad-Grayling, but we found no standalone Toad-Grayling completions.

Analytical Data

While cores have been taken from the Toad-Grayling in numerous wells, most of these targeted the Chinkeh and sampled only the uppermost Toad-Grayling (Map TG1). Older source rock analysis data are available from about a dozen older wells, mostly as part of long-interval drill cutting evaluation programs (Appendix 1).

In the seven wells cored and sampled for this study, the uppermost Toad/Grayling consists of thinly-bedded to finely laminated siltstones, and highly bioturbated siltstones to mudstones (Appendix 3). Mineralogical analyses show clay- and quartz-rich sediments in sandy units, interbedded with more clay-rich beds (Fig. TG3).

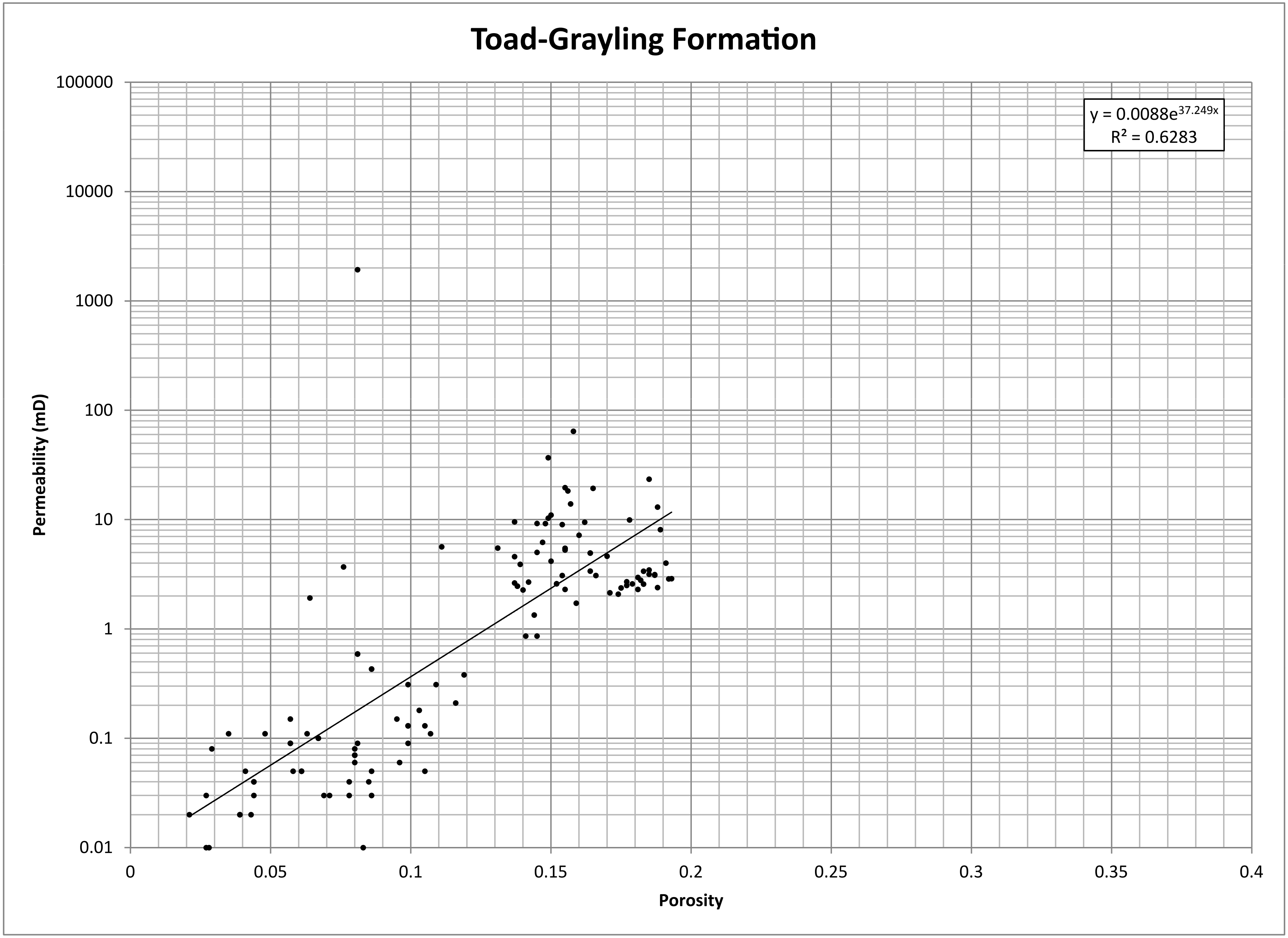

Figure TG2. Porosity / permeability cross-plot, Toad-Grayling Formation, Liard Basin.

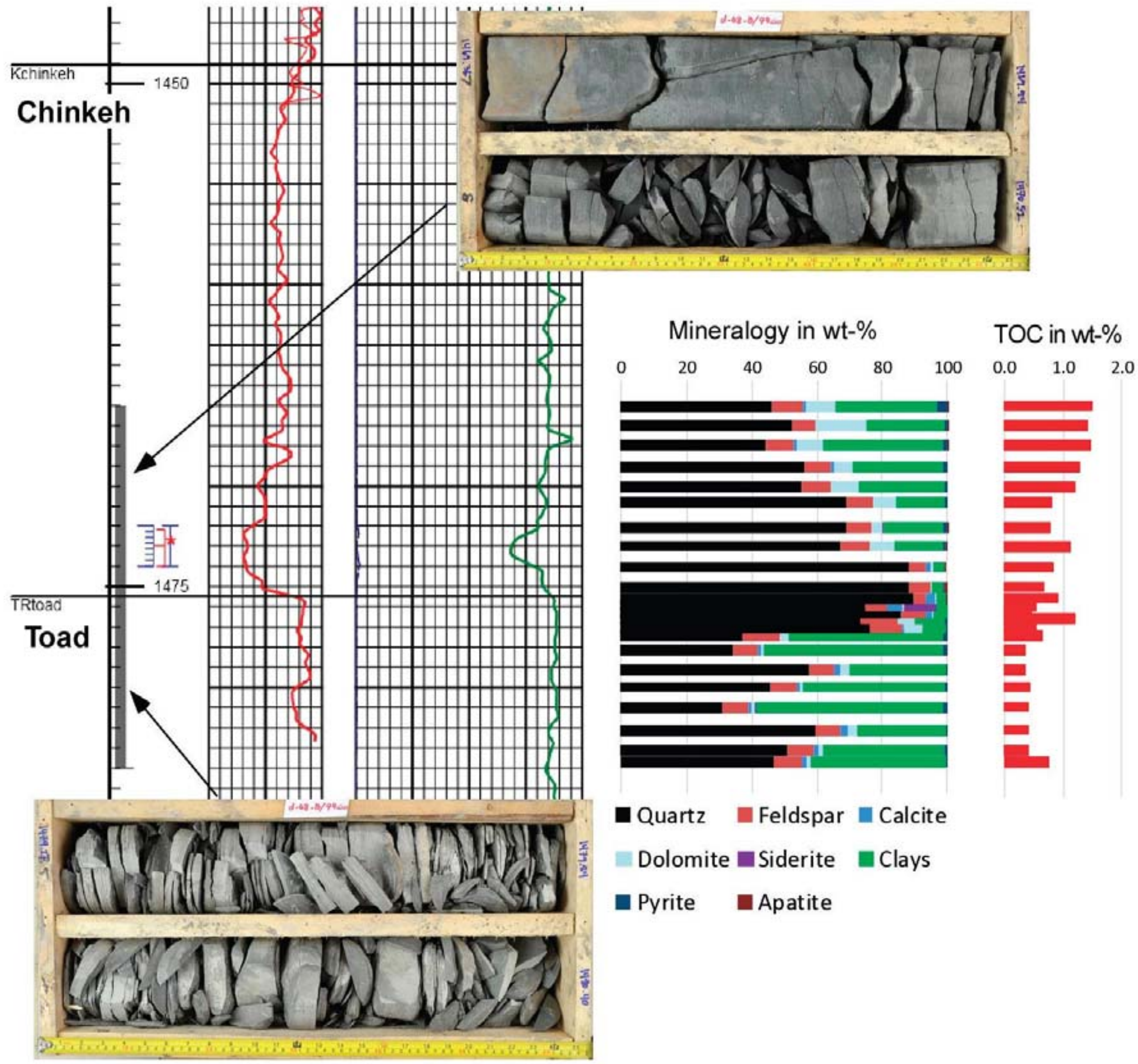

Figure TG3. Mineralogy and TOC plots for samples from the Chinkeh and Toad-Grayling formations, ECA Maxhamish d-48-B/94-O-11.

Feldspar content ranges up to 8%, but some cores completely lack K-feldspars. Calcite, dolomite and siderite are present in minor amounts. Clay minerals include illite and mica clays and chlorite, and in most cores kaolinite is present as well. Pyrite is present in very small amounts.

Total Organic Carbon (TOC) values are generally low, rarely exceeding 0.6 wt%. T_{max} values range between 430-480°C, with an average of around 450°C – a range indicating oil-generating to dry gas generation (Appendix data).

Petrographically, the Toad/Grayling contains clay-rich siltstones to very fine-grained sandstones. Most samples show extensive bioturbation and sediment mixing (Fig. TG4), but bioclasts are absent. Organic matter, including bituminous material, is commonly finely dispersed or in thin short streaks. Under the SEM, clay minerals cover all other mineral phases including quartz and the few feldspars (Fig. TG5).

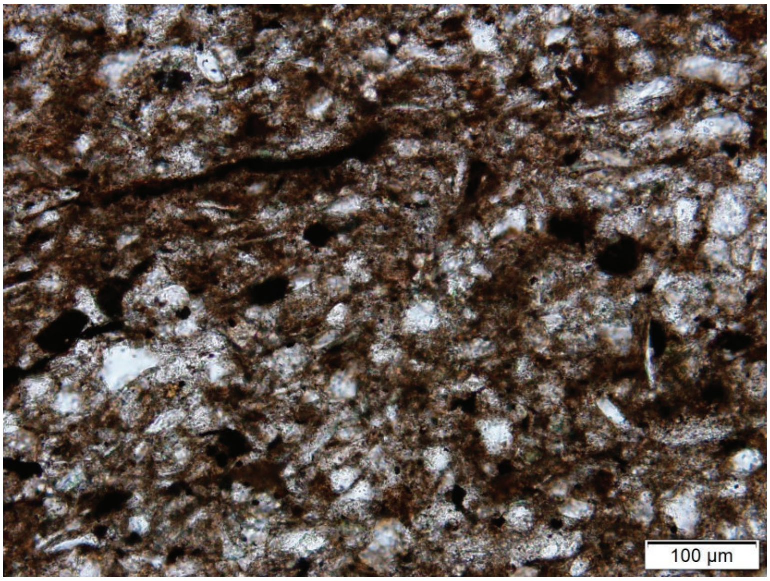

Figure TG4. Photomicrograph, Toad-Grayling Formation, ECA Maxhamish d-48-B/94-O-11 (1480.06-1480.09 m) under plane polarized light. Bioturbated argillaceous siltstone consisting of silt-sized quartz grains in a clay-rich matrix. Organic material and pyrite opaques occur finely dispersed and in streaks.

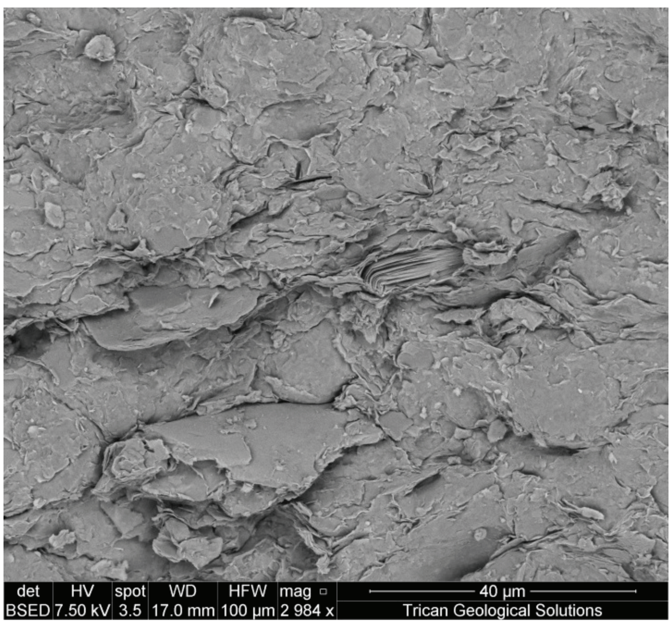

Figure TG5. BSED SEM photomicrograph, Chinkeh Formation, ECA Maxhamish d-48-B/94-O-11 (1480.06-1480.09 m), showing mica and clay minerals embedded in quartz grains coated in clay material. Iron- and magnesium-rich micas may be biotite altering to chlorite.

Unconfined porosities range between 3-8% with a few values up to 17%. Matrix permeability also ranges widely, from 1->100 nD (Table TG1). MICP conformance-corrected porosity is much lower and ranges between 1-3.5%, with one sample having 4.7% (Table TG2). Pore throats in these samples are often very small (<20 nm) (Fig. TG6).

Unconfined Porosity and Matrix Permeability										
Well Name	Well Location	Core Depth (m)	Fm	Density		Porosity (%)	GRI Matrix Permeability (md)		GRI Matrix Permeability (nd)	
				Bulk Density (g/cc)	Skeletal Density (g/cc)		Avg	Std Dev	Avg	Std Dev
AEC Maxhamish	c-016-G/094-O-14	1264.48	Toad/Grayling	2.542	2.702	5.93	8.83E-04	3.80E-04	883.29	379.77
AEC Maxhamish	c-016-G/094-O-14	1265.72	Toad/Grayling	3.010	3.160	4.75				
AEC Maxhamish	c-016-G/094-O-14	1265.73	Toad/Grayling	2.624	2.744	4.38	2.61E-05	1.38E-05	26.08	13.79
AEC Maxhamish	c-016-G/094-O-14	1265.99	Toad/Grayling	2.659	2.746	3.20				
AEC Maxhamish	c-016-G/094-O-14	1267.49	Toad/Grayling	2.629	2.735	3.88				
AEC Maxhamish	c-016-G/094-O-14	1267.62	Toad/Grayling	2.589	2.713	4.59				
AEC Maxhamish	c-016-G/094-O-14	1268.79	Toad/Grayling	2.627	2.725	3.62	1.54E-05	4.79E-06	15.38	4.79
AEC Maxhamish	c-095-J/094-O-11	1516.06	Toad/Grayling	2.501	2.707	7.62	1.17E-04	6.23E-05	117.03	62.35
AEC Maxhamish	c-095-J/094-O-11	1516.65	Toad/Grayling	2.630	2.716	3.16	3.16E-05	9.96E-06	31.57	9.96
AEC Maxhamish	c-095-J/094-O-11	1518.27	Toad/Grayling	2.624	2.752	4.64	3.61E-05	3.76E-05	36.13	37.57
AEC Maxhamish	c-095-J/094-O-11	1519.51	Toad/Grayling	2.597	2.735	5.04	2.34E-05	8.30E-06	23.38	8.30
AEC Maxhamish	c-095-J/094-O-11	1520.63	Toad/Grayling	2.739	2.758	0.69	3.51E-06	3.13E-07	3.51	0.31
ECA ECOG Maxhamish	b-039-J/094-O-11	1869.14	Toad/Grayling	2.337	2.684	12.94	1.64E-04	9.73E-05	163.55	97.32
ECA ECOG Maxhamish	b-039-J/094-O-11	1870.48	Toad/Grayling	2.602	2.713	4.10	1.20E-05	4.39E-06	12.03	4.39
ECA ECOG Maxhamish	b-039-J/094-O-11	1872.39	Toad/Grayling	2.639	2.749	4.00	6.60E-06	1.72E-06	6.60	1.72
ECA ECOG Maxhamish	b-039-J/094-O-11	1873.06	Toad/Grayling	2.656	2.689	1.25	5.05E-07	7.95E-08	0.51	0.08
ECA ECOG Maxhamish	b-039-J/094-O-11	1875.52	Toad/Grayling	2.650	2.727	2.83	7.85E-06	1.93E-06	7.85	1.93
ECA ECOG Maxhamish	b-039-J/094-O-11	1877.63	Toad/Grayling	2.665	2.750	3.08	6.96E-06	2.07E-06	6.96	2.07
ECA ECOG Maxhamish	b-039-J/094-O-11	1879.60	Toad/Grayling	2.645	2.742	3.53	1.44E-05	3.14E-06	14.44	3.14
ECA ECOG Maxhamish	b-039-J/094-O-11	1881.95	Toad/Grayling	2.655	2.741	3.15	5.77E-06	1.40E-06	5.77	1.40
GSENR Maxhamish	a-064-B/094-O-14	1302.30	Toad/Grayling	2.229	2.706	17.63				
GSENR Maxhamish	a-064-B/094-O-14	1306.07	Toad/Grayling	2.630	2.727	3.57	4.05E-06	5.34E-07	4.05	0.53
GSENR Maxhamish	a-064-B/094-O-14	1310.52	Toad/Grayling	2.676	2.749	2.66	3.12E-06	8.65E-07	3.12	0.87
Imperial Pan American Tattoo	a-026-B/094-O-11	1313.69	Toad/Grayling	2.511	2.677	6.19	4.37E-05	2.49E-05	43.65	24.87
Imperial Pan American Tattoo	a-026-B/094-O-11	1315.21	Toad/Grayling	2.433	2.663	8.61	2.58E-05	1.69E-05	25.83	16.89
Imperial Pan American Tattoo	a-026-B/094-O-11	1316.58	Toad/Grayling	2.498	2.669	6.42	3.96E-05	2.46E-05	39.62	24.55
Imperial Pan American Tattoo	a-026-B/094-O-11	1506.55	Toad/Grayling	2.626	2.732	3.89	8.42E-06	2.56E-06	8.42	2.56
Imperial Pan American Tattoo	a-026-B/094-O-11	1507.44	Toad/Grayling	2.602	2.767	5.95	1.41E-05	7.13E-07	14.11	0.71
Imperial Pan American Tattoo	a-026-B/094-O-11	1508.76	Toad/Grayling	2.649	2.733	3.05	6.31E-06	1.59E-06	6.31	1.59
Imperial Pan American Tattoo	a-026-B/094-O-11	1511.22	Toad/Grayling	2.619	2.743	4.54	1.19E-05	1.43E-06	11.88	1.43

Table TG1. Toad-Grayling – unconfined porosity and GRI matrix permeability measurements from core samples in five wells.

MICP Porosity											
Well Name	Well Location	Core Depth (m)	Fm	Density g/cc		Porosity (%)	Corrected Porosity (%)	Peak Range		Stem Volume Used (%)
				Bulk Density (g/cc)	Skeletal Density (g/cc)			Peak Range	Modal Peak	
ECA ECOG Maxhamish	b-039-J 094-O-11	1870.48	Toad/Grayling	2.610	2.656	2.07	1.72	4 - 170	12	5
ECA ECOG Maxhamish	b-039-J 094-O-11	1875.52	Toad/Grayling	2.667	2.698	1.47	1.14	4 - 40	5	3
ECA ECOG Maxhamish	b-039-J 094-O-11	1879.60	Toad/Grayling	1.750	1.765	1.09	0.86	15 - 160	23	11
Imperial Pan American Tattoo	a-026-B 094-O-11	4310.00	Toad/Grayling	2.522	2.620	4.20	3.75	4 - 150	5	25
Imperial Pan American Tattoo	a-026-B 094-O-11	4319.00	Toad/Grayling	2.512	2.604	3.59	3.56	4 - 100	11	8
GSENR Maxhamish	a-064-B 094-O-14	1302.30	Toad/Grayling	2.654	2.707	1.95	1.67	8 - 460	12, 105	20
GSENR Maxhamish	a-064-B 094-O-14	1306.07	Toad/Grayling	2.622	2.715	3.43	2.76	<3 - 190	7	38
GSENR Maxhamish	a-064-B 094-O-14	1310.52	Toad/Grayling	2.621	2.722	3.70	2.56	<3 - 220	5	41
Legacy Maxhamish	d-099-G 094-O-11	1635.35	Toad/Grayling	2.696	2.741	1.66	1.28	10 - 490	135	18
Legacy Maxhamish	d-099-G 094-O-11	1639.71	Toad/Grayling	2.674	2.727	1.97	1.34	4 - 520	11	25
AEC Maxhamish	c-016-G 094-O-14	1264.48	Toad/Grayling	2.546	2.675	5.13	4.82	5 - 370	18	29
AEC Maxhamish	c-016-G 094-O-14	1265.72	Toad/Grayling	3.009	3.092	2.96	2.71	6 - 110	25	32
AEC Maxhamish	c-016-G 094-O-14	1265.99	Toad/Grayling	2.673	2.729	2.13	2.04	6 - 40	13	13
AEC Maxhamish	c-016-G 094-O-14	1268.79	Toad/Grayling	2.628	2.688	2.51	2.23	6 - 250	12	34
AEC Maxhamish	c-095-J 094-O-11	1519.51	Toad/Grayling	2.615	2.671	2.98	2.12	4 - 50	6	38
AEC Maxhamish	c-095-J 094-O-11	1520.63	Toad/Grayling	2.651	2.712	2.84	2.25	4 - 90	7	45

Table TG2. Toad-Grayling – MICP porosity and conformance-corrected porosity measurements from core samples in six wells.

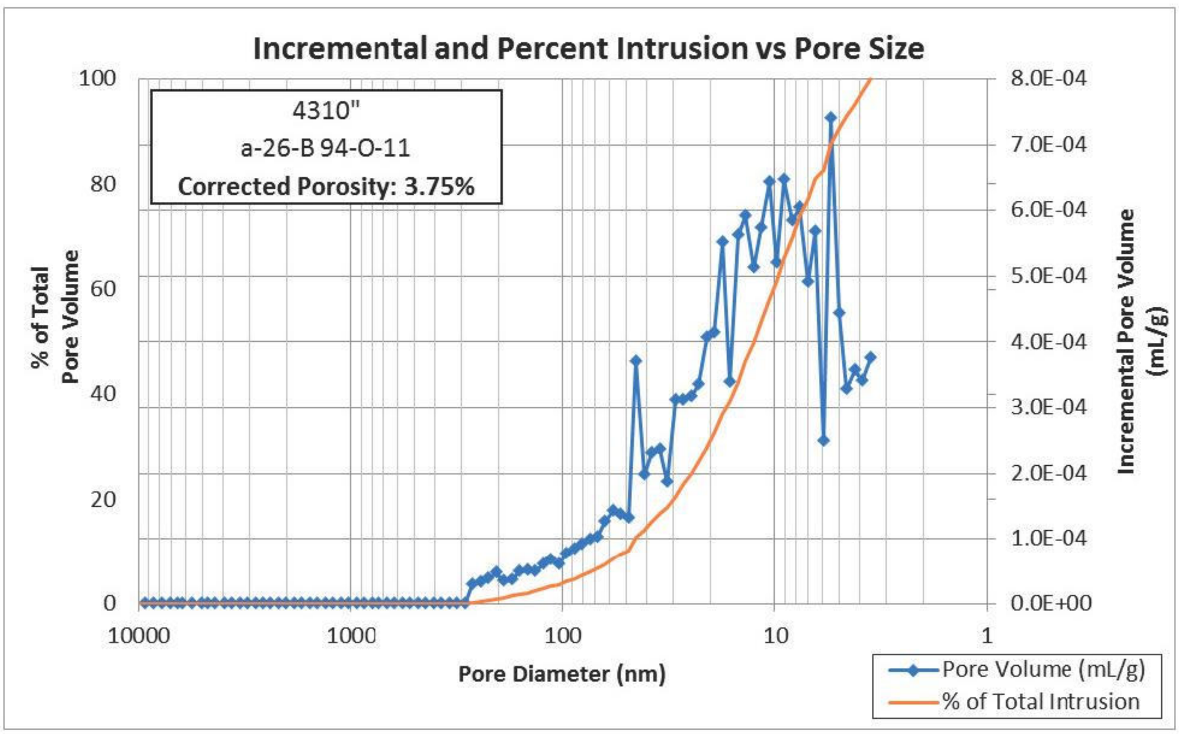

Figure TG6. Incremental and percent intrusion vs pore size, Imperial Pan American Tattoo a-26-B/94-O-11 (4310 ft), highlighting small pore throat diameters, most less than about 20 nm.

Hydrocarbon analysis (S1) of core samples from five wells show a wide range of residual hydrocarbons (Fig. TG7). Samples from b-39-J/94-O-11 show calculated specific gravity of 0.85 and calculated API gravity of 30-36° (Table TG3). Heavy condensates dominate the composition with some biomarkers (Fig. TG7). Unfortunately, the majority of samples yielded poor data, and results must be regarded with caution.

Hydrocarbon Analysis Summary Table
Toad/Grayling Formations

TRICAN Trican Geological Solutions

UWI	Well Name	Sample Type	Sample Depth (m)	Paraffins: % Light Condensate	Paraffins: % Heavy Condensate	% Naphthenes	% Aromatics	% Biomarkers	Peak	Simulated Distillation: Initial Boiling Point (°C)	Simulated Distillation: Carbon Number	Simulated Distillation: Final Boiling Point (°C)	Simulated Distillation: Carbon Number	Calculated Specific Gravity	Calculated API gravity	Chromatogram Quality
c-016-G/094-O-14	AEC Maxhamish	Toad/Grayling	1265.87	11.74	2.17	57.08	29.01	0.00	methylcyclohexane	46	<C6	390	C24	0.756	55.6	poor
c-016-G/094-O-14	AEC Maxhamish	Toad/Grayling	1268.79	6.30	0.00	55.85	37.85	0.00	cyclohexane	45	<C6	374	C22	0.727	63.2	poor
a-064-B/094-O-14	GSENR Maxhamish	Toad/Grayling	1302.90	7.70	11.30	80.10	0.90	0.00	cyclohexane	48	<C6	322	C18	0.711	67.6	no good
d-048-B/094-O-11	ECA Maxhamish	Toad/Grayling	1480.70	24.43	0.00	34.75	40.82	0.00	m,p,xylene	62	<C6	322	C18	0.776	50.8	poor
c-095-J/094-O-11	AEC Maxhamish	Toad/Grayling	1519.89	2.32	15.28	79.10	3.30	0.00	cyclohexane	1	<C6	380	C23	0.709	68.0	no good
b-039-J/094-O-11	ECA ECOG Maxhamish	Toad/Grayling	1867.53	0.02	88.06	0.01	0.03	11.88	C22	236	C13	475	C33	0.874	30.4	best
b-039-J/094-O-11	ECA ECOG Maxhamish	Toad/Grayling	1869.71	4.61	74.83	1.31	3.07	16.18	C15	52	<C6	542	C40	0.842	36.5	best
b-039-J/094-O-11	ECA ECOG Maxhamish	Toad/Grayling	1871.81	3.84	79.74	8.47	7.96	0.00	C15	8	<C6	553	C40	0.807	43.8	very poor
b-039-J/094-O-11	ECA ECOG Maxhamish	Toad/Grayling	1875.98	5.39	19.48	22.42	52.71	0.00	benzene	34	<C6	553	C40	0.834	38.3	very poor
b-039-J/094-O-11	ECA ECOG Maxhamish	Toad/Grayling	1881.14	3.42	32.19	9.48	54.92	0.00	benzene	32	<C6	553	C40	0.838	37.4	very poor

*<u>Light Condensates</u> consist of nC6 through nC12
*<u>Heavy Condensates</u> consist of nC13 through nC40
*<u>Naphthenes</u> consist of Cyclopentane, Methylcyclopentane, Cyclohexane, Methylcyclohexane
*<u>Aromatics</u> consist of Benzenes, Toluene, Ethylbenzene, Xylenes
*<u>Biomarkers</u> consist of Pristane & Phytane

Table TG3. Toad-Grayling – S1 analyzer data from five wells. Note a number of samples yielded poor quality chromatograph data.

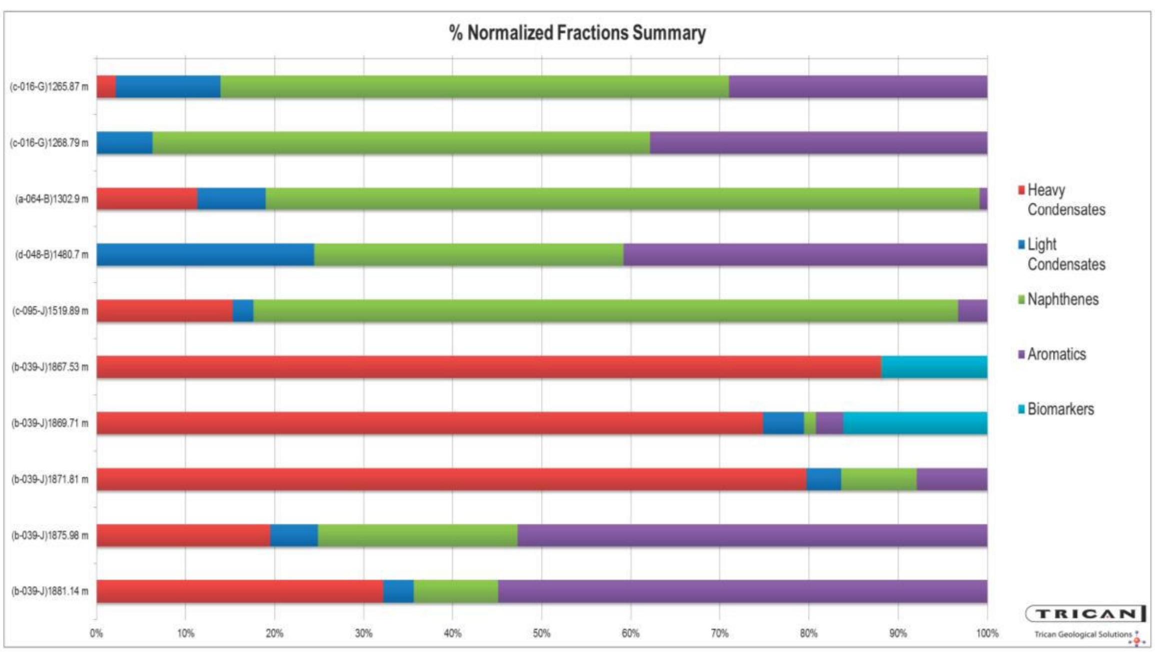

Figure TG7. Normalized fraction plot of hydrocarbon groups, Toad-Grayling, five wells (10 samples listed by well and depth). Data quality is generally poor, and heavy condensates dominate high-quality data points.

Mechanical properties of samples from three wells show average to high compressive strength (170-380 MPa) and residual strength (100-345 MPa). Poisson's Ratio is ~0.14-0.33 and Young's Modulus ~25-42 (Table TG4). These ranges reflect more competent fine sandstones and siltstones from which core plugs were successfully retrieved, but are not representative of shalier intervals.

Well Name	Zone/Fm	Depth (m)	Confining Pressure (MPa)	Axial Strain at Failure (%)	Compressive Strength (MPa)	Residual Strength (MPa)	Static Young's Modulus (GPa)	Static Poisson's Ratio	Static Bulk Modulus (GPa)	Static Shear Modulus (GPa)
b-019-J 94-O-11	Toad/Grayling	1638.81	21.0	1.058	226.97	103.91	25.32	0.213	14.69	10.44
b-039-J 94-O-11	Toad/Grayling	1869.29	21.0	0.953	288.83	121.23	37.47	0.334	37.53	14.05
b-039-J 94-O-11	Toad/Grayling	1873.18	21.0	0.603	178.35	116.36	28.74	0.175	14.73	12.23
d-048-B 94-O-11	Toad/Grayling	1478.76	19.0	0.941	382.67	345.38	42.31	0.144	19.79	18.50

Table TG4. Toad-Grayling - Rock mechanical analyses from three cores showing confining pressure, compressive strength, Young's modulus, Poisson's ratio and bulk and shear modulii.

Resource Oil Assessment

We have little definitive data to assess tight oil potential in the Toad-Grayling. Sandstone-dominated intervals, if mappable using new wells logs associated with deeper play development tied to seismic, may be viable tight oil reservoirs, but this potential cannot be quantified using existing data sets. Tight oil prospectivity in the overlying Chinkeh encourages us that similar prospectivity may exist in Toad-Grayling sandstones that are juxtaposed with oil-bearing basal Chinkeh sands.

DOIG FORMATION

Age and Play Type

Middle Triassic – Tight Oil Play (tight sandstone) and Shale Oil Play
Prospectivity: 'A/B' Play – Proven productivity in tight sandstones, prospective areas may host analogous sandstone reservoirs that can be assessed with stratigraphic and structural work

Regional Geology

The Doig and Halfway Formations are genetically-related facies tracts of a prograding clastic coastal system, deposited along the western margin of the North American craton in proximal to distal marine environments (Gibson and Edwards, 1990). The Doig comprises offshore to lower shoreface shales, siltstones, and sandstones, with thick, cleaner, more proximal sandstones – dubbed "Anomalously Thick Sandstone Bodies (ATSB's)" – occuring in shoreline-related linear trends (Cross-section HDoig-HDoig'; Map D1). Specific ATSB bodies have been analyzed in detail (e.g., Wittenberg, 1993; Evoy and Moslow, 1995; Evoy, 1997, 1998; Harris and Bustin, 2000; see Dixon (2011) for a comprehensive list).

Dixon (2006, 2010, 2011) summarized Doig ATSB's:

> Interpretations vary from incised valleys, deltaic, barrier islands, turbidites in slope slumps, to shallow-water gravity flow beds overlain by shoreface deposits … The most probable explanation is that during late regression, structural depressions formed on a muddy shelf and were filled by sandy sediment. Initial deposits commonly are debris-flow and/or slump deposits that filled the deeper parts of the depressions. As the depression filled, sediment entered wave- and current-influenced water depths and more typical shoreface deposits began to form.

Figure D1 illustrates a number of ATSB's at various stratigraphic levels within the Doig in northeastern B.C. Figure D2 is a sample core log from the Wembley Field, and Fig. D3 shows isopach maps of ATSB's at Buick Creek and Dawson Creek. Dixon (2006, 2010, 2011) mapped the distribution of ATSB's in NEBC and adjacent Alberta, and suggested that older structures related to the Peace River Embayment / Fort St John Graben complex may have guided structural depressions and hence depositional trends (Map D1). Several more ATSB's have been identified (e.g., Noel (93-P-8), Swan Lake (93-P-9), Inga (87-23W6)) since Dixon (2011) produced his last compilation. Chopra *et al*. (2015) demonstrated that Doig ATSB's can be mapped seismically, although their highly variable development makes mapping each ATSB reservoir a different challenge.

At the base of the Doig, the "Doig Phosphate Zone" consists of variably phosphatic, thinly-bedded argillaceous siltstone, interbedded calcareous siltstone, and minor dark grey shale (Riediger *et al*., 1990a). It is characterized by high spiky gamma log values and generally high resistivities on logs, typical of a regional condensed section (Cross-section HDoig-HDoig'). The Doig Phosphate Zone is recognized as a major source rock in the WCSB, and has been developed as a shale gas reservoir in some areas coincident with the Montney unconventional play trend.

Doig strata are preserved across the southern Deep Basin and Peace River areas, thinning to a northeasterly subcrop edge (Map D1). The edge is not sharply defined because of complex stratigraphic relationships, including numerous closely-spaced unconformities, within the Triassic section. Zonneveld *et al*. (1997) discussed distal outcrop equivalents (Toad Formation) in the B.C. Foothills. Burial depths range from <1000m in the northeast to more than 4000 metres in the southern Deep Basin (Map D1).

Reservoir Description

Doig ATSB sandstones range up to 60m thick, and can be entirely sandstone, or may contain mudstone-dominated intervals, ranging from shales to argillaceous sandstones to sandstones with abundant mud clasts. Harris and Bustin (2000) described Doig

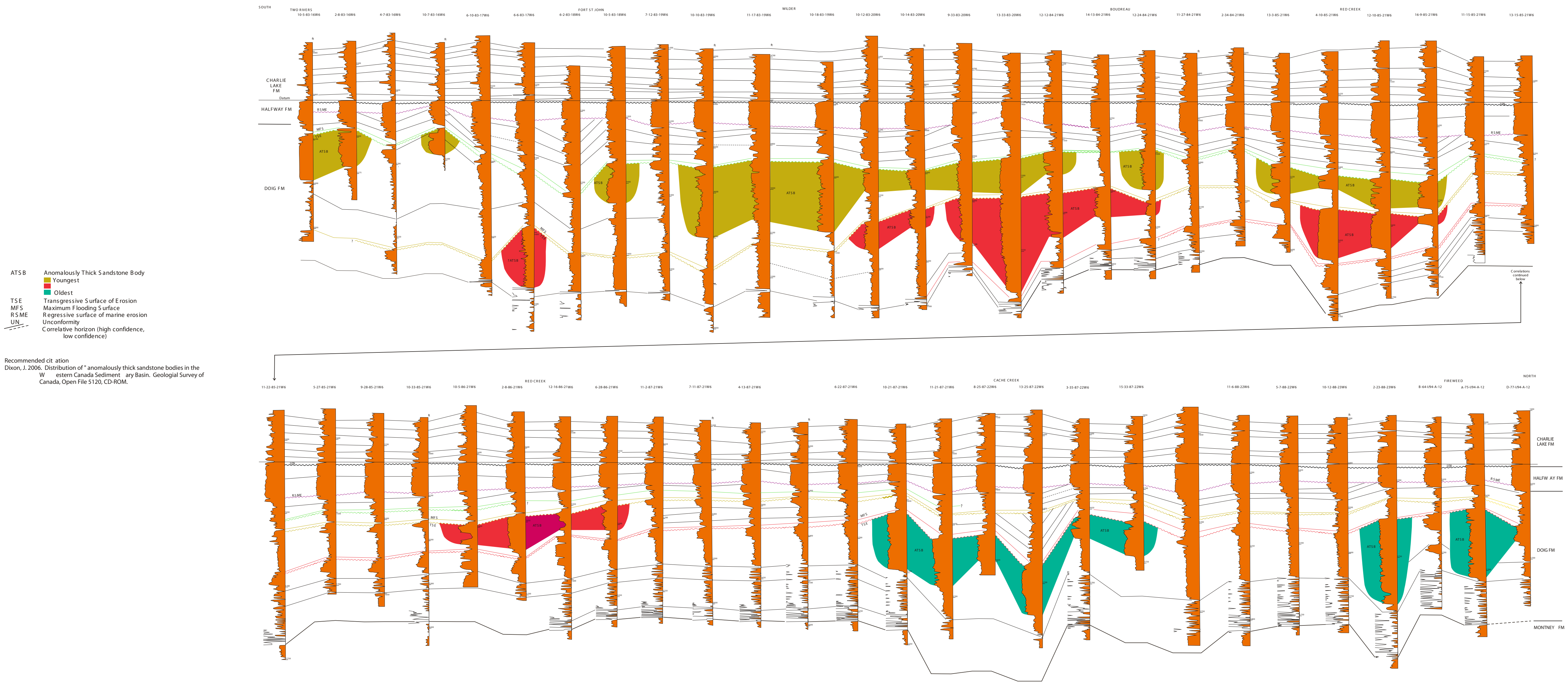

A: Correlations in the Doig-Halfway interval along a strike-oriented stratigraphic cross section. Gamma-ray logs. All depths in metres unless otherwise indicated.

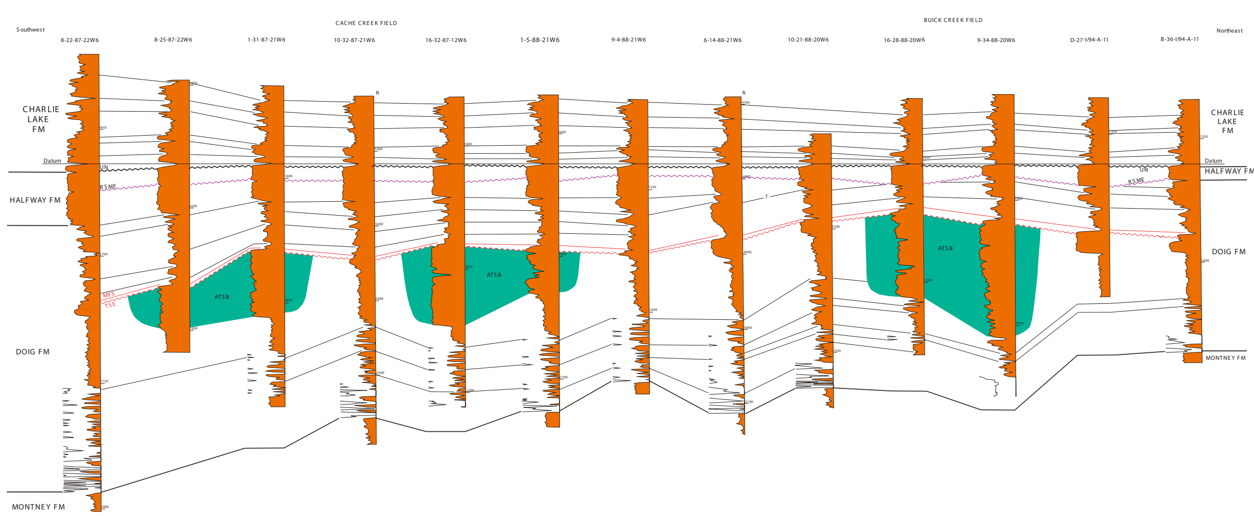

B: Correlations in the Doig-Halfway interval along a dip-oriented stratigraphic cross section, between Buick Creek and Cache Creek fields. All depths in metres unless otherwise indicated.

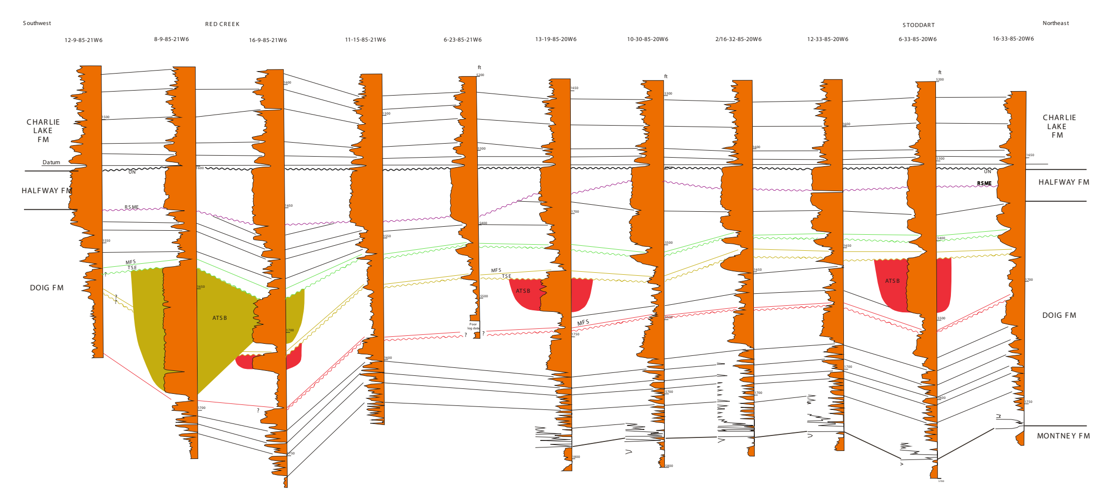

C: Correlations in the Doig-Halfway interval along a dip-oriented stratigraphic cross section, between Stoddart South and Red Creek fields. Gamma-ray logs. All depths in metres unless otherwise indicated.

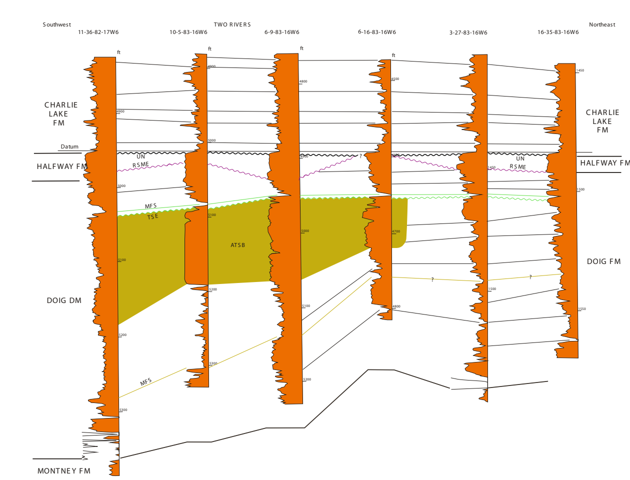

D: Correlations in the Doig-Halfway interval along a dip-oriented stratigraphic cross section across the Two Rivers Field. Gamma-ray logs. All depths in metres unless otherwise indicated.

Figure D1. Doig correlations in NEBC, highlighting occurrences of ATSB's. Cross-section locations on Map D1 (from Dixon, 2006).

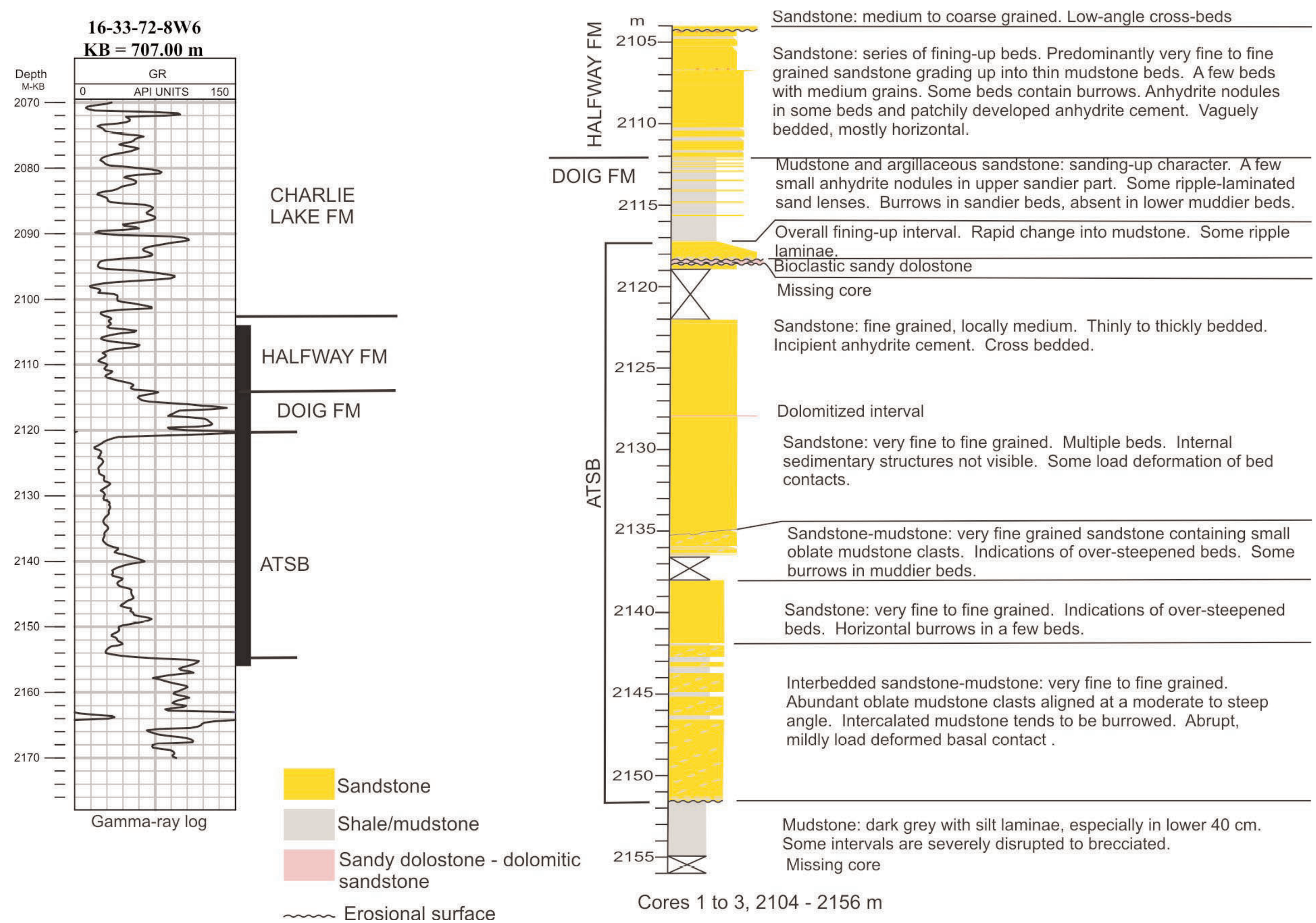

Figure D2. Core description, Doig ATSB at Wembley 16-33-72-8W6 (from Dixon, 2011).

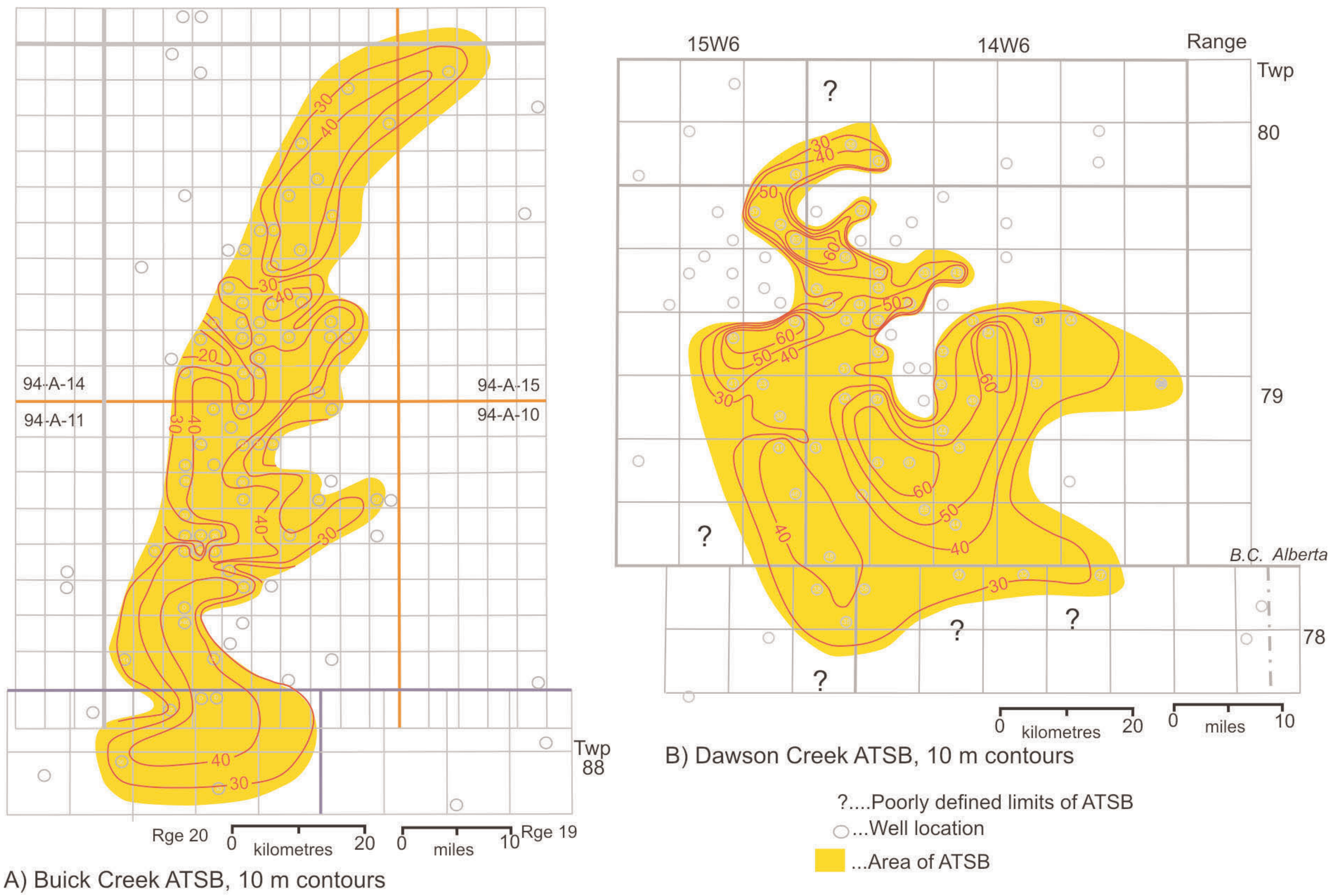

Figure D3. Isopach maps, Doig ATSB's at Buick Creek and Dawson Creek (from Dixon, 2011).

sandstones as well-sorted, very fine- to fine-grained sublithic to quartz arenites, with interbedded bioclastic (coquinoid) packstones and grainstones. Coquinas or moldic porosity after coquinas have been noted at Buick Creek (Evoy and Moslow, 1995) and Valhalla (Wittenberg, 1993).

Harris and Bustin (2000) documented a complex diagenetic history for Doig sandstones.. Porosity is dominantly primary intergranular, but is commonly reduced by calcite, quartz, dolomite, and anhydrite cements. They noted no consistent relationship between reservoir quality and present-day burial depths. Reservoir fracturing was seen as an early event, occurring where early calcite cementation lithified sediments at a shallow depth. Open fractures are abundant in core only at West Stoddart and Cache Creek (Harris and Bustin, 2000).

A permeability vs porosity cross-plot for Doig sandstones shows the main population (Population 1) to fall on a trend line dominated by porosities of <10% and permeabilities <10mD (Fig. D4). A smaller population of better-quality rocks (Population 2) features porosities of 10-25% and permeabilities of 20 to several hundred millidarcies, and comes almost exclusively from cores in the northeast (Peejay-Wildmint area), updip from almost all Doig production.

Conventional well logs depict Doig blocky sandstone reservoir quality reasonably well, but for quantitative petrophysical evaluations, complex mineralogies including feldspars and carbonate grains and cements must be modelled. Reservoir mineralogies may vary abruptly on a fine (cm) scale, particularly in coquinoid sandstone facies.

At Groundbirch in the northern Deep Basin (Twp 78-79, Rge 19W6; Map D1), the Doig produces gas from a siltstone facies more closely resembling Montney reservoirs than Doig ATSB's, but this appears to be a relatively isolated reservoir type.

As noted above, the Doig Phosphate Zone is an interbedded shale / siltstone interval with high organic content, and should be evaluated as a shale reservoir.

Production and Test Data

Doig reservoirs produce oil and gas in the Peace River Plains and the southern Deep Basin, and along the deformation front as far north as Tommy Lakes (Map D1). Oil dominates in northeasterly updip areas, generally shallower than 2000m present day burial depth, while gas production dominates deeper areas. Harris and Bustin (2000) related this pattern to maturity of Doig Phosphate Zone source rocks. Significant oil

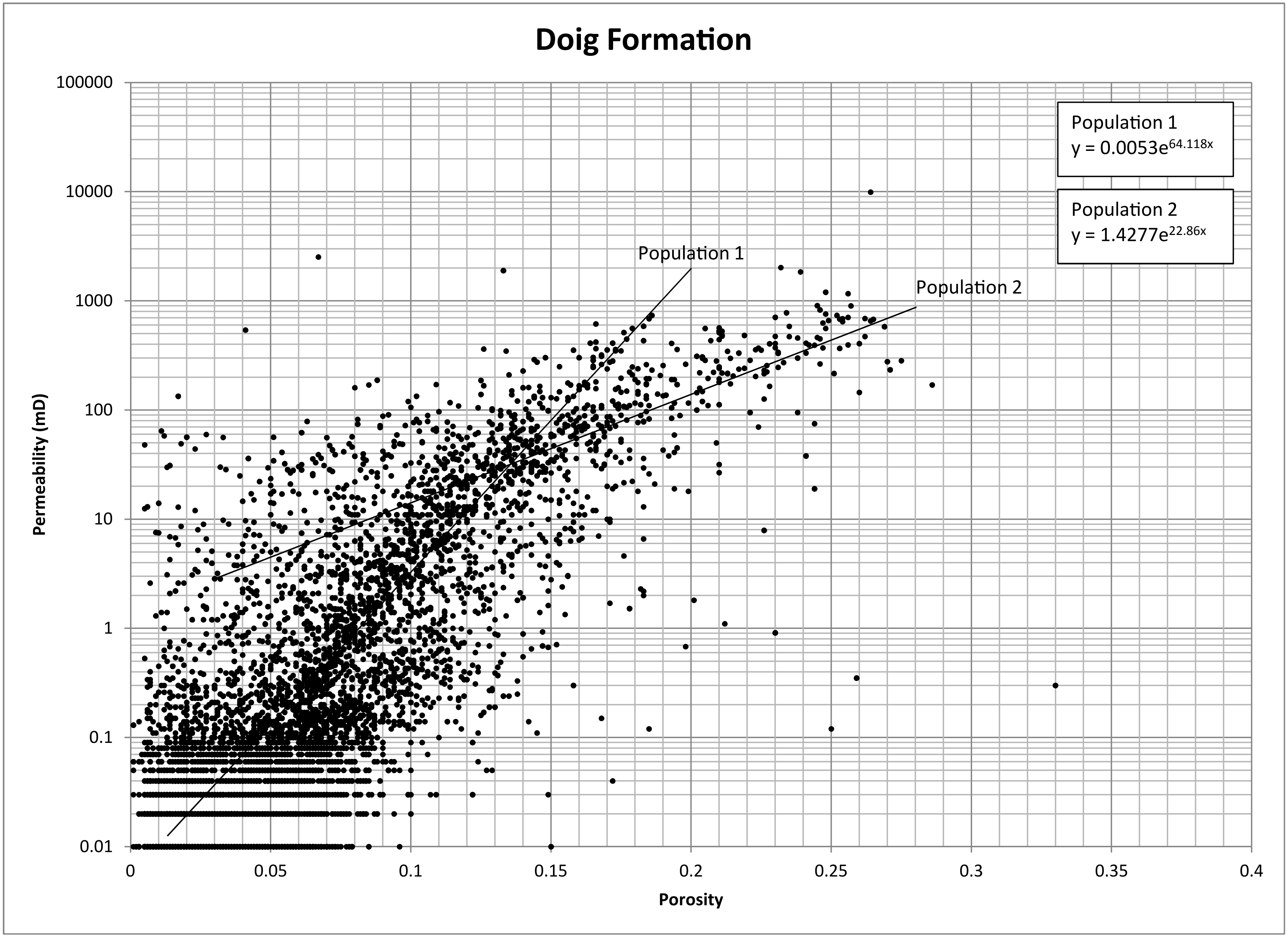

Figure D4. Porosity / permeability cross-plot, Doig Formation sandstones.

pools occur primarily in ATSB reservoirs, as at Buick Creek, Fireweed, and West Stoddart; note that official pool nomenclature mistakenly places some of this production in the “lower Halfway”.

Appendix 9 summarizes characteristics of B.C. Doig oil pools.

- The largest existing field is at Buick Creek, where “Lower Halfway” pools contain 75 million barrels of oil originally in place (MMBOOIP) ($12e^6m^3$ oil). Seven other pools contain >20 MMBOOIP, while the next 18 pools contain 1 to 7 MMBOOIP each.
- Net pays are quite variable (1-18m), and average 5.45m. Pool boundaries are sharply defined vertically and horizontally by facies and cementation boundaries.
- Most pools are very mature and remaining reserves are relatively small.
    - Discovery statistics are dominated by the many individual pools making up the Buick Creek “Lower Halfway” and Cache Creek Doig accumulations, which were drilled up in the 1990’s and 2005-2007 time periods, respectively. There have been very few discoveries since 2007. Like the Baldonnel, primary exploration focus for the Doig has moved to gas-prone areas.
- Oil gravities are light to very light (almost all >40 API)
- Average porosities (3.5-19%, average 11.1%) and permeabilities (1.3-150mD) by pool range from modestly tight to conventional.
- Recovery factors are generally low (<20%). Only Muskrat and Red Creek pools are under waterflood.

Horizontal Drilling

Horizontal drilling dominates most current Doig gas development – in siltstones at Groundbirch, sandstones in the Deep Basin (Noel area), and in Phosphate Zone reservoirs in the western reaches of the Montney fairway at Altares and Townsend (Map D1). Recent horizontals at Inga produce high-liquids gas from Doig ATSB’s; a few of these have been classified as oil wells.

Major ATSB sandstones, as at Buick Creek, Fireweed and West Stoddart, have been exploited almost exclusively with horizontal wells. These areas were first developed in 1977, but only ten wells were drilled prior to 1995, when drilling accelerated. By 2000 there were 70 wells on production. Many horizontals were drilled during this time, followed by another small boom in about 2007.

Vertical wells were typically perfed and frac'd with small, single-stage fracs; some were also acidized. Most horizontal wells were drilled open hole and were left unstimulated.Ten horizontals drilled in 2011-2012 were treated with multistage fracs, averaging 8 stages per well (maximum 13). Average horizontal length is 760m, meaning frac stage intervals of about 100m. Of the 10 multi-frac wells, six are at Fireweed; these are all the horizontals in the pool, so we cannot make a comparison between frac'd and unfrac'd wells. The other four multi-frac wells are widely distributed, with only one in Buick Creek, so meaningful performance comparisons are not possible here either. Some horizontals with open hole completions were also perfed through casing above the open hole and this interval was then fracked with a single stage. No discernable advantage can be attributed to this procedure.

New horizontal drilling of the Doig ATSB at Red Creek was proposed by a junior operator in 2016 but has not taken place.

Northern Oil Pools (Buick Creek / Stoddart West / Fireweed / Cache Creek

Initial production rates were very good for both verticals and horizontals in these pools (Table D1) (Appendix 5). At Buick Creek, ultimate recovery volumes from the horizontals are spectacular. For the depth and cost, recoveries in the other three areas are likely economic, although horizontal well declines are very steep. Horizontals show twice the average recovery of verticals except at Buick, where they are 5 times better. However, at Fireweed and Cache Creek, the best vertical wells are better than the best horizontals, by a fairly wide margin (Fig. D5). As most wells are now non-producing or are near the end of life, cumulative production is a good proxy for EUR.

Doig Area Summary								Vertical			Horizontal		
Field	API	Pressure psi	Depth m	Gradient psi/ft	Cum. Oil mstb	GOR scf/bbl	WOR bbl/bbl	Wells	IP bbl/d	EUR mstb	Wells	IP bbl/d	EUR mstb
Stoddart W	46	2600	1600	0.50	5116	7750	0.02	11	75	74	37	476	120
Cache Ck	49.8	3000	1700	0.54	881	21200	0.03	22	163	35	2	349	56
Buick Ck	42.7	1830	1280	0.44	12871	5960	0.07	23	136	58	38	551	307
Fireweed	44.6	1920	1550	0.38	1484	2660	0.8	16	113	58	6	230	123

Table D1. Oil pool summaries, Doig Formation ATSB's, Stoddart / Buick Creek / Fireweed area.

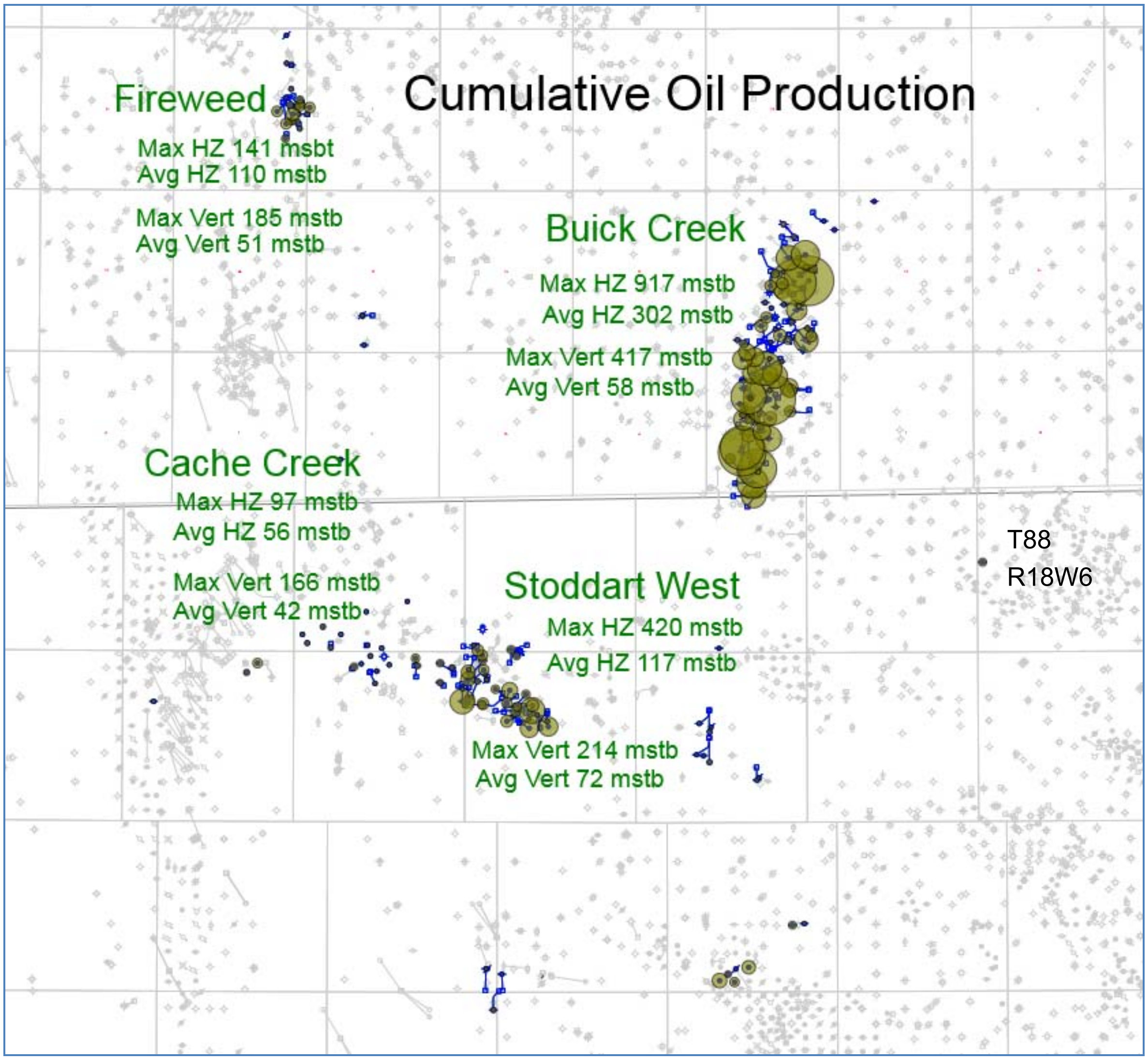

Figure D5. Cumulative oil production bubble map, Doig Formation, northern oil pools.

Although depths in all pools are between 1300 and 1700m, pressures and pressure gradients vary widely (Table D1). API gravity and GOR follow the spread in pressures; i.e., higher pressure gradients host more volatile oils. Stoddart and Cache Creek are overpressured, Buick is normally-pressured, and Fireweed slightly underpressured (Fig. D6). Two isolated overpressured wells (in D/94-A-14) lie between Buick and Fireweed in D/94-H-14. To the southeast of Stoddart West, two pools are underpressured and one is overpressured. From this disparity in pressure gradients, it appears no strong connections or a single pressure system can be inferred.

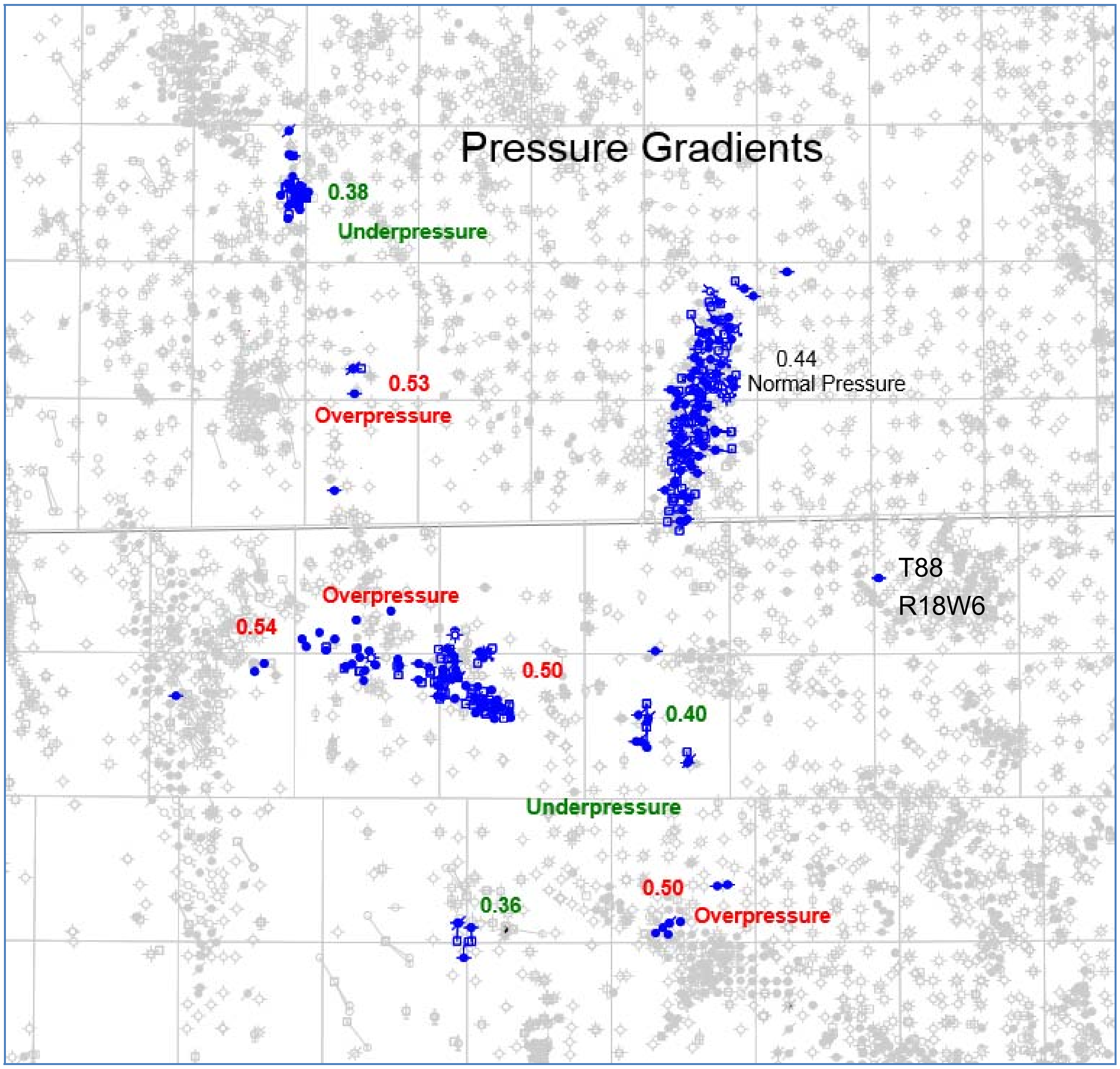

Figure D6. Distribution of pressure gradients, Doig Formation, northern oil pools.

Cache Creek and Stoddart West have produced negligible water and have had no water injection. Fireweed, on the other hand, shows cumulative water production of almost 1 bbl water per bbl oil, but there has been no injection. Virtually all the water production comes from three horizontal wells, d-43-H, a-52-H, b-A52-H located on the western side of the pool.

Doig sandstones at Buick Creek were developed as 16 Lower Halfway pools, but this appears to be for administrative reasons more than systematic reservoir distinction. Altogether there are 86 wells, of which 49 are horizontal. Fourteen wells are listed as injectors at some point during their lives (Fig. D7). There were never more than eight injectors on injection at one time during the peak around year 2000. Cumulative injection was 2.3 MMBW, compared to 15.3 MMB oil production and less than 1 MMB water production, so it appears water injection had minimal effect.

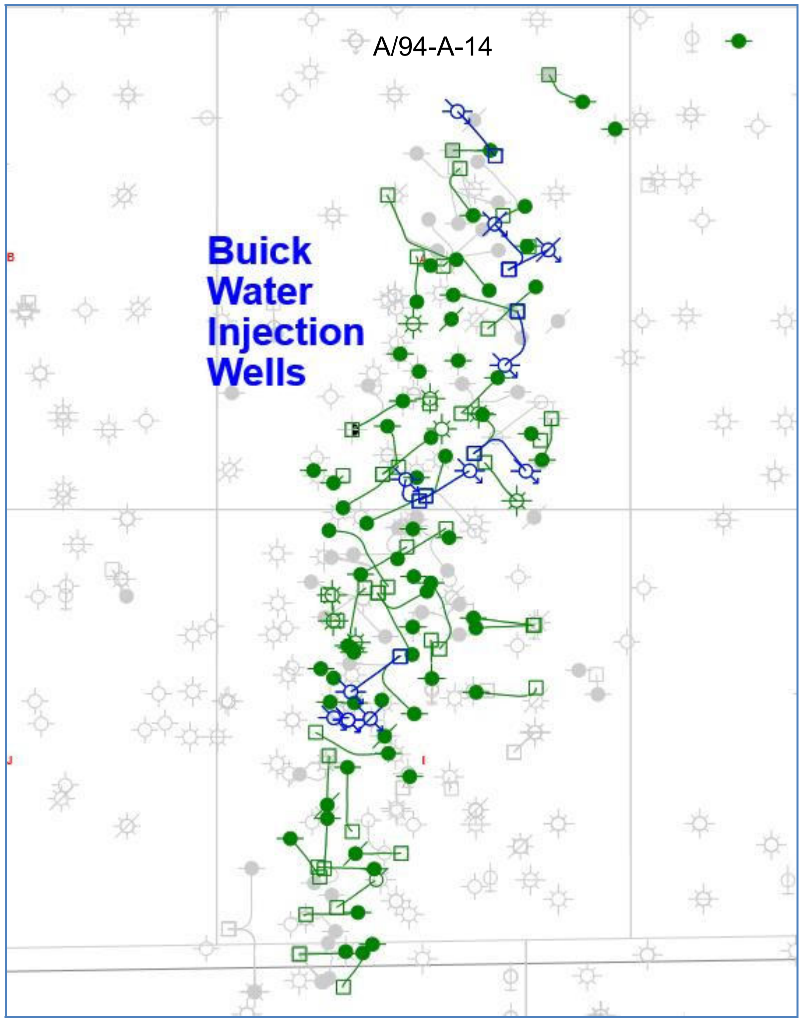

Figure D7. Water injection wells, Doig Formation, Buick Creek Field.

Analytical Data

Using all available data from the literature and OGC analysis files, we constructed TOC (organic richness) and T_{max} (maturity) maps for the Doig Formation (Maps D2, D3) (Appendix 6). Source rock data were selected from the Doig Phosphate Zone only, as we judged samples from upper Doig clastics would not properly reflect source rock potential. For TOC mapping, where multiple data points are available from a wellbore, we selected the median value. T_{max} figures are selected from the sample with the highest S2 value; if the maximum S2 value is <1mg/g, we judged there to be no valid T_{max} figure.

Map D2 demonstrates that there is abundant organic-rich rock in the Doig – but most of the richest values are in medial or downdip positions, which is somewhat unexpected. Normally, we would expect higher maturity levels in these areas to have caused much of the organic material to have been converted to hydrocarbons and expelled. One possible explanation is that the Phosphate Zone becomes much thicker and more likely to be sampled adequately in western areas, and hence may be better represented.

Map D3 shows the Doig to be mature for oil generation in the east, with a general westward increase with depth to gas-mature values. This pattern corresponds well with the occurrence of oil and gas in upper Doig reservoirs. Lower T_{max} values in the southern Deep Basin may reflect a westward decrease in maturity at the eastern edge of the Foothills documented by Bustin and Bustin (2016), but comparing Map 1, we see that Doig reservoirs are gas-prone throughout this area.

Silva and Bustin (2018) showed preliminary results on a comprehensive Doig petroleum systems analysis project in progress, evaluating potential of the Doig with focus on the distribution of producible liquids. Their preliminary TOC and maturity mapping show distributions broadly similar to those mapped here, but will have far more control points upon project completion.

Reviewing well locations and report types in Appendix 1, we see that available analytical work on the Doig focuses on source rock analysis and characterization of shale gas potential; there is relatively little work on the sandstone reservoirs.

Rokosh *et al*. (2012) did not address Doig unconventional potential in Alberta. Walsh *et al*. (2006) calculated total in-place shale gas potential (in NEBC) of 40-200 TCF for the upper Doig, and 70 TCF for the Doig Phosphate, but made no attempt to quantify liquids potential. Chalmers and Bustin (2012a) analyzed mineralogy of the Doig siltstone / sandstone reservoir at Groundbirch with the perspective of understanding sorbed gas capacity and porosity/permeability controls. Silva and Bustin (2017) documented progress on a study to characterize Doig unconventional hydrocarbon potential through a comprehensive petroleum systems analysis – with a focus on delineating the potential for producible liquids.

Resource Oil Assessment

Doig sandstones appear to have additional resource and conventional oil potential in NEBC, but intensive regional stratigraphic work is required to understand its scope. Township-scale ATSB's host several large oil accumulations, several of which have been exploited successfully using horizontal wells. Reservoir pressures and formation waters are quite variable and not well understood on a regional basis. The distribution of ATSB's is also not well understood, and complex Halfway / Doig stratigraphic relationships, including the assignment of some Doig ATSB's to the "lower Halfway" further confuses the situation.

A hundred-kilometre gap between Doig ATSB production in western Alberta and pools at Buick Creek / Fireweed suggest an exploration fairway, although prospects might be even better north of Buick Creek, where Doig Phosphate TOC values are high

(Map D2). In the north, however, more conventional reservoir quality appears to dominate, and prospects may be confined to discrete conventional accumulations.

HALFWAY FORMATION

Age and Play Type

Middle Triassic – Halo Oil Play;
Prospectivity: 'A' Play – Lower-permeability but oil-bearing shoreface sandstones appear to have been largely ignored in multi-field development schemes.

Regional Geology

The Halfway Formation consists of a series of southwestward prograding, regressive barrier-island shorefaces reworked by tidal channels (Gibson and Edwards, 1990; Caplan and Moslow, 1997). Sandstone bodies within individual parasequences can be stratigraphically isolated in updip areas ("discontinuous" Halfway), but pass southwestward into a broad, continuous shelfal sandstone complex (Bird *et al*., 1994; Dixon, 2008). The Halfway is regionally extensive throughout the southern part of northeastern British Columbia, and grades westward into thick stacked marine fine-grained clastics of the Liard Formation (Zonneveld *et al*., 1997) (Map H1).

Although precise stratigraphic relationships have been debated, Halfway sandstones parasequences overlie the Doig more or less conformably. In the west, restricted strata of the lower Charlie Lake interfinger with the Halfway, but both the lower Charlie Lake and the Halfway are eroded beneath intra-Charlie Lake unconformities to the east (Fig. H1, H2; Map H1). While we have shown a defined updip edge of Halfway porous sandstones (from Moslow and Davies, 1993), stratigraphic relationships become complex and difficult to follow consistently in the east, and there are porous outliers east of this line (Fig. H1; Cross-section HDoig-HDoig').

Halfway burial depths range from <1000 metres in the north, increasing to more than 4000 metres in the southwestern Deep Basin (Map H1). Outcrop equivalents are widespread in the adjacent Deformed Belt.

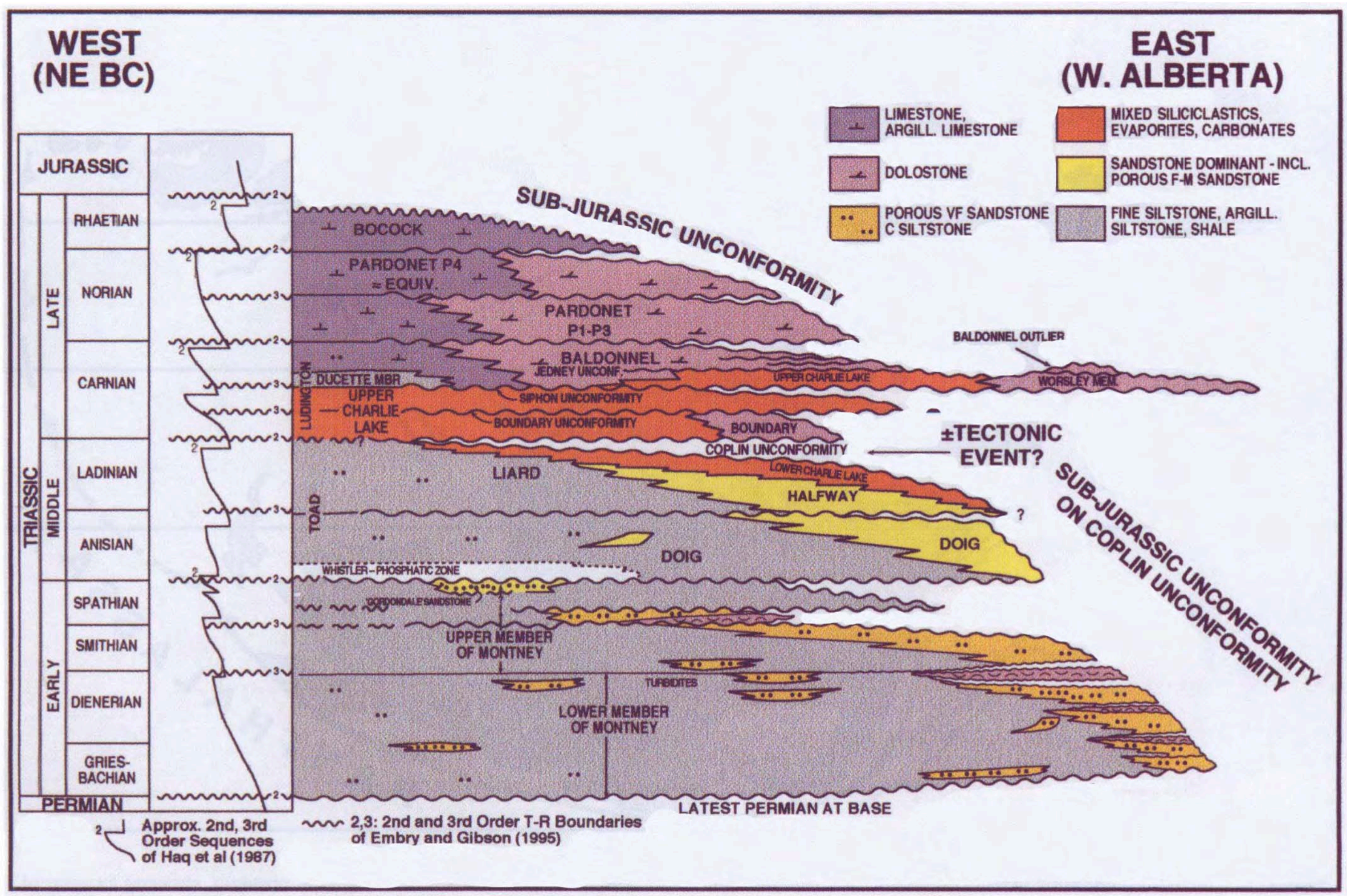

Figure H1. Event stratigraphic summary for Triassic succession of WCSB (same as Fig. CL1). Note conformable, interfingering relationship between the Halfway and lower Charlie Lake in the west; both are removed eastward beneath intra-Charlie Lake unconformities (from Davies, 1997a).

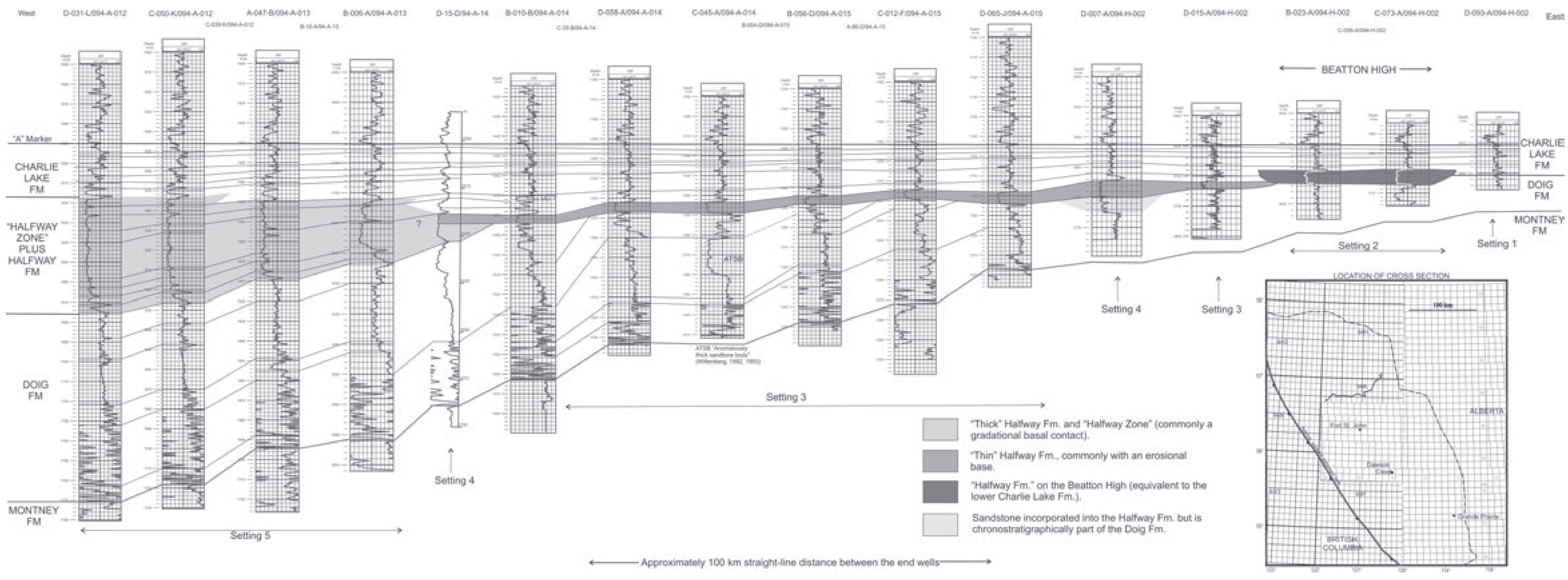

Figure H2. Regional Halfway cross-section illustrating stratigraphic relationships (from Dixon, 2008).

Reservoir Description

Numerous papers have been written on conventional Halfway oil and gas reservoirs (e.g., Caplan and Moslow, 1997, 1999; Labute *et al*., 1997; Norgard, 1997; Spence and Evoy, 1997; Willis and Moslow, 1994; Zonneveld *et al*., 1998). Halfway sandstones are primarily quartzarenites and sublitharenites, with local bioclastic (shell debris) sandstones and coquinas. Major cements include silica, carbonates, and anhydrite. The best reservoir facies in many pools in the updip "discontinuous" Halfway regime are tidal channel fills, exhibiting porosities approaching 20% and permeabilities of hundreds of millidarcies (e.g., Caplan and Moslow, 1997; Willis and Moslow, 1994; Spence and Evoy, 1998). These contrast with much lower reservoir quality in the regional barrier / shoreface sandstones (see Peejay Focus Study, below).

Moving south and west into the gas-dominated "continuous" Halfway regime, reservoir quality generally deteriorates. At Tommy Lakes (94-G-9, Map H1) (present depth about 1000 metres), Zonneveld *et al*. (1998) described Halfway shoreface strata as quartzose, well-sorted, trough to planar cross-stratified, very fine- to medium-grained sandstone, with porosities of 3-12%, and permeabilities ranging between 0.1 and 3 mD. Coquinoid tidal inlet channel fills provide reservoir sweet spots, with porosities of 12-19% and permeabilities ranging between 15 and 90 mD. At Monias (Twp 82-83, Rge 21-23W6) (present depth about 1500 metres), Norgard (1997) calculated average porosity of 8.8% and average permeability of 5.2 mD in quartzose sandstones with secondary solution porosity.

Peejay Field Focus Study

In order to assess "halo" oil potential in the Halfway, we examined production from tidal channel (high-quality) and regional shoreface (generally low-quality) sandstone reservoirs in the Peejay area (94-A-15 and 16), relying on reservoir analysis by Caplan and Moslow (1997, 1999) (Map H1, H2). In addition to Peejay, the focus study area also includes Halfway pools at Beavertail, Currant, Bulrush, Doig Rapids and Osprey. First Halfway oil production in the area dates back to 1959, and so most pools are very mature. Key parameters for the area include (BCOGC, 2015; Appendix 9):

- Original oil in place: 38818 e^3m^3 (244 MMBO);
- Initial reserves: 13650 e^3m^3 (86 MMBO);
- Production to date: 12795 e^3m^3 (80.5 MMBO);
- Porosity: 9-24% (average 17%);
- Water saturation: 13-52% (average 29%);
- Oil density: 810-846 (average 823) kg/m^3 (light oil).

Most of the Halfway reserves in the area are in pools under waterflood; note the abundant water injection wells on Map H2.

Caplan and Moslow (1997, 1999) demonstrated that tidal inlet/channel sublitharenites and bioclastic grainstones are the primary conventional Halfway reservoirs in the Peejay area, and are readily distinguished from regional shoreface sandstone parasequences in core and on logs (Fig. H3, H4). Tidal inlet reservoirs are readily correlated at various stratigraphic levels (Fig. H5-H7; Map H2). Caplan and Moslow (1999) developed a reservoir distribution model, showing tidal channels embedded within regional parasequences as reservoir "sweet spots"; reservoir distribution is further complicated by post-Halfway extension and faulting (Fig. H8). Subsequently, oil migration charged the Halfway reservoir complex, beneath a top seal provided by tight Charlie Lake evaporitic strata (Fig. H9). This situation suggests widespread potential for "halo" oil in lower-quality Halfway shoreface sandstones, outside the tidal channel sweet spots.

We reviewed all wells in the Peejay Field focus area, and mapped the distribution of Halfway shoreface sandstones and tidal inlet deposits (Map H3, H4; stratigraphic data are in Appendix 10). Tidal channel and shoreface intervals were picked as per the Caplan and Moslow cross-sections (Fig. H5-H7). Maps are computer contoured and should be regarded as schematic, as contouring at this scale cannot accurately depict well-to-well variations where drilling is so dense. Both shoreface and tidal channel facies are laterally extensive and continuous in aggregate, although they would appear less continuous if broken out by parasequence. The Halfway erosional edge on Map H3 and H4 is the general eastern limit of Halfway reservoir sandstones; they are removed to the east by post-Halfway erosion (Cross-section HDoig-HDoig'; Fig. H7).

Reviewing core analysis data by facies, tidal channel reservoir quality is clearly better – most values lie in the 10-25% porosity range with permeabilities ranging from a few millidarcies up to a Darcy, whereas most shoreface sandstone samples measure porosities of 5-20% and permeabilities of 100mD or less (Fig. H10, H11). Scattered high poro/perm values on the shoreface plot may represent isolated coquinas in the shoreface (e.g., Fig. H4).

Reservoir Engineering Analysis

Examining test and production data, we discovered (not surprisingly) that almost all evaluations and completions were conducted on the tidal channel reservoirs, which are readily distinguished from tighter shoreface sandstones on density and sonic logs. Shoreface sandstones were tested in a number of wells, but we found only nine wells where they were DST'd alone, and five where they were completed alone – either separately from tidal channel facies in the same well, or in wells where there are no tidal channel facies (Map H5, Appendix 5). Most test results showed the shoreface to be tight by conventional standards, but oil has been produced from all five Halfway shoreface completions:

1. **d-81-H/94-A-15**: Section cored, analysis shows low permeabilities characteristic of the shoreface throughout. A three-foot section at the base of the Halfway shoreface was acidized and frac'd, and 1033 barrels oil produced over four

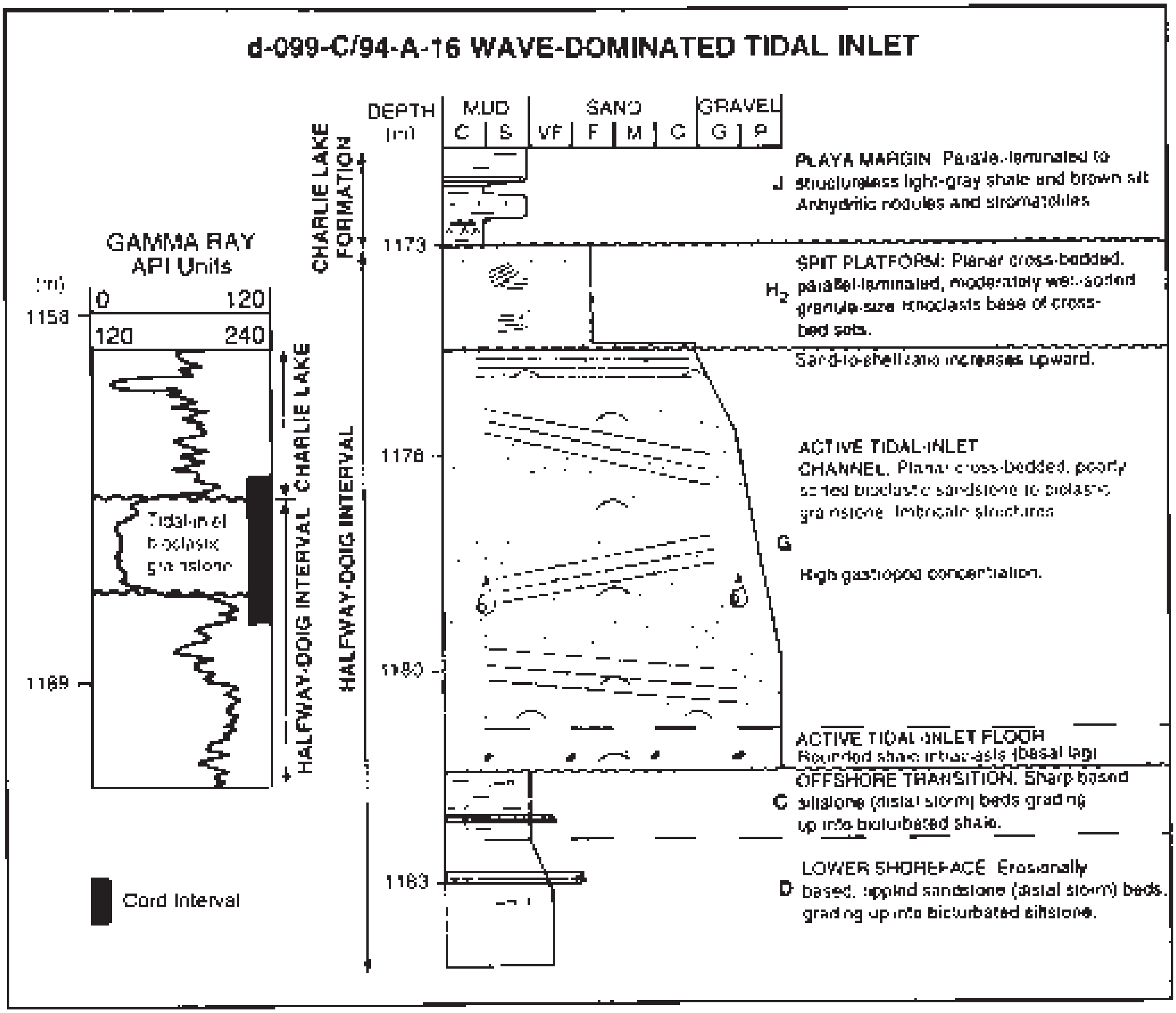

Figure H3. Core and well log, wave-dominated tidal inlet reservoir sandstone, Peejay Field (from Caplan and Moslow, 1999).

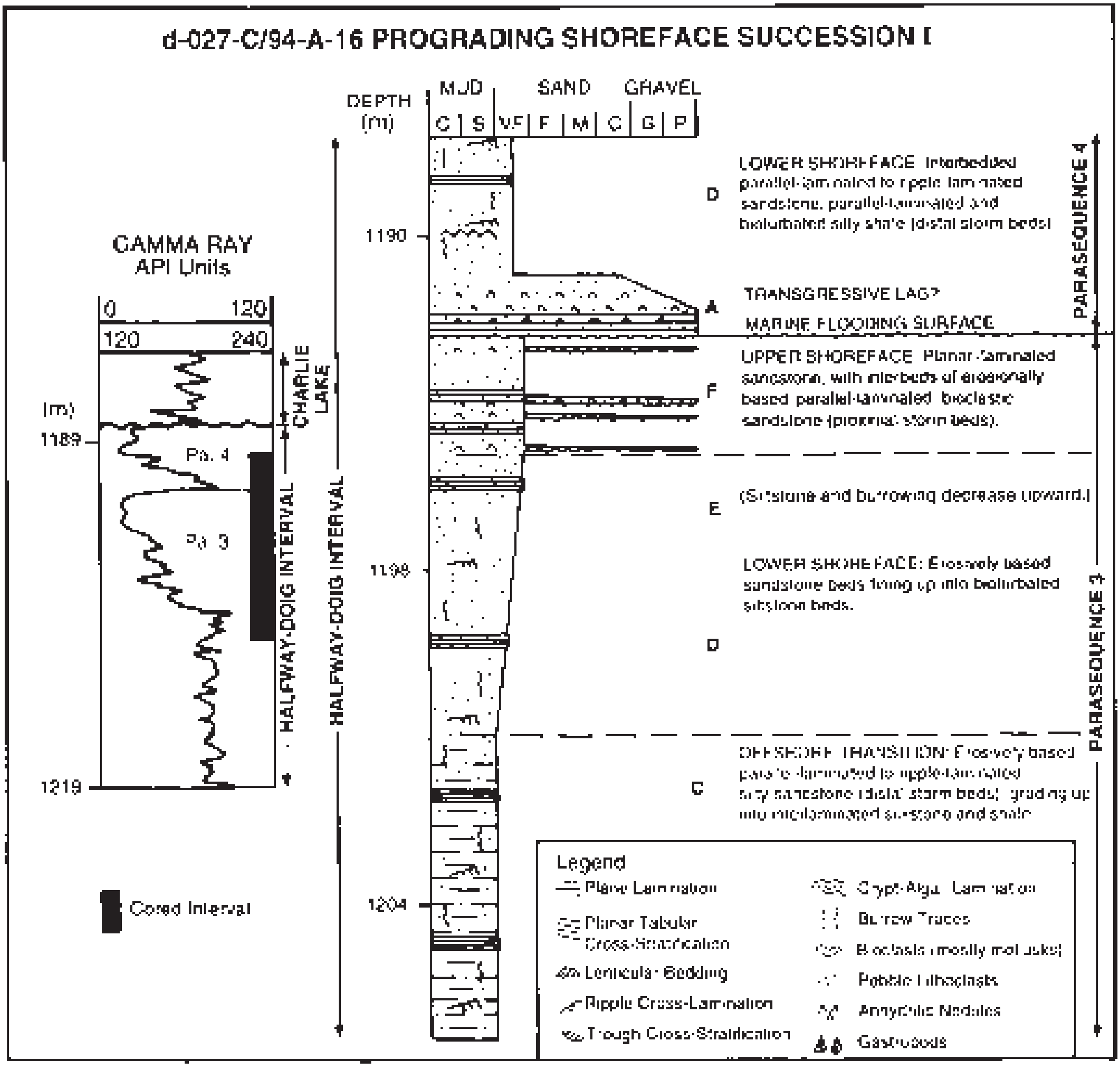

Figure H4. Core and well log, prograding shoreface succession, Peejay Field area (from Caplan and Moslow, 1999).

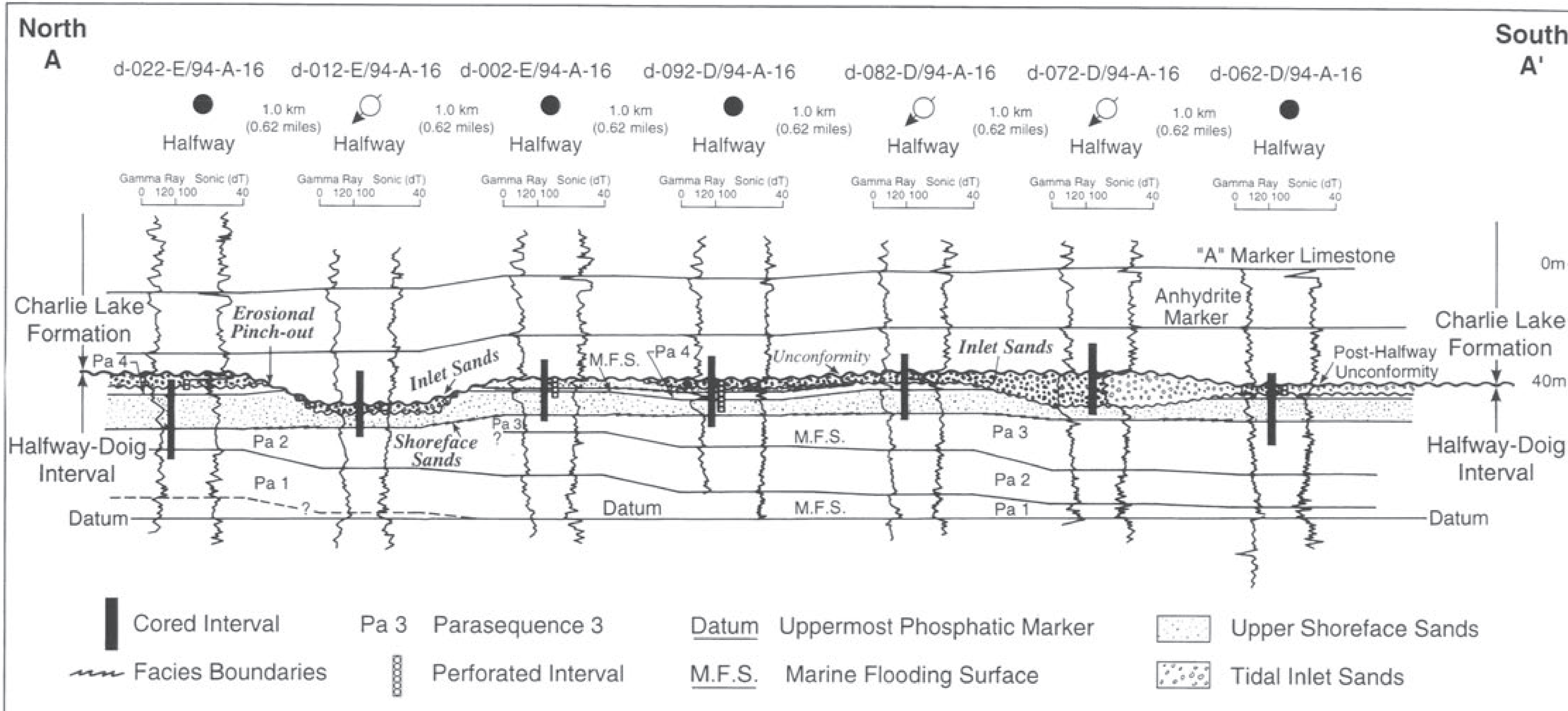

Figure H5. Stratigraphic cross-section A-A', Peejay area, demonstrating sequence stratigraphy of the Halfway/Doig succession, and highlighting occurrence of tidal channel/inlet reservoirs (from Caplan and Moslow, 1997).

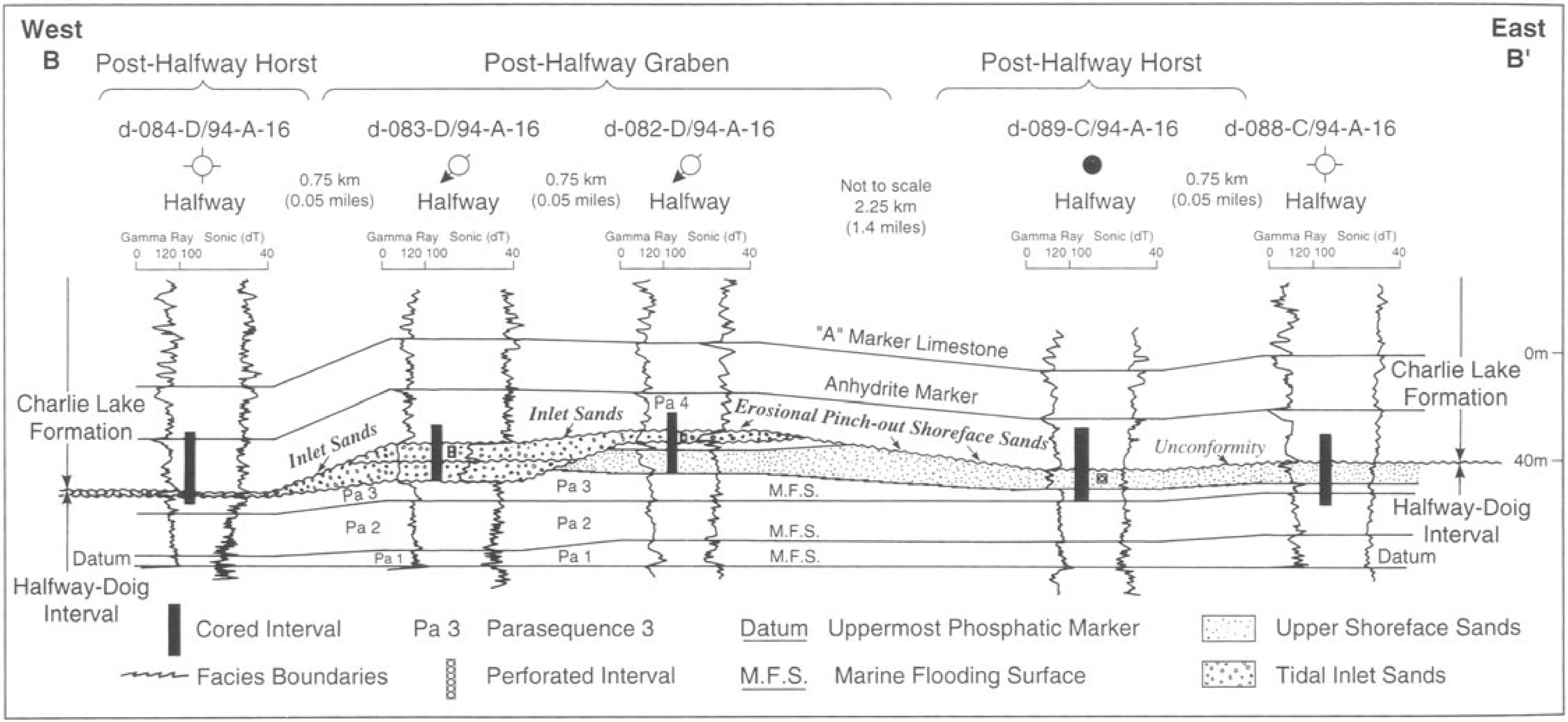

Figure H6. Stratigraphic cross-section B-B', Peejay area, demonstrating sequence stratigraphy of the Halfway/Doig succession, and highlighting occurrence of tidal channel/inlet reservoirs (from Caplan and Moslow, 1997).

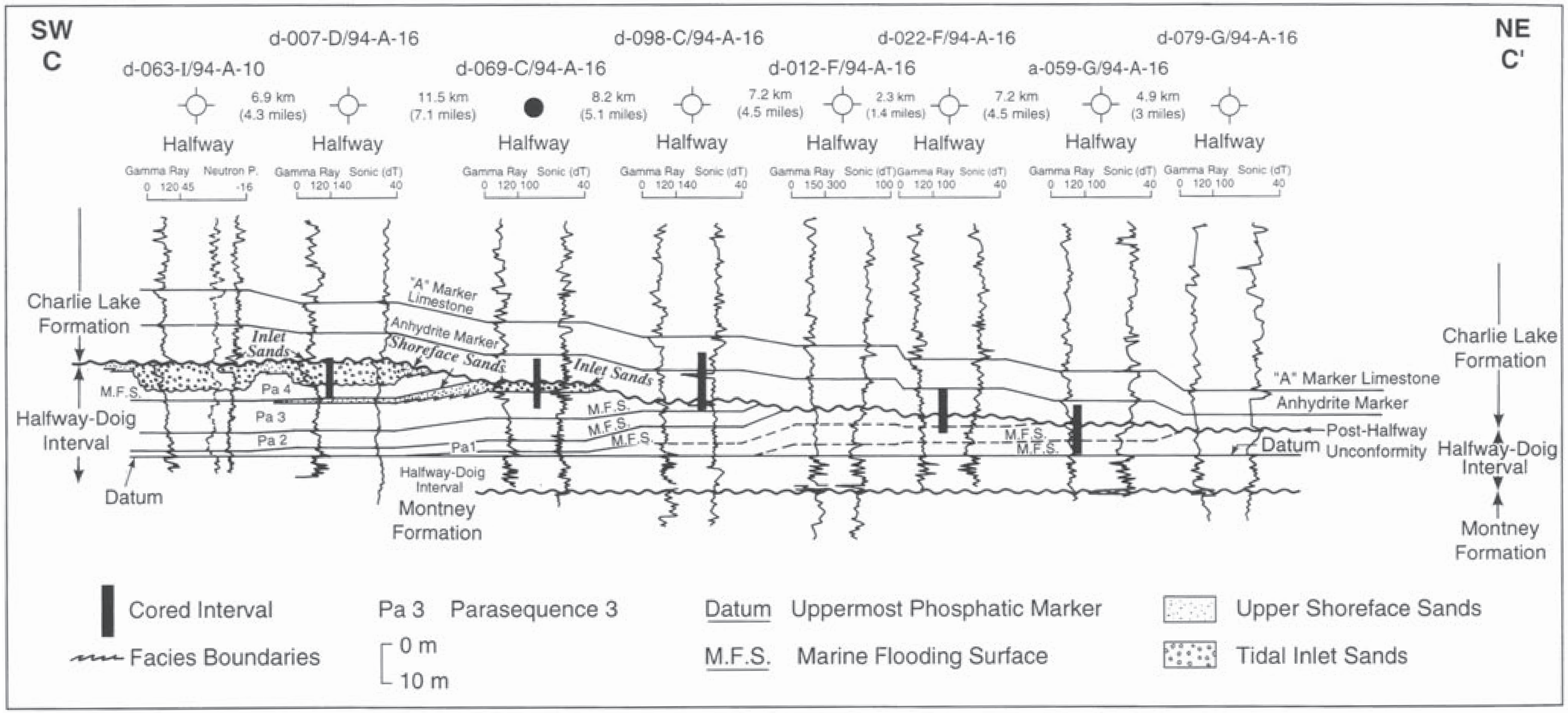

Figure H7. Stratigraphic cross-section C-C', Peejay area, demonstrating sequence stratigraphy of the Halfway/Doig succession, and highlighting occurrence of tidal channel/inlet reservoirs (from Caplan and Moslow, 1997).

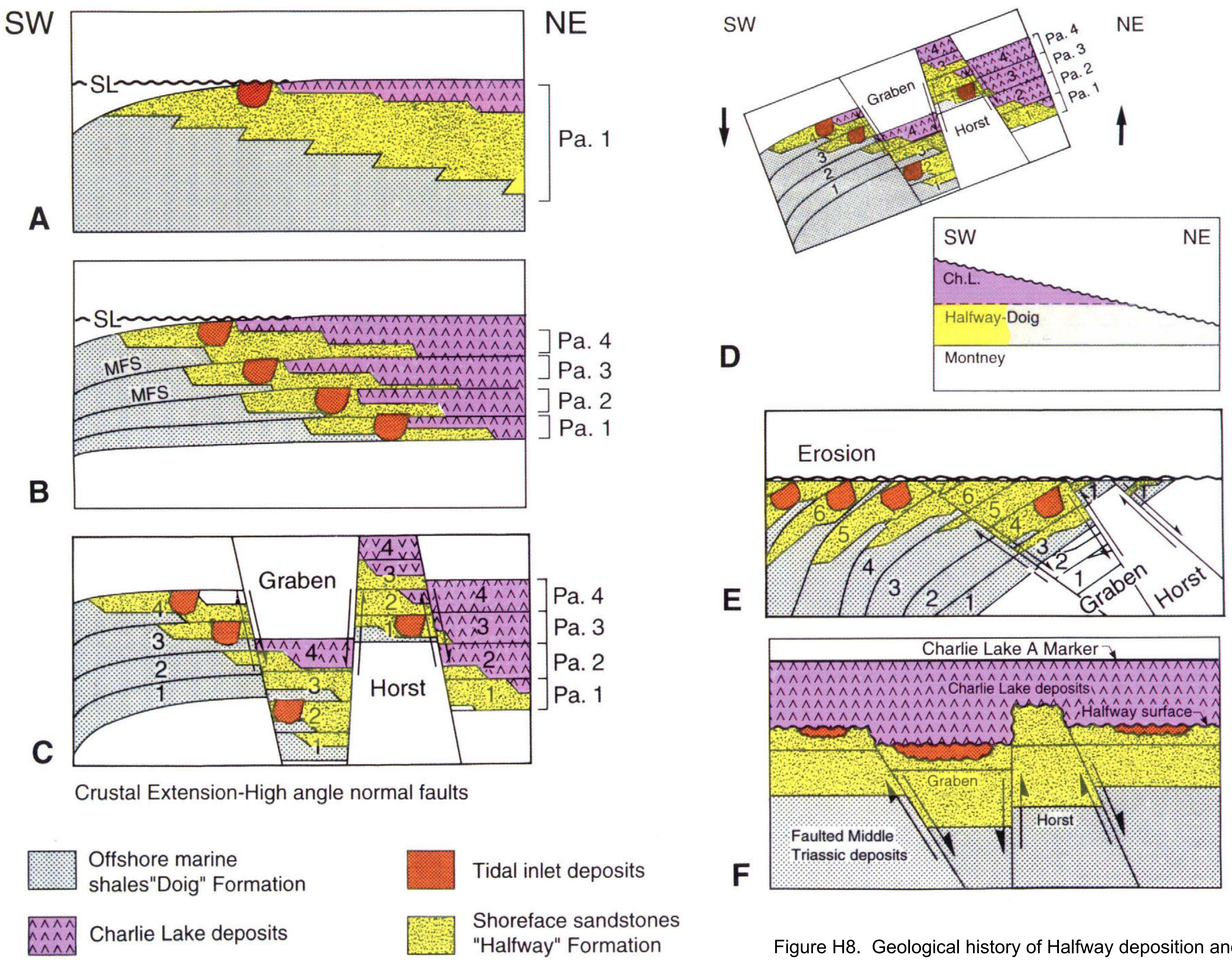

Figure H8. Geological history of Halfway deposition and subsequent structural deformation in the Peejay area (from Caplan and Moslow, 1999).

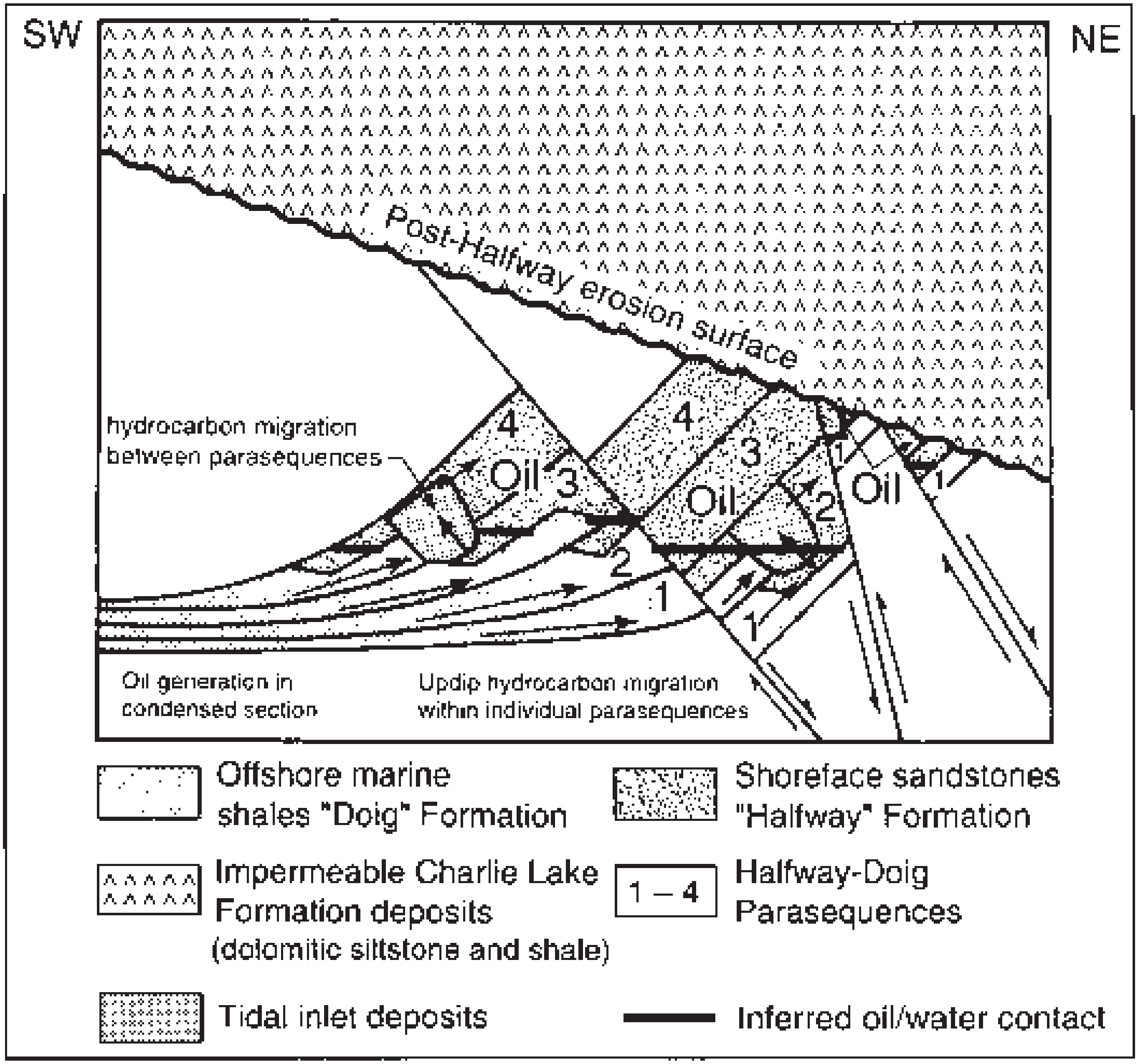

Figure H9. Idealized hydrocarbon exploration framework for Halfway reservoirs at Peejay (from Caplan and Moslow, 1999). Note that regional shoreface sandstones, in addition to tidal channel “sweet spot” reservoirs, are hydrocarbon-charged.

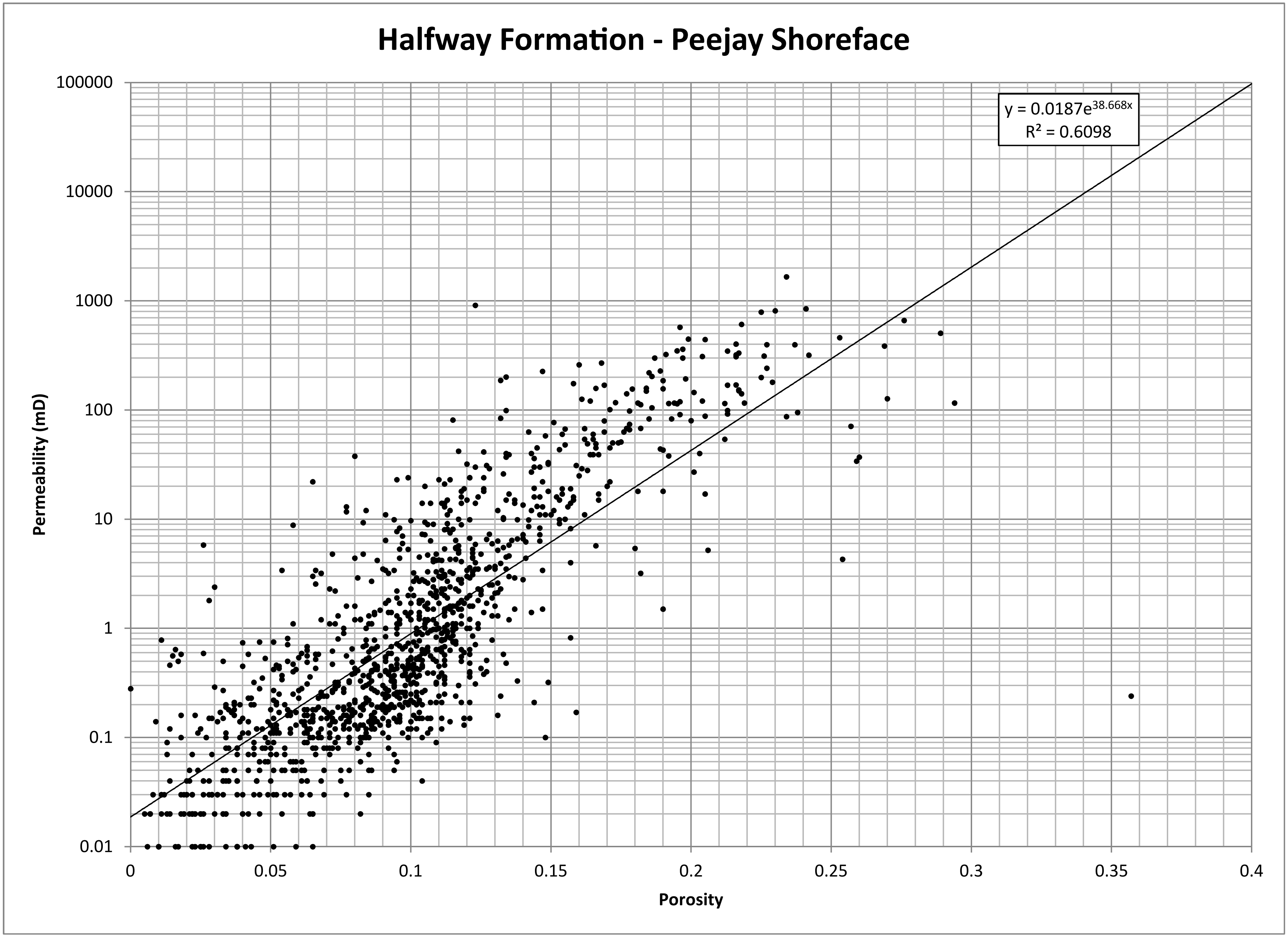

Figure H10. Porosity / permeability cross-plot, Halfway shoreface facies, Peejay Field focus area.

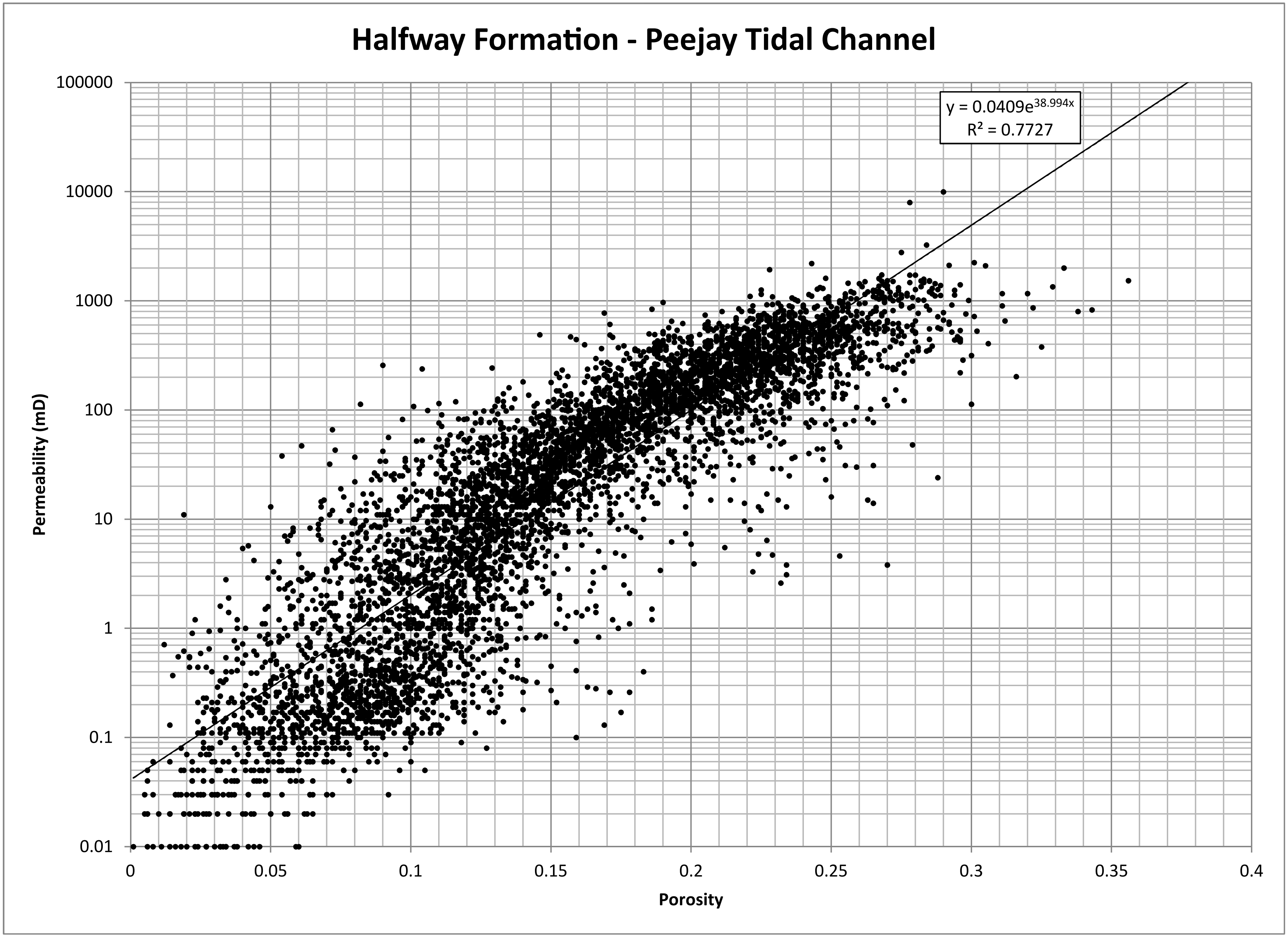

Figure H11. Porosity / permeability cross-plot, Halfway tidal inlet facies, Peejay Field focus area.

production months between 1962 and 1968. Reservoir pressure upon shut-in was 10363 kPa (1503 psia), and in May 1987 had risen to 10549 kPa (1530 psia) with no further production.

Examining five Halfway producers to the southeast (two of which were converted to water injectors), we found pressure and production responses to demonstrate that d-81-H is not in communication with the other wells, which jointly produced about 58.3 e^3m^3 oil and injected about 540 e^3m^3 water (Fig. H12, H13). We interpret the lack of communication to reflect production from the shoreface reservoir at d-81-H and tidal channel reservoirs in the other wells. See Appendix 5 for a more detailed discussion.

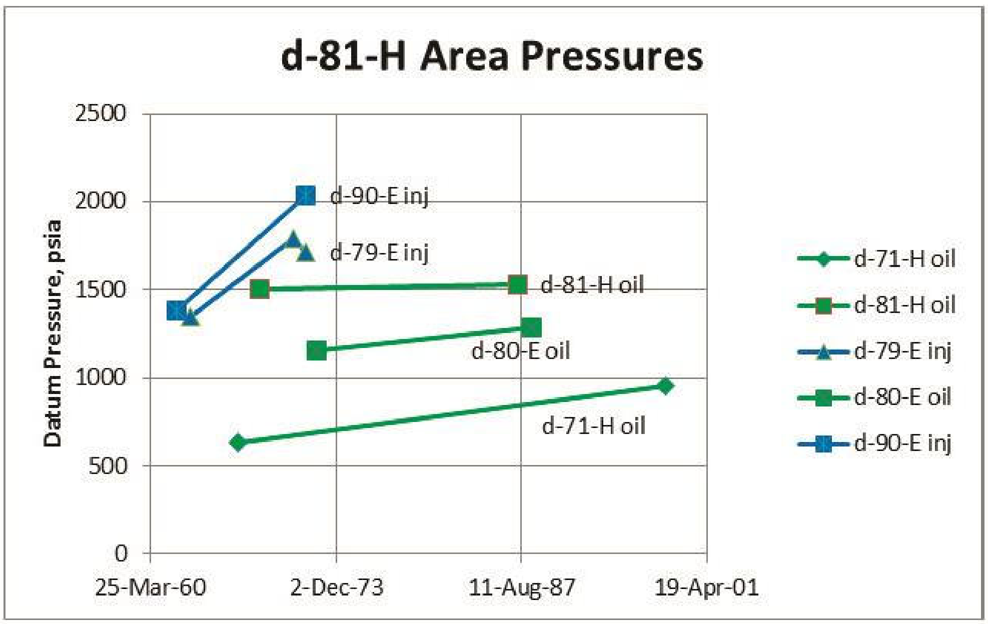

Figure H12. Historical reservoir pressures in Halfway at d-81-H/94-A-15 and adjacent wellbores.

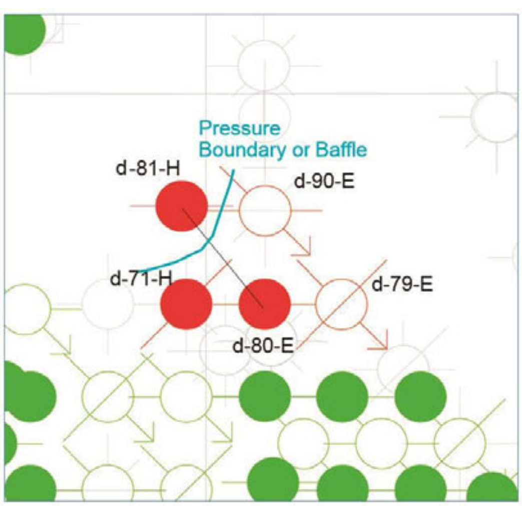

Figure H13. Schematic map showing reservoir pressure boundary or baffle in the Halfway reservoir between d-81-H/94-A-15 and adjacent producing / injecting wells.

2. **d-39-C/94-A-16**: Section cored, analysis shows low permeabilities characteristic of the shoreface throughout except for a one-foot section (3926.5-3927.5'), having 15% porosity and 58mD permeability, about eight feet below a high-quality tidal channel section. This one-foot section was acidized and frac'd in 1963, production tested in 1971, and produced 0.22 BCF and 16,349 barrels condensate during 1996-1999. Reservoir pressures measured 9763 kPa (1416 psia) in 1962, 7736 kPa (1122 psia) in 1987, and 6805 kPa (987 psia) in 1995.

   Pressure and production behaviour in offsetting wells is complex (Fig. H14, H15). Oil production from d-28-C appears to have drawn down pressures at both d-37-C and d-39-C before both wells were put on production in 1996. While both d-28-C and d-37-C were completed in the upper tidal channel facies, the tidal channel at d-37-C is thick and blocky, and appears to have incised the entire underlying shoreface section. We interpret this incision to have put the tidal channel reservoir locally in pressure and fluid communication with the shoreface reservoir at d-39-C.

   Much different pressure values and histories in wells to the north indicate the presence of a no-flow boundary (Fig. H15). See Appendix 5 for a more detailed discussion.

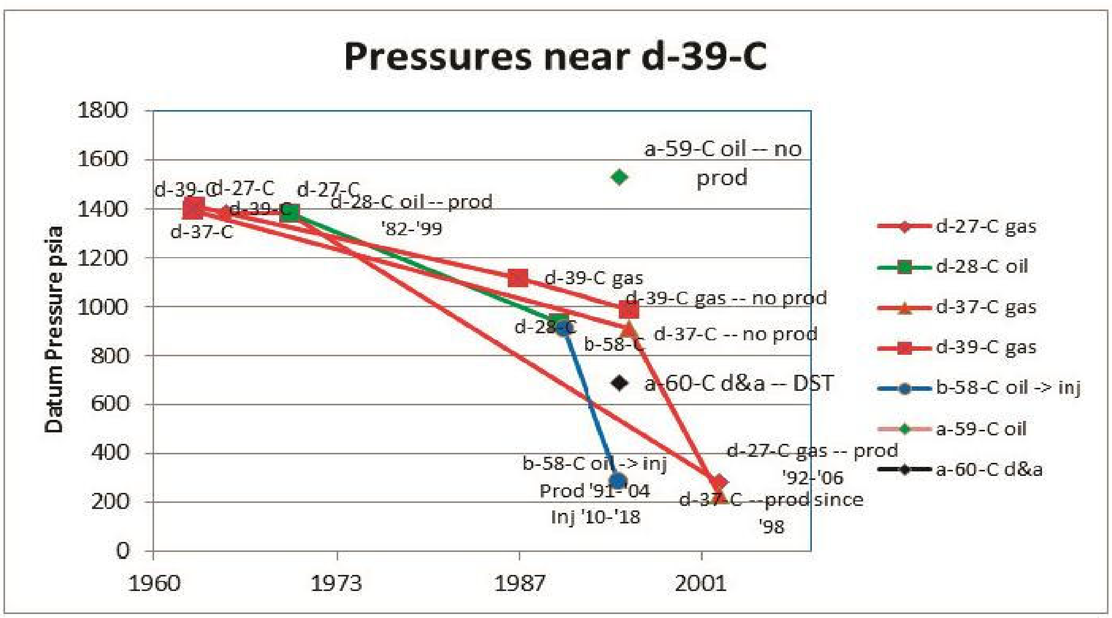

Figure H14. Historical reservoir pressures in Halfway at d-39-C/94-H-16 and adjacent wellbores.

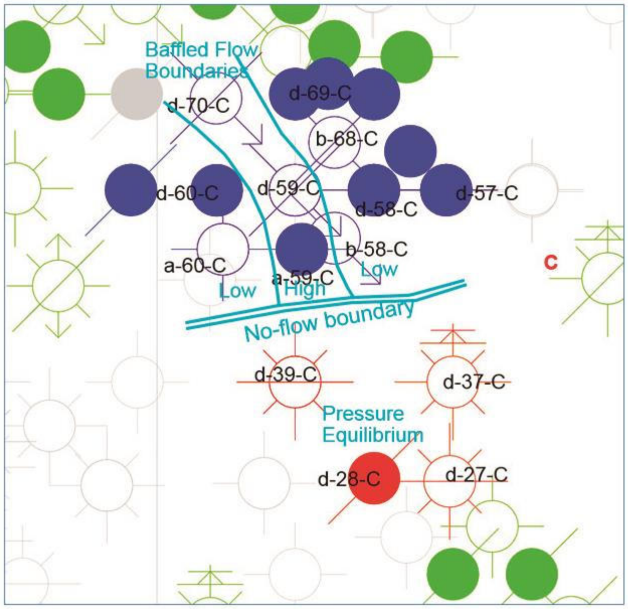

Figure H15. Schematic map showing reservoir pressure boundary in the Halfway reservoir between d-39-C/94-H-16, d-59-C/94-H-16 and offsetting wells.

3. **d-59-C/94-A-16**: Section cored, analysis shows low permeabilities characteristic of the shoreface throughout except for four thin intervals (<1') showing better reservoir quality typical of coquinoid sands. A four-foot section at the base of the Halfway was acidized and frac'd, and produced 14,459 barrels oil during nine months in 1966. In 1967, the entire Halfway was perfed and acidized and converted to water injection. Pool discovery pressure was 9487 kPa (1376 psia), and in 1995, a reservoir pressure of 13755 kPa (1995 psia) was measured.

   Reservoir pressures in Halfway wells surrounding d-59-C show quite variable behaviours (Fig. H15, H16). Wells were converted from production to injection at different times, adding to the complexity of the analysis. Water injection has met or exceeded voidage requirements, but very little water has been produced. There are steep pressure gradients between injectors and producers, but permeability at wells seems generally good, demonstrated by high production rates and good cumulative production volumes, and the apparent ease of injecting large volumes of water. We interpret these behaviours to indicate compartmentalization with baffles impeding flow between wells, or groups of wells (Fig. H15). See Appendix 5 for a more detailed discussion.

   Regarding d-59-C specifically, early oil production confirms oil charge and productive capacity in the shoreface section. After recompletion and conversion to water injector, the well's behaviour presumably was dominated by the upper tidal channel reservoir. However, the pressure gradients and lack of significant water breakthrough suggest potential for infill drilling to access undrained compartments and/or improve sweep, even in the higher-quality tidal channel reservoir facies.

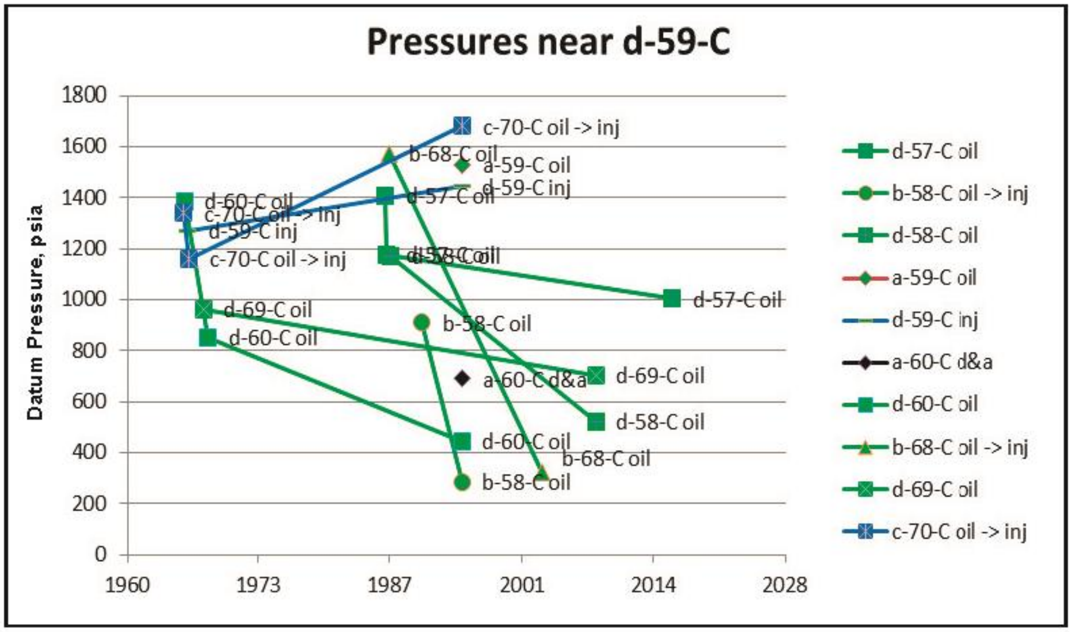

Figure H16. Historical reservoir pressures in Halfway at d-59-C/94-H-16 and adjacent wellbores.

4. **d-89-C/94-A-16**: Section cored, analysis shows permeabilities of 4mD or less throughout. Caplan and Moslow (1997) interpreted the entire section as shoreface facies (Fig. H6). An eight-foot section was acidized and frac'd, and 26.2 e^3m^3 (164,730 barrels) oil produced at rates up to 16 m^3/D (100 BOPD) between 1966 and 1987. A reservoir pressure of 9046 kPa (1312 psia) was taken shortly after production commenced; a measurement in 1986 showed a decline to 3000 kPa (435 psia).

   Surveying seven offsetting Halfway wells (five producers and two water injectors, all completed in the tidal channel facies), we saw fairly consistent pressure behaviour and good waterflood responses, with reservoir pressures mostly within a fairly narrow band of 7585-9650 kPa (1100-1400 psia) (Fig. H17, H18). The five producers show limited gas/oil ratio increases and water breakthrough with increasing water/oil ratios.

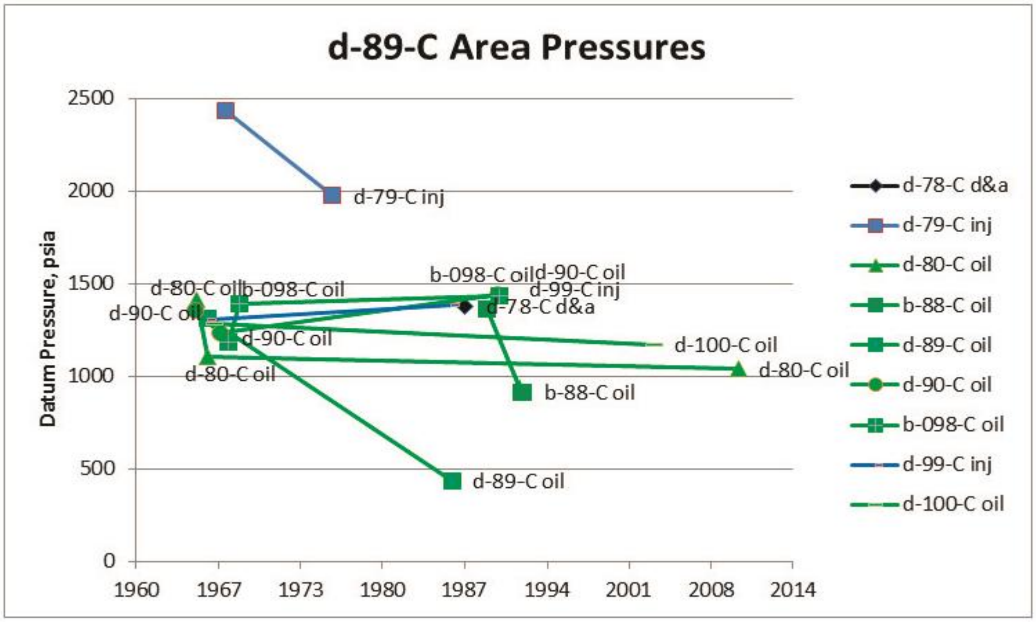

Figure H17. Historical reservoir pressures in Halfway at d-89-C/94-H-16 and adjacent wellbores.

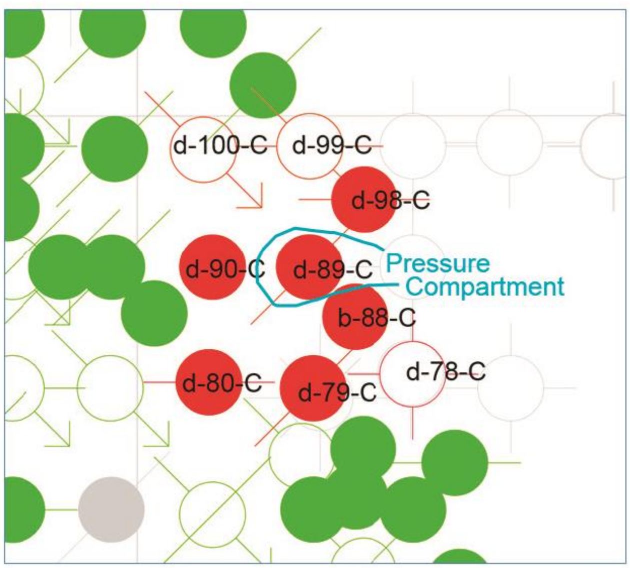

Figure H18. Schematic map showing reservoir pressure boundary in the Halfway reservoir between d-89-C/94-H-16 and offsetting wells.

Production behaviour at d-89-C demonstrates that it is in a separate reservoir compartment; besides the declining reservoir pressures, we see little water production and generally smoothly-declining oil production rates (Fig. H19). We interpret this compartmentalization to result from the stratigraphic separation of the shoreface reservoir at d-89-C from the tidal channel reservoirs producing in the offsetting wells. See Appendix 5 for a more detailed discussion.

5. **d-2-E/94-A-16**: Section cored, analysis shows permeabilities of 7mD or less throughout, except for four intervals of 0.7 feet or less with perms of 10-37mD.

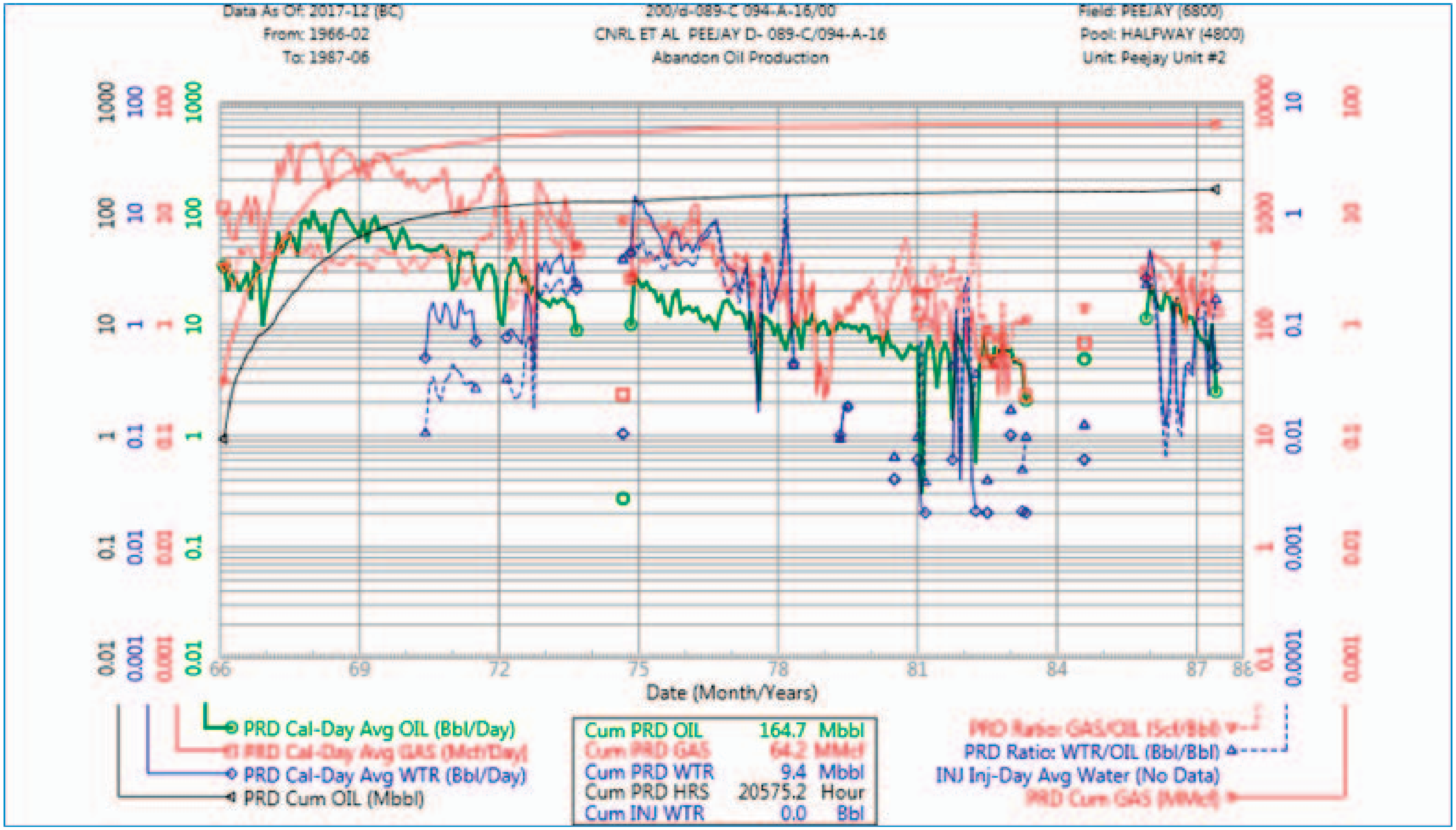

Figure H19. Production history plot, d-89-C/94-H-16, showing no evidence of response to waterflooding in offset wells.

Shoreface interpretation confirmed in Caplan and Moslow (1999), who interpreted the higher-perm streaks as isolated coquina layers in the shoreface (Fig. H5). An eleven-foot section was acidized and frac'd, which produced 95.9 e^3m^3 (602,298 barrels) oil and 47.1 e^3m^3 (295,961 barrels) water between 1965 and 2015.

Numerous Halfway oil producers and water injectors, completed in tidal channel facies, surround the d-2-E well. Its reservoir pressure behaviour indicates close links to a few nearby wells, and significant baffling or compartmentalization compared to other wells (Fig. H20, H21). Reservoir pressure at d-2-E and neighbouring producers, as well as the b-2-E water injector dropped consistently to as low as 1075 kPa (156 psia) by 1991. The production history at d-2-E indicates excellent waterflood response, with significant water breakthrough and increasing water rates until the well was suspended with a water cut of >95% (Fig. H22).

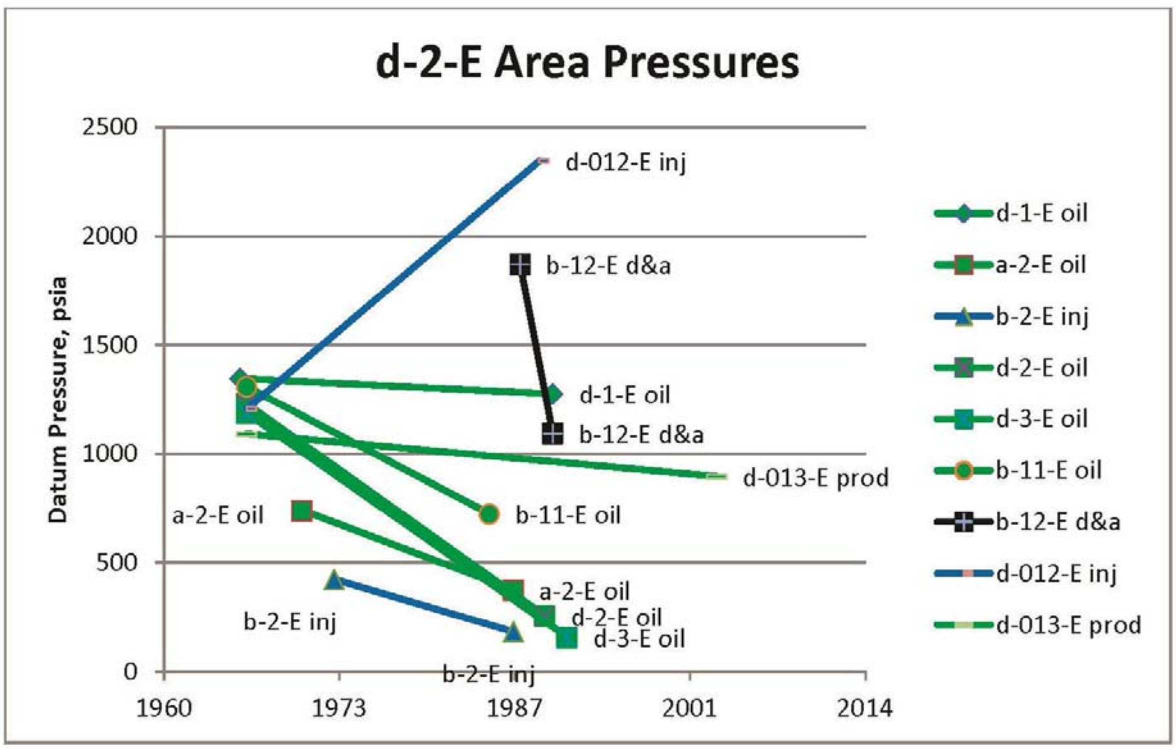

Figure H20. Historical reservoir pressures in Halfway at d-2-E/94-H-16 and adjacent wellbores.

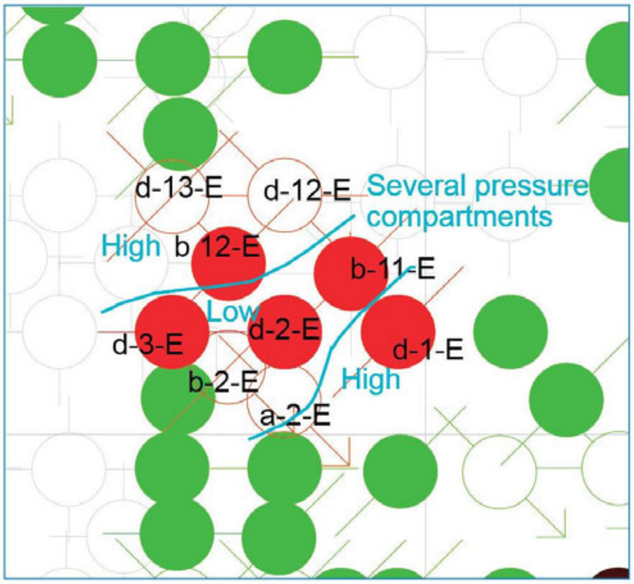

Figure H21. Schematic map showing reservoir pressure boundary in the Halfway reservoir between d-2-E/94-H-16 and offsetting wells.

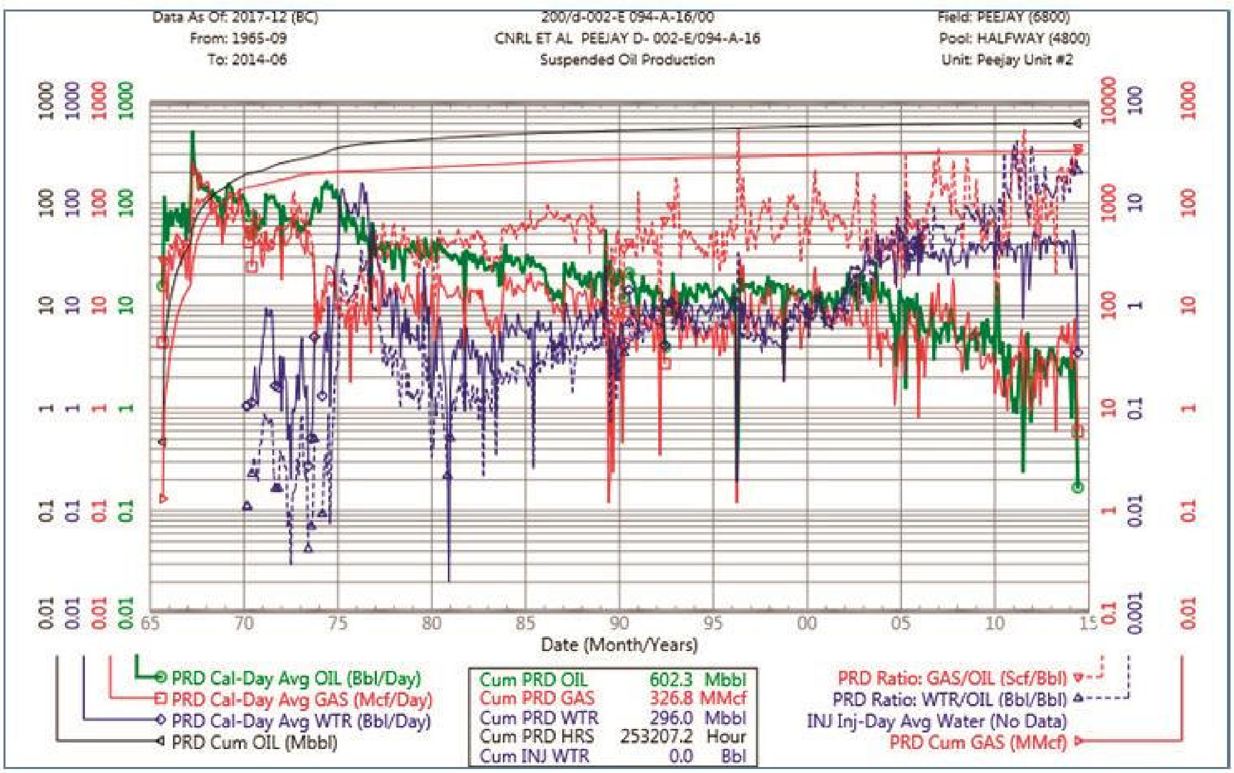

Figure H22. Production history plot, d-2-E/94-H-16, showing excellent waterflood response.

We conclude that the shoreface reservoir at d-2-E is in contact with tidal channel reservoirs in its nearest neighbours, likely through incision of tidal channels into the shoreface. Further work would be required to understand the structural and/or stratigraphic separation that has produced pressure baffles and barriers between the d-2-E group and offsetting wells. See Appendix 5 for a more detailed discussion.

Looking at DST data, eight of the nine wells tested in the shoreface reservoir analyze as low permeability, with no valid reservoir fluid information. At c-59-L/94-A-9, some good permeability is evident, likely from a very thin (<1m) clean porous sandstone in the 5m thick shoreface succession.

We conclude that while high-quality tidal channel reservoirs have been the primary producers in the Halfway in the Peejay area, there exists a substantial body of lower-quality, oil-charged reservoir rock that in places is capable of oil production from vertical wellbores.

Regional Production and Test Data

Halfway reservoirs host gas in western areas, including major accumulations at Tommy Lakes (northern stratigraphic subcrop edge), Bubbles / Jedney / Beg (outer Foothills structural traps), and at Monias and related structurally-trapped pools in the Fort St. John Graben area to the south (Map H1). Oil pools are found updip, generally shallower than 1500m in northeastern B.C., but at considerably greater depths in adjacent Alberta. Maturity of underlying Doig source rocks appears to be the primary control on Halfway reservoir fluid composition (Podruski *et al.*, 1988).

Appendix 9 summarizes important characteristics of conventional Halfway oil pools in British Columbia. Key observations:

- Only one field – Peejay – has more than 100 million barrels of oil originally in place (MMBOOIP), and contains twice as much oil as Milligan Creek Halfway ‘A’, the next largest accumulation.
- Four other pools exceed 30 MMBOOIP, while the next 50 pools tabulated contain 1-18 MMBOOIP. While generally thicker than the Charlie Lake, net pays are thin, and pool boundaries are sharply defined vertically and horizontally by facies and cementation boundaries.
- Most pools are very mature and remaining reserves are relatively small.
    - The largest Halfway discoveries were made in the 1960’s and 1970’s; smaller discoveries were made commonly through the 1990’s. Since 2000, however, the pace of discovery has slowed considerably, and only one Halfway oil pool has been discovered since 2008.
- Oil gravities are light to very light.

- Pool average porosities (8-28%, average 17%) and permeabilities (10-1080mD, average 206mD) are conventional. It appears that oil in place resources in tighter sandstone facies have not been tabulated.
- Recovery factors are highly variable. Waterfloods have been implemented in some of the larger pools; many pools with low recovery factors are too small to justify enhanced recovery.

Janicki (2014) found in a regional hydrogeological analysis of the Halfway in NEBC that the oil-producing region, including our Peejay Field Focus Area, lies within a regional potentiometric low (Fig. H23). This suggests enhanced oil trapping potential in the region, and thus better prospectivity for regionally extensive tight oil accumulations.

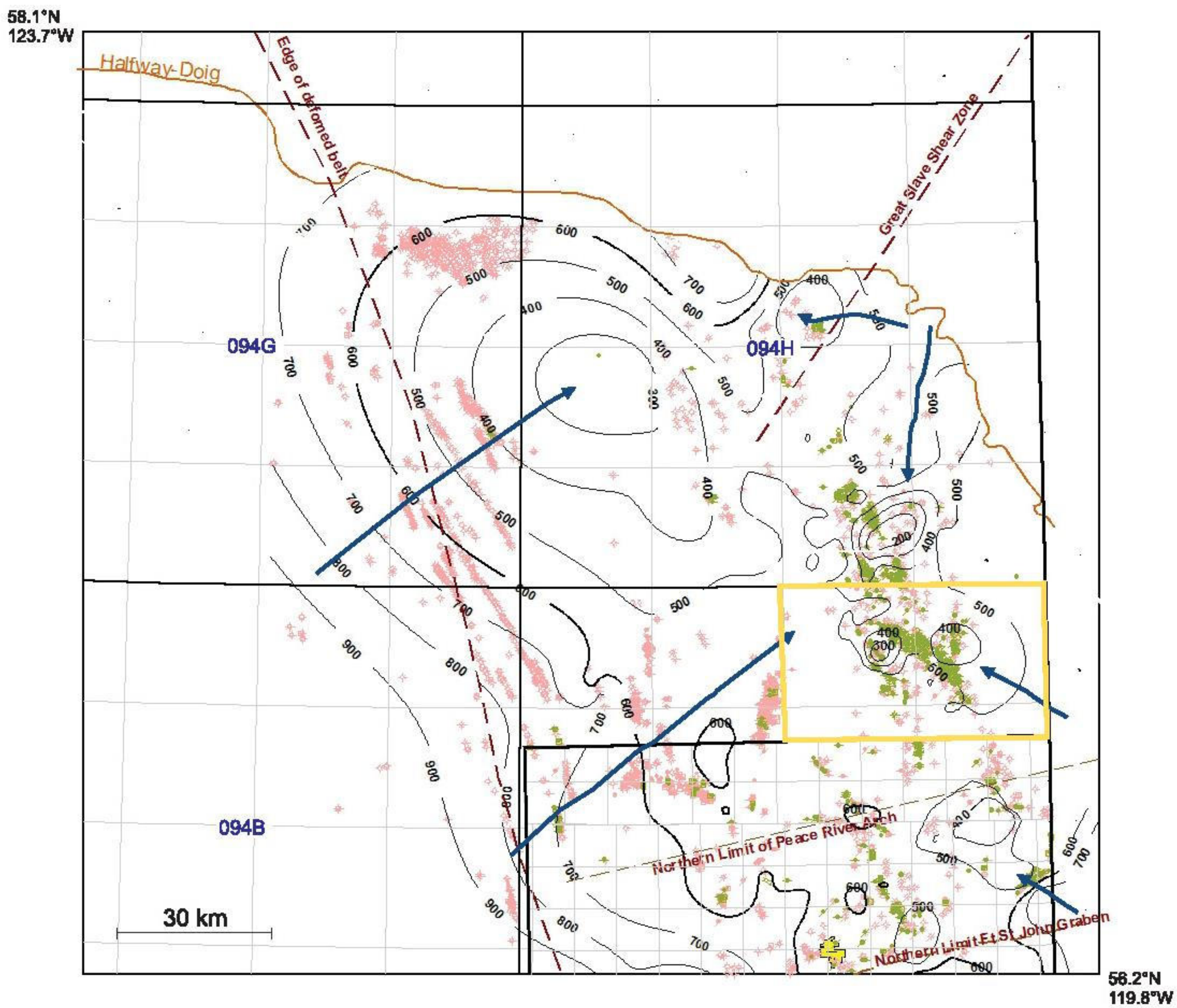

Figure H23. Potentiometric surface on top Halfway Formation (from Janicki, 2014). Potentiometric lows in the oil-producing area assists in regional trapping of oil, and enhances potential for extensive oil accumulations in Halfway shoreface reservoirs.

Horizontal Drilling

Horizontal wells have been drilled in a number of Halfway oil and gas pools in Alberta and B.C., but only the Progress area (Twp 77-78, Rge 9-10W6) has seen significant horizontal development in an oil pool (Map H1). Styan and Shaw (1991) described deltaic and estuarine valley fill reservoirs in the lower and upper Halfway, noting petrographically elongate lenses of coarser sandstones with intergranular and vuggy porosity capping the upper Halfway. Core analysis data demonstrate that most of the Halfway reservoir at Progress is of moderate quality, similar to shoreface reservoirs at Peejay. A round of horizontal drilling between 2011 and 2014 at Progress appears to have targeted both the high-quality and lower-grade sands. A reservoir engineering review of horizontal well performance may be instructive and applicable to similar quality Halfway reservoirs in B.C.

In B.C., there are a number of Halfway horizontal gas wells in the outer Foothills at Altares, Beg, and Tommy Lakes areas, and two or three horizontal oil wells have been drilled in pools at Flatrock, Boundary Lake North, and Rigel. There appears to have been no consistent effort to develop lower-permeability oil-bearing Halfway sandstones.

Analytical Data

Our database search returned analytical reports on the Halfway Formation in 29 wells, which sampled conventional core, sidewall cores, and cuttings (Appendix 1; Map H1). These consist primarily of routine core analyses, standard petrography, and x-ray diffraction work. Source rock analysis work was done in older wells, primarily for GSC studies that sampled large intervals across a number of formations regardless of lithology. There is no record of systematic geomechanical work being done to assess the Halfway for horizontal multi-frac development.

No new analytical work on the Halfway was undertaken in this study.

Resource Oil Assessment

The Halfway may offer halo oil play potential analogous to that in the Cardium of western Alberta. In the broad fairway of Halfway oil production trending from Lapp (94-H-10) in the northwest to Boundary Lake (Twp 85-14W6) in the southeast, and southeastward into Alberta, high-quality tidal channel and upper shoreface reservoirs have been developed in many pools with vertical wells (Map H1). Most Halfway exploration and development work was undertaken in the 1980’s and earlier, and few horizontal wells have been completed in oil pools.

We have demonstrated that Halfway shoreface reservoirs have substantial (although poorer) reservoir quality, are regionally to sub-regionally charged with oil, and are capable of oil production from vertical wells in isolated cases. Existing oil production throughout the formation is strongly compartmentalized by structural and stratigraphic elements. There may be abundant opportunity to develop lower-quality Halfway "halo" shoreface reservoirs in areas undrained or ineffectively drained by existing vertical producers.

Prospective areas for Halfway "halo" oil should be assessed along the oil fairway west of the Halfway erosional limit, particularly offsetting existing conventional production where abundant data are available. Shoreface reservoir thickness, quality, and in-place oil resources should be characterized in detail, and some very targeted analytical work done to characterize geomechanical characteristics in the target areas. Very detailed structural mapping using both well control and seismic should be undertaken to help identify reservoir compartments. Horizontal wells may not only enable economic development of marginal-quality sandstones, but may tap into isolated small tidal channels or better-quality coquinoid sandstone developments in the shoreface (as in the d-39-C, d-59-C and d-2-E wells in the Peejay Focus Area).

CHARLIE LAKE FORMATION

Age and Play Type

Upper Triassic (Carnian).

We investigated Charlie Lake resource oil potential in two settings:

- Halo oil associated with conventional Charlie Lake oil pools, primarily in the Peace River Block and in 94A and 94H (Map CL1, Appendix 9);

- Tight oil in low- to moderate-porosity and permeability upper Charlie Lake sandstones, like those currently under development in the Worsley area about 70 km east of the Alberta border.

Both plays have a 'C' level of prospectivity – there appears to be little potential for significant resource oil discoveries in B.C.

Regional Geology

The Charlie Lake is a thick succession of intercalated siliciclastic, carbonate, and evaporitic rocks, forming the culmination of a major transgressive-regressive cycle begun at the base of the Doig (Gibson and Edwards, 1990). Siliciclastics consist of shale, siltstone and very fine- to medium-grained sandstone; red beds are common to the east. Microcrystalline silty dolostone and skeletal limestone and dolostone are laterally extensive, while anhydrite and gypsum are common, in places forming persistent stratigraphic markers. Up to fourteen locally significant sub-units, most representing producing or potentially productive oil and gas reservoirs, have been recognized and named.

The top of the Charlie Lake occurs at depths as shallow as about 1000 metres near the northern subcrop edge, and as deep as 3700m in the southwestern Deep Basin adjacent to the deformation front (Map CL1).

Charlie Lake strata more or less conformably overlie or interfinger with marine sandstones of the Halfway Formation over much of NEBC, and normal marine carbonates of the Baldonnel Formation overlie the Charlie Lake where the Triassic is fully preserved (Fig. CL1). Eastward and northward, the Baldonnel and then the Charlie Lake are eroded beneath pre-Jurassic and pre-Cretaceous unconformities. Westward, the Charlie Lake grades into open marine carbonates and sandstones of the Ludington Formation (Fig. CL1, Gibson and Edwards, 1990).

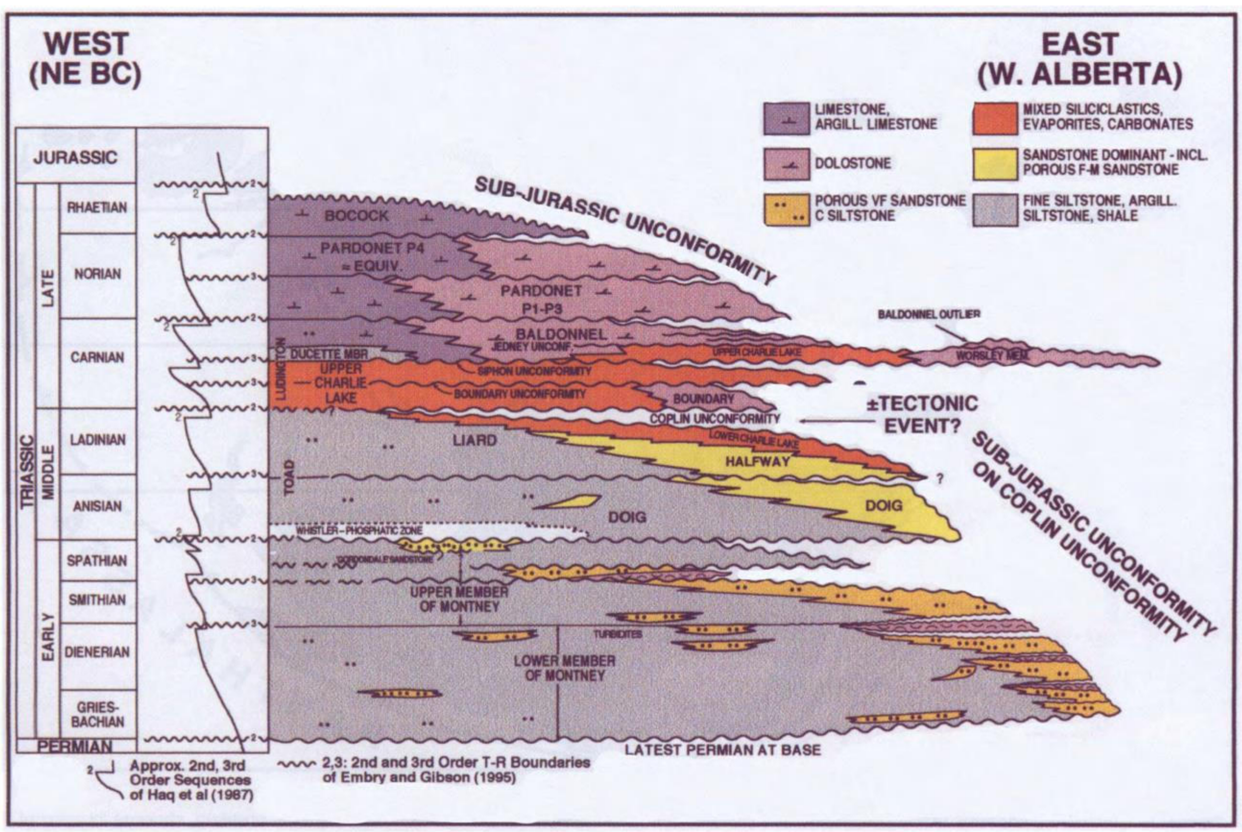

Figure CL1. Event stratigraphic summary for Triassic succession of WCSB (same as Fig. H1). Note numerous unconformities within the Charlie Lake Formation, particularly beneath the upper Charlie Lake and Worsley members in the east (from Davies, 1997a).

Internal regional to sub-regional unconformities subdivide the Charlie Lake (Fig. CL1). Unconformities are particularly important in the distribution of reservoir facies in the undifferentiated upper Charlie Lake and Worsley Member in west-central Alberta, as discussed below (Davies, 1997a).

Charlie Lake strata were deposited in restricted marine, shallow water lagoon, tidal flat and sabkha environments. The bulk of the formation is cemented by evaporitic and carbonate cements; most conventional reservoir sandstones were deposited as subaerial dunes, and feature very good reservoir quality where porosity is not occluded by evaporite / carbonate cements or pyrobitumen.

Reservoir Geology – Regional Charlie Lake

Sandstone members – Light oil and gas occur primarily in relatively small stratigraphic traps at various stratigraphic levels within the Charlie Lake (Map CL1). Quartzose sandstones deposited as aeolian dunes are the primary reservoir facies in numerous pools, such as in the Artex Member at Brassey (Fefchak and Zonneveld, 2010; Higgs, 1990), the Inga Member at Inga (Fitzgerald and Peterson, 1967; Arnold and Moslow, 1996), the Cecil Member at Boundary Lake, Oak, Rigel, and Cecil Lake, and the North Pine sandstone at Stoddart, North Pine and Fort St. John (Janicki, 2013) (Map CL1). Stratigraphic traps are formed by the pinchout of reservoir facies, and/or cementation by evaporitic and carbonate cements. Net pay thicknesses are generally only a few metres; producing pools are sharply bounded, and are rarely more than 1-2 km wide and a few kilometres long. The Artex member at Brassey is a good example (Fig. CL2, CL3, CL4).

The Inga sandstone at Inga Field was deposited in a similar aeolian setting, but covers a much larger area. It hosted original oil in place of 19,838 e^3m^3 (125 MMBO) in a broad structural / stratigraphic trap in the outer Foothills (Fitzgerald and Peterson, 1967; Janicki, 2013) (Fig. CL5).

Charlie Lake sandstones have been cored extensively, in most cases by short cores targeting a single thin reservoir interval. Looking at core analysis samples with grain densities <2.675 g/cm^3 (clean sandstones with little or no carbonate / evaporite cement) we see a reasonable linear relationship and very good to excellent reservoir quality, with porosities to 25% and permeabilities to just over a Darcy (Fig. CL6). Low porosity/permeability samples make up a fairly small fraction of the total.

Boundary Limestone – At Boundary Lake, Roy (1972) described the Boundary Member as a multi-cyclic stromatolitic limestone and dolomite complex, preserved as an erosional remnant in a paleostructural low. In B.C., the Boundary Lake ‘A’ Pool covers more than two townships, but has been eroded outside of pool-bounding faults (Map CL1; Fig. CL7). A number of structurally-controlled outliers have been identified, primarily in Alberta. Janicki (2013) interpreted Boundary Lake Field to be a conventional structural / stratigraphic trap.

Looking at Charlie Lake limestones in core analysis data, chosen as those samples with grain densities >2700 g/cm^3 (which will include some noise from cemented samples with mixed mineralization), we see a reasonable linear relationship, with some porosities >30%, but permeabilities significantly lower than in the sandstones (Fig. CL8).

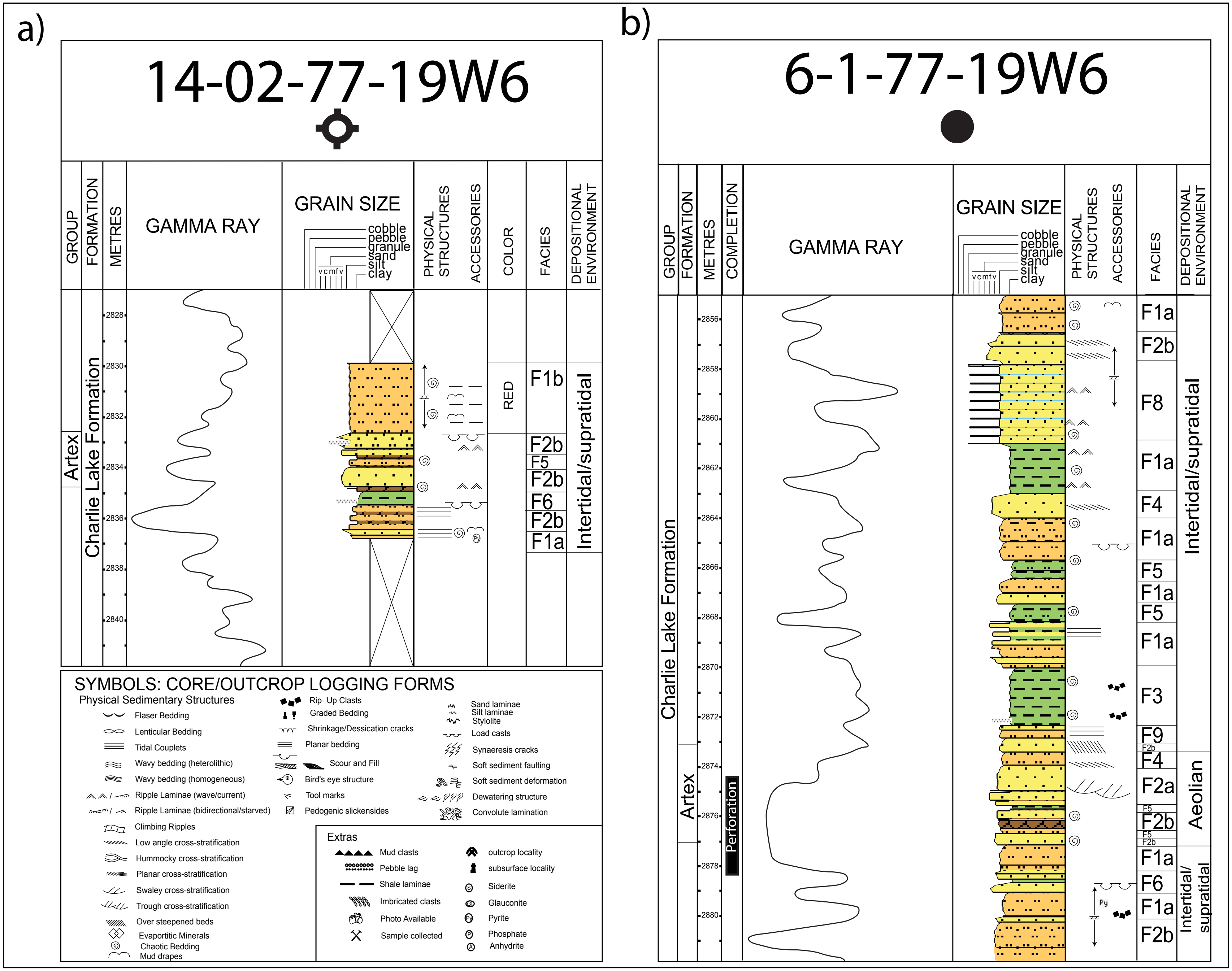

Figure CL2. Core descriptions for the productive Artex Member at Brassey Field. Producing facies F2a is less than 2m thick at producing well 6-1-77-19W6. Well 14-2-77-19W6, at the pool boundary, shows thinner, more cemented, lower-quality sandstones. From Fefchak and Zonneveld (2010).

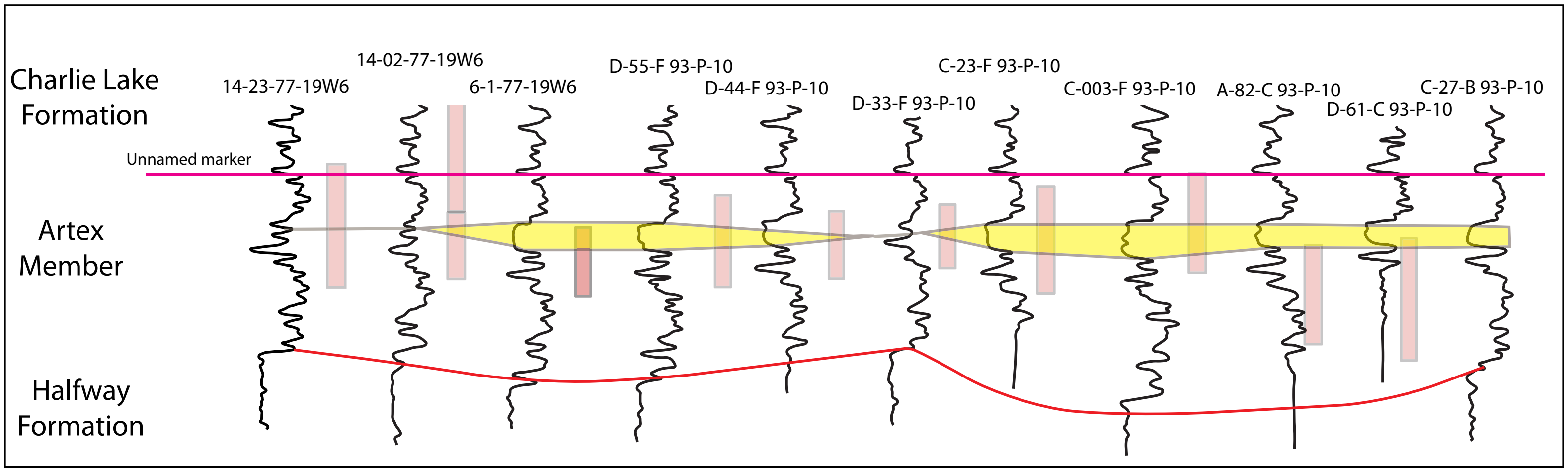

Figure CL3. Northwest-southeast cross-section through pools B and D of the Brassey Field, highlighting thin reservoir sandstones of the Artex Member. Line of section shown in Fig. CL4. From Fefchak and Zonneveld (2010).

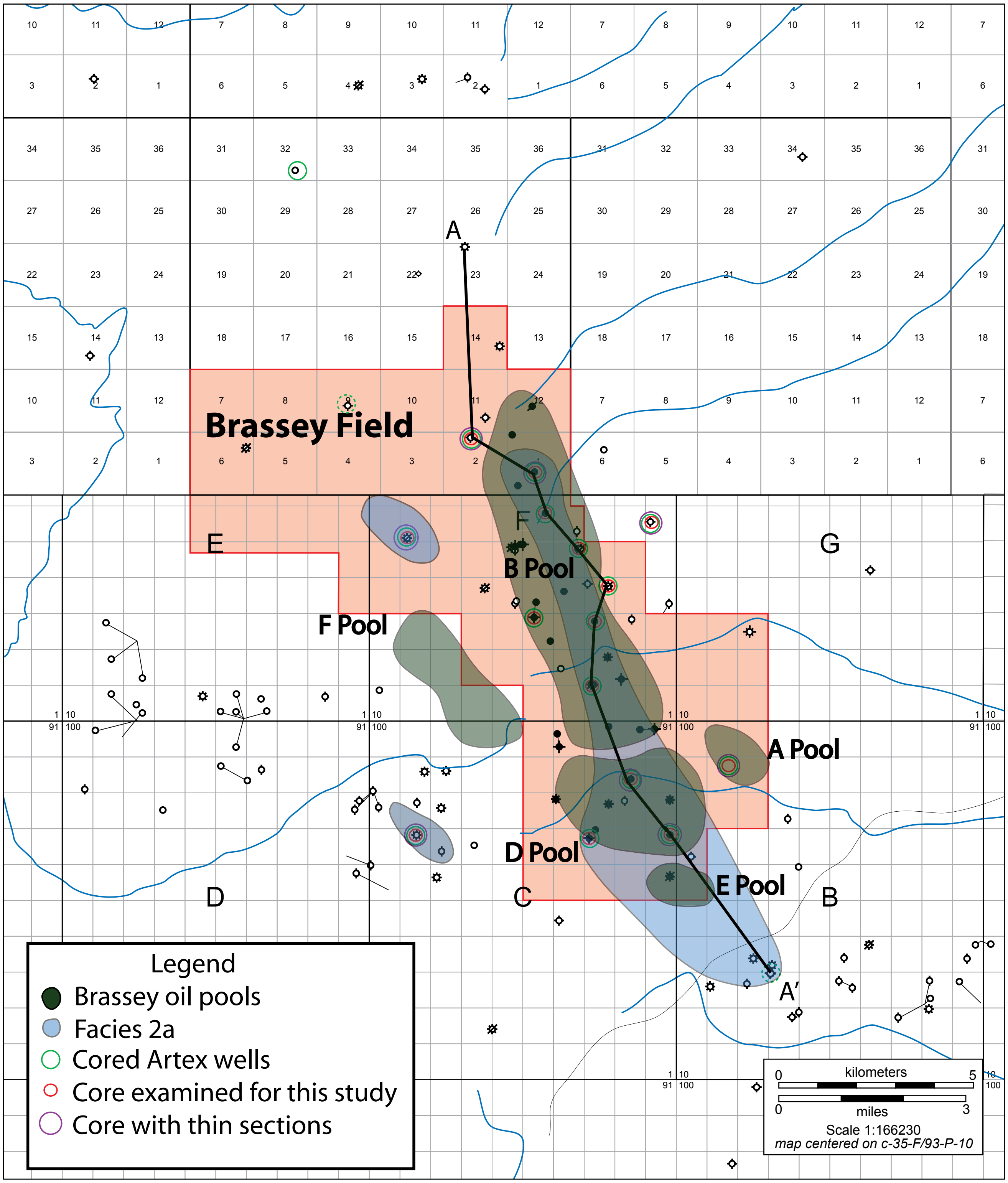

Figure CL4. Facies and pool map, Brassey Field. Note the main producing trend is only about 2km wide and less than 10km long. From Fefchak and Zonneveld (2010).

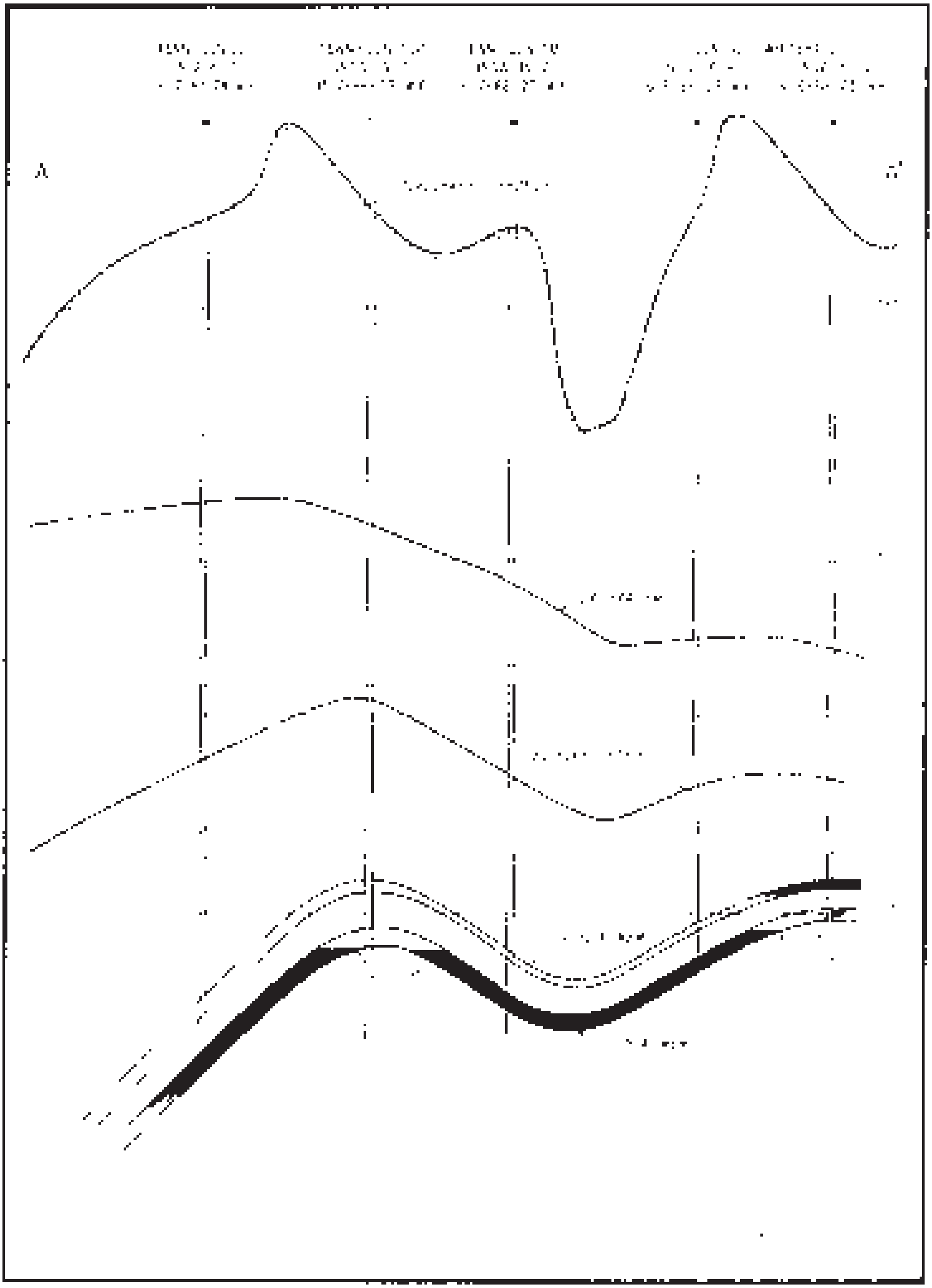

Figure CL5. Structural cross-section through Inga Field.
From Fitzgerald and Peterson (1967).

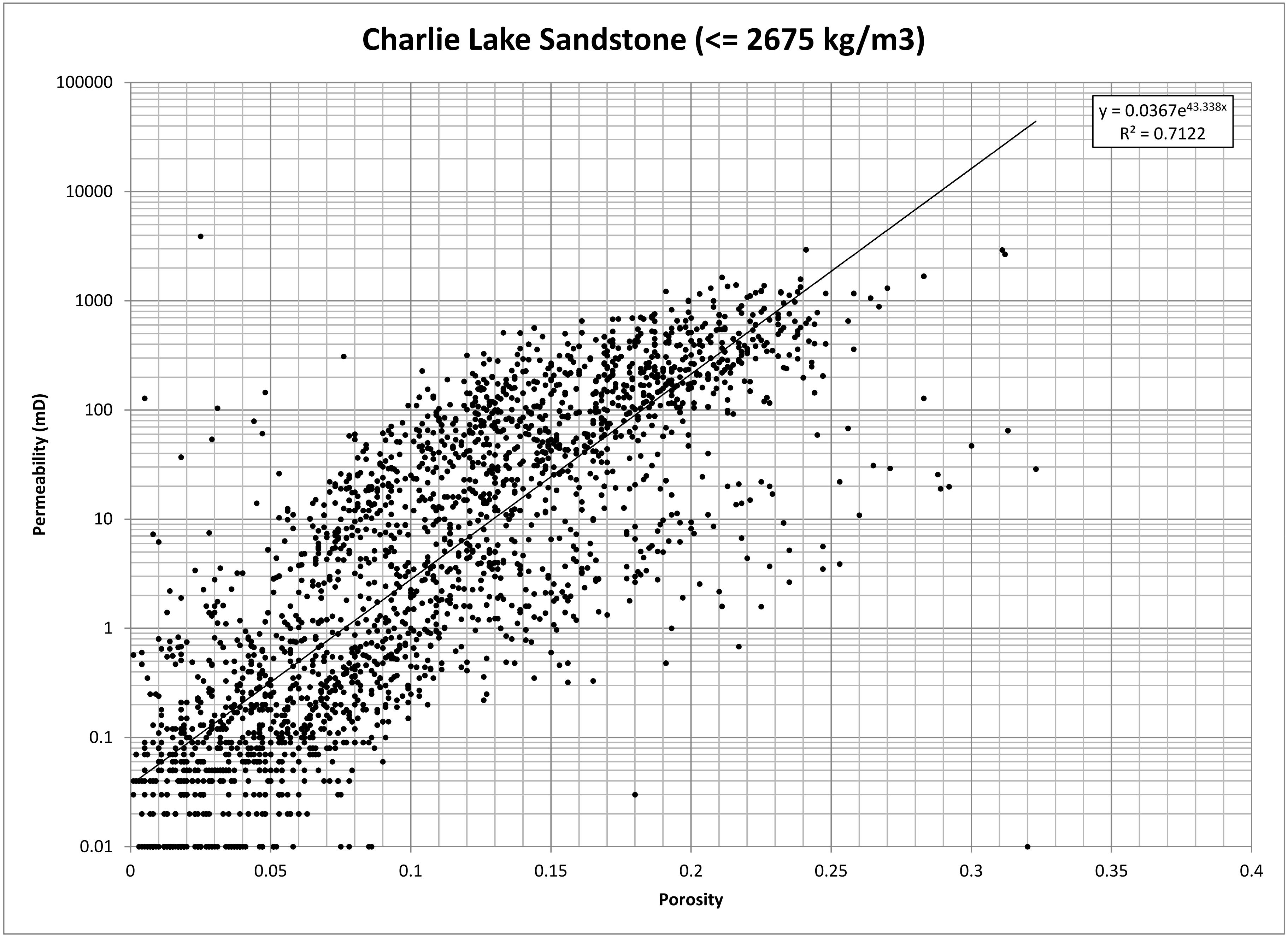

Figure CL6. Porosity / permeability cross-plot, Charlie Lake sandstone.

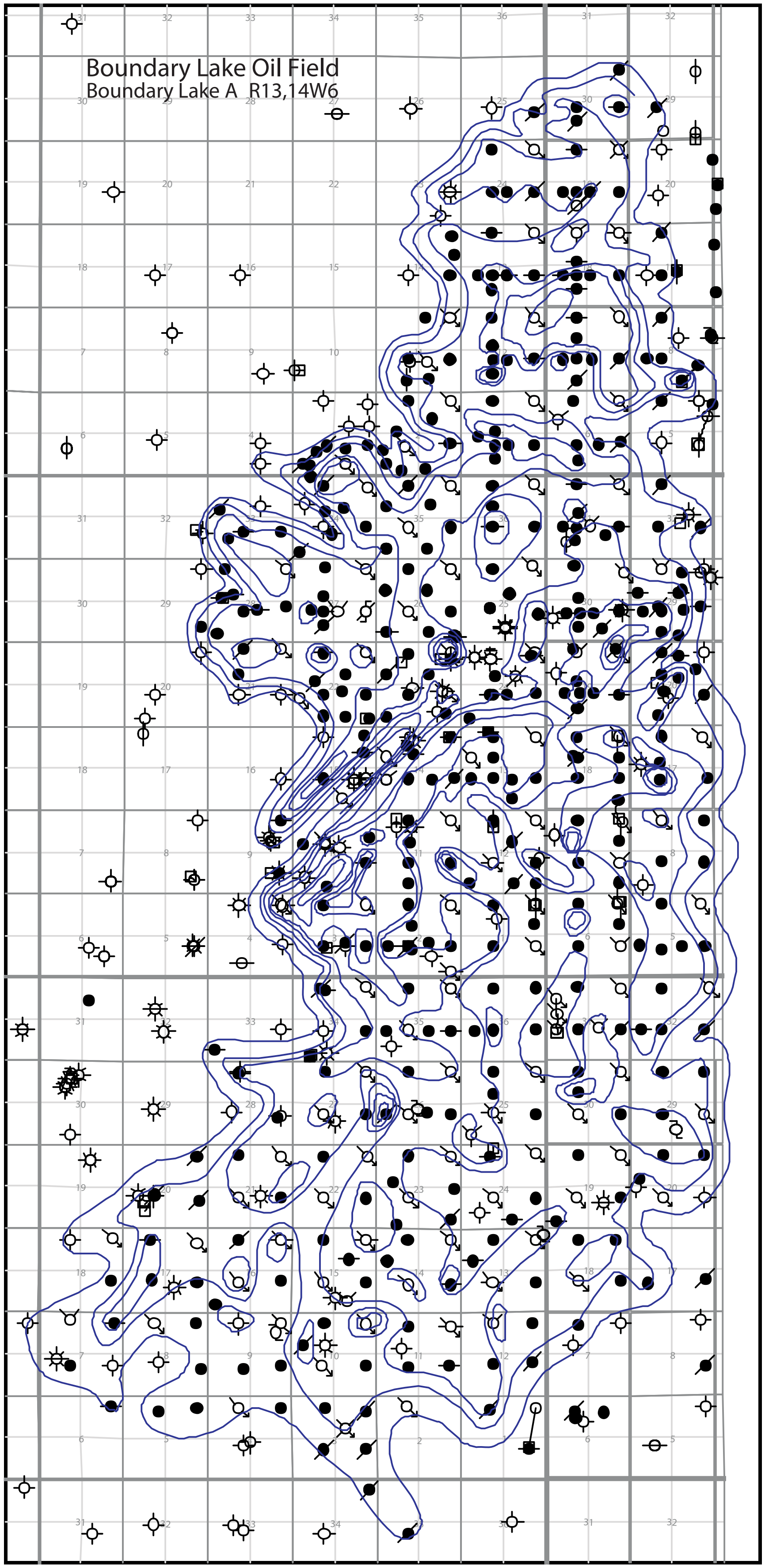

Figure CL7. Net oil pay isopach map, Boundary Lake 'A' Pool. Contour interval is 2m. From Janicki (2013).

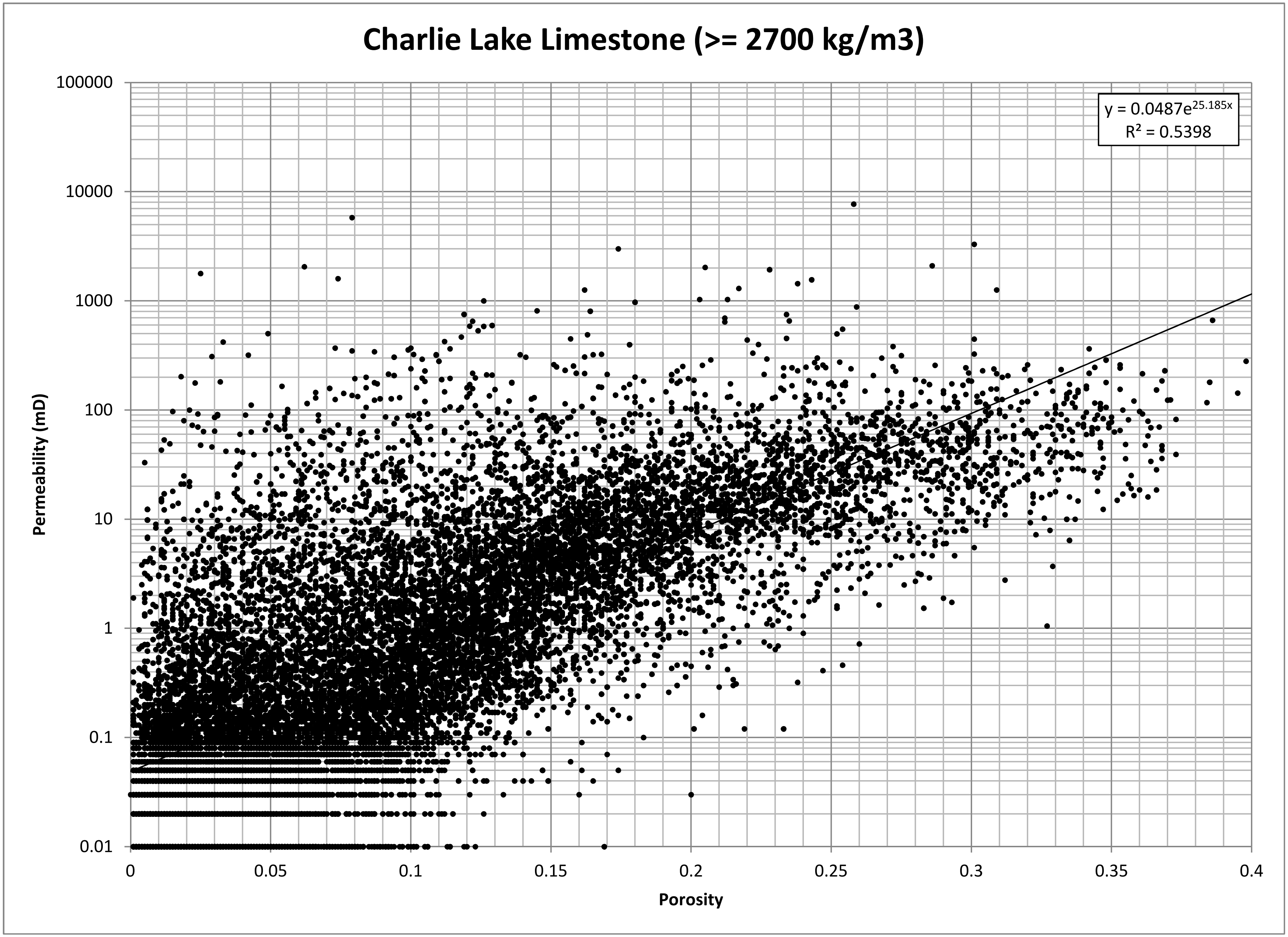

Figure CL8. Porosity / permeability cross-plot, Charlie Lake limestone.

There are many data points in the low porosity/permeability range, although some of these are likely sandstones cemented by carbonate and/or evaporite minerals.

Appendix 9 summarizes reservoir parameters for Charlie Lake oil pools, all of which exhibit conventional reservoir characteristics.

Reservoir Geology – Eastern Upper Charlie Lake Play

Shell Canada (1990) described the occurrence of light oil in the dolomitic Worsley Member at Worsley, Alberta (Twp 87-7W6; east of Map CL1). The reservoir is a stromatolitic sucrosic dolomite about 5m thick, with excellent lateral permeability supporting high sustained production rates. The original Worsley pool is a conventional structural/stratigraphic trap with strong aquifer support. Figure CL1 shows the Worsley Member as an eastern equivalent to the upper part of the Charlie Lake Formation, but Cross-sections CL1-CL1' and CL2-CL2' demonstrate that it is a distinct unit lying unconformably on the upper Charlie Lake. It is in turn overlain unconformably by the Nordegg and is truncated to the north by the pre-Cretaceous unconformity (at 6-21-90-11W6, Cross-section CL2-CL2'). Thus, the Worsley Member is found only east of Rge 11W6, and not at all in B.C.

A distinct upper Charlie Lake tight oil play, developed using horizontal multi-frac wells, has been pursued aggressively in the Spirit River – Worsley area of west-central Alberta since 2010 (Map CL1, Fig. CL9). Tourmaline Oil has booked reserves of 84.4 MMBOE on the play, and projects 1606 horizontal locations on their lands, while Birchcliff Energy has booked 2P (proven and probable) reserves of 41.1 MMBOE, with more than 200 horizontal locations forecast to be drilled.

The Tourmaline / Birchcliff upper Charlie Lake reservoir lies beneath the Worsley Member, and consists of stacked heterolithic sandier-upward successions of fine-grained sandstones and siltstone/mudstone, reaching log and core porosities up to 15%, and permeabilities of generally less than 10mD (Fig. CL10). A permeability-porosity cross-plot from core analysis data shows that the Worsley Member proper is dominated by rocks with modest porosities and permeabilities, while upper Charlie Lake sandstones in the western Alberta play fairway show generally good porosities but lower permeabilities (Fig. CL11).

Following Cross-section CL1-CL1' southwestward from Birchcliff's Worsley development (Twp 88-10W6), we lose the distinctive sandier-upward cycles and grade to tight regional carbonate- and evaporite-cemented facies in the upper Charlie Lake. We also see the Doig, Halfway and lower Charlie Lake thicken westward beneath the Coplin unconformity, producing a "normal" B.C. Charlie Lake section at 10-10-84-15W6 in the Boundary Lake area. Following CL2-CL2' northwestward from Worsley, the sandier-upward cycles become less distinct and are essentially lost as we get to d-44-H/94-H-1. At the northwestern end of the section (a-74-A/94-H-8), the small Chinchaga River Lower Charlie Lake / Montney 'A' pool produces from a thin remnant Charlie Lake / Doig interval just above the Montney, which does not appear to be related

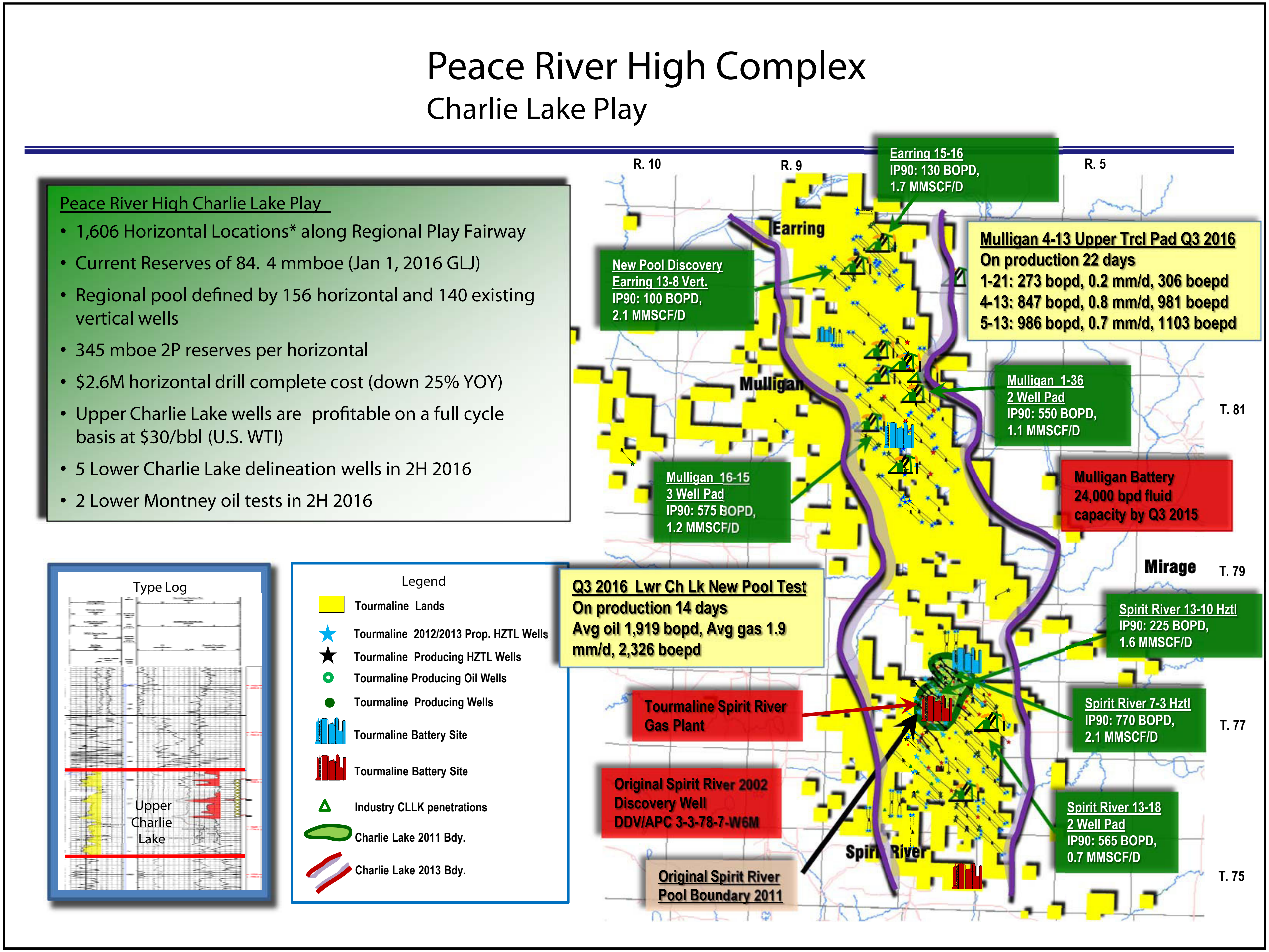

Figure CL9. Upper Charlie Lake play fairway, west-central Alberta. From Tourmaline Oil, 2016. (http://www.tourmalineoil.com/investor-relations/httptourmalineoil-comassetscorp-overview-nov-2014v4-pdf/).

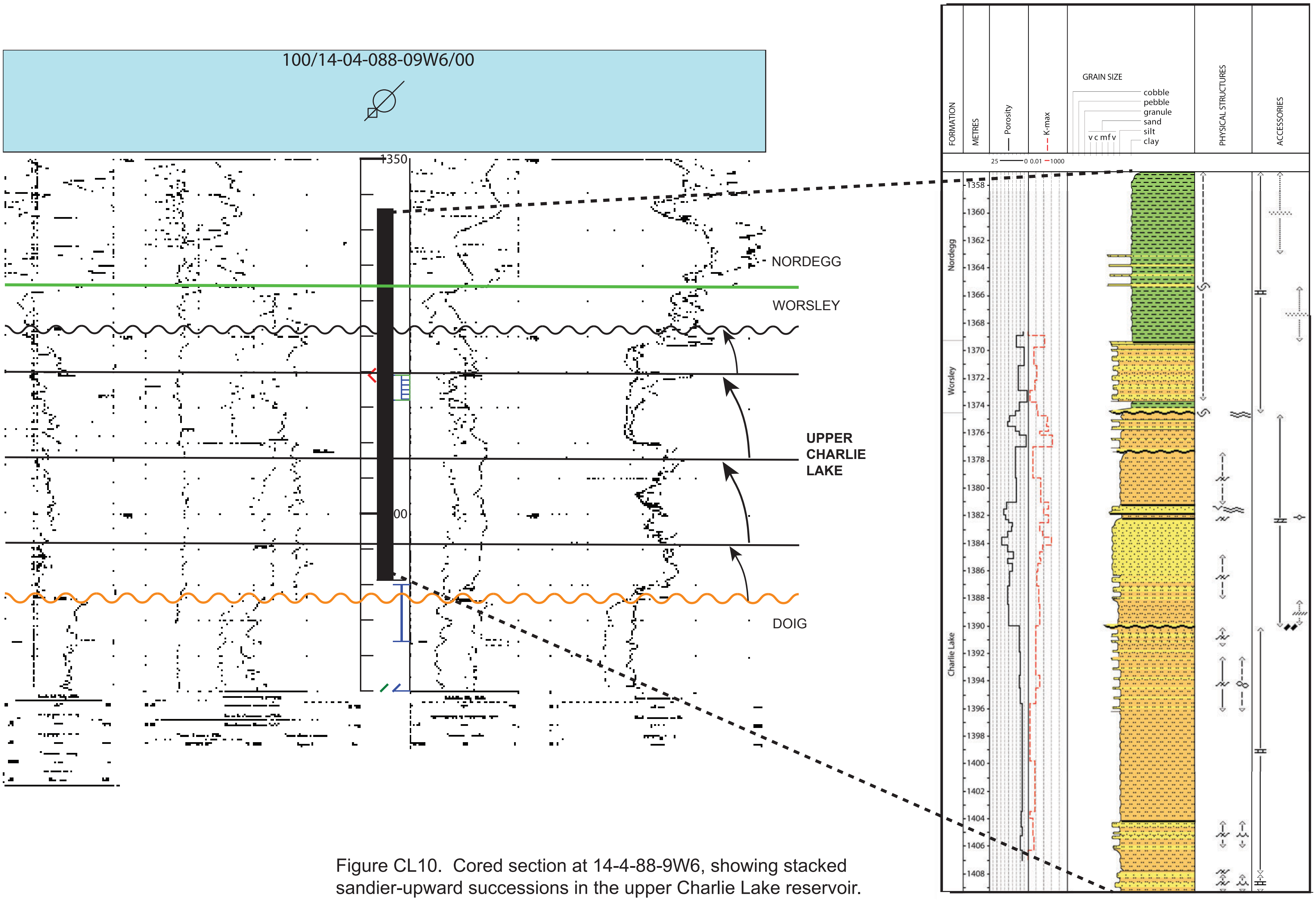

Figure CL10. Cored section at 14-4-88-9W6, showing stacked sandier-upward successions in the upper Charlie Lake reservoir.

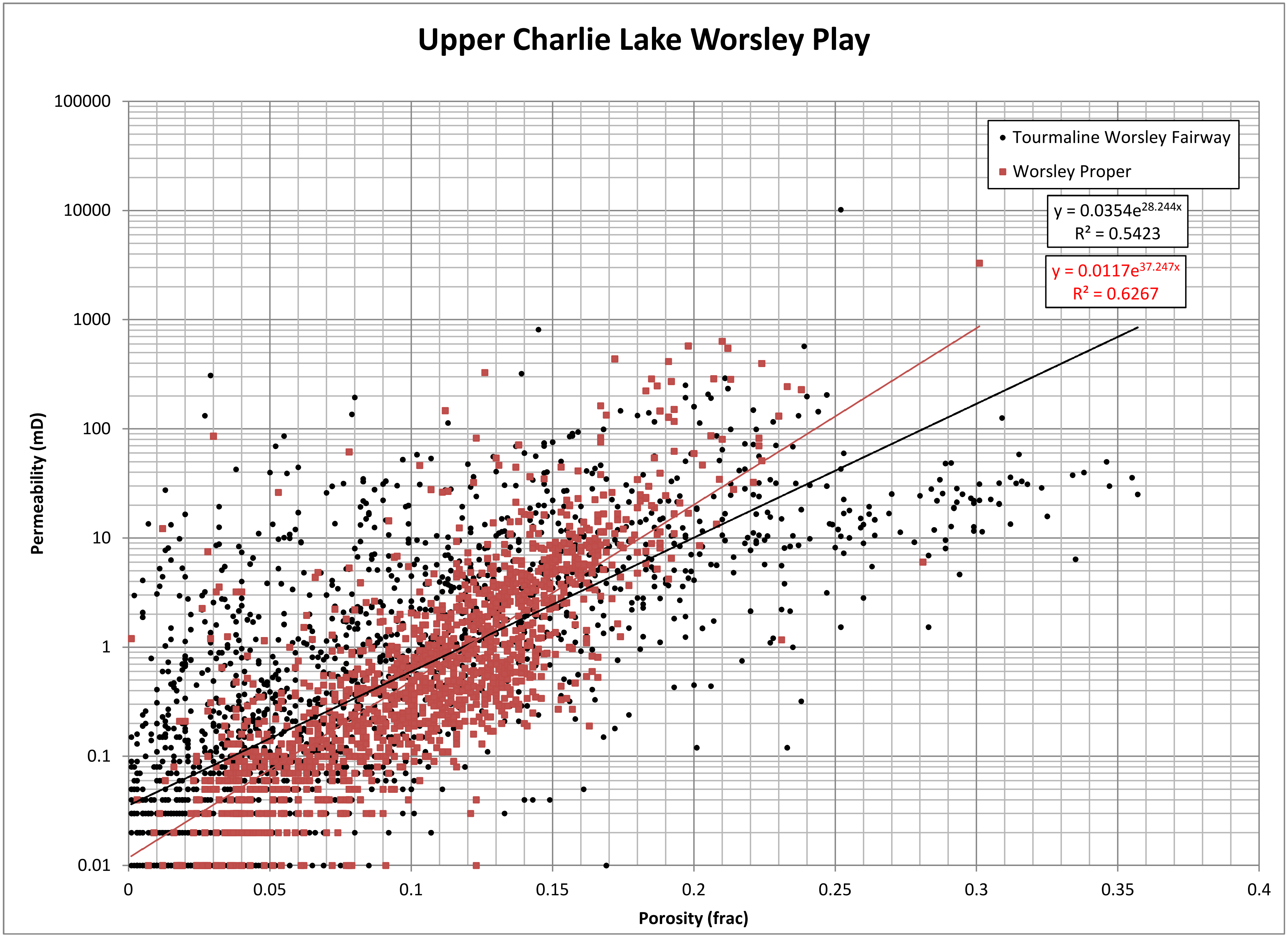

Figure CL11. Porosity / permeability cross-plot, Upper Charlie Lake reservoir units.

stratigraphically to the upper Charlie Lake in the Worsley fairway. Moving southwestward from Chinchaga River along Cross-section CL3-CL3', stratigraphic relationships are made more complex by incision beneath the pre-Cretaceous unconformity, but we do not see the sandier-upward Worsley reservoir cycles developed.

We conclude that the upper Charlie Lake section containing tight oil resources in sandier-upward successions occurs only in western Alberta, and does not extend into British Columbia. This relationship was illustrated by Davies (1997a) (Fig. CL1), although our work shows that the upper Charlie Lake is more extensive, and older than the Worsley Member (Fig. CL12). Tectonic controls exerted by faults bounding the Peace River Embayment / Dawson Creek Graben Complex may govern the limits of the upper Charlie Lake resource oil fairway (Fig. CL13).

Production and Test Data

On Map CL1, the designation of Charlie Lake oil wells is fairly reliable, but a number of gas wells designated as Charlie Lake producers actually produce from other units. For example, at Laprise Creek (94-H-5 and 94-G-8, many wells in the Baldonnel / Upper Charlie Lake pool produce only from the Baldonnel, but all are captured in a search for Charlie Lake gas wells.

The Charlie Lake petroleum system is dominated by oil; most gas pools occur in the west, at or near the regional deformation front. It is interesting to note on Map CL1 that most Charlie Lake production lies south of the Nordegg subcrop edge, leading one to speculate that the Nordegg cap is an essential ingredient of the Charlie Lake petroleum system. One would therefore expect most resource oil prospectivity also to occur south of the Nordegg edge.

Appendix 9 summarizes important characteristics of Charlie Lake oil pools in British Columbia. Key observations relevant to resource oil potential include:

- Two fields – Boundary Lake and Inga – have more the 100 million barrels of oil originally in place (MMBOOIP). Each is structurally complex and is really an aggregate of numerous smaller compartments, some of which are recognized as separate pools on advanced reservoir and performance data.
- Most pools are quite small - <10 MMBOOIP. Net pays are thin, and pool boundaries are sharply defined vertically and horizontally by facies and cementation boundaries.
- Most pools are very mature and remaining reserves are relatively small.
    - Major discoveries were made in the 1950's and 1960's, and new pools were discovered most years up to 2006. Since that time, however, there have been only four single-well discoveries in the Charlie Lake.

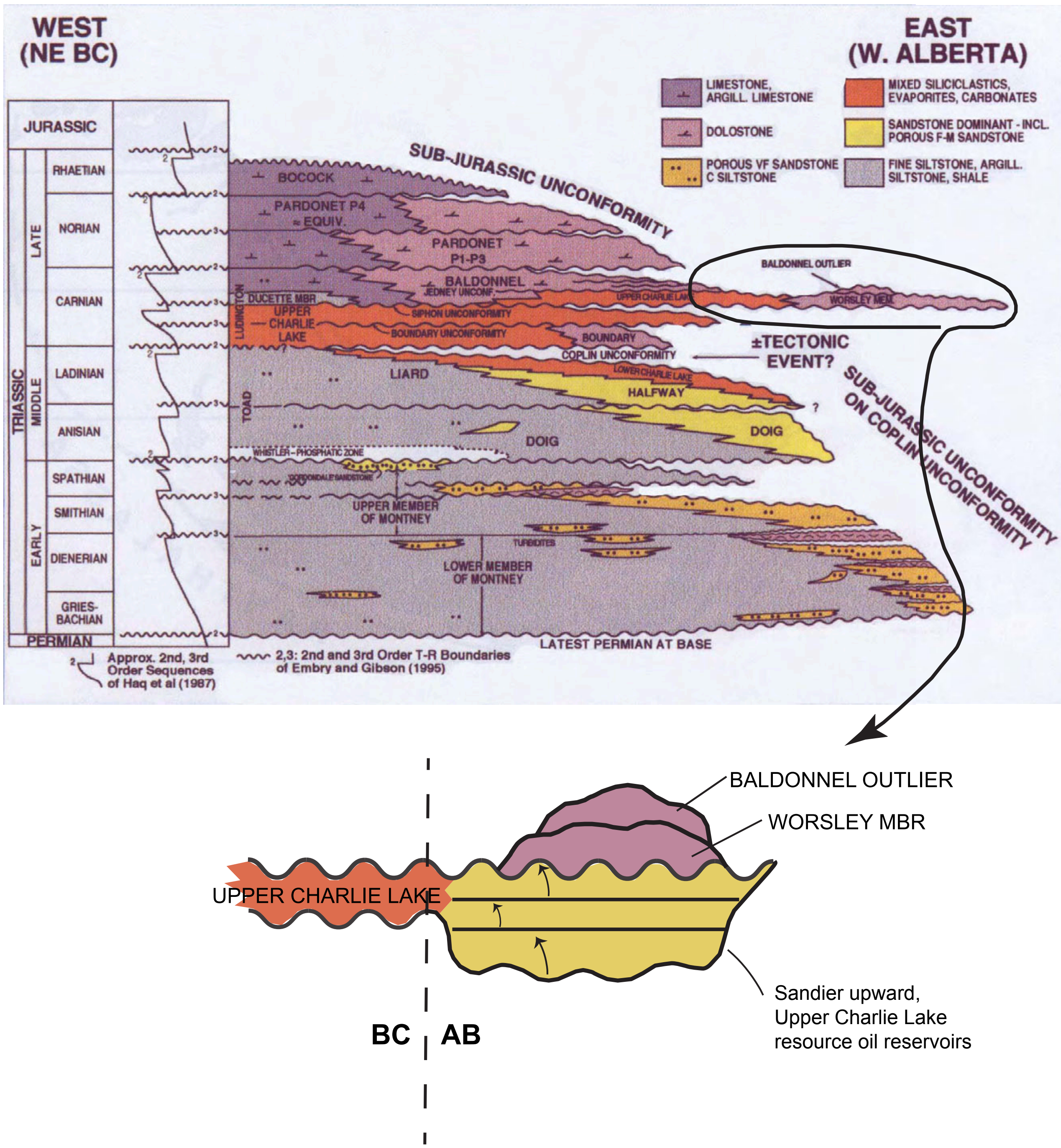

Figure CL12. Revised stratigraphic relationships of the upper Charlie Lake and Worsley Member in west-central Alberta. After Davies (1997a).

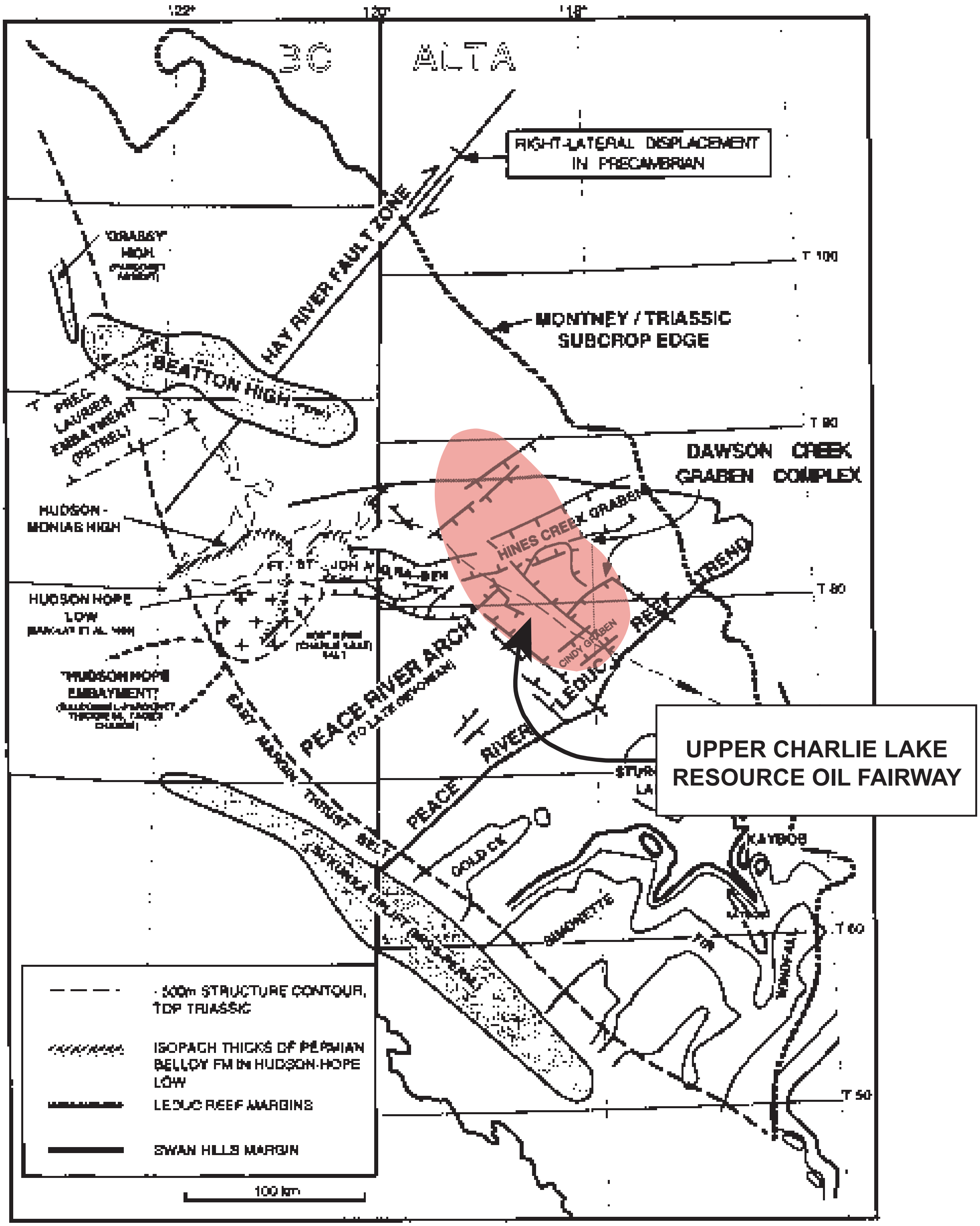

Figure CL13. Compilation of tectonic and depositional elements that influenced Triassic sedimentation. From Davies (1997a).

- Oil gravities are light to very light.
- Pool average porosities (5-27%, average 13%) and permeabilities (5-610mD, average 113mD) are conventional.
- Recovery factors are highly variable. Waterfloods have been implemented in many of the larger pools (see water injection wells, Map CL1); many pools with low recovery factors are too small to justify enhanced recovery.

Horizontal Drilling

Horizontal wells have been used to develop tight, laterally continuous sandstone reservoirs of the eastern Upper Charlie Lake play in Alberta, and Tourmaline Oil has reported recent horizontal development of a “lower Charlie Lake” oil play in Alberta.

Database searches for horizontal wells in the Charlie Lake in B.C. identified more than 100 wells. Many search “hits” were found not to be valid Charlie Lake horizontals. Most problems arise from complex drilling histories, particularly where a vertical pilot hole is drilled to some point in the Charlie Lake in the first (/00) event, and then in the second event the well is either plugged backed and drilled horizontally into the Baldonnel, or deepened to be drilled horizontally in the Halfway, Doig or Montney.

Manual checking shows that a limited number of Charlie Lake oil zones have been drilled horizontally in NEBC:

- Artex zone at Brassey – primarily recompletions of old vertical producers;
- Cecil zone at Groundbirch / Sunset Prairie;
- Mica zone at Mica;
- Siphon zone at Two Rivers;
- Cecil zone at Oak and Rigel – including a number of horizontal water injectors;
- Boundary Lake zone at Muskrat;
- A Marker zone at Zaremba.

As well, Whitecap Resources acquired the Boundary Lake Field as a long-term, low-decline light oil asset under waterflood (5% annual decline over 30 years with little development capital). They are drilling very selected horizontal wells to maximize oil recovery where available within defined pool boundaries, but they are not undertaking systematic stepout from existing production. Whitecap is claiming to boost recovery factor in the Boundary reservoir from the current 34.4% to 43-46%, but is making no specific claims about accessing tight oil resources.

Analytical Data

Drill cuttings have been analyzed for source rock potential in five wells where the GSC surveyed a thick continuous section (Map CL1, Appendix 1). Standard petrography and XRD work has been submitted on cores from eight wells, but no geomechanical or other specialized core analysis.

Resource Oil Assessment

Halo oil potential associated with conventional Charlie Lake pools appears very limited. Small, sharply-bounded reservoirs have little tighter but still viable reservoir rock – they tend to be either good-quality rock or highly cemented. Limited data sets and concurrent waterfloods make it difficult to assess results from horizontal developments at Rigel and Boundary Lake, but activity has been slow and it seems reasonable to assume that results are not sufficiently good to justify accelerating horizontal programs.

Charlie Lake resource oil being developed in adjacent Alberta occurs in regional low-permeability sandstone facies associated with the Peace River Arch, but only 20 km and more eastward from the border. We see little potential to extend the play westward into B.C.

If there is new potential to be found in the Charlie Lake, it may be most likely in chance discoveries encountered with intensive development of the deeper Montney, in areas south of the Nordegg subcrop edge.

BALDONNEL FORMATION

Age and Play Type

Upper Triassic – Tight Oil play (tight carbonate);
Prospectivity: 'C' Play – Areas of oil charge are limited; basin-centred accumulations and regional stratigraphic traps are not present.

Regional Geology

Upper Triassic Baldonnel strata subcrop beneath the pre-Jurassic and pre-Gething unconformities in southern NEBC (Fig. BD1, Map BD1). They comprise a series of shallowing-upward bioclastic marine carbonate parasequences, variably dolomitized, and exhibiting good reservoir quality over large areas. Davies (1997b) illustrated a number of stratigraphic units and internal unconformities that he correlated regionally within the Baldonnel and overlying Pardonet formations (Fig. BD2).

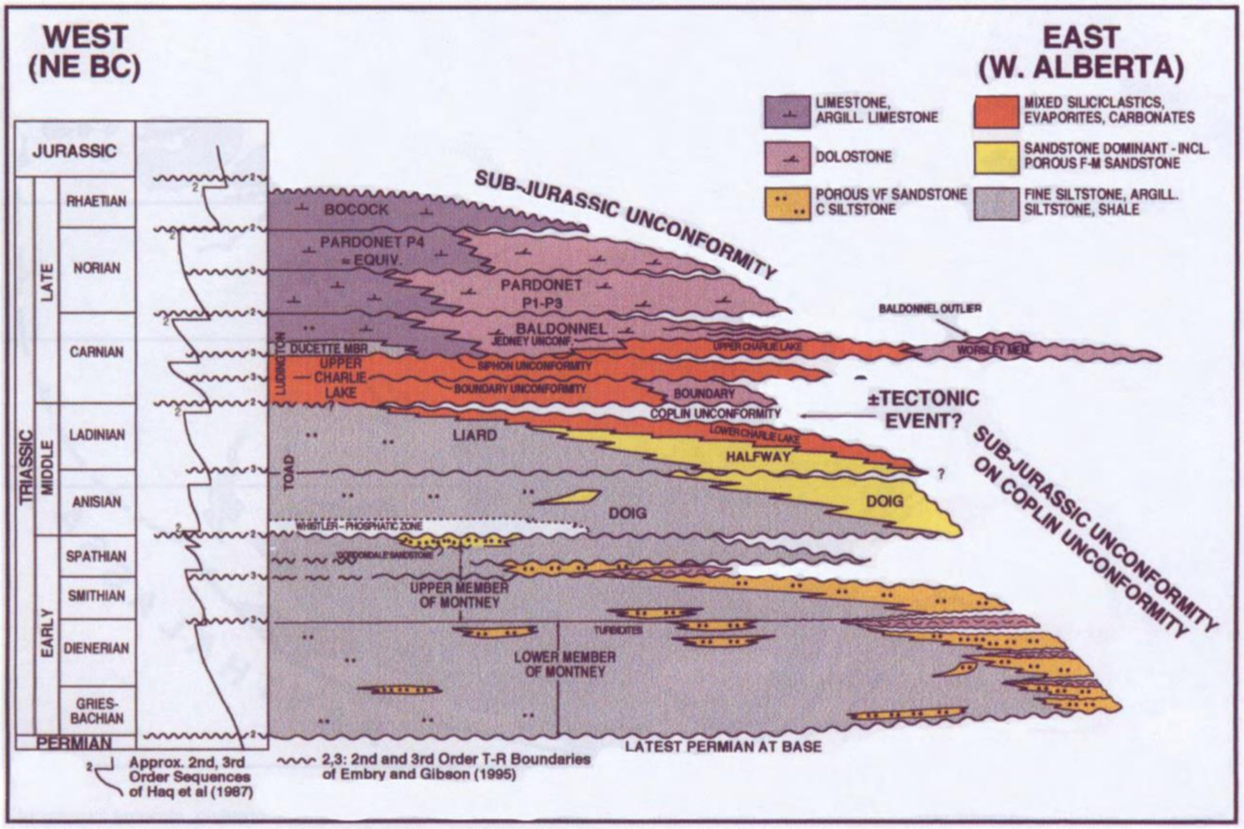

Figure BD1. Event stratigraphic summary for Triassic succession of WCSB (same as Fig. H1, CL1). Note eastward bevelling of Pardonet and Baldonnel strata beneath the sub-Jurassic unconformity, which is itself incised in the east by the pre-Cretaceous unconformity (from Davies, 1997a).

Baldonnel strata include a variety of interbedded limestones, dolostones, and fine-grained siliciclastics, with common mixed lithologies (Texaco Boundary 11-30-87-14W6, Appendix 4). It is difficult to characterize reservoir lithologies and porosities from well logs, even those with modern log suites containing a photoelectric (PE) curve. Regional thickness maps are difficult to draw consistently because of the complex internal stratigraphic relationships and cyclicity of the Baldonnel; in many places, industry places the base Baldonnel / top Charlie Lake at the base of good continuous porosity (see sonic log 2-18-84-19W6, Fig. BD2). Edwards et al. (1994) showed a very generalized thickness and lithology map for the Pardonet-Baldonnel section (Fig. BD3).

Baldonnel burial depths range from less than 1500m near the subcrop edge to >4000m in the Deep Basin adjacent to the deformation front (Map BD1).

Reservoir Geology

At Laprise Creek gas field (Map BD1), Bever (1980) subdivided the Baldonnel reservoir into five informal mappable subunits separated by flooding surfaces. He characterized

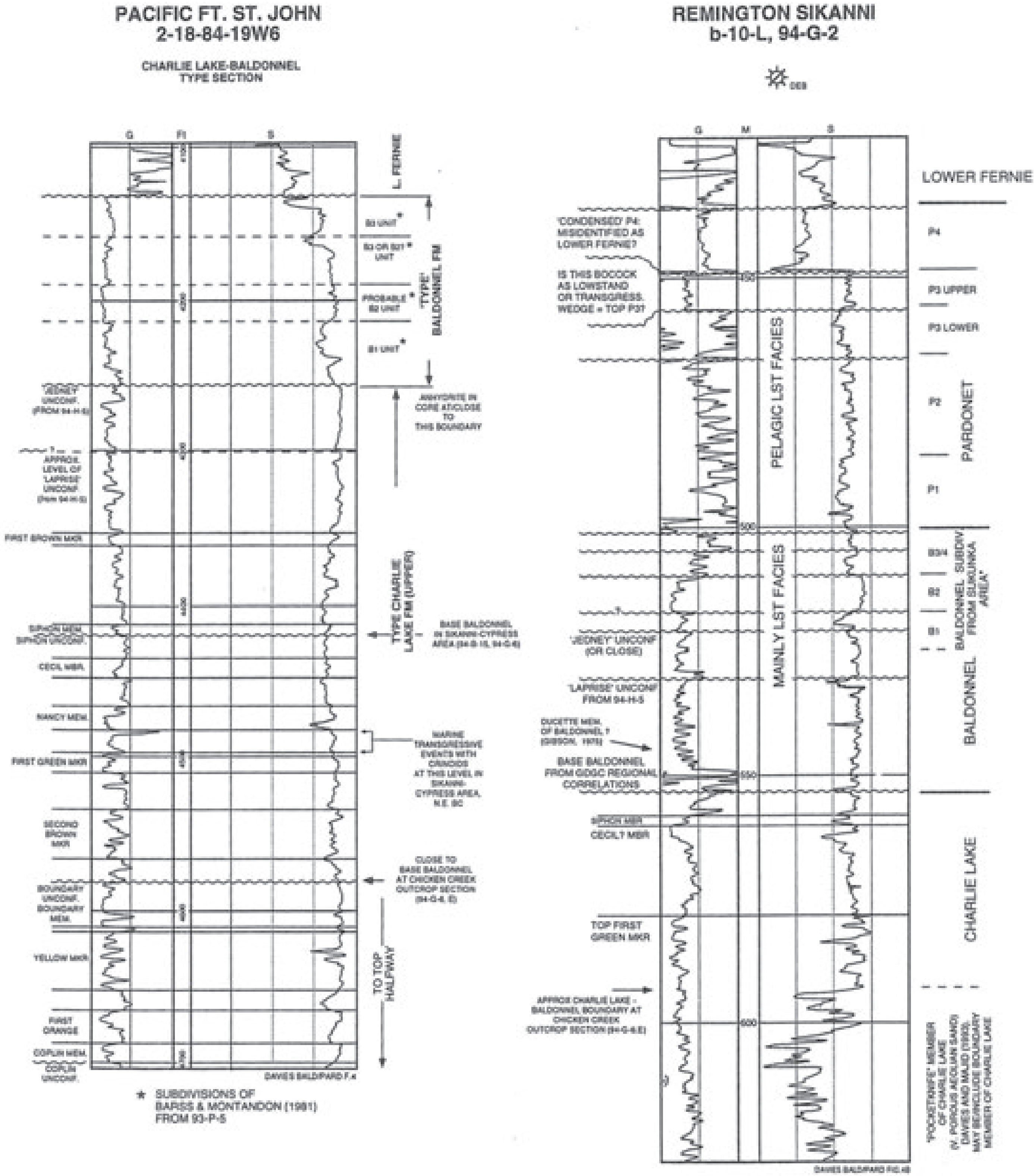

Figure BD2. Baldonnel and Pardonet internal stratigraphy (from Davies, 1997b).

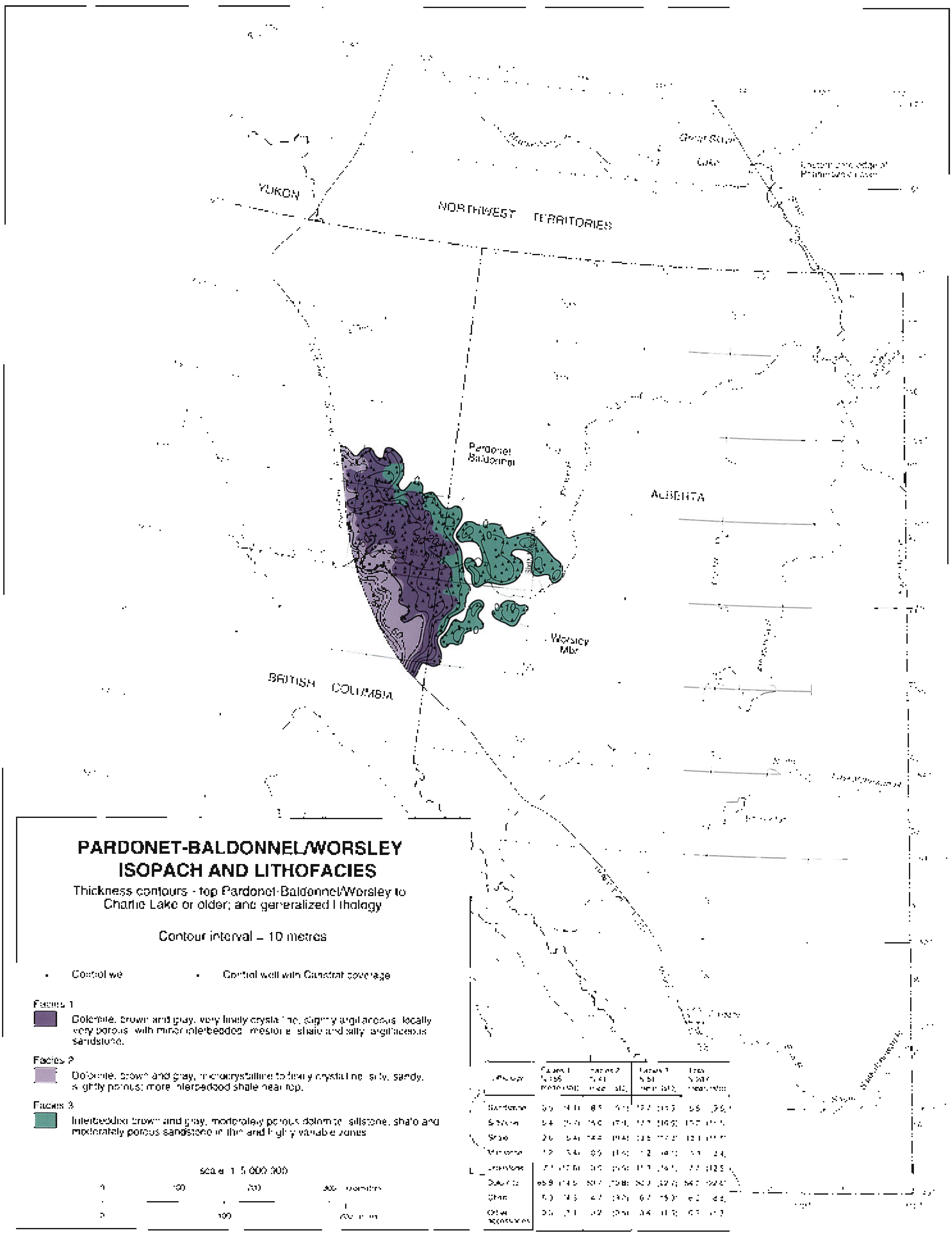

Figure BD3. Pardonet-Baldonnel isopach and lithofacies (from Edwards et al., 1994).

the reservoir rock as highly dolomitized calcarenite, with best reservoir development in coquinas with moldic vuggy porosity.

A permeability / porosity cross-plot from core analysis data shows an immense amount and spread of data, with most samples exhibiting porosities of <20% and permeabilities ranging up to several hundred millidarcies (Fig. BD4). There is a significant tail of high-quality reservoir rock trending from 25-35% porosity and 50-800mD permeability. More detailed and locally-focused work would be required to extract meaningful information from this plot.

Production and Test Data

The Baldonnel is primarily a gas reservoir; oil production in B.C. is limited largely to a triangular area bounded on the southeast at Oak (Twp 86-18W6), on the southwest at Inga (Twp 86-23W6), and on the north at Birch (94-A-13) (Map BD1). Appendix 9 summarizes important characteristics of Baldonnel oil pools in British Columbia. Key observations relevant to resource oil potential include:

- The largest existing field is at Birch, where the Baldonnel 'C' pool contains 10.9 million barrels of oil originally in place (MMBOOIP). Only four other pool contain more than 5 MMBOOIP.
- Net pays are quite variable (2.7-14.4m), and average 5.55m.
- Most pools are very mature and remaining reserves are relatively small.
    - 24 pools were discovered between 1954 and 2009; the largest pool at Birch was discovered in 1979. Regionally, the Baldonnel is a much more significant gas target, and relatively little attention is paid to oil.
- Oil gravities are light to very light.
- Pool average porosities (9-19%, average 11.8%) and permeabilities (only two measured, at 36 and 41mD) range from somewhat tight to conventional. Internal heterogeneities related to degree of dolomitization are common.
- Recovery factors are generally low (<20%), except at Birch, where a natural water drive is present and water is re-injected for pressure maintenance.

Kelt Exploration claimed that in the Inga / Fireweed area (Twp 86-88, Rge 23W5 and north into 94-A-13), the Baldonnel hosts substantial oil in structural lows and gas in structural highs (Daily Oil Bulletin, 17/04/20). Leucrotta Exploration has promoted regional Baldonnel oil potential offsetting its horizontal producer at West Stoddart (4-1-88-21W6), but there is substantial associated water production.

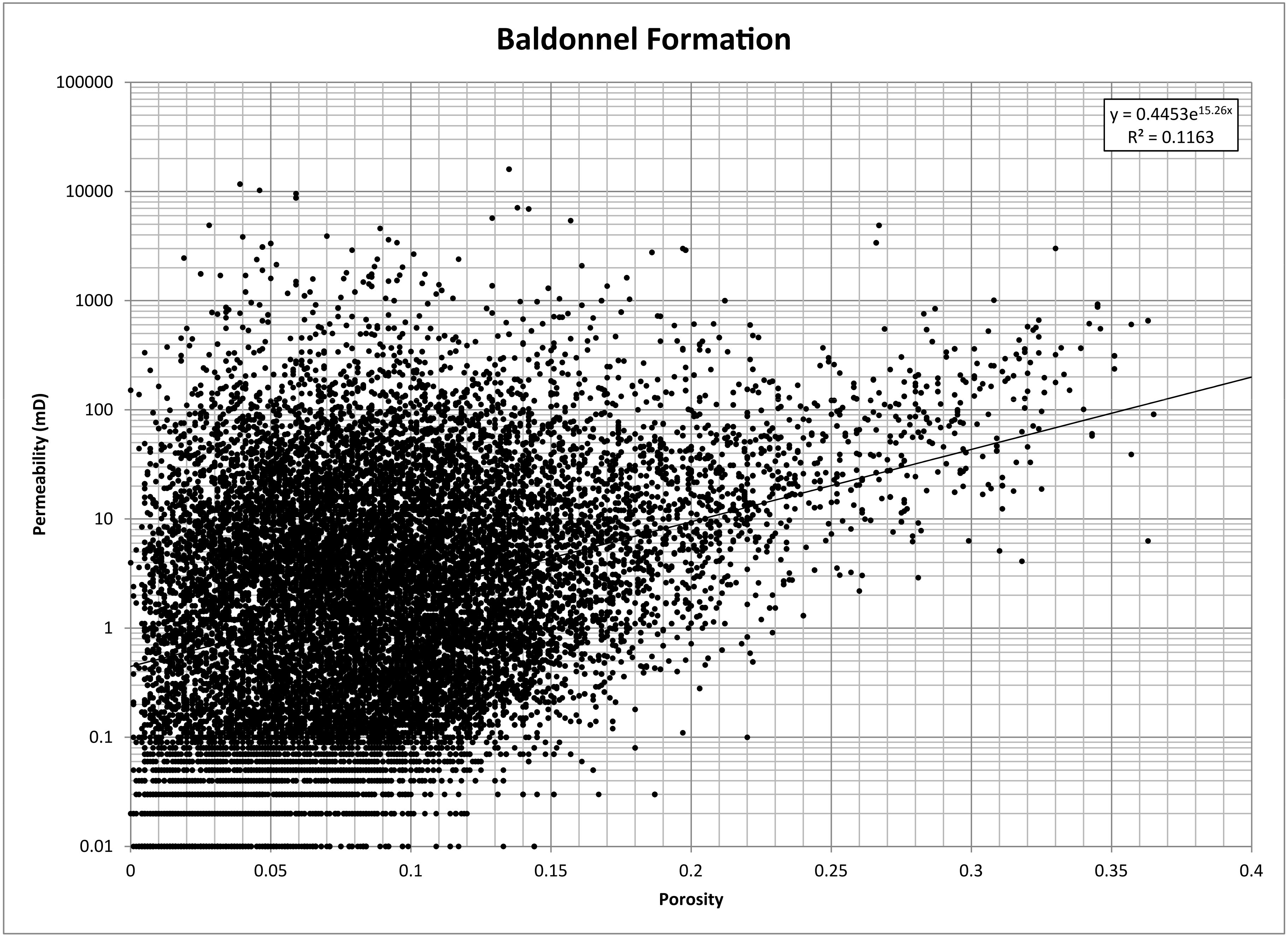

Figure BD4. Porosity / permeability cross-plot, Baldonnel Formation.

Horizontal Drilling

There are well over 250 Baldonnel horizontal completions in NEBC; about 100 of these are into structurally-deformed fractured sections in Foothills gas pools, and are not relevant to this study. In the Plains, Baldonnel horizontal oil and gas wells have been drilled over a broad area ranging from Fort St John in the southeast (Twp 83-17W6) to Laprise Creek (94-H-5) in the northwest (Map BD1). Most of the horizontal oil wells have been drilled at Birch (94-A-13), many as early as 1993, and many have been suspended or converted to water injectors. Adams et al. (2016) noted that CNRL drilled three horizontal development wells in 2014 at Birch in order to improve oil recovery from the pool – although pool boundaries are generally well-established and considerable waterflooding has taken place.

Outside of Birch, Baldonnel horizontal oil wells are sprinkled over a broad area. Many were drilled as far back as 1993; most were drilled in the 1990's, and very few have been drilled since 2010. In some areas – e.g., Nig Creek, Oak – horizontal oil wells and gas wells have been drilled in close proximity, and there are no sizeable continuous accumulations. As noted above, a recent horizontal well at West Stoddart by Leucrotta has produced significant oil, but high water production suggests it is not an areally-extensive tight oil accumulation.

Analytical Data

Searching available OGC core report files, we found a limited number of source rock analysis and other analytical work done on Baldonnel core (Appendix 1; Map BD1). Much of the source rock is from cuttings, and was done in older wells sampled throughout the wellbore, and thus not focused on the Baldonnel. Standard petrography and XRD work focuses on conventional reservoir characteristics, and essentially no geomechanical work has been conducted on the Baldonnel.

Riediger *et al*. (2004) interpreted the Baldonnel to have only poor to fair initial hydrocarbon source rock potential because of generally low organic richness (TOC) values in predominantly clean carbonate facies. The Pardonet Formation overlies the Baldonnel in the west, and contains relatively continuous source rock intervals (Davies, 1997b). Riediger *et al*. (2004) judged the Pardonet to have had fair to excellent initial hydrocarbon source rock potential, but showed it to be overmature and gas-prone throughout its range (Fig. BD5).

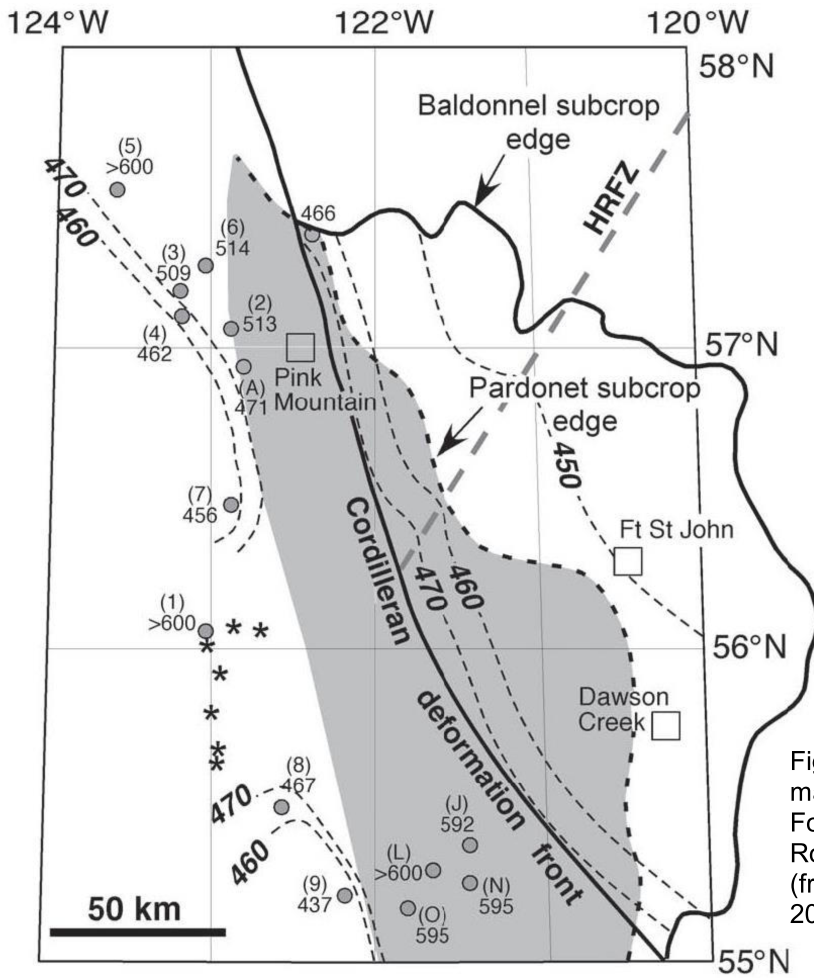

Figure BD5. Thermal maturity, Pardonet Formation, based on Rock-Eval T_{max} data (from Riediger *et al.*, 2004).

For the current study, we examined one short Baldonnel core at Texaco Boundary 11-30-87-14W6, which consists of light grey dolomitic mudstone to muddy limestone (Appendix 4). Our review is tempered by the single data source and small number of samples analyzed. Mineralogical analysis shows dolomite content to be >90%, with some calcite and small amounts of quartz, pyrite and apatite (Fig. BD6; Table BD1). Total Organic Carbon (TOC) content is low (<1.7 wt%), and T_{max} values range between 425-435°C, an early oil window maturity level. Source rock analyses show that several samples have elevated S1 values (>4mg/g) indicating the presence of residual free hydrocarbons (Table BD2).

Petrographically the Baldonnel is a light grey, finely crystalline dolostone with minor preserved bioclastic. Bioclasts are recrystallized and species identification is difficult, although shell and crinoidal remains may be identified (Fig. BD7, BD8). SEM data show microcrystalline minerals to be dolomite, calcite and quartz (Fig. BD9).

Unconfined porosities of two Baldonnel samples range between 9.5-14.9%, with matrix permeabilities of 22-70 nD (Table BD3). MICP conformance-corrected porosity for one sample is similar to the unconfined value (9.09 vs 9.57%) (Table BD4), and the pore throat size distribution is predominantly in the 50-100 nm range (Fig. BD10).

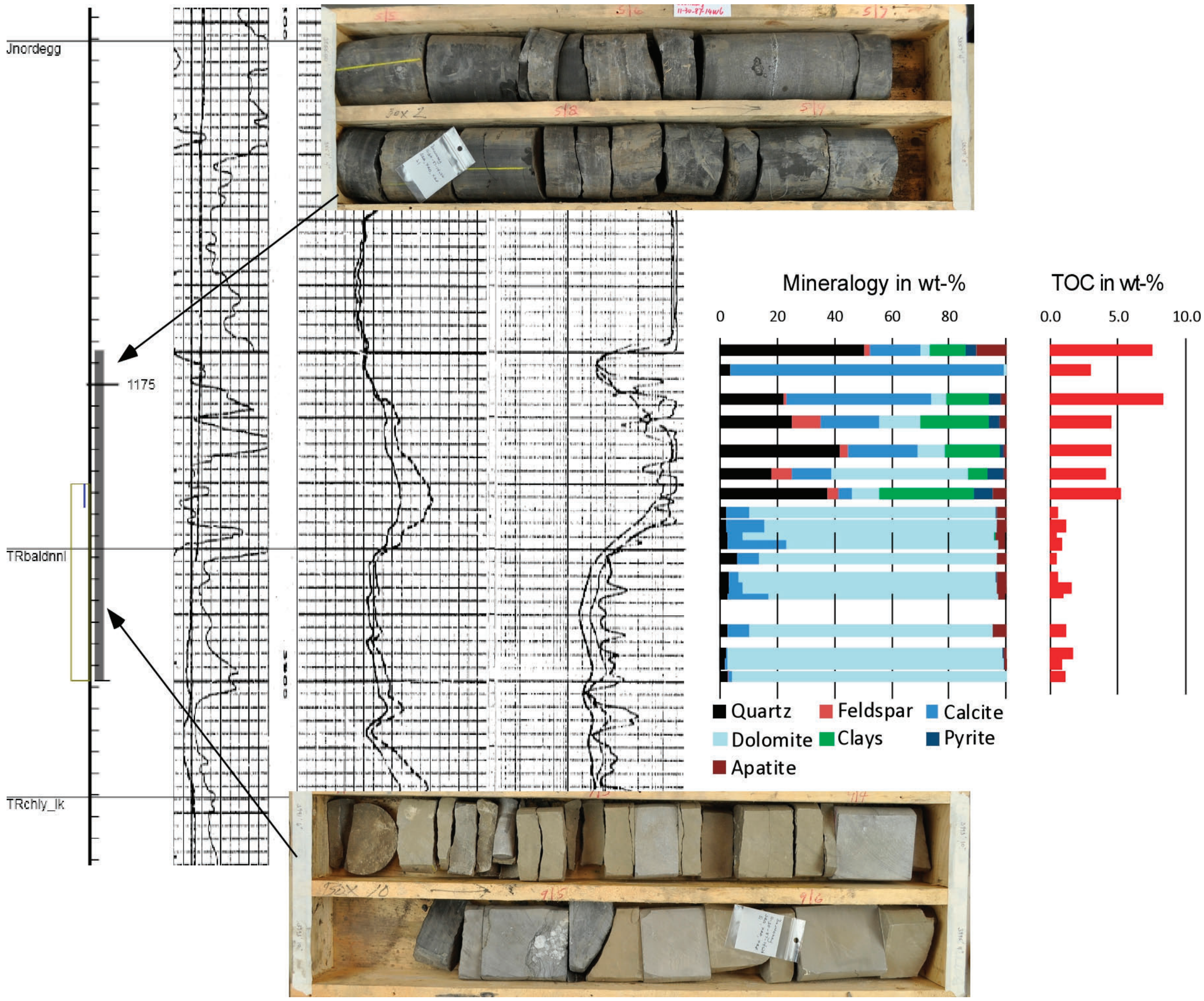

Figure BD6. Mineralogy and TOC plots for samples from the Baldonnel Formation, Texaco Boundary 11-30-87-14W6.

MICP Porosity

Well Name	Well Location	Core Depth (m)	Fm	Density g/cc: Bulk Density (g/cc)	Density g/cc: Skeletal Density (g/cc)	Porosity (%)	Corrected Porosity (%)	Peak Range: Peak Range	Peak Range: Modal Peak	Stem Volume Used (%)
AEC Maxhamish	200/c-016-G 094-O-14/00	1252.91	Upper Chinkeh	2.548	2.657	4.30	4.09	8 - 470	32	53
AEC Maxhamish	200/c-016-G 094-O-14/00	1254.14	Upper Chinkeh	2.542	2.662	4.74	4.49	6 - 1130	27	61
AEC Maxhamish	200/c-016-G 094-O-14/00	1255.16	Upper Chinkeh	2.572	2.658	3.60	3.26	7 - 220	23	43
AEC Maxhamish	200/c-016-G 094-O-14/00	1263.50	Top Porosity Chinkeh	2.425	2.648	8.70	8.41	15 - 430	174	98
GSENR Maxhamish	200/a-064-B 094-O-14/00	1293.57	Top Porosity Chinkeh	2.258	2.542	11.16	10.75	58 - 2460	58, 711	94
GSENR Maxhamish	200/a-064-B 094-O-14/00	1295.04	Top Porosity Chinkeh	2.482	2.657	6.57	6.25	6 - 890	29	51
GSENR Maxhamish	200/a-064-B 094-O-14/00	1295.39	Top Porosity Chinkeh	2.557	2.666	4.10	3.31	<3 - 370	14	44
GSENR Maxhamish	200/a-064-B 094-O-14/00	1300.91	Top Porosity Chinkeh	2.5089	2.659	5.63	5.26	6 - 250	35	48
ECA Maxhamish	200/d-048-B 094-O-11/00	1466.95	Upper Chinkeh	2.563	2.659	3.62	3.03	4 - 120	10	36
ECA Maxhamish	200/d-048-B 094-O-11/00	1467.85	Upper Chinkeh	2.562	2.664	3.81	3.46	<3 - 190	6	36
AEC Maxhamish	200/c-095-J 094-O-11/00	1503.76	Upper Chinkeh	2.556	2.626	3.23	2.68	4 - 70	8	41
AEC Maxhamish	200/c-095-J 094-O-11/00	1505.43	Upper Chinkeh	2.530	2.632	4.54	3.87	5 - 240	11	53
AEC Maxhamish	200/c-095-J 094-O-11/00	1506.78	Upper Chinkeh	2.566	2.636	2.95	2.66	4 - 110	4	41
AEC Maxhamish	200/c-095-J 094-O-11/00	1508.15	Upper Chinkeh	2.566	2.641	3.28	2.87	4 - 130	11	36
AEC Maxhamish	200/c-095-J 094-O-11/00	1511.32	Top Porosity Chinkeh	2.271	2.623	14.05	13.44	9 - 3220	2218	61
AEC Maxhamish	200/c-095-J 094-O-11/00	1513.52	Top Porosity Chinkeh	2.107	2.395	13.26	12.04	8 - 5170	2870	49
AEC Maxhamish	200/b-049-J 094-O-11/00	1616.79	Upper Chinkeh	2.550	2.622	2.74	2.38	<3 - 210	5	31
Legacy Maxhamish	200/b-019-J 094-O-11/00	1623.61	Upper Chinkeh	2.572	2.658	3.25	2.51	<3 - 70	5	34
Legacy Maxhamish	200/b-019-J 094-O-11/00	1627.74	Top Porosity Chinkeh	2.595	2.640	1.71	1.53	<3 - 490	4	21
Legacy Maxhamish	200/b-019-J 094-O-11/00	1634.10	Top Porosity Chinkeh	2.598	2.691	3.47	3.25	6 - 870	18, 96	42

Table BD1. Baldonnel Formation – thermal maturity and mineralogical data from samples in Texaco Boundary 11-30-87-14W6.

Hydrocarbon Composition by Thermal Desorption Gas Chromatography

Well Name	Well Location	Core Depth (m)	Fm	% Light Condensate	% Heavy Condensate	% Naphthenes	% Aromatics	% Biomarkers	Peak	Initial Boiling Point (°C)	Carbon Number	Final Boiling Point (°C)	Carbon Number	Calculated Specific Gravity	Calculated API gravity	Chromatogram Quality
GSENR Maxhamish	200/a-064-B 094-O-14/00	1293.57	Top Porosity Chinkeh	1.78	82.18	0.43	0.39	15.22	C20	61	<C6	434	C28	0.85	34.64	okay
GSENR Maxhamish	200/a-064-B 094-O-14/00	1295.04	Top Porosity Chinkeh	6.41	81.13	0.47	0.79	11.21	C15	61	<C6	482	C34	0.85	35.43	good
ECA Maxhamish	200/d-048-B 094-O-11/00	1466.95	Upper Chinkeh	13.69	63.55	3.02	5.51	14.23	C16	75	C6	393	C24	0.83	39.68	good
ECA Maxhamish	200/d-048-B 094-O-11/00	1467.85	Upper Chinkeh	11.97	67.89	1.80	4.30	14.04	C16	116	C8	385	C23	0.83	38.87	good
AEC Maxhamish	200/c-095-J 094-O-11/00	1505.59	Upper Chinkeh	14.26	62.89	3.71	6.50	12.64	C16	49	<C6	440	C29	0.83	37.98	poor
AEC Maxhamish	200/c-095-J 094-O-11/00	1510.83	Top Porosity Chinkeh	17.19	41.51	11.86	23.27	6.16	C15	48	<C6	423	C27	0.82	41.41	good
AEC Maxhamish	200/c-095-J 094-O-11/00	1514.17	Top Porosity Chinkeh	0.04	90.27	0.22	0.06	9.42	C22	56	<C6	473	C33	0.86	32.58	poor
AEC Maxhamish	200/b-049-J 094-O-11/00	1616.79	Upper Chinkeh	7.79	72.81	1.04	2.03	16.33	C16	82	C6	474	C33	0.84	37.71	excellent

Table BD2. Baldonnel Formation – source rock analysis data from samples in Texaco Boundary 11-30-87-14W6

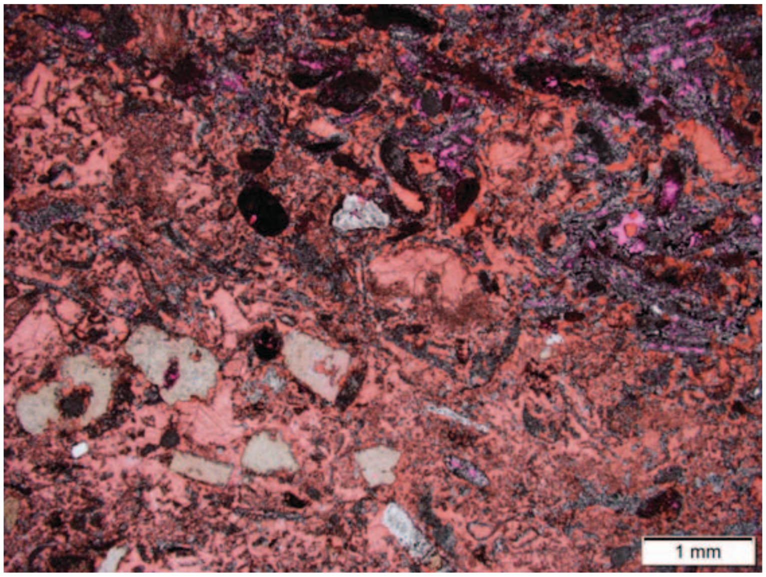

Figure BD7. Photomicrograph, Baldonnel Formation, Texaco Boundary 11-30-87-14W6 (3887.5 ft) under plane polarized light. Bioclastic dolomitic limestone with patches of recrystallized calcite. A few shell fragments have been replaced by chert.

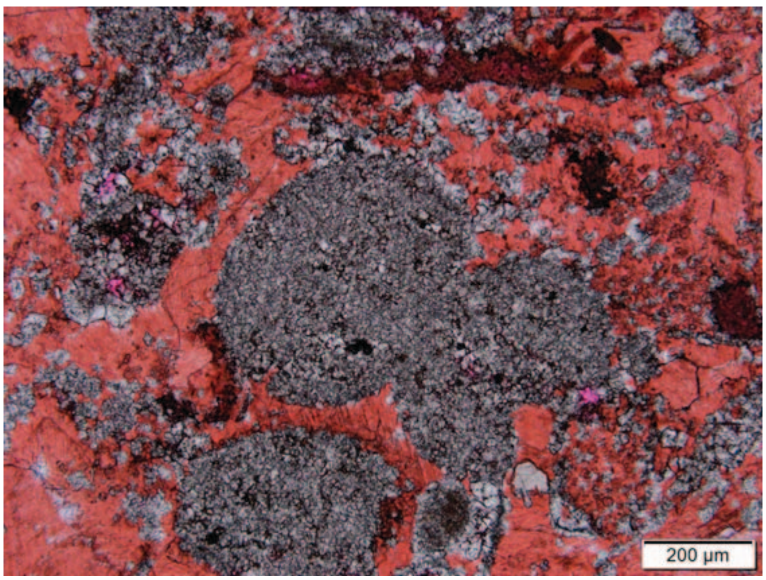

Figure BD8. Photomicrograph, Baldonnel Formation, Texaco Boundary 11-30-87-14W6 (3887.5 ft) under plane polarized light. Spherical bioclasts have been replaced by fine crystalline dolomite, and are embedded in sparry calcite.

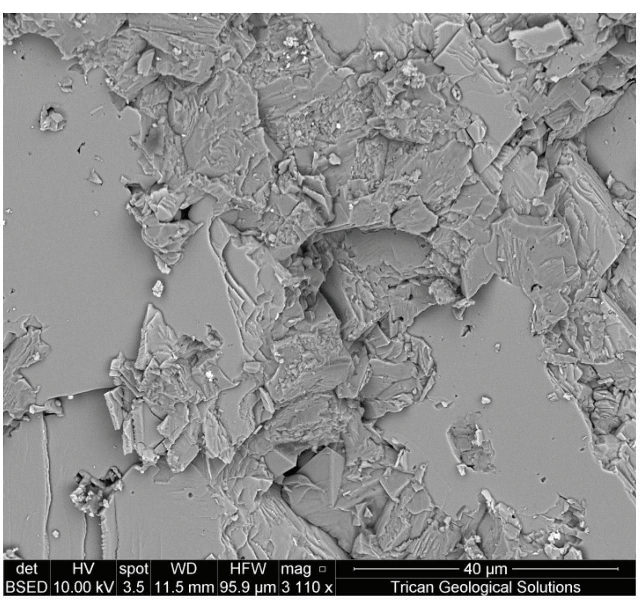

Figure BD9. BSED SEM photomicrograph, Baldonnel Formation, Texaco Boundary 11-30-87-14W6 (3887.5 ft), showing interlocking calcite (smooth surfaces) and dolomite (rough surfaces).

Unconfined Porosity and Matrix Permeability										
Well Name	Well Location	Core Depth (m)	Fm	Density		Porosity (%)	GRI Matrix Permeability (md)		GRI Matrix Permeability (nd)	
				Bulk Density (g/cc)	Skeletal Density (g/cc)		Avg	Std Dev	Avg	Std Dev
Texaco Boundary	100/11-30-087-14W6/00	1185.14	Baldonnel	2.415	2.840	14.94	6.93E-05	2.96E-05	69.26	29.58
Texaco Boundary	100/11-30-087-14W6/00	1187.53	Baldonnel	2.569	2.841	9.57	2.23E-05	1.04E-05	22.25	10.45

Table BD3. Baldonnel Formation – unconfined porosity and GRI matrix permeability measurements from two core samples in Texaco Boundary 11-30-87-14W6.

MICP Porosity										
Well Name	Well Location	Core Depth (m)	Fm	Density g/cc		Porosity (%)	Corrected Porosity (%)	Peak Range		Stem Volume Used (%)
				Bulk Density (g/cc)	Skeletal Density (g/cc)			Peak Range	Modal Peak	
Texaco Boundary	100/11-30-087-14W6/00	1187.53	Baldonnel	2.526	2.778	9.61	9.09	8 - 150	75	59

Table BD4. Baldonnel Formation – MICP porosity and conformance-corrected porosity measurements from one core sample in Texaco Boundary 11-30-87-14W6.

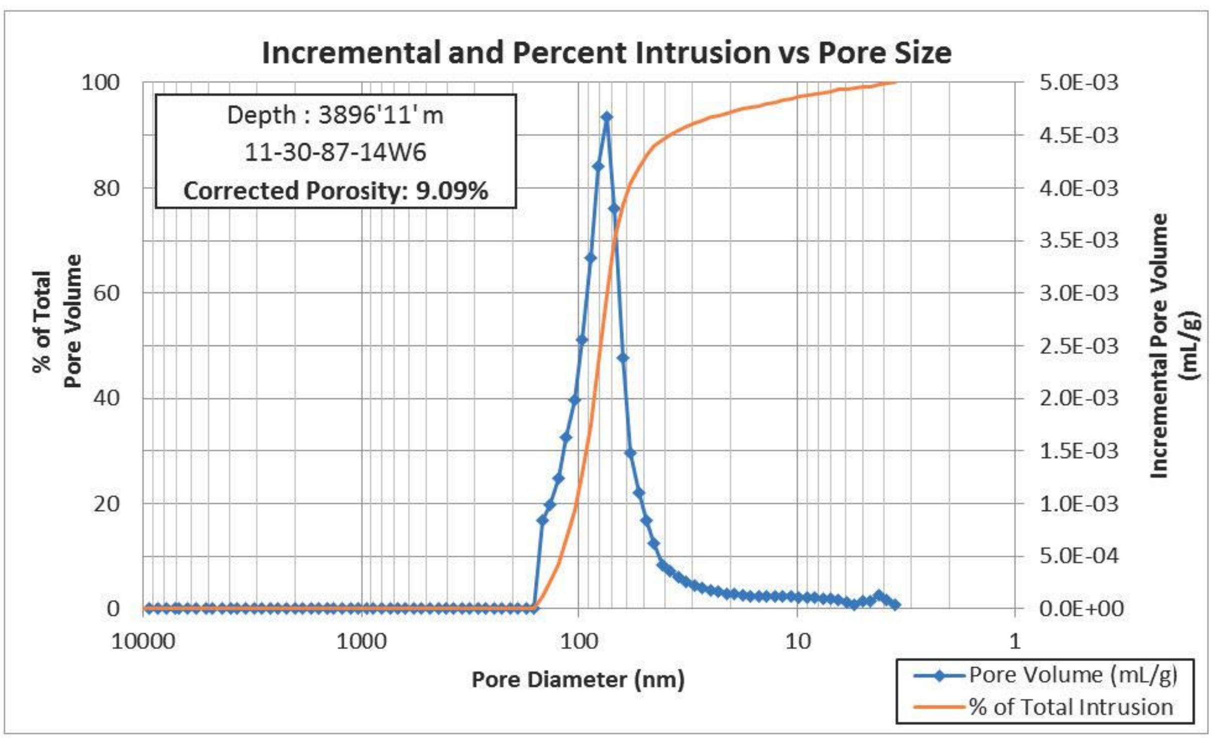

Figure BD10. Incremental and percent intrusion vs pore size, Texaco Boundary 11-30-87-14W6 (3896'11"). Pore throat diameters are primarily in the 50-100 nm range.

Hydrocarbon analysis (S1) shows that residual hydrocarbons are present and most commonly contain heavy C_{17}-C_{38} chains with a calculated API gravity of ~29°; calculated specific gravity is ~0.88, indicating heavy condensates (Table BD5, Fig. BD11).

Hydrocarbon Composition by Thermal Desorption Gas Chromotography

Well Name	Well Location	Core Depth (m)	Fm	% Light Condensate	% Heavy Condensate	% Naphthenes	% Aromatics	% Biomarkers	Range >2%	Peak	Initial Boiling Point (°C)	Carbon Number	Final Boiling Point (°C)	Carbon Number	Calculated Specific Gravity	Calculated API gravity	Chromatogram Quality
Texaco Boundary	100/11-30-087-14W6/00	1184.78	Baldonnel	0.08	96.36	0.01	0.17	3.38	C17-C38	C20	190	C11	546	C40	0.88	29.78	best
Texaco Boundary	100/11-30-087-14W6/00	1187.27	Baldonnel	0.05	98.07	0.01	0.15	1.72	C19-C38	C35	208	C12	553	C40	0.88	28.41	best

Table BD5. Baldonnel Formation – hydrocarbon composition data from two samples in Texaco Boundary 11-30-87-14W6.

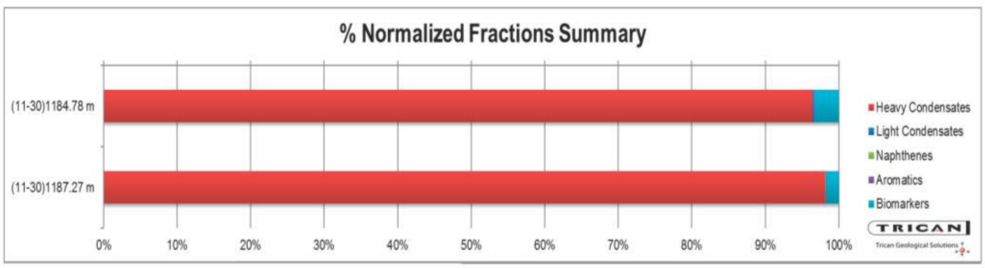

Figure BD11. Normalized fraction plot of hydrocarbon groups identified in two Baldonnel core samples, Texaco Boundary 11-30-87-14W6.

Mechanical properties of a single Baldonnel sample show compressive strength of 29 MPa and residual strength of 21.8 MPa. Poisson's ratio is ~0.23, and Young's modulus 8.42 (Table BD6; Fig. BD12). The sample has considerable visible porosity, and compression of void space is likely the dominant control on strength and compressibility properties. Integrating static (lab triaxial) and dynamic (lab ultrasonic/dipole sonic) measurements can be difficult in lithologies with high or variable amount of porosity, and caution must be used in interpreting results from a single sample.

Triaxial Data

Well Name	Well Location	Core Depth (m)	Fm	Confining Pressure (MPa)	Axial Strain at Failure (%)	Compressive Strength (MPa)	Residual Strength (MPa)	Static Young's Modulus (GPa)	Static Poisson's Ratio	Static Bulk Modulus (GPa)	Static Shear Modulus (GPa)
Texaco Boundary	100/11-30-087-14W6/00	1184.63	Baldonnel	13.0	0.403	28.98	21.81	8.42	0.232	5.23	3.42

Table BD6. Baldonnel Formation – rock mechanical analysis data from one sample in Texaco Boundary 11-30-87-14W6.

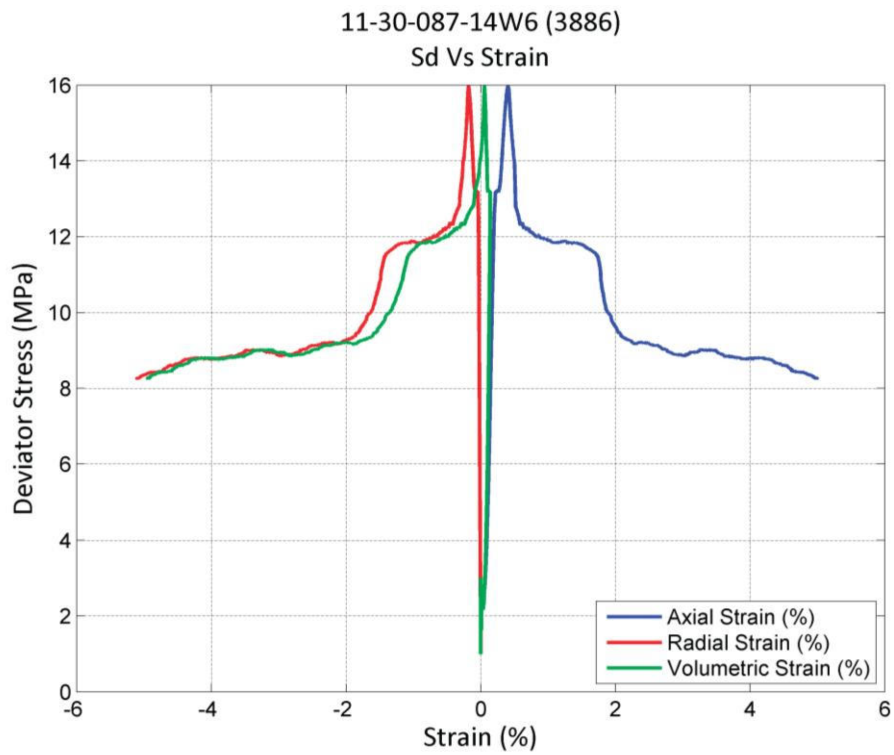

Figure BD12. Mechanical stress-strain graph, Texaco Boundary 11-30-87-14W6 (3886’7”).

Resource Oil Assessment

Existing Baldonnel production is conventional – stratigraphic and structural traps in a variety of settings, but all featuring conventional reservoir quality and hydrocarbon traps over regional aquifers. Like the Charlie Lake, Baldonnel reservoirs tend to feature good conventional quality, or to be tightly cemented by carbonate / evaporite cements. We see no evidence for continuous hydrocarbon accumulations.

Gas production dominates throughout the Baldonnel; oil pools occur in a northwest-southeast fairway from Birch (I/94-A-13) to Oak (86-18W6) but except for Birch are areally small and interspersed with gas pools. Controls on oil charge are unclear, but the southern part of the oily area overlaps with Belloy-Kiskatinaw oil production at Stoddart and Eagle, suggesting a specific charge mechanism related to structural controls.

Adams *et al*. (2016) referenced a CNRL Birch Baldonnel project, “investigating the possibility of a regional ‘resource style’ oil play” – but we have seen no targeted horizontal drilling activity from CNRL beyond very limited drilling at Birch. Similarly, Leucrotta has promoted their Stoddart Baldonnel discovery as being an indicator of regional Baldonnel oil potential, but has not followed up with more drilling.

In summary, the Baldonnel does not offer significant resource oil potential.

“NORDEGG” (GORDONDALE) MEMBER

Age and Play Type

Lower Jurassic – Shale Oil Play;
Prospectivity: ‘C’ Play – While most rock properties appear to favour resource oil prospectivity, horizontal multi-frac completions have not been attempted in the Nordegg in B.C., largely because of lack of success in Alberta.

Regional Geology

The “Nordegg” Member in northwestern Alberta and adjacent British Columbia is a highly-mappable, regionally continuous shale at the base of the Fernie Formation (Map N1, Cross-section Nordegg-Nordegg’). Asgar-Deen *et al*. (2004) mapped the unit regionally, and formally named it the Gordondale Member to distinguish it from the type Nordegg, which is a cherty carbonate package found in the Alberta Foothills and adjacent south-central Plains (Fig. N1). Observing long-term industry usage, we refer to the Nordegg Member in this report, but the correct nomenclature is now Gordondale.

Ross and Bustin (2006, 2007), described the Nordegg in northeastern BC as mudstones, calcareous mudstones, phosphatic mudstones and phosphatic marlstones, which they subdivided into four lithological units: a basal mudstone conglomerate/breccia, phosphatic calcareous mudstone, calcareous mudstone grading to siliceous mudstone, and capped by a phosphatic marlstone to mudstone (Fig. N2). Fossil material, including fish fragments, bivalves, belemnoids, ammonites, coccoliths, and radiolarians, is abundant.

We examined Nordegg cores from Texaco Boundary 11-30-87-14W6 and Murphy Heritage 16-1-78-18W6 (photos in Appendix 4). We have not posted all available Nordegg core on our maps, because many are very short sections taken where under- or overlying strata were the primary targets; note that many of the more complete Nordegg cored sections are indicated on Maps N3 and N4 where analytical data locations are posted.

Log signatures – particularly spiky and elevated gamma log readings and high resistivities – are highly distinctive and enable confident correlation of the Nordegg (Cross-section Nordegg-Nordegg’). High gamma log values are produced by radioactive elements (particularly phosphate and uranium) associated with very high organic content.

The Nordegg lies unconformably on Triassic strata – primarily the Baldonnel Formation in the current study area, and on the Pardonet Formation to the southwest and in the Foothills. There is a relatively minor unconformity between the Nordegg and the overlying Poker Chip Shale, marked by a mudstone conglomerate (Fig. N2). The pre-

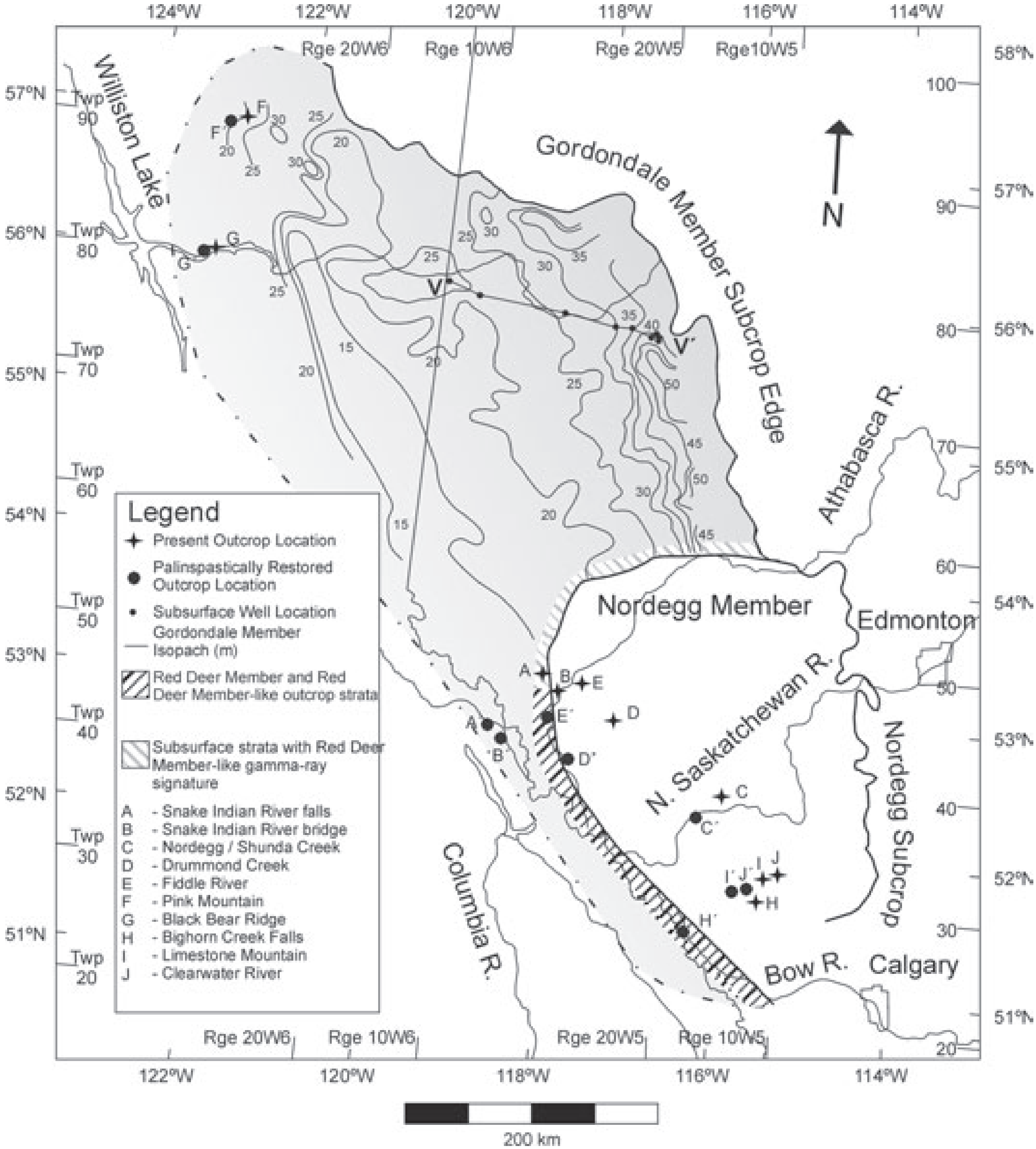

Figure N1. Nordegg / Gordondale stratigraphic relationship (from Asgar-Deen et al., 2004).

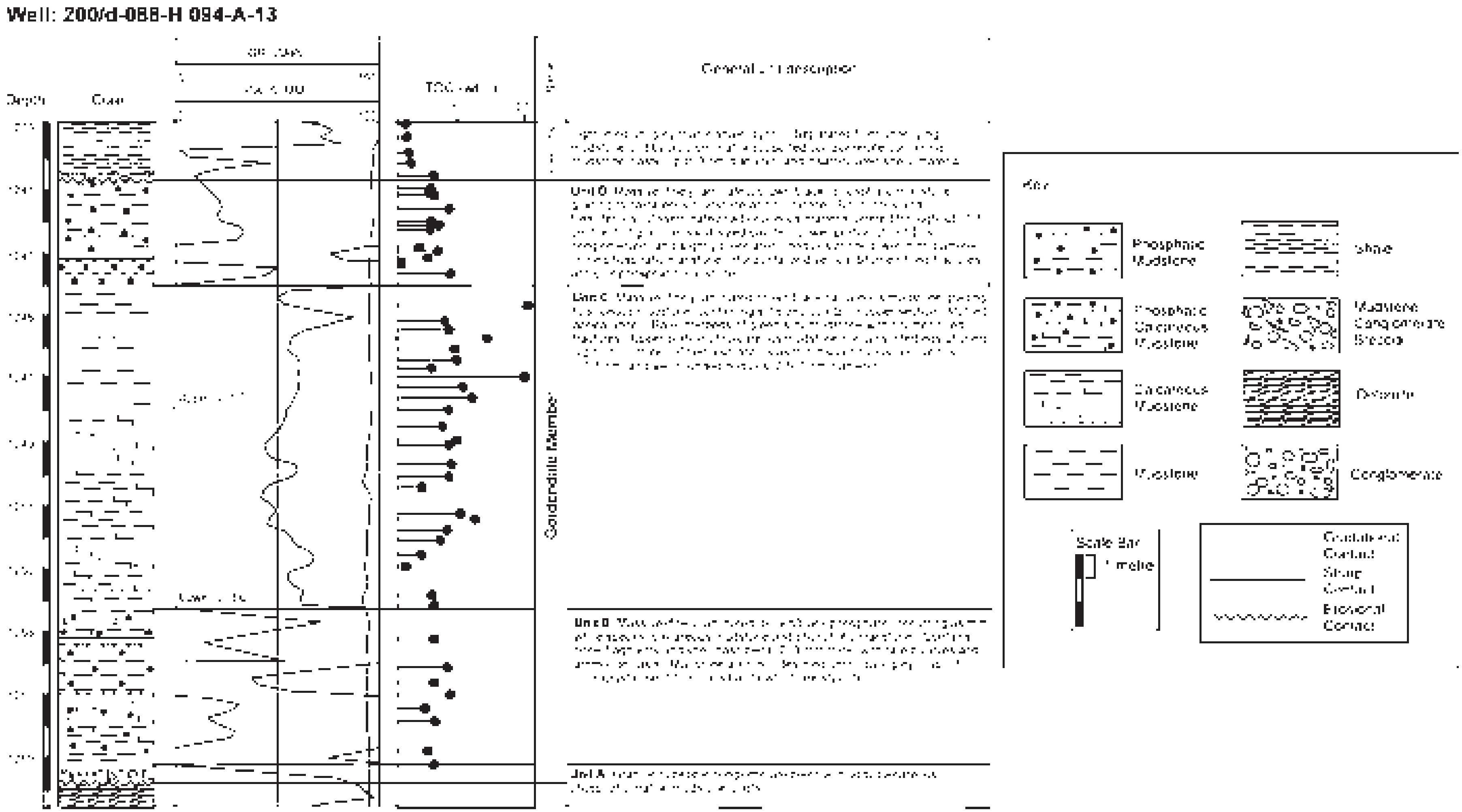

Figure N2. Core description, stratigraphic subdivision, gamma-log response and total organic carbon (TOC) of a completely-cored Nordegg section at d-88-H/94-A-13 (from Ross and Bustin, 2007).

Cretaceous unconformity incises the Jurassic section northeastward, producing an abrupt Nordegg subcrop edge (Cross-section Nordegg-Nordegg’, Map N1). North of the subcrop edge, highly radioactive basal Gething detrital sections are commonly mistaken for the Nordegg (e.g., well c-80-B/94-A-16, Cross-section Nordegg-Nordegg’, Fig. N3), and local sandstone reservoirs in this basal section are in places called the “Nordegg-Baldonnel”.

Where completely preserved, the Nordegg in NEBC ranges in excess of 30m thick (Map N1), and is buried to depths of <1100m to more than 3500m thick (Map N2).

Production and Test Data

Only two completions have been attempted in the Nordegg in NEBC:

- At 16-1-78-18W6, Murphy perfed and frac’d a 20m vertical section of the Nordegg in 2009, and did not recover the load fluid. No further work has been undertaken, and the well is onstream as a Doig gas producer.
- At b-24-H/94-B-8, Canbriam completed a horizontal Nordegg section in 2012, but detailed information is held confidential under terms of an Experimental Scheme. Some gas flow was achieved; note that this location is in the outer Foothills, where structural deformation, natural fracturing, and high organic maturity levels would be expected.

Most DST’s straddling the Nordegg in NEBC were run to test the underlying Baldonnel conventional reservoir, and impart no meaningful information on the Nordegg. The few DST’s completely contained in the Nordegg generally show very poor permeability.

The Nordegg shale play has been pursued as an unconventional target in Alberta, primarily south of Twp 80, where a few naturally-fractured wells have produced oil. Activity peaked in 2010-2012 with several tests yielding minor oil and gas production, but industry has been unable to systematically design economic completions in the Nordegg.

Analytical Data

The Nordegg is regarded as an important conventional oil and gas source rock in western Canada (Riediger *et al*., 1990b; Riediger, 1994; Riediger and Bloch, 2005). Extensive analytical datasets have been acquired, historically in evaluating the Nordegg as a conventional source rock, and more recently in evaluating it as a shale gas / shale oil reservoir. Rokosh *et al*. (2012) mapped mean oil resources in place in the “north Nordegg shale” of Alberta, contiguous with the Nordegg fairway of NEBC, of $6459e^6m^3$ (40.6 billion barrels) (Fig. N4). Note, however, that the northern limit of the oil-prone Nordegg in Alberta is governed by maturity (as measured by vitrinite reflectance) – and

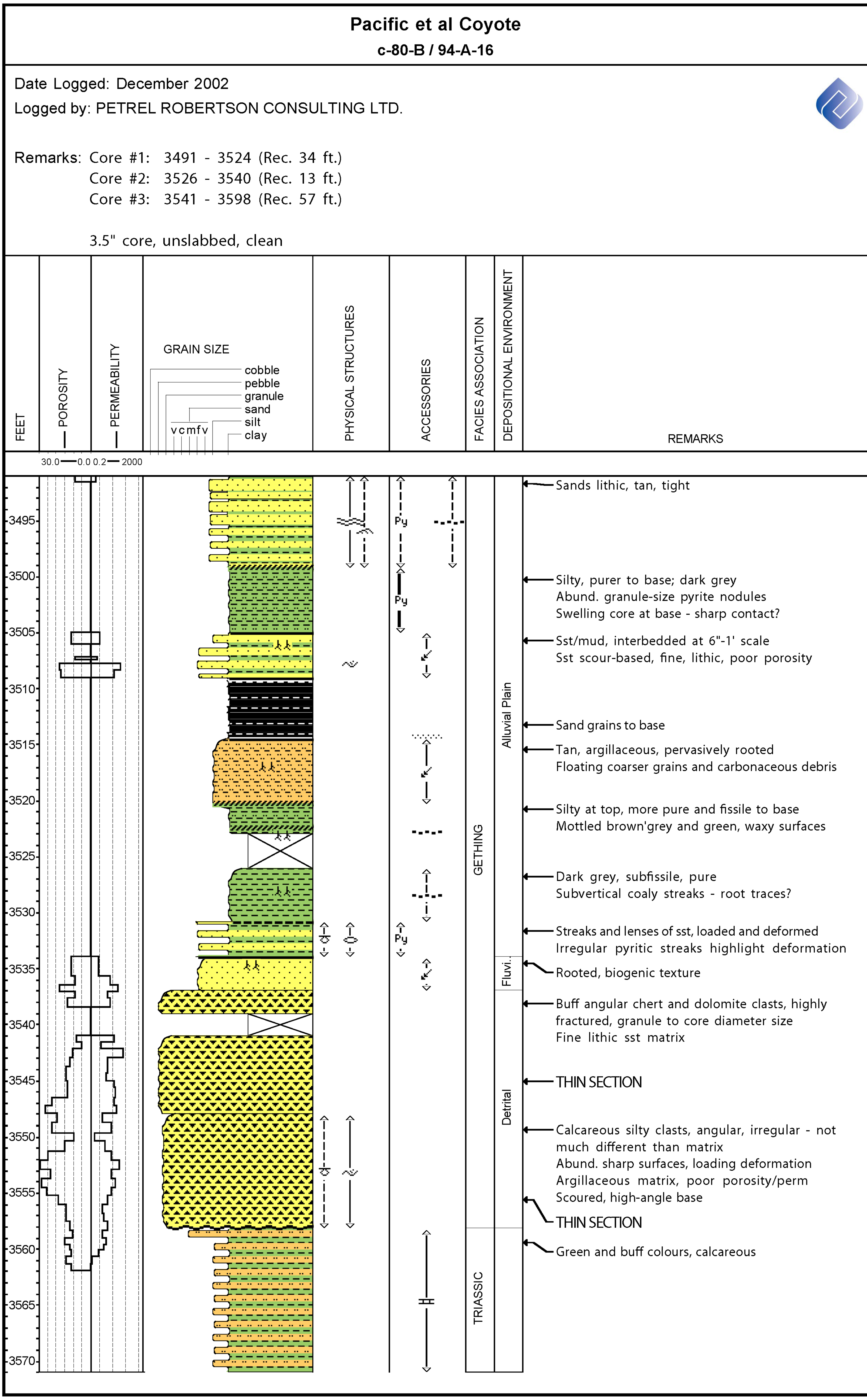

Figure N3. Core log, well c-80-B/94-A-16, showing basal Gething detrital section often mistakenly correlated as Nordegg because of elevated gamma log signatures.

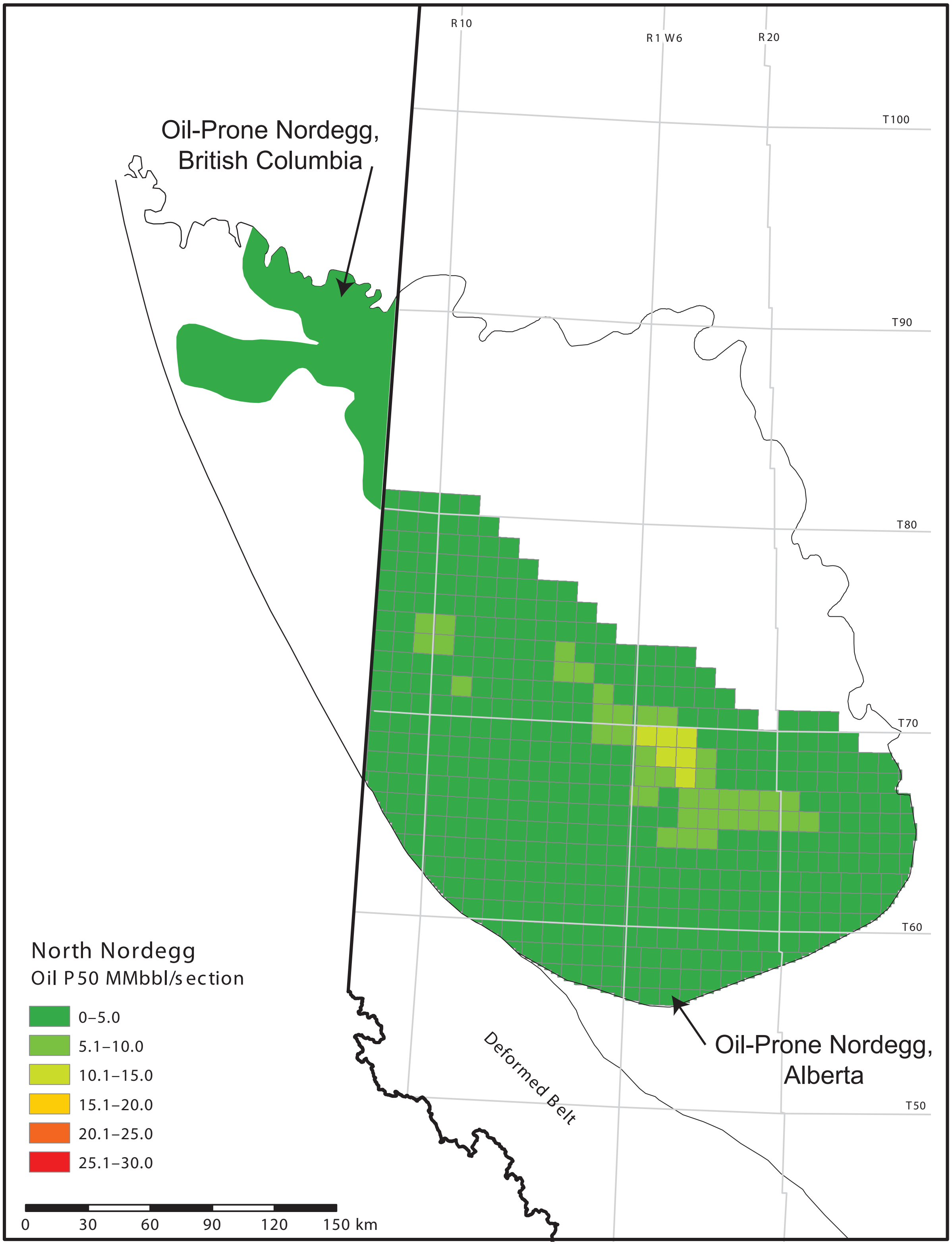

Figure N4. P50 shale oil initially in place in the north Nordegg shale play of Alberta, contiguous with the Nordegg project area of the current project (after Rokosh et al., 2012). Compare the oil-prone area in British Columbia mapped in this study.

substantially disagrees with the oil-prone area in B.C. measured by T_{max} in this study (Fig. N4).

Maps N3 and N4 show T_{max} and TOC values respectively from Nordegg core and cuttings data. Where multiple data points are available from one wellbore, median TOC value was selected, while the T_{max} value from the sample with the highest S2 value was used (if maximum S2 < 1mg/g, no Tmax value was plotted) (Appendix 6). The Nordegg exhibits very high TOC values near the subcrop edge, and lower values with greater burial depth southwestward, where it is more mature and has expelled most of its original hydrocarbon content (Map N3). The maturity (T_{max}) map shows the Nordegg to be mature for oil generation in updip areas and overmature downdip (Map N4). Bustin and Bustin (2016), using T_{max} and vitrinite data, documented a reversal of southwestward-increasing maturity in the Nordegg on a more regional scale (Fig. N5).

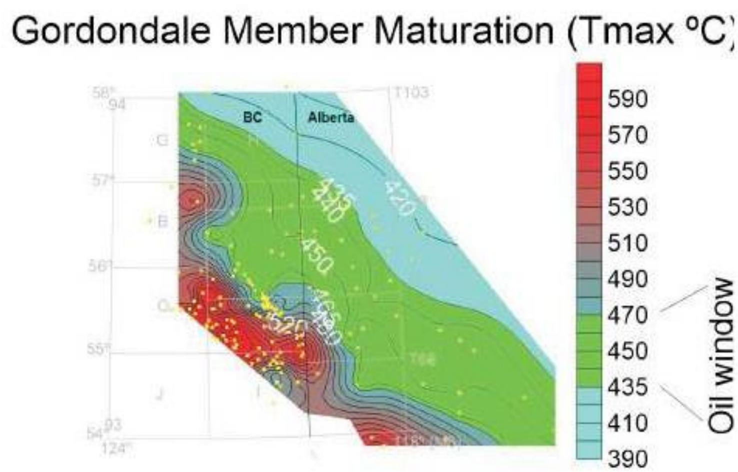

Figure N5. Regional isomaturity map for Nordegg / Gordondale (from Bustin and Bustin, 2016).

Ross and Bustin (2007) evaluated the Nordegg as a shale gas reservoir in northeastern B.C. , with a primary focus on understanding sorbed and free gas capacity. They did note, however, that their unit C (central section of the formation (Fig. N2)) contains abundant silica and small amounts of ductile clay, making it most amenable to frac stimulation.

Analysis of Nordegg Core

We examined Nordegg core from two wells – Texaco Boundary 11-30-87-14W6 and Murphy Heritage 16-1-78-18W6. In both locations, the Nordegg comprises thinly bedded to finely laminated siliceous mudstones/shales and calcareous limestones (Appendix 4). Anhydrite-cemented zones showing brittle fracturing are also present. At 16-1, we also noted thin carbonate beds to finely laminated mudstones/shales with abundant recrystallized, cm-scale shell fragments.

Mineralogical trends throughout the section illustrate diverse origins and diagenetic pathways, like those documented by Ross and Bustin (2007) (Fig. N6, N7; Table N1). The upper section features organic-rich siliceous shale overlying calcite-rich mudstones.

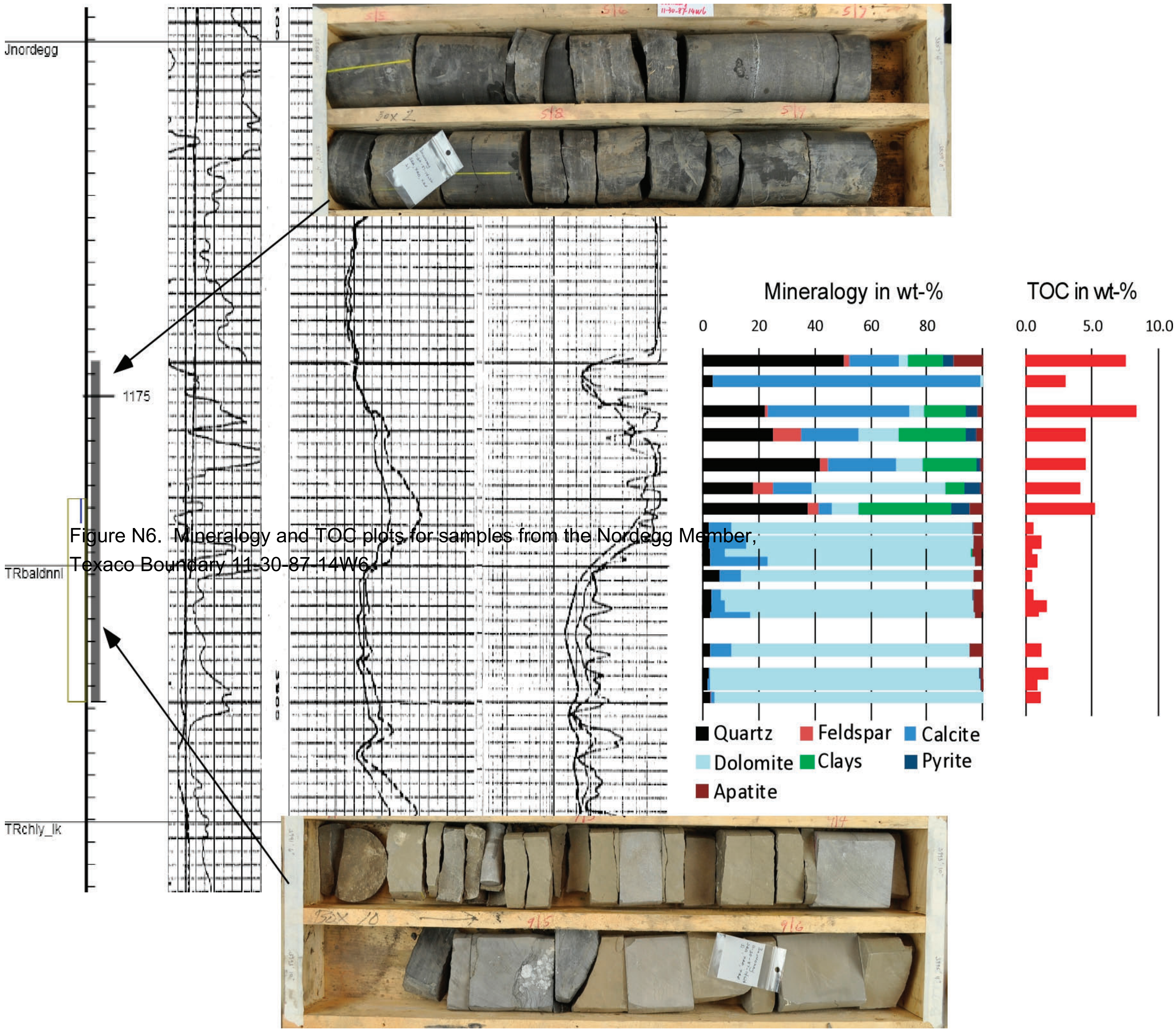

Figure N6. Mineralogy and TOC plots for samples from the Nordegg Member, Texaco Boundary 11-30-87-14W6.

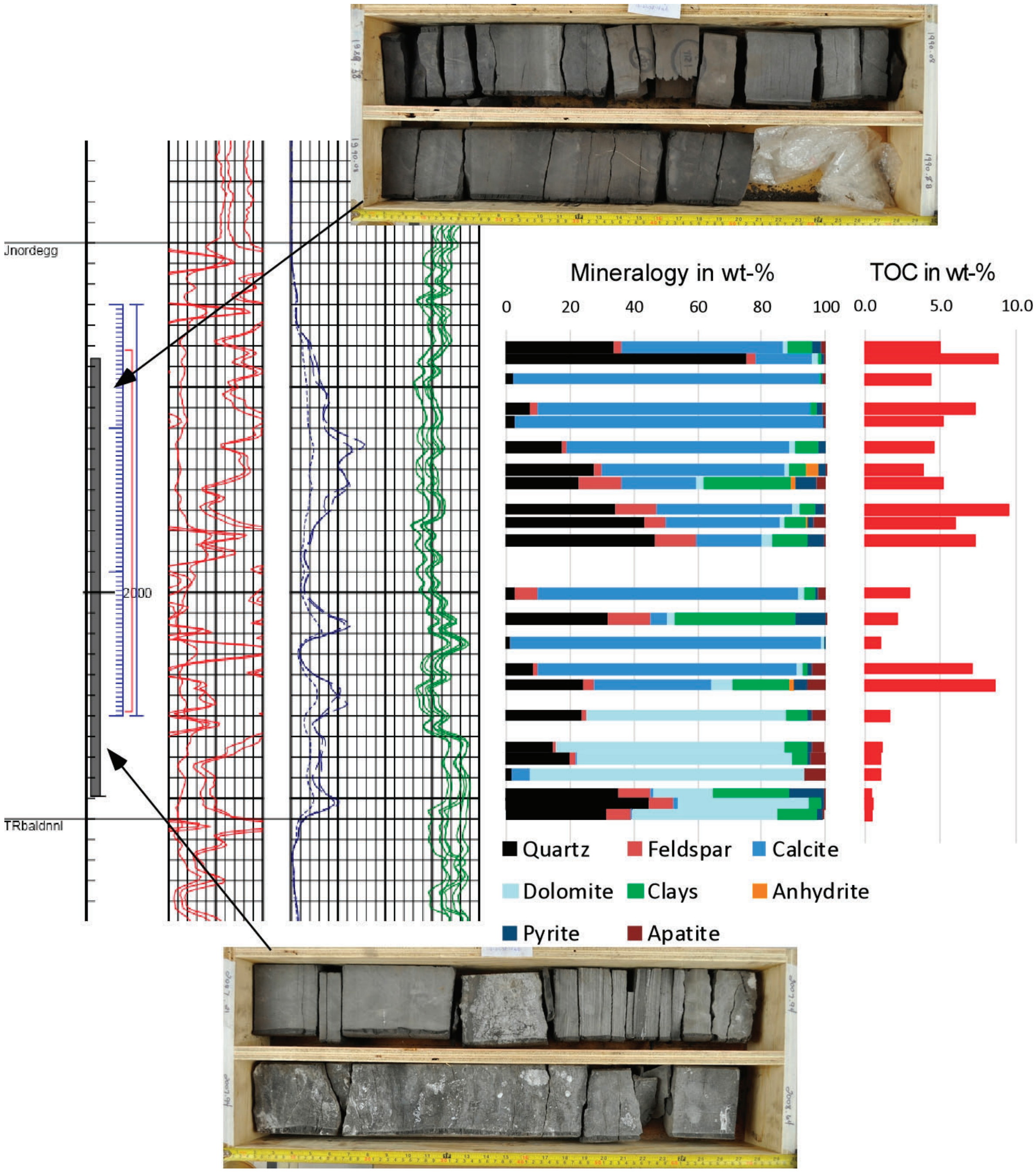

Figure N7. Mineralogy and TOC plots for samples from the Nordegg Member, Murphy Heritage 16-1-78-18W6.

Below, quartz, feldspar and clay minerals increase downhole to the top of the Baldonnel, where dolomite dominates.

Petrographically, the Nordegg comprises finely laminated, organic-rich siliceous shale interbedded with packstones with abundant macro- to nanofossils (Fig. N8, N9). SEM images show the matrix to contain microcrystalline to sparry calcite and dolomite, and abundant coccoliths and pseudo-spherical fossils (likely radiolaria) (Fig. N10). Algal material occurs as short streaks or clusters of opaque organics, including bituminous material.

Well ID	Sample ID	Zone	Sample Type	Depth (m)	Tmax in °C	TOC %	Quartz	Feldspar		Carbonates		Clays	Sulphate	Sulphides		Apatite
								Albite	Microcline	Calcite	Dolomite, Fe-dolomite	Illite/mica	Anhydrite	Pyrite	Marcasite	
Murphy Heritage 100/16-01-078-18W6/00 WA: 24334	1988.16	Nordegg	Core	1988.16	475	5.05	33.6	2.5		50.4	1.7	7.8		2.3	0.3	1.3
	1988.97	Nordegg	Core	1988.97	494	8.86	75.1	3.2		17.4	2	0.9		0.8	0.1	0.5
	1989.85	Nordegg	Core	1989.85	492	4.45	2.3			95.9		0.6		0.4		0.7
	1991.03	Nordegg	Core	1991.03	481	7.32	7.5	2.5		85.1		2		2		0.9
	1991.9	Nordegg	Core	1991.90	500	5.23	2.6			96.6				0.2		0.5
	1992.99	Nordegg	Core	1992.99	475	4.56	17.4	1.7		69.3	2	7.1		2.4		
	1993.2	Nordegg	Core	1993.20	481	3.87	27.4	2.5		57.4	1.2	5.2	4.2	2		0.1
	1994	Nordegg	Core	1994.00	485	5.19	22.9	13.1		23.6	2.4	27.1	1.2	6.9		2.8
	1994.8	Nordegg	Core	1994.80	486	9.50	34.4	12.5		42.8	2.4	4.6		2.8		0.5
	1996.09	Nordegg	Core	1996.09	479	6.02	43.4	6.4		36	1.5	6.4	0.7	2		3.5
	1996.84	Nordegg	Core	1996.84	488	7.30	46.8	12.6		20.7	3.5	10.5		5.4		0.5
	1997.6	Nordegg	Core	1997.60	476	2.98	2.9	6.9		81.5	2.1	3.2		1.3		2
	2000.4	Nordegg	Core	2000.40	499	2.19	32	13		5.4	2.4	37.6		9.6		0.1
	2001.27	Nordegg	Core	2001.27	526	1.09	1.2	0.3		97.3	0.8	0.1		0.2		
	2002.5	Nordegg	Core	2002.50	571	7.13	8.5	1.4		80.9	2.1	1.6		1.4		4
	2003.85	Nordegg	Core	2003.85	579	8.63	24.1	3.5		36.6	6.8	17.8	1.2	4.5		5.4
	2004.52	Nordegg	Core	2004.52	568	1.68	23.8	1.6			62.3	6.6		1.4		4.3
	2006.08	Nordegg	Core	2006.08	569	1.21	14.9	0.9			71.4	7		1.6		4
	2007.75	Nordegg	Core	2007.75		1.08	20	1.7		0.8	67	4.9		0.8		4.8
	2008.08	Nordegg	Core	2008.08	428	1.05	2			5.6	85.7			0.1		6.5
	2009.97	Nordegg	Core	2009.97	549	0.53	35.2	3.8	6.4	0.6	18.6	23.9		11		0.4
	2010.25	Nordegg	Core	2010.25		0.57	44.9	2.7	4.6	1.6	40.9	4.1		0.9		0.2
	2010.92	Nordegg	Core	2010.92		0.45	31.4	3.6	4.2	0.5	45.2	12.2		2.2		0.5
Texaco Boundary 100/11-30-087-14W6/00 WA: 03098	3850'2"	Nordegg	Core	1173.52	444	7.56	50.3	2.1		17.5	3.3	12.6		3.9		10.2
	3853'3"	Nordegg	Core	1174.47	442	2.96	3.9			95	1.1					
	3857'10"	Nordegg	Core	1175.87	440	8.33	22.5	0.6	0.1	50.7	5.3	14.5		4.6		1.7
	3861'6"	Nordegg	Core	1176.99	446	4.50	25.4	3.8	5.9	20.8	14.2	23.8		3.6		2.5
	3865'4"	Nordegg	Core	1178.15	440	4.50	42.1		2.5	24.4	9.8	18.8		1.3		1.1
	3868'6"	Nordegg	Core	1179.12	441	4.13	18	7.2		13.9	47.7	6.8		5.5		0.8
	3871'10"	Nordegg	Core	1180.13	440	5.19	37.4		4.1	4.5	9.5	33.1		6.5		4.8
	3874'9"	Nordegg	Core	1181.02	433	0.60	2.5			7.9	86			0.1		3.6
	3876'4"	Nordegg	Core	1181.51	426	1.17	2.4			13.1	81.3			0.1		3.2
	3877'10"	Nordegg	Core	1181.96	421	0.47	2.8			5.2	87.9	0.4		0.1		3.7
	3878'8"	Nordegg	Core	1182.22	427	0.91	2.8			20.3	74.2			0.1		2.7
	3881'8"	Baldonnel	Core	1183.13	434	0.49	6			7.8	82.9			0.1		3.2
	3884'4"	Baldonnel	Core	1184.05	435	0.60	3.3			3.1	90			0.1		3.4
	3887'1"	Baldonnel	Core	1184.78	426	1.63	3.2			4.8	88.8			0.1		3.1
	3887'2"	Baldonnel	Core	1184.80	446	0.97	2.8			14.4	79.9			0.1		2.8
	3891'1"	Baldonnel	Core	1186.00	426	1.18	2.9			7.5	84.7			0.1		4.9
	3895'3"	Baldonnel	Core	1187.27	429	1.74	2.4			0.2	96.2			0.1		1.2
	3897'	Baldonnel	Core	1187.81	433	0.87	1.7			0.9	96.3			0.1		1.1
	3898'11"	Baldonnel	Core	1188.39	433	1.06	2.6	0.1		1.7	95.7					

Table N1. Nordegg Member – thermal maturity and mineralogical data from samples in Texaco Boundary 11-30-87-14W6 and Murphy Heritage 16-1-78-18W6.

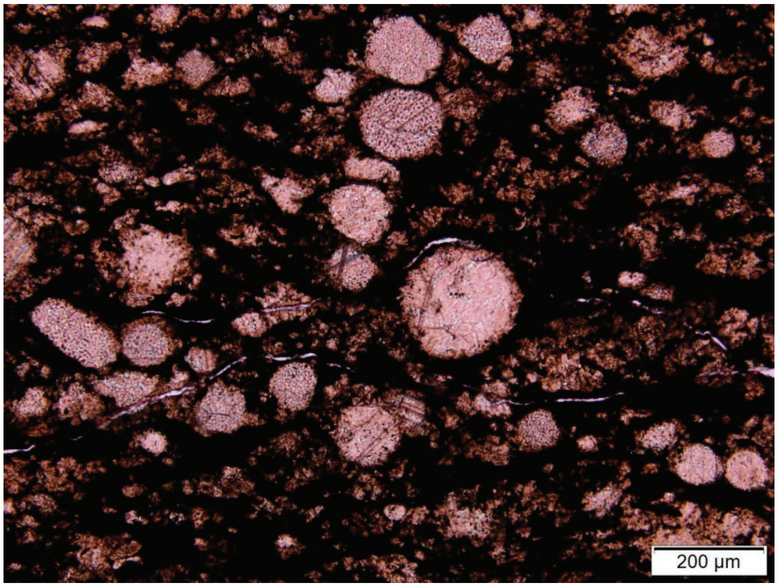

Figure N8. Photomicrograph, Nordegg Member, Murphy Heritage 16-1-78-18W6 (1989.96 m) under plane polarized light. Typical organic-rich bioclastic packstone, highlighting abundant radiolarians (40-220 um) and other recrystallized nannofossils composed of sparry calcite.

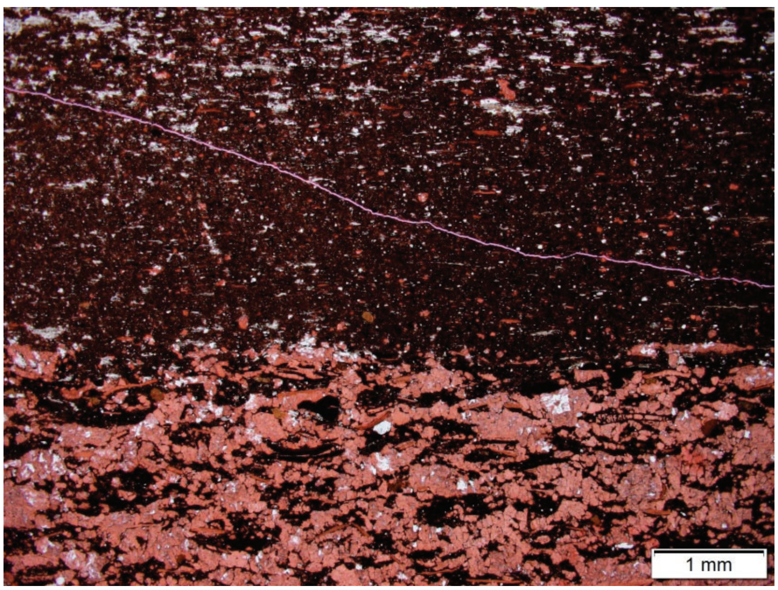

Figure N9. Photomicrograph, Nordegg Member, Texaco Boundary 11-30-87-14W6 (3856'2") under plane polarized light. Very fine-grained calcareous-argillaceous bed overlying bioclastic limestone bed.

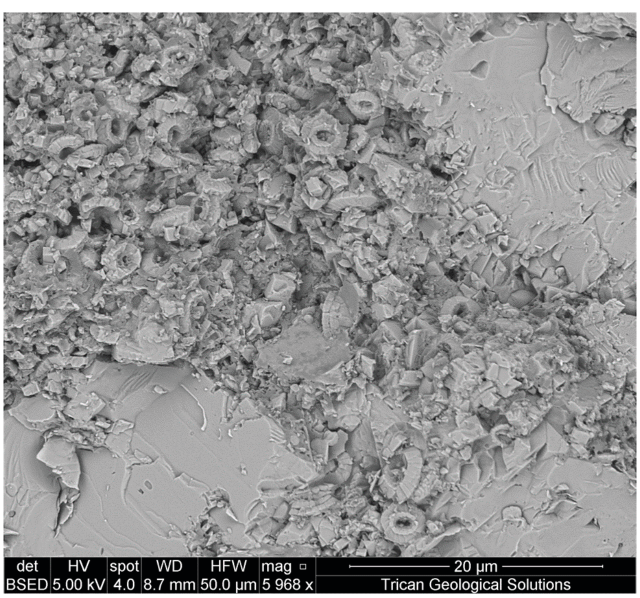

Figure N10. BSED SEM photomicrograph, Nordegg Member, Murphy Heritage 16-1-78-18W6 (1989.96 m), showing fine crystalline calcite with abundant coccolith plates.

Unconfined porosity values range between 1.5-7.4%, and matrix permeabilities range from 6.5-14 nD (Table N2). In general, pervasive carbonate cementation has reduced porosity and permeability. MICP conformance-corrected porosity values are similar to the unconfined values, and range between 0.4-6.4% (Table N3). Most pore throat sizes are <50 μm (Fig. N11).

Unconfined Porosity and Matrix Permeability										
Well Name	Well Location	Core Depth (m)	Fm	Density		Porosity (%)	GRI Matrix Permeability (md)		GRI Matrix Permeability (nd)	
				Bulk Density (g/cc)	Skeletal Density (g/cc)		Avg	Std Dev	Avg	Std Dev
Texaco Boundary	100/11-30-087-14W6/00	1175.03	Nordegg	2.431	2.577	5.65	1.32E-05	2.29E-06	13.24	2.29
Texaco Boundary	100/11-30-087-14W6/00	1178.86	Nordegg	2.359	2.527	6.63	9.59E-06	2.36E-06	9.59	2.36
Murphy Heritage	100/16-01-078-18W6/00	1989.42	Nordegg	2.413	2.450	1.52	4.36E-07	7.82E-08	0.44	0.08
Murphy Heritage	100/16-01-078-18W6/00	1994.81	Nordegg	2.303	2.355	2.22	1.03E-06	1.41E-07	1.03	0.14
Murphy Heritage	100/16-01-078-18W6/00	1998.14	Nordegg	2.526	2.611	3.25	7.56E-06	1.57E-06	7.56	1.57
Murphy Heritage	100/16-01-078-18W6/00	2001.69	Nordegg	2.242	2.328	3.71	1.41E-06	3.85E-07	1.41	0.39
Murphy Heritage	100/16-01-078-18W6/00	2005.61	Nordegg	2.605	2.812	7.38	1.49E-05	1.65E-06	14.93	1.65

Trican Geological Solutions

Table N2. Nordegg Member – unconfined porosity and GRI matrix permeability measurements from core samples in Texaco Boundary 11-30-87-14W6 and Murphy Heritage 16-1-78-18W6.

MICP Porosity										
Well Name	Well Location	Core Depth (m)	Fm	Density g/cc		Porosity (%)	Corrected Porosity (%)	Peak Range		Stem Volume Used (%)
				Bulk Density (g/cc)	Skeletal Density (g/cc)			Peak Range	Modal Peak	
Texaco Boundary	100/11-30-087-14W6/00	1178.86	Nordegg	2.376	2.432	2.37	2.30	4 - 40	7	19
Murphy Heritage	100/16-01-078-18W6/00	1989.42	Nordegg	2.402	2.439	1.63	1.52	4 - 30	4	0
Murphy Heritage	100/16-01-078-18W6/00	1998.14	Nordegg	2.590	2.601	0.92	0.43	6 - 110	18	12
Murphy Heritage	100/16-01-078-18W6/00	2005.61	Nordegg	2.590	2.771	6.83	6.56	5 - 150	75	39

Trican Geological Solutions

Table N3. Nordegg Member – MICP porosity and conformance-corrected porosity measurements from core samples in Texaco Boundary 11-30-87-14W6 and Murphy Heritage 16-1-78-18W6.

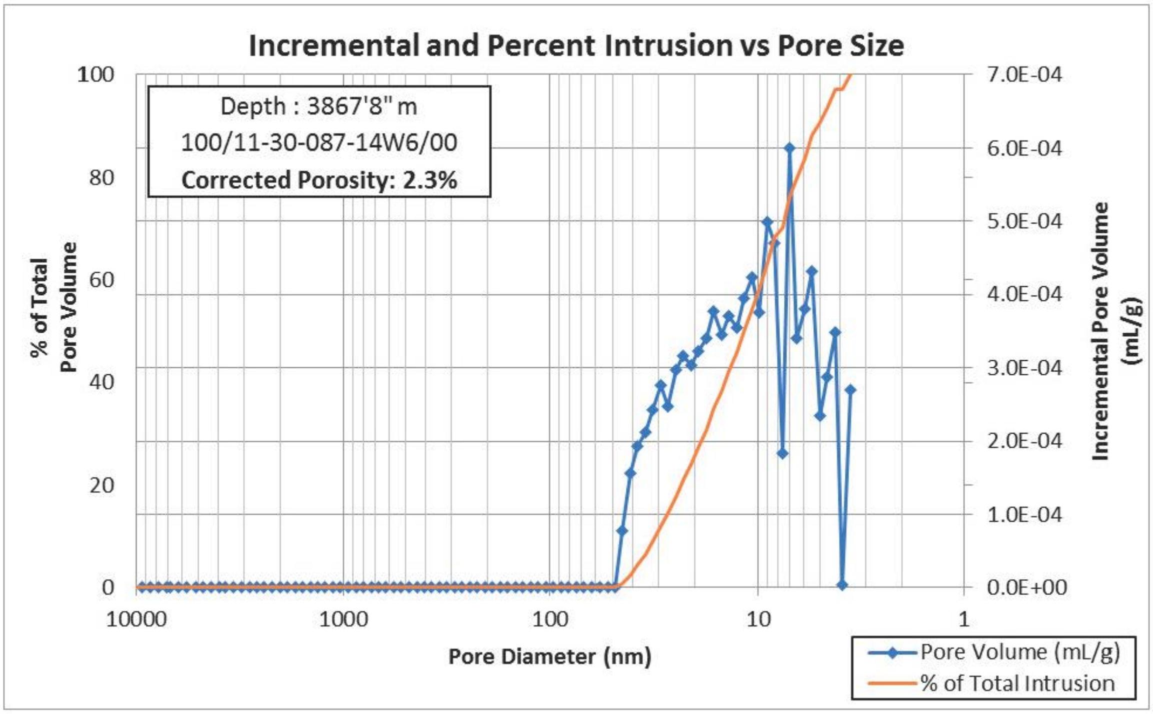

Figure N11. Incremental and percent intrusion vs pore size, Texaco Boundary 11-30-87-14W6 (3867’8”). Pore throat diameters are very small (<40 nm).

Hydrocarbon analysis (S1) shows abundant residual hydrocarbons, most commonly containing C_{10}-C_{35} chains with calculated API gravities of 33-49°; most samples are around 30-33°. Calculated specific gravities range between 0.78-0.88 (Table N4). Heavy hydrocarbons dominate with high aromatics in two samples from Murphy 16-1-78-18W6 and light condensates in all samples at lower concentrations (Fig. N12).

Hydrocarbon Composition by Thermal Desorption Gas Chromatography

TRICAN Trican Geological Solutions

Well Name	Well Location	Core Depth (m)	Fm	% Light Condensate	% Heavy Condensate	% Naphthenes	% Aromatics	% Biomarkers	Peak	Initial Boiling Point (°C)	Carbon Number	Final Boiling Point (°C)	Carbon Number	Calculated Specific Gravity	Calculated API gravity	Chromatogram Quality
Texaco Boundary	100/11-30-087-14W6/00	1174.42	Nordegg	0.18	95.01	0.12	0.31	4.39	C20	95	C7	538	C40	0.88	28.39	best
Texaco Boundary	100/11-30-087-14W6/00	1178.15	Nordegg	0.62	93.14	0.14	0.79	5.31	C20	85	C7	543	C40	0.88	30.04	best
Texaco Boundary	100/11-30-087-14W6/00	1181.51	Nordegg	0.04	96.27	0.02	0.17	3.50	C20	192	C11	542	C40	0.88	30.13	best
Murphy Heritage	100/16-01-078-18W6/00	1989.85	Nordegg	4.22	78.92	0.41	1.51	14.94	C15	70	C6	545	C40	0.85	34.46	best
Murphy Heritage	100/16-01-078-18W6/00	1994.00	Nordegg	14.80	25.53	10.38	44.01	5.29	toluene	41	<C6	549	C40	0.78	49.54	excellent
Murphy Heritage	100/16-01-078-18W6/00	1997.60	Nordegg	5.60	65.32	2.55	11.47	15.05	phytane	45	<C6	544	C40	0.85	35.47	best
Murphy Heritage	100/16-01-078-18W6/00	2001.27	Nordegg	3.22	73.79	1.26	7.07	14.66	C20	43	<C6	549	C40	0.86	33.65	good
Murphy Heritage	100/16-01-078-18W6/00	2003.85	Nordegg	3.50	45.27	4.42	42.27	4.54	toluene	38	<C6	551	C40	0.79	47.06	good
Murphy Heritage	100/16-01-078-18W6/00	2009.97	Nordegg	0.00	65.89	0.14	0.52	33.45	C16	48	<C6	552	C40	0.86	33.12	good

Table N4. Nordegg Member – hydrocarbon composition data from samples in Texaco Boundary 11-30-87-14W6 and Murphy Heritage 16-1-78-18W6.

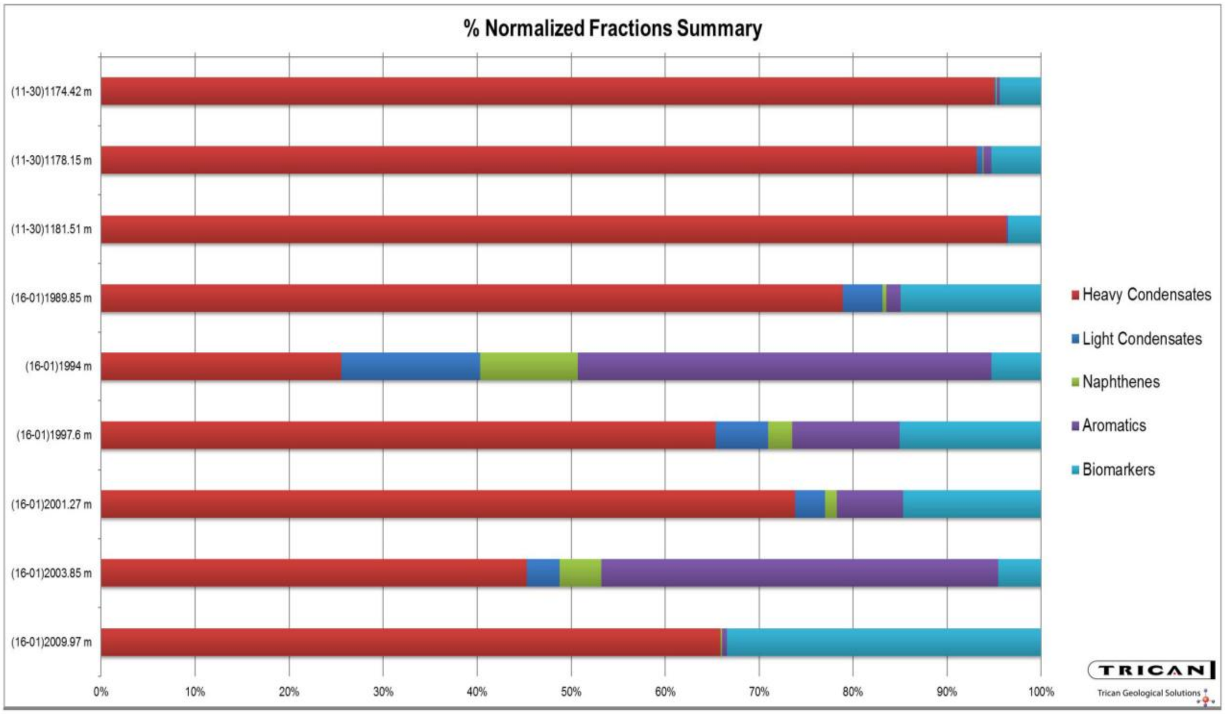

Figure N12. Normalized fraction plot of hydrocarbon groups identified in nine Nordegg core samples.

Mechanical properties show a wide range of compressive strength (57-310 MPa) and residual strength (38-182 MPa); Poisson's ratio is ~0.24-0.30 and Young's modulus ~14-54 (Table N5). However, the 1989.67m sample from 16-1 was severely damaged prior to testing and consequently yielded a significantly lower compressive strength and Young's modulus, as well as an erroneous (and therefore excluded) Poisson's ratio. Other samples may have similar flaws that create a wide spread in the data; however, mechanical damage may be representative of the zone itself.

Triaxial Data (TRICAN Trican Geological Solutions)											
Well Name	Well Location	Core Depth (m)	Fm	Confining Pressure (MPa)	Axial Strain at Failure (%)	Compressive Strength (MPa)	Residual Strength (MPa)	Static Young's Modulus (GPa)	Static Poisson's Ratio	Static Bulk Modulus (GPa)	Static Shear Modulus (GPa)
Texaco Boundary	100/11-30-087-14W6/00	1175.16	Nordegg	13.0	0.753	224.18	117.66	34.19	0.255	23.22	13.63
Murphy Heritage	100/16-01-078-18W6/00	1989.67	Nordegg	17.0	0.331	57.82	38.27	13.59	NA	NA	NA
Murphy Heritage	100/16-01-078-18W6/00	1998.02	Nordegg	17.0	0.821	178.97	102.69	34.34	0.240	22.03	13.84
Murphy Heritage	100/16-01-078-18W6/00	2005.80	Nordegg	17.0	0.626	310.66	182.28	54.38	0.297	44.60	20.97

Table N5. Nordegg Member – rock mechanical analysis data from samples in Texaco Boundary 11-30-87-14W6 and Murphy Heritage 16-1-78-18W6.

Figures N13 and N14 show mechanical stress-strain relationships for samples from the two wells.

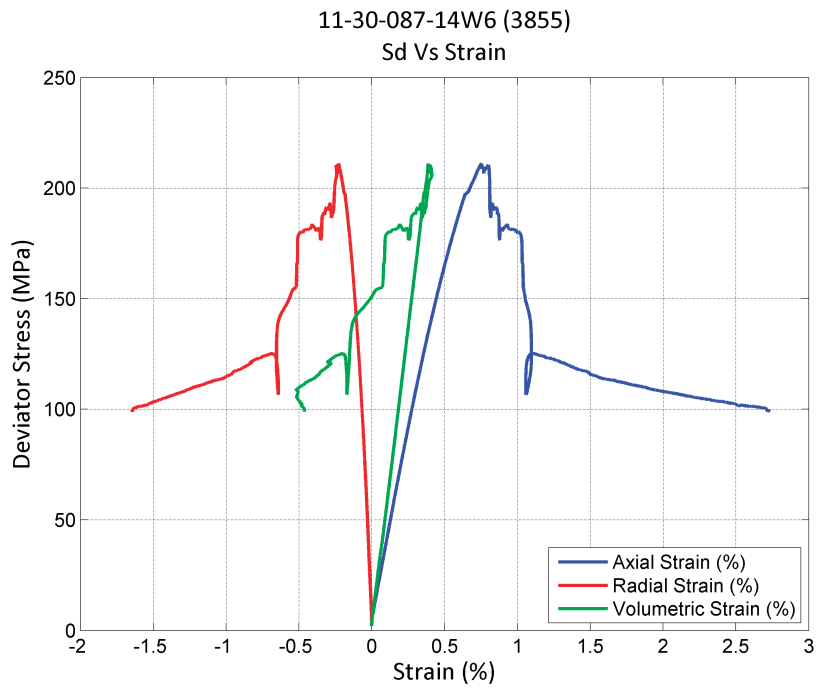

Figure N13. Mechanical stress-strain graph, Nordegg Member, Texaco Boundary 11-30-87-14W6 (3855’6”).

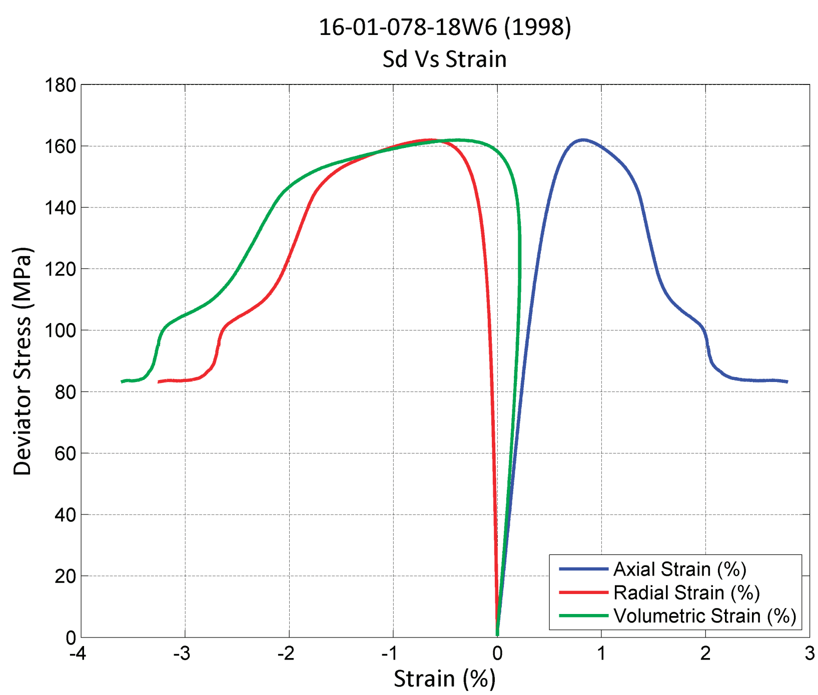

Figure N14. Mechanical stress-strain graph, Murphy Heritage 16-1-78-18W6 (1998.02m).

Resource Oil Assessment

The lack of success to date in stimulating Nordegg shales to be shale oil (or at least shale gas) producers is not clear. There is no question that the unit is an excellent conventional source rock, and its geomechanical properties appear favourable in terms of frackability. Regional resource assessments (e.g., Rokosh *et al*. (2012)) has assigned large in-place oil volumes, while others such as Ross and Bustin (2007) interpreted significant shale gas potential in more thermally mature areas.

While only two Nordegg completions have been attempted in NEBC, much more effort has been put into horizontal drilling and multi-frac completions in adjacent Alberta. There has been essentially no economic success, despite some oil production from naturally-fractured Nordegg shales further to the south in the Simonette area.

There appears to be little point in further data acquisition on the Nordegg play, unless one can define some very specific procedures to assess geomechanical properties and / or stress conditions that might address the lack of productivity seen to date.

FERNIE FORMATION ("Rock Creek" Sandstone)

Age and Play Type

Lower Jurassic – Tight Oil Play (Tight sandstone);
Prospectivity: 'C' Play – No evidence of oil charge, no targeted evaluations exist.

Regional Geology

Petrel Robertson (1997) described the Fernie Formation in the Buick Creek – Laprise area as dark grey marine to prodeltaic shales, relatively pure at the base, but incorporating more coarse clastics towards the top. Uppermost Fernie beds are silty, and contain abundant nodular and disseminated pyrite, scattered highly glauconitic beds, and disseminated fine to medium sand grains. The Fernie lies unconformably on the "Nordegg", and there is some evidence in more complete sections to the west of interfingering with the overlying Buick Creek sandstone. To the south in the Peace River Block and Deep Basin areas, the Fernie passes more or less gradationally up into Nikanassin sandstones. Beyond the Nikanassin and Buick Creek subcrop edges, the Fernie is eroded beneath the pre-Cretaceous unconformity.

Burial depth to top of the Fernie ranges from <1100m in the north to more than 3500m in the southwestern Deep Basin (Map RC1).

Fernie shales are not regarded as shale reservoir targets because of their relatively low organic content.

In the Peace River Block, Janicki and Balogun (2015) described the “Fernie sand”, also informally termed the Rock Creek, in the lower part of the Fernie Formation above the Nordegg Member (Cross-section RC-RC’ traverses the thickest and most extensive development). Where clean and fully-developed, the Rock Creek stands out on logs as a conventional sandstone, but it is more commonly interbedded with shales, and presents a subdued, shaly log response. Janicki and Balogun (2015) mapped clean, fine-grained Fernie sand sections (Fig. RC1), which we have reproduced on Map RC1. Systematic mapping and reconstruction of depositional environments and trends have not been undertaken.

Core analysis data show most Rock Creek samples to be tight, with porosities <10% and permeabilities <0.1 mD (Fig. RC2).

Production and Test Data

After perf and frac, the Rock Creek in 13-32-78-14W6 produced 1.51e^{6}m^3 (0.054 BCF) gas. A followup horizontal Rock Creek completion at 5-33-78-14W6 produced 27.9 e^{6}m^3 (0.989 BCF) gas between 2010 and 2016. Janicki and Balogun (2015) showed b-36-C/94-A-13 as a Rock Creek gas producer too, but this well in fact produced from the Baldonnel, although there is a Rock Creek sand developed.

Analytical Data

Map RC1 shows locations where analytical data were acquired from Fernie shales and Rock Creek sandstones. A limited amount of petrographic work has been done in the Rock Creek in Twp 77-79, Rge 14-16W6, in the area of maximum sand thickness and in or offsetting the gas producers in 78-14W6. While analytical work in the Fernie is shown in a number of wells, many of these are in older wells where long sections of cuttings were analyzed, or in wells where reservoirs above or below the Fernie were analyzed and the cored interval overlapped the Fernie.

Comparing Map RC1 with Nordegg maturities (Map N3), Rock Creek sandstones are best developed in areas where the underlying Nordegg source rock is overmature for oil.

In the Rock Creek core at 7-1-80-15W6, % pore volume oil values are variable, ranging from 0.04 to 0.41, with most values <0.25, and % pore volumes water values are generally higher . We interpret this to mean that there has been some oil charge, but it has been relatively ineffective.

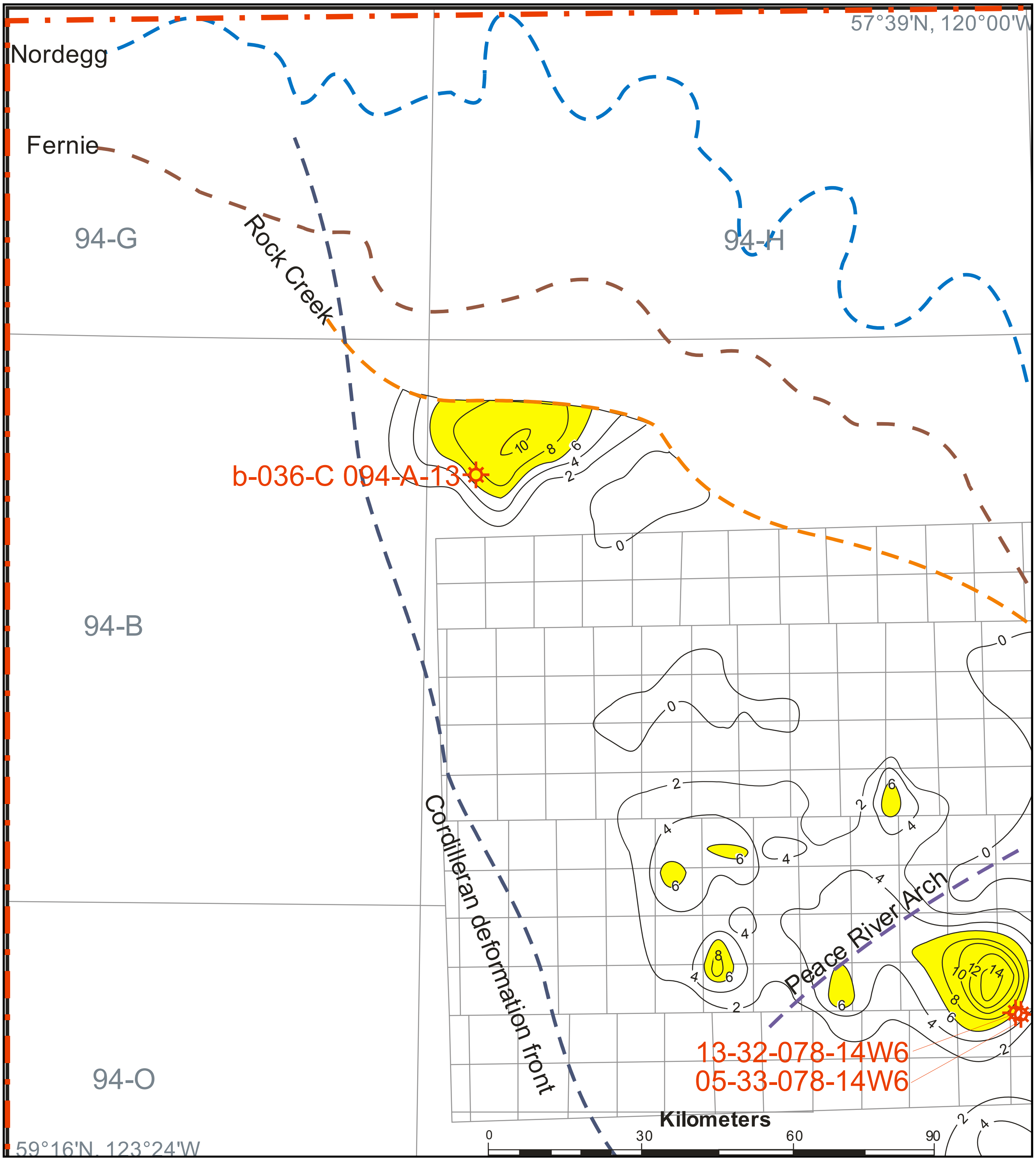

Figure RC1. Isopach map of Rock Creek sandstone in NEBC (from Janicki and Balogun, 2015).

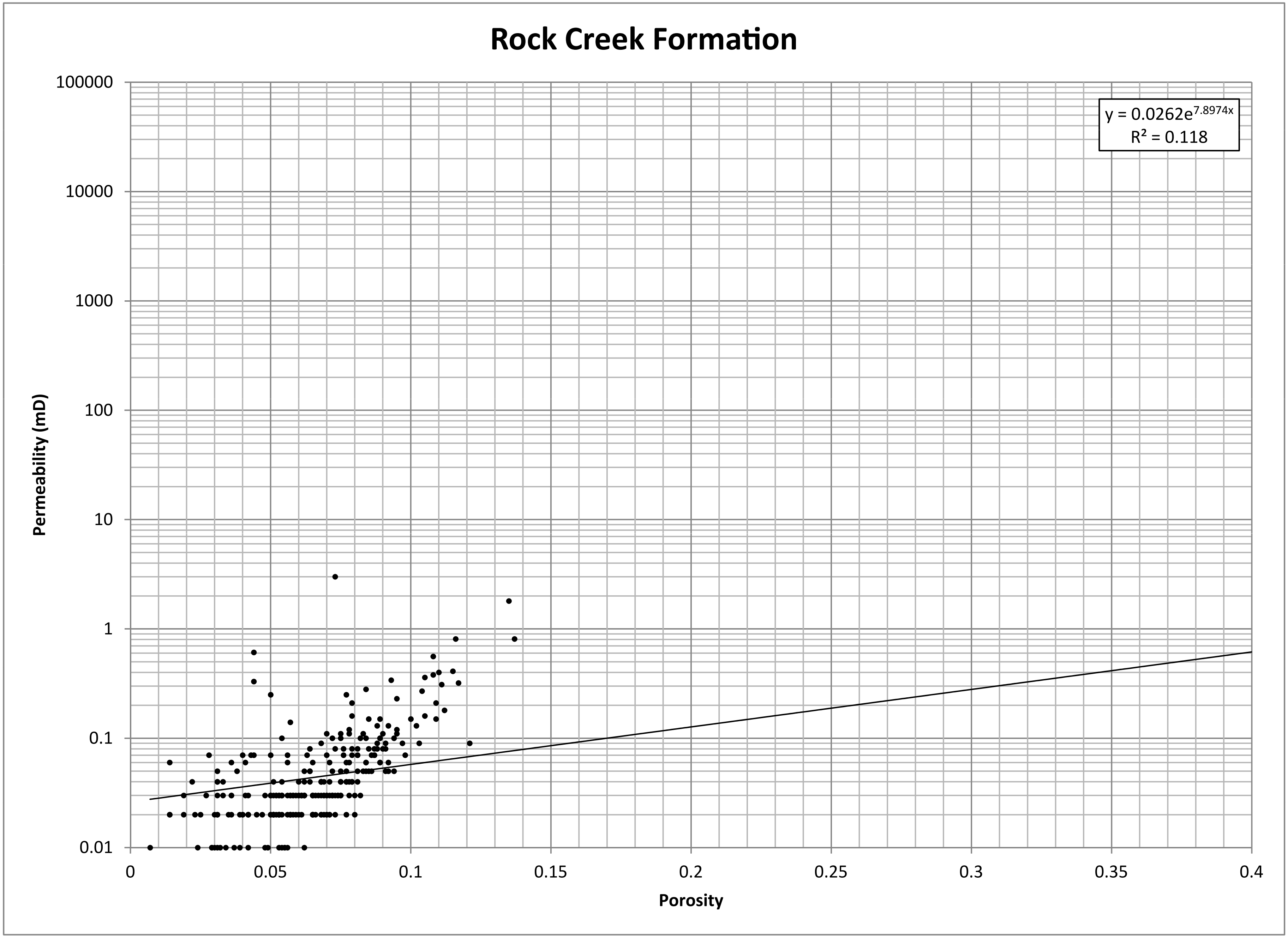

Figure RC2. Porosity / permeability cross-plot, Rock Creek Formation.

Resource Oil Assessment

We have no evidence to suggest that the Rock Creek is a viable resource oil target. While there may have been some oil charge, we see no convincing evidence of potential produceability.

CHINKEH FORMATION

Age and Play Type

Lower Cretaceous – Tight Oil Play (Tight sandstone);
Prospectivity: 'A' Play – there is oil production from a broad reservoir fairway downdip of, but compartmentalized from, a major gas pool. A regionally extensive resource oil target may exist.

Regional Geology

Sandstones and finer-grained clastics of the Chinkeh Formation were named, described and mapped in outcrop and the subsurface of the Liard Basin by Leckie *et al.* (1991) and Frank (2002). McMechan *et al*. (2016) analyzed biostratigraphic and detrital zircon data to determine an Early Albian age, and to distinguish the Chinkeh from underlying Triassic sandstones. Hayes and Stewart (2017) characterized the Chinkeh in the Liard Basin in adjacent Northwest Territories.

The Chinkeh lies on the pre-Cretaceous unconformity, which cuts strata ranging from Mississippian carbonates in the east to Triassic siltstones over most of the basin (Cross-section Ch1-Ch1', Liard1-Liard1'; Core photos Legacy Maxhamish b-19-J/94-O-11, Appendix 4)). Chinkeh sandstones are transgressed more or less conformably by marine shales of the Garbutt Formation.

Chinkeh deposition was confined to the Liard Basin, and so is found only west of the Bovie Fault Zone (Map Ch1, Cross-section Ch1-Ch1'). On the isopach map, we have posted Triassic outcrop for reference on the western flank of the basin, as the Chinkeh has not been systematically broken out on regional surface geology maps. Selected outcrop locations logged by Leckie *et al*. (1991) lie adjacent to Triassic outcrop areas.

Where well control is abundant in the Maxhamish Field, the Chinkeh is generally 20-30m thick and correlations are straightforward (Cross-section Ch2-Ch2'). Westward, correlations are less certain, and the Chinkeh appears to be absent in some areas. There may be some fine-grained equivalents not distinguishable on older log suites, which might be picked up with detailed drill cuttings analysis. Leckie *et al*. (1991) mapped the Chinkeh continuously throughout the basin, while Frank (2002) interpreted the eastern (Maxhamish) Chinkeh to be younger than the outcrop Chinkeh. McMechan *et al*. (2016) recognized the physical separation of Chinkeh sands on the eastern and western flanks of the basin, but judged them to be equivalent.

Chinkeh sandstones lie at depths ranging from <800 metres at the eastern edge of the Liard Basin to more than 2200 metres near the basin centre (Map Ch2). Very scant well control west of Maxhamish area makes burial depth uncertain over most of the basin, although important control points have been added as shale gas wells (targeting the Besa River) drilled after 2011 came off confidential status.

Reservoir Analysis

Chinkeh deposition took place in shoreface to channelized settings, described by Leckie et al. (1991) and Frank (2002) (Fig. Ch1). The best reservoir quality is in clean basal Chinkeh sandstones that are the primary completion interval in the Maxhamish Field, interpreted as shoreface deposits running north-south through the centre of 94-O-11 and 94-O-14 (Frank, 2002) (Fig. Ch1, Cross-section Ch2-Ch2'). Core and outcrop logs by Leckie *et al*. (1991) show more diverse depositional environments, including a variety of breccias and conglomerates in channelized settings, and generally poorer-quality sands (Fig. Ch2). Chinkeh core analysis data show two populations:

- Tight samples with porosities up to 15% but permeabilities below 0.1mD, and;
- Higher-quality samples, primarily from the clean basal sandstones, featuring porosities of 15-21% and permeabilities up to 10mD (Fig. Ch3).

We examined and photographed Chinkeh cores from six locations (Appendix 4):

- ECA Maxhamish d-48-B/94-O-11;
- Legacy Maxhamish b-19-J/94-O-11;
- AEC Maxhamish b-49-J/94-O-11;
- AEC Maxhamish c-95-J/94-O-11;
- GSENR Maxhamish a-64-B/94-O-14;
- AEC Maxhamish c-16-G/94-O-14.

Clean, fine-grained basal Chinkeh sandstones are prominent in all these cores.

Petrographically, Chinkeh sandstones were described by Leckie *et al*. (1991) as: "fine- to medium-grained, well-sorted, slightly glauconitic, matrix-poor, moderately porous sublitharenite to quartzarenite. The majority of the sandstone is mineralogically very mature and texturally mature". Quartz overgrowths are the dominant cement, particularly in the most quartzose sandstones (Leckie *et al.*, 1991). Pyrobitumen, calcite, and clays are volumetrically less important.

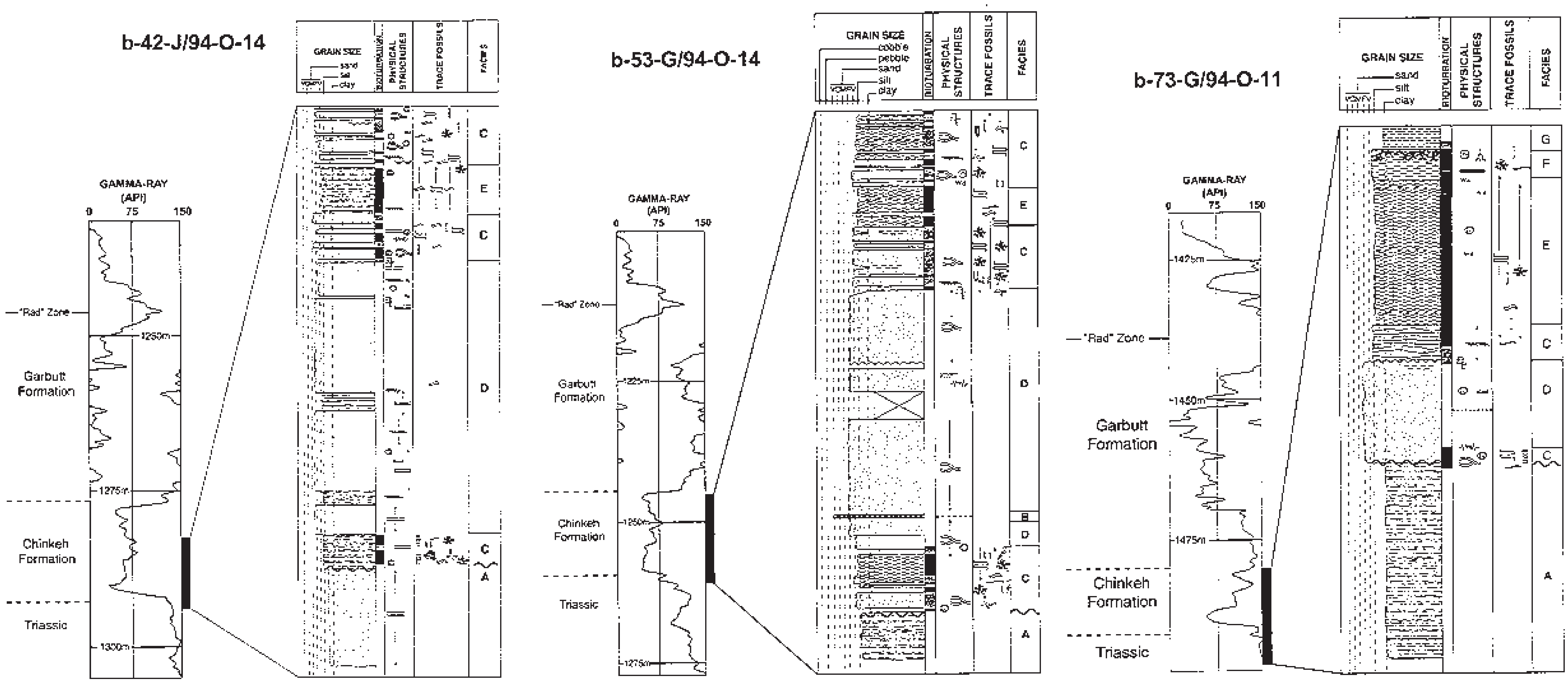

Figure Ch1. Core logs of typical Chinkeh sections in the Maxhamish Field area (from Frank, 2002).

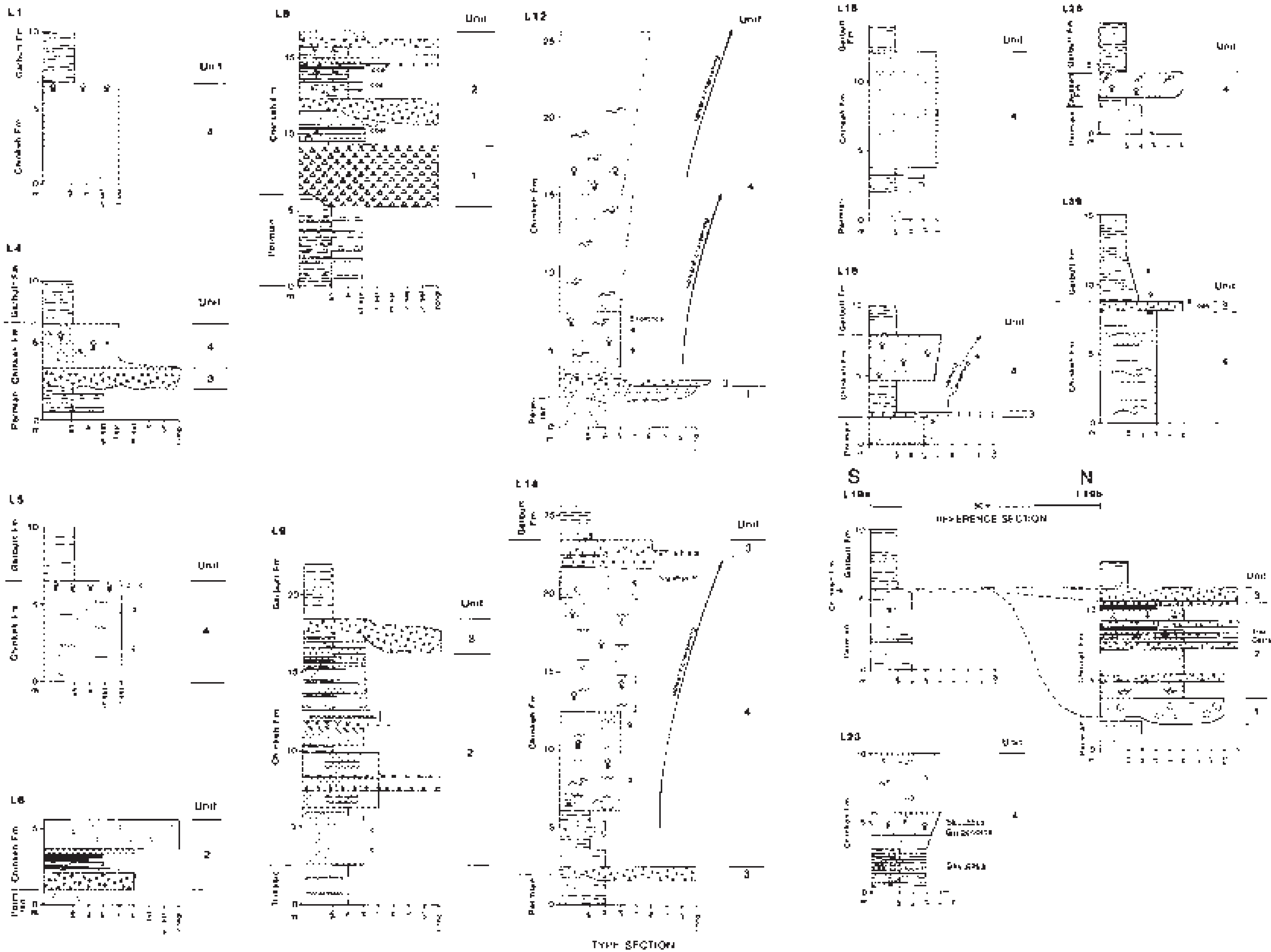

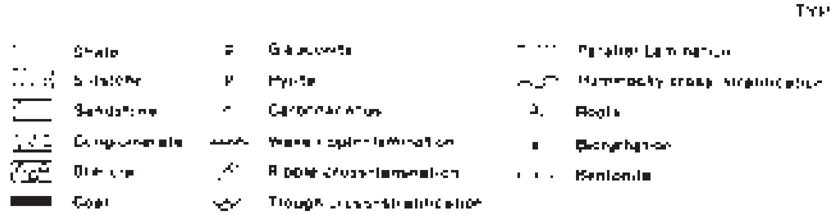

L1 N67260 E4485;
L4 N67337 E4463;
L5 N67211 E4043;
L6 N67336 E3994;
L8 N671715 E4394;
L9 N64825 E4460;
L12 N67177 E4316;
L14 N67395 E4106;
L16 N67348 E4375;
L18 N67348 E4458;
L19 N67423 E4287;
L23 N67338 E4078;
L26 N66895 E4965;
L33 N67256 E4494;
L37 N64899 E4429;
L39 N65931 E3944.

Figure Ch2. Graphic logs from outcrop sections of the Chinkeh Formation (from Leckie et al., 1991).

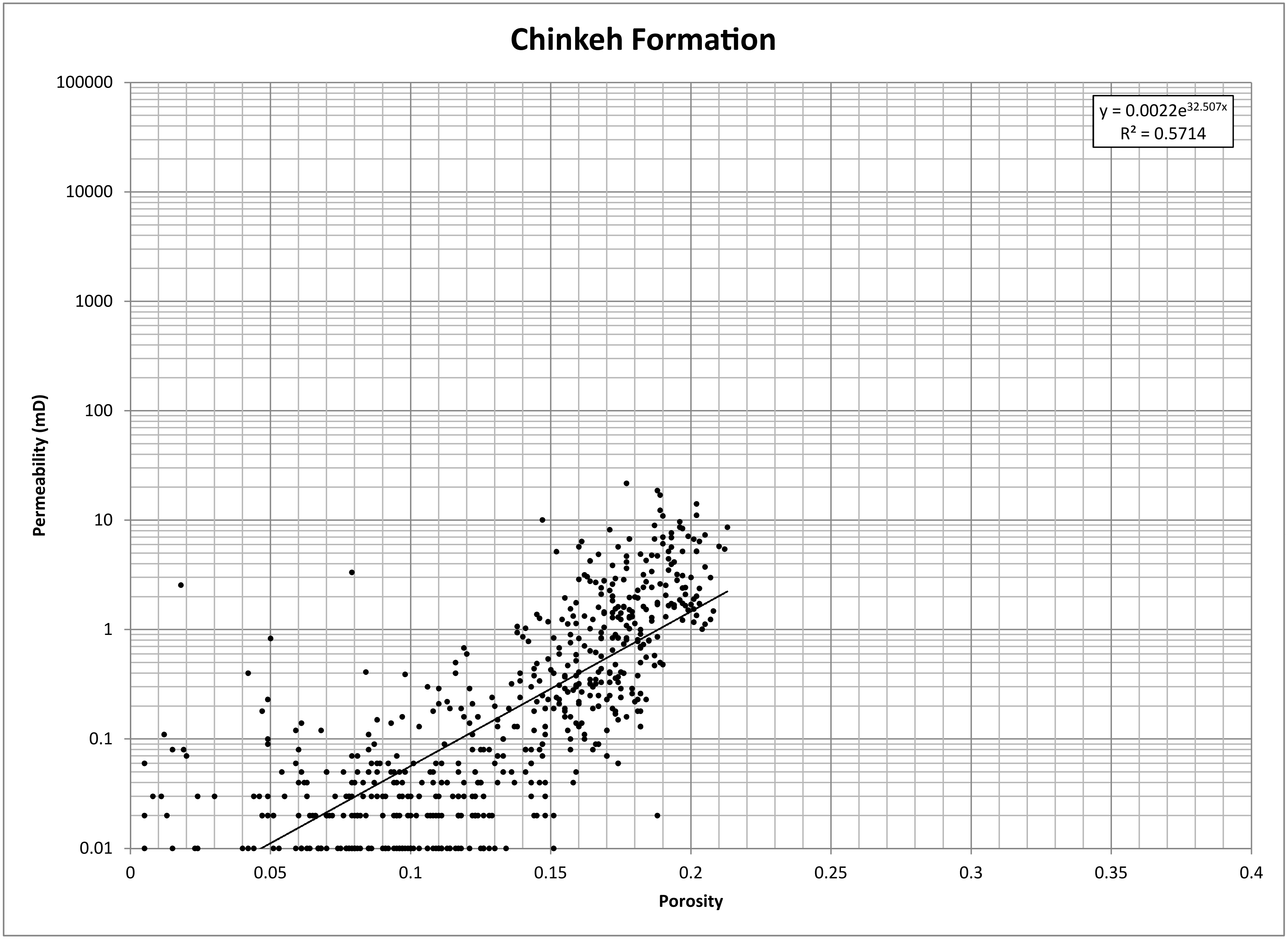

Figure Ch3. Porosity / permeability cross-plot, Chinkeh Formation.

Production and Test Data

The Chinkeh produces gas from the Maxhamish Lake Chinkeh A Pool (Map Ch1), featuring 129 gas wells, many now shut in. Very little water has been co-produced, suggesting water of condensation only. A preliminary Pressure-Elevation plot was not useful in delineating a regional aquifer, as there are no water tests, and we conclude that there is no evidence for a regional Chinkeh aquifer. As well, reservoir pressures are significantly lower than would be expected for a conventional reservoir in contact with an aquifer. These observations suggest that the Chinkeh is in a Deep Basin (hydrocarbon-saturated) regime.

Nine wells (two verticals, three deviated, and four horizontals) produce oil from the Chinkeh on the western (downdip) flank of Maxhamish (Map Ch3). Four more wells are used for pressure observation. The regulator has approved a concurrent production scheme from both the oil and gas areas.

Production Analysis

Oil production began in 2003, and as of November 2017 the nine oil wells have produced about $58.5e^3m^3$ (368 MBO). Water production continues to be very low, and there does not appear to be water drive or aquifer support.

BCOGC (2016) assigned $888e^3m^3$ (5.6 MMBO) oil in place and a recovery factor of 10% to the concurrent production area, which they measured as 325 ha. Looking at the present distribution of oil wells, we estimated a 1250 ha productive area with oil in place of about $4.7e^6m^3$ (30 MMBO), using parameters similar to BCOGC (2016) but with a thicker net pay (3.1m vs OGC 2.1m). Production to date is thus only 1.2% of the oil in place. The oil gravity is 42 API (814 kg/m^3), and at reservoir conditions, industry correlations give a B_o of 1.25 and a saturation pressure (bubble point) of 1200 to 1500 psia. Original reservoir pressure is 9197 kPa (1334 psia), indicating that the gas and oil areas were likely originally in pressure and phase equilibrium.

We performed decline analysis on all nine oil wells, and on some gas wells adjacent to the oil leg. Production is extremely flat, and it was difficult in some cases to get the decline analysis routine to converge to an answer. The four horizontal wells averaged initial production of $9.2m^3$/day (58 BOPD) and estimated ultimate recovery of $30.5e^3m^3$ (192 MBO) (Fig. Ch4). Two vertical wells averaged IP $9.2m^3$/day (47 BOPD) and EUR $21.9e^3m^3$ (138 MBO) (Fig. Ch5). Three deviated, almost-vertical wells performed poorly, with average IP $2.7m^3$/day (17 BOPD) and EUR $3.3e^3m^3$ (21 MBO). One additional vertical well is listed as producing, but has never produced. Total EUR for the nine wells is $175e^3m^3$ (1.1 MMBO), or 4% of volumetric OOIP, indicating potential for infill drilling. Current production from all wells together is $17.5m^3$/day (110 MBO). The horizontals average $3.2m^3$/day (20 BOPD), the verticals $1.8m^3$/day (11 BOPD), and deviated, $0.5m^3$/day (3 BOPD).

Representative Horizontal Oil Well

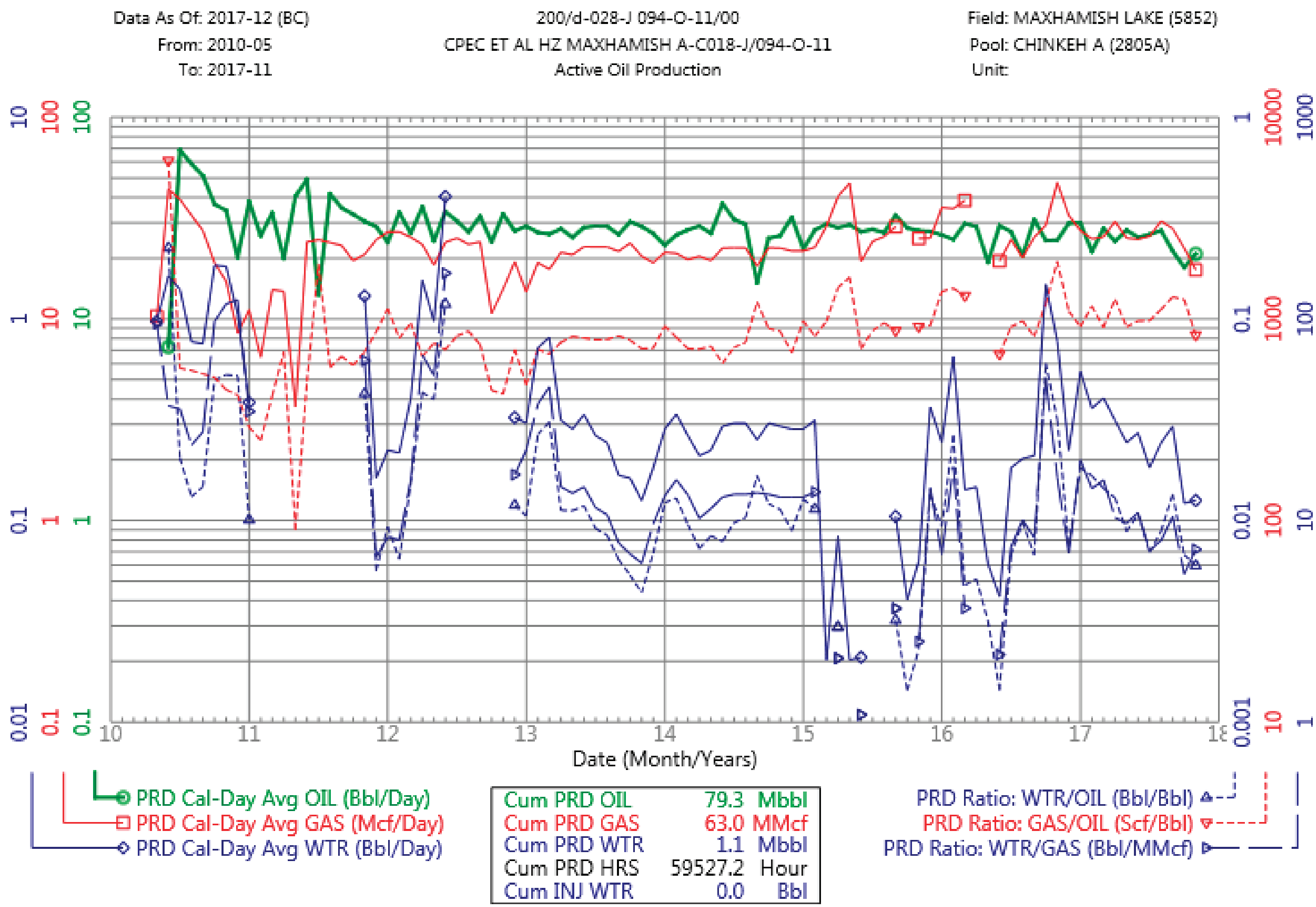

Figure Ch4. Production plot, representative horizontal Chinkeh oil well.

Representative Vertical Oil Well

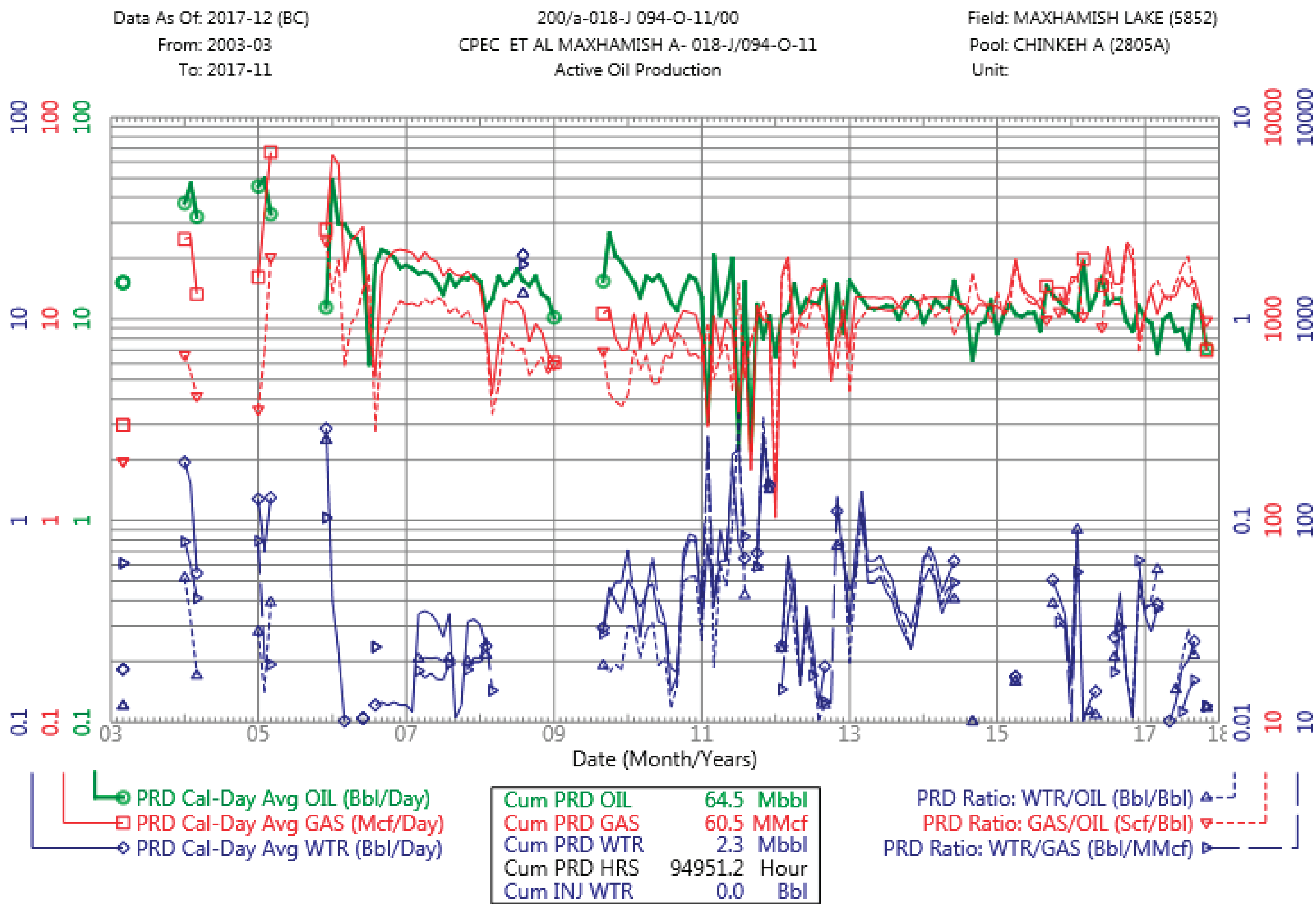

Figure Ch5. Production plot, representative vertical Chinkeh oil well.

Gas wells offsetting the oil area generally produce at low rates (below 2.8e^{3}m^3/d (100 MCF/D)), and have become erratic due to lifting water of condensation (Fig. Ch6). Thus, gas production is almost at an end, while oil production continues to be robust. Gas-oil ratio was initially 500 scf/bbl, and has increased only modestly over 10-15 years of production, currently averaging 1700 scf/bbl. Flat declines and large estimated ultimate recovery oil volumes indicate significant pressure support. Modest increases in GOR also indicate pressure support from somewhere, but the lack of rapidly rising GOR indicates minimal support from the gas cap. The lack of significant water production in either the gas or oil areas suggests that there is not an active aquifer.

A large amount of pressure data is available from the gas wells, two of the vertical oil wells have pressure data, and four observation wells to the north, northwest, west, and south of the oil area also provided data (Map Ch3; Fig. Ch7). Oil pressures are not declining as rapidly as pressures in the gas area, particularly in the vicinity of the northern-most vertical oil well, b-49-J/94-O-11. In addition, observation wells to the west and northwest are maintaining pressures significantly above pressure in either the oil or gas areas. Observation wells on the north and south ends of the oil area, and the vertical oil well at the south end, a-18-J/94-O-11, are declining more quickly than the b-49-J oil well and westerly observation wells, but not as quickly as most of the adjacent gas wells.

We conclude that there is a source of pressure to the west of the oil wells, and that pressure communication with the updip gas area is weak.

DST Analysis

Thirteen DSTs conducted in the Chinkeh Formation were reviewed, most within or flanking the Maxhamish Lake Chinkeh 'A' Pool. There are additional tests in field wells not used in our mapping, but these were judged not to offer significant additional information. Of the thirteen tests, six have useable pressures and can be plotted on a Pressure-Elevation plot. Pressure gradients for valid tests range from 5.69 to 8.23 kPa/m (0.251 to 0.364 psi/ft). Most tests show relatively low (0.1-2 mD) to very low/virtually no (<0.01 mD) qualitative permeability, and only two tests (both in B/94-O-14) are rated relatively high (10-20 mD) and high (20-50 mD). All of the tests recovered mud or gas, and no tests reported any water recovery.

Analytical Data

New analytical work was undertaken on samples from the six cores examined for this study (Appendix 3).

At a-64-B/94-O-14, the Chinkeh contains >60% quartz with some dolomite, feldspar and clay minerals (Fig. Ch8). At d-48-B/94-O-11, the mineralogical profile shows that quartz content increases to >80% at the base, and clay mineral content decreases concurrently (Fig. Ch9). At b 19-J/94-O-11 (d-99-G/94-O-11), quartz content increases

Representative Adjacent Gas Well

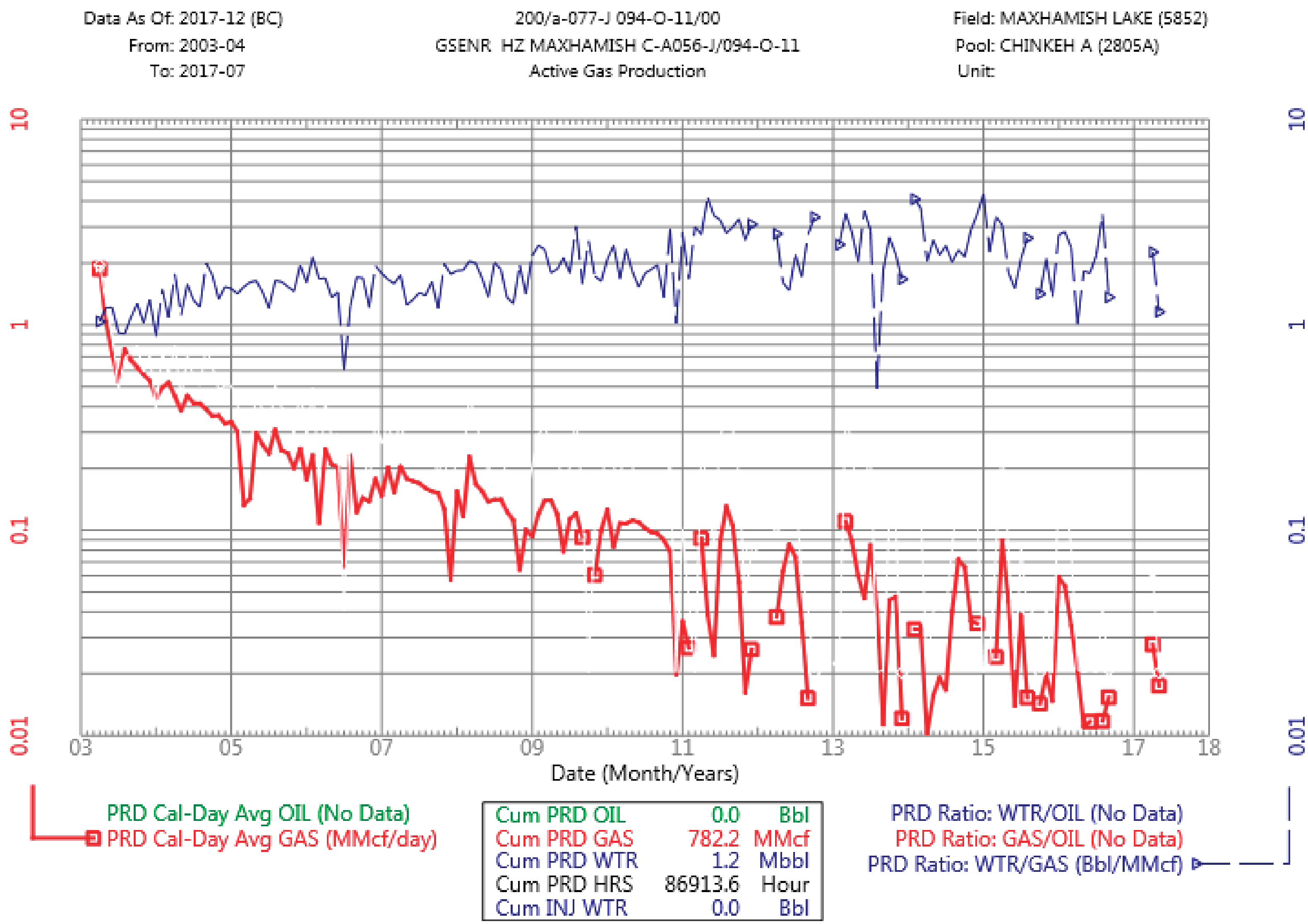

Figure Ch6. Production plot, representative vertical Chinkeh gas well.

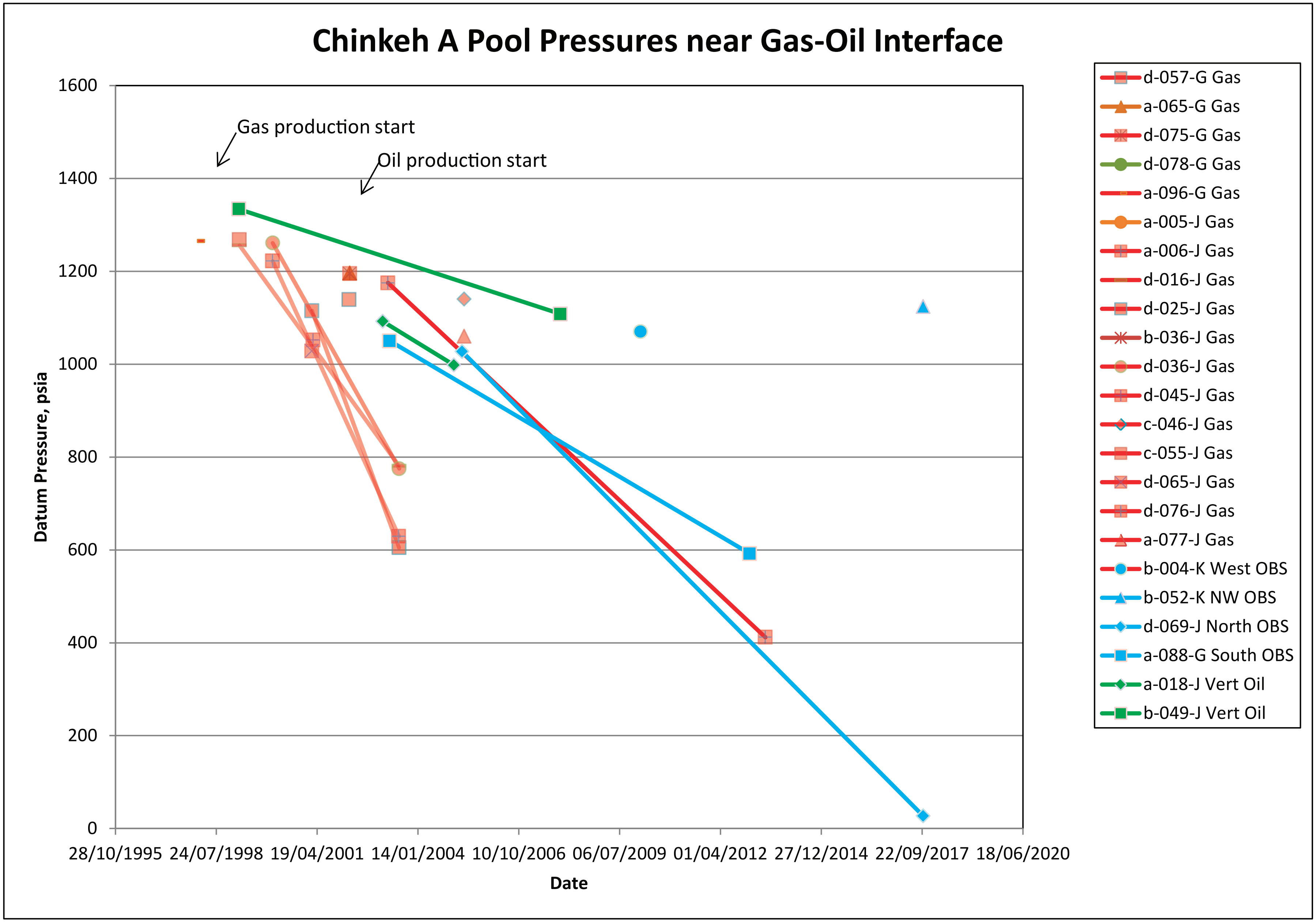

Figure Ch7. Chinkeh pressure versus time plots for oil, gas and observation wells near the gas-oil interface in the Maxhamish Chinkeh 'A' Pool.

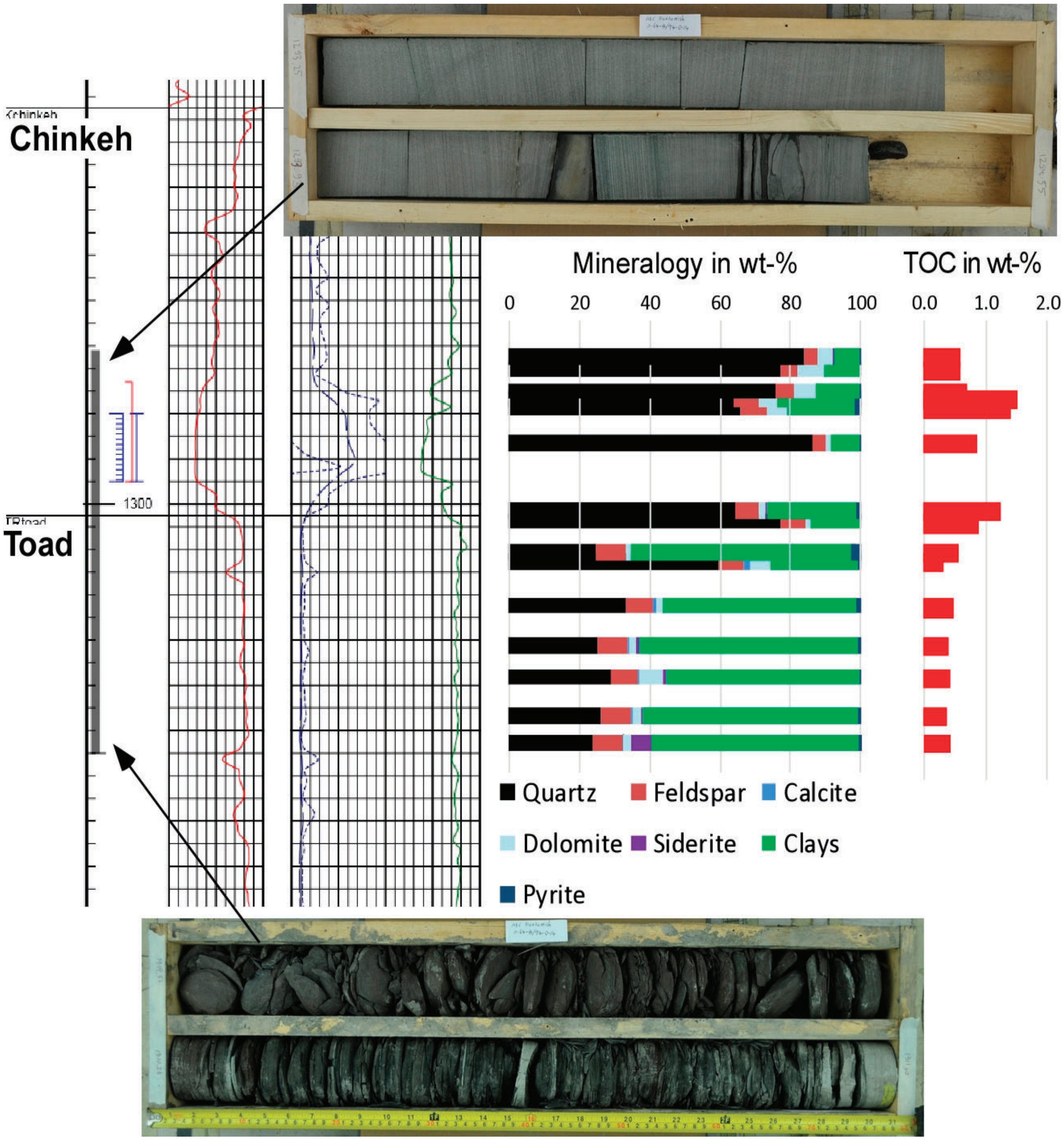

Figure Ch8. Mineralogy and TOC plots for samples from the Chinkeh and Toad formations, GSENR Maxhamish a-64-B/94-O-14.

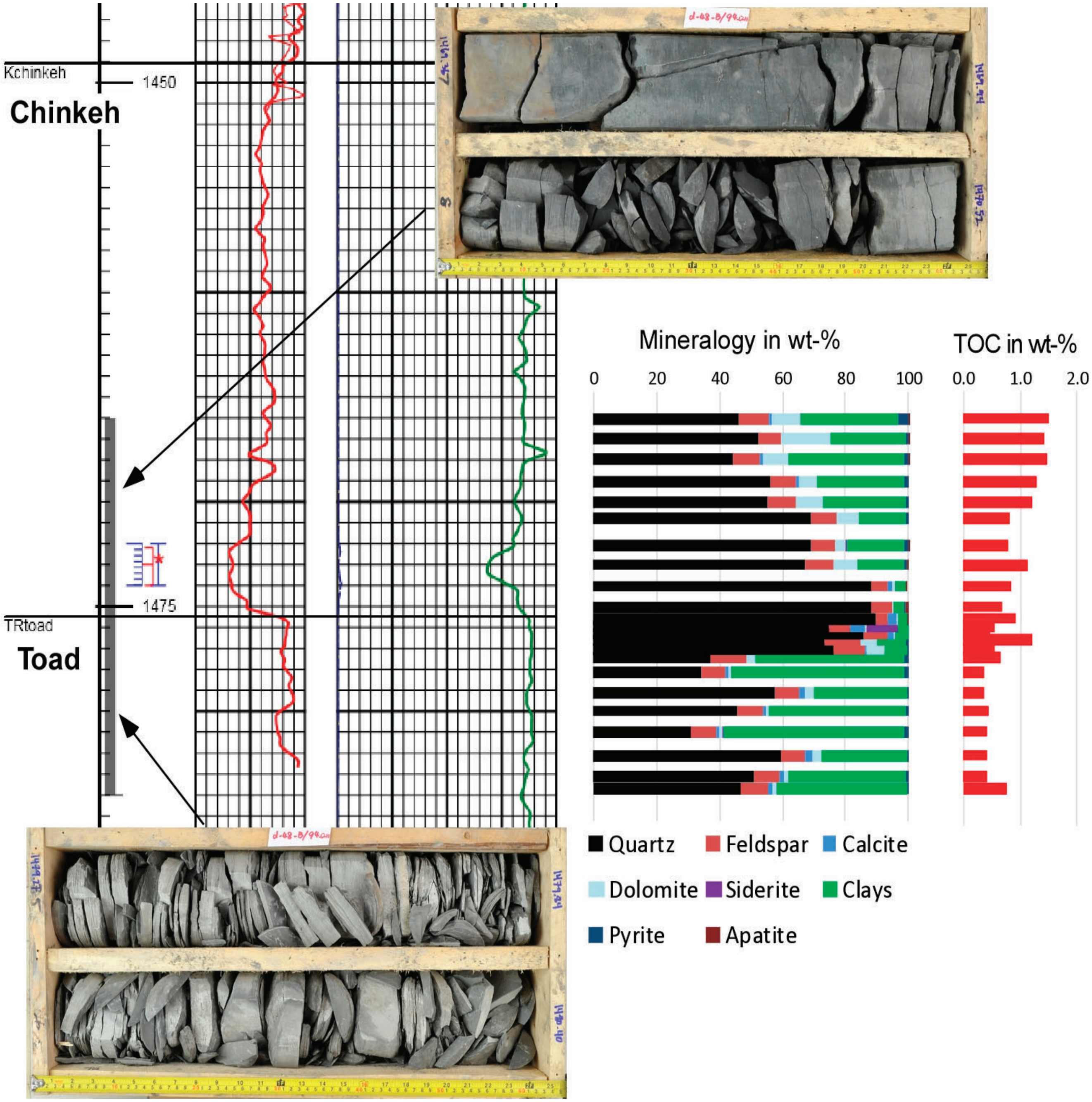

Figure Ch9. Mineralogy and TOC plots for samples from the Chinkeh and Toad formations, ECA Maxhamish d-48-B/94-O-11.

towards the base; sandstones in the basal porous Chinkeh unit have >85% quartz, with a few highly carbonate-cemented streaks (Fig. Ch10).

In these three wells, Chinkeh sandstones exhibit relatively low TOC values, ranging generally between 0.5-1.5 wt%. T_{max} values range from 435-459°C, much in the oil-generating window.

Thin section and SEM petrography show the Chinkeh to contain both mudstones and very fine-grained sandstones (Fig. Ch11-16). Quartz grains range in size up to ~140 µm; various shapes and roundnesses indicate both detrital and diagenetic origins, and some quartz grains have diagenetic overgrowth rims. Clay minerals are abundant and occur dispersed between other mineral matter and organics. Dolomite, (as cements or detrital grains), feldspars, and glauconite (up to 5%) are present. Opaque minerals include pyrite and organics.

Unconfined porosities measured from Chinkeh core samples range from 2.9% to 23%, and matrix permeabilities range from 3 to 850 nD (Table Ch1). Mercury injection capillary pressure (MICP) conformance-corrected porosity of the same samples shows slightly lower values between 1.5-13.4% (Table Ch2).

Unconfined Porosity and Matrix Permeability

Well Name	Well Location	Core Depth (m)	Fm	Density		Porosity (%)	GRI Matrix Permeability (md)		GRI Matrix Permeability (nd)	
				Bulk Density (g/cc)	Skeletal Density (g/cc)		Avg	Std Dev	Avg	Std Dev
AEC Maxhamish	200/c-016-G 094-O-14/00	1252.91	Upper Chinkeh	2.547	2.689	5.25				
AEC Maxhamish	200/c-016-G 094-O-14/00	1254.14	Upper Chinkeh	2.538	2.687	5.54				
AEC Maxhamish	200/c-016-G 094-O-14/00	1255.16	Upper Chinkeh	2.582	2.699	4.33				
AEC Maxhamish	200/c-016-G 094-O-14/00	1255.36	Upper Chinkeh	2.570	2.688	4.37	3.62E-05	3.67E-06	36.23	3.67
AEC Maxhamish	200/c-016-G 094-O-14/00	1257.41	Top Porosity Chinkeh	2.338	2.705	13.55	1.91E-05	1.29E-05	19.12	12.94
AEC Maxhamish	200/c-016-G 094-O-14/00	1257.70	Top Porosity Chinkeh	2.258	2.705	16.54				
AEC Maxhamish	200/c-016-G 094-O-14/00	1258.38	Top Porosity Chinkeh	2.242	2.683	16.45				
AEC Maxhamish	200/c-016-G 094-O-14/00	1260.74	Top Porosity Chinkeh	2.178	2.681	18.76				
AEC Maxhamish	200/c-016-G 094-O-14/00	1262.22	Top Porosity Chinkeh	2.121	2.681	20.87				
AEC Maxhamish	200/c-016-G 094-O-14/00	1263.50	Top Porosity Chinkeh	2.429	2.731	11.05				
GSENR Maxhamish	200/a-064-B 094-O-14/00	1293.57	Top Porosity Chinkeh	2.257	2.685	15.92				
GSENR Maxhamish	200/a-064-B 094-O-14/00	1295.04	Top Porosity Chinkeh	2.512	2.700	6.93	7.17E-06	1.17E-06	7.17	1.17
GSENR Maxhamish	200/a-064-B 094-O-14/00	1295.39	Top Porosity Chinkeh	2.648	2.719	2.58	3.19E-06	5.59E-07	3.19	0.56
GSENR Maxhamish	200/a-064-B 094-O-14/00	1297.42	Top Porosity Chinkeh	2.477	2.716	8.79	2.82E-05	1.64E-06	28.20	1.64
GSENR Maxhamish	200/a-064-B 094-O-14/00	1300.91	Top Porosity Chinkeh	2.566	2.642	2.87	1.12E-06	2.35E-07	1.12	0.24
ECA Maxhamish	200/d-048-B 094-O-11/00	1466.95	Upper Chinkeh	2.558	2.696	5.12	1.39E-04	1.06E-04	139.42	105.54
ECA Maxhamish	200/d-048-B 094-O-11/00	1467.85	Upper Chinkeh	2.551	2.697	5.40	3.96E-05	6.25E-06	39.63	6.25
AEC Maxhamish	200/c-095-J 094-O-11/00	1503.76	Upper Chinkeh	2.536	2.680	5.38	2.76E-05	1.70E-05	27.63	16.97
AEC Maxhamish	200/c-095-J 094-O-11/00	1505.43	Upper Chinkeh	2.532	2.682	5.59	4.39E-05	5.48E-06	43.90	5.48
AEC Maxhamish	200/c-095-J 094-O-11/00	1506.78	Upper Chinkeh	2.560	2.688	4.77	8.51E-05	6.62E-05	85.10	66.24
AEC Maxhamish	200/c-095-J 094-O-11/00	1508.15	Upper Chinkeh	2.566	2.706	5.17	3.42E-05	1.31E-05	34.24	13.10
AEC Maxhamish	200/c-095-J 094-O-11/00	1509.57	Upper Chinkeh	2.544	2.700	5.76	5.31E-05	1.66E-05	53.09	16.62
AEC Maxhamish	200/c-095-J 094-O-11/00	1511.32	Top Porosity Chinkeh	2.287	2.722	15.99	6.20E-04	3.12E-04	619.89	311.90
AEC Maxhamish	200/c-095-J 094-O-11/00	1513.52	Top Porosity Chinkeh	2.102	2.689	21.82	8.47E-04	6.64E-04	847.39	663.77
AEC Maxhamish	200/c-095-J 094-O-11/00	1514.75	Top Porosity Chinkeh	2.078	2.688	22.70	2.75E-04	1.18E-04	275.08	118.07
AEC Maxhamish	200/b-049-J 094-O-11/00	1616.79	Upper Chinkeh	2.554	2.697	5.31	3.36E-05	7.40E-06	33.62	7.40
Legacy Maxhamish	200/b-019-J 094-O-11/00	1616.79	Top Porosity Chinkeh	2.561	2.711	5.51	3.17E-05	1.60E-05	31.69	16.03
Legacy Maxhamish	200/b-019-J 094-O-11/00	1627.74	Top Porosity Chinkeh	2.583	2.686	3.87	1.51E-05	3.54E-06	15.06	3.54
Legacy Maxhamish	200/b-019-J 094-O-11/00	1628.56	Top Porosity Chinkeh	2.578	2.686	4.03	1.90E-05	1.84E-06	18.99	1.84
Legacy Maxhamish	200/b-019-J 094-O-11/00	1631.60	Top Porosity Chinkeh	2.222	2.695	17.55	6.36E-04	2.56E-04	636.46	256.29

Table Ch1. Chinkeh Formation – unconfined porosity and GRI matrix permeability measurements from core samples in various wells.

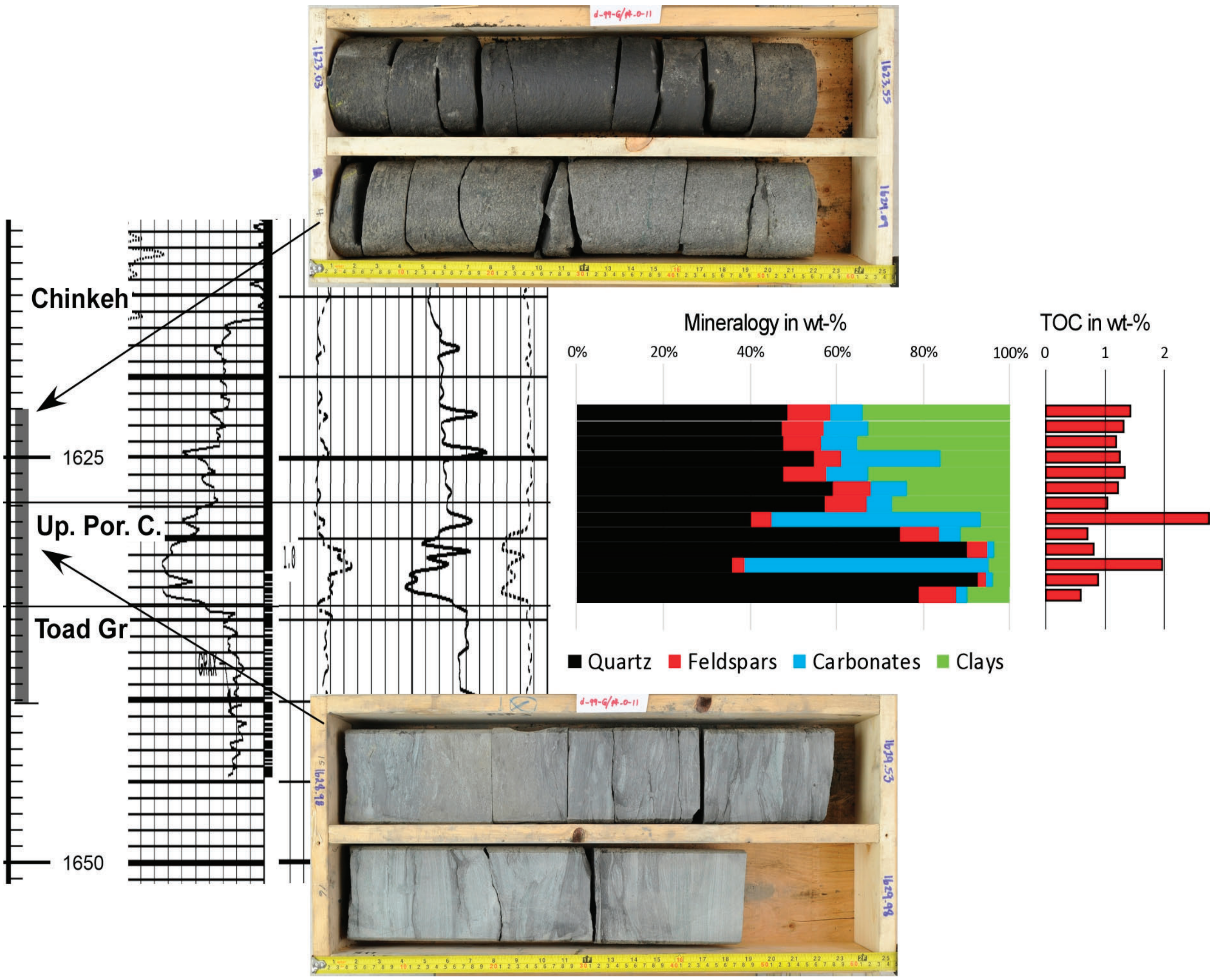

Figure Ch10. Mineralogy and TOC plots for samples from the Chinkeh Formations, Legacy Maxhamish b 19 J/94 O 11.

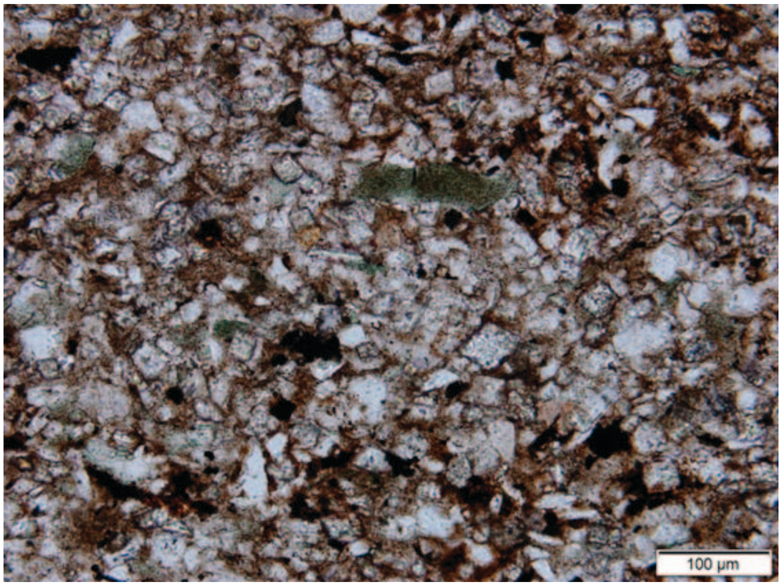

Figure Ch11. Photomicrograph, Chinkeh Formation, AEC Maxhamish c-95-J/94-O-11 (1504.60-1504.68 m) under plane polarized light. Argillaceous dolomitic siltstone with angular to subrounded quartz grains; glauconite grains (green) are deformed and/or disaggregated pellets or clasts with a sugary texture; silt-size crystals of dolomite (grey).

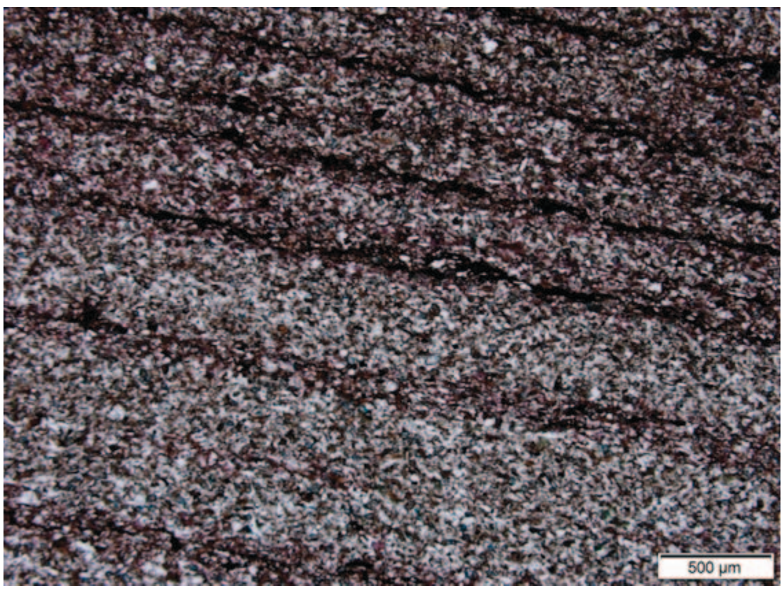

Figure Ch12. Photomicrograph, Chinkeh Formation, AEC Maxhamish c-95-J/94-O-11 (1510.25-1510.35 m) under plane polarized light. Finely laminated argillaceous siltstone consisting primarily of silt-size quartz with local porosity development (pink). Clay material is finely distributed throughout, and laminations are defined by layers with elevated organic matter (opaque).

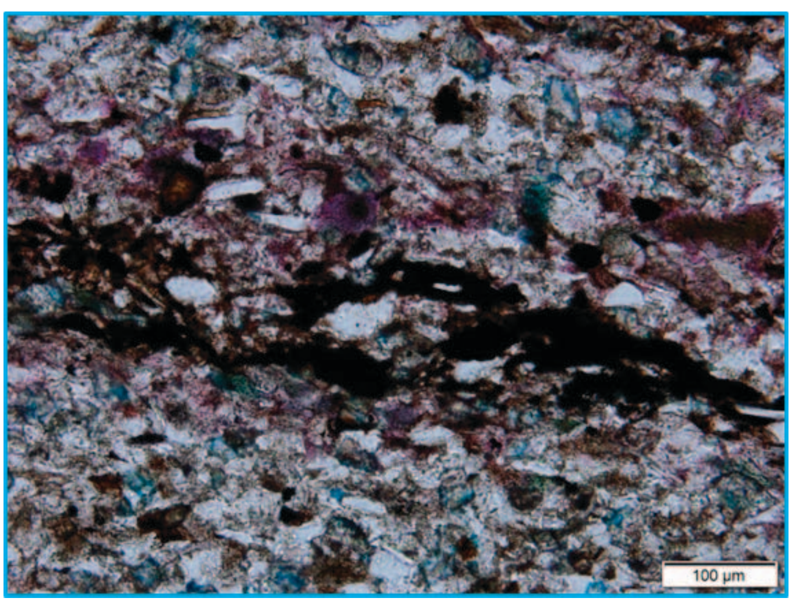

Figure Ch13. Photomicrograph, Chinkeh Formation, AEC Maxhamish c-95-J/94-O-11 (1510.25-1510.35 m) under plane polarized light. Quartz and dolomite dominate sand-rich laminae. Quartz grains are angular to subangular quartz; irregular shapes suggest authigenic (i.e. diagenetic) origin. Ferroan dolomite is stained blue. Green glauconite (green) grains are deformed or disaggregated pellets or clasts with a sugary texture. The image shows the contact of two sandy laminae divided by an organic-rich thin lamina.

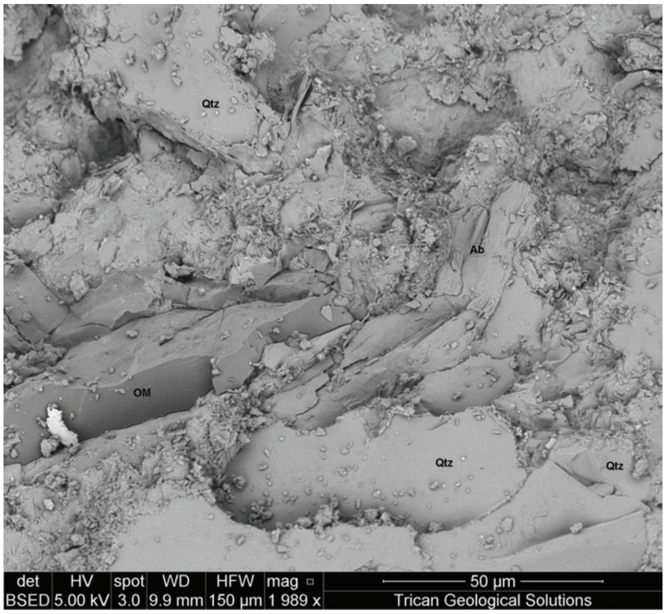

Figure Ch14. BSED SEM photomicrograph, Chinkeh Formation, AEC Maxhamish c-95-J/94-O-11 (1510.25-1510.35 m), showing angular quartz and smooth surfaces, some of which indicates diagenetic growth. Minor amounts of albite and solid organic matter (<1%) are present.

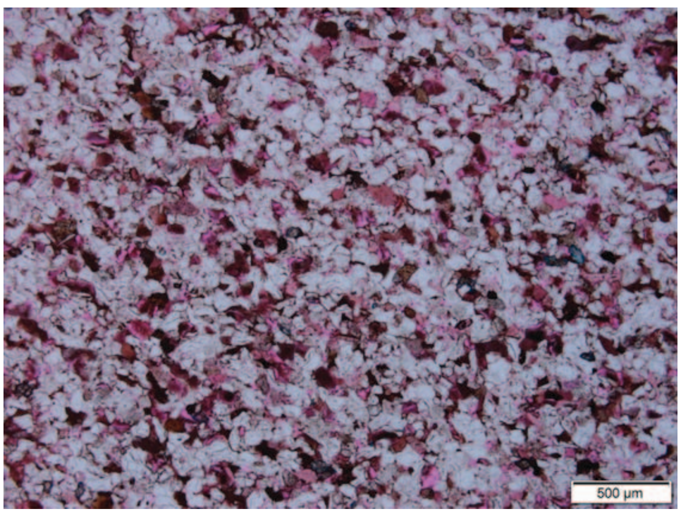

Figure Ch15. Photomicrograph, Chinkeh Formation, AEC Maxhamish c-16-G/94-O-14 (1260.37-1260.41m) under plane polarized light. Very fine- to fine-grained (up to 140 µm), quartzose sandstone; light-coloured minerals are predominantly quartz, with minor chert and rare feldspar. Disaggregated and degraded glauconite pellets/clasts (greenish) occur throughout, and dolomite cement is patchy. Pink epoxy highlights pervasive pore network.

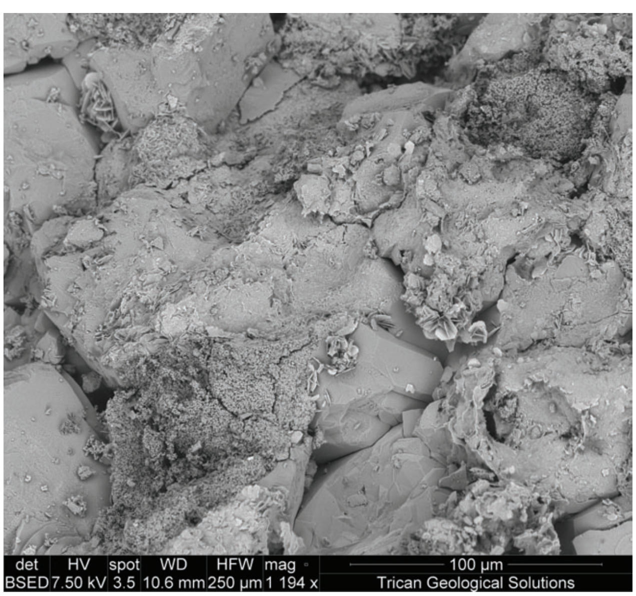

Figure Ch16. BSED SEM photomicrograph, Chinkeh Formation, AEC Maxhamish c-16-G/94-O-14 (1260.37-1260.41 m), featuring both detrital (rounded edges) and neomorph (diagenetic with euhedral shapes) quartz. Open pore space is also present. Euhedral pseudohexagonal Fe-phyllosilicate (glauconite) sheets form clusters perpendicular to grain surfaces within pore spaces. Intergranular porosity is estimated at up to 3% volume.

MICP Porosity										
Well Name	Well Location	Core Depth (m)	Fm	Density g/cc: Bulk Density (g/cc)	Density g/cc: Skeletal Density (g/cc)	Porosity (%)	Corrected Porosity (%)	Peak Range: Peak Range	Peak Range: Modal Peak	Stem Volume Used (%)
AEC Maxhamish	200/c-016-G 094-O-14/00	1252.91	Upper Chinkeh	2.548	2.657	4.30	4.09	8 - 470	32	53
AEC Maxhamish	200/c-016-G 094-O-14/00	1254.14	Upper Chinkeh	2.542	2.662	4.74	4.49	6 - 1130	27	61
AEC Maxhamish	200/c-016-G 094-O-14/00	1255.16	Upper Chinkeh	2.572	2.658	3.60	3.26	7 - 220	23	43
AEC Maxhamish	200/c-016-G 094-O-14/00	1263.50	Top Porosity Chinkeh	2.425	2.648	8.70	8.41	15 - 430	174	98
GSENR Maxhamish	200/a-064-B 094-O-14/00	1293.57	Top Porosity Chinkeh	2.258	2.542	11.16	10.75	58 - 2460	58, 711	94
GSENR Maxhamish	200/a-064-B 094-O-14/00	1295.04	Top Porosity Chinkeh	2.482	2.657	6.57	6.25	6 - 890	29	51
GSENR Maxhamish	200/a-064-B 094-O-14/00	1295.39	Top Porosity Chinkeh	2.557	2.666	4.10	3.31	<3 - 370	14	44
GSENR Maxhamish	200/a-064-B 094-O-14/00	1300.91	Top Porosity Chinkeh	2.5089	2.659	5.63	5.26	6 - 250	35	48
ECA Maxhamish	200/d-048-B 094-O-11/00	1466.95	Upper Chinkeh	2.563	2.659	3.62	3.03	4 - 120	10	36
ECA Maxhamish	200/d-048-B 094-O-11/00	1467.85	Upper Chinkeh	2.562	2.664	3.81	3.46	<3 - 190	6	36
AEC Maxhamish	200/c-095-J 094-O-11/00	1503.76	Upper Chinkeh	2.556	2.626	3.23	2.68	4 - 70	8	41
AEC Maxhamish	200/c-095-J 094-O-11/00	1505.43	Upper Chinkeh	2.530	2.632	4.54	3.87	5 - 240	11	53
AEC Maxhamish	200/c-095-J 094-O-11/00	1506.78	Upper Chinkeh	2.566	2.636	2.95	2.66	4 - 110	4	41
AEC Maxhamish	200/c-095-J 094-O-11/00	1508.15	Upper Chinkeh	2.566	2.641	3.28	2.87	4 - 130	11	36
AEC Maxhamish	200/c-095-J 094-O-11/00	1511.32	Top Porosity Chinkeh	2.271	2.623	14.05	13.44	9 - 3220	2218	61
AEC Maxhamish	200/c-095-J 094-O-11/00	1513.52	Top Porosity Chinkeh	2.107	2.395	13.26	12.04	8 - 5170	2870	49
AEC Maxhamish	200/b-049-J 094-O-11/00	1616.79	Upper Chinkeh	2.550	2.622	2.74	2.38	<3 - 210	5	31
Legacy Maxhamish	200/b-019-J 094-O-11/00	1623.61	Upper Chinkeh	2.572	2.658	3.25	2.51	<3 - 70	5	34
Legacy Maxhamish	200/b-019-J 094-O-11/00	1627.74	Top Porosity Chinkeh	2.595	2.640	1.71	1.53	<3 - 490	4	21
Legacy Maxhamish	200/b-019-J 094-O-11/00	1634.10	Top Porosity Chinkeh	2.598	2.691	3.47	3.25	6 - 870	18, 96	42

Table Ch2. Chinkeh Formation – MICP porosity and conformance-corrected porosity measurements from core samples in various wells.

Hydrocarbon analysis (S1) data show significant hydrocarbons to be present, commonly containing C_{10}-C_{35} chains with calculated API gravities of 33-41° and calculated specific gravities between 0.82-0.86 (Table Ch3). Heavy condensates dominate the residual compositions with biomarkers, aromatics and light condensates (Fig. Ch17), demonstrating that liquid hydrocarbons are present within the Chinkeh Formation.

Hydrocarbon Composition by Thermal Desorption Gas Chromotography																	
Well Name	Well Location	Core Depth (m)	Fm	% Light Condensate	% Heavy Condensate	% Naphthenes	% Aromatics	% Biomarkers	Peak	Initial Boiling Point (°C)	Carbon Number	Final Boiling Point (°C)	Carbon Number	Calculated Specific Gravity	Calculated API gravity	Chromatogram Quality
GSENR Maxhamish	200/a-064-B 094-O-14/00	1293.57	Top Porosity Chinkeh	1.78	82.18	0.43	0.39	15.22	C20	61	<C6	434	C28	0.85	34.64	okay
GSENR Maxhamish	200/a-064-B 094-O-14/00	1295.04	Top Porosity Chinkeh	6.41	81.13	0.47	0.79	11.21	C15	61	<C6	482	C34	0.85	35.43	good
ECA Maxhamish	200/d-048-B 094-O-11/00	1466.95	Upper Chinkeh	13.69	63.55	3.02	5.51	14.23	C16	75	C6	393	C24	0.83	39.68	good
ECA Maxhamish	200/d-048-B 094-O-11/00	1467.85	Upper Chinkeh	11.97	67.89	1.80	4.30	14.04	C16	116	C8	385	C23	0.83	38.87	good
AEC Maxhamish	200/c-095-J 094-O-11/00	1505.59	Upper Chinkeh	14.26	62.89	3.71	6.50	12.64	C16	49	<C6	440	C29	0.83	37.98	poor
AEC Maxhamish	200/c-095-J 094-O-11/00	1510.83	Top Porosity Chinkeh	17.19	41.51	11.86	23.27	6.16	C15	48	<C6	423	C27	0.82	41.41	good
AEC Maxhamish	200/c-095-J 094-O-11/00	1514.17	Top Porosity Chinkeh	0.04	90.27	0.22	0.06	9.42	C22	56	<C6	473	C33	0.86	32.58	poor
AEC Maxhamish	200/b-049-J 094-O-11/00	1616.79	Upper Chinkeh	7.79	72.81	1.04	2.03	16.33	C16	82	C6	474	C33	0.84	37.71	excellent

Table Ch3. Chinkeh Formation – hydrocarbon composition data.

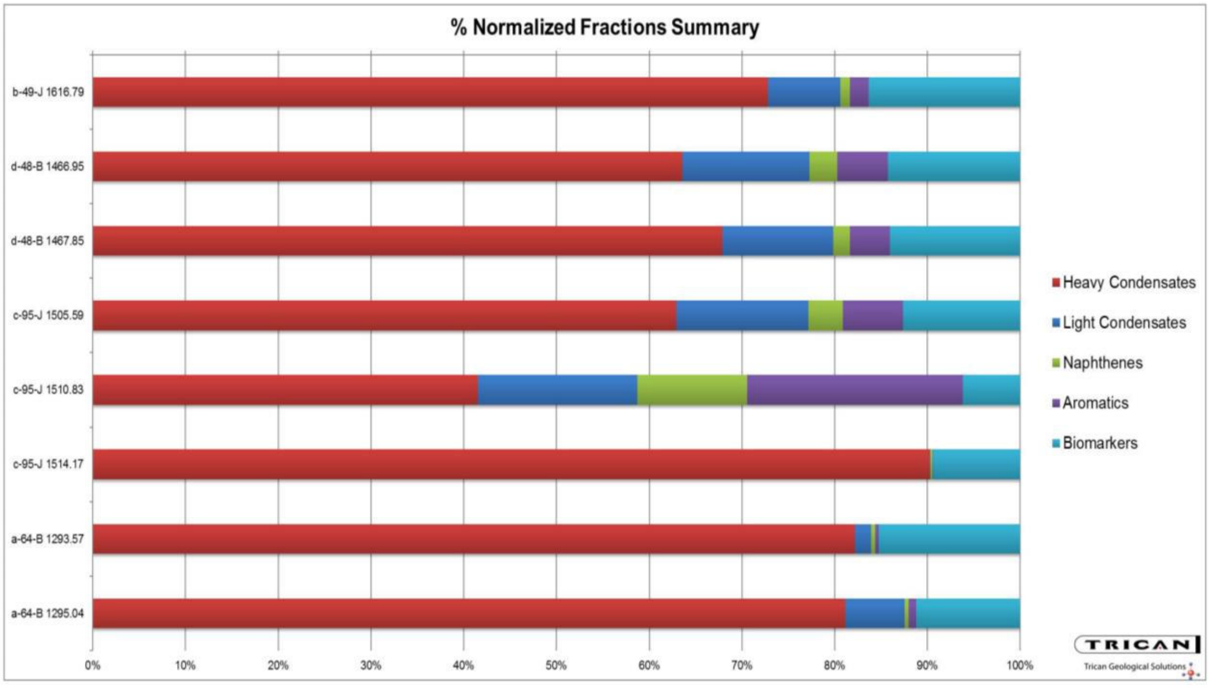

Figure Ch17. Normalized fraction plot of hydrocarbon groups identified in Chinkeh core samples.

Rock mechanics data show a bimodal distribution, with samples falling into a "low Young's Modulus" group (ranging from 20-30 GPa) and a "high Young's Modulus" group (~30-45 GPa) (Table Ch4; Fig. Ch18). A distinguishing factor between the groups appears to be mineralogy; the low YM group exhibits significantly higher amounts of quartz (~80% from offset samples) while the high YM group exhibits more albite and illite/mica. Mineralogical analysis of the post-failure core samples would greatly increase the understanding of how composition affects mechanical properties.

Triaxial Data											
Well Name	Well Location	Core Depth (m)	Fm	Confining Pressure (MPa)	Axial Strain at Failure (%)	Compressive Strength (MPa)	Residual Strength (MPa)	Static Young's Modulus (GPa)	Static Poisson's Ratio	Static Bulk Modulus (GPa)	Static Shear Modulus (GPa)
AEC Maxhamish	200/c-016-G 094-O-14/00	1254.76	Upper Chinkeh	16.0	1.206	224.00	97.31	22.94	0.160	11.23	9.89
AEC Maxhamish	200/c-016-G 094-O-14/00	1259.69	Top Porosity Chinkeh	16.0	0.920	154.63	106.09	20.00	0.192	10.83	8.39
ECA Maxhamish	200/d-048-B 094-O-11/00	1467.21	Upper Chinkeh	19.0	0.708	179.68	110.49	28.45	0.153	13.68	12.33
ECA Maxhamish	200/d-048-B 094-O-11/00	1473.50	Top Porosity Chinkeh	19.0	1.022	274.93	19.00	31.64	0.166	15.77	13.57
AEC Maxhamish	200/c-095-J 094-O-11/00	1507.28	Upper Chinkeh	20.0	0.752	308.79	172.80	44.49	0.163	21.99	19.13
AEC Maxhamish	200/c-095-J 094-O-11/00	1514.82	Top Porosity Chinkeh	20.0	0.998	179.73	94.59	22.06	0.174	11.28	9.39
Legacy Maxhamish	200/b-019-J 094-O-11/00	1624.26	Upper Chinkeh	21.0	0.697	191.54	153.81	27.22	0.171	13.77	11.62
Legacy Maxhamish	200/b-019-J 094-O-11/00	1632.26	Top Porosity Chinkeh	21.0	1.058	226.97	103.91	25.44	0.238	16.18	10.27
AEC Maxhamish	200/b-049-J 094-O-11/00	1617.09	Upper Chinkeh	21.0	0.609	206.06	144.92	33.10	0.172	16.83	14.12

Table Ch4. Chinkeh Formation - Rock mechanical analyses showing confining pressure, compressive strength, Young's Modulus, Poisson's Ratio and bulk and shear modulii.

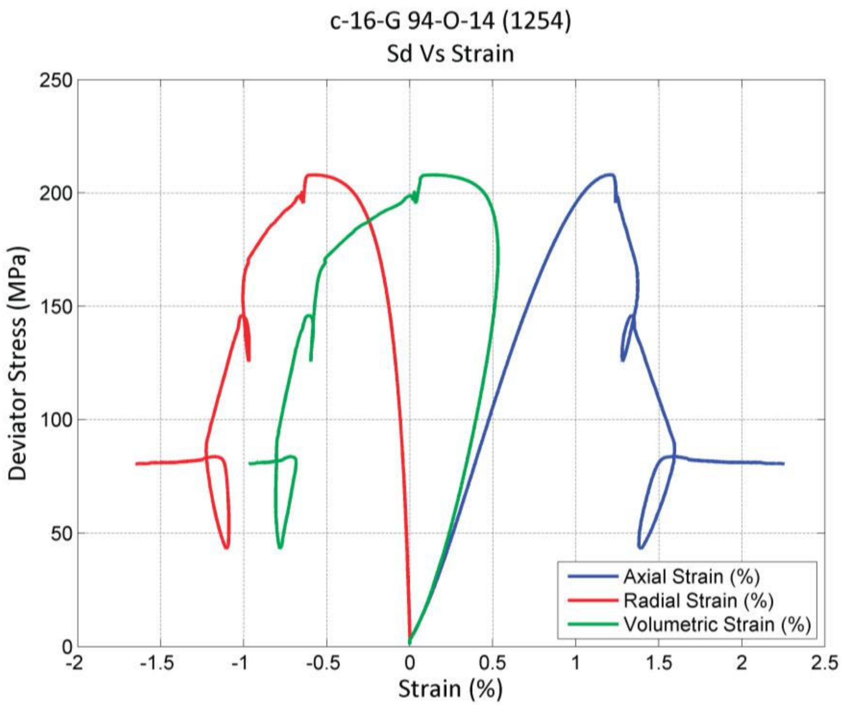

Figure Ch18. Mechanical stress-strain relationship graph, Chinkeh Formation, c-16-G/94-O-14.

Resource Oil Assessment

Chinkeh sandstones are found in a hydrocarbon-saturated (Deep Basin) setting on the eastern flank of the Liard Basin. A large gas pool at Maxhamish is largely depleted, but nine oil wells on the western (downdip) flank exhibit variable productive behaviour, and do not appear to have been drawn down by the updip gas production. Only a small percentage of the oil in place has been produced, suggesting good infill potential. Geological mapping suggests reservoir sandstones should extend westward and southward from the existing production, so there could conceptually be a large oil leg present. Reservoir pressures are in accordance with this idea, suggesting pressure support from downdip hydrocarbons, but no associated aquifer.

Jiang *et al*. (2015) projected 400-500 million barrels of light oil in place in the Chinkeh, likely sourced from the overlying Garbutt Shale. Several years ago, Strategic Oil & Gas Ltd. mapped an extensive light oil fairway with >500 MMBOIP. In March 2018, Strategic was marketing their 38.5% non-operated working interest in the Maxhamish Chinkeh ‘A’ oil pool, which they described as having “potential to further develop the oil leg of the pool with multi-frac horizontal wells”, and further upside through initiation of a waterflood.

We recommend the western flank of the Chinkeh gas and oil pools be mapped in detail to support new Chinkeh horizontal drilling in the best-quality and thickest sandstones. Drilling and completion programs should build on the existing analytical dataset to design the most effective and efficient penetration and stimulation of the reservoir.

Poorer-quality Chinkeh sandstones above the basal clean unit, and possibly underlying Toad-Grayling sandstones should be assessed for their potential contribution.

BUCKINGHORSE FORMATION (GARBUTT FORMATION)

Age and Play Type

Lower Cretaceous – Shale Oil Play
Prospectivity: 'B' Play – Potentially prospective reservoir characteristics, but has not been tested.

Regional Geology

Regional transgression from the north during Early Cretaceous time initiated clastic sedimentation across the Western Canada Sedimentary Basin after a long period of exposure during the latest Jurassic and earliest Cretaceous. In southern and central areas, continental and shallow marine coarse-grained clastics derived from rising western orogenic highlands, included in the Blairmore / Mannville / Bullhead / Spirit River / Peace River units, were deposited along the southern margin of the Boreal sea. These become increasingly marine northward, and north of about Twp 90 (southern 94A, H), the entire package grades to marine Buckinghorse shales (Fig. BU1).

Organic-rich condensed sections marking transgressive events at the top of the Bullhead, Spirit River, and Peace River units can be correlated as radioactive log markers throughout the northern part of the basin (Fig. BU2). Although organic-rich sections are widespread and readily mapped, they have received very little attention as potential shale reservoirs except in the outer Foothills west of Fort St John (see discussion under Production and Test Data), and in the Liard Basin.

Liard Basin

In the Liard Basin, Garbutt Formation shales represent the earliest stages of transgression above basal clastics of the Chinkeh Formation. Leckie and Potocki (1998) described the Garbutt in outcrop as:

> "black silty shale and mudrock … The basal contact is sharp, resting either conformably on the Chinkeh Formation or unconformably on underlying [Toad-Grayling or] Paleozoic strata … Bentonite beds, 1 to 20 cm thick, are common … The upper contact is gradational and is marked by the first occurrence of thick-bedded sandstone of the overlying Scatter Formation." (see Fig. BU3 for outcrop sections).

Garbutt core photos from wells a-26-B/94-O-11and b-53-B/94-O-14 are shown in Appendix 4.

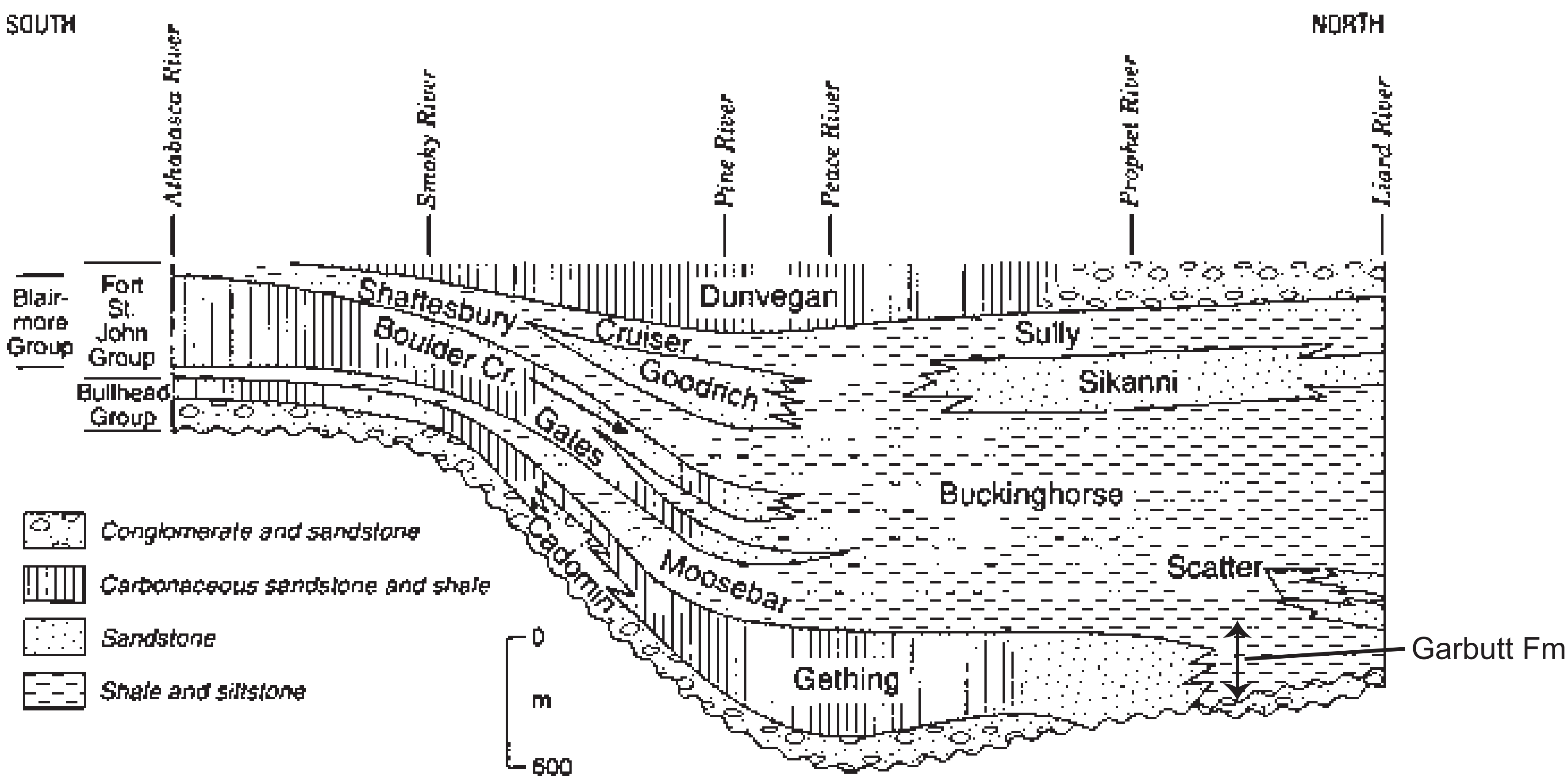

Figure BU1. Stratigraphic relationships of Buckinghorse and Garbutt shales (from Leckie and Potocki, 1998).

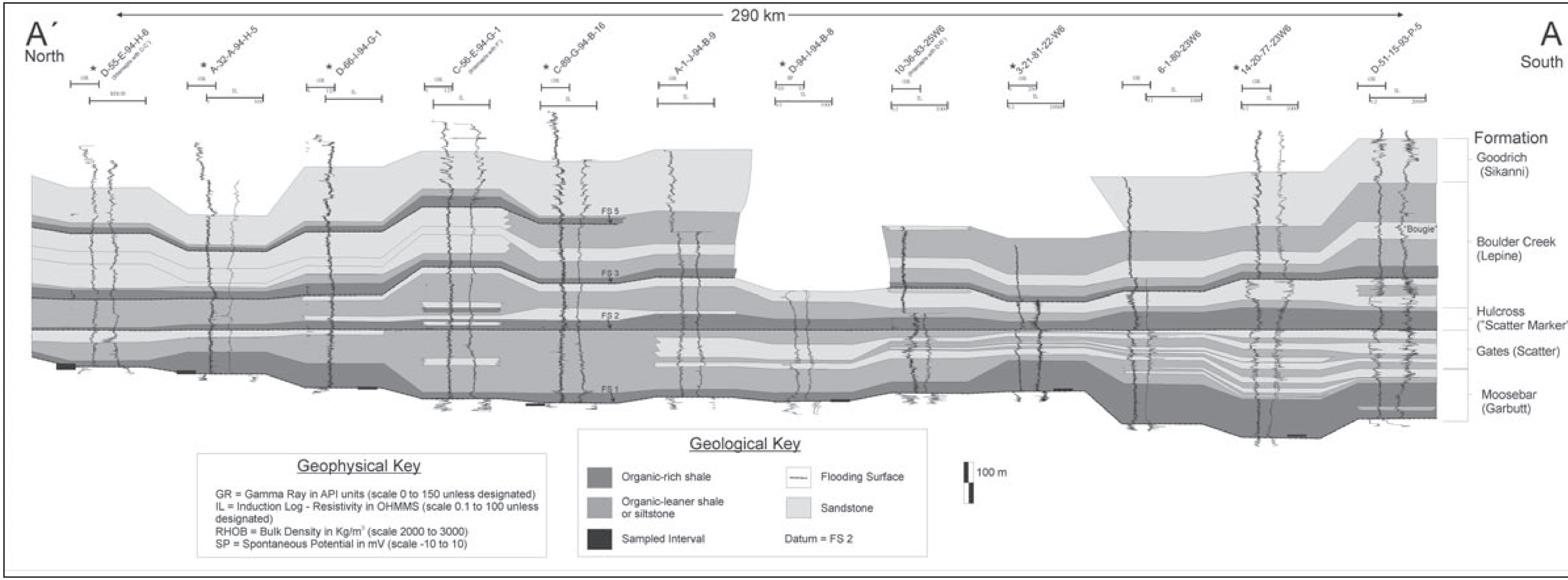

Figure BU2. South to north cross-section A-A', highlighting organic-rich shales in transgressive sections that converge northward as radioactive markers as the intervening clastic packages shale out (from Chalmers and Bustin, 2008).

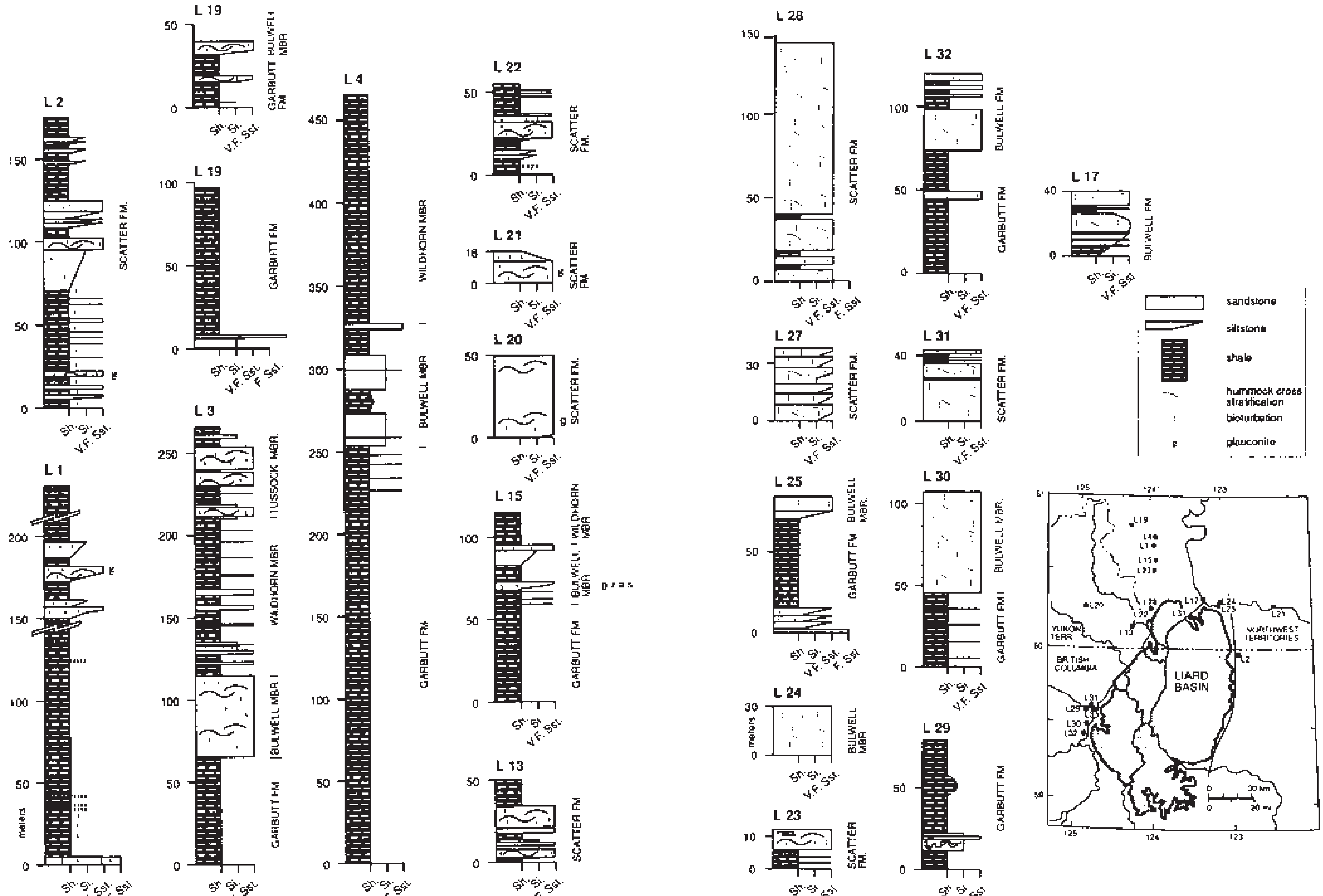

Figure BU3. Measured sections of the Garbutt and Scatter formations, Liard Basin (from Leckie and Potocki, 1998).

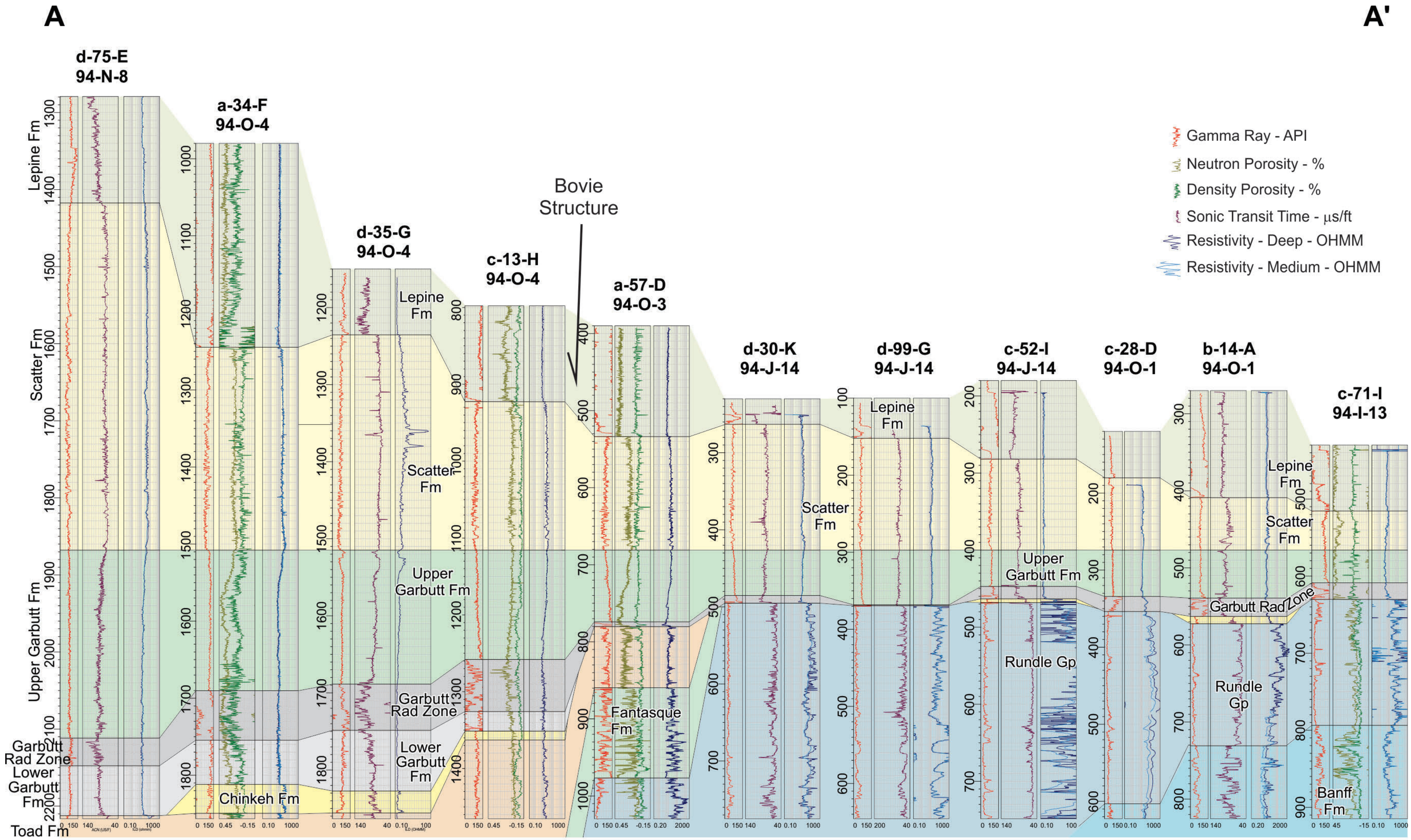

Figure BU4. West-east cross-section straddling Liard Basin and Horn River Basin to the east; note abrupt thinning of Garbutt Formation shales at the Bovie Fault Zone (from Ferri et al., 2017).

In the subsurface, Leckie and Potocki noted a lower radioactive shale interval, recognized regionally as “Radioactive Marker No. 1” on well logs. The upper third of the Garbutt consists of several coarsening- and sandier-upward cycles, each 4 to 20m thick. Ferri *et al*. (2017) recommended subdivision of the Garbutt into the lower Garbutt shale, a middle organic-rich, high gamma ray interval (Radioactive Zone, containing Radioactive Marker No. 1), and the upper Garbutt shale / siltstone / sandstone, which grades conformably into the overlying Scatter Formation (Fig. BU4). Ferri *et al*. (2017) mapped thickness of the Radioactive Zone and lower Garbutt Formation (Fig. BU5).

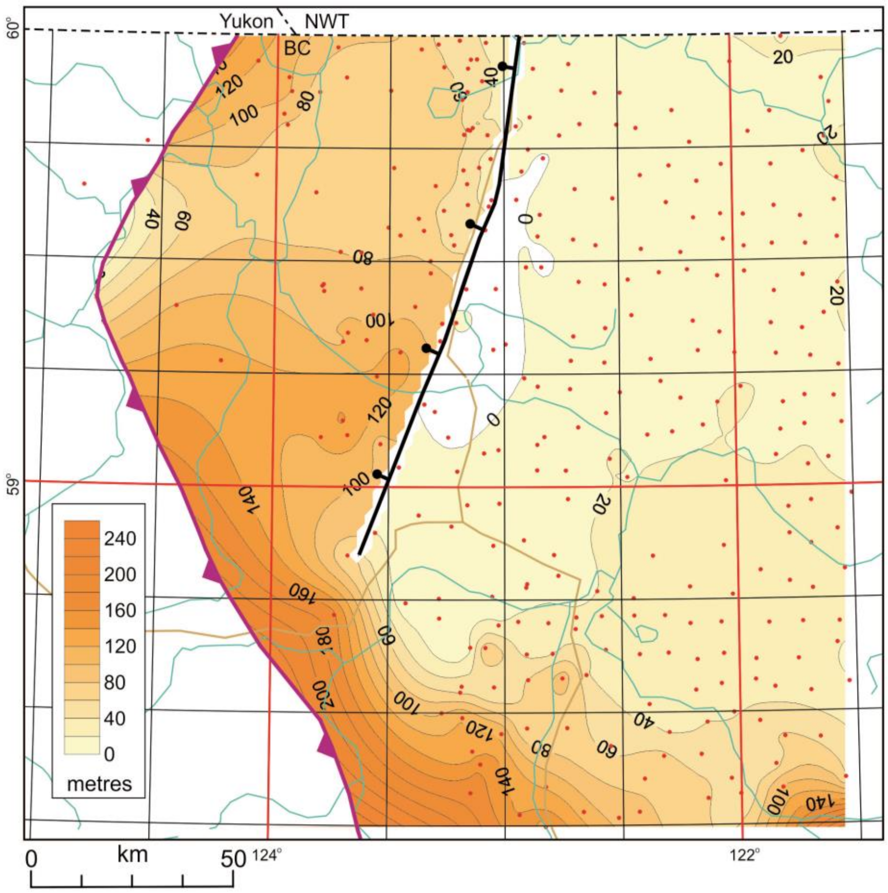

Figure BU5. Isopach map of the Radioactive Zone and lower Garbutt Formation, Liard Basin and surrounding areas (from Ferri *et al*., 2017).

Deposition took place in an offshore marine setting, predominantly below storm wave base. The radioactive shale represents a condensed section deposited at the peak of the transgression above the basal transgressive surface, and overlying highstand progradational beds were deposited in shallowing marine waters.

Radioactive Marker #1 serves as the datum for Chinkeh cross-sections Ch1-Ch1’ and Ch2-Ch2’, and illustrates the relationship of the lower Garbutt to underlying strata. Cross-sections Liard1-Liard1’ and Liard2-Liard2’ illustrate correlation of the Garbutt across the basin, and clearly show the middle radioactive interval and upper Garbutt transition to the overlying Scatter Formation. Relatively little work has been done on the Lepine Formation, which lies immmediately above the Scatter Formation (Cross-sections Liard1-Liard1’ and Liard2-Liard2’), but it is a regional marine shale similar to the Garbutt, and was sampled in core from well b-6-C/94-O-11 (Appendix 4).

Map BU1 illustrates thickness of the Garbutt Formation across the NEBC portion of the Liard Basin. It thins abruptly at the eastern margin, suggesting the Bovie Fault Zone was active at the time of Garbutt deposition (Fig. BU4); we have not mapped the Garbutt east of the Bovie FZ. Within the basin, the Garbutt thickens southwestward to more than 350m. A composite thickness of about 280m at an outcrop section measured by Ferri *et al*. (2011b) in northwestern 94-N-10 conforms to this pattern, but we did not measure thicknesses in the few wells west of the deformation front because of the potential for structural distortion.

Drill depth to the top of the Garbutt increases abruptly moving westward across the Bovie FZ, and increases westward to more than 2000m in 94-O-13 (Map BU2).

Production and Test Data

Adams *et al*. (2016) reviewed exploration / assessment activity in Cretaceous shales in the Beg-Jedney, Blair Creek, and Farrell Creek regions – all in the outer Foothills west of Fort St. John, from 94-B-8 northward to 94-G-1. Operators are focused on shale gas potential, and realize cost efficiencies in pursuing the play uphole from and in the same area as gas development in the Montney Formation.

While Cretaceous shale gas and oil potential has been studied throughout the Western Canada Sedimentary Basin, there has been very little drilling and testing, other than in established plays such as the naturally-fractured Second White Specks (Upper Cretaceous) shales in the southern and central Alberta Foothills. No horizontal drilling / multi-frac completion testing has been undertaken in the Garbutt Shale of the Liard Basin.

Analytical Data

Chalmers and Bustin (2012b) assessed light volatile liquid and gas shale reservoir potential in the Lower-Upper Cretaceous Shaftesbury Formation southeast of Fort St John (eastern 93P, 94A). They concluded that there is substantial liquid hydrocarbon in place in these shales, but in relatively shallow sections that are generally regarded as too shallow and clay-rich to offer reservoir potential. Rokosh *et al*. (2012) mapped relatively low concentrations of oil in place in the Lower Cretaceous Wilrich Member in Alberta adjacent to the B.C. Deep Basin – a southern equivalent of the lower Buckinghorse (Moosebar shale in Fig. BU1; Fig. BU6).

We sampled Garbutt core from AEC Maxhamish b-53-B/94-O-14 and the Lepine core from ECA Maxhamish b-6-C/94-O-11 (Appendix 4). Quartz and clay minerals dominate, with carbonates typically absent, although elevated siderite values are seen toward the base of the core at b-53-B (Fig. BU7, BU8). Clay minerals are typically 60-80% of the samples, including mixed-layer clays and smectites. Feldspars are generally <6% and pyrite ranges between 2-4%.

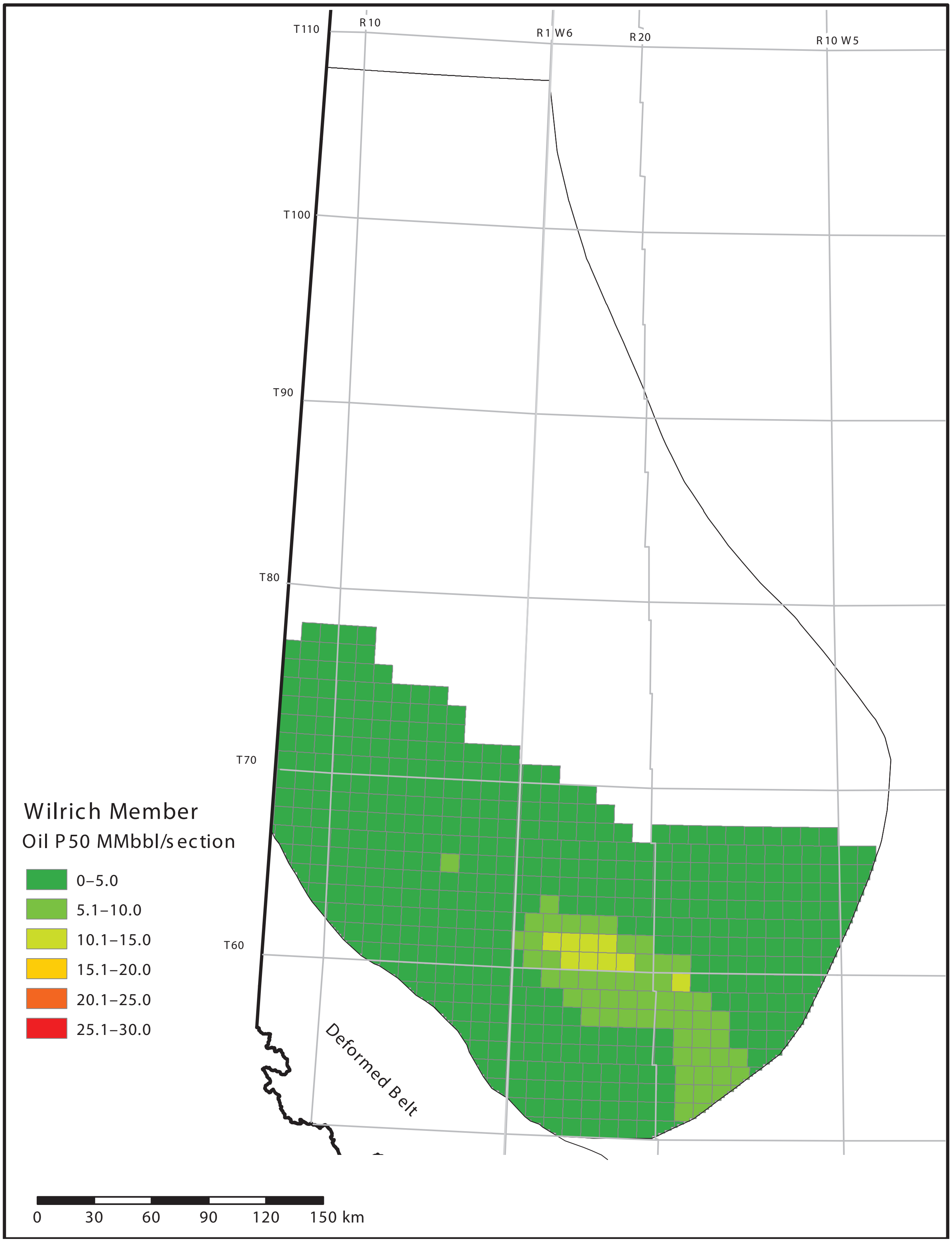

Figure BU6. P50 shale-hosted oil in place, Wilrich Member, Alberta (from Rokosh et al., 2012).

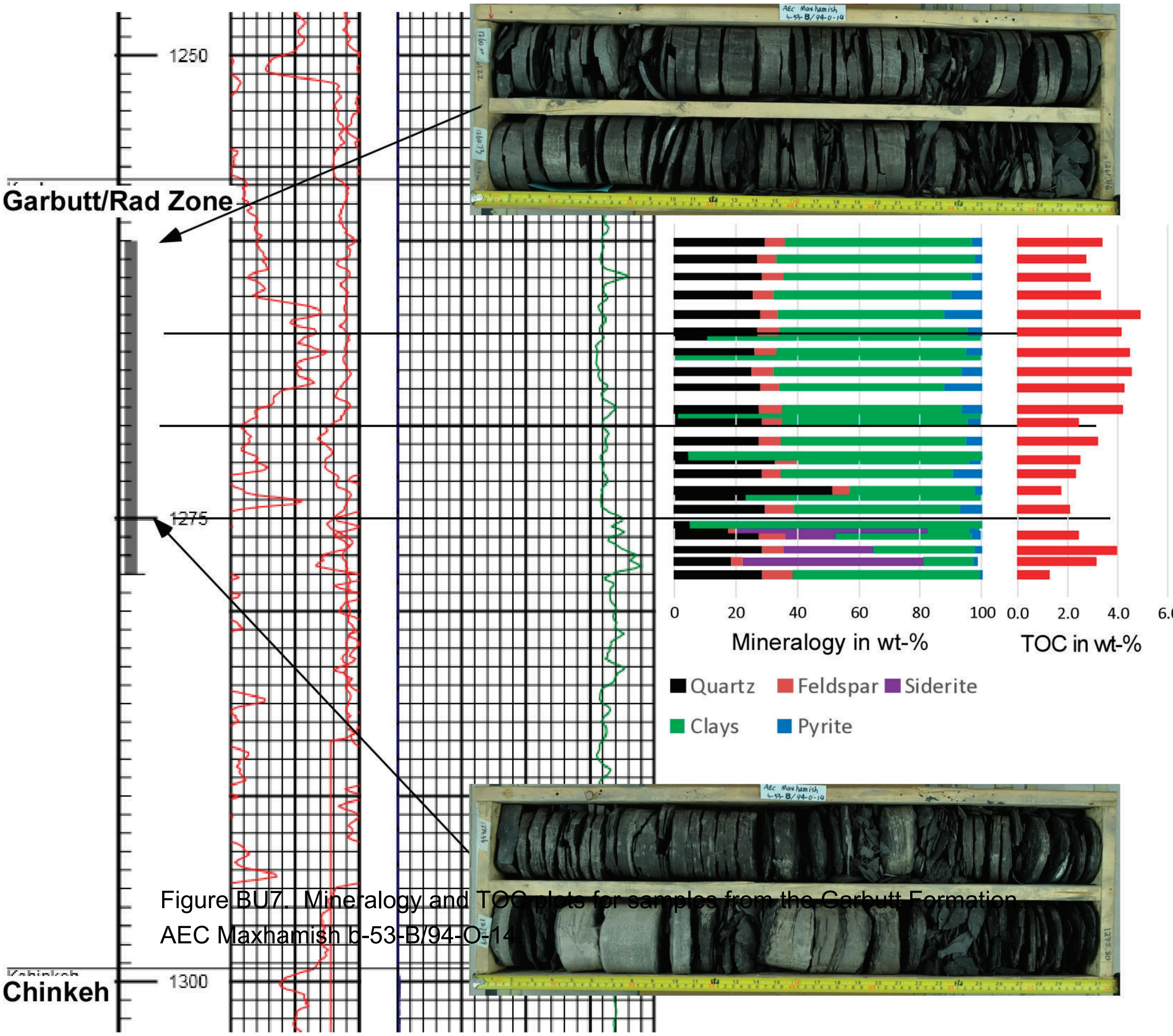

Figure BU7. Mineralogy and TOC plots for samples from the Garbutt Formation, AEC Maxhamish b-53-B/94-O-14.

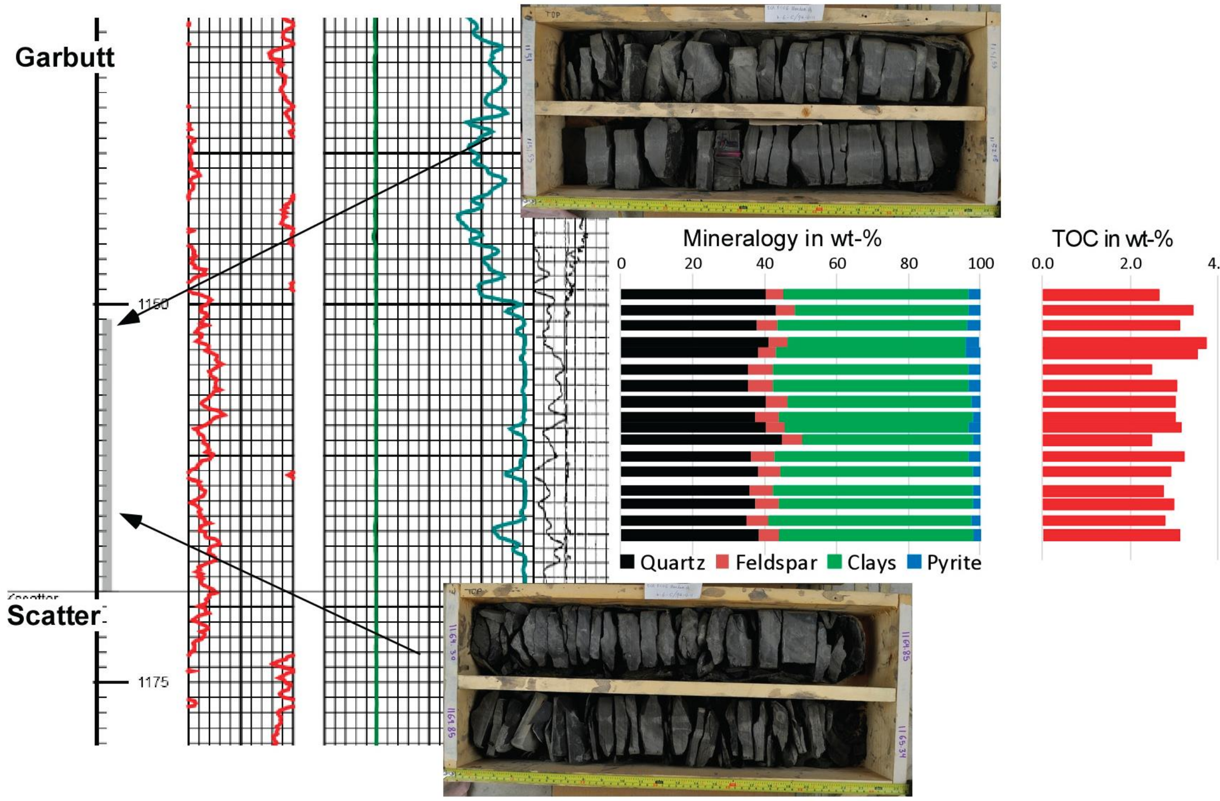

Figure BU8. Mineralogy and TOC plots for samples from the Lepine Formation, ECA Maxhamish b-6-C/94-O-11.

TOC ranges generally between 2-4 wt%, and T_{max} values range between 438-447°C, indicating maturity within the oil window (Table BU1, BU2).

Thin section and SEM petrography show finely laminated organic-rich shale with abundant small silt-size quartz and abundant opaque streaks and dispersed material (Fig. BU9, BU10). Quartz clusters are also present in lenticular shapes or wavy forms and bioturbation appears to have been subtle but common. Under SEM, most grains are fully embedded in illitic clay minerals (Fig. BU11).

Unconfined porosities range between 3.2-8.8%, and matrix permeabilities are 0.5-38 nD (Table BU3). MICP conformance-corrected porosities are slightly lower, ranging between 2.4-5.2% (Table BU4). Pore openings are narrowly confined to a range of <20 nm (Fig. BU12).

Well ID	Sample ID	Zone	Sample Type	Depth (m)	Tmax in °C	TOC %	Quartz	Feldspar		Carbonates		Clays				Sulphate	Sulphides
								Albite	Microcline	Calcite	Siderite	Illite/mica	Ill/Mont	Chlorite	Kaolinite	Barite	Pyrite
AEC Maxhamish 200/b-053-B 094-O-14/00 WA 9950 (Int: 1260-1278m)	1260	Garbutt Rad Zone	Core	1260.00	442	3.36	29.6	3.6	3			37.9		8.5	14		3.4
	1261.03	Garbutt Rad Zone	Core	1261.03	447	2.74	27	3.5	2.6			41.7		8.6	14.4		2.2
	1261.96	Garbutt Rad Zone	Core	1261.96	444	2.90	28.6	3.7	3.2			40.2		9	11.8		3.5
	1263.01	Garbutt Rad Zone	Core	1263.01	437	3.30	25.7	3.7	3.1			37.9		9	10.5		10
	1264.03	Max Rad Marker	Core	1264.03	438	4.88	28.2	3.1	2.5			36.7		7.9	9.3		12.4
	1265.02	Max Rad Marker	Core	1265.02	441	4.13	27	4.5	2.9			41.7		8.7	10.6		4.6
	1265.14-.20	Max Rad Marker	Core	1265.14			11.1						29.2		59.7		
	1265.99	Max Rad Marker	Core	1265.99	442	4.90	26.1	4.1	3			40.9		8.6	11.9		5.4
	1266.13	Max Rad Marker	Core	1266.13			0.5						87.4		12.2		
	1267.03	Max Rad Marker	Core	1267.03	441	4.56	25.1	4	3.3			39.1		11.1	10.9		6.6
	1267.99	Max Rad Marker	Core	1267.99	439	4.24	27.8	3.7	2.9			35.3		9.3	8.6		12.5
	1269.04	Max Rad Marker	Core	1269.04	440	4.22	27.6	4	3.8			38.7		10.2	9.1		6.6
	1669.4	Max Rad Marker	Core	1669.40			1.5						40.9		57.6		
	1269.81	Max Rad Marker	Core	1269.81	445	2.45	28.3	4	3.1			40.6		10.7	8.6		4.5
	1270.8	Max Rad Marker	Core	1270.80	442	3.23	27.5	3.9	3.3			39.1		11.1	9.7		5.5
	1271.5	Max Rad Marker	Core	1271.50			4.9						71.3		23.8		
	1271.7	Max Rad Marker	Core	1271.70	443	2.52	32.8	4	3.3			37.2		10	8.7		4.1
	1272.74	Max Rad Marker	Core	1272.74	441	2.33	28.6	2.9	3.1			36.9		9.7	9.2		9.7
	1273.61	Max Rad Marker	Core	1273.61	442	1.73	51.3	2.6	3.1			29.8		6.3	4.8		2.2
	1273.82	Max Rad Marker	Core	1273.82			23.1						66.2		10.7		
	1274.69	Max Rad Marker	Core	1274.69	442	2.10	29.5	4.2	5.3			37.9		11.9	4.3		6.9
	1275.23	Max Rad Marker	Core	1275.23			5.1						54.6		40.4		
	1275.45-.50	Max Rad Marker	Core	1275.45			17.7	2			62.6	9		3.3	1.3	1.2	3
	1275.77	Max Rad Marker	Core	1275.77	444	2.46	27.6	3.8	4.9			27.6		10.8	5.9		3.5
	1276.59	Max Rad Marker	Core	1276.59	441	3.99	28.6	3.4	3.9		28.7	25		3.3	4.9		2.1
	1277.49	Max Rad Marker	Core	1277.49	446	3.17	18.4	1.8	2	1.3	58.9	10.1		4.8	1.3		1.3
	1278	Max Rad Marker	Core	1278.00	444	1.29	28.4	4.3	5.7			45.9		6.1	8.5		1.2

Table BU1. Garbutt Formation – Thermal maturity and mineralogical data from samples in AEC Maxhamish b-53-B/94-O-14.

Well ID	Sample ID	Zone	Sample Type	Depth (m)	Tmax in °C	TOC %	Quartz	Feldspar		Clays			Sulphides
								Albite	Microcline	Illite/mica*	Chlorite	Kaolinite	Pyrite
ECA Maxhamish 200/b-006-C 094-O-11/00 WA 18890	1151	Garbutt	Core	1151.00	441	2.67	40.3	2.9	2.3	33.7	7.9	9.7	3.1
	1151.98	Garbutt	Core	1151.98	441	3.45	43.2	3	2.3	32.4	7	8.8	3.4
	1153.05	Garbutt	Core	1153.05	440	3.12	38	3.2	2.6	34.1	8	10.5	3.5
	1154.24	Garbutt	Core	1154.24	438	3.73	41.1	3	2.3	32.7	7.9	9	3.8
	1155.02	Garbutt	Core	1155.02	436	3.53	38.4	2.9	2.1	36	7	9.7	4
	1156.03	Garbutt	Core	1156.03	442	2.50	35.5	4	3	35.1	8.2	11.1	3.1
	1157	Garbutt	Core	1157.00	443	3.06	35.3	3.9	3.1	34.4	8.4	11.8	3.1
	1157.97	Garbutt	Core	1157.97	442	3.05	40.2	3.8	2.5	34.1	7.4	9.7	2.2
	1158.95	Garbutt	Core	1158.95	441	3.05	37.4	3.7	2.9	35.2	7.8	10.9	2.2
	1160	Garbutt	Core	1160.00	440	3.18	40.2	3.3	2.4	34.2	7.4	9.2	3.2
	1160.92	Garbutt	Core	1160.92	442	2.50	44.9	3.6	2.3	33.6	5.4	8	2.3
	1162	Garbutt	Core	1162.00	441	3.25	36.4	3.7	2.7	36	7.5	10.3	3.5
	1163	Garbutt	Core	1163.00	443	2.92	38.2	3.5	2.7	36.8	6.9	9.7	2.1
	1164	Garbutt	Core	1164.00	443	2.76	35.8	3.8	3	38.4	7.3	9.6	2.2
	1165	Garbutt	Core	1165.00	443	3.00	37.6	3.6	2.8	37.6	7.4	9.1	2
	1166	Garbutt	Core	1166.00	443	2.81	35.1	3.4	2.9	37.8	7.6	10.6	2.6
	1166.8	Garbutt	Core	1166.80	446	3.15	38.3	3.2	2.4	38.9	5.7	9.4	2

Table BU2. Garbutt Formation – Thermal maturity and mineralogical data from samples in ECA Maxhamish b-6-C/94-O-11.

Unconfined Porosity and Matrix Permeability										
Well Name	Well Location	Core Depth (m)	Fm	Density		Porosity (%)	GRI Matrix Permeability (md)		GRI Matrix Permeability (nd)	
				Bulk Density (g/cc)	Skeletal Density (g/cc)		Avg	Std Dev	Avg	Std Dev
ECA Maxhamish	200/b-006-C 094-O-11/00	1151.57	Garbutt	2.411	2.578	6.47	1.32E-05	9.21E-07	13.16	0.92
ECA Maxhamish	200/b-006-C 094-O-11/00	1154.72	Garbutt	2.417	2.593	6.76	1.39E-05	2.70E-06	13.90	2.70
ECA Maxhamish	200/b-006-C 094-O-11/00	1158.40	Garbutt	2.422	2.630	7.90	1.77E-05	4.40E-06	17.67	4.40
ECA Maxhamish	200/b-006-C 094-O-11/00	1162.48	Garbutt	2.432	2.667	8.83	9.82E-06	1.21E-06	9.82	1.21
ECA Maxhamish	200/b-006-C 094-O-11/00	1165.67	Garbutt	2.434	2.569	5.24	1.33E-05	2.76E-06	13.29	2.76
AEC Maxhamish	200/b-053-B 094-O-14/00	1260.47	Garbutt Rad Zone	2.462	2.556	3.70	1.13E-05	7.33E-07	11.33	0.73
AEC Maxhamish	200/b-053-B 094-O-14/00	1262.57	Garbutt Rad Zone	2.471	2.578	4.18	1.95E-05	2.67E-06	19.47	2.67
AEC Maxhamish	200/b-053-B 094-O-14/00	1263.89	Max Rad Marker	2.414	2.527	4.47	1.18E-05	5.00E-07	11.81	0.50
AEC Maxhamish	200/b-053-B 094-O-14/00	1264.55	Max Rad Marker	2.405	2.499	3.75	1.32E-05	2.32E-06	13.21	2.32
AEC Maxhamish	200/b-053-B 094-O-14/00	1266.99	Max Rad Marker	2.438	2.522	3.33	1.79E-05	2.16E-06	17.90	2.16
AEC Maxhamish	200/b-053-B 094-O-14/00	1268.45	Max Rad Marker	2.435	2.624	7.18	3.91E-05	1.51E-05	39.11	15.05
AEC Maxhamish	200/b-053-B 094-O-14/00	1270.50	Max Rad Marker	2.459	2.652	7.26	4.99E-05	1.77E-05	49.86	17.71
AEC Maxhamish	200/b-053-B 094-O-14/00	1272.75	Max Rad Marker	2.517	2.718	7.41	4.00E-05	1.82E-05	39.98	18.17
AEC Maxhamish	200/b-053-B 094-O-14/00	1274.31	Max Rad Marker	2.457	2.654	7.41	7.41E-05	1.53E-05	74.05	15.28
AEC Maxhamish	200/b-053-B 094-O-14/00	1275.27	Max Rad Marker	2.693	2.783	3.23	4.38E-05	1.71E-05	43.79	17.13
AEC Maxhamish	200/b-053-B 094-O-14/00	1276.60	Max Rad Marker	3.066	3.215	4.61	5.06E-05	3.88E-05	50.60	38.82
AEC Maxhamish	200/b-053-B 094-O-14/00	1277.25	Max Rad Marker	2.929	3.026	3.22	1.52E-05	6.73E-06	15.23	6.73

Trican Geological Solutions

Table BU3. Garbutt Formation– unconfined porosity and GRI matrix permeability measurements from core samples in AEC Maxhamish b-53-B/94-O-14 and ECA Maxhamish b-6-C/94-O-11.

MICP Porosity										
Well Name	Well Location	Core Depth (m)	Fm	Density g/cc		Porosity (%)	Corrected Porosity (%)	Peak Range		Stem Volume Used (%)
				Bulk Density (g/cc)	Skeletal Density (g/cc)			Peak Range	Modal Peak	
ECA Maxhamish	200/b-006-C 094-O-11/00	1151.57	Garbutt	2.404	2.519	4.99	4.55	4 - 100	5	25
ECA Maxhamish	200/b-006-C 094-O-11/00	1158.40	Garbutt	2.410	2.544	5.89	5.25	4 - 80	8	36
ECA Maxhamish	200/b-006-C 094-O-11/00	1165.67	Garbutt	2.435	2.557	5.13	4.80	4 - 100	5	26
AEC Maxhamish	200/b-053-B 094-O-14/00	1260.47	Garbutt Rad Zone	2.482	2.566	3.28	2.70	<3 - 130	11	37
AEC Maxhamish	200/b-053-B 094-O-14/00	1262.57	Garbutt Rad Zone	2.485	2.587	3.94	3.28	<3 - 130	5	32
AEC Maxhamish	200/b-053-B 094-O-14/00	1263.89	Max Rad Marker	2.412	2.514	4.06	3.41	<3 - 160	4	52
AEC Maxhamish	200/b-053-B 094-O-14/00	1264.55	Max Rad Marker	2.398	2.520	4.83	3.71	<3 - 140	<3	45
AEC Maxhamish	200/b-053-B 094-O-14/00	1266.99	Max Rad Marker	2.430	2.538	4.25	3.61	<3 - 160	8	51
AEC Maxhamish	200/b-053-B 094-O-14/00	1268.45	Max Rad Marker	2.443	2.574	5.09	4.69	<3 - 130	6	42
AEC Maxhamish	200/b-053-B 094-O-14/00	1270.50	Max Rad Marker	2.483	2.638	5.88	5.15	<3 - 100	7	52
AEC Maxhamish	200/b-053-B 094-O-14/00	1272.75	Max Rad Marker	2.559	2.700	5.21	4.47	<3 - 110	6	48
AEC Maxhamish	200/b-053-B 094-O-14/00	1274.31	Max Rad Marker	2.490	2.613	4.70	4.31	<3 - 160	7	49
AEC Maxhamish	200/b-053-B 094-O-14/00	1275.27	Max Rad Marker	2.695	2.773	2.79	2.29	11 - 820	38372	19
AEC Maxhamish	200/b-053-B 094-O-14/00	1276.60	Max Rad Marker	3.159	3.247	2.71	2.45	8 - 220	23	24

Trican Geological Solutions

Table BU4. Garbutt Formation – MICP porosity and conformance-corrected porosity measurements from core samples in AEC Maxhamish b-53-B/94-O-14 and ECA Maxhamish b-6-C/94-O-11.

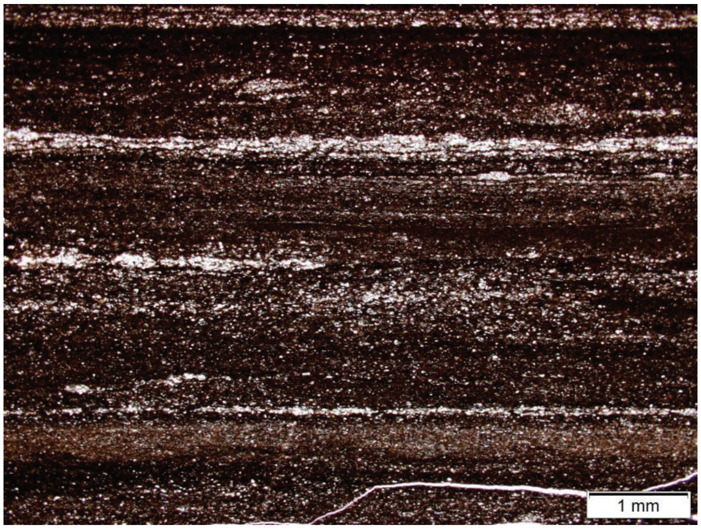

Figure BU9. Photomicrograph, Garbutt Formation, ECA Maxhamish b-6 C/94-O-11 (1152.65 m) under plane polarized light. Bioturbated, finely-laminated siliceous shale with alternating light (quartz-rich) layers and dark (high-organic and opaque) layers. Bioturbation causes minor disruption of some layers.

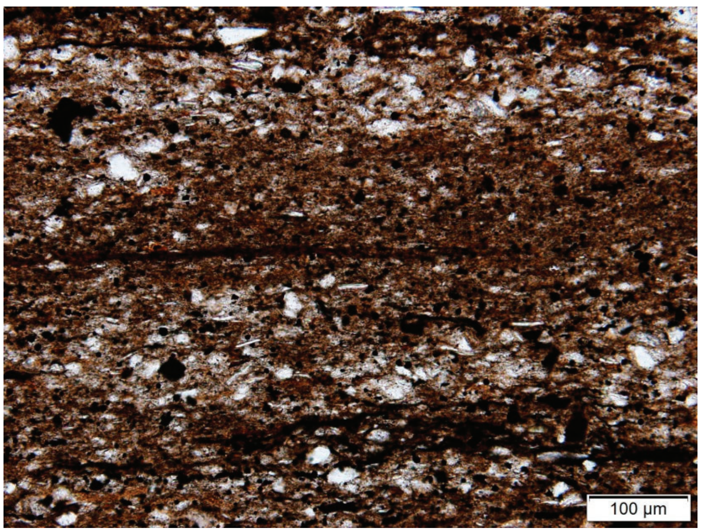

Figure BU10. Photomicrograph, Garbutt Formation, ECA Maxhamish b-6 C/94-O-11 (1152.65 m) under plane polarized light. Bioturbated, finely-laminated siliceous shale with a greater percentage of quartz-rich laminae.

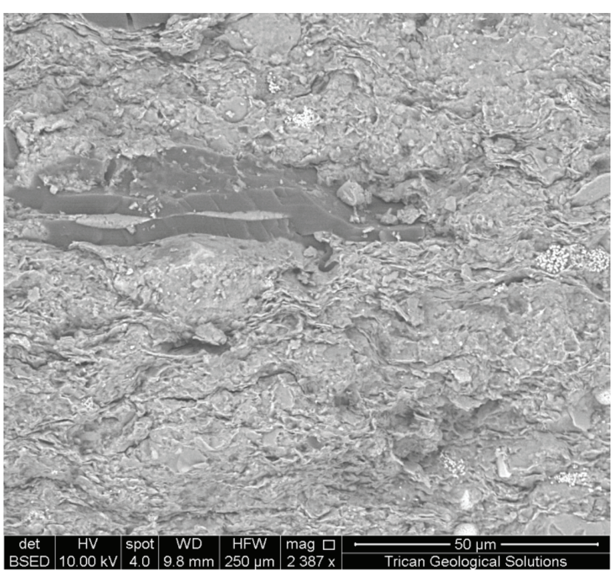

Figure BU11. BSED SEM photomicrograph, Garbutt Formation, ECA Maxhamish b-6 C/94-O-11 (1152.65 m) featuring laminated texture and coated silt-sized quartz grains.

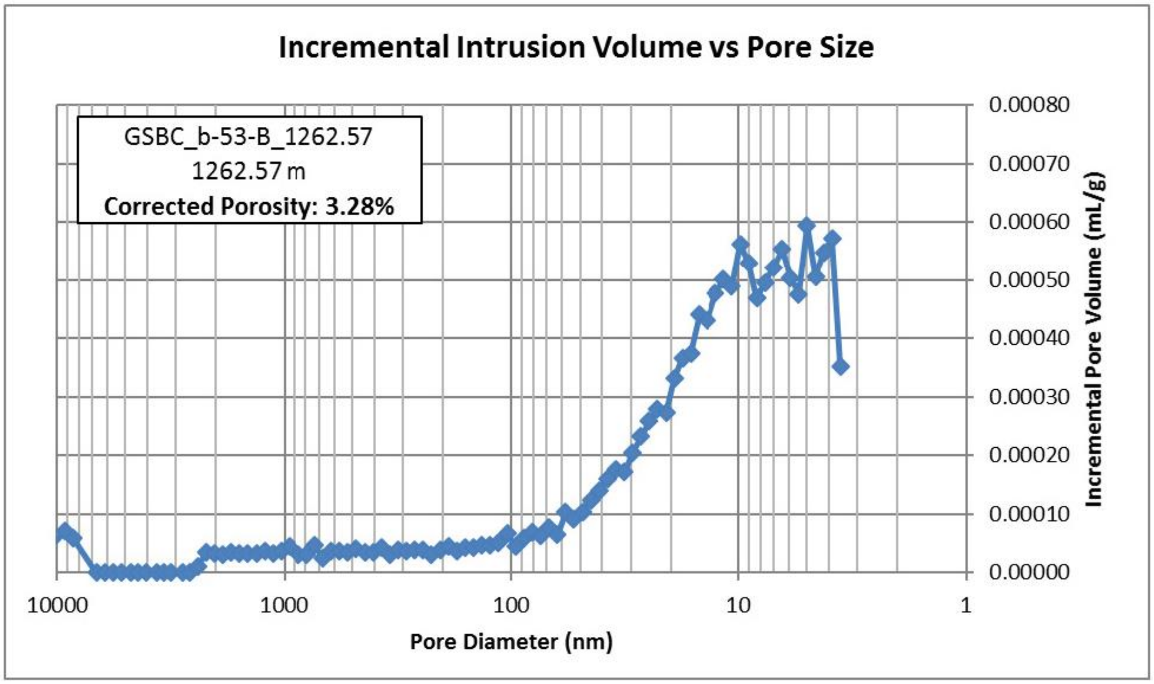

Figure BU12. Incremental and percent intrusion versus pore size, Garbutt Formation, AEC Maxhamish b-53-B/94-O-14 (1262.57 m) highlighting very small pore throat diameters (generally <20 nm).

Hydrocarbon analysis (S1) show that residual hydrocarbons are present and most commonly contain C_{10}-C_{55} chains with calculated API gravities of 37-39° and calculated specific gravities between 0.83-0.84 (Table BU5, Fig. BU13). Hydrocarbon liquids thus appear to be present in the Cretaceous shale section.

Hydrocarbon Composition by Thermal Desorption Gas Chromatography																	Trican Geological Solutions
Well Name	Well Location	Core Depth (m)	Fm	% Light Condensate	% Heavy Condensate	% Naphthenes	% Aromatics	% Biomarkers	Range >2%	Peak	Initial Boiling Point (°C)	Carbon Number	Final Boiling Point (°C)	Carbon Number	Calculated Specific Gravity	Calculated API gravity	Chromatogram Quality
ECA Maxhamish	200/b-006-C 094-O-11/00	1151.98	Garbutt	15.83	68.68	1.80	4.98	8.72	C10-C26	C13	59	<C6	442	C29	0.84	37.55	excellent
ECA Maxhamish	200/b-006-C 094-O-11/00	1154.24	Garbutt	19.14	64.25	2.49	6.99	7.13	C10-C25	C13	55	<C6	453	C30	0.84	37.91	best
ECA Maxhamish	200/b-006-C 094-O-11/00	1157.00	Garbutt	20.25	62.31	2.81	6.84	7.78	C10-C23	C13	54	<C6	427	C28	0.83	39.04	excellent
ECA Maxhamish	200/b-006-C 094-O-11/00	1160.92	Garbutt	22.17	61.52	2.13	6.32	7.86	C9, C10-C23	C13	57	<C6	422	C27	0.83	38.64	best
ECA Maxhamish	200/b-006-C 094-O-11/00	1163.00	Garbutt	20.90	61.12	2.82	6.76	8.40	C9-C23	C13	58	<C6	402	C25	0.83	39.62	excellent
ECA Maxhamish	200/b-006-C 094-O-11/00	1166.80	Garbutt	21.47	63.58	2.07	5.45	7.43	C9-C24	C13	58	<C6	429	C28	0.83	38.91	best

Table BU5. Garbutt and Lepine Formations – hydrocarbon composition data from samples in AEC Maxhamish
b-53-B/94-O-14 and ECA Maxhamish b-6-C/94-O-11.

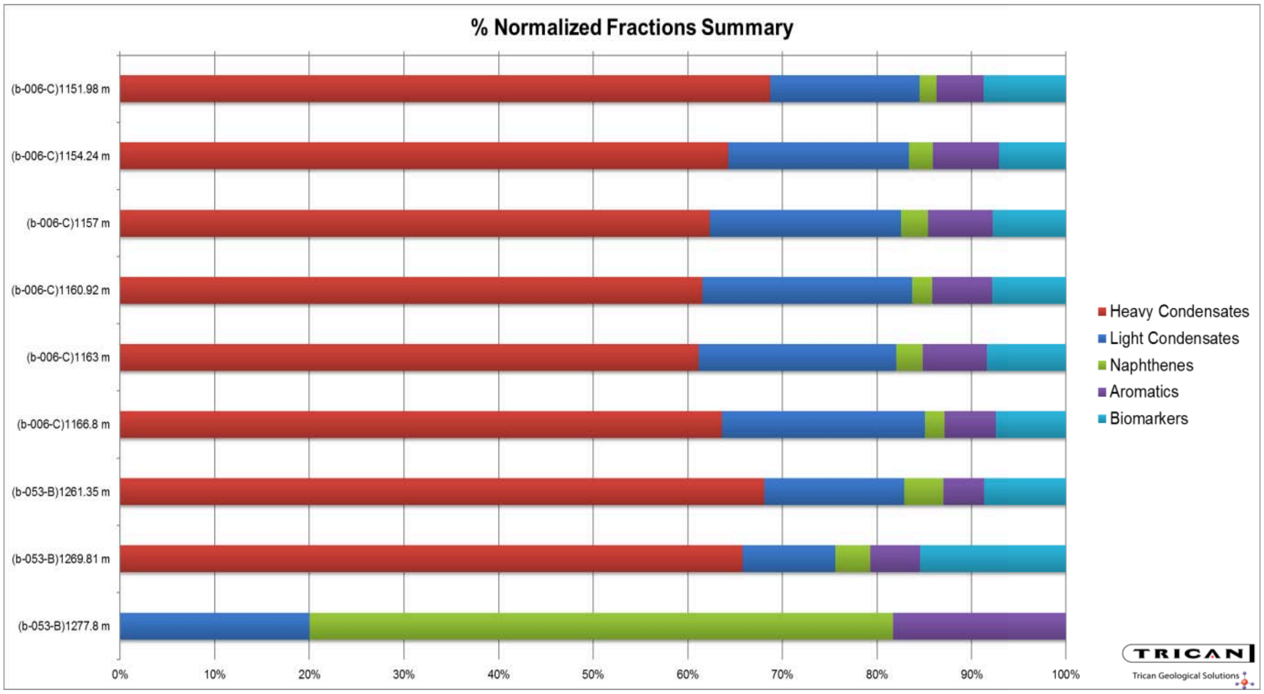

Figure BU13. Normalized fraction plot of hydrocarbon groups identified in nine core samples from two wells. Most samples are dominated by heavy condensates.

Mechanical properties of Garbutt rocks from the b-53-B well show compressive strengths of 88-275 MPa and residual strengths of 16-63 Mpa; Poisson's ratio is ~0.14-0.28 and Young's modulus ~5-61 (Table BU6). However, the 1274m sample was below the recommended length to diameter ratio (1.42 vs recommended ratio of 2.0-2.5), and results are thus not reliable. Results from the 1261.74 sample are reliable, and show higher than average (relative to the rest of the study) Young's modulus and brittleness.

Triaxial Data (TRICAN, Trican Geological Solutions)											
Well Name	Well Location	Core Depth (m)	Fm	Confining Pressure (MPa)	Axial Strain at Failure (%)	Compressive Strength (MPa)	Residual Strength (MPa)	Static Young's Modulus (GPa)	Static Poisson's Ratio	Static Bulk Modulus (GPa)	Static Shear Modulus (GPa)
AEC Maxhamish	200/b-053-B 094-O-14/00	1261.74	Garbutt Rad Zone	16.0	0.449	275.31	16.00	61.05	0.288	48.10	23.69
AEC Maxhamish	200/b-053-B 094-O-14/00	1274.01	Max Rad Marker	16.0	1.996	88.81	63.65	5.28	0.140	2.45	2.32

Table BU6. Garbutt Formation, AEC Maxhamish b-53-B/94-O-14 - Rock mechanical analyses showing confining pressure, compressive strength, Young's Modulus, Poisson's Ratio and bulk and shear modulii.

Ferri *et al*. (2017) published a significant study of Garbutt prospectivity in the Liard Basin after initiation of our current project. Rather than duplicate their compilation and interpretation of available data, we summarize key points from their report. They did include Rock-Eval (TOC and maturity) and mineralogical (XRD) data from the two wells we examined for our study.

Key findings include:

- TOC values generally increase with depth, and are highest in the Radioactive Zone adjacent to the Bovie FZ (Fig. BU14). Values locally exceed 6%, dropping to about 2% in the central Liard Basin. In the underlying lower Garbutt, TOC values exceed 3% adjacent to the Bovie FZ, and decrease to 1.5-2% elsewhere. Kerogens are dominantly Type II (oil-prone).

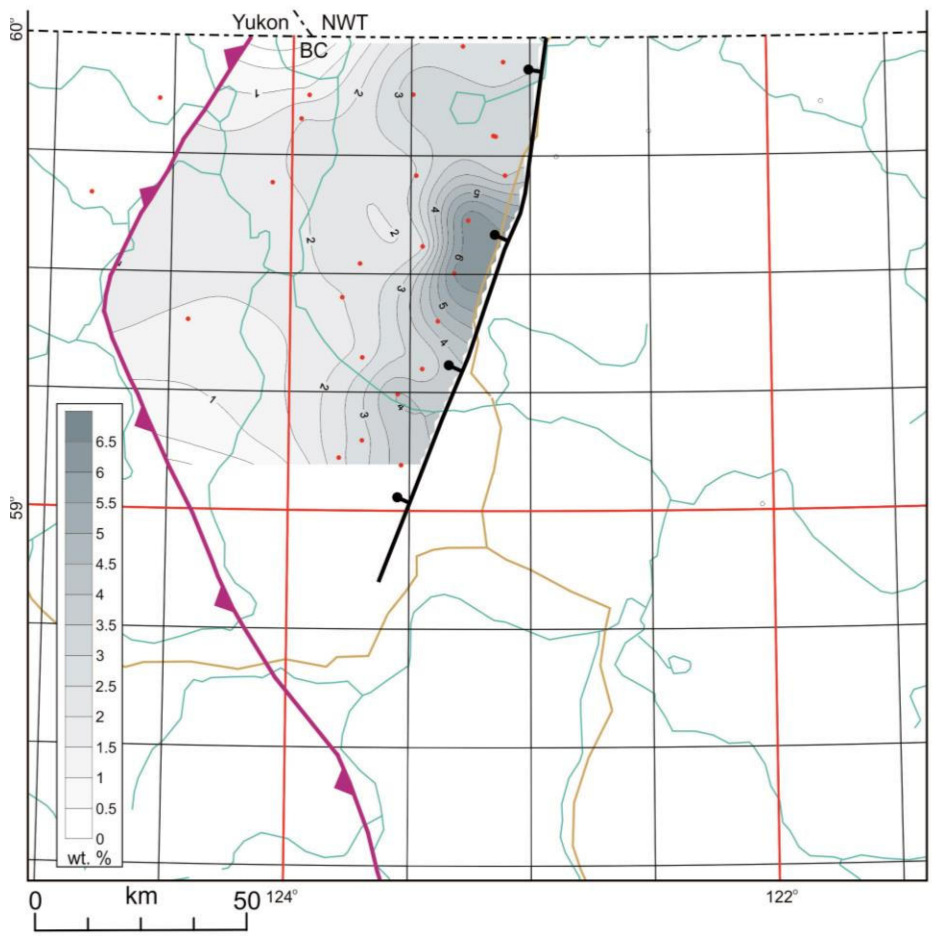

Figure BU14. Average TOC for the Garbutt Formation Radioactive Zone in the Liard Basin (from Ferri *et al*., 2017).

- T_{max} values show the Radioactive Zone to be thermally immature east of the Bovie FZ, mature for oil in the northeastern Liard Basin, and mature for wet gas to the southwest (Fig. BU15). Similar patterns are evident in the lower Garbutt.

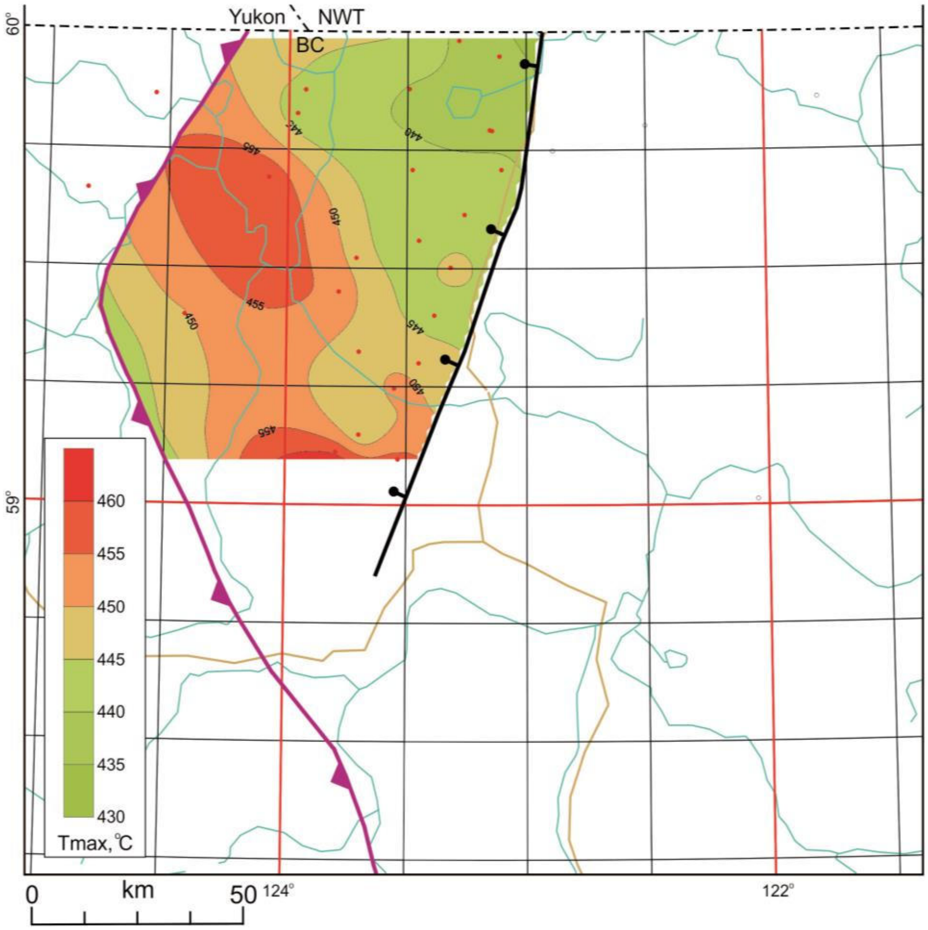

Figure BU15. Average T_{max} for the Garbutt Formation Radioactive Zone in the Liard Basin (from Ferri *et al*., 2017).

- MIneralogical analyses (XRD) of samples across the Radioactive Zone and lower Garbutt indicate average quartz content of 39 weight% and average clays at 53 weight% (Fig. BU16).

Finally, Haeri-Ardakani *et al*. (2015) reported that Garbutt core samples in the oil window have high S2 values and exude oil under fluorescent light; and that oil fills intercrystalline porosity in framboidal pyrites and pores in microfossil skeletons.

Resource Oil Assessment

Ferri *et al*. (2017) noted that the Radioactive Zone has been recognized in the literature as a potential oil and gas source rock, and likely generated the oil in the Maxhamish Chinkeh oil pool. Thickness, burial depth, TOC and maturity values all suggest that the Garbutt (particularly the Radioactive Zone and lower Garbutt) could be a resource oil target in the northern Liard Basin, transitioning to a wet gas target to the southwest. From a mineralogical and geomechanical point of view, while there is abundant silica in the formation, its clay-rich nature may inhibit effective fracturing. However, as

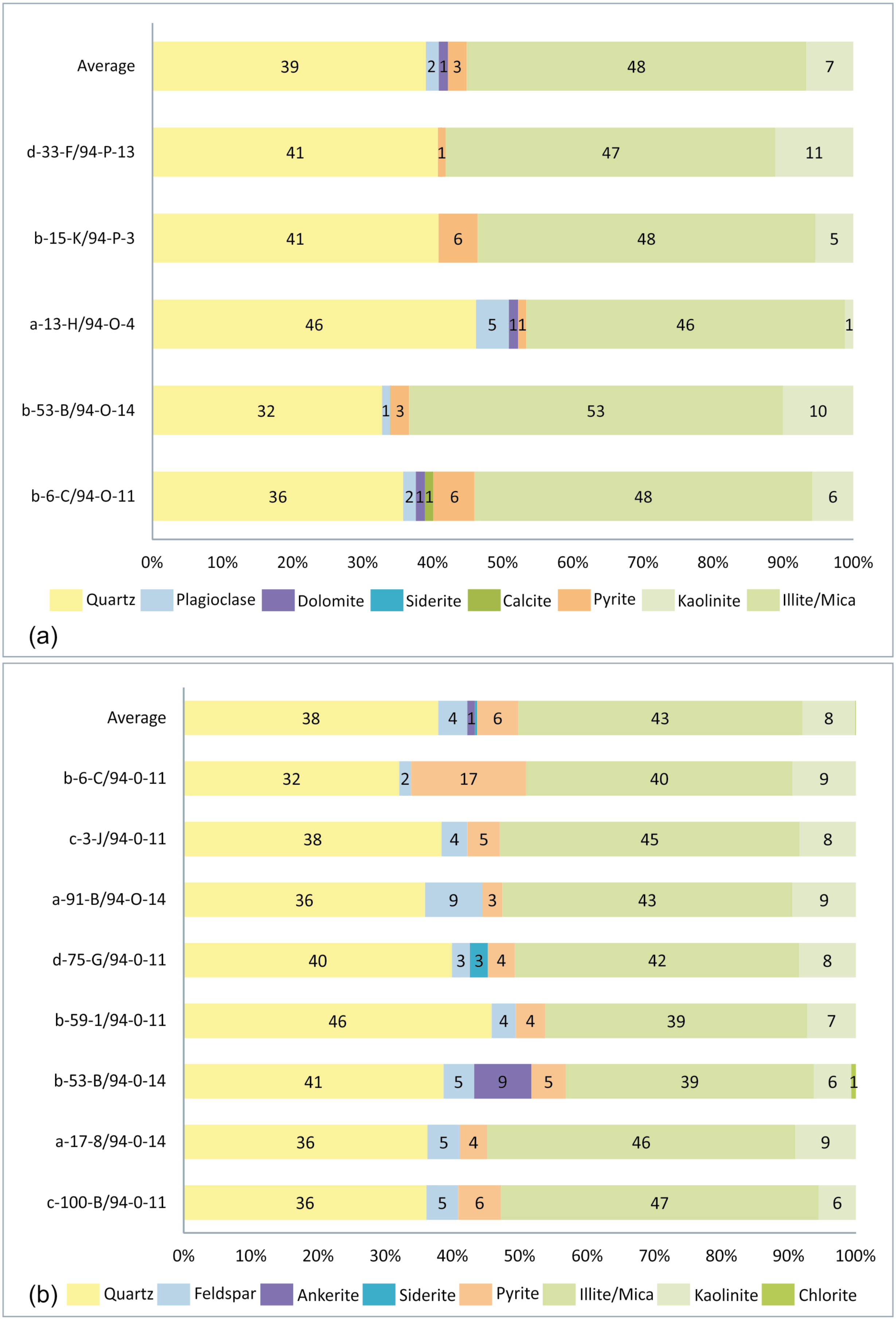

Figure BU16. Compositional analysis by X-ray diffraction of samples from the Radioactive Zone (samples in (a) analyzed in the Ferri *et al.* (2017) study, and samples in (b) reported in Nexen and Encana well reports) highlighted by Ferri *et al*. (2017), modern fracturing techniques may produce effective stimulation.

Ferri *et al*. (2017) speculated that the Garbutt may be overpressured, considering early Tertiary uplift of the Liard Basin. However, as the underlying Chinkeh appears to be subnormally pressured, this may not be the case.

Chalmers and Bustin (2008b) calculated average gas-in-place values of $28.3e^6m^3$/section (30 BCF/section) for the Radioactive Zone where mature for gas. Comparable values for oil and liquids-rich gas have not been generated, but the resource oil prize looks to be large considering the thickness and richness of the Zone and its large areal extent. Unlocking this potential awaits an effective and systematic horizontal drilling and hydraulic fracturing program.

CONCLUSIONS AND RECOMMENDATIONS

Muskwa Formation (Shale, Prospectivity: **B**)

- Muskwa shales are productive shale gas reservoirs in the Horn River Basin, and appear to have favourable shale reservoir characteristics and wet gas to liquids-level maturity near the Alberta border and into Alberta. Large oil-in-place volumes have been mapped on the Alberta side.

- Horizontal / multi-frac wells drilled in 2009-2012 have yielded uneconomic oil production, and there is no apparent current activity.

- Re-assessment of Muskwa potential using current drilling and completions technology may be justified, referencing recent success in producing oil from the East Shale Basin Duvernay.

Jean Marie Formation (Tight Carbonate, Prospectivity: **B**)

- Jean Marie platform carbonates are widespread and prolific tight gas reservoirs, with thousands of horizontal completions in a regionally underpressured system.

- Local oil production appears controlled by maturity of underlying Muskwa source rock, and possibly preferred migration of fluids along regional fault trends.

- More regional resource oil prospectivity requires a systematic understanding of oil migration and emplacement. There may be better Jean Marie resource oil prospectivity in Alberta where the Muskwa source rock is oil-mature.

Kakisa Formation (Tight Carbonate, Prospectivity: **C**)

- Kakisa platform carbonates, lying just above the Jean Marie, lack the well-documented reservoir sweet spots of the Jean Marie, but have produced gas from horizontal multi-frac wells

- It is unclear why Kakisa carbonates have not produced oil when the Jean Marie below and Tetcho above have; perhaps a function of where wells have been tested in an area where oil charge appears to be very local. Regardless, lack of production leads us to rank the Kakisa lower than the others.

Kotcho / Tetcho Formations (Tight Carbonate, Prospectivity: **B**)

- The Tetcho and Kotcho appear to lack the well-developed reefal buildups present on the Jean Marie platform, and hence are dominated by limestones with fewer reservoir sweet spots. Nevertheless, limited oil production from the Tetcho points to some level of oil prospectivity.
- As for the Jean Marie, regional resource oil prospectivity requires a systematic understanding of oil migration and emplacement. There may be better Kotcho / Tetcho resource oil prospectivity in Alberta where the Muskwa source rock is oil-mature.

Exshaw Formation (Shale, Prospectivity: **C**)

- The Exshaw is a well-known source rock throughout the Western Canada Sedimentary Basin, but in northeastern BC is very thin in eastern and central areas where oil-prone. It thickens westward into the Liard Basin to become part of the Besa River shale package, but is definitely gas-prone.

Banff Formation (Tight Carbonate and Sandstone, Prospectivity: **C**)

- Thin and discontinuous conventional-quality sandstones and more continuous but tight clean carbonate reservoirs exist in the upper Banff. The sandstones host several gas pools near their subcrop edge, but there are only a couple of isolated oil shows in the Desan area (where the overlying Rundle produces oil) in both reservoir types. Most completions show the interval to be tight.
- Resource oil prospectivity is poor because regional mapping shows little potential for consistently developed oil-charged reservoir.

Rundle Group (Tight / Halo Carbonate, Prospectivity: **B**)

- At Desan, the area producing oil from Rundle carbonates is much larger than producing areas for other Paleozoic reservoir intervals. Most productive intervals exhibit conventional reservoir quality, but structural and stratigraphic controls are complex. Many of the newer horizontal wells drilled into waterflood areas have been economic, but horizontals into non-waterflooded areas have not.
- While resource oil potential may exist, we see no strong evidence suggesting systematic and extensive halo oil prospectivity in lower-grade reservoir. Instead, new potential probably lies in more efficient access to stratigraphic and structural compartments in the Desan reservoir complex – built on improved and detailed stratigraphic and structural mapping.

Golata Formation (Shale, Prospectivity: **C**)

- A widespread, dark marine shale mappable throughout the Fort St John Graben. The Golata is not prospective as a resource oil target because of low organic content and elevated maturity levels.

Kiskatinaw / Taylor Flat Formations (Halo / Tight Sandstone, Prospectivity: **C**)

- While thick channelized sandstones in the basal Kiskatinaw produce gas over a large area, local oil production at Eagle raises the possibility of more widespread halo oil production, either in tight facies stratigraphically equivalent to the main producing sands, or in thinner interbedded reservoir successions higher in the section.

- Existing oil producers are tightly bounded, both structurally and stratigraphically, and hold out little potential for marginal / halo facies. Sandstones higher in the section are thin and tend to be carbonate cemented, with little reservoir capacity.

Belloy Formation (Halo / Tight Sandstone, Prospectivity: **C**)

- The Belloy is less structurally compartmentalized than the underlying Kiskatinaw, but existing oil pools are similarly limited to the Eagle and Stoddart area. They are tightly delineated and under waterflood, leaving little halo oil potential.

- Limited horizontal drilling before 2010 appears to have targeted field extension and/or halo oil, but only one well appears to have reached payout.

Toad-Grayling Formation (Tight Sandstone, Prospectivity: **B**)

- Resource oil potential in the Toad-Grayling is highly speculative, as there is insufficient well and test control to map reservoir bodies or assess their fluid content.

- We speculate that tight oil potential delineated in the overlying Chinkeh Formation may, at least locally, be continuous through reservoir-quality sandstones in the underlying Toad-Grayling.

Doig Formation (Tight Sandstone, Prospectivity: **A/B**)

- Discrete thick sandstone bodies in the Doig (ATSB's) produce oil in updip areas where the underlying Doig Phosphate source rock is mature for oil. In the Buick Creek – West Stoddart area, which hosts the largest oil pools, Doig reservoirs exhibit a variety of pressure gradients and water production. Horizontal / multi-frac wells greatly enhance production performance.

- We saw no evidence for oil production from Doig Phosphate shales, although the interval produces gas along the western flank of the Peace River Block.

- Additional tight oil potential may lie in new Doig ATSB's in the northeastern Peace River Block, between oil production at Buick – West Stoddart and pools in Alberta. To the north, new Doig oil discoveries may be in more conventional pools with better reservoir quality. In both cases, prospectivity will occur in discrete pools as opposed to continuous accumulations.

Halfway Formation (Halo Sandstone, Prospectivity: **A**)

- Halfway reservoirs offer the best halo / tight oil prospectivity in northeastern B.C. Conventional production is extensive and well-documented, and is controlled by both tidal channel reservoir facies distribution and related syndepositional structuring.

- Careful analysis of test and production data show that Halfway shoreface sandstones, while demonstrating poorer reservoir quality, are capable of independent oil production in some places – suggesting more widespread halo oil potential.

- Detailed reservoir mapping may suggest areas where undrained shoreface sandstones in separate structural / stratigraphic compartments can be exploited. Horizontal / multi-frac drilling would likely be most efficient. Some analogous drilling in the Halfway at Progress (Alberta) may be instructive.

Charlie Lake Formation (Halo / Tight Sandstone, Prospectivity: **C**)

- Tight oil potential in the Charlie Lake is very limited – most conventional pools consist of high-quality reservoir rock tightly constrained by depositional and/or diagenetic contacts.

- Regional tight oil trends being developed using horizontal multi-frac wells in western Alberta are confined largely to the Peace River Arch / FSJ Graben area in Alberta, and cannot be mapped into northeastern B.C.

Baldonnel Formation (Tight Carbonate, Prospectivity: **C**)

- Baldonnel production is primarily gas and primarily from conventional-quality reservoirs. Oil pools are small and areally interspersed with gas pools, except for one sizeable accumulation at Birch. While horizontal wells have been drilled into the Birch Baldonnel pool, these optimize local productivity and do not suggest more regional resource oil potential.

Nordegg Member (Shale, Prospectivity: **C**)

- Nordegg / Gordondale strata are excellent regional source rocks and appear highly prospective for oil and gas, depending on local maturation. However, drilling results to date, primarily in Alberta, have yielded no success in systematically producing oil (or gas) from the Nordegg. We have abundant log and analytical data in B.C., but none suggests new resource oil exploitation strategies.

Fernie Formation / Rock Creek Mbr (Tight Sandstone, Prospectivity: **C**)

- Rock Creek sandstones occur locally in the middle of Fernie shales, suggesting good potential for well-sealed tight reservoirs a short distance above Nordegg source rocks. However, very little work has been done on evaluating the unit, and there is little to suggest systematic charge or productive potential.

Chinkeh Formation (Tight Sandstone, Prospectivity: **A**)

- Chinkeh sandstones occur in a hydrocarbon-saturated setting, and there appears to be a broad area prospective for oil on the downdip flank of the Maxhamish gas field. Nine existing wells confirm the presence of an oil pool, and reservoir pressures indicate isolation from the largely depleted gas pool. Geochemical work indicates abundant source potential in the overlying Garbutt shales.

- Previous workers have suggested hundreds of millions of barrels of oil potential in the Chinkeh downdip of Maxhamish. New drilling is required to map out the prospective area in more detail, and modern horizontal drill / complete technologies should be applied to maximize recovery. Early-stage waterflooding may be important in building an economic venture.

Garbutt Formation (Shale, Prospectivity: **B**)

- The Radioactive Zone of the Garbutt is rich in organic material, and is mature for oil and liquids in northeastern Liard Basin. Although the unit has substantial silica, abundant clay content calls its frackability into question.
- A systematic horizontal drilling and fracturing program is required to assess the economic viability of a Garbutt development.

REFERENCES

Adams, C., 2014. Northeast BC industry activity update. 8th B.C. Unconventional Gas Technical Forum, Victoria.

Adams, C., E. Janicki, and A. Balogun, 2016. Summary of shale gas activity in Northeast British Columbia 2014. In: Oil and Gas Reports 2016, B.C. Ministry of Natural Gas Development, p. 1-39.

Arnold, K.J., and T.F. Moslow, 1996. Sedimentologic controls of reservoir characteristics in the Inga oil field, Charlie Lake Formation, northeastern British Columbia. *In*: Pools '96, Proceedings 1996 CSPG Annual Conference.

Asgar-Deen, M., C. Riediger, and R. Hall, 2004. The Gordondale Member: designation of a new member in the Fernie Formation to replace the informal "Nordegg Member" nomenclature of the subsurface of west-central Alberta. Bulletin of Canadian Petroleum Geology, v. 52, no. 3, p. 201-214.

Balogun, A., 2014. Organic shale potential of the Muskwa-Otter Park interval within the Cordova Embayment area of northeastern British Columbia using sonic and resistivity logs. In Geoscience Reports 2014, B.C. Ministry of Natural Gas Development, p.1-6.

Barclay, J.E., 1988. The Lower Carboniferous Golata Formation of the Western Canada Basin, in the context of sequence stratigraphy. *In* Sequences, Stratigraphy, Sedimentology: Surface and Subsurface. CSPG Memoir 15, D.P. James and D.A. Leckie (eds.), p. 1-14.

Barclay, J.E., L.A. Dunn, F.F. Krause, and M.R. Staniland, 2002. Estuarine valley fill and interfluve strata at a significant sequence boundary, Kiskatinaw and Golata formations, Lower Carboniferous (Upper Visean), north-western Alberta. Extended abstract, CSPG Diamond Jubilee Convention, Calgary.

Barclay, J.E., G.D. Holmstrom, P.J. Lee, R.I. Campbell, and G.E. Reinson, 1997. Carboniferous and Permian gas resources of the Western Canada Sedimentary Basin, Interior Plains. Geological Survey of Canada Bulletin 515.

Barclay, J.E., F.F. Krause, R.J. Campbell, and J. Utting, 1990. Dynamic casting and growth faulting: Dawson Creek Graben Complex, Carboniferous-Permian Peace River Embayment, western Canada. Bulletin of Canadian Petroleum Geology, v. 38A, p. 115-145.

Belyea, H.R., and D.J. McLaren, 1962. Upper Devonian formations, southern part of Northwest Territories, northeastern British Columbia, and northwestern Alberta. Geological Survey of Canada Paper 61-29.

Bever, J.M., 1990. Laprise Creek and East Laprise Creek. In: M.L. Rose (editor), Oil and Gas Pools of Canada, Canadian Society of Petroleum Geologists.

Birchcliff Energy, November 2016 Corporate Presentation. http://birchcliffenergy.com/media/uploads/documents/pdfs/CorporatePresentation/2016.11.09%20Corporate%20Presentation%20-%20FINAL.pdf

Bird, T.D., J.E. Barclay, R.I. Campbell, and P.J. Lee, 1994. Triassic gas resources of the Western Canada Sedimentary Basin, Interior Plains. Geological Survey of Canada Bulletin 483.

Bloy, G., and B. Scott, 1993. Characterization of the Belloy Formation reservoir, Boundary Lake pool, northeastern British Columbia. *In* Carboniferous to Jurassic Pangea, Core Workshop. J. Den Haan, K. Jang, and T. Webb (eds.). Calgary, p. 73-87.

British Columbia Ministry of Energy and Mines and CBM Solutions, 2005. Gas shale potential of Devonian strata, northeastern British Columbia. Petroleum Geology Special Paper 2005-1.

British Columbia Ministry of Natural Gas Development, 2015. Unconventional natural gas assessment for the Cordova Embayment in northeastern British Columbia. Oil and Gas Report 2015-1.

British Columbia Ministry of Energy and Mines, and National Energy Board, 2011. Ultimate potential for unconventional natural gas in northeastern British Columbia's Horn River Basin. Oil and Gas Reports 2011-1.

British Columbia Oil and Gas Commission, 2015. Pool Reserves Report – Oil. https://www.bcogc.ca/industry-zone/documentation/reserves

Bustin, R.M., and A.M.M. Bustin, 2016. Potential for natural-gas liquid from western Canadian shales: regional variation in thermal maturity and gas composition, northeastern British Columbia. *In*: Geoscience BC Summary of Activities 2015, Geoscience BC Report 2016-1, p. 49-54.

Caplan, M.L. and T.F. Moslow, 1997. Tectonic controls on preservation of Middle Triassic Halfway reservoir facies, Peejay Field, northeastern British Columbia: a new hydrocarbon exploration model. Bulletin of Canadian Petroleum Geology, v. 45, no. 4, p. 596-613.

Caplan, M.L. and T.F. Moslow, 1999. Depositional origin and facies variability of a Middle Triassic barrier island complex, Peejay Field, northeastern British Columbia. American Association of Petroleum Geologists Bulletin, v. 83, p. 128-154.

Chalmers, G.R.L., and R.M. Bustin, 2008a. Lower Cretaceous gas shales in northeastern British Columbia, Part I: geological controls on methane sorption capacity. Bulletin of Canadian Petroleum Geology, v. 56, p. 1-21.

Chalmers, G.R.L., and R.M. Bustin, 2008b. Lower Cretaceous gas shales in northeastern British Columbia, Part II: evaluation of regional potential gas reserves. Bulletin of Canadian Petroleum Geology, v. 56, p. 22-61.

Chalmers, G.R.L., and R.M. Bustin, 2012a. Geological evaluation of Halfway-Doig-Montney hybrid gas shale-tight gas reservoir, northeastern British Columbia. Marine and Petroleum Geology, v.38, p.53-72.

Chalmers, G.R.L., and R.M. Bustin, 2012b. Light volatile liquid and gas shale reservoir potential of the Cretaceous Shaftesbury Formation in northeastern British Columbia, Canada. AAPG Bulletin, v. 96, no. 7, p. 1333-1367.

Chen, Z., and K.G. Osadetz, 2013. An assessment of tight oil resource potential in Upper Cretaceous Cardium Formation, Western Canada Sedimentary Basin. Petroleum Exploration and Development, v. 40 (3), p. 344-353.

Chopra, S., R.K. Sharma and J. Keay, 2015. Mapping Middle Triassic Doig Sandstone reservoirs in northeast British Columbia using seismic attributes. Search and Discovery Article #51080.

Clarkson, C.R., and P.K. Pedersen, 2011. Production analysis of Western Canadian unconventional light oil plays. Proceedings, Canadian Unconventional Resources Conference, Calgary. CSUG/SPE Paper 149005.

Davies, G.R., 1997a. The Triassic of the Western Canada Sedimentary Basin: tectonic and stratigraphic framework, paleogeography, paleoclimate and biota. Bulletin of Canadian Petroleum Geology, v 45, no. 4, p. 434-460.

Davies, G.R., 1997b. The Upper Triassic Baldonnel and Pardonet formations, Western Canada Sedimentary Basin. Bulletin of Canadian Petroleum Geology, v 45, #4, p. 643-674.

Dembicki, H. (2014): Challenges to black oil production from shales; American Association of Petroleum Geologists/Datapages, Inc., Search and Discovery Article #80355, 22 p.

Dixon, J., 2006. Distribution of "anomalously thick sandstone bodies" in the Middle Triassic of the Western Canada Sedimentary Basin. Geological Survey of Canada Open File 5120.

Dixon, J., 2008. Stratigraphic relationships of the Triassic Halfway Formation in the Western Canada Sedimentary Basin. Bulletin of Canadian Petroleum Geology, v. 56, no. 1, p. 62-68.

Dixon, J., 2010. Character and origin of thick sandstone bodies in the Middle Triassic Doig Formation of Western Canada. Geological Survey of Canada Open File 6431.

Dixon, J., 2011. A review of the character and interpreted origins of thick, mudstone-encased sandstone bodies in the Middle Triassic Doig Formation of western Canada. Bulletin of Canadian Petroleum Geology, v.59, no.3, p.261-276.

Dong, T., N.B. Harris, K. Ayranci, and S. Yang, 2017. The impact of rock composition on geomechanical properties of a shale formation: Middle and Upper Devonian Horn River Group shale, northeast British Columbia, Canada. AAPG Bulletin, v.101, no.2, p.177-204.

Edwards, D.E., J.E. Barclay, D.W. Gibson, G. Kvill and E. Halton, 1994. Triassic strata of the Western Canada Sedimentary Basin. In: Geological Atlas of the Western Canada Sedimentary Basin, edited by G.D. Mossop and I. Shetsen. Calgary, Canadian Society of Petroleum Geologists / Alberta Research Council.

Energy Information Administration, 2013. Technically recoverable shale oil and shale gas resources: an assessment of 137 shale formations in 41 countries outside the United States. United States Department of Energy, Washington, DC.

Evoy, R.W., 1997. Lowstand shorefaces in the Middle Triassic Doig Formation: implications for hydrocarbon exploration in the Fort St. John area, northeastern British Columbia. Bulletin of Canadian Petroleum Geology, v. 45, p. 537-552.

Evoy, R.W., 1998. Reservoir sedimentology of the Doig Formation, Buick Creek Field, northeastern British Columbia. In: Oil and Gas Pools of the Western Canada Sedimentary Basin, edited by J.R. Hogg. Canadian Society of Petroleum Geologists Special Publication S-51, p. 127-135.

Evoy, R.W., and T.F. Moslow, 1995. Lithofacies associations and depositional environments in the Middle Triassic Doig Formation, Buick Creek Field, northeastern British Columbia. Bulletin of Canadian Petroleum Geology, v. 43, #4, p. 461-475.

Fefchak, C., and J.-P. Zonneveld, 2010. Sedimentary geology of the Artex Member, Brassey Field, northeastern British Columbia. Geoscience Reports 2010, BC Ministry of Energy, Mines, and Petroleum Resources, p. 1-10.

Ferri, F., M.L. Golding, J.K. Mortensen, J-P Zonneveld, and M.J. Orchard, 2010. Toad Formation (Montney and Doig equivalent) in the northwestern Halfway River area, British Columbia (NTS 094B/14). Geoscience Reports 2010, B.C. Ministry of Energy, Mines and Petroleum Resources, p. 21-34.

Ferri, F., and M. Griffiths, 2014. Thermal maturity and regional distribution of the Muskwa Formation, northeastern British Columbia. *In* Geoscience Reports 2014, British Columbia Ministry of Natural Gas Development, p. 37-45.

Ferri, F., Hayes, M. and Nelson, A., 2013. Liquids potential of the Lower to Middle Triassic Montney and Doig Formations, British Columbia. *In* Geoscience Reports 2013, British Columbia Ministry of Natural Gas Development, p. 1-11.

Ferri, F., A.S. Hickin and D.H. Huntley, 2011a. Besa River Formation, western Liard Basin, British Columbia (NTS 094N): geochemistry and regional correlations. *In* Geoscience Reports 2011, BC Ministry of Energy and Mines, p. 1-18.

Ferri, F., A.S. Hickin and D.H. Huntley, 2011b. Geochemistry and shale gas potential of the Garbutt Formation, Liard Basin, British Columbia. *In* Geoscience Reports 2011, BC Ministry of Energy and Mines, p. 19-36.

Ferri, F., M. McMechan and R. Creaser, 2015. The Besa River Formation in Liard Basin, British Columbia. *In* Oil and Gas Geoscience Reports 2015, British Columbia Ministry of Natural Gas Development, p.1-27.

Ferri, F., M. McMechan, O. Haeri Ardakani, and H. Sanei, 2017. The Garbutt shale of the B.C. Liard Basin: a potential liquids-rich play? Bulletin of Canadian Petroleum Geology, v.65, p.279-306.

Fitzgerald, E.L., and D.J. Peterson, 1967. Inga Oil Field, British Columbia. Bulletin of Canadian Petroleum Geology, v. 15(1), p. 65-81.

Fossenier, K.N., 2001. Stratigraphic framework of the Pennsylvanian to Permian, Belloy Formation in the Peace River Embayment of northeastern British Columbia: a multidisciplinary approach. M.Sc Thesis, University of Calgary.

Frank, J.H., 2002. Sedimentology, ichnology and stratigraphy of the lowermost Cretaceous, Liard Basin, Canada. M.Sc thesis, University of Alberta.

Frank, J., K. Aulstead, M. Edmonds, and G. Pemberton, 1999. Stratigraphy and ichnology of the Lower Cretaceous Chinkeh Formation, Liard Basin, northeastern B.C. 1999 CSPG and Petroleum Society Joint Convention Proceedings, Abst. 99-117C.

Gibson, D.W., and D.E. Edwards, 1990. An overview of Triassic stratigraphy and depositional environments in the Rocky Mountain Foothills and western interior Plains, Peace River Arch area, northeastern British Columbia. Bulletin of Canadian Petroleum Geology, v. 38A, p. 146-158.

Glass, D.J., 1990 (editor). Lexicon of Canadian stratigraphy. Volume 4, Western Canada. Canadian Society of Petroleum Geologists.

Goldthorpe, A.G., 1996. Significance of mixed carbonate-siliciclastic sedimentation in the Banff Formation, greater Cessford area, southeastern Alberta. In: Pools ’96, Canadian Society of Petroleum Geologists Core Conference Guidebook, p. 6-1 to 6-8.

Haeri-Ardakani, O., H. Sanei, M. McMechan, N. Van de Wetering, J. Reyes and R. Ferri, 2015. Hydrocarbon potential and depositional environment of the Lower Cretaceous Garbutt Formation, Liard Basin, Canada. Geoconvention 2015: New Horizons.

Halbertsma, H.L., 1994. Devonian Wabamun Group strata of the Western Canada Sedimentary Basin. In: Geological Atlas of the Western Canada Sedimentary Basin, edited by G.D. Mossop and I. Shetsen. Calgary, Canadian Society of Petroleum Geologists / Alberta Research Council.

Hamilton, W.D., D.R. Van Alstine, J.E. Butterworth, and G. Raham, 1995. Paleomagnetic orientation of fractures in Jean Marie Member cores from NE British Columbia/NW Alberta. Proceedings Canadian Society of Petroleum Geologists Annual Conference.

Harris, R.G., and R.M. Bustin, 2000. Diagenesis, reservoir quality, and production trends of Doig Formation sand bodies in the Peace River area of Western Canada. Bulletin of Canadian Petroleum Geology, v. 48, #4, p. 339-359.

Hayes, B.J.**,** 2005. Revisiting the Early Cretaceous paleogeography of N.E. British Columbia – important stratigraphic controls on large gas fields. CSPG Reservoir, v. 32, no. 1.

Hayes, B., and R. Stewart, 2017. Deep Subsurface Saline Aquifer Characterization, Deh Cho Area, Northwest Territories; Northwest Territories Geological Survey, NWT Open File 2015-07.

Higgs, R., 1990. Sedimentology and petroleum geology of the Artex Member (Charlie Lake Formation), northeastern British Columbia. B.C. Ministry of Energy, Mines and Petroleum Resources Petroleum Geology Special Paper 1990-1.

Hutton, A.N., 1995. An integrated geological, geophysical and hydrodynamic evaluation of the Mississippian in northeast British Columbia. Petrel Robertson Ltd. multiclient report.

Janicki, E., 2013. Conventional oil pools of northeastern British Columbia. BC Ministry of Natural Gas Development, Petroleum Geology Open File 2013-2, 222 p.

Janicki, E., 2014. Petroleum geology of the Halfway Formation, northeastern British Columbia. *In*: Geoscience Reports 2014, British Columbia Ministry of Natural Gas Development, p. 7-24.

Janicki, E. and A. Balogun, 2015. Distribution of arenites in the Fernie Formation in northeastern British Columbia. In: Oil and Gas Geoscience Reports 2015, British Columbia Ministry of Natural Gas Development, p. 28-44.

Jiang, C., A. Mort, M. McMechan and Z. Chen, 2015. Source of Chinkeh oil from Maxhamish Field, Liard Basin, northeastern British Columbia. Geoconvention 2015 Proceedings.

Jones, R.M.P., 1980. Basinal isostatic adjustment faults and their petroleum significance. Bulletin of Canadian Petroleum Geology, v. 28, p. 211-251.

Kirkland, I.K., and I.E. Hutcheon, 1991. Diagenesis and porosity distribution in the Upper Mississippian Kiskatinaw Formation, Peace River Region (abstract). Bulletin of Canadian Petroleum Geology, v. 39, no. 2, p. 216.

Labute, G.J., R.W. Evoy, and M. Clegg, 1998. The Middle Triassic Rigel Halfway “C” Pool, northeastern British Columbia. In: Oil and Gas Pools of the Western Canada Sedimentary Basin, edited by J.R. Hogg. Canadian Society of Petroleum Geologists Special Publication S-51, p. 111-125.

Law, J., 1971. Regional Devonian geology and oil and gas possibilities, upper Mackenzie River area. Bulletin of Canadian Petroleum Geology, v. 19, no. 2, p. 437-484.

Law, J., 1981. Mississippian correlations, northeastern British Columbia, and implications for oil and gas exploration. Bulletin of Canadian Petroleum Geology, v. 29, no. 3, p. 378-398.

Leckie, D.A., D.J. Potocki, and K. Visser, 1991. The Lower Cretaceous Chinkeh Formation: a frontier-type play in the Liard Basin of western Canada. Bulletin of the American Association of Petroleum Geologists, v. 75, no. 8, p. 1324-1352.

Leckie, D.A. and D.J. Potocki, 1998. Sedimentology and petrography of marine shelf sandstones of the Cretaceous Scatter and Garbutt formations, Liard Basin, northern Canada. Bulletin of Canadian Petroleum Geology, v. 46, no. 1, p. 30-50.

Leggett, S.R., F.G. Young, and D. Elbenschutz, 1993a. The Stoddart West oil field, Fort St. John, B.C.: an example of oil accumulation in a Permian shallow marine setting. Proceedings, CSPG Pangaea Conference, Calgary, p. 175.

Leggett, S.R., F.G. Young, and D. Elbenschutz, 1993b. Facies of the Belloy Formation (Lower Permian), northeastern British Columbia. *In* Carboniferous to Jurassic Pangea, Core Workshop. J. Den Haan, K. Jang, and T. Webb (eds.). Calgary, p. 88-108.

Letourneau, J.P., 1991. Petroleum hydrogeology of the Jean Marie Member, northeastern British Columbia (Abstract). Proceedings, Opportunities for the Nineties, CSPG Annual Convention, p. 92.

Macquarie Equities Research, 2010. Going straight to the “Source” – a spotlight on the emerging Canadian shale oil plays.

McAdam, K., 1993. The Jean Marie Member in the Hossitl-Ring area, British Columbia. Petroleum Geology Branch, Ministry of Energy, Mines and Petroleum Resources, Special Paper 1993-1.

McMechan, M., W. Matthews, F. Ferri, and B. Guest, 2016. Maximum age of the basal Cretaceous Chinkeh Formation sandstones, Maxhamish Lake area, Liard Basin, British Columbia. Bulletin of Canadian Petroleum Geology, v. 64, no. 3, p. 467-476.

McMechan, M.E., M. Obermajer, and F. Ferri, 2016. Rock-Eval / TOC data for selected samples of the Garbutt and Toad Formation from boreholes in the Liard Basin area, northeast British Columbia and southwest Northwest Territories. Geological Survey of Canada Open File 8109.

Moslow, T.F., and G.R. Davies, 1993. Triassic reservoir facies and exploration trends: Western Canada Sedimentary Basin. CSPG Short Course #4, course notes.

National Energy Board and Northwest Territories Geological Survey, 2015. Energy briefing note: an assessment of the unconventional petroleum resources of the Bluefish Shale and the Canol Shale in the Northwest Territories.

Norgard, G.T., 1997. Structural inversion of the Middle Triassic Halfway Formation, Monias Field, northeast British Columbia. Bulletin of Canadian Petroleum Geology, v. 45, no. 4, p. 614-623.

Northwest Territories Geological Survey, Yukon Geological Survey, British Columbia Oil and Gas Commission, and British Columbia Ministry of Natural Gas Development, 2016. The unconventional gas resources of Mississippian-Devonian shales in the Liard Basin of British Columbia, the Northwest Territories, and Yukon. Energy Briefing Note, March 2016

O’Connell, S.C., G.R. Dix, and J.E. Barclay, 1990. The origin, history, and regional structural development of the Peace River Arch, western Canada. Bulletin of Canadian Petroleum Geology, v. 38A, p. 4-24.

Petrel Robertson Consulting Ltd., 1997. Exploration and development assessment of the Lower Cretaceous section, Buick Creek-Laprise area, northeastern British Columbia. Non-exclusive report.

Petrel Robertson Consulting Ltd., 2000. Exploration study of Mississippian and Cretaceous strata, Bivouac area, NEBC and adjacent Alberta. Non-exclusive report.

Petrel Robertson Consulting Ltd., 2010. Horn River Basin Aquifer Characterization Project – Geological Report. Geoscience BC, Report 2010-11, http://www.geosciencebc.com/s/2010-011.asp

Petrel Robertson Consulting Ltd., 2015. Characterization of Belloy, Kiskatinaw and Debolt water disposal zones in the Montney Play Area, northeastern British Columbia. Geoscience BC Report 2015-3, http://www.geosciencebc.com/s/Report2015-03.asp .

Podruski, J.A., J.E. Barclay, A.P. Hamblin, P.J. Lee, K.G. Osadetz, R.M. Proctor, and G.C. Taylor, 1988. Conventional oil resources of western Canada (light and medium). Geological Survey of Canada Paper 87-26.

Pyle, L.J., L.P. Gal, and K.M. Fiess, 2014. Devonian Horn River Group: a Reference Section, lithogeochemical characterization, correlation of measured sections and wells, and petroleum-potential data, Mackenzie Plain area (NTS 95M, 95N, 96C, 96D, 96E, 106H and 106I), NWT. Northwest Territories Geoscience Office, NWT Open File 2014-06, 70p.

Reimer, J.D., 1994. Speculations concerning reservoir diagenesis and sourcing of Upper and Middle Devonian gas fields, northeastern British Columbia: a hydrogeological perspective (Abstract). CSPG Reservoir, v. 21, #10, p. 1-2.

Reinson, G.E., P.J. Lee, W. Warters, K.G. Osadetz, L.L. Bell, P.R. Price, F. Trollope, R.I. Campbell, and J.E., Barclay, 1993. Devonian gas resources of the Western Canada Sedimentary Basin. Geological Survey of Canada Bulletin 452.

Richards, B.C., J.E. Barclay, D. Bryan, A. Hartling, C.M. Henderson and R.C. Hinds, 1994. Carboniferous strata of the Western Canada Sedimentary Basin. *In* Geological Atlas of the Western Canada Sedimentary Basin, edited by G.D. Mossop and I. Shetsen. Canadian Society of Petroleum Geologists and Alberta Research Council, Calgary, Alberta, p. 221-250.

Riedger, C.L., 1994. Migration of “Nordegg” oil in the Western Canada Basin. How much and how far? Bulletin of Canadian Petroleum Geology, v. 42, no. 1, p. 63-73.

Riedger, C.L., and J.D. Bloch, 1995. Depositional and diagenetic controls on source-rock characteristics of the Lower Jurassic “Nordegg Member”, western Canada. Journal of Sedimentary Research, v. A65, no. 1, p. 112-126.

Riediger, C.L., P.W. Brooks, M.G. Fowler, and L.R. Snowdon, 1990a. Lower and Middle Triassic source rocks, thermal maturation, and oil-source rock correlations in the Peace River Embayment area, Alberta and British Columbia. Bulletin of Canadian Petroleum Geology, v.38A, p.218-235.

Riediger, C.L., G.G. Carrelli and J-P Zonneveld, 2004. Hydrocarbon source rock characterization and thermal maturity of the Upper Triassic Baldonnel and Pardonet formations, northeastern British Columbia, Canada. Bulletin of Canadian Petroleum Geology, v. 52, no. 4, p. 277-301.

Riediger, C.L., M.G. Fowler, L.R. Snowdon, F. Goodarzi, and P.W. Brooks, 1990b. Source rock analysis of the Lower Jurassic “Nordegg Member” and oil-source rock correlations, northwestern Alberta and northeastern British Columbia. Bulletin go Canadian Petroleum Geology, v. 38A, p. 235-249.

Rocheleau, J., K.M. Fiess, L.J. Pyle, F. Ferri, and T.A. Fraser, 2014. Source rock characterization of the Carboniferous Golata Formation and Devonian Besa River Formation outcrops, Liard Basin, Northwest Territories. Proceedings, Geoconvention 2014: Focus.

Rokosh, C.D., Lyster, S., Anderson, S.D.A., Beaton, A.P., Berhane, H., Brazzoni, T., Chen, D., Cheng, Y., Mack, T., Pana, C. and Pawlowicz, J.G., 2012. Summary of Alberta's shale- and siltstone-hosted hydrocarbon resource potential; Energy Resources Conservation Board, ERCB/AGS Open File Report 2012-06, 327 p.

Ross, D.J.K, and R.M. Bustin, 2006. Sediment geochemistry of the Lower Jurassic Gordondale Member, northeastern British Columbia. Bulletin of Canadian Petroleum Geology, v. 54, no. 4, p. 337-365.

Ross, D.J.K. and R.M. Bustin, 2007. Shale gas potential of the Lower Jurassic Gordondale Member, northeastern British Columbia, Canada. Bulletin of Canadian Petroleum Geology, v. 55, no. 1, p. 51-75.

Roy, K.J., 1972. The Boundary Member: a buried erosional remnant of Triassic age in northeastern British Columbia. Bulletin of Canadian Petroleum Geology, v. 20, #1, p. 27-57.

Shell Canada, 1990. Worsley Alberta Triassic oil pool. *In*: Oil and Gas Pools of Canada, edited by M.L. Rose. Canadian Society of Petroleum Geologists.

Silva, P.L. and R.M. Bustin, 2018. Preliminary liquid hydrocarbon potential assessment of the Doig Formation, northeastern British Columbia and west-central Alberta, based on thickness, organic richness and maturity.. In: Geoscience BC Summary of Activities 2017: Energy. Geoscience BC Report 2018-4, p. 39-50.

Smith, M.G., and R.M. Bustin, 2000. Late Devonian and Early Mississippian Bakken and Exshaw black shale source rocks, Western Canada Sedimentary Basin: a sequence stratigraphic interpretation. AAPG Bulletin, v.84, no.7, p.940-960.

Spence, L.M. and R.W. Evoy, 1998. Discovery history and sedimentological framework of the Grande Prairie Halfway “A” Pool, west-central Alberta: an example of a Middle Triassic barrier island/tidal inlet reservoir. In: Oil and Gas Pools of the Western Canada Sedimentary Basin, edited by J.R. Hogg. Canadian Society of Petroleum Geologists Special Publication S-51, p. 99-110.

Stasiuk, L.D., and M.G. Fowler, 2004. Organic facies in Devonian and Mississippian strata of Western Canada Sedimentary Basin: relation to kerogen type, paleoenvironment and paleogeography. Bulletin of Canadian Petroleum Geology, v.52, no.2, p.234-255.

Stoakes, F.A., 1992. Winterburn megasequence. In: Devonian-Early Mississippian carbonates of the Western Canada Sedimentary Basin: a sequence stratigraphic framework. SEPM Short Course #28, p. 207-224.

Stoneburner, R.K., 2015. The exploration, appraisal and development of unconventional reservoirs: a new approach to petroleum geology. Search and Discovery Article #110181.

Styan, W., and J. Shaw, 1991. An overview of Triassic Halfway pools in the Progress area (Abst). Bulletin of Canadian Petroleum Geology, v. 39, p. 226.

Tourmaline Oil Corporation, November 14 2016 Corporate Presentation. http://www.tourmalineoil.com/assets/Tourmaline-Oil-Corp-Overview-NOV-14-2016.pdf

Walsh, W., C. Adams, B. Kerr, and J. Korol, 2006. Regional “Shale Gas” potential of the Triassic Doig and Montney formations, northeastern British Columbia. B.C. Ministry of Energy, Mines and Petroleum Resources, Petroleum Geology Open File 2006-02.

Wendte, J.C., 2004. Jean Marie stratigraphic cross-sections, Cordova Embayment area, northeast British Columbia. Geological Survey of Canada Open File 4541.

White, T. and Al-Aasm, I.S. 1997. Hydrothermal dolomitization of the Mississippian Upper Debolt Formation, Sikanni gas field, northeastern British Columbia, Canada. Bulletin of Canadian Petroleum Geology, 45, no. 3, p. 297-316.

Willis, A.J., and T.F. Moslow, 1994. Sedimentology and stratigraphy of tidal inlet reservoirs in the Triassic Halfway Formation, Wembley Field, Alberta. Bulletin of Canadian Petroleum Geology, v. 42, p. 245-262.

Wilson, T.K., and R.M. Bustin, 2017. Unconventional petroleum system analysis of Upper Devonian organic-rich shale units in the Horn River and Liard Basins, northeastern British Columbia and adjacent western Alberta: Preliminary report. In: Geoscience BC Summary of Activities, Report 2017-1, p. 29-36.

Wittenberg, J., 1993. The significance and recognition of mass wasting events in cored sequences, impact on the genesis of several anomalously thick sandstones bodies in the Middle Triassic Doig Formation of west-central Alberta. Carboniferous to Jurassic Pangea – CSPG Core Workshop volume, edited by R. Karvonen et al., p. 131-161.

Young, F.G., S.R. Leggett, and D. Elbenschutz, 1993. Belloy Formation (Lower Permian), Fort St. John, B.C.: condensed, mixed siliciclastic-carbonate-chert sequences of channelized, marginal marine origin. Proceedings, CSPG Pangaea Conference, Calgary, p. 353.

Zonneveld, J-P., T.F. Moslow, and C.M. Henderson, 1997. Lithofacies associations and depositional environments in a mixed siliciclastic-carbonate coastal depositional system, upper Liard Formation, Triassic, northeastern British Columbia. Bulletin of Canadian Petroleum Geology, v. 48, no. 4, p. 553-575.

Zonneveld, J.-P., S.M. Hubbard, and T.F. Moslow, 1998. Middle Triassic reservoir facies, Tommy Lakes Field, northeastern British Columbia. Geo-Triad conference core workshop volume, p. 503-506.